Synthetic and Structural Investigation of Copper, Molybdenum and Nickel Complexes Derived from Polyfunctional Disalicylaldehyde Oxaloyldihydrazone

ABSTRACT

By

SANJESH CHOUDHURY

DEPARTMENT OF CHEMISTRY

SCHOOL OF PHYSICAL SCIENCES

A THESIS SUBMITTED

IN FULFILLMENT OF THE REQUIREMENT FOR THE

DEGREE OF

DOCTOR OF PHILOSOPHY IN CHEMISTRY

TO

NORTH-EASTERN HILL UNIVERSITY

SHILLONG – 793022

MEGHALAYA (INDIA)

MAY, 2009

ABSTRACT

CHAPTER I

Introduction and Literature Survey

This chapter gives a brief account of the importance of copper, molybdenum and nickel complexes. Pertinent literature on the transition and non-transition metal complexes of acyl, aroyl and pyridoyl dihydrazones derived from condensation of acyl-, aroyl-, and pyridoyl dihydrazines, respectively, with variety of aldehydes and ketones has also been presented in this chapter. An attempt has been made to survey literature on these ligands upto date.

CHAPTER II

Experimental

In this chapter the experimental details regarding the preparation of disalicylaldehyde oxaloyldihydrazone have been described. Procedure for elemental analyses, physico-chemical techniques and the instruments used are also presented.

CHAPTER III

Synthesis and Characterization of Monometallic Molybdenum (VI) Complexes derived from Polyfunctional Disalicylaldehyde oxaloyldihydrazone

This chapter deals with the synthesis and characterization monometallic molybdenum (VI) complexes derived from polyfunctional disalicylaldehyde oxaloyldihydrazone (H_4slox).

The monometallic complexes of the compositions: $[MoO_2(H_2slox)(A)]$ {where A = H_2O **(3.1)**, py **(3.2)**, 2-pic **(3.3)**, 3-pic **(3.4)** and 4-pic **(3.5)**} and

$[(MoO_2)_2(H_2slox)_2(NN)]$ {where NN = phen **(3.6)** and bpy **(3.7)**}, have been isolated and described.

All the complexes are either yellow or white in colour, air stable and decompose above 300°C. The complexes are non-electrolyte in DMSO. They are diamagnetic in nature consistent with d^0 electronic configuration of molybdenum.

The electronic spectrum of the free ligand shows bands in the region 290-342 nm assigned to $\pi \rightarrow \pi^*$ and $n \rightarrow \pi^*$ transitions. The complexes show an additional band in the region 413-431 nm assigned to ligand-to-metal charge transfer (LMCT) transition.

The free ligand shows two proton resonance at δ 12.64 (s), 11.00 (s), 8.81 (s) and eight proton resonance in the region 7.57-6.84 (m) ppm, respectively. The signals at δ 12.64, δ 11.00 and δ 8.81 ppm are assigned to arise due to -OH, >NH and -CH=N- protons, respectively, in the ligand. The multiplet in the region δ 7.57-6.84 ppm is assigned to arise due to protons of phenyl ring of the ligand molecule. The ^{1}H NMR spectra of the complexes show one proton resonances in the regions δ 12.64-12.67 and δ 10.98-11.31 ppm, respectively, due to -OH and >NH protons and two proton resonances in the region δ 8.63-9.06 due to -CH=N- protons. The complexes **(3.2)** to **(3.5)** also show an additional resonance in the region δ 8.35-8.54 ppm which have been assigned to arise due to the o-proton of pyridyl ring of the nitrogen donor bases. The ^{1}H NMR spectra of complexes **(3.6)** and **(3.7)** shows new signals at δ 7.89 and δ 8.80 due to phenanthroline and bipyridine protons. The resonance in the region 2.27-2.50 in the complexes **(3.3)** to **(3.5)** has been assigned to methyl protons of substituted pyridine molecules.

The IR spectrum of the ligand shows two bands at 3278 and 3204 cm^{-1}, respectively. The essential feature of this band suggests that they arise from phenolic -OH and >NH groups. A strong band at 1667 cm^{-1} is due to ν (>C=O) group while those at 1627 and 1603 cm^{-1} is due to ν (>C=N-) group. The IR spectra of the complexes also

show bands due to ν (-OH), ν (>NH), ν (>C=O) and ν (>C=N-) groups. Further, the complexes show new band in the region 1518-1533 cm^{-1}. This band is assigned to stretching vibration of NCO group produced as a result of enolization of the half part of the dihydrazone ligand upon coordination to the metal centre. The appearance of strong bands in the region 883-939 cm^{-1} in the IR spectra of the complexes is due to the presence of cis-MoO_2^{2+}. Complexes **(3.2)** to **(3.5)** show an additional new band in the region 1060-1003 cm^{-1} assigned to the ring stretching mode of pyridine and substituted pyridine molecules. Complex **(3.6)** shows two new strong bands at 725 and 840 cm^{-1} while complex **(3.7)** shows only one band at 758 cm^{-1}. These bands are due to the out-of-plane motion of the hydrogen atoms on the heterocyclic rings. The in-plane ring deformation mode of the phenanthroline and bipyridine occurs at 634 and 632 cm^{-1} in complexes **(3.6)** and **(3.7)** respectively.

On the basis of results obtained from various physico-chemical and spectral studies, the tentative structures for the complexes have been proposed at the end of the chapter.

CHAPTER IV

Synthesis and Characterization of Homobimetallic Molybdenum (VI) Complexes derived from Polyfunctional Disalicylaldehyde oxaloyldihydrazone

This chapter deals with the synthesis and characterization of homobimetallic molybdenum (VI) complexes derived from polyfunctional disalicylaldehyde oxaloyldihydrazone.

On the basis of various analytical and physico-chemical data, the complexes isolated in the present chapter are suggested to have the compositions: $[(MoO_2)_2(slox)(A)_2]$ {where A = H_2O **(4.1)**, py **(4.2)**, 2-pic **(4.3)**, 3-pic **(4.4)** and 4-pic **(4.5)**}.

All the complexes are yellow coloured and are air stable. They decompose above 300°C and have molar conductance value in the range 1.8-5.0 $ohm^{-1}cm^2mol^{-1}$ in

DMSO indicating that they are non-electrolyte in this solvent. All the complexes are diamagnetic in nature.

The electronic spectra of the complexes show three bands in the region 292 – 341 nm and an additional broad band in the region 417 – 432 nm. The bands in the region 292 – 341 nm are assigned to intraligand $\pi \rightarrow \pi^*$ and $n \rightarrow \pi^*$ and that in the region 417 – 432 nm is assigned to ligand-to-metal charge transfer (LMCT) transition.

The two proton -OH and >NH signals in the uncoordinated dihydrazone ligand at δ 12.64 and δ 11.00 ppm disappear in the complexes indicating the coordination of the ligand to the metal via deprotonation of phenolic -OH group and via enolized carbonyl group. The singlet at δ 8.81 ppm in the ligand undergoes splitting in the metal complexes. One signal is downfield shifted by about 0.24 ppm and the other signal remains at almost the same position as that in the free ligand. The splitting of >CH=N- signal into two in the ^{1}H NMR of the complexes is a good evidence of the existence of ligand molecule in anti-cis configuration. The complexes **(4.1)** to **(4.5)** show triplet in the region 1.04 -1.25 ppm, quartet in the region 3.21-3.46 ppm and another triplet in the region 4.35-4.37 ppm which are assigned to the $-CH_3$, $-CH_2$ and -OH protons of ethanol molecule. The o-proton signal of pyridyl ring of pyridine or substituted pyridine occurs in the region 8.30-8.58 ppm in the complexes **(4.2)** to **(4.5)**. These complexes except complex **(4.1)** and **(4.2)** also show a new signal in the region 2.30-2.50 ppm which are assigned to arise due to the protons of methyl group of substituted pyridine molecules.

The bands due to phenolic -OH and >NH groups are absent in the IR spectra of the complexes suggesting its involvement in coordination with the metal centre. A new broad band at 3448 cm^{-1} in the IR spectrum of the complex **(4.1)** is due to stretching vibration of -OH group of coordinated water molecules. The IR spectra of the complexes do not show bands due to stretching vibration of (>C=O) group suggesting its involvement in coordination with the metal centre via enolization. Enolization of the ligand is also evident from the appearance of new band due to ν

(NCO) group in the region 1535-1537 cm^{-1} in the complexes. The ν (>C=N-) band on an average shifts to lower frequency by 11-13 cm^{-1} in the metal complexes suggesting the coordination of azomethine nitrogen atom to the metal centre. The complexes **(4.2)** to **(4.5)** also show a weak intensity band in the region 1060-1003 cm^{-1}, which is assigned to ring stretching mode of pyridine, 2-picoline, 3-picoline and 4-picoline molecules. Two strong bands appearing in the region 951 – 912 cm^{-1} in complexes are assigned to the stretching vibration of the cis-MoO_2^{2+} group. The band in the region 951 – 933 cm^{-1} is due to the symmetric stretching vibration of cis-MoO_2^{2+} group while the band in the region 916 – 902 cm^{-1} is due to the asymmetric stretching vibration of the cis-MoO_2^{2+} group.

Based on physico-chemical data and spectral studies, the tentative structures of the complexes have also been suggested at the end of the chapter.

CHAPTER V

Synthesis and Characterization of Monometallic Copper (II) Complexes derived from Polyfunctional Disalicylaldehyde oxaloyldihydrazone

This chapter deals with the synthesis and characterization of monometallic copper (II) complexes derived from polyfunctional disalicylaldehyde oxaloyldihydrazone.

On the basis of various analytical and physico-chemical data, the complexes are suggested to have the compositions: [Cu(H_2slox)] **(5.1)**, [Cu(H_2slox)(A)] {where A = py **(5.2)**, 2-pic **(5.3)**, 3-pic **(5.4)** and 4-pic **(5.5)**}, respectively.

All the complexes are dark green in colour, air stable and decompose above 300°C. The complexes have molar conductance value in the range 1.2-1.8 $ohm^{-1}cm^2mol^{-1}$ in DMSO at 10^{-3} M dilution indicating their non-electrolytic nature. The room temperature magnetic moment values for the complexes are in the range 1.69-1.75 BM which is close to the spin only value of 1.73 BM indicating no appreciable spin-spin interaction between copper atoms.

Apart from the ligand bands, the complexes show a single broad band in the 636 – 661 nm regions with a comparatively very low molar extinction coefficient in the range 59 – 90 $dm^3mol^{-1}cm^2$. Hence, this band is assigned to d-d transition. The essential feature of this band in the 630 – 660 nm regions suggests that it is the combination of three transitions ($^2B_{1g} \rightarrow {}^2A_{1g}$, $^2B_{1g} \rightarrow {}^2B_{2g}$ and $^2B_{1g} \rightarrow {}^2E_g$) It is concluded that all the copper (II) complexes have square-planar geometry.

The $g_{\|}$ value for the copper (II) complexes **(5.1)** to **(5.5)** lies in the range 2.318 – 2.330 at RT and 2.314 – 2.339 at LNT, while the $g_{|}$ value lies in the range 2.111 – 2.119 at RT and 2.104 – 2.125 at LNT, respectively. The EPR spectra of the complexes at RT as well as at LNT in DMSO solution show copper hyperfine splitting due to interaction of unpaired electron of copper (II) ion with the nuclear spin (I = 3/2). The superhyperfine structure at high field has been observed in the copper (II) complex **(5.1)** at LNT and is attributed to the interaction of the unpaired electron of copper (II) ion with the nuclear spin of the N atom from the ligand molecule. The superhyperfine coupling constant $A_{|N}$ = 12G, corresponds to the coupling of electron spin with the nuclear spin of two nitrogen atoms.

The α^2_{Cu} values for the copper (II) complexes **(5.1)** to **(5.5)** are in the range of 0.878 – 0.929 < 1 indicating that the copper (II) complexes have some covalent character. The $A_{\|}$ values for the copper (II) complexes **(5.1)** to **(5.5)** are in the range of 174 - 180 cm^{-1}. The $g_{\|}/A_{\|}$ for the copper (II) complexes **(5.1)** to **(5.5)** lies in the range 129.9 – 132.9 cm, which falls in the range 90 – 140 cm for square-planar copper (II) complexes. All of the copper (II) complexes have $g_{\|}>g_{|}>2.0023$ indicating that the unpaired electron lies in the d_{x2-y2} orbital. G value for the complexes **(5.1)** to **(5.5)** lies in the range 2.80-2.94 at RT and 2.74-3.09 at LNT which is in good agreement with the result reported for the square planar complexes of copper (II).

The essential features of the IR spectra of the complexes **(5.1)** to **(5.5)** in the region 3000 – 3300 cm^{-1} is almost same as that of the ligand. The υ (>NH) band in the complexes remains almost unshifted in position ruling out the possibility of

coordination of ligand to the metal centre through secondary >NH nitrogen atom. The complexes show a very strong band in the region 1533-1527 cm^{-1} in the IR spectra. Although the IR spectrum of the ligand also shows a strong band at 1534 cm^{-1}, yet the intensity of the band in the region 1533-1527 cm^{-1} in the complexes is considerably enhanced as compared to that in the uncoordinated ligand. Hence this band appears to have contribution due to both υ (C-O) (phenolate) and υ (NCO) produced as a result of enolization. The presence of both υ (NCO) group and υ (>C=O) group in the complexes suggests that only one >C=O group undergoes enolization and the other >C=O group remains as such. The υ (>C=N-) band observed at 1627 and 1603 in the free dihydrazone shifts to lower frequency on an average by 2-8 cm^{-1} in the complexes indicating coordination through azomethine nitrogen atom to the metal centre.

The redox behaviors of copper (II) complexes **(5.1)** to **(5.5)** have been studied with the help of cyclic voltammetry.

Based on physico-chemical data and spectral studies, the tentative structures of the complexes have also been suggested at the end of the chapter.

CHAPTER VI

Synthesis and Characterization of Homotrimetallic Copper (II) Complexes derived from Polyfunctional Disalicylaldehyde oxaloyldihydrazone

This chapter deals with the synthesis and characterization of homotrimetallic copper (II) complexes derived from polyfunctional disalicylaldehyde oxaloyldihydrazone.

The complexes were isolated and characterized on the basis of various physico-chemical and spectral studies and were suggested to have the composition $[Cu_3(slox)Cl_2(A)_2]$ {where A = H_2O **(6.1)**, py **(6.2)**, 2-pic **(6.3)**, 3-pic **(6.4)** and 4-pic **(6.5)**}.

The complexes are either green or dark green in colour and decompose above 300°C without melting. The molar conductance values for the complexes in DMSO lies in the region 1.3 – 2.0 $ohm^{-1}cm^2mol^{-1}$ indicating their non-electrolytic nature in this solvent. The magnetic moment value of the complexes **(6.1)** to **(6.5)** lies in the region 2.23-2.56 BM i.e. 0.74 – 0.85 BM per copper atom indicating considerable amount of interaction between the copper atoms in these complexes.

The electronic spectra of the complexes show a new non-ligand band in the region 429 – 435 nm which have high molar extinction coefficient. This band has been assigned to arise due to ligand-metal charge transfer (LMCT) transition. The band in the region 628 – 660 nm is due to d-d transition which indicates square planar environment around copper (II) atom with $^2B_{1g}$ ground state.

The EPR spectra of the complexes in the present study are isotropic in DMSO solution at room temperature. The complexes show anisotropic spectra at LNT characteristic of the systems having axial symmetry. LNT EPR spectra are typical for S = ½ spin systems. The hyperfine splitting constants fall in the region 120-150 G. The $g_{\|}$ values fall in the region 2.407-2.442 while the $g_{|}$ values fall in the range 2.176-2.208. Further, the $g_{\|}/A_{\|}$ values are also found to lie in agreement with the proposed distorted square planar geometry around copper atom. The $g_{\|}/A_{\|}$ values for the present complexes are found to lie in the range 162 – 200 cm, slightly higher than that required for a square planar geometry. Such EPR spectra are typical of a d^9 complex possessing axial symmetry with the unpaired electron present in a $d_{x^2-y^2}$ orbital. The spectra of these complexes do not show any half field ($\Delta Ms = 2$) transition or fine structure and look like a spectrum associated with isolated S = ½ states.

The υ (-OH) and υ (>NH) vibrations disappear in the complexes indicating the coordination of -OH group via deprotonation and involvement of >NH group in coordination via enolization. The disappearance of band due to >C=O group and appearance of new band in the region around 1533 cm^{-1} due to newly created (NCO)

group further supports the enolization of the ligand molecule upon coordination with the metal centre. The bands due to azomethine (>C=N-) group appears in the region 1613-1606 cm^{-1} in the complexes **(6.1) - (6.5)** which is shifted to lower frequency on an average by 7-12 cm^{-1}. The shift of this band to lower frequency indicates the coordination of azomethine nitrogen atom to the metal centre. Complexes **(6.1)** to **(6.5)** show two new bands in the low frequency region ~ 180 and ~200 cm^{-1} assigned to arise due to stretching vibration of bridged Cu-Cl group.

The redox behaviors of copper (II) complexes **(6.1)** to **(6.5)** have been examined by cyclic voltammetry.

On the basis of various physico-chemical data and spectral studies, the tentative structures of the complexes have been suggested at the end of the chapter.

CHAPTER VII

Synthesis and Characterization of Nickel (II) Complexes derived from Polyfunctional Disalicylaldehyde oxaloyldihydrazone

This chapter describes the synthesis and characterization of monometallic and homobimetallic nickel (II) complexes derived from polyfunctional disalicylaldehyde oxaloyldihydrazone.

The complexes of the compositions $[Ni(H_2slox)(H_2O)_3]$ **(7.1)**, $[Ni_2(slox)(A)_4]$ {where A = H_2O **(7.2)**, py **(7.3)**, 2-pic **(7.4)**, 3-pic **(7.5)** and 4-pic **(7.6)**, $[Ni_2(slox)(NN)_2]$ {where NN = phen **(7.7)** and bpy **(7.8)**} have been described in this chapter.

The complexes are light greenish yellow, greenish yellow or brown in colour, air stable and have a very high decomposition point (>300°C). The complexes are non-electrolyte in DMSO. The magnetic moment values for the complexes at room temperature is found to lie in the range 2.94-3.10 BM i.e. 1.47-1.55 BM per nickel

(II) ion in complexes **(7.2)** to **(7.6)** while complex **(7.1)** has magnetic moment value of 3.10 BM which falls in the range reported for high-spin octahedral nickel (II) complexes. The magnetic moment values for complexes **(7.2)** to **(7.6)** are considerably less than the values expected for two spin-free nickel (II) ions present in the same molecular unit. This indicates strong metal-metal interaction in the structural unit of the complexes via oxo-bridging which causes substantial lowering of magnetic moment. Complexes **(7.7)** and **(7.8)** have magnetic moment value of 4.95 and 4.80 BM, respectively. The magnetic moment value for these complexes is very near to the theoretical value for four electron spin systems.

Apart from the ligand and charge transfer bands the nickel (II) complexes **(7.1)** to **(7.8)** show two bands in the 615-950 nm range corresponding to the transition $^3A_{2g} \rightarrow {}^3T_{2g}$ (F) (ν_1), and $^3A_{2g} \rightarrow {}^3T_{1g}$ (F) (ν_2), respectively. These two low energy bands observed in the complexes are characteristic of nickel (II) in octahedral environment. The octahedral environment around nickel (II) in these complexes is further supported by the value of ν_2/ν_1 ratio which lies in the region of 1.49-1.51.

The IR spectra of the complexes **(7.2)** to **(7.8)** do not show any band due to ν (-OH) and ν (>NH) groups suggesting the involvement of -OH group in coordination via deprotonation and destruction of amide structure via enolization. The ν (>C=O) band occurs at 1668 cm^{-1} in the complex **(7.1)** with reduced intensity whereas in the rest of the complexes this band is absent. The absence of band due to ν (>C=O) group indicates enolization of the ligand molecule and its coordination to the metal centre via enolized >C=O group in these complexes. The ν (>C=N-) band appears as a single strong band at 1608 cm^{-1} in the complex **(7.1)** while in the remaining complexes it appears as a couple of strong intensity band in the region 1626-1598 cm^{-1}. The appearance of ν (NCO) group in the IR spectra of all the complexes confirms the presence of dihydrazone in enol form. The presence of both ν (>C=O) and ν (NCO) bands in the IR spectrum of the complex **(7.1)** indicates that in this complex only one hydrazone part is enolized while the other hydrazone part remains uncoordinated in keto-form. The nickel (II) complexes **(7.3)** to **(7.6)** also show a

weak intensity band in the region 1020-1010 cm^{-1}, characteristic of ring stretching mode of pyridine, 2-picoline, 3-picoline and 4-picoline molecules.

Based on the various physico-chemical and spectral studies, the tentative structures of the complexes have been assigned at the end of the chapter.

CHAPTER VIII

Synthesis and Characterization of Heterobimetallic Copper, Molybdenum and Nickel Complexes derived from Polyfunctional Disalicylaldehyde oxaloyldihydrazone

This chapter describes the synthesis and characterization of heterobimetallic nickel (II)-molybdenum (VI) and copper (II)-molybdenum (VI) complexes derived from polyfunctional disalicylaldehyde oxaloyldihydrazone.

The complexes of the compositions $[Ni(slox)MoO_2(A)_4]$ {where A = H_2O **(8.1)**, py **(8.2)**, 2-pic **(8.3)**, 3-pic **(8.4)** and 4-pic **(8.5)**}, $[Ni(slox)MoO_2(NN)_2]$ {where NN = bpy **(8.6)** and phen **(8.7)**}, $[Cu(slox)MoO_2(A)_2]$ {where A = H_2O **(8.8)**, py **(8.9)**, 2-pic **(8.10)**, 3-pic **(8.11)** and 4-pic **(8.12)**} and $[Cu(slox)MoO_2(NN)_2]$ {where NN = bpy **(8.13)** and phen **(8.14)**} have been described in this chapter.

The Ni(II)-Mo(VI) complexes are yellow while Cu(II)-Mo(VI) complexes are green or dark green in color. All the complexes are air stable, decompose above 300°C and are non-electrolytic in nature in DMSO. The room temperature magnetic moment for the heterobimetallic complexes **(8.1)** to **(8.7)** is in the range 2.87-3.10 BM while for the complexes **(8.8)** to **(8.14),** it is in the range 1.69-1.82 BM.

Three non-ligand bands are observed in the nickel (II)-molybdenum(VI) heterobimetallic complexes **(8.1)** to **(8.7)** in the region 413-423, 618-626 and 931-952 nm respectively, whereas in the copper (II)-molybdenum(VI) heterobimetallic complexes **(8.8)** to **(8.14)** only two non-ligand bands are observed in the region 414-

424 and 608-666 nm respectively. The two low energy bands observed in the region 618-626 and 931-952 nm in the complexes **(8.1)** to **(8.7)** correspond to $^3A_{2g} \rightarrow {}^3T_{2g}$ (F) (ν_1) and $^3A_{2g} \rightarrow {}^3T_{1g}$ (F) (ν_2) transitions, characteristic of nickel (II) in octahedral environment. The band in the 610 – 670 nm regions in the complexes (8.8) to (8.14) suggests that it is the combination of three transitions ($^2B_{1g} \rightarrow {}^2A_{1g}$, $^2B_{1g} \rightarrow {}^2B_{2g}$ and $^2B_{1g} \rightarrow {}^2E_g$).

The EPR spectra of the complexes **(8.8)** to **(8.14)** give g values in the order $g_{\|} > g_{|} >$ 2.0023 indicating square planar stereochemistry around copper centre with the unpaired electron lying predominantly in the $d_{x^2-y^2}$ orbital, as evident from the value of the exchange interaction term G.

The IR spectra of the complexes do not show any band due to ν (-OH), ν (>NH) and ν (>C=O) groups. The ν (>C=N-) band appears in the region 1602-1609 cm^{-1}. This band remains either unshifted or shifts to lower frequency in the complexes as compared to the precursor complexes. The band in the region 1512-1552 cm^{-1} is due to ν (NCO) obtained as a result of enolization of the ligand. The couple of new strong intensity bands appearing in the region 881-948 cm^{-1} are characteristic of occurrence of cis-MoO_2^{2+} group in the complexes. A weak intensity band in the region 1000-1070 cm^{-1} is assigned to ring stretching mode of pyridine and substituted pyridine molecules. Complexes **(8.7)** and **(8.14)** show two strong intensity bands at 725-727 and 841-849 cm^{-1} region which are assigned to the out-of-plane motion of the hydrogen atoms on the heterocyclic rings and the hydrogen atoms on the central ring, respectively. In the complexes **(8.6)** and **(8.13)** only one strong band is observed at 756 - 758 cm^{-1} due to out-of-plane motion of the hydrogen atoms as expected for two identical groups of four hydrogen atoms each.

Based on the various physico-chemical and spectral studies, the tentative structures of the complexes have been assigned at the end of the chapter.

Synthetic and Structural Investigation of Copper, Molybdenum and Nickel Complexes Derived from Polyfunctional Disalicylaldehyde Oxaloyldihydrazone

By

SANJESH CHOUDHURY

DEPARTMENT OF CHEMISTRY

SCHOOL OF PHYSICAL SCIENCES

A THESIS SUBMITTED

IN FULFILLMENT OF THE REQUIREMENT FOR THE

DEGREE OF

DOCTOR OF PHILOSOPHY IN CHEMISTRY

TO

NORTH-EASTERN HILL UNIVERSITY

SHILLONG – 793022

MEGHALAYA (INDIA)

MAY, 2009

Dedicated to my beloved parents

DECLARATION

I, Mr. Sanjesh Choudhury, hereby declare that the subject matter of the thesis entitled "*Synthetic and Structural Investigation of Copper, Molybdenum and Nickel Complexes Derived from Polyfunctional Disalicylaldehyde Oxaloyldihydrazone*" is the record of work done by me and the content of this thesis did not form the basis of the award of any previous degree to me or to anybody else to the best of my knowledge and that the thesis has not been submitted by me for any research degree in any other University/Institution.

This is being submitted to the North-Eastern Hill University for the degree of Doctor of Philosophy in Chemistry.

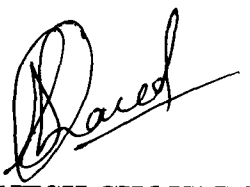

Place: Shillong

(SANJESH CHOUDHURY)

Date: 21/05/09

पूर्वोत्तर पर्वतीय विश्वविद्यालय
पू० प० विवि० परिसर, शिलांग-७९३०२२ (मेघालय)
North-Eastern Hill University
NEHU Campus, Shillong - 793 022 (Meghalaya)

Phone :
Grams : NEHU

Dr. R. A. Lal
Professor
Department of Chemistry

Phone: 0364-2722617(O)
E-mail: ralal@rediffmail.com

CERTIFICATE

This is to certify that the thesis entitled "*Synthetic and Structural Investigation of Copper, Molybdenum and Nickel Complexes Derived from Polyfunctional Disalicylaldehyde Oxaloyldihydrazone*" submitted by Mr. Sanjesh Choudhury for the degree of Doctor of Philosophy of the North-Eastern Hill University, Shillong, embodies the record of original investigation carried out by him under my supervision. He has been duly registered, and the thesis presented is worthy of being considered for the Ph.D. degree in Chemistry.

The work described in this thesis is original and has not been submitted for any other degree or diploma in this or any other university.

Ralal
21/05/09
(Prof. R. A. Lal)
SUPERVISOR

Professor
Department of Chemistry
North-Eastern Hill University
Shillong - 793022

Countersigned

(Prof. B. Myrboh)

Head, Department of Chemistry

Head
Department of Chemistry
North - Eastern Hill University
Shillong - 793022

ACKNOWLEDGEMENT

At the outset, I express my heartfelt gratitude to Dr. R. A. Lal, Professor in the Department of Chemistry, NEHU, Shillong, for suggestion of the problem and for his able guidance and supervision throughout the course of this investigation.

I am grateful to the Dean, School of Physical Sciences and the Head of the Department of Chemistry, NEHU, for providing me the facility to carry out this work. I am thankful to all the faculty members for their good wishes. My special thanks are due to Head and staff of RSIC, NEHU, Shillong, for allowing me to avail various instrumentation facilities needed during the course of my work.

I am also thankful to Head, NMR research centre, Indian Institute of Science, Bangalore and IIT Bombay for recording 1H NMR, and EPR spectra of the complexes. I am very much thankful to University Grants Commission, New Delhi for providing financial assistance through UGC fellowship.

It is my pleasure to acknowledge the help and generous cooperation extended by my fellow workers in the laboratory, Mr Mithun Chakrabarty and Mr. Aziz Ahmed. My thanks are also due to all my Research Scholar friends for the help they rendered on various occasions during the course of my work.

I am grateful to Ms. Priya Juving Rai Dkhar for her moral support and valuable suggestions.

I will be failing in my duty if I do not convey my thanks to the non-teaching staff of the Department of Chemistry, NEHU, and the staff of library, for their cooperation.

Last but not the least, I express my deepest sense of gratitude to my parents for the sacrifice they did to mould my carrier and who were always a source of inspiration to me, I am thankful to all my brothers and sisters for their good wishes.

PREFACE

Studies on synthesis and characterization of copper (II), molybdenum (VI) and nickel (II) complexes derived from polyfunctional disalicylaldehyde oxaloyldihydrazone are the focal theme of the work described in the present thesis. The entire matter of the thesis is distributed over eight chapters (**Chapter I-VIII**). Each chapter is virtually complete in itself. The description of the results of the work undertaken for the present research work is presented in **Chapter III** through to **Chapter VIII**. These chapters (**III-VIII**) include a short Introduction justifying the specific objective of the work followed by experimental describing the synthesis and then Results and discussion and finally the tentative structures of the complexes.

The first chapter (**Chapter I**) dealing with introduction provides a background pertaining to the work described in the thesis. The significance, interest and scope of some polyfunctional Schiff bases have been portrayed in this chapter with citations from contemporary literature. Diversity of structures, synthesis procedures and characterization of coordination compounds has found particular attention in this chapter.

Chapter II includes the details of instruments used, synthetic methods of preparation of principal ligands and analytical methods for solid-state characterization of the complexes.

Chapter III of this thesis is concerned with synthesis and characterization of monometallic molybdenum (VI) complexes of disalicylaldehyde oxaloyldihydrazone incorporating pyridine, 2-picoline, 3-picoline, 4-picoline, 1,10-phenanthroline and 2,2'-bipyridine as co-ligands. The complexes reported here are of type $[MoO_2(H_2slox)(A)]$ {*where A = H_2O* **(3.1)**, *pyridine (py)* **(3.2)**, *2-picoline (2-pic)* **(3.3)**, *3-picoline (3-pic)* **(3.4)** *and 4-picoline (4-pic)* **(3.5)**}; $[(MoO_2)_2(H_2slox)_2(NN)]$ {*where NN = 1,10-phenanthroline (phen)* **(3.6)** *and 2,2'-bipyridine (bpy)* **(3.7)**}.

Chapter IV of this thesis deals with synthesis and characterization of homobimetallic molybdenum (VI) complexes of disalicylaldehyde oxaloyldihydrazone incorporating

nitrogen donor co-ligands. The complexes mentioned here are $[(MoO_2)_2(slox)(A)_2]$ {*where A = H_2O* **(4.1)**, *pyridine (py)* **(4.2)**, *2-picoline (2-pic)* **(4.3)**, *3-picoline (3-pic)* **(4.4)** *and 4-picoline (4-pic)* **(4.5)**}.

Chapter V describes the synthesis and characterization of monometallic copper (II) complexes derived from disalicylaldehyde oxaloyldihydrazone incorporating pyridine, 2-picoline, 3-picolin and 4-picoline as co-ligands. The complexes reported here are of the type $[Cu(H_2slox)]$ **(5.1)**, $[Cu(H_2slox)(A)]$ {*where A = pyridine (py)* **(5.2)**, *2-picoline (2-pic)* **(5.3)**, *3-picoline (3-pic)* **(5.4)** *and 4-picoline (4-pic)* **(5.5)**}.

Synthesis and characterization of homotrimetallic copper (II) complexes of disalicylaldehyde oxaloyldihydrazone with nitrogen donor co-ligands forms the subject matter of **Chapter VI**. The complexes mentioned here are $[Cu_3(slox)Cl_2(A)_2]$ {*where A = H_2O* **(6.1)**, *pyridine (py)* **(6.2)**, *2-picoline (2-pic)* **(6.3)**, *3-picoline (3-pic)* **(6.4)** *and 4-picoline (4-pic)* **(6.5)**}.

Chapter VII of this thesis presents an account of synthesis and characterization of monometallic and homobimetallic nickel (II) complexes of disalicylaldehyde oxaloyldihydrazone with pyridine, 2-picoline, 3-picolind, 4-picolind, 1,10-phenanthrolind and 2,2'-bipyridine as co-ligands. The complexes are of the type $[Ni(H_2slox)(H_2O)_2]$ **(7.1)**, $[Ni_2(slox)(A)_4]$ {*where A = H_2O* **(7.2)**, *pyridine (py)* **(7.3)**, *2-picoline (2-pic)* **(7.4)**, *3-picoline (3-pic)* **(7.5)** *and 4-picoline (4-pic)* **(7.6)**}, $[Ni_2(slox)(NN)_3]$ {*where NN = 1,10-phenanthroline (phen)* **(7.7)**, *and 2,2'-bipyridine (bpy)* **(7.8)**}.

The final chapter (**Chapter VIII**) deals with synthesis and characterization of heterobimetallic copper, molybdenum and nickel complexes of disalicylaldehyde oxaloyldihydrazone with the nitrogen donor co-ligands. The complexes reported here are of the type $[Ni(slox)MoO_2(A)_4]$ {*where A = H_2O* **(8.1)**, *pyridine (py)* **(8.2)**, *2-picoline (2-pic)* **(8.3)**, *3-picoline (3-pic)* **(8.4)** *and 4-picoline (4-pic)* **(8.5)**}, $[Ni(slox)MoO_2(NN)_2]$ {*where NN = 2,2'-bipyridine (bpy)* **(8.6)** *and 1,10-phenanthroline (phen)* **(8.7)**}, $[Cu(slox)MoO_2(A)_2]$ {*where A = H_2O* **(8.8)**, *pyridine (py)* **(8.9)**, *2-picoline (2-pic)* **(8.10)**, *3-*

picoline (3-pic) **(8.11)** *and 4-picoline (4-pic)* **(8.12)**} and [Cu(slox)$MoO_2(NN)_2$] {*where NN = 2,2-bipyridine (bpy)* **(8.13)** *and 1,10-phenanthroline (phen)* **(8.14)**}.

A summary (**Abstract**) describing the research highlights have been given at the end followed by the **list of publication**.

CONTENTS

CHAPTER I

Introduction and literature survey

Introduction

The present thesis embodies the results of investigations of reactions of metal salts of copper, molybdenum and nickel salts with disalicylaldehyde oxaloyldihydrazone and the characterization of the resulting complexes. The structural assessment of the complexes described in this thesis is based on the data from conductivity measurements, magnetic susceptibility measurement, electronic, IR, ^{1}H NMR and EPR measurements. Accordingly, the present chapter gives a brief account of importance of copper, molybdenum and nickel in monometallic and heterometallic systems followed by literature survey on metal complexes of dihydrazones.

Molybdenum is the only element of the second transition series, being essential for life **[1]**. The element molybdenum is present in two types of enzymes. One of these is nitrogenase **[2]** which is found in free living and symbiotic microorganisms and catalyses reduction of dinitrogen to ammonia. The other category of molybdenum enzymes consists of hydroxylases or oxotransferases **[3]** which catalyze a variety of two electron oxidation reduction reactions. As a constituent of enzymes, molybdenum also participates in redox reactions e.g. oxidation of aldehydes, xanthine and other purines **[4]**, and reduction of nitrate to molecular nitrogen **[5, 6]**. Biochemical role of molybdenum is based on its ability to facilitate electron exchanges and to form stable complexes with oxygen, nitrogen and sulfur containing ligands **[2]**. Further, the polyoxomolybdenum compounds have potential application in medicine, including anti-tumor, antibacterial and antivirus activity **[7]**. Molybdenum compounds have been shown to suppress the tumor growth in mice bearing several human tumors. They also exhibit anti-tumor activity against human gastric cancer **[8]**. Molybdenum compounds are also used as heterogeneous photocatalysts **[9]**. Homogeneous molybdenum (VI) catalysts containing the cis-

[MoO_2^{2+}] unit are the basis of important industrial oxidation processes such as epoxidation using alkyl hydroperoxides as the oxygen source **[10]**.

Mixed metal molybdenum oxides are used as efficient and selective catalysts for potential oxidation of light alkanes in petrochemistry **[11]**. A cobalt, nickel or platinum promoted catalysts are used in the hydrosulfurization and hydrodenitrogenation processes **[12]** whereby organo-sulfar and nitrogen compounds in petroleum feedstocks are heterogeneously desulfurized and denitrogenated. Molybdenum and copper based heterometal systems are important in molecular scale memory devices **[13]**, or switches **[14]** or ferroelectrics **[15]**. A high spin molecule $MoCu_6$ based on copper and octacyanomolybdate shows photoswitchable property **[16]**. Another Mo and Cu based compound $Cu_2^{II}[Mo(CN)_8].8H_2O$ shows property of ferroelectricity **[17]**. The coordination nanoparticles like $[Mo(CN)_8CuNi]$ act as photomagnetic particles **[18]** and have revealed the possibility of triggering supermagnetism **[19]** by ligand.

Nickel occurs in the enzyme urease. Urease catalyzes the hydrolysis of urea to ammonia and carbonic acid **[20]**. Nickel occurs widely in bacterial hydrogenase which catalyzes the combination of hydrogen and oxygen, the reduction of sulphate ion, the production of methane and other reductive processes such as reduction of alkyl halides **[21]**. Nickel complexes are also used as antioxidants **[22]** and are also used as catalysts for the oligomerization of ethylene **[23]**. The other nickel-dependent enzymes are E.Coli glyoxalase I (E. Coli Glx I), [NiFe]-hydrogenase, methyl-CoM reductase (MCR), Co dehydrogenase (CODH) and acetyl CoA synthase (ACS) **[24]**.

Nickel plays a prominent role in several areas of material chemistry. Some topical interplay between nickel coordination chemistry and material science exists in the use of Ni-containing alkoxides for the synthesis of ceramic materials by MOCUD and Sol-gel processes, the preparation and nanoscopic dendrimers incorporating Ni, the construction of 3D hybrid inorganic-organic porous materials with Ni

coordination units and the fabrication of supported Ni catalysts and Ni nano structures through nanotechnology. Paramagnetic high spin Ni^{II} has found particular attention in the field of molecular magnetism, culminating in the recent discovery of the first single molecule magnets based on Ni^{II} centres **[24]**.

Copper is an essential bioelement responsible for numerous catalytic processes in living organism where it is often present in di- and trinuclear assemblies **[25]** like ascorbate oxidase, copper dioxygenase, copper monooxygenase and blue and non-blue oxidase etc. Copper is the constituent of redox enzymes and O_2 transfer pigments. Polynuclear copper centres are widespread in biological systems, occurring in type 3 cuproproteins such as tyrosinase and hemocyanin **[26]**. The trinuclear copper centres occur in luccase, ascorbate oxidase and particulate methanol monooxygenase (pMMO) **[27]**. In all these enzymes, copper is present either alone or in combination with atoms of its own kind. Copper is also present in the multimetallic enzymes in combination with other metals. Thus copper occurs in superoxide dismutase in combination with zinc and in cytochrome C oxidase in combination with iron. In humans also, multicopper oxidase is present in ceruloplasmin in which copper is present in combination with iron **[28]**. Ceruloplasimin effectively catalyses the oxidation of Fe (II) to Fe (III) under physiological conditions **[29]**. Recently, copper has been reprted to occur at the active site of the heterobimetallic enzyme carbon monoxide dehydrogenase (CODH) from Oligotropha carboxidovoraus in combination with molybdenum **[30-32]**.

Heterobimetallic complexes are important from several points of view. Firstly the heterobimetallic complexes have been successfully used as precursors in the synthesis of ceramic materials favoring an intimate mixing of the elements which can enable reactions at lower temperatures rather than for traditional route or the preparation of purer inaccessible solid state phases. Secondly, the molecular complexes containing two or more different metal ions are of interest in metalloenzymes, homogeneous and heterogeneous catalysis. The formation of metal enzyme complexes is universal in nature and many reactions in living systems occur

via metal complex formation with large molecules. In homogeneous catalysis, a heterobimetallic complex containing an electron deficient metal atom and an electron rich metal atom presents the possibility of lewis acid activation of a substrate molecule bound to the electron rich metal centre. The heterobimetallic complexes which have such types of properties are usually derived from widely divergent transition metals. Further, the heterobimetallic complexes have the potential to mediate cetain chemical reactions of industrial relevance either more efficiently than or in a different manner to isolated metal centres. They exhibit different reactivity pattern as compared to the corresponding monometallic and homobimetallic complexes as well.

Literature Survey

Hydrazine is a potential ligand which functions in metal complexes as monodentate, bidentate chelating and bridging ligand. The coordination behavior of hydrazone is modified by substitution of one of the hydrogen in hydrazine by an acyl group, which provides additional bonding sites of carbonyl oxygen atoms, the resulting -CONH- group is capable of existing in keto-enol equilibrium. In such monoacyl hydrazines, the bridging character of hydrazine is lost and the studies have revealed that such derivatives act as bidentate ligands coordinating through carbonyl oxygen and $-NH_2$ groups.

Further, condensation of N-acyl hydrazines with aldehyde and ketones give acyl-hydrazones (Schiff bases). In such ligands basicity of nitrogen atoms in hydrazine residue is considerably reduced by substitution on either side. A variety of such hydrazones can be prepared in which the number of bonding sites can be increased as desired by changing alkyl groups. Condensation of acylhydrazines with o-hydroxyaromatic aldehydes and ketones enhances chelating tendencies of the acylhydrazones. These compounds have been shown to act as monodentate, bidentate and tridentate [**33-36**] ligands. Closely related to monoacyl-, aroyl-, and pyridoyl-, hydrazones are acyl-, aroyl-, and pyridoyl-, dihydrazones containing same

donor groups but each in duplicate, which increases their bonding potentialities. In such dihydrazones, the two hydrazone parts may be linked to one another either directly or by methylene chains of varied length or phenyl or pyridyl- groups.

The dihydrazones can be obtained from condensation of acyl-, aroyl-, and pyridoyl-, dihydrazines [$R(CONHNH_2)_2$]; (R = O, -$(CH_2)_n$-, $C_6H_4<$, $C_6H_3N<$) with o-hydroxyaromatic aldehydes and ketones. Another category of the dihydrazones can be obtained from condensation of dialdehydes [$R(CR'O)_2$]; (R = O, -$(CH_2)_n$-, $C_6H_4<$, $C_6H_3N<$, R' = alkyl groups) with monoacyl-, aroyl-, pyridoyl- and quinaldenoyl-, hydrazines. Accordingly, the literature survey is presented under the following two major sections.

A) Complexes of dihydrazones derived from condensation of acyl-, aroyl-, and pyridoyl-, dihydrazines with simple and o-hydroxyaromatic aldehydes and ketones.

B) Complexes of dihydrazones derived from condensation of dialdehydes with monoacyl-, aroyl-, pyridoyl- and quinaldinoyl-, hydrazines.

Sacconi **[37]** has isolated a seies of diamagnetic dinuclear nickel (II) complexes of dihydrazones obtained from condensation of aliphatic dicarboxylic acid dihydrazides with salicylaldehyde, 2-hydroxy-1-naphthaldehyde, o-aminobenzaldehyde, and o-hydroxyacetophenone. He showed that the hydrazones react in their enol forms with $Ni(OAc)_2$ in aq. alc. ammonia as bis-tridentate complexing agents.

Aggarwal and coworkers **[38]** isolated complexes of the compositions $[VO(LH_2)]SO_4$, $[VO(LH_2)]Cl_2$, $[VO(LH_2)py]SO_4$ from reaction of vanadyl sulphate and chloride and metal (II) chloride with bis(acetone)oxaloyldihydrazone, bis(acetone)malonoyldihydrazone and bis(acetone)succinoyldihydrazones in alcoholic medium. The complexes $[VO(LH_2)]SO_4$ and $[VO(LH_2)]Cl_2$ were proposed to have square pyramidal stereochemistry while the remaining complexes were proposed to have octahedral stereochemistry.

Iskander and coworkers **[39]** isolated the metal (II) complexes of the composition $M(LH_3)X.nH_2O$, $M_2(LH_2)X_2.nH_2O$, $M(LH_2).nH_2O$ and $M(LH_3)_2.nH_2O$ (where M = Cu (II), Ni (II) and Co (II); X = Cl^-, Br^-, I^-)from reaction of the metal (II) salts with dihydrazones (LH_4) derived from condensation of salicyaldehyde with acyldihydrazines with the methylene backbone varying from 1 to 5 under different experimental conditions. They assigned a pseudo-octahedral stereochemistry for the nickel (II) complexes $[Ni(LH_3)X].nH_2O$ (X = Cl^-, Br^-, I^-) and $[Ni_2(LH_2)Cl_2].2H_2O$ on the basis of magnetic moment data and spectral studies. The latter complexes change to penta-coordinated state on dehydration. However, five coordinate structure was proposed for the nickel (II) complexes $Ni(LH_2).nH_2O$ as against a distorted octahedral structure for the corresponding cobalt (II) analogues. On the other hand, Kapoor and coworkers **[40]** suggested that the nickel (II) complexes $Ni(LH_2).nH_2O$ have octahedral stereochemistry. Anomolous magnetic behaviour of the nickel complexes $Ni_2(L).nH_2O$ (μ_{eff} values lying in the range 1.65-1.70 BM) is ascribed to arise due to the presence of two magnetically non-equivalent sites in the same unit cell. This is confirmed from electronic spectral study of the complexes as well which show bands characteristic of octahedral and square planar nickel (II) sites in the complexes. All the cobalt (II) complexes are proposed to have octahedral stereochemistry. The copper complexes $Cu(LH_3)X.nH_2O$ and $Cu_2(LH_2)X_2.nH_2O$ are proposed to have square pyramidal stereochemistry. The low magnetic moment values than the spin only value is attributed to superexchange interactions through the oxygen bridges. The complex $Cu(LH_2).nH_2O$has been suggested to have square planar stereochemistry.

Narang and Lal **[41]** have described complexes of disalicyaldiminesuccinamide (H_2L) and N,N-Bis(o-hydroxyacetophenoneimine)succinamide (H_2J) of the types ML, MJ, M(HL)Cl, M(HJ)Cl and $M'(HL)_2$ (where M = Cu (II), Ni (II), or Co (II) and = Ni (II) or Co (II) and M' = Ni (II) or Co (II)). The complexes are proposed to have either octahedral stereochemistry or square planar stereochemistry.

Narang and Lal **[42]** have reported mono and binuclear zinc (II) complexes Zn(HL)Cl and Zn_2(L-2H) derived from multidentate acyldihydrazone ligands. The reaction medium, zinc salts and ligand geometry are shown to influence the composition and stereochemistry of the complexes. The zinc centres were proposed to have octahedral as well as tetrahedral stereochemistry.

Polymeric metal (II) complexes **[43]** of the type M_2L derived from dihydrazones obtained from condensation of oxaloyldihydrazide, succinoyldihydrazide and phthaloyldihydrazide with salicylaldehyde or o-hydroxyacetophenone have been described by the above authors. Copper complexes and few nickel and cobalt complexes are proposed to have square planar stereochemistry while other nickel and cobalt complexes are proposed to have distorted octahedral and square pyramidal stereochemistry. The anomalously low magnetic moments of some complexes are related to M-M interactions via oxo-bridge structure.

Narang and Lal **[44]** have prepared and characterized the metal (II) complexes $M(H_2J)$, $M(H_2K)$, $M(H_3J)Cl$, $M(H_3K)Cl$, M_2J, M_2K and M_2 (HK) (CH_3COO) (where M = Cu (II), Ni (II) and Co (II)) derived from di(salicylaldimine}malonamide(H_4J) and di(o-hydroxyacetophenoneimine}malonamide (H_4K) and the zinc (II) complexes ZnH_2L and Zn_2L from a number of multidentate acyldihydrazones (H_4L). The copper complexes are shown to have square pyramidal and pseudo-octahedral stereochemistry. The cobalt complexes are shown to have square planar, square pyramidal, mixed octahedral and tetrahedral and distorted octahedral stereochemistry in the solid state whereas zinc complexes have octahedral and tetrahedral stereochemistry.

Narang and coworkers **[45]** synthesized new series of polymeric cobalt (II) complex of the type $Co_2(L).nH_2O$ from reaction of metal (II) acetate and dihydrazone (LH_4) where LH_4 is bis(o-hydroxyacetophenone)oxaloyldihydrazone, bis(salicylaldehyde) oxaloyldihydrazone, bis(o-hydroxyacetophenone)succinoyldihydrazone in the ratio 4: 1 (metal: ligand) in ethanol under reflux. The complexes have been proposed to

have polymeric structure with strong Co-Co interactions with planar disposition of donor atoms around metal centres.

Sahni and coworkers **[46]** synthesized and characterized complexes of the type $[M(LH_2)]X_3$ (where M = Cr (III), Mn (III), Fe (III) or Co (III); X = Cl^-, NO_3 or OAc) from reaction of metal (III) salts with N-N-dibenzylidene dipicolinic acid hydrazone (LH_2) in ethanol medium. The ligand acts as a pentadentate unit having coordination sites at pyridine nitrogen, amide oxygen and hydrazinic nitrogens or azomethine nitrogens. In this context, it is important to mention that these authors **[47]** have also claimed that dipicolinic acid dihydrazine behaves as pentadentate ligand. On the otherhand, Dutta and Sarkar **[48]** have argued in favour of neutral tridentate behaviour of this ligand in which it can function either as a (NNN) or as a (ONO) donor.

Kapoor and coworkers **[49]** have studied reaction of vanadyl chloride and dipicolinic acid dihydrazone in presence of acetylacetone or other β-diketones in ethanol and acetic acid.

They isolated brown solid complexes of macrocylic ligand bis (β-diketone) dipicolinoyldihydrazones. On the other hand they isolated a non-macrocyclic pyrazole derivative when reaction of vanadyl chloride was carried out with the preformed bis (β-diketone) dipicolinic acid dihydrazone. Similar products **[50]** were isolated in case of zirconium (IV) also.

Teotia and Rana **[51]** synthesized complexes $[M(L).2H_2O]$ (M = Cu (II), Ni (II) and Co(II)) of the above macrocyclic ligands by treating a methanol solution containing a mixture of acetylacetone and 2, 6-dipicolinic acid hydrazide and the appropriate metal chloride. The IR spectra indicated condensation of both the oxygen atoms of acetylacetone with NH groups of dihydrazine. The electronic spectral bands agree reasonably well with five coordinated geometry.

Kapoor and coworkers **[52]** synthesized a number of metal (II) and metal (III) complexes from reaction of metal (II) and metal (III) salts with dihydrazones obtained from condensation of salicylaldehyde with oxaloyldihydrazine, malonoyldihydrazine and succinoyldihydrazine under different experimental conditions. The trivalent metal ions are found to yield complexes having compositions $[M_2LX_2].nH_2O$ and $[M_2 (LH_2)X_4] .nH_2O$ (M = Cr (III), Fe (III) and Mn (III)) (X = Cl^-, NO_3^-, OAc, OH) while the bivalent metal ions were found to form complexes having compositions $[M(LH_2)]$ and $[ML(H_2O)_4]$ (M = Mn (II) and Fe (II)). The dihydrazones are suggested to function as dibasic and tetrabasic hexadentate binucleating ligands. Iron (III) complexes were characterized by Mossbauer spectroscopy as well. The complexes have been suggested to have distorted octahedral stereochemistry.

Narang and Yadav **[53]** studied reaction of aluminium (III) salts with several dihydrazone ligands in aqueous medium at controlled pH and characterized the resulting complexes by infrared spectroscopy. The complexes are suggested to be polymeric with dihydrazones coordinated in the keto form.

Narang and Dubey **[54]** have described Zn (II), Cu (II), Ni (II) and Co (II) complexes of solid polymers derived from glyoxal and organic acid dihydrazides. They have discussed the structure of the complexes in light of magnetic moment, electronic and IR spectral studies.

Yacouta and coworkers **[55]** studied the complexation behaviour of uranyl ion with various dihydrazides and their diydrazones obtained from condensation of simple and o-hydroxy aromatic aldehydes and ketones with dihydrazides. They isolated several monometallic and bimetallic uranyl complexes and characterised by various physico-chemical data and spectroscopic studies. They also studied the effect of excess acetate ion on complex formation.

Lal and coworkers **[56]**, have prepared several homotrinuclear complexes having general formula $[M_3LCl_2(H_2O)_3]$ (M = Mn (II), Co (II) or Ni (II)) from bis(acetophenone)-2,6-dipicolinoyldihydrazone(LH_4) in alcoholic medium by adjusting pH to ~8 by KOH. The complexes show low μ_{eff} values much less than those expected for the high-spin metal ions possibly due to metal-metal interaction and anti- ferromagnetic exchange. The complexes are proposed to have mixed six-coordinate octahedral and five coordinate square pyramidal stereochemistry.

Narang and Singh **[57]** have synthesized polymeric complexes $M(L\text{-}2H).nH_2O$ (where M = Fe (II), Mn (II), Co (II), Ni (II), Cu (II), Zn (II), Cd (II) and Hg (II), L = A, B) from bis(2-hydroxy-1naphthaldehyde)oxaloyldihydrazone (A) and bis(2-hydroxy-1naphthaldehyde) malonoyldihydrazone (B) by solid-solution reaction. All of the complexes were suggested to have distorted octahedral stereochemistry.

Lal and coworkers **[58]** studied reaction of uranyl acetate with the above dihydrazones (H_4L) in aqueous-alcoholic media and isolated complexes of the type $(UO_2)_2L.6H_2O$. The dihydrazones coordinate to the metal centre in enol form. They have studied the effect of complexation on the coupling of >C=O vibrations, in an enolized form and of ligand coordination to the uranyl ion as a function of the number of methylene groups by comparing the asymmetric stretching vibrations of the uranyl ion in various complexes recorded under identical conditions.

Lal and Das **[59]** studied reaction of uranyl nitrate and acetate with dihydrazones (H_4L) (where H_4L = disalicylaldehydeoxaloyldihydrazone (H_4A), malonoyldihydrazone (H_4B), succinoyljihydrazone (H_4C), glutoyldihydrazone (H_4D), adipoyldihydrazone (H_4E), and phthaloyldihydrazone (H_4F) in 3: 1 molar ratio in alcoholic medium. The complexes $[(UO_2)_2(H_2L)\ (NO_3)_2\ (H_2O)_4].2H_2O$ and $[(UO_2)_2(H_2L)(CH_3COO)_2(C_2H_5OH)_2].C_2H_5OH$ have been isolated and characterized.

Lal and coworkers **[60]** synthesized copper (II) complexes $Cu_2(L).nH_2O$ and dioxouranium (VI) complexes $[(UO_2)_2(H_2L)(C_2O_4)].2nH_2O$ of the above

dihydrazones. The $C_2O_4^{2-}$ group is suggested to cooordinate to the uranium centre retaining its D_{2h} symmetry.

Lal and coworekers **[61]** synthesized a series of uranyl complexes of the composition $[UO_2(H_3L)_2].nH_2O$ from above dihydrazones from reaction of uranyl nitrate with salicylaldehyde and acyl- and aroyl- dihydrazines in 1: 4: 2 molar ratio in ethanol medium.

Lal and coworkers **[62]** studied reactions of disalicylaldehyde adipoyldihydrazone with uranyl njtrate and uranyl acetate in aqueous and ethanol media under different experimental conditions. The resulting complexes of the compositions $[UO_2(H_2L)(H_2O)]_n$, $[UO_2(H_2L)_2]_n.3nH_2O$, $[UO_2(H_3L)(CH_3COO)]_n.3nH_2O$, $[UO_2Zn(L)(H_2O)_2]_n.2nH_2O$, $[(UO_2)_2(H_2L)(C_2O_4)].nH_2O$, $[(UO_2)_2(L)(py)_2(H_2O)_4]$, $[(UO_2)_2(HL)(CH_3COO)(H_2O)_3]_3.nH_2O$ $[(UO_2)_3(L)(CH_3COO)_2(H_2O)_2]_n.2nH_2O$, $[(UO_2)_2(L)(py)_2(H_2O)_2]_n.xnH_2O$, (where py = pyridine or α-, β-, γ-picoline, X = 0, 1) have been isolated and characterized. In the complexes the ligand functions as a bridging monobasic tetradentate, dibasic hexadentate and tetrabasic hexadentate ligand and exhibits keto-enol tautomerism. In the heterobimetallic complexes $[UO_2Zn(L)(H_2O)_2]_n.2nH_2O$, the uranium and zinc atoms are considered to have hexagonal bipyramidal and tetrahedral stereochemistry respectively.

Lal and coworkers **[63]** have described dioxouranium (VI) and zinc (II) complexes $M(H_2L)(H_2O)_2]_2.2nH_2O$ (where M = UO_2^{2+}, Zn^{2+})of bis(o- hydroxynaphthaldehyde) oxaloyldihydrazone(H_4L). The complexes are obtained from reaction of metal acetate with oxaloyldihydrazine in 1: 1 molar ratio in ethanol followed by reaction of excess o-hydroxynaphthaldehyde under reflux. Dioxouranium (VI) complex is proposed to be eight coordinate involving coordination of dihydrazone in the enolic fom with cis-configuaration while the zinc complex is proposed to be octahedral involving coordinated dihydrazone in enolic fom in the staggered configuration. The naphtholic-OH is proposed to be non-coordinated.

They **[64]** have, further, synthesized dioxouraninum (VI) complexes $[UO_2(H_2L)]_n.2nH_2O$ and $[(UO_2)_2(L)(H_2O)_6]_n$ from reaction of uranyl nitrate with preformed dihydrazone bis (o-hydroxynaphthaldehyde)oxaloyldihydrazone in a 3: 1 molar ratio in aqueous and ethanol media, respectively, under reflux. Based on the splitting of the δ NH signal in monometallic complex and δCH=N in both complexes into quartet as compared to the singlet in free dihydrazone, the complexes are proposed to exist in chair formation with the anti-cis-configuration of dihydrazone involving eight and nine coordinated uranium atoms, respectively.

The complexes **[65]** $Na_4[(UO_2)_4(L)_2(CH_3COO)_4(H_2O)_4].4H_2O$ and $Na_4[(UO_2)_4(L)_2F_4(H_2O)_4]$ have been obtained from the same ligand have also been described by them.

Patil and Kulkarni **[66]** and others **[67]** obtained complexes of the type $[UO_2L].nH_2O$ from interaction of uranyl acetate disalicylaldehyde thiocarbohydrazone (H_2L) and established their structure by ^1H NMR and IR spectroscopic studies.

Kapoor and coworkers **[68]** studied reaction of malonoyldihydrazine and phthaloyldihydrazine with β-diketones in presence of the dioxouraninum (VI) cation which appears to function as a metal template. This facilitates condensation of dihydrazide with diketones resulting in the formation of several dioxouranium (VI) complexes of macrocylic ligands. The formation of a macrocyclic ring was confirmed from infrared spectroscopic studies. However, when dioxouranium (VI) nitrate is treated with the condensation product of phthaloyldihydrazine and acetylacetone, an entirely different pyrazole derivative is formed.

Sahoo and coworkers **[69]** have synthesized several first series transition metal complexes from several dihydrazones. The complexes were characterized by elemental analysis, physicohemical data and spectral studies.

Pandey **[70]** reported a number of organometallic complexes derived from pyridoyldihydrazones. In. this study, he showed from IR spectral data that dihydrazones coordinate to the metal centre in keto form through both >C=O and >C=N groups.

Mahale and Havanur **[71]** studied dioxomolybdenum (VI) complexes of the composition $(MoO_2)_2(L)(py)_2$ synthesized from dihydrazones (H_4L) obtained from condensation of the several acyl dihydrazines and substituted salicylaldehyde.

Panda and coworkers **[72]** synthesized heterobimetallic complexes $[MNiM(BTDO)_2X_2(H_2O)_4].nH_2O$ (where M = Ni (II), Co (II) and Cu (II); X = Cl^-, NO_3^-, n = 0 or 0.5 and BTDO = 1,8-bis(2'-oxophenyl)-2,3,6,7-tetraza-4,5-dimethyl-1,3,5,7-octatetraene) from the precursor nickel complex nickel-[bis(diacetyldihydrazone)]. The metal centres have been proposed to have octahedral stereochemistry.

Gopinathan and coworkers **[73]** synthesized a tin complex of disalicylaldehyde malonoyldihydrazone and studied its structure by X-ray crystallography.

Sacconi **[74]** studied reactions of biacetyl-bis(benzoylhydrazone) with nickel (II) acetate in alcohol in the presence of concentrated ammonia and isolated orange coloured biacetylbis(benzoylhydrazonato)nickel (II) complex and studied its reaction with pyridine **[75]**. The formation constant of complexes formed between biacetyl bis(benzylhydrazonato)nickel (II) and various alkyl amines **[76]** have been studied. Complexes of lead (II), lead (IV) and tin (IV) of the types [Pb(L)], $[ph_2Pb(L)]$, $[Sn(L)_2]$, [phSn(L)Cl] and $[ph_2Sn(L)]$ have been obtained by mixing methanol solutions of the appropriate metal salts and the ligand **[77]** .

Pelizzi and coworkers **[78]** have studied reaction of copper (II) chloride dihydrate with 2, 6-diacetylpyridinebis(picoloylhydrazone) (LH_2) in refluxing ethanol yielding dark green crystal of $Cu_2(L)Cl_2.H_2O$. IR spectral data indicate coordination of all the

three pyridine nitrogens. The ligand behaves as an octadentate bridging (NONNNNNN) donor. The authors have established the square pyramidal structure of the complex unequivocally by X-ray crystallography. The environment about one Cu (II) is made up of a basal plane consisting of a chloride, two nitrogen atoms from the ligand (LH_2), an oxygen atom from second adjacent ligand molecule and another nitrogen from the same adjacent ligand molecule taking up the axial position. The environment around the second Cu (II) is made up of four nitrogen atoms from the first ligand molecule, while a chlorine ion takes up the apical site. Same authors **[79]** have isolated another series of complexes of the type $M(LH_2)Cl_2.nH_2O$ (M = Mn (II), Co (II), Ni (II) and Cu (II)) by mixing chloroform solution of LH_2 and ethanolic solution of the metal chlorides in 1: 1 molar ratio. Another Mn (II) compound $MnL.9H_2O$ was obtained by adding dropwise, a dilute NaOH solution to a warm ethanol-water solution containing LH_2 and $MnCl_2.4H_2O$(1: 1) molar ratio until pH~ 8.0. The compounds were characterized by magnetic moment data, electronic and IR spectroscopic studies.

The complex $Mn(LH_2)Cl_2.5H_2O$ was shown to have pentagonal bipyramidal stereochemistry by X-ray crystallography **[80]**. On the basis of similarity of IR spectra of Cu (II), Ni (II) and Zn (II) complexes with that of Mn (II) complexes, a similar pentagonal bipyramidal stereochemistry was proposed for them also with ligand acting as ONNNO donor and chloride or water molecules occupying apical positions. The complex $MnL.9H_2O$ was also characterized by X-ray crystallography and shown to have pentagonal bipyramidal stereochemistry.

Curtis and coworkers **[81]** and others **[82]** studied Cu (II) and Ni (II) complexes of acetylacetonebis(picoloylhydrazone) and acetylacetonebis(isonicotinoylhydrazone). They carried out X-ray structural analysis of copper (II) complex of acetylacetone bis(isonicotinoylhydrazone) obtained from reaction of metal (II) salt, isonicotinoylhydrazine and acetyl acetone and confirmed the square pyramidal stereochemistry.

Giordano and coworkers **[83]** isolated cobalt (II) and nickel (II) complexes of compositions $[Co(LH_2)(H_2O)(NO_3)]NO_3$ and $[Ni(LH_2)(H_2O)_2](NO_3)2.2H_2O$ from reaction of metal nitrates with 2,6-diacetylpyridine bis(benzoylhydrazone) (LH_2) in 95% ethanol. The X-ray crystallographic study confirmed that the metal atoms are in a pentagonal bipyramidal arrangement in the structural unit of the complexes.

Palenik and coworkers **[84]** isolated lanthanum complex of composition $[La(LH_2)(NO_3)_3]$ from reaction of lanthanum nitrate and the ligand in ethanol at 55^0C in the presence of water. The complex was studied by infrared spectroscopy and X-ray crystallographic studies. They showed lanthanum to be eleven coordinated in these complexes. A decahedral arrangement of the donor atoms of the ligand is proposed around the lanthanum atom in the complexes.

Paolucci and coworkers **[85]** prepared a series of dioxouranium (VI) complexes of 2,6-acetylpyridine bis(4-methoxybenzoylhydrazone) (H_2dapmb). The neutral compound of the composition UO_2(dapmb) was formed in two different crystalline forms, α and β depending upon the experimental conditions. The geometry of $[UO_2(dapmb)]$ which was formed in two forms is very similar, the only significant difference being the difference in the conformation of carbon atoms in a methoxy group. Seven fold coordination of uranium (VI) was established with the five donor nitrogen atoms in the equatorial plane.

Pelizzi and coworkers **[86]** isolated tin (IV) complexes of the composition $[Snpr_2(LH_2)]$ from reaction of n-propyltinchloride in anhydrous acetone, under nitrogen atmosphere with boiling suspension of 2,6-diacylpyridine-bis(salicylhydrazone) (LH_4) in dry methanol. X-ray crystal structure study has established that tin atom is seven coordinated in the complex with pentagonal bipyramidal arrangement of ligand atoms. The -OH groups remain uncoordinated.

Teotia and coworkers **[87]** have studied reactions of metal (II) salts (M = Cu (II), Ni (II)) with picolinoyl/isonicotinoylhydrazine in presence of acetylacetone. They

isolated complexes of the compositions [M(LH)X] (M = Ni (II), Cu (II), X = Cl^-, Br^- NO_3^- and NCS, LH_2 = acetylacetonebis(picolinoylhydrazone) or acetylacetone bis(isonicotinoylhydrazone). All the complexes have been established to have square pyramidal stereochemistry. Complexes $[M(LH)X_2]$ [X = Cl^-, Br^- NO_3^- and NCS for M = Cu (III); X = OAc, Cl^-, Br^-, NCS for Mn (III) and OH for Co (III) were also prepared similarly **[88]** by them. The complexes have been suggested to have six-coordinate tetragonal structure.

Paolucci and coworkers **[89]** synthesized several complexes of 2, 6-diformylphenol bis(benzoylhydrazone) and its substituted derivatives with the bivalent metal ions (M = Co (II), Ni (II), Cu (II) and Zn (II) and established their molecular structure by various physico chemical techniques. A fascinating aspect of these ligands is the coordinating and bridging ability of phenolic-OH of the 2, 6-formylphenol moiety plus the very subtle behaviour of acidic protons.

Dutta and coworkers **[90]** isolated complexes of the composition [VO(L)] from reaction of $VO(acac)_2$ with acetylacetone bis(benzoylhydrazone) (LH_2) in acetone. The same ligand on reaction with CoX_2 (X = Cl^-, Br^-) in anhydrous medium yield blue coloured tetrahedral polymeric complexes $[Co(LH_2)X_2]$ **[91]**. However, in the presence of lattice water, bromide salt yields pink coloured pseudo-octahedral $[Co(LH_2)Br_2]$ complexes.

The dihydrazone reacts with nickel (II) chloride in rectified spirit and yields diamagnetic, orange yellow complex [Ni(L)] **[92]**. However reaction with anhydrous $NiCl_2$ in warm anhydrous methanol gives a paramagnetic complex $[Ni(LH_2)Cl_2]$ having a trans-dichloro pseudo-octahedral structure. When this complex is exposed to moist atmosphere and over KOH, the partial dechlorination occurs giving the complex [Ni(LH)Cl]. This complex is proposed to have a five-coordinate structure. They also isolated complexes [Zn(L)], [Cd(L)] $.2H_2O$ and [Pb(L)] from the interaction of appropriate metal acetate with the ligand in ethanol.

Snow and coworkers **[93]** studied the reaction of bis(acetylacetonato)oxovanadium (IV) with benzoylhydrazine in dry ethanol under dry nitrogen. They isolated bis(acetylacetone benzoylhydrazonato)vanadium (IV). A trigonal prismatic geometry was verified for this complex.

Dutta and coworkers **[94]** showed that the reaction of $VO(acac)_2$ with benzoylhydrazine and related ligands in methanol, ethanol and methyl acetate yielded violet or almost black coloured bis(acetylacetonebenzoylhydrazonato)-vanadium (IV) whereas reaction in acetone or methyl ethyl ketone yielded (acetylacetonebenzoylhydrazonato)oxovanadium (IV). While in the former complex, the abstraction of oxo-group has been suggested to occur; in the latter complex it is retained.

Lanthanide complexes **[95]** of the type $[Ln(L)(OH)(H_2O)]$ (Ln = La (III), Pr (III), Nd (III), Sm (III), Gd (III), Ho (III), Er (III)) have been obtained in situ by refluxing biacetyl, benzoylhydrazine and the appropriate metal chloride in ethanol in the presence of a regulated quantity of NH_4OH. The ligand acts as a quadridentate ONNO donor in its enol form.

Pelizzi and coworkers **[96]** have isolated a new series of metal (II) complexes of the type $[M(LH_2)(OH_2)Cl]$ (M = Co (II), Ni (II), Mn (II), Cu (II) and Zn (II)) by mixing ethanol solutions of LH_2 with ethanol solutions of metal(II) chloride in 1: 1 molar ratio. With metal (II) acetates, the compounds of the type [ML] are obtained. The ligand reacts with metal centres in keto form in complexes $[MLH_2(OH_2)Cl]Cl$ and enol form in complexes [ML]. Some of the complexes are characterized by X-ray crystallographic method as well. The complexes are shown to have pentagonal bipyramidal stereochemistry.

Dutta and coworkers **[97]** have studied the reaction of $MoO_2(acac)_2$ with benzoylhydrazine and related ligands in different solvents. They isolated the complex (benzoyldrazine)(benzoylhydrazido)(acetylacetonato)molybdenum (VI) in

dry methanol while in ordinary methanol the complexes (acetylacetonato)(cis-dioxo)molybdenum (VI)-μ-diol-(benzoylhydrazino) (cis-dioxo)molybdenum (VI) dihydrate was isolated. They have shown that in dry methanol acetylacetone and hydrazines condense to give Schiff base complexes whereas no Schiff base formation occurs in ordinary methanol.

The Schiff bases derived from acetylacetone and 2-picolinoylhydrazide or isonicotinoylhydrazide are similar to above, but they give complexes of the $[UO_2L]Cl$ (where LH = Schiff base), in which Schiff bases coordinate through both azomethine nitrogen and pyridine nitrogen (in the case of 2-picolinoylhydrazone) or carbonyl oxygen (in the case of isonicotinoylhydrazone) **[98]**.

On the basis of IR and conductivity data Day et.al **[99]** have reported the formation of $[UO_2(LH_2)](NO_3)_2$ (where LH_2 represents 1,2-dimethyl bis(4-methoxybenzoylhydrazone)). Similarly they hay reported the formation of $[UO_2(LH_2)(NO_3)]NO_3$ upon acidification of $[UO_2L]$ with HNO_3. Ligands are proposed to coordinate to the metal centres in keto as well as enol forms. Interaction of these complexes with neutral mono and bidentate ligands lead to the formation of $[UO_2L(A)_2]$ and $[UO_2L(AA)]$ (where A = pyridine, picoline, methylamine, aniline, ph_3PO; AA = en, ph, phen).

Marangoni and coworkers **[100]** synthesized mercury (II) complex with 2,6-diacetylpyridinebis(2-pyridoylhydrazone). They carried out X-ray structural analysis of the complex, and confirmed its pentagonal bipyramidal stereochemistry.

Pelizzi and coworkers **[101]** synthesized nickel(II) complex $[\{Ni(H_2apsh)(OH_2)(I)\}_2C1_2].2dmf.5H_2O$, and cobalt (II) and copper (II) complexes, viz., $[Co(H_2dpsah)(OH_2)_2]Cl.4H_2O$ of 2,6-diacetylpyridinebis[2-(semicarbozono) propionylhydrazone] (H_4apsh) and H_2dpsah = 2,6-diacetylpyridinebis[2-(semicarbazono) acetophenoylhydrazone] (H_2dpash) respectively. In the nickel complex, the four atoms of the semicarbazone system are involved in coordination

while in the cobalt complex semicarbazone system does not participate in coordination. They established the structure of the complexes by IR spectroscopy and X-ray crystallography.

Pelizzi and coworkers **[102]** studied the structure of a tetranuclear copper (II) complex $[Cu_2(dappc)(OH_2)_3]_2$, $[Cu_2(dappc)(OH_2)_2(ClO_4)]_2(ClO_4)_6.2H_2O$ (I) and $[(Cu_2(dapip)Br]_2$ (II) derived from the polyfunctional ligand 2,6-diacetylpyridinebis-(2-pyridinecarbonylhydrazone) (H_2dappc) and 2,6-diacetylpyridinebis(2-pyridinecarbonylhydrazone phenylacetohydrazone] (H_4dapip) respectively . The structure of compound (I) is built up of complex cations of formula $[Cu_2(dappc)(OH_2)_3]_2$ and $[Cu_2(dappc)(OH_2)_2\ ClO_4]^{2+}.ClO_4$ anions and uncoordinated H_2O molecule while that of the compound (II) consists of neutral unit of formula $[Cu_2(dapip)Br]_2$ and solvating H_2O molecules. In both compounds, two metal atoms for one hydrazone molecule are present and the ligand is bideprotonated in complex (I) and trideprotonated in complex (II).

A monoperoxo complex of Schiff base $(H_5C_6C{=}N\text{-}NHC(S).SCH_2C_6H_5)_2$, ($LH_2$) has been reported by Tarafder et.al **[103]**. The complex $[UO_2(O_2)L]$ was prepared by treating uranyl nitrate with the Schiff base dissolved in a solution of KOH in 30% H_2O_2. The Schiff base behaves as dibasic NNSS tetradentate ligand, while peroxo group is bonded to the metal centre as bidentate chelating ligand.

Toshev and coworkers **[104]** reported the dioxouranium complex of diacetylbis (thio-benzoylhydrazone) in which uranium has a distorted pentagonal bipyramidal structure with the uranyl oxygen atoms at the axial positions.

Pelizzi and coworkers **[105]** synthesized copper complexes of di-2-pyridylketone(phenylsemicarbazone)acetylhydrazone (H_2psah) and studied their structure by X-ray crystallography. They showed that the copper complex $[Cu_2(psah)Cl].H_2O$ consists of a pair of structurally distinct metal centres with

different environments bound to the heptadentate hydrazone ligand and held together by a -N-N- bridge.

Katti and coworkers **[106]** synthesized a number of Palladium (II) complexes from series of phosphorous hydrazide and hydrazones. The complexes were characterized by elemental analysis. The structural assessment was carried out by NMR and IR spectroscopic studies. They established the structure of one complex by X- ray crystallography as well.

Lukyanenko and coworkers **[107]** have determined complex stability of Na^+, K^+, Rb^+, and Cs^+ ions with bis(benzo-15-crown-5) with acylhydrazide fragments in the linking chain in 95% aqueous methanol. In all cases, the formation of 1: 1 complex was observed. The studied bis-crown ethers form more stable complexes than benzo-15-crown-5. The stability of biscrown ether complexes is substantially determined by the length of the linking chain. Biscrown ether with a glutaric acid residue in the linking chain exhibits striking potassium selectivity. High selectivity and stability of the complexes are due to the increase of their sandwich structure rigidity resulting from the formation of H-bonds between acylhydrazide fragments.

Ji and coworkers **[108]** studied several dinuclear yttrium (III) and lanthanide (III) picrate complexes derived from acetylferrocenepyridine-2,6-diformylhydrazone having the stoichiometric formula $Ln_2L_2pic_6.n(1\text{-}C_3H_7OH).mH_2O$ (pic = picrate anion, Ln = Y, La, Pr, Nd, Sm, Eu, Gd, Tb, Dy, Ho, n = 2, m = 4; Ln = Er, Tm, Yb, n = 0, m = 2). These complexes were characterized by EA, IR, UV, ^1H NMR spectra and molar conductance data. It was found that the ligand coordinates in keto form to the lanthanide ions. All the complexes described in the present study are 1: 6 electrolytes in methanol.

Xianzeng and coworkers **[109]** synthesized zinc (II) complex $[Zn_2L(CH_3COO)_2].CH_3CH_2OH$, from binucleating ligand L, 2,6-diformylpyridine N-oxidebis(benzoylhydrazone) via template reaction in alcohol. They characterized

the complex by X-ray crystalljographic studies. The dihydrazone ligand was found to be present in doubly deprotonated form. They established that all the coordinated atoms of the Schiff base ligand and two zinc atoms with the same bond length of 2.24(1) Å. The two acedtato ions act as bidentate ligands linking two zinc atoms. Both the zinc atoms have a distorted trigonal-bipyramidal environment. The complex crystallizes in the triclinic space group P1.

Pelizzi and coworkers **[110]** synthesized six complexes of copper (II), nickel (II), and iron (II) from a chiral ligand 2, 6-diacetyl pyridine bis{[DL-hydroxy-(phenyl)acetic]hydrazone (H_4dapm) and characterized them by spectroscopic studies. They established the structure of the nickel complex [Ni(H_4dapm)-(H_2dapm)].13H_2O by X-ray diffraction methods. The complex crystallizes in the monoclinic space group C2/c. The complex has two fold crystallography imposed symmetry with the nickel atom in a distorted octahedral environment consisting of six nitrogen atoms from two ligand molecules. With the help of ^{1}H NMR spectroscopic studies, the existence of the ligand in therr forms i.e the meso DL and the two enantiomeric DD and LL ones were established. They attributed the doublets at 6.40 and 5.58ppm to the OH groups. The ^{1}H NMR spectrum of the complex [Ni(H_4dapm)(H_2dapm)].13H_2O showed the presence of two inequivalent ligand molecules i.e. one in meso form and the other in the DD or LL form. The complexes were characterized by IR spectroscopic studies.

Rana and cowoekers **[111]** synthesized several manganese (II), iron (II), cobalt (II), nickel (II), and copper (II) complexes of 2, 6-diacetylpyridine-(benzylacetone)-hydrazone (H_2L). The complexes have been shown to have composition [M(H_2L)X_2] (where M = Mn, Fe, Co, Ni and Cu; X = Cl, Br, NO_3, SCN) and have been characterized by molar conductance , magnetic moment data, infrared, and electronic spectroscopy. The dihydrazone has been shown to function as a tridentate ligand bonding to the metal centre through pyridyl nitrogen and azomethine nitrogen atoms. All the complexes have been proposed to be five coordinate having trigonal

bipyramidal stereochemistry in which the dihydrazone donor atoms occupy equatorial position while the anions occupy axial positions.

Paolucci and coworkers **[112]** studied the interactions of potentially binucleating ligand, 2, 6-diacetylpyridine-bis(1-phthalazinylhydrazone) (H_2dapz), containing only nitrogen donor atoms, with nickel (II), copper (II), and zinc (II) salts. They showed that depending on the nature of the counter ions, Ni (II) and Cu (II) ions selectively enter in one of the two compartments present in the ligand. They isolated five series of mononuclear complexes [dapzM], [H_2dapzMCl_2], [HdapzMCl], [(H_2dapz)$_2$M][ClO_4]$_2$, [HdapzM][ClO_4], from reactions of metal acetates, metal chlorides and metal perchlorates, respectively and the ligand. They established that the dihydrazone is present in the bisdeprotonated, monodeprotonated and undeprotonated forms, respectively in the complexes. They also studied some interconversion reactions. The complexes were characterized by analytical techniques and spectroscopic methods. Some tentative stereochemical assignments of these compounds are reported on the basis of their physico-chemical properties. Different behaviour has been observed in the case of zinc (II) chloride and perchlorate. Crystal structure analysis on the bisdeprotonated complex [dapzNI]$_2$ shows that the compound is dimeric with the metal ions octahedrally coordinated into the upper compardtment and the pyridine nitrogens bridging the two nickel atoms.

Maurya and coworkers **[113]** synthesized binuclear dioxotungsten (VI) complexes of the type [(WO_2)$_2$L], where L is a flexibly bridged hexadentate tetra anionic Schff base derived from the condensation of methylene or dithiobissalicylaldehyde with isonicotinoylhydrazine, benzoylhydrazine, p-nitrobenzoylhydrazine and furoylhydrazine are reported. The IR and NMR spectral data suggest an oligomeric structure for these complexes in which each tungsten atom achieves a pseudo-octahedral structure via W—O→W bridging. Cyclic voltammetric measurements indicate irreversible to quasireversible reduction of the dioxotungsten (VI) complexes to oxotungsten (V) with a cathodic reduction potential of -1.0 to -1.1V vs

SCE at the scan rate of 500mV/s. The bridging methylene ($-CH_2$) or dithio (-S-S-) group has very little effect on the thermodynamic stability of the complexes.

Lal and coworkers **[114]** synthesized the bimetallic manganese (II, III) and dioxouranium(VI) complexes $[Mn_4(H_2L)(OAc)_4].4H_2O$, $[Mn_4(L)_2(H_2O)_8].4H_2O$, $K_4[Mn_4(L)_2F_6(H_2O)_2].2H_2O$, $[UO_2(H_2O)_4[Mn_4(L)_2(OAc)_4].4H_2O$ and $K_4[(UO_2)Mn_3(L)_2F_5(H_2O)_3]$ from bis(2-hydroxy-1-naphthaldehyde)oxaloyl-dihydrazone (H_4L). The complexes have been characterized by physical and spectral data. IR spectral data indicate that the dihydrazone coordinates to the metal centres in keto as well as in enol forms in the anti-cis-configuration in all of the complexes.

Lal and Adhikari **[115]** synthesized the compound $[(MoO_2)_2(L)(H_2O)].2H_2O$ from the reaction of $MoO_2(acac)_2$ with bis(2-hydroxy-1-naphthaldehyde)oxaloyl-dihydrazone (H_4L) in ethanol-acetonitrile in 3: 1 molar ratio under reflux. The complex is proposed to be a hexamer in which ligands are arranged in sets of three in two parallel planes one above the other. The intra-planer metal atoms are bonded to each other by naphthoxo-bridges whereas the inter-planer metal atoms are bonded to each other by M=O···Mo type bridging. The anti-cis-configuration of the dihydrazone moieties leads to the chair conformation of the complexes.

Lal and coworkers **[116]** isolated the homobimetallic complex $[(MoO_2)_2(L)].4H_2O$ from bis(2-hydroxy-1-naphthaldehyde)oxaloyldihydrazone (H_4L) in the solid state. It reacts with Lewis bases pyridine and 3-picoline to form the complexes $[\{\mu_2\text{-}O)MoO_2\}MoO_2(H_2L)].2D.4H_2O$ (where D = pyridine (py) (2), 3-picoline (3-pic) (3) and with proton bases salicyloylhydrazine ($sylshH_3$) and isonicotinoylhydrazine ($inhH_3$) to yield the Mo (V) compounds $[Mo_2(L)(sylsh)_2].5H_2O$ (4), and $[Mo_2(L)(inh)_2(H_2O)_2].3H_2O$ (5), respectively. The complexes have been characterized by elemental analysis, molecular weight determinations, molar conductance, magnetic moment, ESR, electronic, infrared, and ^1H NMR spectral studies. IR and ^1H NMR data indicate that the dihydrazone coordinates to the metal centre in and anti-cis-configuration in all the complexes. The dihydrazone is present in the enol form in the complexes (1), (4), and (5) but in the keto form in the

complexes (2) and (3). The complexes (4) and (5) are paramagnetic to the extent of 3.02 and 3.16 μ_B respectively.

Lal and coworkers **[117]** have synthesized the complexes of the type $[(UO_2)_4(L)_2(H_2O)_8].4H_2O$ (1), $K_4[(UO_2)_4(L)_2(OAc)_4(H_2O)_4].4H_2O$ (2), and $K_4[(UO_2)_4(L)_2F_4(H_2O)_4]$ (3), from bis(2-hydroxy-1-naphthaldehyde)oxaloyl-dihydrazone (H_4L) and characterized by elemental analysis, molecular weight determinations, molar conductance, electronic, IR and ^1H NMR spectroscopic studies. The dihydrazone coordinates to the metal centre in the anti-cis-configuration in enol form in the complexes (1) and (3) which contain water and fluoro groups as co-ligands in the coordination sphere functioning as terminal monodentate ligand. The dihydrazone isomerizes to syn-cis-configuration when the bridging bidentate acetate group is introduced into the first coordination sphere in the complex (2). The coordination of both azomethine groups of the dihydrazone to the same metal centre in anti-cis- configuration in complexes (1) and (3) leads to coupling between azomethine protons suggesting their chair conformation. However, no such coupling occurs when different hydrazone parts of the dihydrazone coordinates to different metal centres in syn-cis-configuration in complex (2) eliminating the possibility of its existence in chair conformation.

Lal and Kumar **[118]** have synthesized an unstable monomeric yellow complex of the type $[(MoO_2)_2(CHsalmlhH_4)(H_2O)_2].H_2O$ {complex (A)} from the reaction between bis(acetylacetonato)dioxomolybdenum (VI) and disalicyldehyde malonoyldihydrazone (CH_2salmlhH) in ethanol. This is transformed into an intermediate complex $[(MoO_2)_2(CHsalmlhH)(H_2O)]_2.4H_2O$ {complex (AB)} after sometime. Ultimately a stable brown isomer complex $[(MoO_2)_2(CH_2salmlh)(H_2O)_2].4H_2O$ {complex (AB)} is obtained. All the products have been characterized by various physico-chemical techniques and IR and ^1H NMR spectroscopic studies.

Lal and coworkers **[119]** isolated the complexes of the composition $[UO_2(H_3salligh)(OAc)].3H_2O$ and $[UO_2Zn(salligh)(H_2O)_2].2H_2O$, where $H_4salligh$ refers to disalicylaldehydeoxaloyldihydrazone ($H_4saloxlh$), malonoyldihydrazone ($H_4salmlh$), succinoyldihydrazone ($H_4salsuch$), glutaroyldihydrazone ($H_4salgluth$), and phthaloyldihydrazone ($H_4salphth$). The complexes have been characterized by molar conductance and spectral data.

Lal and coworkers **[120]** have synthesized the complexes, $Na_4[(UO_2)_4(L)_2(OAc)_4(H_2O)_4].4H_2O$ (1) and $Na_4[(UO_2)_4(L)_2F_4(H_2O)_4]$ (2) from bis(o-hydroxynaphthaldehyde)oxaloyldihydrazone ($napoxlhH_4$) and characterized by elemental analysis, molar conductance, electronic, IR and ^1H NMR spectroscopic studies. On the basis of these studies, it is suggested that the fluoro complex exists in chair conformation in which coordination of both azomethine nitrogen atoms of the dihydrazone in cis-configuration to the same metal centre leads to coupling between azomethine protons. In the acetato complex, the coordination of two hydrazone parts of the dihydrazone even in cis-configuration to different metal centres eliminates the possibility of azomethine proton coupling and thus, its existence in chair conformation. All the complexes involves eight-coordinated uranium atom with the dihydrazone in the enol form.

Lal and coworkers **[121]** have synthesized the monometallic complexes of the type $[Zn_2(H_4L)_2(SO_4)_2]$ (1), $[Zn_2(H_2L)_2(H_2O)_2]$ (2), $K_2[Zn_2(H_2L)_2F_2]$ (2a), and the heterometallic complexes of the type compound $[(UO_2)_2Zn_2(H_2O)_6]$ (3), $[(UO_2)_2Zn_2(L)_2F_4(H_2O)_2]$ (3a), $[Cu_2Zn_2(L)_2(H_2O)_4]$ (4), $K_4[Cu_2Zn_2(L)_2F_4(H_2O)_2]$ (4a), and characterized by analytical, molar conductance and magnetic moment data and electronic, ESR, IR, and ^1H NMR spectroscopic studies. All of the complexes have been proposed to be dimmer on the basis of molecular weight determinations. Monometallic complexes have been shown to contain the coordinated dihydrazone in syn-cis- configuration while the heterobimetallic complexes contain the coordinated dihydrazone in the anti-cis- configuration. In these complexes, copper and zinc metal

centres have been shown to be five coordinate square-pyramidal whereas uranium centres have been shown to be eight-coordinate hexagonal bipyramidal.

Ma Yongxiang and coworkers **[122]** synthesized the chelates $Na_2[Ln(C_{34}H_{28}N_8O_8)Cl].nH_2O$ of the malonoyl dihydrazone of salicylaldehyde with the lanthanides and characterized them by elemental analysis, IR, UV, molar conductance and TGA. They showed that the ligand coordinates to the central ion with one hydrazone unit in the keto form and one chloride ion participates in coordination to the metal ion. These chelates are 1: 2 electrolytes in DMF and are more thermostable than their ligand due to the formation of chelate rings.

Bolgar and coworkers **[123]** synthesized a series of dihydrazone and substituted dihydrazone derivatives of biacetyl and of hydrazone and phenylhydrazone derivatives of 2-acetylpyridine. They studied the reactions of those dihydrazones with $[Ru(bpy)_2Cl_2]$ and isolated the products of the composition $[Ru(bpy)_2(L\text{-}L)][PF_6]_2$ {bpy = 2,2'-bipyridine; L-L = biacetyl di(phenylhydrazone) 1a, biacetyl di[methyl(phenyl)hydrazone] 1b, biacetyl di(o-tolylhydrazone) 1c, biacetyl di(methylhydrazone) 1d, biacetyl dihydrazone) 1e, biacetyl di(benzaldehyde azine) 1f, 2-acetylpyridine phenylhydrazone 1g, or 2-acetylpyridine hydrazone 1h}. The structures of all complexes were determined using IR, UV/VIS, NMR and microanalysis. The proton NMR spectra of 1a-1c showed an unusual dependence on probe temperature with broadened aromatic resonances, sharpening at both high and low temperatures in the case of 1b and 1c. No emission was observed for complexes with two hydrazone moieties, whereas it was observed for 1g and 1h with one hydrazone. The molecular structure of 1a was determined and it was shown that a hydrazone phenyl group lies over each of the bipyridyl rings: space group C2/c, a = 25.895(3), b = 10.505 (1), c = 17.431(2) Å, β = 106.03 (2) and Z = 4.

Khan and coworkers **[124]** synthesized a new class of tetraiminetetraamide macrocyclic (Ph_4[20]tetraene, N_8O_4, and Ph_6[20]tetraene, N_8O_4) complexes through the metal ion controlled reaction of 1,2-diphenylethane-1,2-dione dihydrazone

(DPEDDH) with succinic acid [ML_1X_2] or phthalic acid [ML_2X_2] [M = Co, Ni, Cu or Zn; X = Cl or NO_3]. They elucidated the structure of the complexes on the basis of IR, ^1H NMR, EPR and electronic spectral data and conductance, as well as magnetic, properties. An octahedral geometry was assigned for all the complexes, involving coordination of the all-imine nitrogens.

Labib and coworkers **[125]** synthesized a series of polyacylhydrazones by condensing diacetyl with oxalic, malonic, succinic, glutaric and adipic dihydrazides and characterized them by conventional spectroscopic studies. They reacted these dihydrazones of general formula $\{[Cu_2(L)(OAc)_2(OH)(H_2O)_2].yH_2O\}_n$, $\{[Cu(L)(OAc)_2(HO)(H_2O)].yH_2O\}_n$, $\{[Ni_2(L)(OAc)_2(HO)_2].yH_2O\}_n$, $\{[Ni(L)(OAc)$-$(HO)].yH_2O\}_n$, where L refers to the neutral dihydrazone unit. Magnetic susceptibility measurements in the 4.2-300 K range indicated significant antiferromagnetic coupling between the Cu^{II} centers in the metallopolymers. The results might indicate the presence of two polymer chains crosslinked by bis-μ-acetatocopper (II) bridges. Based on IR, spectral and magnetic measurements, tentative structures of the Cu^{II} and Ni^{II} metallopolymers were proposed. The dihydrazone units in these polymers were found to be coordinated to the metal (II) via the azomethine nitrogen(s) whereas the amide group was found to remain uncoordinated. Each Cu^{II} is penta-cordinated in a distordted square pyramidal environment and is neutralized by bridged acetate and a hydroxide ion, while the fifth coordination site is occupied by a water molecule. In the nickel (II) metallopolymers, the metal ions were in a tetrahedral environment and were coordinated to azomethine nitrogen, two bridged acetate oxygens and to the hydroxide ion.

Larin and coworkers **[126]** synthesized the dinuclear copper (II) complexes with 2-hydroxypropiophenone, 2-hydroxy-5-methyl and 5-chloro-2-hydroxyacetophenone acyldihydrazones (H_4L) having the composition [$Cu_2L.mPy$], where L ligand contains the polymethylene chain with different lengths (from two to five units). The crystal and molecular structure of the 2-hydroxypropiophenone adipoylhydrazone

complex $[Cu_2L.4Py].Py$ were established by X-ray diffraction analysis. Copper atoms were found to be separated from one another by a distance of 8.212Å. Their nearest environment was found to have tetragonal pyramidal geometry. The ESR spectra of solutions of the complexes based on acyldihydrazones of succinic, malonic, glutaric, and adipic acids contain seven HFS lines with the constant ~ 40×10^{-4} cm^{-1} from two equivalent copper atoms. The spectra were interpreted as a result of the spin-spin exchange interaction of two unpaired electrons. An increase in the polymethylene chain length of five units prevents exchange interactions. The ESR spectrum of the complex with acyldihydrazone of pimelic acid contains a signal of four HFS lines with $A_{Cu} = 73.4\times10^{-4}$ cm^{-1}, which is typical of mononuclear copper (II) complexes.

Andelkovic and coworkers **[127]** synthesized complexes of Zn (II), Pd (II) and Pt (II) with 2'-[1-(2-pyridinyl)ethylidene]oxamohydrazide (Hapsox). The complexes were characterized and their structures were determined. All the complexes were found to be neutral type with two apsox ligands coordinating to Zn (II) and one apsox ligand coordinating to Pd (II) or Pt (II). In each case, the polydentate ligand was coordinated via pyridine and hydrazone nitrogens and α-oxyazine, forming an octahedral geometry around Zn (II), and a square planer one around Pd (II) and Pt (II). The structure determination was performed by IR, ^1H NMR and ^{13}C NMR spectroscopy, and for the Zn (II) complex by X-ray structure analysis.

Para etal **[128]** synthesized dialdehyde starch dihydrazone DASHZ from reaction of dialdehyde starch with hydrazine. The dihydrazone (DASHZ) coordinated to Ca, Cd, Co (II), Cu (II), Fe (II), Mg, Mn (II), Ni (II), Pb (II), and Zn ions. The nitrogen atoms of the >C=N moiety in dihydrazone as well as the oxygen atom of the fomer pyranose ring were the coordination sites. Metal ions were chelated to a different extent. One mole of a metal ion could coordinate with 3 [Cu (II)] to 50 [Mn (II)] mole of the DASHZ units. The ligand DASHZ and the metal complexes decomposed thermally in four steps but the rates of decomposition of the ligand and chelates in

relevant steps were different. Except the complex with Mg, these rates for complexes were lower.

Zhao and coworkers **[129]** synthesized polynuclear manganes e(II), cobalt (II)/(III), iron (II)/(III) and nickel (II) complexes of a group of flexible polydentate dihydrazone ligands, based on pyridine-2,6-dipicolinic (A), oxalic (B) and malonic (C) subunits. They reported the structural details for the linear dinuclear complexes $[Ni_2(2poap)_2(H_2O)_2](NO_3)_2.2CH_3OH.2H_2O$ (1), $[Mn_2(pttp)_2(NO_3)_2(CH_3OH)_2$-$(H_2O)_2](NO_3)_2.2H_2O$ (2), and $[Mn_2(mapttp)_2(NO_3)_2(H_2O)_2](NO_3)_2.10H_2O$ (3), a square tetranuclear complex $[Co_4(pttp)_4]Br_6.9H_2O$, a tetranuclear tetrahedral complex $[Ni_4(pttp)_6](BF_4)_6F_2.14H_2O$ (7), and a mixed spin state tetranuclear Ni(II) complex $[(2pyoap)_2Ni_4(CH_3OH)_4].1.5CH_3OH$ (10), with a diamond-like arrangement of metal ions. The paramagnetic metal centres are well separated in each case, leading to weak antiferromagnetic coupling or non-existent spin exchange.

Tirosh and coworkers **[130]** synthesized the cadmium (II) complex $[Cd(C_4H_{10}N_4)_3(ClO_4)_2$ from the reaction of $Cd(ClO_4)_2.H_2O$ with biacetyl dihydrazone in methanol. They established the structure of the compound with the help of X-ray crystallography. The cation was found to be located on a 3 axis and was characterized by an approximate octahedral geometry, with each of the ligands occupying two coordination sites around the metal.

Carcelli and coworkers **[131]** synthesized a novel series of lanthanide (III) complexes with two potentially hexadentate ligands containing a rigid phenanthroline moiety and two flexible hydrazonic arms with different donor atom sets (NNN'N'OO and NNN'N"N", respectively. These hydrazones (2,9-diformylphenanthroline)bis(benzoyl)hydrazone (H_2L^1), (2, 9-diformylphenanthro-line)bis(2-pyridyl)hydrazone (H_2L^2). They prepared both both nitrate and acetate complexes of H_2L^1 with La, Eu, Gd, and Tb and fully characterized. They presented the X-ray crystal structure of the complex $[Eu(HL^1)(CH_3COO)_2].5H_2O$. The stability constants of the equilibria $Ln^{3+} + H_2L^1 = [Ln(H_2L^1)^{3+}$ and $Ln^{3+} + (L^1)^{2-} = [Ln(L_1)^+$

(Ln = La (III), Eu (III), Gd (III), and Tb (III) were determined by UV spectrophotometric titrations in DMSO at t = 25°C. They also synthesized the nitrate complex of H_2L^2 with La, Eu, Gd and Tb. The X-ray crystal structure of the complex $[La(H_2L^2)(NO_3)_2(H_2O)](NO_3)$, $[Eu(H_2L^2)(NO_3)_2](NO_3)$ and $[Tb(H_2L^2)(NO_3)_2](NO_3)$ were also established.

Salem **[132]** synthesized a series of acyldihydrazones, H_2L^n from condensation of ethylpyruvate with oxalic, malonic, succinic, glutaric and adipic dihydrazides. The author isolated dicopper(II) complexes of the general formula $[Cu(L'^n).H_2O].x\ H_2O$, where L'^n refers to the quadruply deprotonated pyruvic acid dihydrazone ligand and n refers to the number to number of carbon atoms of the aliphaticspacer between the two acylhydrazone units. The isolated complexes were characterized by elemental analysis, infrared spectra, mass spectra, as well as variable temperature magnetic susceptibility measurements. Magnetic susceptibility measurements in the 4.2-298 K range indicate significant antiferromagnetic coupling between copper (II) centers and suggest association of the coordinated copper (II) units Cu(ONO) via oxazine oxygen bridges. This leads to a polymeric structure where the dimeric units are connected together with aliphatic spacer. From the best fit values of the mole fraction of paramagnetic uncoupled copper (II) centers (ρ), the degree of association in these polynuclear copper (II) complexes was estimated.

Elengoz etal **[133]** synthesized the zinc complex tris(biacetyldihydrazone-κ^2N,N')zinc(II) bis(perchlorate) at 110 K and determined its crystal structure precisely.The metal-organic cation, which is located on a 3 axis, is characterized by an approximate octahedral geometry, with each of the ligands occupying two coordination sites around the metal. The title compound, crystallizes in the trigonal space group P3c1 with two units of the $[Zn(C_4H_{10}N_4)_3]^{2+}$ cationic complex and four ClO_4^- anions in the unit cell. The Zn^{II} atom is located on a 3axis, while the perchlorate anion is located on a theefole rotation axis. The cation is characterized by perfect symmetry, in which three chelating ligands occupy the octahedral coordination sites of the zinc metal ion. The imine N atoms of the lignd provide the

coordination sites to the central metal ion. The conformation about the central C—C bond of the ligand is cis, with the two C=N bonds being nearly coplanar, to direct the two imine coordinating sites towards the metal centre. The N—Zn—N bond angle involving two coordinating N atoms of a given ligand is 74.33 (11). In the free form of the ligand, the N—N=C—C=N—N backbone adopts a planer anti conformation (Hauer et al, 1987).

V. P. Singh and P. Gupta **[134]** synthesized and characterized the Complexes of diacetyl salicylaldehyde oxalic acid dihydrazone, $CH_3COC(CH_3)$= NNHCOCONHN=CHC_6H_4(OH), (dsodh) and diacetyl salicylaldehyde malonic acid dihydrazone, $CH_3COC(CH_3)$=NNHCOCH_2CONHN=CHC_6H_4(OH), (dsmdh) by elemental analyses, molar conductance, magnetic moments, electronic, ESR and infrared spectra and X-ray diffraction data. and were found to have the general compositions [M(L)]Cl, [M'(L)Cl], [M(L')]Cl and [M'(L')Cl] (where M = Co (II), Cu (II), Zn (II), Cd (II) and M'= Ni (II); HL = dsodh and HL' = dsmdh). With the help of magnetic moments and electronic spectral data they predicted a six-coordinate octahedral geometry for Co (II) and square planar geometry for Ni (II) complexes. They also found that the ESR spectral data of Cu (II) complexes in DMF solution reveal a tetragonally distorted octahedral geometry. Both ligands bond through >C=O, >C=N and deprotonated phenolate groups in all octahedral complexes and through >C=N and deprotonated phenolate groups in Ni (II) square planar complexes. The lattice parameters for Cu(dsodh) and Co(dsmdh) correspond to an orthorhombic and Ni(dsodh) corresponds to a tetragonal crystal lattice. The complexes were found to exhibit significant antifungal activity against a number of pathogenic fungi viz. Stemphylium, Myrothecium and Alternaria. The antibacterial activity was studied against Pseudomonas fluorescence (gram -ve) and Clostridium thermocellum (gram +ve).

C. T. Yang and coworkers **[135]** synthesized the complexes of dioxouranium (VI) with four dipyridoxal hudrazone ligands $H_{4PL}{}^n$ and characterized them by various analytical and spectroscopic methods including x-ray crystallography. The ligands

and the UO_2^{VI} complexes were also tested for cytotoxicity. They found that the solid-state structure of $[(UO_2)_4(PL')_2(H_2O)_4].12H_2O$ is a cyclic tetramer.

M. F. Iskander and coworkers **[136]** synthesized and characterized two series of dicopper(II) complexes derived from bis(N-salicylidine)dicarboxylic acid dihydrazides ($H4L^n$) of general formula $[Cu_2(L_n).xH_2O].yH_2O$ and $[Cu_2(H_2L^n)Cl_2.xH2O].yH2O$ where n refers to the number of carbon atoms in the aliphatic spacer between the two N-salicylideneacylhydrazine units. Magnetic susceptibility measurements for neutral dicopper (II) complexes $[Cu_2(L^n).xH_2O].yH_2O$ indicate significant antiferromagnetic coupling between copper(II) centers. The –2J values obtained from the Bleany–Bowers equation are within the range 121–223cm^{-1}, suggesting association of the coordinated copper (II) units Cu(ONO) via phenoxy bridges. This leads to a polynuclear structure in which the dimeric units are connected with the aliphatic spacer. From the best-fit values of the mole fraction of paramagnetic uncoupled copper (II) centers (ρ), the degree of association in these polynuclear copper (II) complexes has been estimated. The chloro dicopper (II) complexes $[Cu_2(H_2L^n)Cl_2.xH_2O].yH_2O$ with n = 0, 2 and 3 also show strong antiferromagnetic exchange coupling (2J = 215–423cm^{-1}), suggesting a polynuclear structure in which the copper (II) is in a distorted square-pyramidal environment, bound in the equatorial plane with a monoanionic ONO tridentate acylhydrazone unit and the μ-phenoxy oxygen and the axial site occupied by a chloride. The dicopper (II) complexes with n¼1 and 4 show weak antiferromagnetic exchange coupling (2J = 16–20 cm^{-1}). In these complexes the chloride ion may occupy the fourth equatorial site while the μ-phenoxy is in the apical position.

V. P. Singh and P. Gupta **[137]** synthesized and characterized the Complexes of diacetyl salicylaldehyde oxalic acid dihydrazone, CH3COC(CH3)= NNHCOCONHN=CHC6H4(OH), (dsodh) and diacetyl salicylaldehyde malonic acid dihydrazone CH3COC(CH3)=NNHCOCH2CONHN=CHC6H4(OH), (dsmdh) of general compositions[M(L)]Cl, [M'(L)Cl], [M(L')]Cl and [M'(L')Cl] (where M = Co (II), Cu (II), Zn (II), Cd (II) and M' = Ni (II); HL = dsodh and HL' = dsmdh)

were prepared and characterized by elemental analyses, molar conductance, magnetic moments, electronic, ESR and infrared spectra and X-ray diffraction data. The magnetic moments and electronic spectra indicate six-coordinate octahedral geometry for Co (II) and square planar geometry for Ni (II) complexes. The ESR spectral data of Cu (II) complexes in DMF solution reveal a tetragonally distorted octahedral geometry. Both ligands bond through >C=O, >C=N and deprotonated phenolate groups in all octahedral complexes and through >C=N and deprotonated phenolate groups in Ni (II) square planar complexes. The lattice parameters for Cu(dsodh) and Co(dsmdh) correspond to an orthorhombic and Ni(dsodh) corresponds to a tetragonal crystal lattice. The complexes were found to exhibit significant antifungal activity against a number of pathogenic fungi viz. Stemphylium, Myrothecium and Alternaria. The antibacterial activity was studied against Pseudomonas fluorescence (gram -ve) and Clostridium thermocellum (gram +ve).

V. P. Singh and co-workers **[138]** isolated the metal (II) complexes of the general formula [M(Bsodh)]Cl and [MBsmdh]Cl where M = Co (II), Ni (II), Cu (II), Zn (II) and Cd(II) (HBsodh = benzyl salicylaldehyde oxalic acid dihydrazone and HBsmdh = benzyl salicylaldehyde malonic acid dihydrazide) and characterized them by elemental analyses, molar conductance, magnetic moment, ESR, IR and X-ray diffraction studies. The ligands and their metal complexes were found to exhibit significant antibacterial activity against Bacilus subtilis and Pseudiomonas fluiorescens.

L. D. Popov and co-workers **[139]** synthesized the dihydrazone ligand 2,6-diformyl-4-tert-butylphenol bis(8-quinolylhydrazone) and its transition meta complexes of the compositions $[Cu_2(H_2L)Cl]Cl_2$, $[Ni_2(H_2L)Cl_3]$ and $[Mn_2(H_2L)Cl_3]$, where H_2L is the monodeprotonated form of the hydrazone. They studied the conformations of sthe bis-hydrazone, geometries of the complexes, and parameters of exchange coupling between the ferromagnetic centres using quantum –chemical calculations. They also

compared the calculated results with the results of the physicochemical study of the complexes.

S. Naskar and D. Mishra **[140]** synthesized a Ni(II) complex of 2,6-diacetyljpyridine bis(anthraniloyl hydrazone) and characterized it by various physico-chemical methods. The structure of the complex was determined by X-ray crystallography. They also found that, in the solid state, the compound exist as a dimer and two coordinated ligand moieties form a double helix around the two metal ions.

R. M. Issa and co-workers **[141]** studied the thermal stabilities of bis salicylidine adipic dihydrazone derivatives and their complexes with divalent Mn, Ni, Cu and Zn ions and discussed them in terms of structure and type of metal ions. They also found that, the TG curves display mostly four steps of thermal decomposition.

V. F. Shulgin and co-workers **[142]** synthesized and characterized dinuclear copper (II) complexes with acyldihydrazones of 2-hydroxy-5-nitroacetophenone (H_4L) of the composition $Cu_2(py)_xL.mEtOH$. It was found that, in the complexes, the coordination polyhedra ofs the copper atoms are linked to each other by a polymethylene chain of different lengths, from one to five monomer units. They also established the structure for $[Cu_2L.4Mrf]$ complex (where Mrf is morpholine) based on acyldihydrazone of malonic acid by X-ray diffraction.

M. Salavati-Niasari and A. Sobhani **[143]** isolated the monomer transition metal complexes, [ML] (M = Mn (II), Co (II), Ni (II) and Cu (II)) from the reaction of metal acetates with bis(salicylaldehyde)oxaloyldihydrazone (H_2L) in 1: 1 molar ratio in ethanol under reflux. It was suggested that, in all of the complexes, the principal dihydrazone ligand coordinate to the metal centres in the *anti-cis* configuration. These metal complexes were entrapped in the nano cavity of zeolite-Y. The new Host-Guest Nano Composite Materials (HGNM) was characterized by chemical analysis and spectroscopic methods. They also reported the catalytic activities for the oxidation of cyclohexane with HGNM.

Da-Yu Wu and co-workers **[144]** isolated three ligands, di(2-pyridylcarbaldehyde)-6,6'-dicarboxylic acid hydrazone-2,2'-bipyridine (H_2L^1), di(2-acetylpyridyl)-6,6'-dicarboxylic acid hydrazone-2,2'-bipyridine (H_2L^2) and di(2-pyridyketone)-6,6'-dicarboxylic acid hydrazone-2,2'-bipyridine (H_2L^3) with flexible bis-terdentate coordination sites and their cobalt complexes. The complexes were obtaine via self-assembly and their structures were determined by FT-IR, elemental analyses, ESI-MS and X-ray diffraction method.

Lal and coworkers **[145]** synthesized the complexes $[(UO_2)(CH_2L)(H_2O)_4].4H_2O$, $[M_4(H_2L)_2(H_2O)_4].4H_2O$ (M = Zn, Cu), $(M')_2[(UO_2F)(CH_2L)(H_2O)_2]$ [M' = K, Na], $M'[(UO_2)_2(CH_2L)(OAc)(H_2O)_2]$ [M' = K, Na], $K_4[(MF)_2(CH_2L)_2].4H_2O$ [M Zn, Cu] from the reaction of appropriate metal salts with bis(2-hydrowy-1-naphthaldehyde)oxaloyldihydrazone (CH_2LH_4) under different experimenatal conditions in ethanol/methnol media. The complexes have been characterized by elemental analyses, molecular weight, molar conductance, magnetic and EPR data. The structural assessments of the complexes have been carried out on the basis of electronic, infrared, ^1H NMR and ^{13}C NMR sprectral studies.

Lal and coworkers **[146]** synthesized and characterized zinc (II), copper (II), nickel (II) and manganese (II) complexes derived from bis(2-hydroxy-1-naphthaldehyde)malonoyldihydrazone. In their study, they have shown that the reaction of different salts of the same metal with stericallly crowded dihydrazone bis(2-hydroxy-1-naphthaldehyde)malonoyldihydrazone (CH_2LH_4) in ethanol/ aqueous media gives complexes of different stereochemistry. While the reaction of Zn (II) and copper (II) sulphate with dihydrazone yields tetrahedral complexes, the zinc (II) and copper (II) chlorides give square pyramidal and distorted octahedral complexes respectively. On the other hand, nickel (II) sulphate and chloride, both gave high-spin octahedral complexes. They also investigated the reaction of these complexes with KF. All of the products were characterized by analytical, magnetic moment and molar conductance data. The structure of the complexes has been established by spectroscopic studies.

Lal and coworkers **[147]** synthesized the monomer molybdenum (VI) complex $[MoO_2(napoxlhH_2)].2H_2O$ (1) from the reaction of $MoO_2(acac)_2$ with bis(2-hydroxy-1-naphthaldehyde)oxaloyldihydrazone ($napoxlhH_4$) in 1: 1 molar ratio in ethanol under reflux. Thes complex on reaction with pyridine /3-picoline/4-picoline yielded the dimmer molybdenum (VI) complex $[Mo_2O_4(napoxlhH_2)(A)_2].2H_2O$ (A = py (2), 3-pic(3), 4-pic(4)), whereas the reaction with isonicotinoyl hydrazine ($inhH_3$) and salicyloyl hydrazine ($sylshH_3$) led to the reduction of the metal centre yielding monomeric molybdenum (V) complexes $[Mo(napoxlhH_2)(hzid)].2H_2O$ (Where $hzidH_3$ = $inhH_3$ (5) and ($sylshH_3$ (6)). The complexes have been characterized by elemental analyses, molecular weight determinations, molar conductance data, magnetic moment data, electronic, IR, ESR, ^1H NMR spectroscopic data.

Singh and co-workers **[148]** studied the reaction of bis(2-hydroxy-1-naphthaldehyde) oxaloyldihydrazone ($naohH_4$) with manganese (II) acetate in methanol followed by addition of KOH to get the complex $[Mn^{IV}(naoh)(H_2O)_2]$. They also studied the reaction of activated ruthenium (III) chloride with $naohH_4$ in methanol to get the complex $[Ru^{III}(naohH_4)(H_2O)Cl_2]$ and characterized them by elemental analyses, IR, electronic, ESR and cyclic voltammetric studies. They observed the replacement of aquo by heterocyclic nitrogen donor in these complexes when the reaction was carried out in presence of heterocyclic nitrogen donors such as pyridine, 3-picoline and 4-picoline.

From the survey of literature presented above, it is evident that although mono and bimetallic complexes of various types of dihydrazones have been synthesized and characterised, in some detail, those derived from dihydrazones containing bulky fragments in their molecular skeleton have been much less studied. Further, the heterobimetallic complexes of such dihydrazones are almost non-existent. In view of limited number of investigations on metal complexes of dihydrazones containing bulky fragments in their molecular skeleton, the project has been undertaken. It is quite possible to extend and develop such a study, with the help of variety of metal ions into a major field, but because of time factor, it has been restricted to

monometallic, homobimetallic and heterobimetallic complexes of disalicylaldehyde oxaloyldihydrazone with copper (II), molybdenum (VI) and nickel (II).

References

1. E. Kahrovic, K. Molcanov, L. T. Bozic and B. K. Prodic, *Polyhedron,* **25**, 2459 (2006).
2. W. H. Orome-Jhonson, *Ann. Rev., Biophys. Chem.,* **14**, 419 (1985); T. G. Spiro (Ed) Molybdoenzymes, *Wiley Interscience,* New York, 1985.
3. R. C. Brevy, *Q. Rev. Biophys.,* **21**, 299 (1988); R. H. Holm and J. M. Berg, *Acc. Chem. Res.,* **19**, 363 (1986).
4. E. I. Stiefel, *Science,* **272**, 1599 (1996).
5. D. Sellman, *Angew. Chem., Int. Ed.,* **32**, 64 (1993).
6. J. Kim, D. Wood, D. C. Ress, *Biochemistry,* **32**, 7104 (1993).
7. C. Litos, A. Terzis, C. Rapotopoulou, A. Rontoyianni and A. Karaliota, *Polyhedron*, **25**, 1337 (2006); T. Yamase, *J. Mater. Chem.*, **15**, 4773 (2005).
8. S. Mitusi, A. Ogata, H. Kasano, T. Hisa, T. Yamase and M. Eriguchi, *Biomed. Pharmacother.*, **60**, 353 (2006).
9. W. Yao and J. Ye, *Catal. Today*, **116**, 18 (2006).
10. Z. Petrovoski, A. A. Valente, M. Pillinger, A. S. Dias, S. S. Rodrigues, C. C. Romao and I. S. Gonsalves, *J. Mol. Catal. A: Chem.*, **249**, 166 (2006); F. E. Kuhn, J. Zhao and W. A. Herrmann, *Tetrahedron: Asymmetry*, **16**, 3469 (2005); S. M. Bruno, C. C. L.Pereira, M. S. Balula, M. Nolasco, A. A. Valente, A. Hazell, M. Pilinger, P. R. Claro, I. S. Gonsalves, *J. Mol. Catal. A: Chem.*, **261**, 79 (2006).
11. P. Concepcion, P. Botella, J. M. Nieto, *Appl. Catal., A: Gen,* **278**, 45 (2004).
12. R. R. Chianeli, *Catal., Rev. Sci. Eng.,* **26**, 361 (1984); R. J. Angelici, *Acc. Chem. Res.*, **21**, 387 (1988); M. Lewandowski, A. Kolasa, P. Da Costa and C. Sayag, *Catal. Today*, **119**, 31 (2007).
13. S. Saha and J. F. Stoddart, *Chem. Soc. Rev.*, **36**, 77-92 (2007).
14. M. Ire, *Chem. Rev.*, **100**, 1683 (2000).
15. "*Ferroelectric Polymers: Chemistry, Physics and Applications*", H. S. Nalwa, Ed., Marcel dekkar, Inc: New York (1995); M. E. Lines and A. M. Glass, "*Principles and Applications of Ferroelectrics and Related*

Materials", The International Series of Monographs on Physics, Clarendon Press: Oxford, U.K. (1977).

16. J.-M. Harrera, V. Mariand, M. Verdagner, J. Manot, M. Kalisz and C. Mathoniere, *Angew. Chem., Int. Ed.*, **43**, 5468-5471 (2004).
17. K. Nakagawa, H. Tokoro and S. Ohkoshi, *Inorg. Chem.*, **47**, 10810 (2008).
18. D. Brinzei, L. Catala, C. Mathoniere, W. Weinsdorfer, A. Gloster, O. Stephan and T. Mallah, J. Am. Chem. Soc., 129, 3778-3779 (2007).
19. J. Long, L.-M. Chamorean, C. Mathoniere and V. Marvard, *Inorg. Chem.*, **48**, 22 (2009).
20. R. K. Andrews, R. L. Blakely and B. Zenner, *Advances in Inorganic Biochemitry*, Vol. **5**; G. L Ei Chhorn and L. G. Marzilli, Ed. Elsevier, New York, (1984), p- 245.
21. A. M. Stolzenberg and Z. Zhang, *Inorg. Chem.*, **36**, 593 (1997).
22. W. Nau, S. J. Back, K. Ah. Lee, B. T. Ahn, J. G. Muller, C. J. B urrows and J. S. Valentine, *Inorg. Chem.*, **35**, 6632 (1996).
23. C.Muller, L. J. Ackerman, J. N. H. Reck, P. C. J. Kamer and P. W. N. M Vanleeuwen, *J. Am. Chem. Soc.*, **126**, 14960 (2004).
24. Comprehensive Coordination Chemistry II, Vol. **6**, p-249 – 554, *Elsevier* (Pergamon) (2004).
25. M. Casarin, C. Corvaja, C. Di Nicola, D. Falcomer, L. Franco, M. Monair, L. Pandorfo, C. Pettinari and F. Piccinelli, *Inorg. Chem.*, **44**, 6265 (2005).
26. H. Sigel, Eds., "*Metal Ions in Biological Systems*", Marcel Dekker: New York, Vol. **13** (1981).
27. E. I. Solomon, U. M. Susidaram and T. E. Machonkin, *Chem. Rev.*, **96**, 2563 (1996); A. Messerschmidt, *Struct. Bonding (Berlin)*, **90**, 37 (1998).
28. T. E. Machonkin, H. H. Zhang, B. Hedmam, K. O. Hodgson and E. I. Solomon, *Biochemistry*, **37**, 9570 (1998).
29. F. J. Carver, D. L. Farb and E. Frieden, *Biol. Trace Elem. Res.*, **4**, 1 (1982); A. E. Palmer, L. Guintanar, S. Severance, T. P. Wang, D. J. Kosman and E. I. Solomon, *Biochemistry*, **41**, 6438 (2002).

30. H. Dobbek, L. Gremer, O. Meyer and R. Huber, "*In Handbook of Metallo-proteins*", A. Messerschmidt, R. Huber, K. Wieghardt and T. Poulos, Eds., Wiley: Chichester, U.K., Vol. **2**, pp. 1136-1147 (2001).

31. A. Siegel and H. Siegel, Eds., "*Metal Ions in Biological Systems*", Marcel Dekkar: New York, Vol. **39** (2002).

32. C. Gourlay, D. J. Nielsen, J. M. White, S. Z. knottenbelt, M. L. Kirk and C. G. Young, *J. Am. Chem. Soc.*, **128**, 2164 (2006).

33. I. Ramade, O. Khan, Y. Jeannin and F.Robert, *Inorg. Chem.*, **36**, 930 (1997).

34. C. Benilli, A. Caneschi, D. Gatteschi, O. Guillon, and L. Pardi, *Inorg. Chem*, **29**, 1750 (1990).

35. A. Nanthakumar, S. Fox, N. N. Murthy and K. D. Karlin, *J. Am. Chem. Soc.*, **119**, 3898 (1097).

36. N. N. Murthy, K .D. Karlin, I. Bertini and C. Luchinat, *J. Am. Chem. Soc.*, **119**, 2156 (1097).

37. L. Sacconi, *J. Chem. Soc.*, 1326 (1954).

38. R. C. Aggarwal and B. Singh, *Transition Met. Chem.*, **1**, 275 (1976); *Curr. Sci.*, **46**, 836 (1977); *J. Inorg. Nucl. Chem.*, **40**, 1174 (1978).

39. A. EL-Toukhy, A. F. M. Henry, L. El-Sayad and M. F. Iskandar, *Mh. Chem.*, **113**, 171 (1982); M. F. Iskander, A. F. M. Hefny, L. El-Sayad and S. E. Zayan, J. *Inorg. Nucl. Chem.*, **38**, 2209 (1976).

40. S. Chandra and R. N. Kapoor, *Acta Chim. Hung.*, **112**, 11 (1983).

41. K. K. Narang and R. A. Lal, *Transition Met. Chem.*, **1**, 260 (1976).

42. K. K. Narang and R. A. Lal, *Transition Met. Chem.*, **2**, 100 (1977).

43. K. K. Narang and R. A. Lal, *Transition Met. Chem.*, **3**, 272 (1978).

44. K. K. Narang and R. A. Lal, *Curr. Sci.*, **46 (12)**, 401 (1977); **47**, 793 (1978).

45. K. K. Narang and R. A. Lal, *J. Scient, Res., BHU.* **28 (2)**, 1 (1978); **31**, 259 (1980-81).

46. S. K. Sahni, S. P. Gupta, V. B. Rana, *J. Indian. Chem. Soc.*, **54**, 200 (1977).

47. S. K. Sahni, S. K. Sanyal, S. P. Gupta and V. B. Rana, *J. Inorg. Nucl. Chem.*, **39**, 1098 (1977).

48. R. L. Duttta and A. K. Sarker, *J. Inorg. Nucl. Chem.*, **43**, 180 (1981).

49. S. Kher, S. K. Sahni and R. N. Kapoor, *Inorg. Chim. Acta,* **37**, 121 (1979).

50. S. Kher, S. K. Sahni, V. Kumari and R. N. Kapoor, Synth. React. *Inorg.Met-Org.Chem.,* **10 (5)**, 431 (1980).

51. V. B. Rana and M. P. Teotia, *Indian J. Chem.,* **19A**, 267 (1980).

52. R. Chandra, S. K. Sahni and R. N. Kapoor, *Acta. Chim. Hung.,* **112 (4)**, 385 (1983); S. Chandra and R. N. Kapoor, *Acta. Chim. Hung.,* **112**, 11 (1983).

53. K. K. Narang and U. S. Yadav, *Indian J. Chem.,* **19A**, 697 (1980).

54. K. K. Narang, and R. M. Dubey, *Indian J. Chem.,* **21A**, 830 (1982).

55. A. Yacouta Nour, M. M. Mostafa and A. K. T. Maki, *Transition Met. Chem.,* **15**, 34 (1990); *Spectrochim Acta.,* **44A**, 1291 (1988).

56. D. L. Arora, K. Lal, S. P. Gupta and S. K. Sahni, *Polyhedron,* **5**, 1499-1501 (1986); *Indian J. Chem.,* 24A, 980 (1987).

57. K. K. Narang and M. K. Singh, *Transition Met. Chem.,* **12**, 385 (1987).

58. R. A. Lal, S. Das and R. K. Thapa, *Inorg. Chim. Acta,* **132**, 129 (1987).

59. R. A. Lal and S. Das, *Indian J. Chem.,* **27A**, 225 (1988).

60. R. A. Lal, K. N. Srivastava and S. Das, *Synth. React. Inorg. Met-Org. Chem.,* **18**, 837 (1988); R. A. Lal, A. N. Siva, R. K. Thapa, M. K. Singh and S. S. Bhattacharjee, Synth. React. *Inorg. Met-Org. Chem.,* **25**, 357 (1995).

61. R. A. Lal, *Polyhedron,* **8**, 2527, (1989).

62. H. Hussain, S. S. Bhattacharjee, K. B. Singh and R. A. Lal, *Polyhedron,* **10**, 779 (1991); R. A. Lal, A. N. Siva, S. Adhikari, M. K. Singh and U. S. Yadav, , Synth. React. *Inorg. Met-Org. Chem.,* **26 (2)**, 321-337 (1996).

63. R. A. Lal, L. M. Mukherjee, A. N. Siva, A. Pal, S. Adhikari, K. K. Narang and M. K. Singh, *Polyhedron,* **12**, 235 (1993).

64. R. A. Lal, A. N. siva, L. M. Mukherjee, K. K. narang, M. K. Singh and R. K. Thapa, *Spectrochim. Acta,* **50A**, 1005 (1994).

65. R. A. Lal, A. N. Siva, S. Adhikari and A. Pal, *Indian J. Chem.,* **34A**, 1000 (1995).

66. S. A. Patil and V. H. Kulkarni, *Inorg. Chim. Acta,* **95**, 195 (1984).

67. T. R. Goudar, S. M. Shindagi and G. S. Nadagauda, *J. Indian Chem. Soc.,* **64**, 636 (1987).

68. V. Kumar, S. K. Sahni, S. Kher and R. N. Kapoor, *Transition Met. Chem.*, **5**, 85 (1980).

69. B. Sahoo, A. K. Rout, B. Sahoo, *Indian J. Chem.*, **25A**, 609 (1986); B. Sahoo and B. K. Mohapatra, *Indian J. Chem.*, **22A**, 494 (1983); **23A**, 8444 (1984); **24A**, 653 (1985).

70. O. P. Pandey, *Polyhedron*, **6**, 1021 (1987).

71. G. H. Havanur and V. B. Mahale, *Indian J. Chem.*, **26A**, 1063 (1987).

72. A. K. Panda, S. Rout and H. Mohanty, *Indian J. Chem.*, **33A**, 788 (1994).

73. S. Gopinathan, S. S. Tavale, V. G. Puranik and M. P. Degaonkar, *Bull. Chem. Soc., Japan*, **41**, 1797 (1994).

74. L. Sacconi, *Z Anorg. Allg. Chem.*, **275**, 249 (1954).

75. L. Sacconi, G. Lombardo and P. Paoletti, *J, Chem, Soc.*, 848 (1960).

76. L. Sacconi, G. Lombardo and R. Ciofalo, *J. Am. Chem. Soc.*, **82**, 4182 (1960).

77. R. Cefalu, F. Maggio, L. Pellerito and V. Romano, *Inorg. Nucl. Chem. Lett.*, **10**, 529 (1974).

78. A. Mangia, C. Pelizzi, G. Pellizzi, *Acta. Crystallogr.*, **30B**, 2146 (1974).

79. C. Pelizzi, G. Pelizzi, G. Predieri and S. Resola, *J. Chem. Soc.*, 1349, (1982).

80. M. Nardelli, C. Pelizzi, G. Pelizzi, *Transition Met. Chem.*, **2**, 35 (1997).

81. J. W. J. Martin, J. H. Johnston and N. F. Curtis, J. Chem. Soc., *Dalton Trans*, 68, (1978).

82. L. Sacconi and I. Bertini, *J. Am. Chem. Soc.*, **88**, 5180 (1966).

83. T. J. Giordano, G. J. Palenik, R. C. Palenik and D. A. Sullivan, *Inorg. Chem.*, **18**, 2445 (1979).

84. J. E. Thomas, R. C. Palenik and G. J. Palenik, *Inorg. Chim. Acta*, **37**, 2459 (1979).

85. G. Paolucci, G. Marangoni, G. Bandli and D. D. Clemente, J. Chem. Soc., *Dalton Trans*, 1304, (1980).

86. C. Pelizzi and G. Pelizzi, *J. Chem. Soc., Dalton Trans*, 1970, (1980).

87. M. P. Teotia, I. Singh and V. B. Rana, *Transition Met. Chem.*, **6**, 60 (1981).

88. V. B. Rana, I. Singh and M. P. Teotia, *Croat. Chim. Acta.*, **54(3)**, 267 (1981).

89. G. Paolucci, P. A. Vigato, G. Rossetto, V. Casellato, *Inorg. Chem. Acta.*, **65**, L71 (1982).

90. R. L. Dutta and Md. M. Hossain, *Indian J. Chem.*, **21A**, 746 (1982).

91. R. L. Dutta and A. K. Sarkar, Indian J. Chem., **19A**, 1188 (1980); *J. Indian Chem. Soc.*, **57**, 332 (1980).

92. R. L. Dutta and A. Bhattacharya, *J. Indian Chem. Soc.*, **54**, 239 (1977).

93. A. A. D. Mathis, M. R. Snow and J. A. Vanzo, *Chem. Commun.*, **7**, 264 (1976).

94. R. L. Dutta and A. K. Pal, *Indian J. Chem.*, **21A**, 1130 (1982).

95. V. B. Singh, D. P. Singh, P. Singh and M. P. Teotia, *Indian J. Chem.*, **21A**, 528 (1982).

96. C. Lorenzini, C. Pelizzi, G. Pelizzi, and G. Predieri, *J.Chem. Soc., Dalton Trans*, 1304 (1980).

97. R. L. Dutta, A. K. Pal, *Indian J. Chem.*, **22A**, 871 (1983).

98. V. B. Rana, V. K. Chauhan, D. P. Singh and M. P. Teotia, *Orient J. Chem.*, **1**, 24 (1985).

99. K. Day, A. K. S. Roy, K. K. Bhasin and R. D. Verma, *Indian J. Chem.*, **26A**, 230 (1987).

100. G. Marangoni, G. Chessa, B. Pitteri, V. Bertolasi, V. Ferrotti and G. Gilli, *J. Chem. Soc., Dalton Trans,* 1479, (1988).

101. S. Ianelli, G. Minardi, C. Pelizzi, G. Pelizzi, R. Reverbari, C. Solinas and P. Tarasconi, *J. Chem. Soc., Dalton Trans*, 2113 (1991); D. Belletti, M. Carcelli, c. Pelizzi and G. Pelizzi, *J. Crystallogr. Spectross. Res.*, **22**, 185 (1992).

102. A. Bonardi, S. Ianelli, C. Pelizzi and G. Pelizzi, *Inorg. Chim. Acta*, **187**, 1617 (1991).

103. M. T. H. Tarafder and A. R. Khan, *Polyhedron*, **10**, 973 (1991).

104. M. T. Toshev, V. G. Yusupov, M. M. Karimov and R. N. Shehelokov, *Koord. Khim.*, **18**, 202 (1992) .

105. A. Bacchi, L. P. Bhattaghia, M. Carcelli, C. Pelizzi, G. Pelizzi, C. Solinas and M. A. Zorundu, *J. Chem. Soc., Dalton Trans*, 773 (1993).

106. P. K. Singh, H. Jimerez, K. V. Katti, W. A. Vokert and C. Barnes, *Inorg. Chem.*, **33**, 736 (1994).

107. N. G. Lukyanenko, N. Y. Nazarova, V. I. Vetrogen, H. J. Holdt, J. Aurich and G. Kurntoch, *Inorg. Chim. Acta*, **155**, 35 (1989).

108. B. Ji, Q. Du, K. Ding, Y. Li and Z. Zhou, *Polyhedron*, **15**, 403 (1996).

109. L. Xiaozeng, W. Genglin, L. Zaizheng, Y. Shiping, J. Zonghui, W. Honggen and Y. Xinkan, *Polyhedron*, **14**, 511- 514 (1995).

110. A. Bonardi, S. Ianelli, C. Pelizzi and C. Solinas, *Inorg. Chim. Acta*, **232**, 211 (1995).

111. D. P. Singh, M. N. Ansari and V. B. Rana, *J. Indian Chem. Soc.*, **74**, 448 (1997).

112. G. Paolucci, S. Telluto, S. Sitran, D. Aju, F. Benetollo, A. Polo and G. Bombieri, *Inorg. Chim. Acta.*, **193**, 57- 75 (1992).

113. M. R. Maurya, D. C. Antony, S. Gopinathan and C. Gopinathan, *Indian J. Chem.*, **34A**, 967- 970 (1995).

114. R. A. Lal, S. Adhikari, A. Kumar and M. L. Pal, *J. Indian Chem. Soc.*, **75**, 345- 348 (1998).

115. R. A. Lal and S. Adhikari, *Indian J. Chem.*, **35A**, 607 - 610 (1996).

116. R. A. Lal, S. Adhikari and A. Pal, A. N. Siva and A. Kumar, *J. Chem. Res.* (S), 122 – 123 (1997); *J. Chem. Res.* (M), 0749 – 0772 (1997).

117. R. A. Lal, S. Adhikari and A. Kumar, *Indian J. Chem.*, **36A**, 1063 - 1067 (1997).

118. R. A. Lal and A. Kumar, *Indian J. Chem.*, **37A**, 921 - 926 (1998).

119. R. A. Lal, A. Kumar and M. L. Pal, *J. Indian Chem. Soc.*, **76**, 71- 75 (1999).

120. R. A. Lal, A. N. Siva, S. Adhikari and A. Pal, *Indian J. Chem.*, **34A**, 1000 - 1002 (1995).

121. R. A. Lal and A. Kumar, *Indian J. Chem.*, **34A**, 839 (1999).

122. Yongmin, H. guosheng and Ma Yongxiang; *Polyhedron*, **12**, 1043-1046 (1993).

123. A. Bolger, G. Ferguson, J. P. James, C. Long, P.McArdle and J. G. Vos; *J.Chem.Soc., Dalton Trans.*, 1577-1583 (1993).

124. A.Khan, S.S. Hasan, S.P. Varkey, M.A. Rather, N.Jahan and M. Shakir; *Trans. Met. Chem.*, **22**, 4 (1997).

125. L.Labib, L.A. Mohamed, M.F. Iskander, K.Grieser and W. Hasse; *Trans. Met. Chem.*, **25**, 700 (2000).

126. G. M. Larin, V.F. Shul"gin, A.N. Gusev and A.N. Chernega; *Russ. Chem. Bull.*, **53**, 775 (2004); 52, 1301 (2003).

127. K. Andelkovic, G. Jakovljevic, M. Zlatovic, Z. Tesic, D. Sladic, J. Howing and R. Tellgren; *J.Serb. Chem. Soc.* **69 (8-9)**, 651-660 (2004).

128. A. Para, S. Karolczyk-Kostuch and M. Fiedorowicz; *Carbohydrate Polymers*, **56**, 187-193 (2004).

129. L. Zhao, V. Niel, L.K. Thompson, Z. Xu, V. A. Milway, R.G. Harvey, D.O. Miller, G.Wilson, M. Leech, J. A. K. Howard and S. L. Heath; *Dalton Trans.*, 1446-1455 (2004).

130. E. Tirosh, R. Maman and I. Goldberg; *Acta Crystallogr., Sect. E,* E61, m541-m542 (2005).

131. M. Carcelli, S. Ianelli, P. Pelagatti, G. Pelizzi, D. Rogolino, C. Solinas and M. Tegoni; *Inorg. Chim. Acta*, **358**, 903-911 (2005).

132. M. H. Salem; *Synthetic and Reactivity in Inorganic, Metal-Organic and Nano-Metal Chemistry*, **35**, 369-377 (2005).

133. H. Elengoz, R. Shoshnik and I. Goldberg; Acta Crystallogr., Sect. E, E61, m538-m540 (2005).

134. V. P. Singh and P. Gupta, *J. Coord. Chem.* **59**, 1483 (2006).

135. C.T. Yang, J. D. Ranford, and J. J. Vittal, *Syn. React. Inorg. Met-Org. Nano-Met. Chem.* **35**, 71(2005).

136. R. Werner and W. Haase, *J. Coord. Chem.* **58**, 125 (2005).

137. V. P. Singh, P. Gupta, *J. Coord. Chem.* **59**, 1483 (2006).

138. V. P. Singh, P. Gupta and N. Lal, Russ. *J. Coord. Chem.* **34**, 270 (2008).

139. L. D. Popov, S. I. Levchenkov, I. N. Shcherbakov, Yu. P. Tupolova and V. A. Kogan, *Russ. J. Gen. Chem.* **78**, 90 (2008).

140. S. Naskar and D. Mishra, *Struct. Chem.* **18**, 217 (2007).

141. R. M. Issa, S. A. Amer, I. A. Mansour and A. I. Abel-Monsef, *J. Therm. Ana. Calo.* **90**, 261 (2007).

142. V. F. Shulgin, A. N. Gusov, A. N. Chernega and G. M. Larin, *Russ.Chem. Bull.* **56**, 236 (2007).

143. M. Salavati-Niasari and A. Sobhani, *J. Mol. Catal. A. Chem.* **285**, 58 (2008).

144. D. Y. Wu, G. Wu, W. Huang and C. Y. Duan, *Polyhedron*, **27**, 947 (2008).

145. R. A. Lal, D. Basumatary, J. Chakrabarty, S. Bhaumik and A. Kumar, *Indian J. Chem.* **45A**, 619 (2006).

146. R. A. Lal, D. Basumatary, A. K. De and A. Kumar, *Trans. Met. Chem.* **32**, 481 (2007).

147. R. A. Lal, D Basumatary, S. Adhikari and A. Kumar, *Spectrochimica Acta A*, **69**, 706 (2008).

148. M. K. Singh, N. K. Kar and R. A. Lal, *J. Coord. Chem.*, **61**, 3158 (2008).

CHAPTER II

Experimental

The present Chapter deals with the experimental details regarding the synthesis of the ligand, methods of analysis, physico-chemical techniques and the instruments employed for the characterization of the ligand as well the complexes. The procedures for the preparation of the complexes are given in respective chapters.

Materials

The metal salts, ammonium molybdate ($(NH_4)_6Mo_7O_{24}.4H_2O$), nickel acetate tetrahydrate ($Ni(OAc)_2.4H_2O$), copper acetate monohydrate ($Cu(OAc)_2.H_2O$), copper chloride hexahydrate $CuCl_2.6H_2O$, diethyl oxalate $(CO_2Et)_2$, hydrazine hydrate ($N_2H_4.H_2O$), salicylaldehyde ($C_6H_4(OH)(CHO)$), and isonicotinoyl hydrazine ($C_6H_4NCONHNH_2$) were E-Merck, Qualigens, Hi-Media or equivalent grade reagents and were used without further purification. Acetyl acetone, pyridine, 2-picoline, 3-picoline, 4-picoline, 2,2'-bipyridine, 1,10-phenanthroline, ethyl salicylate, and ethyl benzoate were Lanchaster or equivalent grade reagents. Bis(acetylacetonato)dioxomolybdenum (VI), $MoO_2(acac)_2$ was prepared by literature method **[1]**. The organic solvents viz., ethanol, methanol, diethyl ether, dimethyl sulphoxide (DMSO) and dimethyl formamide (DMF) were used after purification by standard literature methods.

Preparation of the Ligand

The ligand disalicylaldehyde oxaloyldihydrazone (H_4L) was prepared in two steps. In the first step, oxaloyldihydrazine (ODH) was prepared by reacting diethyl oxalate with hydrazine hydrate in 1: 2 molar ratios. In the second step, oxaloyldihydrazine thus obtained was allowed to react with salicylaldehyde in 1: 2.5 molar ratios in ethanol to get the ligand.

1. Preparation of Oxaloyldihydrazine $(CONHNH_2)_2$

For the preparation of oxaloyldihydrazine (ODH), dilute solution of diethyloxalate in ethanol was reacted with hydrazine hydrate in 1: 2 molar ratios and the mixture was stirred. The precipitate was filtered, washed with ethanol and recrystallized from hot water at ~110°C.

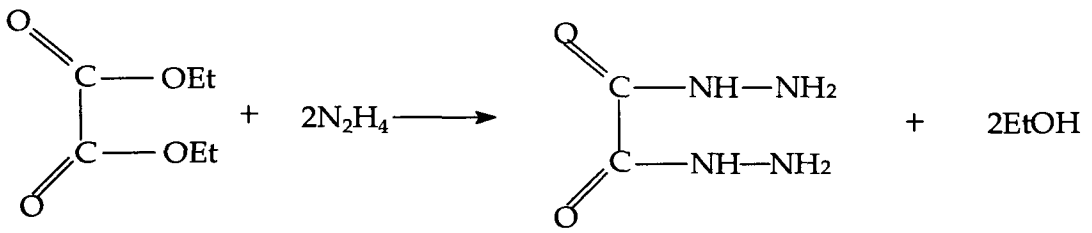

Diethyl oxalate Hydrazine hydrate Oxaloyldihydrazine Ethanol

2. Preparation of Disalicylaldehyde oxaloyldihydrazone

Disalicylaldehyde oxaloyldihydrazone (H_4slox) was prepared from the reaction of oxaloyldihydrazine and salicyaldehyde in 1: 2.5 molar ratios in aqueous ethanol by stirring the reaction mixture for ½ h. The light yellow precipitate thus obtained was purified by washing with hot aqueous ethanol and dried over anhydrous $CaCl_2$.

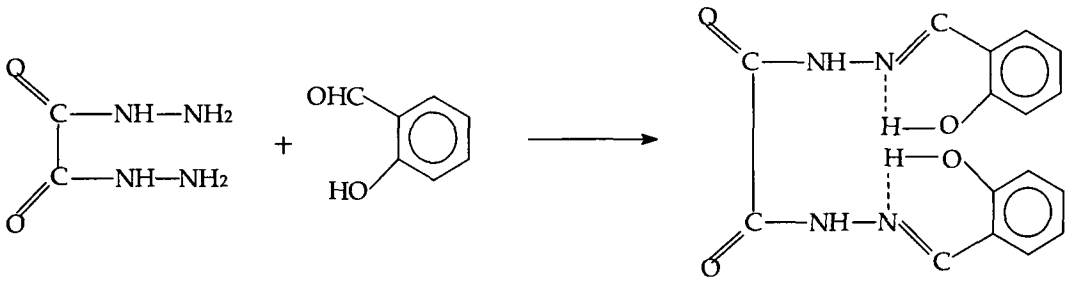

Oxaloyldihydrazine Salicylaldehyde Disalicylaldehyde oxaloyldihydrazone

The purity of the hydrazides and the hydrazone were established by C, H, N analyses and melting points as given in **Table 2.1**.

Table 2.1: Melting point and CHN analyses of the hydrazides and Disalicylaldehyde oxaloyldihydrazone.

Sl No	Hydrazide/Hydrazone	Formula	Melting Point (°C)	Analysis: Expt. (Calc)%		
				C	H	N
1.	Oxaloyldihydrazine	$C_2H_6O_2N_4$	232-234	20.28 (20.34)	5.09 (5.12)	47.38 (47.44)
2.	Disalicyaldehyde oxaloyldihydrazone	$C_{16}H_{14}O_4N_4$	328	59.12 (58.94)	4.31 (4.30)	17.34 (17.18)

Estimation of Metal(s)

The estimation of various metals was done by following standard procedures **[2]** as given below.

Estimation of Molybdenum

Molybdenum content of the complexes was determined by the following procedure. About 0.4g of the complex was accurately weighed in a 250 mL capacity conical flask. To this, 100 mL water and 1.0g of NaOH were added. The solution was boiled for 2 hours. This decomposed the complex which passed into solution. The solution was neutralized with 0.1M H_2SO_4 using methyl red indicator and then further acidified with few drops of 0.1M H_2SO_4. Subsequently 5 mL of 2M ammonium acetate solution was added to it and the solution was diluted to 100mL. The resulting solution was boiled and then oxine solution in dilute acetic acid was added to it until the supernatant liquid became perceptibly yellow. The solution was further boiled and stirred for 3 mins. This yielded precipitate which was filtered through a sintered glass crucible (G-4). The precipitate was washed several times with water until free from oxine and dried to constant weight at 130-140 °C, and is weighed as $MoO_2(C_9H_6ON)_2$.

Estimation of Nickel

The nickel content of the complexes was estimated gravimetrically as nickel dimethyl glyoximate. In a typical procedure, an accurately weighed amount of the nickel compound was dissolved in a hot (70-80 °C) dilute solution of hydrochloric acid (1:40). To this was added the requisite amount of 1% solution of dimethylglyoxime reagent in ethanol followed by the dropwise addition of aqueous ammonia, until the solution was faintly alkaline whereupon nickel dimethyl glyoximate was precipitated. The whole was heated on a boiling water bath ca 30min, and the precipitate was allowed to settle for ca 2hours, while cooling at the same time. Quantitative precipitation of nickel dimethylglyoximate was checked by adding a few drops of dimethyl glyoxime reagent solution. The precipitate was filtered on a weighed sintered Gooch crucible (G-4), washed several times with cold water until free from chloride. The crucible along with the precipitate was dried, to constant weight at 110-120 °C. The precipitate was weighed as nickel dimethylglyoximate $[Ni(C_4H_7O_2N_2)_2]$.

Estimation of Copper

The copper content of the complexes were estimated gravimetrically as copper (I) thiocyanate. About 0.4g of the copper complexes was heated in a cilica crucible at high temperature to remove organic part. This was than added in a beaker containing 50mL of water. To this 20-30 mL hydrochloric acid was added and then diluted to about 200 mL. The mixture was heated to boiling and than freshly prepared 10 percent ammonium thiocyanate solution was added slowly with constant stirring from a burrette until present in slight excess. The precipitate of copper (I) thiocyanate should be white; the mother liquor should be colourless and smell of sulphur dioxide. Allow to stand overnight. Filter through a weighed filtering crucible, and wash the precipitate 10 – 15 times with cold solution prepared by adding to every 100 mL of water 1 mL of a 10 percent solution of ammonium thiocyanate and 5-6 drops of saturated sulphurous acid solution, and finally several

times with 20 percent ethanol to remove ammonium thiocyanate. Dry the precipitate to constant weight. Weigh as CuSCN.

The chloride content of the complexes was determined as silver chloride gravimetrically following standard literature procedure **[2]**.

Physico-Chemical Measurement

CHN Analysis

Elemental Analysis (CHN) was performed by Perkin-elmer 2400 CHNS/O Analyser 11. Water, ethanol, pyridine, 3-picoline and 4-picoline molecules were determined by heating the samples in an electric oven at 110°C or 180°C or 220°C respectively, or in the temperature range 80-250°C and determing the weight loss. Water molecules were identified by passing the vapours through a test tube containing anhydrous copper sulfate which turn blue, while pyridine, 3-picoline and 4-picoline molecules were determined by passing the vapours through a test tube (a) a solution of sodium hydroxide and iodine; (b) a solution of $CHCl_3$ containing a droup of 5M NaOH solution and (c) a test tube containing cyanogens bromide solution which turn green-violet and blue respectively in case of 3-picoline and 4-picoline molecules respectively **[3]**.

Infra red Spectra:

Infra red spectra in the range 4000 – 400/500 cm^{-1} were obtained on either Perkin-Elmer model 983 spectrophotometer or Nicolet-Impact 410 FT-IR Spectrophotometer with samples investigated as KBr discs.

NMR Spectra:

The ^1H Nuclear Magnetic Resonance Spectra were recorded on a Mercury Plus 300

NMR Spectrometer and AMX 400 High Resolution Multinuclear FT-NMR Spectrometer in DMSO-d_6. Tetramethyl silane (TMS) was used as an internal standard.

Magnetic Susceptibility:

Room temperature magnetic susceptibility measurements were made on Sherwood Magnetic Susceptibility Balance MSB-Auto.

Electronic Absorption Spectra:

To record the electronic spectra a Perkin-Elmer Lambda-25 spectrophotometer was made use of.

Electron Paramagnetic Resonance:

For recording electron paramagnetic resonance spectra E-112 ESR Spectrophotometer was made use of.

Conductance:

All conductance measurements were made at 1 KHz using Wayne-Kerr B905 Automatic Precuision Bridge. This LCR meter has 0.01 ns resolution and measures conductance with an accuracy of 0.05%. A dip type conductivity cell having a platinized platinum electrode was used. The cell constant was determined using a standard KCl solution.

Cyclic voltammetry:

Cyclic voltammetric studies were done using CH Instrument Electrochemical Analyzer under nitrogen atmosphere.

References

1. G. J. J. Chen, J. W. McDonald, and W. E. Newton, *Inorg. Chem.*, **15**, 2612, (1976).
2. A. I. Vogel, "*A Text Book of Quantitative Inorganic Analysis Including Elementary Instrumentation Analysis*", (ELBS and Longman), 5th Ed., (1989).
3. R. A. Lal, A. N. Siva, S. Adhikari, M. K. Singh and U. S. Yadav, Synth. React. Inorg. *Met-Org. Chem.*, **26(2)**, 321-337, (1996); F. Feigl, V. Anger and R. E. Oesper, "*Spot Tests in Organic Analysis*", 7th Ed., Elseiver Publishing Company, Amsterdam, Netherland, p 173, 384, (1996) (Indian reprint, 2005).

CHAPTER III

Synthesis and Characterization of Monometallic Molybdenum (VI) Complexes derived from Polyfunctional Disalicylaldehyde oxaloyldihydrazone

Introduction

The present ligand has been derived from condensation of oxaloyldihydrazine with salicyldehyde. Hence, it is relevant to mention the types of complexes formed by acyl-, aroyl- and pyridoyl-dihydrazines and their dihydrazones and examine its bonding modes.

Dutta and Sengupta **[1]** and Sahni et al **[2]** reported that acyl and aroyl dihydrazines derived from aliphatic dicarboxylic acid, containing two $CONHNH_2$ groups coordinate as a neutral bidentate ligand through two imino nitrogen (>NH) although the potentially stronger donor functions like >C=O and $-NH_2$ are present. It has been suggested that strong intramolecular hydrogen bonding as shown below **(Fig. 3.1)**, probably makes them unavailable for coordination.

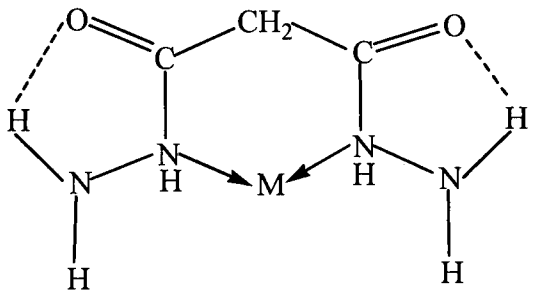

Fig. 3.1

When the terminal $-NH_2$ groups of the dihydrazides are condensed with the aldehydes and ketones, Schiff bases are obtained which possess >C=N- group

instead of $-NH_2$ group in the parent dihydrazides. Further, in such Schiff bases, above type of hydrogen bonding is likely to disappear.

Maki and coworker **[3]** synthesized dioxouranium (VI) complexes of some dicarboxylic acid dihydrazines in ethanol medium in presence or absence of NaOAc. The dihydrazides were found to co-ordinate in a tetradentate fashion in the enol form except adipic acid hydrazide which co-ordinate in the keto form. The existence of dihydroxo bridges for the complexes isolated in the presence of NaOAc or basic medium (N_2H_4) was also established.

Aggarwal and coworkers **[4]** synthesized neutral and cationic complexes from reaction of first row transition metal ions with the dihydrazones derived from condensation of acyldihydrazides and simple aldehydes and ketones. They have established that the dihydrazones behave either as a dibasic tetradentate ligand or neutral tetradentate ligand coordinating through carbonyl oxygen and azomethine nitrogen atoms.

On the other hand, if the dihydrazones are derived from condensation of acyl-, aroyl- and pyridoyl-dihydrazines with o-hydroxy aromatic aldehydes and ketones, they possess –OH groups in addition to >C=O and >C=N- groups **[5]**. In such dihydrazones, the possibility of existence of newer hydrogen bonding as shown in **Fig. 3.2** cannot be ruled out.

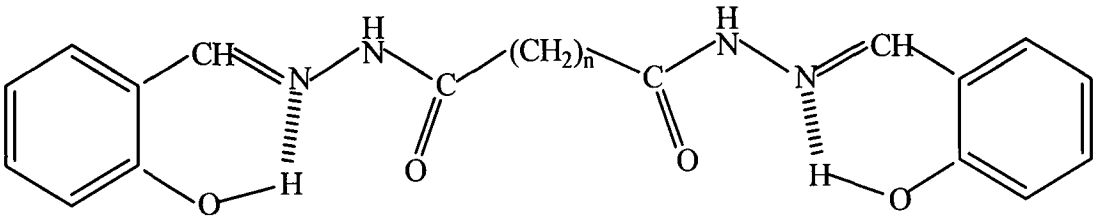

Fig. 3.2

Such dihydrazones can exist in keto form, keto-enol form or enol form and offer several alternate bonding modes and can act as potential multidentate coordinating or

chelating ligands resulting in the formation of complexes having different stoichiometries under different experimental conditions. The molecular model of the dihydrazones indicate their flexible nature in space due to which they are able to offer planar as well as the tetrahedral set of donor atoms depending upon the preferred stereochemical disposition of the metal valences, nature of acyl- and aroyl groups and the bonds formed in the coordination process. The various donor sites in the ligand can bind either to the same metal atom or to the different metal atoms leading to a monomeric or polymeric structure of the complexes **[5]**. However, polymerization may also arise due to oxo-bridged structure **[5, 6]**.

The ligand disalicylaldehyde oxaloyldihydrazone may exist in keto form **(Fig. 3.3)**, keto-enol form **(Fig. 3.4)** and enol form **(Fig. 3.5)** respectively.

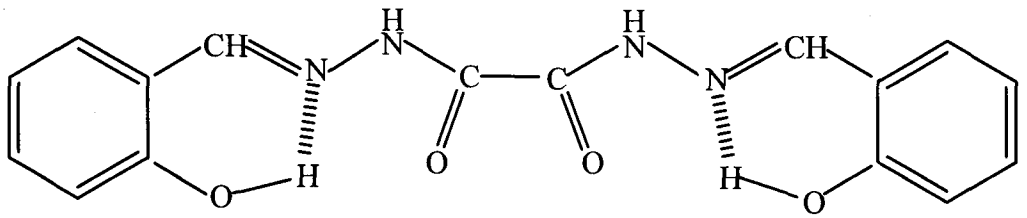

Fig. 3.3

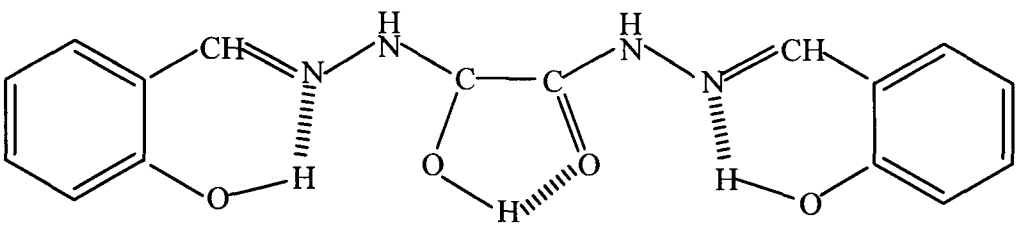

Fig. 3.4

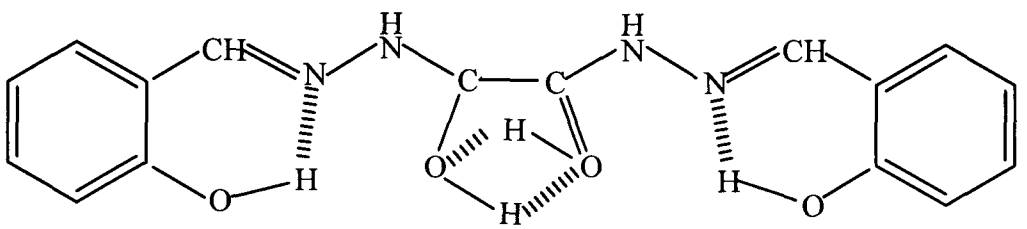

Fig. 3.5

In keto form it may function as:

1. A neutral bidentate ligand coordinates either through the two carbonyl oxygen atoms **(Fig. 3.6)** or the two secondary amine nitrogen atoms **(Fig. 3.7)**, the –OH group remaining hydrogen bonded in the complexes.

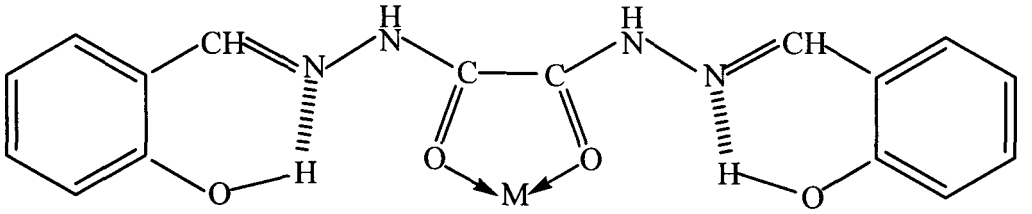

Fig. 3.6

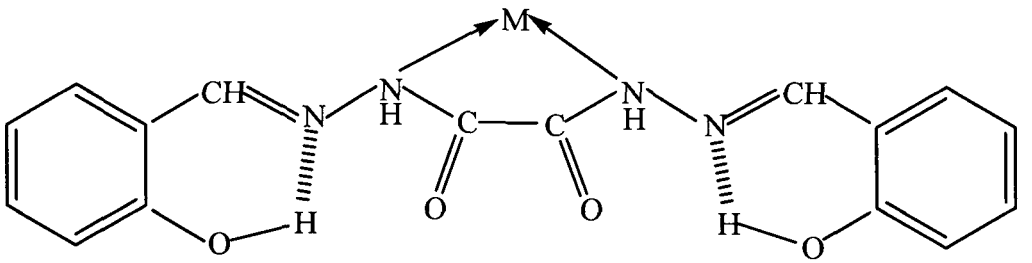

Fig. 3.7

2. A monobasic tridentate ligand coordinating through one hydroxyl oxygen, one azine group nitrogen and one carbonyl group oxygen **(Fig. 3.8)** while the other half portion of the molecule remains unbonded.

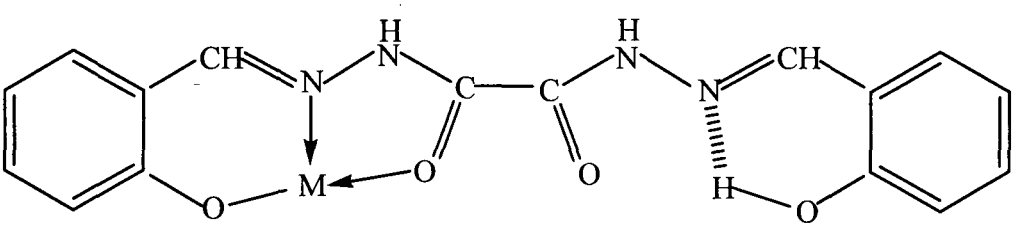

Fig. 3.8

3. A dibasic tetradentate ligand coordinating through two hydroxyl oxygen atoms and the two azine group nitrogen atoms **(Fig. 3.9)**.

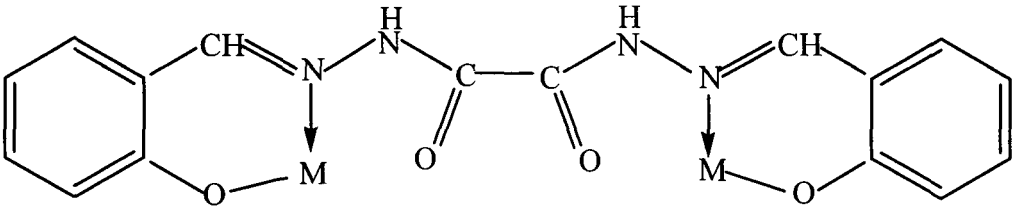

Fig. 3.9

4. A dibasic hexadentate ligand bonding to the two metal ion through the two hydroxyl oxygen, the two azine nitrogen and the two carbonyl oxygen atoms **(Fig. 3.10)**.

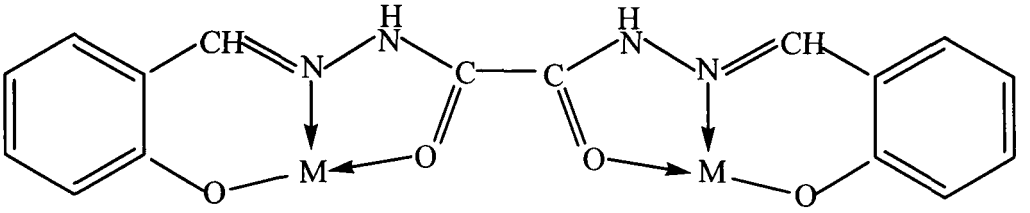

Fig. 3.10

In the keto-enol forms it can act as a dibasic tridentate **(Fig. 3.11)**. In the enol form, it can act as a tetrabasic hexadentate ligand **(Fig. 3.12)**. It can also act as a binucleating or polynucleating ligands.

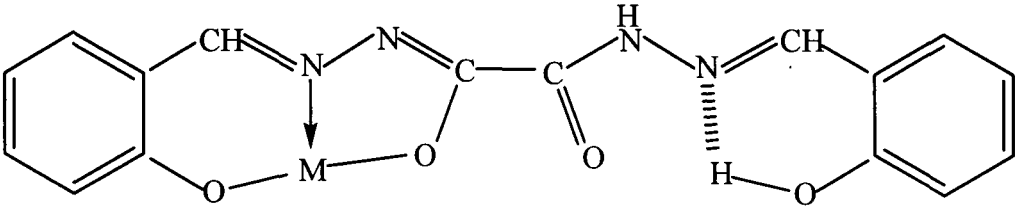

Fig. 3.11

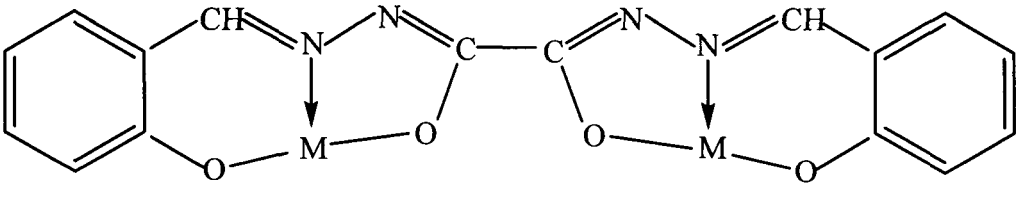

Fig. 3.12

The dihydrazone can exist in the metal complexes either in the staggered-configuration **(Fig. 3.13)** or the cis-configuration. In the cis-configuration, the dihydrazone can adopt either an anti-cis-configuration **(Fig. 3.14)** or syn-cis-configuration **(Fig. 3.15)**.

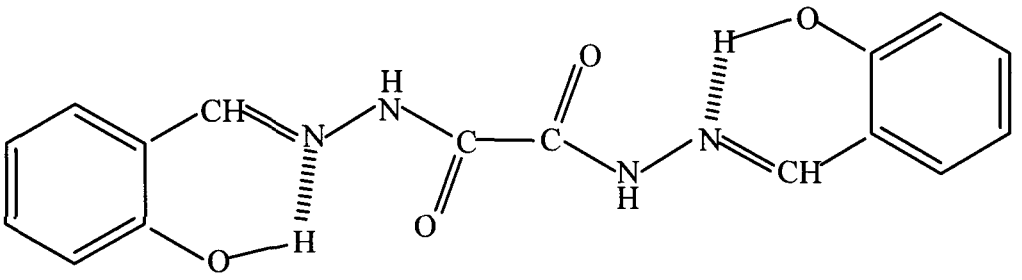

Fig. 3.13

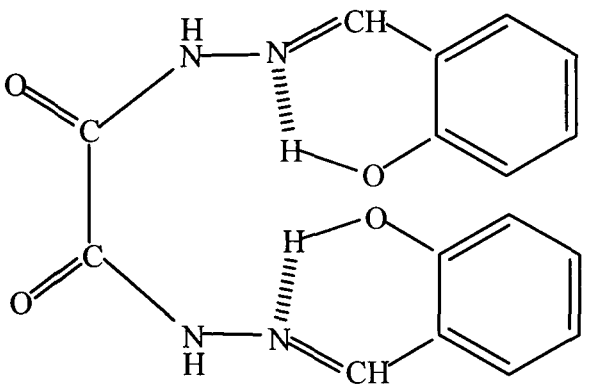

Fig. 3.14

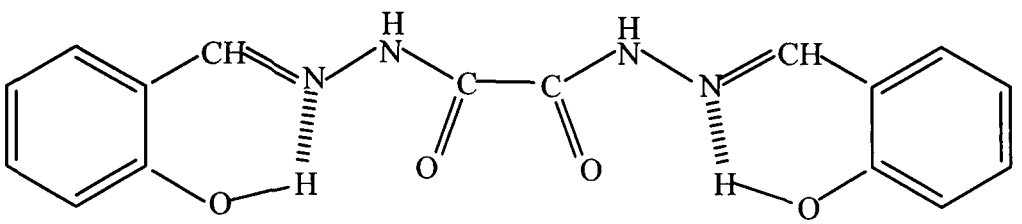

Fig. 3.15

All these possibilities can actually be realized in practice if the nature of the metal salt, mole ratio of the metal ion and the ligand, the nature of the counter cation and anion, reaction medium, pH and temperature are varied.

A survey of literature has disclosed that few complexes of the first row transition metal ions, with the dihydrazones derived from condensation of salicylaldehyde and related o-hydroxy aromatic aldehydes and ketones with malonyldihydrazine and other acyldihydrazines, aroyldihydrazines and pyridoyldihydrazines have been reported, yet it has failed to locate any study on the metal complexes of the title ligand. In view of significant role played by molybdenum in biological systems **[7-12]** and absence of work on metal complexes of disalicylaldehyde oxaloyldihydrazone, the mononuclear molybdenum (VI) complexes from the title ligand have been synthesized by various methods in alcoholic media and are described in the present chapter. The composition of the complexes has been judged mainly from the elemental analyses. The structure of the molybdenum (VI) complexes has been discussed with the help of molar conductance, magnetic moment, electronic spectral data, infrared and ^{1}H NMR data.

Experimental

Preparation of $[MoO_2(H_2slox)(H_2O)]$ (3.1)

To a suspension of H_4slox (1.00 g, 3.07 mmol) in ethanol (60 mL) was added a solution of $MoO_2(acac)_2$ (1.10 g, 3.37 mmol) in 30 mL ethanol containing 1.5 mL H_2O in hot condition by constant stirring for about 30 minutes. The reaction mixture was further stirred for another 2 h with the help of magnetic stirrer. The orange coloured compound thus precipitated was suctioned filtered, washed five to six times with 10 mL ethanol followed by ether and then finally dried over anhydrous $CaCl_2$. Yield: 78.2%

Preparation of $[MoO_2(H_2slox)(A)]$ {*where A = pyridine (py)* **(3.2)**, *2-picoline (2-pic)* **(3.3)**, *3-picoline (3-pic)* **(3.4)** *and 4-picoline (4-pic)* **(3.5)**}.

The complex $[MoO_2(H_2solx)(H_2O)]$ **(3.1)** (1.00 g, 2.13 mmol) was suspended in ethanol (60 mL) in hot condition by constant stirring to make the suspension

homogeneous. To this suspension 1.62 mL of pyridine was added drop by drop over a period of 30 minutes with constant stirring. The resulting mixture was then put to reflux for about 1 h which precipitated a yellow coloured complex. This yellow coloured complex was suctioned filtered in hot condition and purified by washing several times with 10 mL hot ethanol followed by ether and finally dried over anhydrous $CaCl_2$. Yield: 75.4%

The complexes $[MoO_2(H_2slox)(A)]$ {*where A = 2-picoline (2-pic)* **(3.3)**, *3-picoline (3-pic)* **(3.4)** *and 4-picoline (4-pic)* **(3.5)**} were prepared essentially by the above method using 1.9 mL of 2-picoline, 3-picoline and 4-picoline, respectively instead of pyridine. Yield: 69.8-72.8%.

Preparation of $[MoO_2(H_2slox)(NN)]$ {*where NN = 1,10-phenanthroline (phen)* **(3.6)** *and 2,2'-bipyridine (bpy)* **(3.7)**}

The complex $[MoO_2(H_2solx)(H_2O)]$ **(3.1)** (1.00 g, 2.13 mmol) was suspended in ethanol (60 mL) by constant stirring in hot condition to make the suspension homogenous. To this homogeneous suspension, a solution of 1,10-phenanthroline (1.22 g, 6.15 mmol) in 40 mL ethanol, was added drop by drop over a period of about 30 minutes accompanied by vigorous stirring. The resulting mixture was subjected to refluxation for about 1 h when a white coloured complex was isolated. This white coloured complex was then suctioned filtered in hot condition and purified by washing several times with 10 mL hot ethanol followed by ether and finally dried over anhydrous $CaCl_2$. Yield 67.2%

The complex $[MoO_2(H_2solx)(bpy)]$ **(3.7)** was also prepared essentially by following the above procedure using 1.20 g (7.68 mmol) of 2,2'-bipyridine instead of 1.22 g (6.15 mmol) of 1,10-phenanthroline. Yield: 68.4%.

Results and discussion

Disalicylaldehyde oxaloyldihydrazone is a polyfunctional ligand which can coordinate to the metal centre as a monobasic bidentate, monobasic tridentate or dibasic tridentate, dibasic tetradentate and as dibasic hexadentate ligand. Further, this ligand may undergo enolization affording newer bonding possibilities leading to the formation of the binuclear or polynuclear complexes.

The complexes described in this chapter together with color, decomposition point, analytical data, molar conductance and electronic spectral data are set out in the **Table 3.1**.The complexes were isolated by reacting $MoO_2(acac)_2$ with the title ligand in 1.1:1 molar ratio in ethanolic medium either as such or in the presence of pyridine bases. As only one method of preparation for the complexes have been used in the present chapter, only one type of complexes have been obtained. The composition of the complexes has been deduced based on the data obtained from analytical and thermal studies. The general compositions of the complexes are:

$[MoO_2(H_2slox)(A)]$ {*where A = H_2O* **(3.1)**, *pyridine (py)* **(3.2)**, *2-picoline (2-pic)* **(3.3)**, *3-picoline (3-pic)* **(3.4)** *and 4-picoline (4-pic)* **(3.5)**}
$[(MoO_2)_2(H_2slox)_2(NN)]$ {*where NN = 1,10-phenanthroline (phen)* **(3.6)** *and 2,2'-bipyridine (bpy)* **(3.7)**}.

The complexes are white, orange, dark red or yellowish in colour and are air stable. All of the complexes decompose without melting above 300°C.

Thermal analyses

Detailed decomposition studies **[13]** of the complexes were carried out in the temperature range 70 – 250°C and the vapours evolved were identified by passing through a test tube containing anhydrous copper sulfate, a test tube containing a chloroform solution with a drop of 5M sodium hydroxide, a test tube containing a

solution of iodine and sodium hydroxide and a test tube containing cyanogen bromide solution. None of the complexes showed loss of weight in the temperature range 70-150°C ruling out the possibility of presence of water molecules in their lattice structure. The vapours evolved at ~180°C in the complex **(3.1)** turned anhydrous copper sulfate blue confirming that they originate from coordinated water molecule. Complex **(3.1)** shows weight loss at ~180°C corresponding to one water molecule. The vapours evolved in the complex **(3.2)** turned $CHCl_3$ and NaOH solution red at ~ 225°C confirming that they originate from coordinated pyridine molecule **[14]**. The vapours evolved in the complex **(3.4)** at ~ 225°C turned the colour of cyanogen bromide solution to green-violet on treatment with phloroglucinol solution suggesting the presence of 3-picoline molecule in the first coordination sphere around the metal centre **[13, 14]**. Similarly the vapours evolved in the complex **(3.5)** turned the colour of cyanogen bromide solution to blue on treatment with phloroglucinol solution. This suggested the presence of coordinated 4-picoline molecules in the complex **[13, 14]**. The complexes **(3.2)** to **(3.5)** show weight loss corresponding to one pyridine/picoline molecule. However, none of the complexes gave a yellow precipitate with a solution of iodine and sodium hydroxide in any temperature ranges, ruling out the possibility of presence of ethanol molecules in them.

Molar conductance

The molar conductance value for the complexes **(3.1)** to **(3.7)** lies in the range 1.54 – 4.20 $ohm^{-1}cm^2mol^{-1}$.

Molar conductance value for the complexes of different electrolyte types depends on the nature of the solvent. Some of the molar conductance ranges reported for 10^{-3} M dilution of the complexes of different electrolyte types in aqueous and non-aqueous solvents is given below in the **Table 3.2**.

Table 3.2: Molar Conductance ranges for 10^{-3} M solutions of the complexes of different electrolyte types in aqueous and non-aqueous solvents

Solvent	Electrolyte type ($ohm^{-1}cm^2mol^{-1}$)			
	1:1	2:1	3:1	4:1
Water	95	225-270	380-452	Above 520
Nitromethane	75-95	150-180	220-260	Above 320
Nitrobenzene	20-30	50-60	70-82	90-100
Acetone	100-140	160-200	270-?	360-?
Acetonitrile	120-160	220-300	340-420	500-?
DMF	65-90	130-170	200-240	300-?
Methanol	80-115	160-220	290-350	450-?
Ethanol	35-45	70-90	120-?	160-?
DMSO	35-70	-	109-?	-

A comparison of molar conductance data for the complexes with the molar conductance data given in the table suggests that these complexes are non-electrolyte in DMSO **[15]**.

Magnetic moment

The room temperature magnetic moment of the complexes was taken in order to decide upon the magnetic behavior. The complexes **(3.1)** to **(3.7)** are diamagnetic in nature. This suggests that the reduction of the molybdenum centre does not occur under the influence of the ligand and confirms the presence of molybdenum in +6 oxidation state with d^0 electronic configuration in these complexes **[16]**.

Electronic spectra

All of the complexes have been studied by electronic spectroscopy. The positions of the characteristic electronic absorption bands for the dihydrazone ligand (H_4slox)

and the complexes have been set out in **Table 3.1**. The electronic spectra of the dihydrazone ligand and the complexes **(3.1)**, **(3.2)**, **(3.3)** and **(3.6)** have been shown in **Figs. 3.16 – 3.20**. The electronic spectrum of the ligand shows bands at 293 nm, 303 nm and 340 nm which arise due to $\pi \rightarrow \pi^*$ and $n \rightarrow \pi^*$ transition in the free dihydrazone. The electronic spectra of the complexes also show three bands in the region 290 – 342 nm. While the band in the region 290 – 304 nm is assigned to ligand band arising from $\pi \rightarrow \pi^*$ transition, the band in the region 338 - 342 nm is assigned to ligand band arising from $n \rightarrow \pi^*$ transition. All the complexes show another additional broad band in the region 413 – 431 nm (sh). The molar extinction coefficient for this band lying in the region 413 – 431 nm is high indicating that the band in this region arises due to ligand-to-metal charge transfer (LMCT) transition, which may, most probably, be associated with the electronic excitation from the HOMO of phenolate oxygen to the LUMO of molybdenum **[17]**. Since all the complexes mentioned in this chapter are diamagnetic, hence, no bands are expected in the visible region that could be assigned to d-d transition **[18, 19]**. This results are consistent with the results reported **[20, 21]** for dioxomolybdenum (VI) complexes.

Proton nuclear magnetic resonance spectra

The ^1H NMR spectrum of H_4slox has been recorded in DMSO-d_6 as it is insoluble in common organic solvents such as CCl_4 and $CHCl_3$. The assignment of signal has been made to various types of protons in the light of literature records **[22]**. The two proton signal observed at δ12.64 and δ11.00 ppm downfield of TMS has been assigned to -OH and >NH protons, respectively. A two proton singlet appearing at δ8.81 ppm have been assigned to -CH=N- proton. The multiplet appearing in the region δ7.57-6.84 ppm has been assigned to phenyl protons. The resonances in the region δ7.57-6.84 are split into three different signals. The two proton signals appearing at δ7.55 ppm have been assigned to 4a and 4b protons. Due to high electron withdrawing nature of the azomethine group, the 4a and 4b protons are highly downfield shifted as compared to the remaining aromatic protons. The 7a and 7b protons are also downfield shifted due to high electronegativity of oxygen atom

attached to the ring carbon atom adjacent to 7a and 7b proton and appear at δ7.33 ppm but the shift is comparatively less than those of 4a and 4b protons. The four proton signal at δ6.50 ppm is assigned to the remaining four aromatic protons (5a, 5b, 6a, 6b). The fact that the resonances due to δ (-OH), δ (>NH) and δ (-CH=N-) protons appear as a singlet suggests that the ligand adopts staggered configuration, as shown in **Fig. 3.21**.

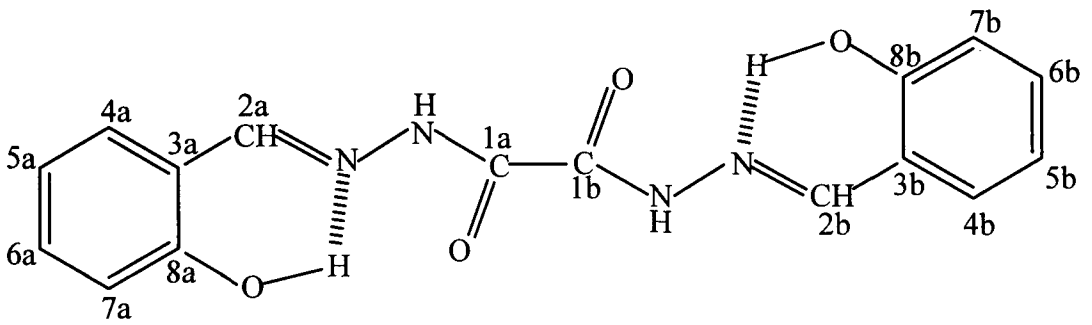

Fig. 3.21: Staggered configuration of H_4slox and its numbering scheme.

The ^{1}HNMR spectra of the complexes **(3.1)** to **(3.7)** show a single resonance in the region δ12.60-12.67 ppm and δ10.98-11.31 ppm, respectively **(Table 3.3)**. The singlets observed in these regions are assigned to arise due to -OH and >NH protons, respectively. The signal due to -OH protons remains almost unshifted in position or shifts upfield in the complexes suggesting the uncoordinated nature of the -OH group to the metal centre. On comparing the integration of various proton signals in the complexes, we find that the signals due to -OH and >NH protons each corresponds to one proton only in the complexes **(3.1)** to **(3.7)** as compared to two proton signals in the free ligand molecule. This suggests that the ligand molecule coordinates to the metal centre through one -OH group only via deprotonation. The fact that δ (>NH) also corresponds to one proton only, suggests that one >NH group is destroyed during complex formation indicating enolization of the ligand and its bonding to the metal centre through enolate oxygen atom. The singlet due to the >NH proton remains either unshifted or is downfield shifted in the complexes.

The two proton singlet due to azomethine group in the ligand is split either into two resonances or two doublets in the complexes which appear in the region δ8.85-9.06

and δ8.63-8.80 ppm respectively. The splitting of the signal due to azomethine proton into two resonances in the complexes as compared to that of a single resonance in the preformed ligand indicates the effect of coordination to the metal centre. Out of the two resonances, one resonance is downfield shifted by ~0.04 – 0.18 ppm while the other resonance is upfield shifted by ~0.01 – 0.18 ppm. The downfield shift of the signal due to the azomethine proton is attributed to the drainage of electron density from the nitrogen atom of the azomethine group to the metal centre and suggests the coordination of one azomethine group to the metal centre **[23]** whereas upfield shift suggests the uncoordinated state of the azomethine group. The upfield shift of the second δ (-CH=N-) signal indicates that although the azomethine group involved in H-bonding in the complexes yet it is weakend in the complexes. Thus, it may be concluded that out of the two hydrazone groups present in the ligand, only one group is involved in bonding with the metal ion through deprotonated phenolate oxygen atom, through enolate oxygen atom and through azomethine nitrogen atom.

The multiplet due to the phenyl protons appears in the region δ6.81-7.74 ppm in the complexes **(3.1)** to **(3.7)**. The ^{1}H NMR spectra of the complexes **(3.2)** to **(3.5)** show an easily identifiable resonance **[24-26]** in the region δ8.35-8.54 ppm. These signals are attributed to arise due to ortho protons of pyridyl ring of pyridine, 2-picoline, 3-picoline and 4-picoline molecules. Whereas in complexes **(3.6)** and **(3.7)** a resonance at δ7.89 and δ8.80 ppm has been identified to arise due o-proton of 1,10-phenanthroline and o-proton of 2,2'-bipyridine molecules respectively, The signal due to ortho proton of pyridyl ring of pyridine/picoline molecules are upfield shifted in the complexes as compared to their positions in free pyridine and free picoline molecules **[27]**. Thus, the upfield shift of ortho proton signal indicates the possible coordination of pyridine, 2-picoline, 3-picoline and 4-picoline molecules to the molybdenum centre through the nitrogen atoms of pyridyl ring of pyridine/picoline molecules. As a result of coordination of the pyridyl nitrogen, the electron density on pyridyl nitrogen decreases which in turn decreases its electronegativity and consequently, the electron density on various bonds of pyridyl ring i.e. C-N, C-C and

C-H drifts away from nitrogen atom. This increases the electron density on various carbon atoms and protons. As a result, the electron density on various types of pyridyl protons is increased which results in the upfield shift of the signals due to these protons in the ^{1}H NMR spectra of the complexes **(3.2)** to **(3.5)**.

The signals due to meta and para protons of pyridine and picoline molecules appear merged with the signals due to phenyl protons. Hence, it is not clearly visible in the ^{1}HNMR spectra of the complexes **(3.2)** to **(3.5)**. Similarly in the complexes **(3.6)** and **(3.7)** the resonance due to the remaining protons of 1.10-phenanthroline and 2,2'-bipyridine also appears merged with the signals due to phenyl protons and azomethine protons. A new signal appearing at δ2.50, δ2.27 and δ2.35 ppm in complexes **(3.3)**, **(3.4)** and **(3.5)** has been assigned to methyl protons of 2-picoline, 3-picoline and 4-picoline molecules respectively. In free picoline molecules, the signal due to methyl protons appears in the region δ2.32-2.55 ppm **[25, 26]**.

Further, these complexes do not show any signal in the downfield region which can be assigned to pyridinium or 2-picolinium or 3-picolinium and 4-picolinium ions. This excludes the possibility of the presence of pyridine, 2-picoline, 3-picoline and 4-picoline as pyridinium, 2-picolinium, 3-picolinium and 4-picolinium ions in the metal complexes. As a representative example the ^{1}H NMR spectra of the dihydrazone ligand and the complexes **(3.1)** to **(3.3)** and **(3.6)** have been shown in **Figs. 3.22 – 3.26**.

Infrared spectra

(OH + NH) stretching vibrations

The IR spectral data of the ligand and its complexes have been set out in **Table 3.4**. The IR spectra of the dihydrazone ligand (H_4slox) and the complexes **(3.1)**, **(3.2)**, **(3.3)** and **(3.6)** have been shown in **Figs. 3.27 – 3.31**. The present ligand shows strong broad band in the region 3300-3200 cm^{-1} which is associated with individual

peaks centered at 3278 and 3204 cm^{-1}. These bands are assigned to arise from stretching vibrations of phenolic -OH and secondary >NH groups. The position of these bands is similar to that observed in salicylaldehyde and o-hydroxyacetophenone **[28, 29]**. This suggests the presence of strong intramolecular hydrogen bonding between secondary amine hydrogen, phenolic -OH hydrogen, the >C=O and >C=N- groups. The IR spectra of the complexes **(3.1)** to **(3.7)** show strong to medium intensity bands in the region 3450-3200 cm^{-1}.The IR spectra of the complexes are complicated in the region 3530-3000 cm^{-1} because of appearance of bands due to stretching vibrations of secondary >NH group, vibrations of lattice and coordinated water molecules and phenolic -OH group. Further, complicacy is added as the spectra of the complexes are recorded in KBr pellets which are moisture sensitive. Hence, the bands in this region might have contributions from bands arising due to water molecules absorbed by KBr pellets as well. In order to decide upon whether the bands in this region arise due to water molecules or phenolic -OH groups, the compounds were subjected to thermal analysis and the resulting products were characterized by IR spectroscopy. Thermal analysis showed the presence of coordinated water molecule in the complex **(3.1)** only while in case of other complexes, the thermoanalytical data ruled out the presence of either coordinated or lattice water molecules. The complex **(3.1)** shows strong intensity bands at 3420 cm^{-1} which is assigned to the stretching vibration of -OH group of coordinated water molecules. On the other hand, a medium intensity band appearing in the region 3300 - 3250 cm^{-1} in the complexes is assigned to phenolic -OH group and another strong band in the region 3250-3000 cm^{-1} is assigned to the stretching vibration of secondary >NH group.

Amide frequency

Amide bands arise due to mixed vibrations and approximate contributions of various modes in amide frequencies **[29]** are as follows:

1667(s) cm^{-1}	AmideI	80%	C=O stretching

1534(s) cm^{-1}	AmideII	60%	N-H stretching
		40%	C-N stretching
1359(s) cm^{-1}	AmideIII	40%	C-N stretching
		30%	N-H in plane bonding
		20%	CH-C stretching
756(s) cm^{-1}	Amide V		N-H out of plane bending
634(s) cm^{-1}	Amide IV	48%	O=C-N stretching
531(s) cm^{-1}	Amide VI		C=O out of plane bending

From the interpretation of various amide bands as given above, it is difficult to assign a particular amide band to a pure stretching or bending vibrations .However based on the interpretation of Mashima **[30]** and Nagano **[31]**, the effect of coordination on amide bands of disalicylaldehyde oxaloyldihydrazone are discussed below.

The ν (>C=O) (amide I) band appearing at 1667 cm^{-1} in the ligand, on an average remains unshifted in position as in the complex **(3.1)** to **(3.7)**. Almost unaltered position of the amide I band indicates the non coordination of dihydrazone to the metal centre through carbonyl oxygen atoms. A single strong band at 1534 cm^{-1} in the present ligand has been assigned to the stretching vibration of amide II+ ν (C-O) group **[32]**. This band is split into two bands in the complexes **(3.1)** to **(3.7)** and one component appears in the region 1534-1554 cm^{-1} while the other component appears in the region 1518-1533 cm^{-1}, respectively. The band in higher frequency region 1534-1554 cm^{-1} has been assigned to the stretching vibration of the amide II + ν (C-O) group whereas the band in the lower frequency region 1518-1533 cm^{-1} is a new band previously not present in the ligand. This band is characteristic of enolization of ligand in the complexes and is assigned to ν (NCO) vibration produced as a result of enolization of the ligand **[33]**. The presence of amide II + ν (C-O) group and ν (NCO) group indicates that only half part of the ligand molecule undergoes enolization on complexation.

>C=N stretching vibrations

The present ligand shows two very strong bands at 1627 and 1603 cm^{-1}. The bands observed in the 1637-1580 cm^{-1} region occurring in hydrazide and dihydrazide Schiff bases and their transition and non-transition metal complexes have been used by us **[34, 35]** and other workers **[36-42]** in the field for the interpretation of the IR spectra of the complexes of the hydrazide Schiff bases. The bands observed at 1627 and 1603 cm^{-1} in the ligand have been assigned to stretching vibration of >C=N- group. The average position of the ν (>C=N-) bands shifts to lower frequency by 3-10 cm^{-1} in all complexes indicating coordination through azomethine nitrogen atom **[43]**.

>C-O stretching vibrations

In the dihydrazone a strong intensity band appears at 1262 cm^{-1}. This band is similar in nature as observed in other ligands containing phenol group. Hence, this band is assigned to ν (C-O) vibration **[44]**. This band is shifted in position to higher frequency in the metal complexes **(3.1)** to **(3.5)** by 7-9 cm^{-1} except in the complexes **(3.6)** and **(3.7)** in which it remains almost unshifted in position. Such a feature associated with ν (C-O) band indicates bonding through oxygen atom of C-O group without involvement of phenoxide oxygen atom in bridging **[45]**.

Aromatic vibrations

The aromatic ring shows a weak absorption at about 1600 cm^{-1}. In the present ligand, it appears at 1571 cm^{-1} as a medium intensity band. In the metal complexes, this band does not show its independent existence, most probably because of its overlapping with ν (>C=N-) band or amide II band or ν (C-O) phenolic/enolic band. The bands at 1486 and 1458 cm^{-1} in the free ligand are characteristic of substitution at α-position of benzene ring **[46]**. The bands around 1220(s), 1161(m) and 1122(w) cm^{-1} are due to C-H in plane deformation vibration which either remains unshifted or slightly shifted in complexes. The 828(s) and 756(s) cm^{-1} bands arise due to the C-H

out-of-plane deformation vibration plus γ (OH) of the phenolic portion of the ligand. Due to the complex nature of the spectra in the 1250-1100 cm^{-1} region, the γ (OH) in the ligand and complexes are difficult to identify.

N-N and C-N stretching vibrations

The ν (N-N) stretching frequency in the hydrazine derivatives has been identified and its shift has been useful in understanding the involvement of nitrogen atoms in coordination. From the ν (N-N) stretching frequency, it is possible to decide whether only one nitrogen atom or both the nitrogen atoms of N-N groups are involved in coordination. The ν (N-N) stretching frequency has been shown to increase from 885 cm^{-1} in N_2H_4 **[47]** to 973 cm^{-1} in $N_2H_5^+$ **[48]** and 1024 cm^{-1} in $N_2H_6^{2+}$ **[49]** due to protonation which is akin to involvement of lone pairs of electrons on nitrogen atoms in coordination to metal ions.

Onyszchuk **[50]** and Sacconi **[51]** have observed υ (N-N) near the above quoted frequencies in the complexes containing unidentate and bidentate hydrazines, respectively. But the above range in no way can be taken as specific for coordination of one or two nitrogen atoms in substituted hydrazine complexes. Further, it appears in the 1014-986 cm^{-1} region in the metal complexes of mono substituted hydrazine of the type NH_2-NH-y **[52]**. But in the metal complexes of N, N-diacylhydrazines υ (N-N) has been observed in 1040-970 cm^{-1} region.

The region below 1299 cm^{-1} is not well defined for hydrazine derivatives and contains bands due to N-N, C-N, C-H bending vibrations **[53]**. Due to several vibrational modes, the region is quite complicated. Eliminating the bands due to C-H in plane deformation in the 1040-900 cm^{-1} region, a weak band at 1054 and 1035 cm^{-1} in the present ligand has been assigned to υ (N-N) vibrations **[54]**. This band either remains unshifted or shifts to higher frequencies by 8-21 cm^{-1} in all the complexes, indicating involvement of only one nitrogen atom of N-N group in coordination **[55]**. The υ (C-N) vibration at 1054 cm^{-1} in the ligand appearing as a weak band is also

shifted to higher frequency in the complexes. Because of complex character of spectra in this region, we have refrained from drawing any conclusion from the position of this band regarding involvement of >C=O group in coordination or otherwise.

MoO_2^{2+} bands

The region 850 – 1000 cm^{-1} in the IR spectra of the complexes is of crucial importance from structural point of view because it contains bands due to υ (M=O) stretching vibrations. The complexes **(3.1)** to **(3.7)** show two to three strong bands in the region 883 - 939 cm^{-1}. The essential features of these bands suggest the presence of cis- MoO_2^{2+} group in the complexes. The appearance of two or more bands in the region 883 - 939 cm^{-1} is due to symmetric and asymmetric stretching vibrations of cis- MoO_2^{2+} group **[56]**. The υ MoO_2^{2+} bands appear at much lower position in the complexes **(3.6)** and **(3.7)** as compared to those in the complexes **(3.1)** to **(3.5)**. This is due to heavy drainage of the electron density from strongly coordinating bidentate ligands phen and bpy.

Water bands

Lattice water absorbs in the 3550-3200 cm^{-1} (antisymmetric and symmetric O-H stretching modes) and 1650-1600 cm^{-1} (H-O-H bending modes) regions while coordinated water besides showing above modes absorbs between 900-750 cm^{-1} regions **[57]**. In the complex **(3.1)** a new band appears in the region 3400 – 3500 cm^{-1} which has been assigned to arise due to stretching vibration of coordinated water molecule. Moreover, this complex shows a weak band at 634 cm^{-1} due to rocking mode of coordinated water molecule.

Pyridine or substituted pyridine coordination

The free pyridine bases absorb at around 604 cm^{-1}due to in-plane ring deformation

mode **[58]**. In the complexes a new medium to weak band is observed in the region 600 – 620 cm^{-1}. This band is assigned to arise due to in-plane deformation mode of pyridine and substituted pyridine ring indicating their coordination to the metal centre. The molybdenum (VI) complexes **(3.2)** to **(3.5)** also show a weak intensity band in the region 1060-1003 cm^{-1}, which is assigned to ring stretching mode of pyridine, 2-picoline, 3-picoline and 4-picoline molecules **[59]**. In the phenanthroline complex **(3.6)**, medium intensity band are observed at 725 cm^{-1} and 840 cm^{-1} which are assigned to the out-of-plane motion of the hydrogen atoms on the heterocyclic rings and the hydrogen atoms on the central ring, respectively **[60]**. In the bipyridyl complex only one band is observed at 758 cm^{-1} due to out-of-plane motion of the hydrogen atoms as expected for two identical groups of four hydrogen atoms each **[61]**. Apart from these bands, complexes **(3.6)** and **(3.7)** also show a very strong broad band at 634 and 632 cm^{-1}which is assigned to arise due to in-plane ring deformation mode of 1,10-phenanthroline and 2,2'-bipyridine indicating their coordination to the metal centre **[60, 61]**.

Conclusion

In the present chapter few monometallic molybdenum (VI) complexes have been prepared and characterized on the basis of data obtained from various physico-chemical and spectroscopic studies. The ligand exists in staggered configuration in the free state and in the complexes the same configuration of the dihydrazone is also retained. The dihydrazone undergoes enolization in which half part of the dihydrazone exist in enol-form whereas the other half part remains in keto-form. The half part of the dihydrazone molecule coordinates to the metal centre through azomethine nitrogen atom, enolate oxygen atom and phenolate oxygen atom as a dibasic tridentate ONO donor whereas the other half part remains uncoordinated. The ^{1}H NMR spectra of the complexes clearly suggest the enolization of half part of the ligand and its subsequent coordination to the metal centre. Enolization of the ligand is further supported by the appearance of a new ν (NCO) band in the IR spectra of the complexes. The molybdenum centre has six coordinated octahedral

geometry in the complexes **(3.1)** to **(3.5)**. On the other hand, the complexes **(3.6)** and **(3.7)** are suggested to have a distorted rhombic structure around the molybdenum centre involving bridging **[62]** 1,10-phenanthroline and 2,2'-bipyridine molecule. The tentative structures for the complexes have been shown in **Figs. 3.32** and **3.33**, respectively.

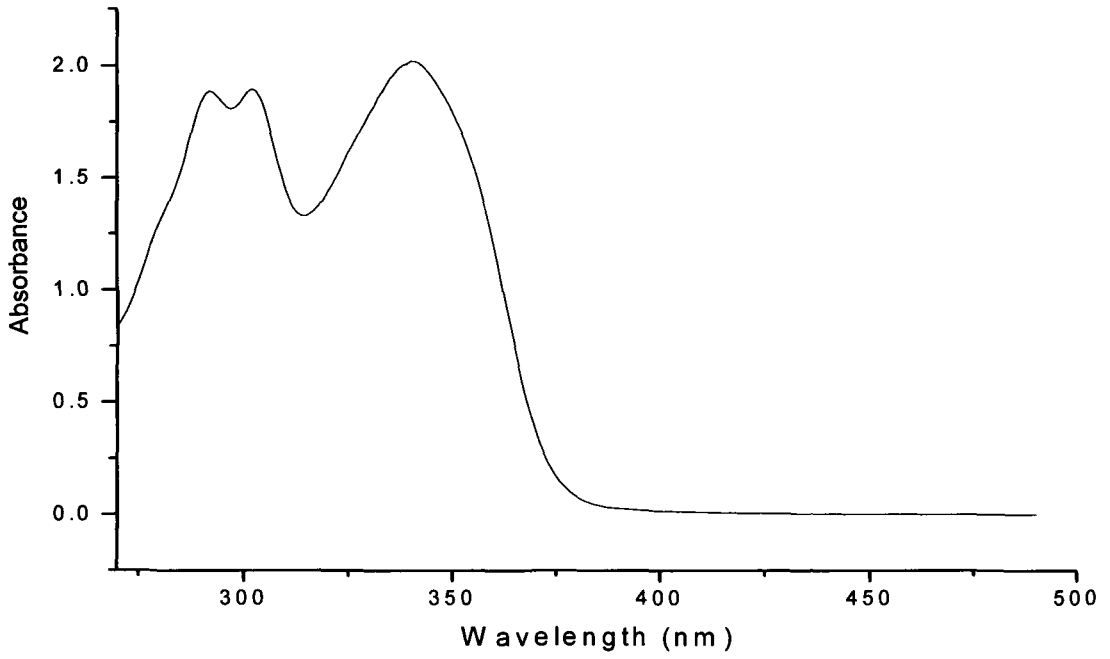

Fig. 3.16 Electronic spectrum of Disalicylaldehyde oxaloyldihydrazone (H_4slox).

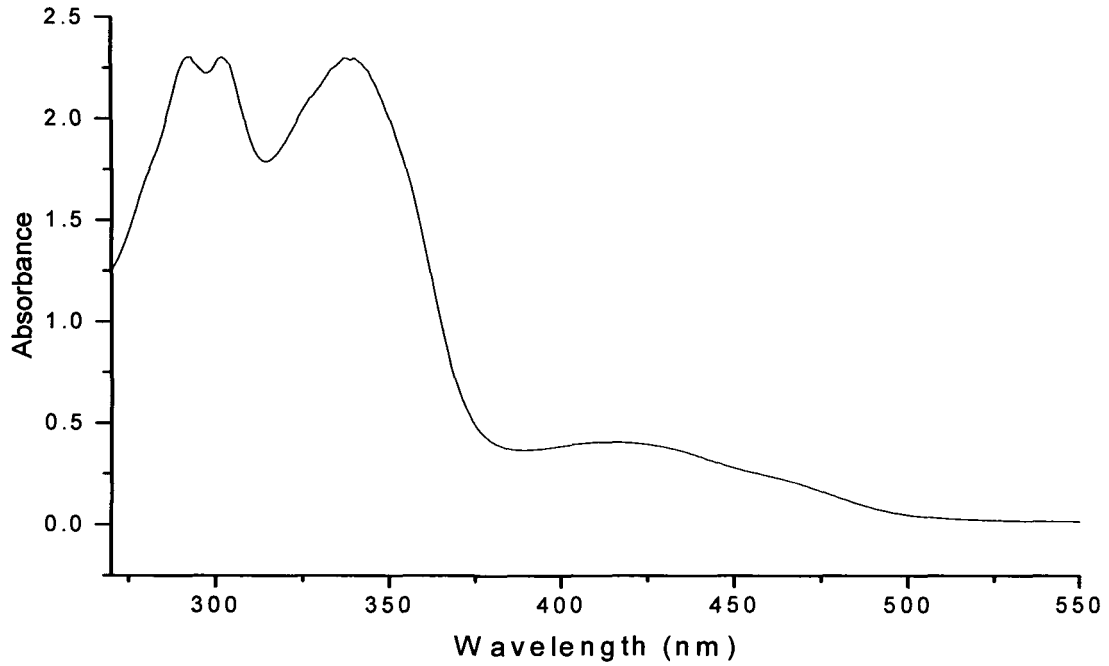

Fig. 3.17 Electronic spectrum of $[MoO_2(H_2slox)(H_2O)]$ **(3.1)**.

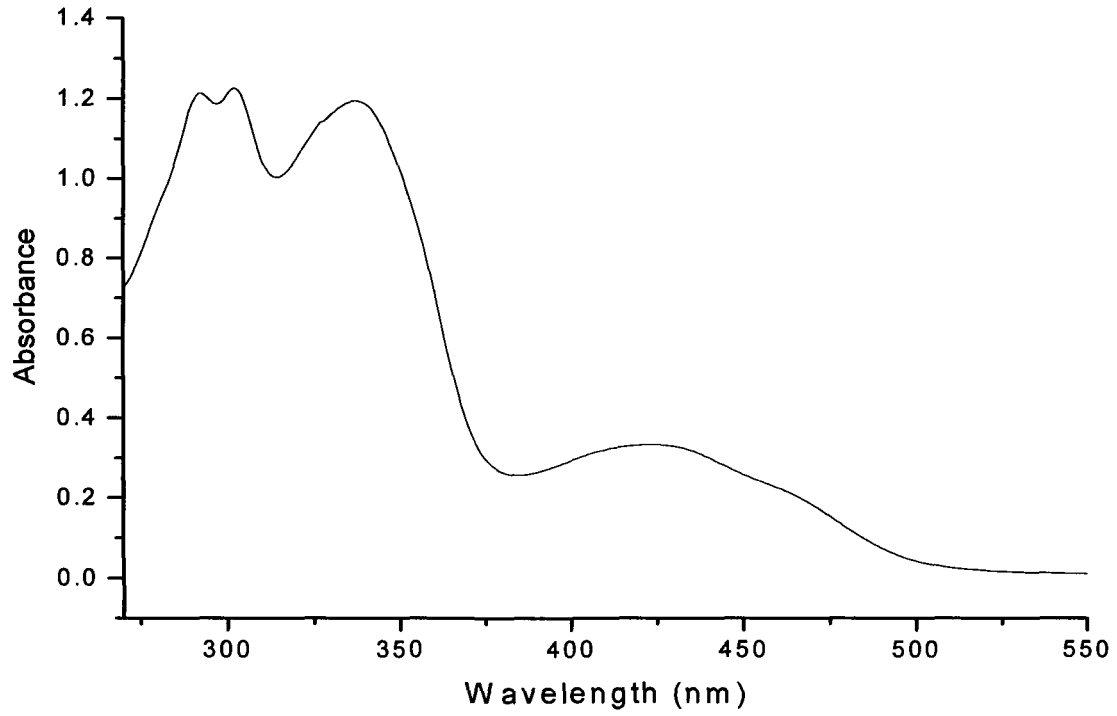

Fig. 3.18 Electronic spectrum of $[MoO_2(H_2slox)(py)]$ **(3.2)**.

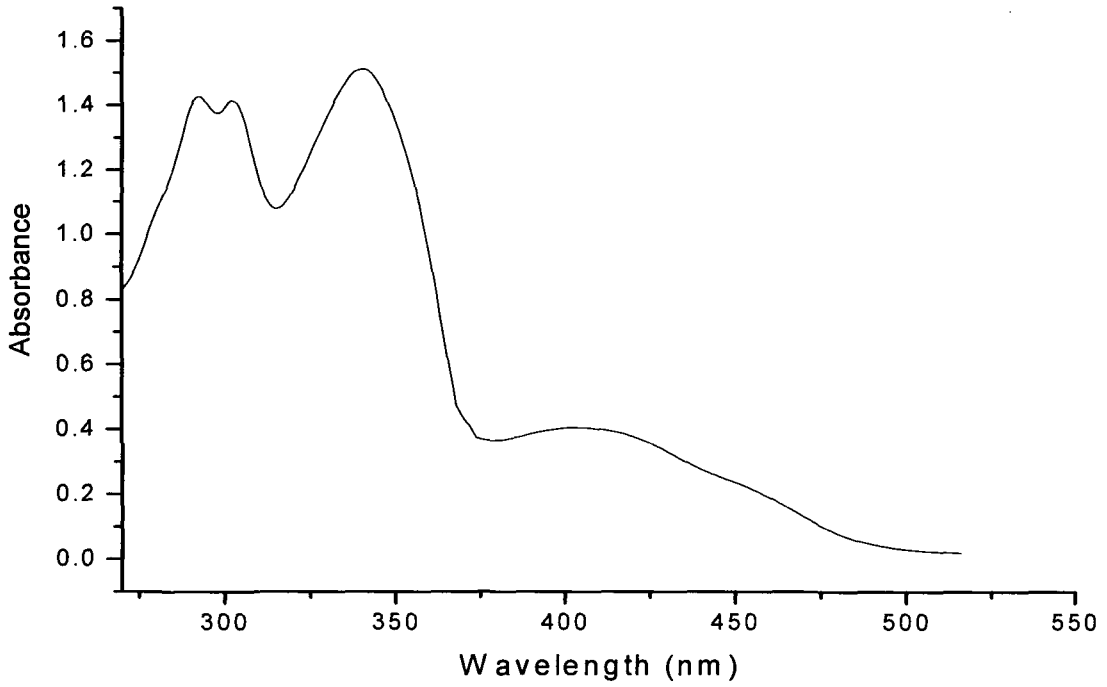

Fig. 3.19 Electronic spectrum of $[MoO_2(H_2slox)(2\text{-pic})]$ **(3.3)**.

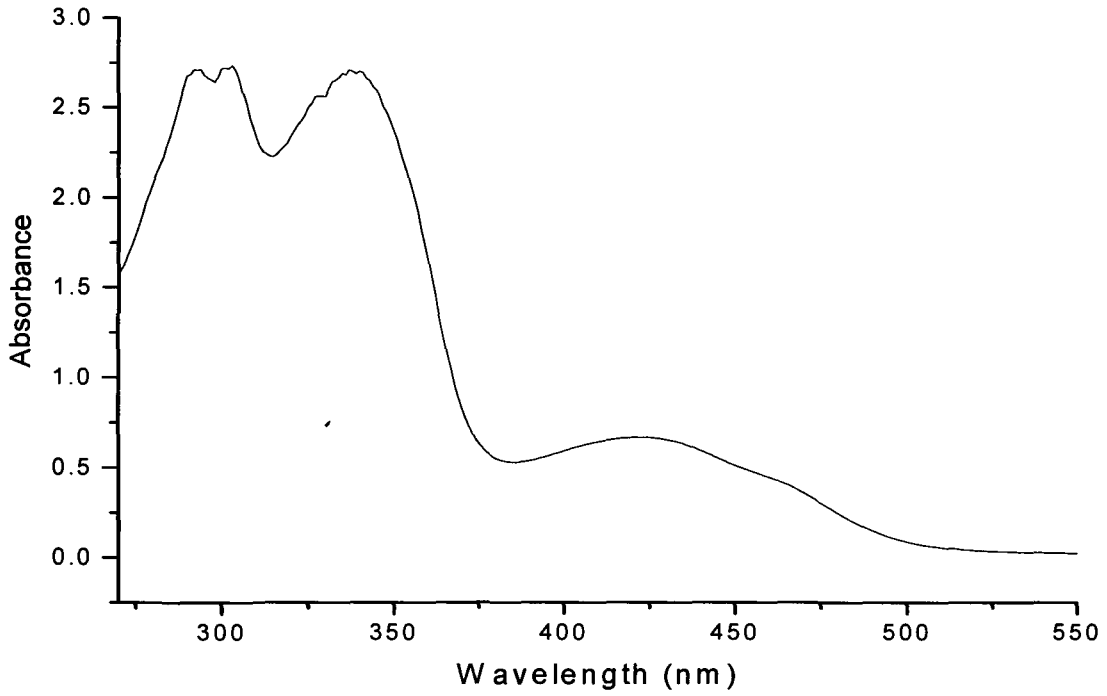

Fig. 3.20 Electronic spectrum of $[(MoO_2)_2(H_2slox)_2(phen)]$ **(3.6)**.

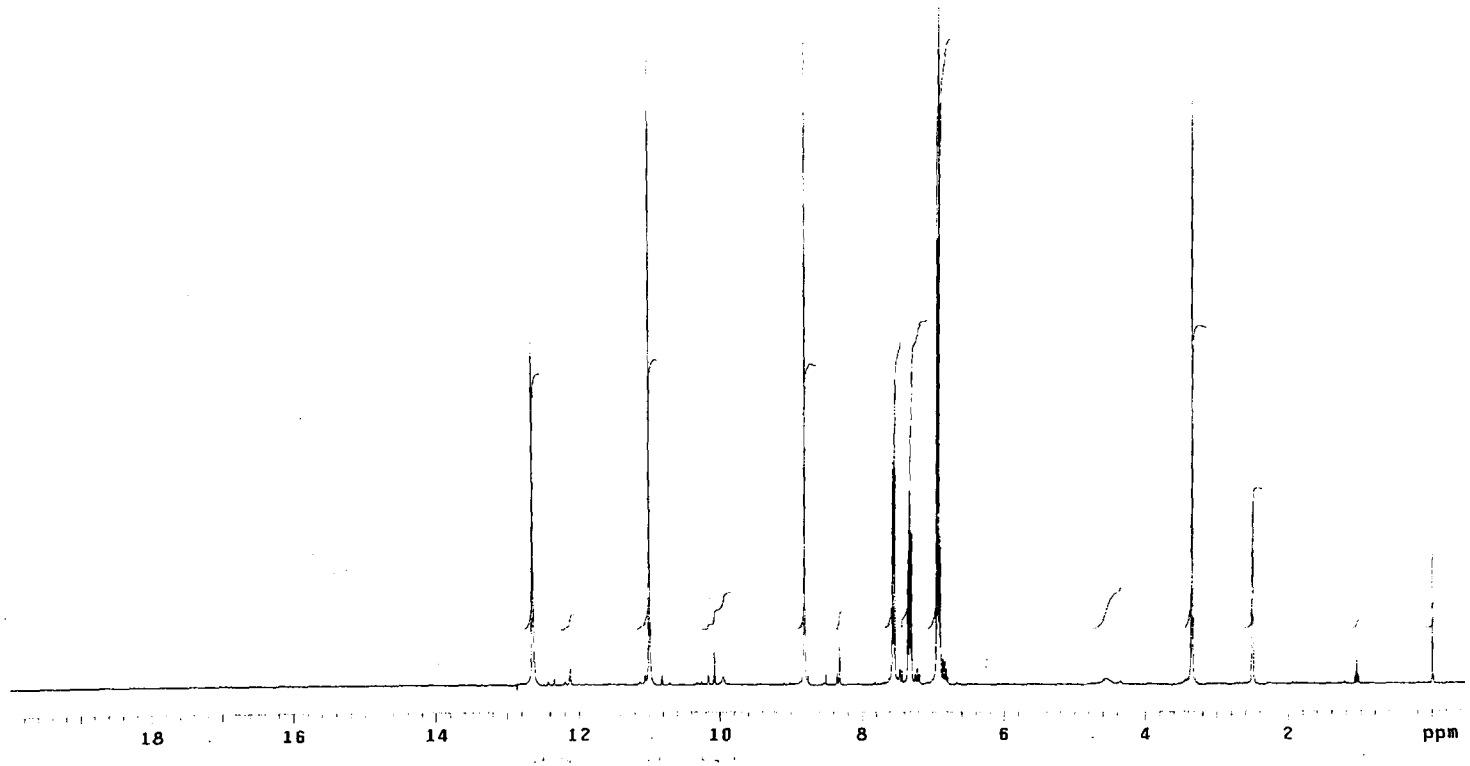

Fig. 3.22 ^{1}H NMR spectrum of disalicylaldehyde oxaloyldihydrazone (H_4slox) in DMSO-d_6.

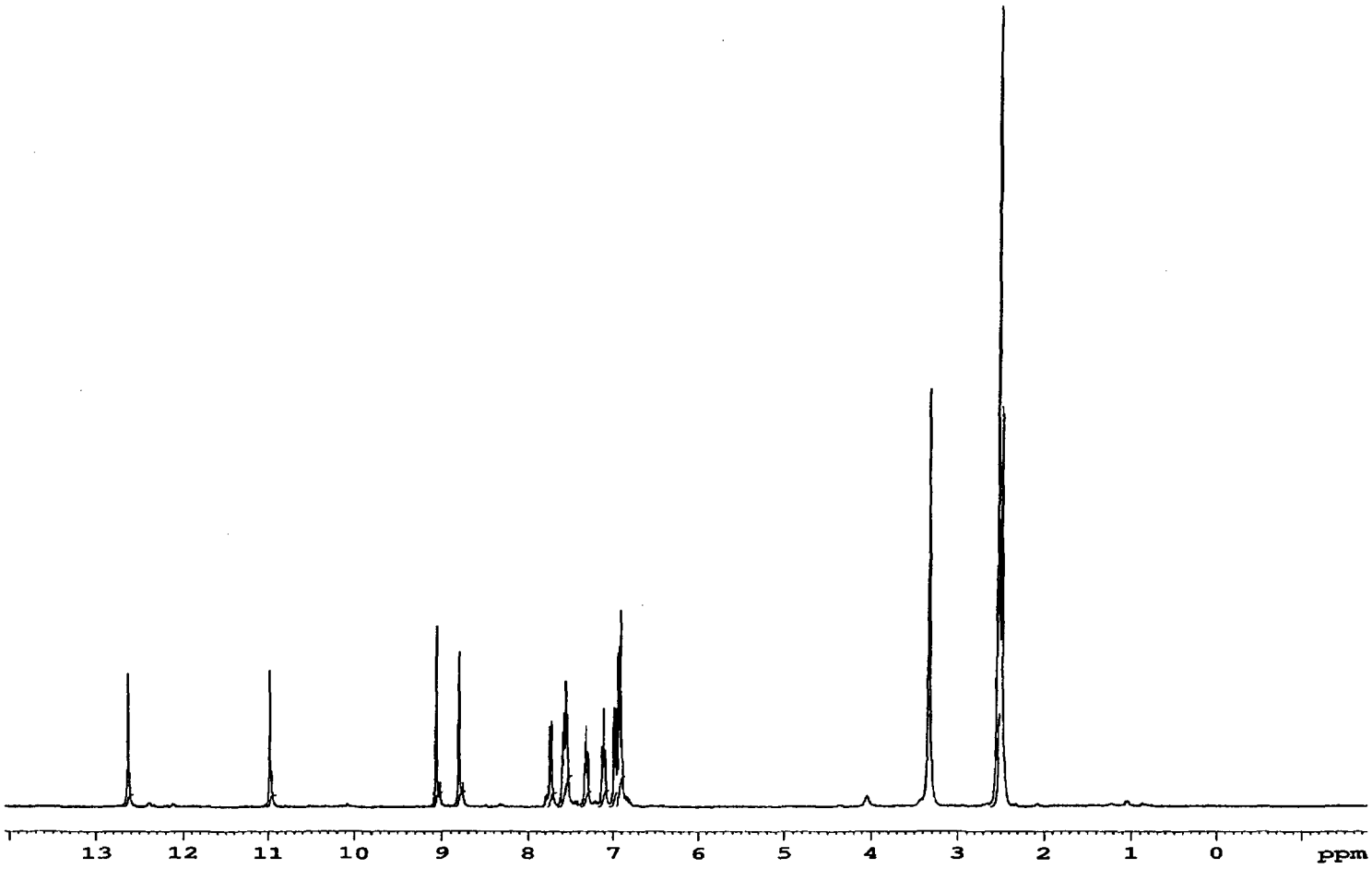

Fig. 3.23 ^{1}H NMR spectrum of $[MoO_2(H_2slox)(H_2O)]$ **(3.1)** in DMSO-d_6.

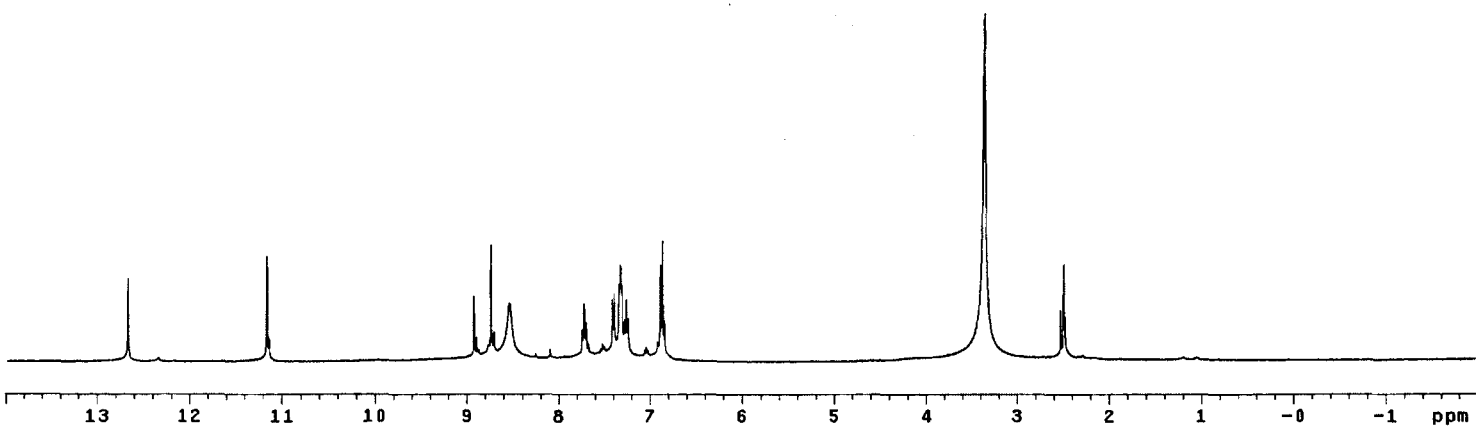

Fig. 3.24 ^{1}H NMR spectrum of $[MoO_2(H_2slox)(py)]$ **(3.2)** in DMSO-d_6.

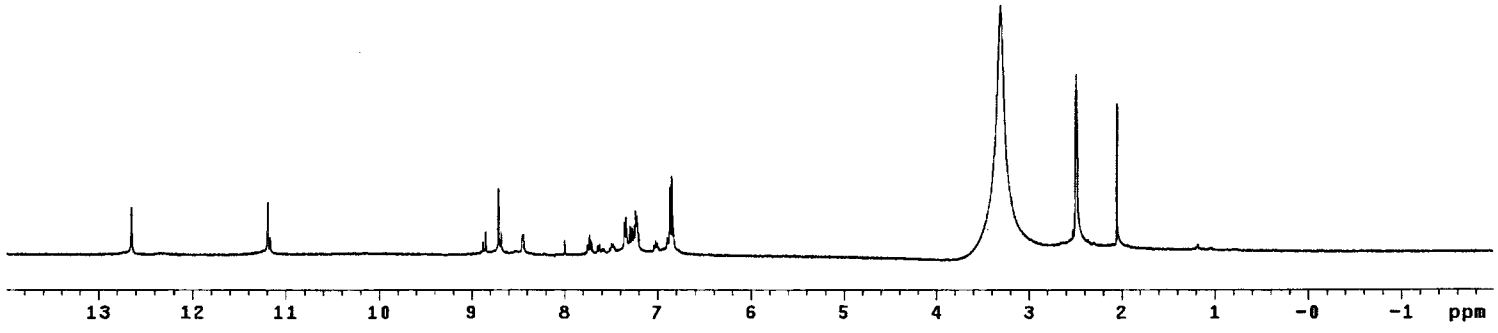

Fig. 3.25 ^{1}H NMR spectrum of $[MoO_2(H_2slox)(2\text{-pic})]$ **(3.3)** in DMSO-d_6.

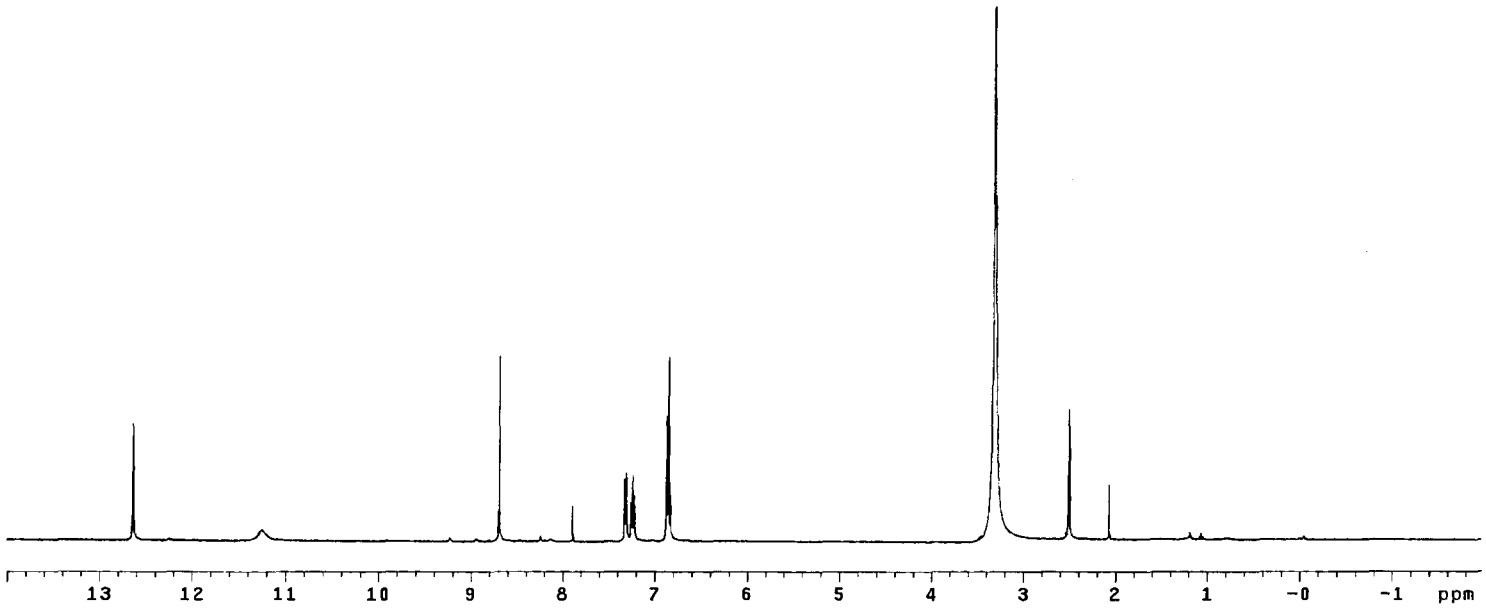

Fig. 3.26 ^{1}H NMR spectrum of $[(MoO_2)_2(H_2slox)_2(phen)]$ **(3.6)** in DMSO-d_6.

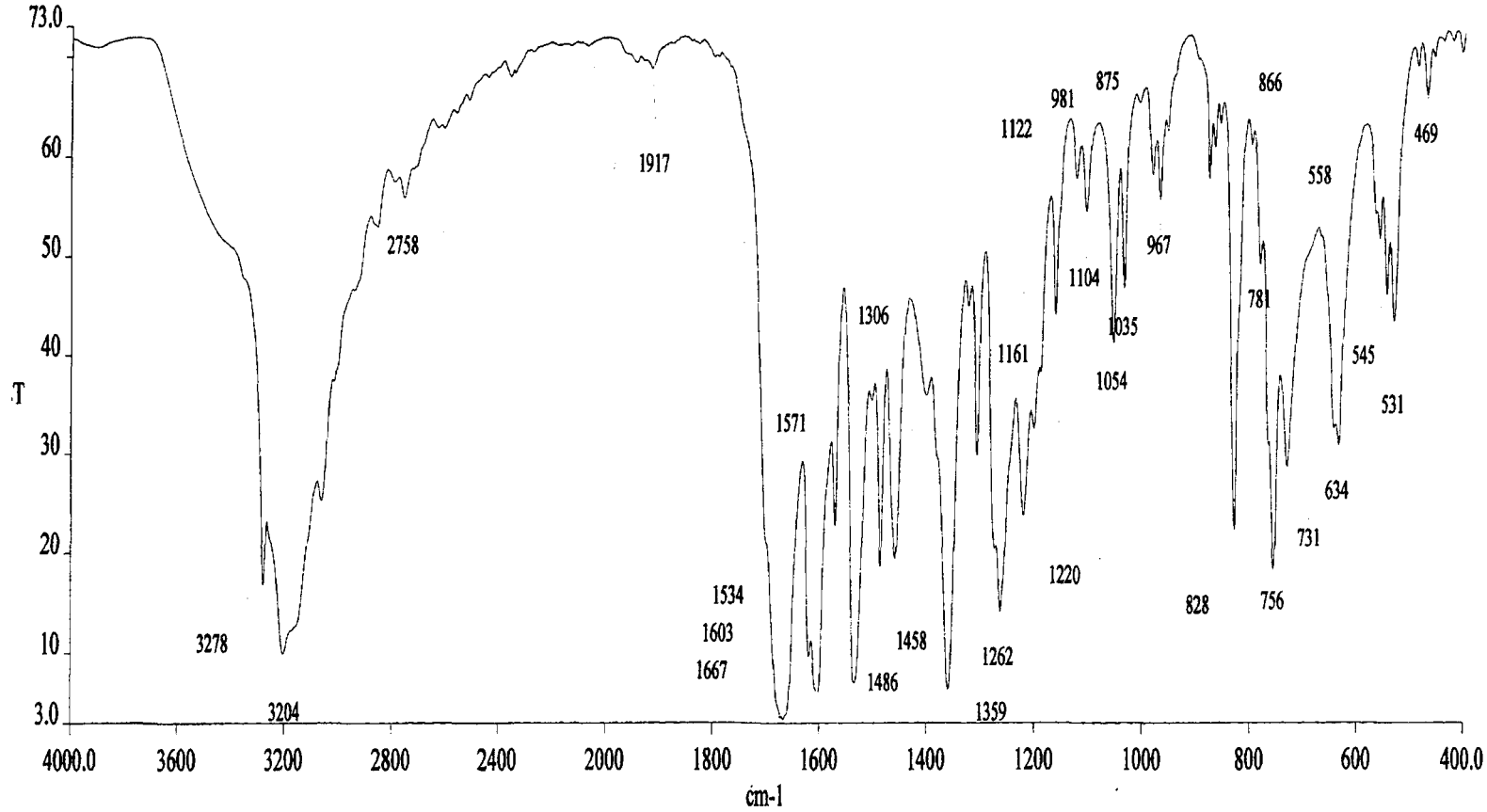

Fig. 3.27 Infrared spectrum of disalicylaldehyde oxaloyldihydrazone (H_4slox).

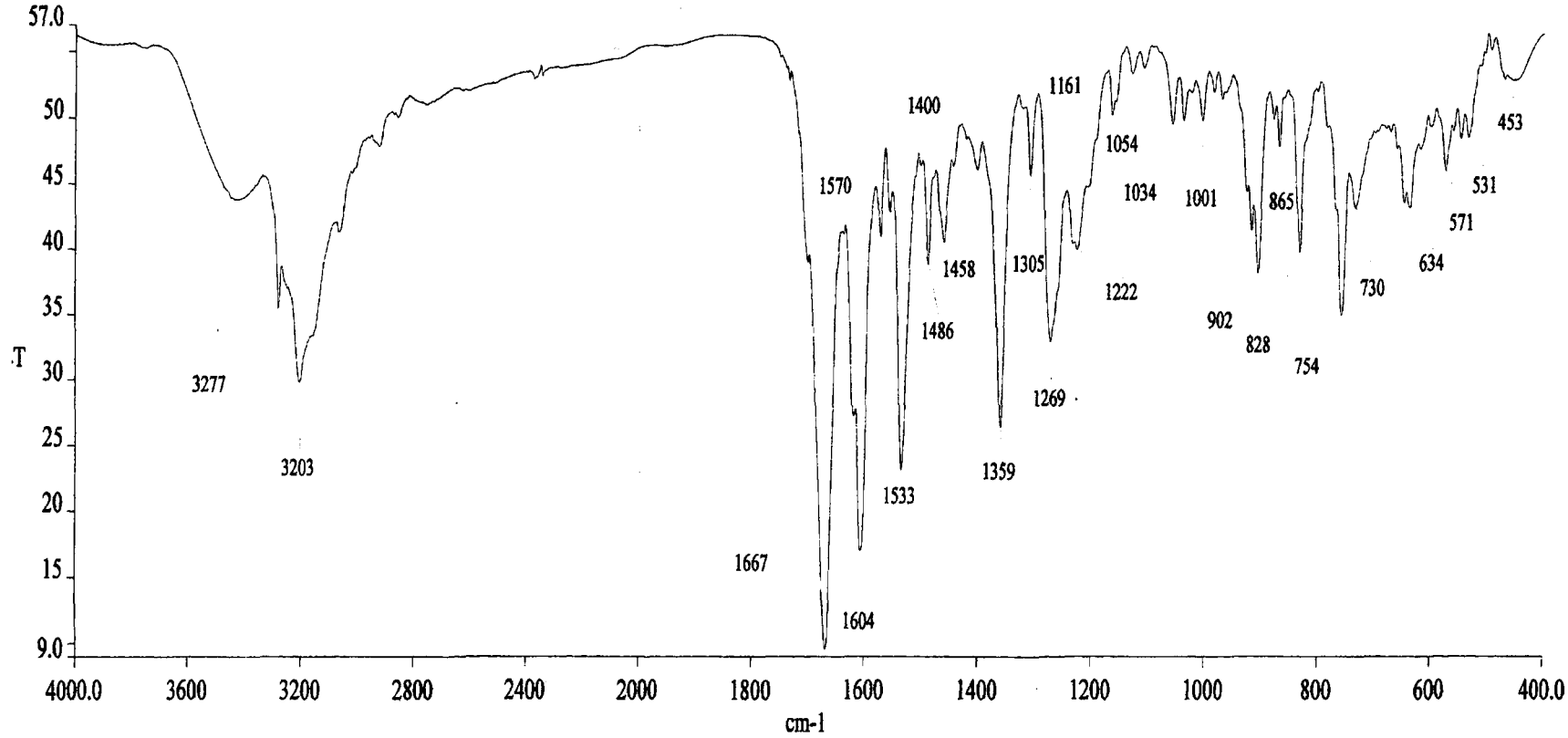

Fig. 3.28 Infrared spectrum of $[MoO_2(H_2slox)(H_2O)]$ **(3.1)** in KBr.

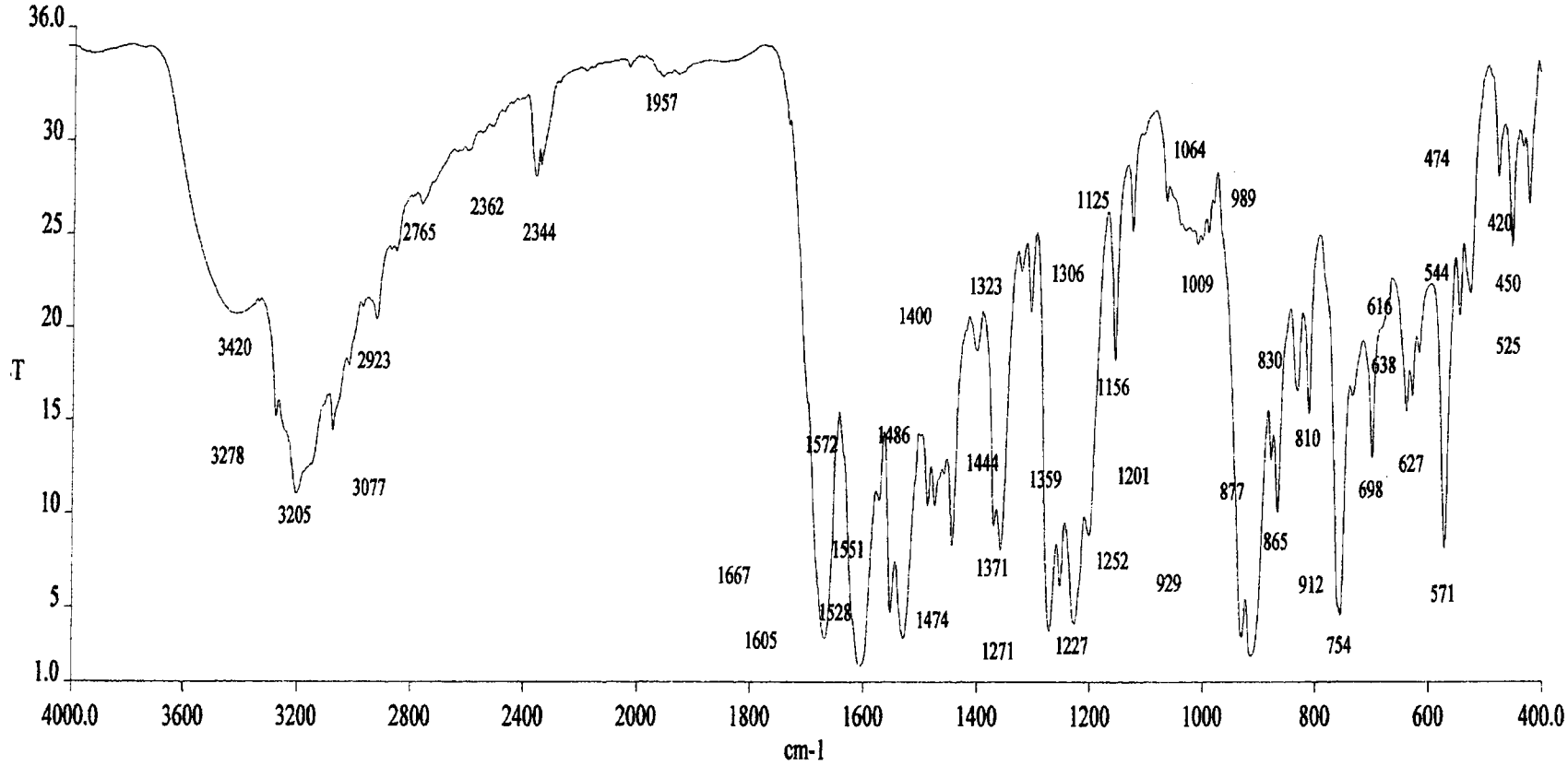

Fig. 3.29 Infrared spectrum of $[MoO_2(H_2slox)(py)]$ **(3.2)** in KBr.

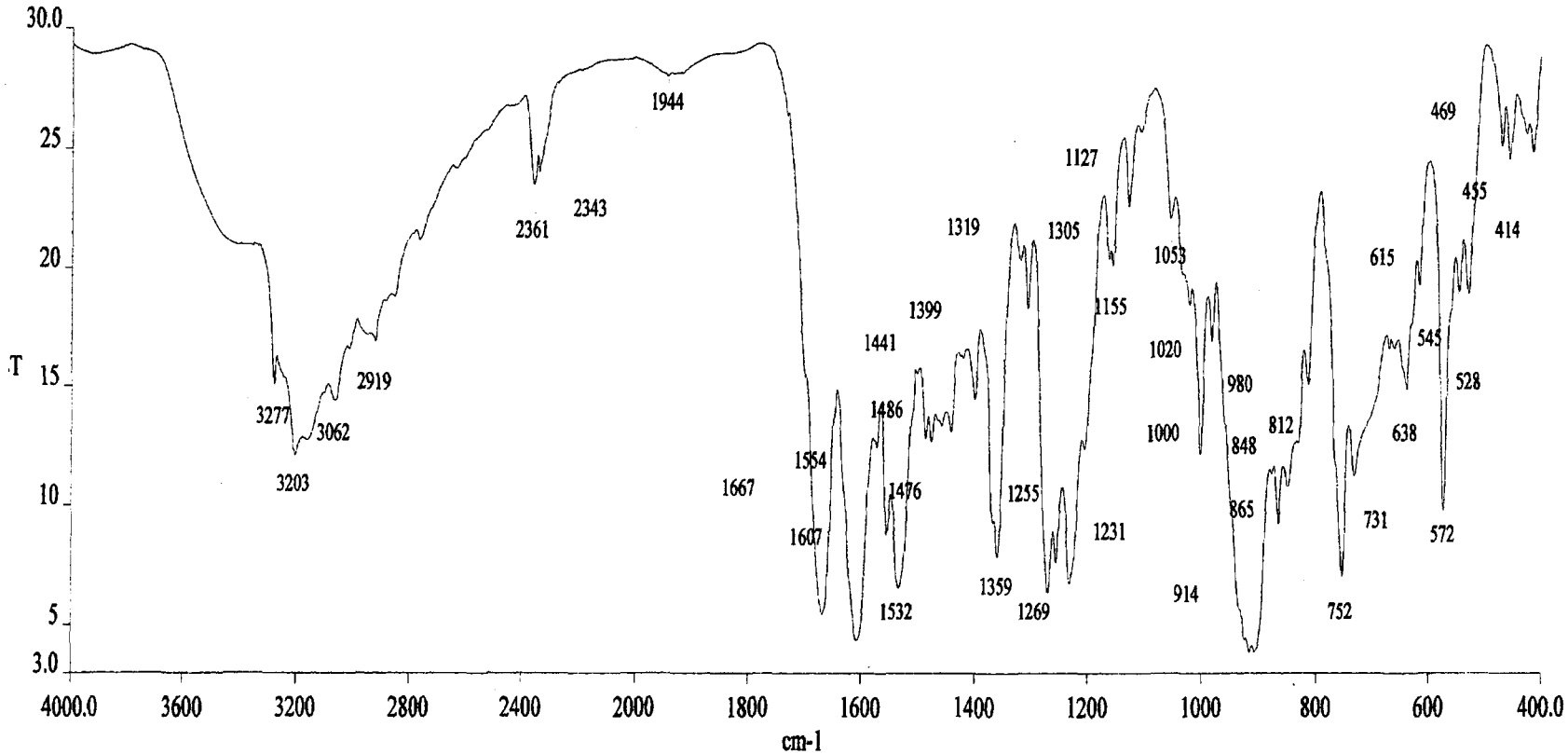

Fig. 3.30 Infrared spectrum of $[MoO_2(H_2slox)(2\text{-pic})]$ **(3.3)** in KBr.

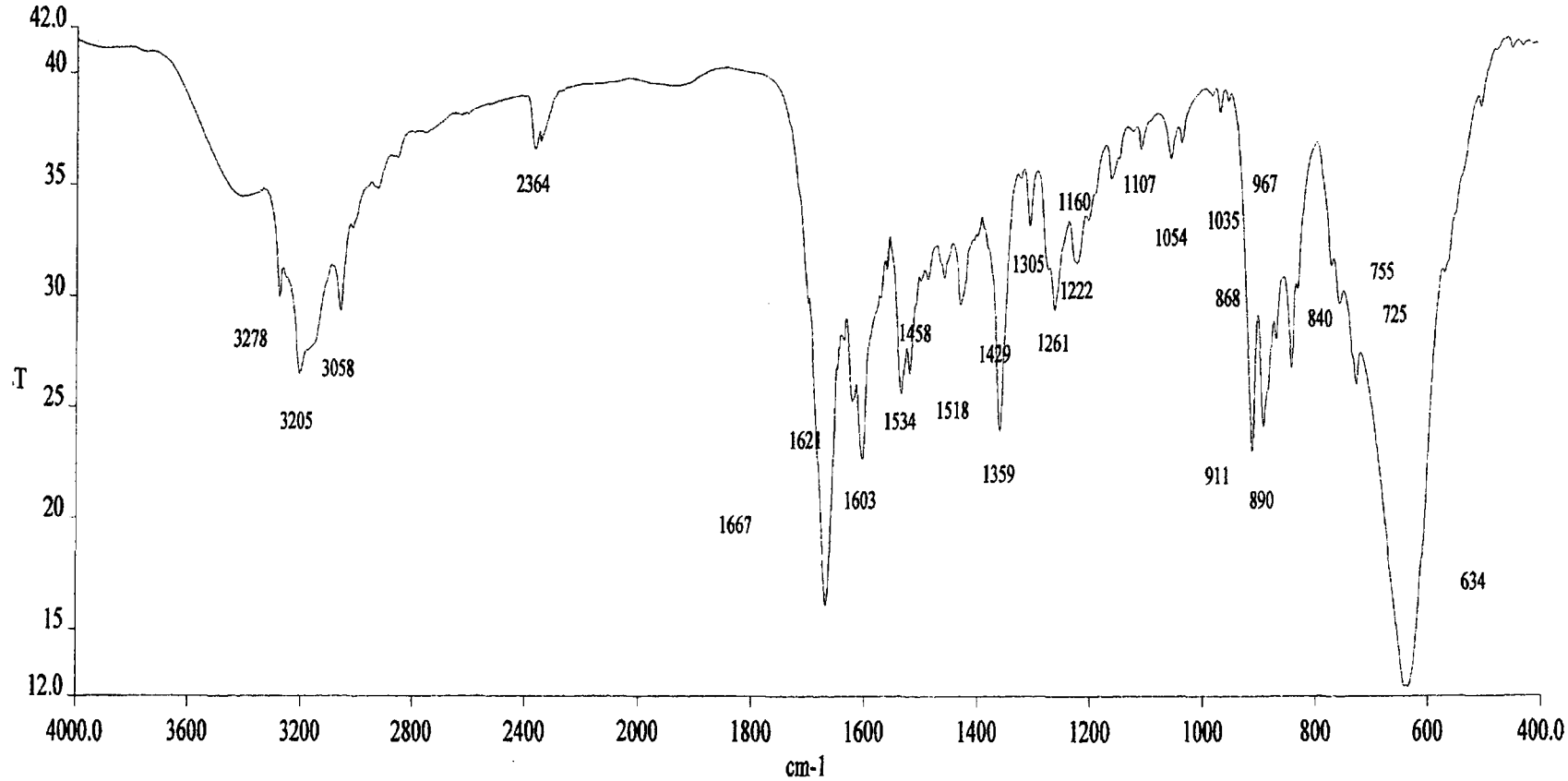

Fig. 3.31 Infrared spectrum of $[(MoO_2)_2(H_2slox)_2(phen)]$ **(3.6)** in KBr.

Table 3.1: Analytical, colour, decomposition point, molar conductance and electronic spectral data for monometallic molybdenum (VI) complexes.

Sl No	Ligand/Complex (Colour)	D.P (°C)	Elemental Analyses: Found (Calcd)%				Molar conductance Λ_M (ohm^{-1} cm^2mol^{-1})	Electronic spectral band λ_{max}(nm) (ε_{max}) (dm^3 $mol^{-1}cm^{-1}$)
			M	C	H	N		
	H_4slox	>300	--	59.12 (58.94)	4.31 (4.30)	17.34 (17.18)	--	293(10461) 303(10494) 340(11225)
3.1	$[MoO_2(H_2slox)(H_2O)]$ (Orange)	>300	19.85 (20.35)	41.33 (40.93)	3.01 (2.98)	12.10 (11.93)	1.54	293(15340) 303(15260) 338(15307) 422(2653)
3.2	$[MoO_2(H_2slox)(py)]$ (Yellow)	>300	17.66 (18.00)	48.02 (47.53)	3.22 (3.20)	13.50 (13.19)	2.36	293(11018) 304(11000) 340(10790) 430(3000)
3.3	$[MoO_2(H_2slox)(2\text{-pic})]$ (Light Orange)	>300	17.00 (17.54)	48.93 (48.51)	3.45 (3.49)	13.00 (12.85)	1.89	294(11891) 304(11775) 341(12608) 413(3308)
3.4	$[MoO_2(H_2slox)(3\text{-pic})]$ (Yellow)	>300	17.12 (17.54)	48.85 (48.51)	3.51 (3.49)	13.11 (12.85)	2.03	293(10041) 304(10191) 340(9892) 423(2783)
3.5	$[MoO_2(H_2slox)(4\text{-pic})]$ (Orange)	>300	16.99 (17.54)	48.91 (48.51)	3.52 (3.49)	13.21 (12.85)	2.16	294(15941) 304(15923) 340(15888) 431(3935)
3.6	$[(MoO_2)_2(H_2slox)_2(phen)]$ (White)	>300	16.87 (17.35)	48.45 (47.99)	2.89 (2.91)	13.10 (12.71)	3.15	294(15958) 304(16100) 342(15817) 427(3912)
3.7	$[(MoO_2)_2(H_2slox)_2(bpy)]$ (White)	>300	17.65 (18.04)	47.90 (47.62)	2.95 (2.91)	13.53 (13.22)	4.20	291(15964) 301(15924) 339(15670) 423(3923)

Table 3.3: ^{1}H NMR spectral data for monometallic molybdenum (VI) complexes.

Sl. No.	Ligand/Complex	δ(OH)	δ(NH)	δ(CH=N)	δ(phenyl protons)	δ(pyridyl protons)	
						o-proton	δ(CH_3)
	H_4slox	12.64(s)	11.00(s)	8.81(s)	7.57 – 6.84(m)	--	--
3.1	[MoO_2(H_2slox)(H_2O)]	12.64(s)	10.98(s)	9.06(d, 4Hz) 8.80(d, 4Hz)	7.74 – 6.92(m)	--	--
3.2	[MoO_2(H_2slox)(py)]	12.67(s)	11.16(d, 6.6Hz)	8.93(d, 9.3Hz) 8.73(d, 9.3Hz)	7.74 – 6.85(m)	8.54 (8.61)[a]	
3.3	[MoO_2(H_2slox)(2-pic)]	12.65(s)	11.18(d, 8.4Hz)	8.87(d, 8.1Hz) 8.69(d, 8.7Hz)	7.74 – 6.83(m)	8.45 (8.48)[a]	2.50 (2.55)[b]
3.4	[MoO_2(H_2slox)(3-pic)]	12.56(s)	11.31(s)	8.70(d, 1.5Hz) 8.63(d, 1.5Hz)	7.62 – 6.81(m)	8.35 (8.44 and 8.42)[a]	2.27 (2.32)[b]
3.5	[MoO_2(H_2slox)(4-pic)]	12.60(s)	11.29(s)	8.75(s) 8.65(s)	7.44 – 6.82(m)	8.43 (8.60)[a]	2.35 (2.32)[b]
3.6	[(MoO_2)$_2$(H_2slox)$_2$(phen)]	12.63(s)	11.25(s)	9.09(d, 59 Hz) 8.75(d, 59 Hz)	7.33 – 6.89(m)	--	--
3.7	[(MoO_2)$_2$(H_2slox)$_2$(bpy)]	12.65(s)	11.21(s)	8.86(s) 8.72(s)	7.37 – 6.84(m)	--	--

a, δ values for o-pyridyl proton of free pyridine and substituted pyridine.
b, δ values for methyl protons of free substituted pyridine molecule.

Table 3.4: Infrared spectral data for monometallic molybdenum (VI) complexes.

Sl. No	Ligand/complex	ν(OH)+ ν(NH)	ν(C=O)	ν(C=N)	Amide II + ν(C-O) (phenolic)	ν(NCO)	ν(C-O)	ν(N-N)	ν(MoO_2^{2+})	ν(M-O) (phenolic)	ν(M-O) (enolic)
	H_4 slox	3278(s) 3204(s)	1667(s)	1627(s) 1603(s)	1534(s)	--	1262(s)	1035(w) 1054(m)	--	--	--
3.1	$[MoO_2(H_2slox)(H_2O)]$	3277(m) 3203(m)	1667(s)	1604(s)	1547(m)	1533(s)	1269(s)	1034(m) 1054(m)	919(s) 902(s)	571(m)	453(w)
3.2	$[MoO_2(H_2slox)(py)]$	3278(m) 3205(s)	1667(s)	1605(s)	1551(s)	1528(s)	1271(s)	1064(w)	929(s) 912(s)	571(s)	450(w)
3.3	$[MoO_2(H_2slox)(2\text{-pic})]$	3277(m) 3203(s)	1667(s)	1607(s)	1554(s)	1532(s)	1269(s)	1053(w)	931(s) 914(s)	572(s)	455(w)
3.4	$[MoO_2(H_2slox)(3\text{-pic})]$	3278(m) 3207(m)	1668(s)	1606(s)	1551(s)	1526(s)	1270(s)	1058(m) 1031(w)	930(s) 913(s)	571(s)	453(w)
3.5	$[MoO_2(H_2slox)(4\text{-pic})]$	3254(m) 3185(m)	1669(m)	1606(s)	1554(s)	1528(s)	1269(s)	1065(w)	939(s) 908(s) 891(s)	575(m)	450(w)
3.6	$[(MoO_2)_2(H_2slox)_2(phen)]$	3278(m) 3205(s)	1667(s)	1621(s) 1603(s)	1534(s)	1518(s)	1261(s)	1054(m) 1035(m)	911(s) 890(s)	569(m)	--
3.7	$[(MoO_2)_2(H_2slox)_2(bpy)]$	3278(m) 3205(s)	1668(s)	1618(s) 1603(s)	--	1534(s)*	1262(s)	1055(m) 1034(w) 1022(m)	914(s) 883(s)	565(m)	442(w)

* Amide II + ν(C-O) merged with ν (NCO)

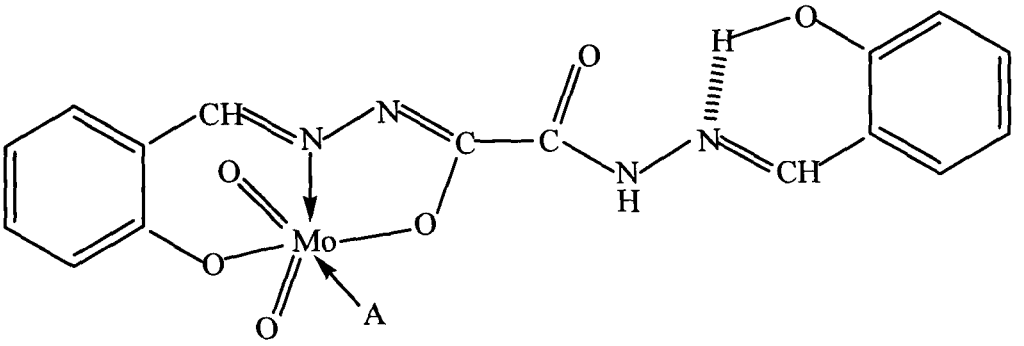

Fig. 3.32 Tentative structure for $[MoO_2(H_2slox)(A)]$ {*where A = H_2O* **(3.1)**, *pyridine* **(3.2)**, *2-picoline* **(3.3)**, *3-picoline* **(3.4)** *and 4-picoline* **(3.5)**}.

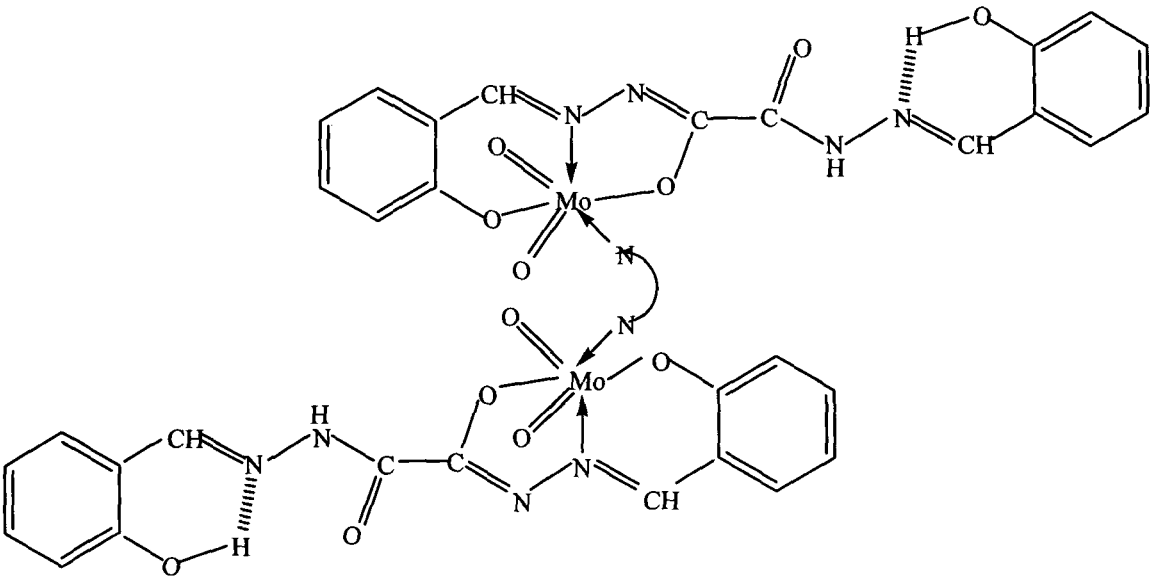

Fig. 3.33 Tentative structure for $[(MoO_2)_2(H_2slox)_2(NN)]$ {*where NN = phenanthroline* **(3.6)** *and bipyridine* **(3.7)**}.

References

1. N. K. Dutta and A. Sengupta, *J. Inorg. Nucl. Chem.*, **33**, 418 (1971).
2. S. Kher, S. K. Sahni and R. N. Kapoor, *Inorg. Chim. Acta*, **37**, 121 (1979).
3. A. Yacouta-Nour, A. K. T. Maki and M. M. Mostafa, J. Indian Chem. Soc., 72, 447 (1995).
4. R. C. Aggarwal and B. Singh, *Trans. Met. Chem.*, 1, 275 (1976); *Curr. Sci.*, **46**, 836 (1977); *J. Inorg. Nucl. Chem.*, **40**, 1174 (1978).
5. A. El-Toukhy, A. F. M. Henry, L. EI-Sayed and M. F. Iskander, *MI. Chem.*, 113, 171 (1982); M. F. Iskander, A. F. M. Henry, L. EI-Sayed and S. E. Zayan, *J. Inorg. Nucl. Chem.*, **38**, 2209 (1976); K. K. Narang and R. A. Lal, *Trans. Met. Chem.*, **3**, 272 (1978).
6. D. L. Arora, K. Lal, S. P. Gupta and S. K. Sahani, *Polyhedron*, **5**, 1499 (1986); *Indian J. Chem.*, **24A**, 980 (1987).
7. P. C. H. Mitchell, *J. Inorg. Biochem.*, **28**, 107 (1986).
8. M. C. Durrant, *Inorg. Chem. Commun.*, **4**, 62 (2001).
9. R. H. Holm, *Chem. Rev.*, **87**, 1401 (1987).
10. J. T. Spence, *Coord. Chem. Rev.*, **48**, 59 (1983).
11. E. W. Harlan, J. M. Berg and R. H. Holm, *J. Am. Chem. Soc.*, **114**, 1086 (1992).
12. M. E. Coughlan, "*Molybdenum and Molybdenum Containing Enzymes*", Pergamon Press, New York (1980).
13. R. A. Lal, A. N. Siva, S. Adhikari, M. K. Singh and U. S. Yadav, Synth. React. Inorg. *Met-Org. Chem.*, **26(2)**, 321-337 (1996); F. Feigl, V. Anger and R. E. Oesper, "*Spot Tests in Organic Analysis*", 7th Ed., Elseiver Publishing Company, Amsterdam, Netherland, p. 173, 384 (1996) (Indian reprint, 2005).
14. R. A. Lal, D. Basumatary, S. Adhikari and A. Kumar, *Spectrochim. Acta A*, **69** 706-714 (2008).
15. J. W. Geary, *Coord. Chem. Rev.*, 7, 81 (1971).

16. E. I. Stiefel, G. Wilkinson, (Ed.) "*Comprehensive Coordination Chemistry*"; R. D. Gillard and J. A. McCleverty (Eds.), Pergamon, Oxford, vol. **1**, p. 1375 (1987).
17. D. G. McCollum, L. Hall, C. White, R. Ostrandor, A. L. Rheingold, J. Whelan and B. Bosnich, *Inorg. Chem.*, **33**, 924 (1994).
18. J. Topich, *Inorg. Chem.*, **20**, 3704 (1981).
19. A. Syamal and M. R. Maurya, *Coord. Chem. Rev.*, **95**, 183 (1989).
20. R. C. Maurya, A. Pandey and D. Sutrashar, *Indian J. Chem.*, **43A**, 763 (2004).
21. R. C. Maurya and S. Rajput, *Int. J. Synth. Charact.* **1**, 49 (2008).
22. R. A. Lal, D. Basumatary, A. K. De and A. Kumar, *Trans. Met. Chem.*, **32**, 481 (2007); L. Xiaozeng, W. Genglin, L. Zaizheng, Y. Shiping, J. Zonghui, W. Hoggen and Y. Xinkan, *Polyhedron*, **14**, 511 (1995).
23. R. A. Lal and A. Kumar, *Indian J. Chem.*, **37A**, 924 (1998).
24. R. A. Lal, D. Basumatary, S. Adhikari and A. Kumar, *Spectrochim. Acta A*, **69**, 706 (2008).
25. L. M. Jackman and S. Sternhell, "*Applications of Nuclear Magnetic Resonance Spectroscopy in Organic Chemistry*", Chapter 3, Vol. **10**, Second Ed., Perganion Press, Amsterdam (1978).
26. J. C. N. Ma, E. W. Warnhoff, *Can. J. Chem.*, **43**, 143 (1961).
27. T. K. Wu, B. P. Daily, *J. Chem. Phys.* **41**, 1849 (1961).
28. R. M. Silverstein and G. C. Bassler, "*Spectroscopic Identification of Organic Compounds*", Wiley, New York (1967).
29. C. N. R. Rao, "*Chemical application of Infrared Spectroscopy*", Academic Press, New York (1963).
30. M. Mashima, *Bull. Chem. Soc. Japan*, **35**, 332, 338, 2020 (1962).
31. K. Nagano, H. Kinosita and A. Hirakawa, *Chem. Pharm. Bull.*, **12(10)**, 1207 (1964).
32. A. Shyamal and K. S. Kale, *Inorg. Chem.*, **18**, 992 (1979); S. Purohit, A. P. Koley, I. S. Prasad, P. T. Manoharan and S. Ghosh, *Inorg. Chem.*, **28**, 3735

(1987); J. M. Beng and R. H. Holm, *Inorg. Chem.*, **22**, 1768 (1983); E. I. Stiefel, *Prog. Inorg. Chem.*, **31**, 511 (1992).

33. G. M. Larin, A. N. Gusev, Y. V. Trush, K. V. Rabotyagov, V. F. Shulgin, G. G. Aleksandrov and I. L. Eremenko, *Russ. Chem. Bull.*, **56 (10)**, 1964 (2007).
34. R. A. Lal, S. Das and R. K. Thapa, *Inorg. Chim. Acta*, **132**, 129 (1987).
35. R. A. Lal, A. N. Siva, S. Adhikari and A. Pal, *Indian J. Chem.*, **34A**, 1000 (1995).
36. A. EL-Toukhy, A. F. M. Henry, L. EI-Sayed and M. F. Iskander, *MI. Chem.*, **113**, 171 (1982); M. F. Iskander, A. F. M. Henry, L. EI-Sayed and S. E. Zayan, *J. Inorg. Nucl. Chem.*, **38**, 220, (1976).
37. S. K. Sahni, S. P. Gupta and V. B. Rana, *J. Indian Chem. Soc.*, **54**, 200 (1977).
38. A. Yacouta Nour, M. M. Mostafa and A. K. T. Maki, *Trans. Met. Chem.*, **15**, 34 (1990); *Spectrochim, Acta A*, **44**, 1291 (1988).
39. C. Pelizzi, G. Pelizzi, G. Predieri and S. Resola, *J. Chem. Soc. Dalton Trans.*, 1349 (1982).
40. G. Paolucci, G. Marangoni, G. Bandoli and D. D. Clemente, *J. Chem. Soc. Dalton Trans.*, 1304 (1980).
41. C. Pelizzi and G. Pelizzi, *J. Chem. Soc. Daltons Trans.*, 1970 (1980).
42. G. Paolucci, P. A. Vigato, G. Rossetto and V. Casellato, *Inorg. Chim. Acta*, **65**, L71 (1982).
43. O. Pouralimardan, A. C. Chamayou, C. Janiak and H. H. Monfarad, *Inorg. Chim. Acta*, **360**, 1599 (2007).
44. K. R. Barnard, M. Bruch, H. Susan, J. H. Enemark, R. W. Gable and A. G. Wedd, *Inorg. Chem.*, **36**, 637 (1997).
45. O. Pouralimardan, A. C. Chamayou, C. Janiak and H. Hosseini-Monfared, *Inorg. Chim. Acta*, **360**, 1599–1608 (2007).
46. J. R. Dyer, "*Applications of Absorption Spectroscopy in Organic Compounds*", 1st Ed., Practice Hall of India Pvt. Ltd., New Delhi (1969).
47. K. Broderson, *Z. Anorg. Chem.*, **290**, 4 (1959).
48. J. C. Decius and D. P. Pearson, *J. Am. Chem. Soc.*, **75**, 2436 (1953).

49. V. J. Goubean and V. Kull, *Z. Anog. Chem.*, **316**, 182 (1962).

50. W. G. Peterson and M. Onyszchuk, *Can. J. Chem.*, **39**, 968 (1961).

51. L. Sacconi and A. Sabatini, *J. Inorg. Nucl. Chem.*, **25**, 1389 (1963).

52. A. Braibanti, F. Dallavalle, M. A. Pellinghelli and E. Leporati, *Inorg. Chem.*, **7**, 1430 (1968).

53. R. Bline and D. Hadzi, *J. Chem. Soc.*, 4536 (1958).

54. G. G. Mohamed and C. M. Sharaby, *Spectrochim. Acta A*, **66**, 949 (2007).

55. R. Gup and B. Kirkan, *Spectrochim. Acta A*, **62**, 1188 (2005).

56. J. Topic and J. C. Bachert, *Inorg. Chem.*, **31**, 511 (1992).

57. G. Sartori, C. Furlani and A. Damiani, *J. Inorg. Nucl. Chem.*, **8**, 119 (1958).

58. K. Nakamoto, "*Infrared and Raman Spectra of Inorganic and Coordination Compounds*", 4th Ed., John Wiley and Sons, New York (1986).

59. R. A. Lal, M. L. Pal and S. Adhikari, *Synth. React. Inorg. Met-Org. Chem.*, **26**, 997 (1996).

60. Mudasir, N. Yoshioka and H. Inoue, *Trans. Met. Chem.*, **24**, 210 (1999).

61. A. K. Boudalis, U. Nastopoulos, S. P. Perlepes, C. P. Raptopoulu and A. Terzis, *Trans. Met. Chem.*, **26**, 276 (2001).

62. R. Uson, J. Fornies, M. Tomas, J. M. Casas and C. Fortuno, *Polyhedron*, **8**, 2209-2211 (1989); S. W. Nag, V. G. Kumardas, C. H. L. Kennard, *Main Group Met. Chem.*, **19**, 107 (1996); S. W. Ng, *Acta Crystallogr.*, **C53**, 1059 (1997).

CHAPTER IV

Synthesis and Characterization of Homobimetallic Molybdenum (VI) Complexes derived from Polyfunctional Disalicylaldehyde oxaloyldihydrazone

Introduction

The dihydrazone selected in the present study is a polyfunctional ligand containing as many as eight bonding sites such as phenolate oxygen atoms, azomethine nitrogen atoms, secondary amine nitrogen atoms and carbonyl oxygen atoms, each in duplicate. The molybdenum compounds described in the previous chapter were isolated from the reaction of $MoO_2(acac)_2$ with ligand in 1.1:1 molar ratio in ethanol. The dihydrazone behaved as a dibasic tridentate ligand coordinating to the metal centre through one phenolate oxygen atom, one enolate oxygen atom and one azomethine nitrogen atom, the remaining coordination sites were unutilized in the complexes. Hence, it was of interest to carry out the reaction of $MoO_2(acac)_2$ with ligand by keeping $MoO_2(acac)_2$ in large quantity and to explore the stoichiometry of the resulting complexes and characterize them by various physico-chemical techniques and spectroscopic studies. Before we proceed to describe the synthesis and characterization of the complexes so isolated, it is pertinent to mention the importance of molybdenum and its complexes.

Molybdenum is a versatile transition element possessing a large number of stable and accessible oxidation states. It is the only element from second transition series which occurs in the biological system **[1]**. In combination with oxo and imido ligands, molybdenum plays a very important role in catalytic chemistry **[2]** and its bio-chemistry **[3]**. The cis-dioxomolybdenum compounds display catalytic activities and are useful material precursors **[4]**. Catalytic activity is frequency linked to coordinative unsaturation and the active site in various molybdenum oxidation catalysts are believed to contain coordinatively unsaturated molybdenum centre **[5]**.

Reactive metal-ligand multiple bonds are now highly important in organic synthesis and catalysis **[6]**. Molybdenum complexes with highly reactive oxo ligands capable of participating in several reactions with saturated/unsaturated organic molecules constitute an active area of research for defining unprecedented bond constructions and functional group transformation. Coordinatively unsaturated molybdenum complexes containing oxo ligands are of interest because Mo is an electron deficient metal centre which can facilitate initial π-coordination of the unsaturated organic molecule and thus may decide to accommodate the desired adduct. An effort will is on to activate the metal-oxo bond of such complexes by using a spectator ligand effect. The oxo ligand has the potential to be six-electron donors through an σ and two degenerate $p\pi$-$d\pi$ bonds to the metal. In certain configuration of the complexes containing multiply bonded ligands, for example, if mutually cis, the ligands compete for three molybdenum π-orbitals originating from the metal dxy, dyz and dxz orbitals **[7]**. Thus one of the multiply bonded ligands can form a triple bond to the metal as a six electron donor ($1\sigma + 2\pi$) while the other can only form a metal ligand double bond with four electron donor ($1\ \sigma + 1\ \pi$).

These spectator ligands effects contribute to the high reactivity of the metal alkylidene fragment in Schrock's olefin metathesis catalyst which contains imido group alongwith other ligands **[8]**. This catalyst is a real example of a transition metal complex that contains two different multiply bonded ligands. The imido group acts as a six-electron donor, stabilizing the coordinatively unsaturated metal centre and the olefin metathesis reaction manifold, of which cycloaddition with an alkene is the first bond forming step. By analogy, we are interested in studying the structure and reactivity of electron-deficient and coordinatively unsaturated oxo complexes of molybdenum that may undergo similar cycloaddition reactions with a range of unsaturated functionality.

The useful role of molybdenum is not restricted to industrial catalysis alone: nature has also incorporated the molybdenum centre in various redox enzymes such as xanthine oxidase and DMSO reductase **[9]**. In all of these biological reactions,

molybdenum plays the role of a catalytic redox site. Molybdenum enzymes can be conveniently divided into three major groups based on the structure about the metal centre; all of such include one or two pyranopterin cofactor **[10]**. The sulfite oxidase (SO) family also contains a dioxo molybdenum centre coordinated to the dithiolene unit of the pyranopterin along with cysteinyl sulfur from the protein. The group exemplified by xanthine oxidase contains one pyranopterin bound to a $MoO(S)(H_2O)$ unit with no direct protein based ligation. The final group, the DMSO reductase family, is characterized by a monooxo (or sulfide, selenido) molybdenum centre with bis dithiolene coordination from two proteins and a coordination from an endogeneous ligand such as a serinate oxygen or a cysteinato sulfur. However, no such coordination was found in arsenite oxidase, which is also a member of the DMSO reductase family. Boyington et al have suggested that the coordination of the different amino acids controls the substrate specificity among the members of the DMSO reductase family **[11]**. Interestingly, the diversity in the coordination features of the prokaryotic enzymes is represented by nitrate reductase.

The polyfunctional ligands containing o-hydroxy aromatic aldehydes and ketones, azomethine and amide functions in their molecular skeleton are of interest because such ligands form complexes with appropriate transition metals which show promise in the field of molecular magnets, bioinorganic chemistry and chemical reactivity. Metal-ligand bonding in such complexes involves σ-/π-electrons of o-hydroxy aromatic aldehydes and ketones.

There have been numerous reports of transition metal complexes containing polufunctional ligands derived from aromatic aldehydes and ketones **[12]**, with two nitrogen and two oxygen donor atoms as well as other similar ligands **[13]** in which one or both aryl rings are electron-withdrawing. Dihydrazones derived from condensation of acyl-, aroyl-, and pyridoyl-dihydrazines with o-hydroxy aromatic aldehydes and ketones are related ligands possessing four oxygen and four nitrogen donor atoms **[14]**. As the growth of interest in use of polyfunctional ligands containing electron withdrawing fragments in their molecular skeleton becomes

more significant **[15]**, we are interested in the synthesis and characterization of the metal complexes derived from polyfunctional ligands containing electron-withdrawing fragments in their molecular skeleton and to see as if they could readily be prepared and how the chemical reactivity of these molecules varies relative to their corresponding non-electron withdrawing counterparts. In addition, as some of these complexes have potential to show several types of properties, it is interesting to explore how this feature could be modified by the presence of electron-withdrawing groups.

The ligand disalicyaldehyde oxaloyldihydrazone, an example of polyfunctional dihydrazone, has been selected in the present study. The ligand has been derived from condensation of oxaloyldihydrazine with salicylaldehyde and possesses as many as eight oxygen and nitrogen donor atoms and an electron-withdrawing salicyl fragment in its molecular skeleton. The most essential constituents of the ligand skeleton are the oxaloyl fragment and the salicyl fragment. While the oxaloyl fragment is associated with planar characteristics, the salicyl fragments are relatively bulky which may introduce steric crowding in the molecule. A combination of such opposite features in the molecular skeleton of the ligand is expected to confer interesting properties upon the resulting complexes. The dihydrazone can exist either in the staggered configuration **(Fig. 4.1)** or syn-cis configuration **(Fig. 4.2)** and anti-cis configuration **(Fig. 4.3)** in the metal complexes.

Although the ligand is a potential polyfunctional ligand, even then the work done on its metal complexes is quite meagre. 1: 1 (metal: ligand) complexes of copper (II) containing the bridging H_4slox ligand in enol form only have been described **[16]**. In view of the above importance of metal ions containing oxo groups and the meager amount of work done on the metal complexes of the title ligand, the present chapter describes the synthesis and characterization of metal complexes derived from reaction of disalicylaldehyde oxaloyldihydrazone with excess molybdenyl acetyl-acetone in ethanol. The complexes isolated in this chapter are characterized by various physico-chemical techniques and spectroscopic methods. The stoichiometry

of the complexes has been judged mainly from elemental analyses and thermogravimetric data. The structure of the complexes has been discussed in the light of conductivity, magnetic moment, electronic, IR and ^{1}H NMR spectral data.

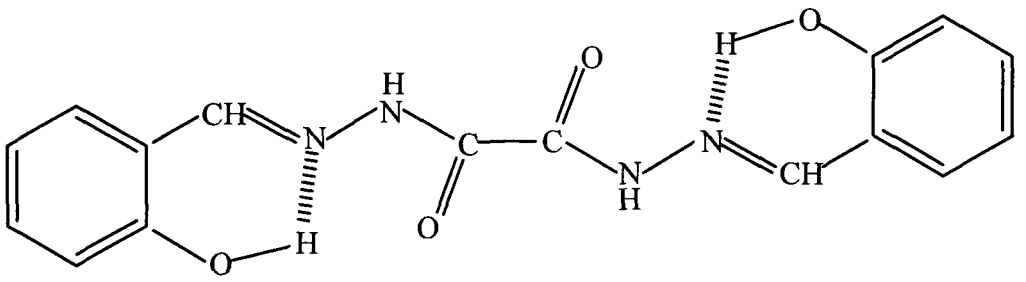

Fig. 4.1: Staggered configuration

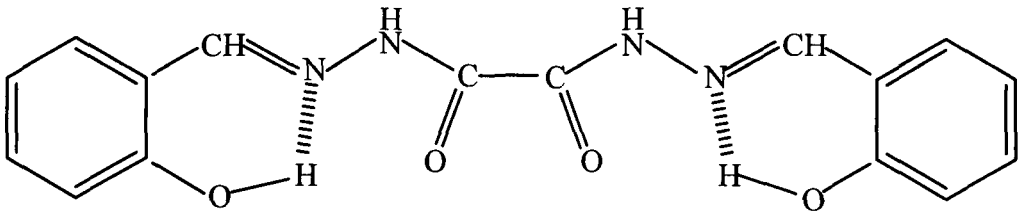

Fig. 4.2: Syn-cis configuration

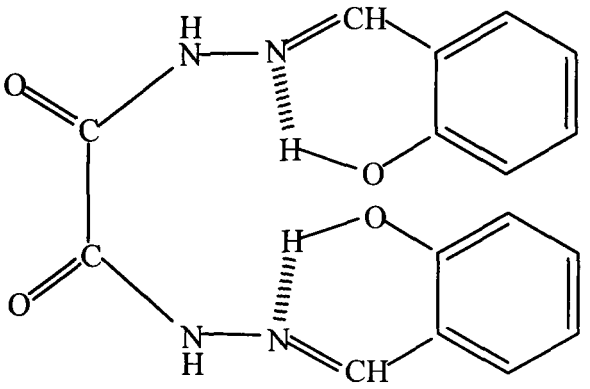

Fig. 4.3: Anti-cis configuration

Experimental

Preparation of $[(MoO_2)_2(slox)(H_2O)_2]$ (4.1)

About 0.50 g (1.53 mmol) of dihydrazone ligand (H_4slox) was suspended in ethanol (30 mL) containing 2.5 mL H_2O with constant stirring to make the suspension homogenous. This homogeneous suspension was then added slowly to $MoO_2(acac)_2$ (1.10 g, 3.37 mmol) solution in ethanol (30 mL) over a period of 15 – 20 minutes with constant stirring. The resulting mixture was refluxed for 1 h which yielded a yellow coloured precipitate. This yellow coloured precipitate was suction filtered, purified by washing several times with 10 mL hot ethanol each time followed by ether and finally dried over anhydrous $CaCl_2$. Yield: 71.7%.

Preparation of $[(MoO_2)_2(slox)(A)_2]$ {*where A = pyridine (py)* **(4.2)**, *2-picoline (2-pic)* **(4.3)**, *3-picoline (3-pic)* **(4.4)** *and 4-picoline (4-pic)* **(4.5)**}

In order to prepare $[(MoO_2)_2(slox)(py)_2]$ **(4.2)**, 0.5 g (1.53 mmol) of H_4slox was suspended in ethanol (30 mL) with constant stirring to make the solution homogenous. This homogeneous suspension was added to $MoO_2(acac)_2$ (1.10 g, 3.37 mmol) solution in ethanol (30 mL) with constant stiiring in hot condition. The resulting mixture was further stirred for another 15-20 minutes and then put to reflux for about 1 h. To this hot mixture was then added 1. 3 mL of pyridine drop by drop accompanied by stirring and refluxed for another 30 minutes when a yellow colured complex was obtained. The yellow coloured complex thus obtained was suction filtered in hot condition, purified by washing several times with 10 mL of hot ethanol each time followed by ether and finally dried over anhydrous $CaCl_2$. Yied: 73.2%.

The complexes $[(MoO_2)_2(slox)(A)_2]$ {*where A = 2-picoline (2-pic)* **(4.3)**, *3-picoline (3-pic)* **(4.4)** *and 4-picoline (4-pic)* **(4.5)**} were also prepared essentially by following the above mentioned procedure using 1.4 mL of 2-picoline, 3-picoline and 4-picoline, respectively., instead of pyridine. Yield: 70.8% - 75.5%.

Results and discussion

The complexes described in the present chapter together with their molecular formula, colour, decomposition point, yield, analytical data, molar conductance values and electronic spectral data are given in **Table 4.1**.

Reaction of $MoO_2(acac)_2$ with the title ligand disalicylaldehyde oxaloyldihydrazone (H_4slox) in 3:1 molar ratio in ethanolic medium as such or in the presence of electron donor bases under reflux resulted in the formation of the complexes with the following compositions:

$[(MoO_2)_2(slox)(A)_2]$ {*where A = H_2O* **(4.1)**, *pyridine (py)* **(4.2)**, *2-picoline (2-pic)* **(4.3)**, *3-picoline (3-pic)* **(4.4)** *and 4-picoline (4-pic)* **(4.5)**}.

The compositions of the complexes have been judged on the basis of elemental analyses, thermo-analytical data and other spectroscopic data. All of the complexes are yellow coloured and air stable and decompose above 300°C. All the complexes are insoluble in water and common organic solvents such as ethanol, methanol, acetone, benzene, chloroform, hexane and ether but are soluble in highly coordinating solvents such as DMSO and DMF.

When the reaction of $MoO_2(acac)_2$ with H_4slox in ethanol in presence of phen and bpy keeping $MoO_2(acac)_2$: H_4slox : NN (NN = phen and bpy) molar ratios at 3:1:3 under reflux, was carried out, the complexes $[(MoO)_2(H_2slox)(NN)]$ described in chapter III only were obtained. Hence, further discussion on these complexes is redundant.

Thermal analyses

Detailed decomposition studies **[17]** of the dioxomolybdenum (VI) complexes **(4.1)** to **(4.5)** were carried out in the temperature range 70 – 250°C and the vapours

evolved were identified by passing through a separate test tube containing anhydrous copper sulfate, chloroform solution with a drop of 5M sodium hydroxide, solution of iodine and sodium hydroxide and cyanogen bromide solution respectively. The complexes showed weight loss in two temperature ranges. The complex **(4.1)** showed weight loss in the temperature range 70-80°C and 150-180°C while the remaining complexes showed weight loss in the temperature range 70-80°C and 220-240°C respectively. All the complexes gave a yellow precipitate with a solution of iodine and sodium hydroxide in temperature range of 70-80°C indicating the possibility of presence of ethanol molecules in their lattice structure **[17]**.

The vapours evolved in the complex **(4.1)** in the temperature range 150-180°C turned a test tube containing anhydrous copper sulfate blue indicating presence of water molecules inside the coordination sphere of the complex **[18]**. The loss of weight was calculated and it was found to be due to two water molecules only. No weight loss occurred in the temperature range 150-180°C in rest of the complexes indicating absence of coordinated water molecules. The vapours evolved in the complex **(4.2)** in the temperature range 220-240°C turned a test tube containing $CHCl_3$ and NaOH solution red confirming that they originate from coordinated pyridine molecule. On the other hand, the vapours evolved in the temperature range 220-240°C in the complex **(4.4)** turned the colour of cyanogen bromide solution to green-violet on treatment with phloroglucinol solution suggesting the presence of 3-picoline molecule **[17]**. Similarly the vapours evolved in the complex **(4.5)** turned the colour of cyanogen bromide solution to blue on treatment with phloroglucinol solution. The weight loss in the temperature range 220-240°C corresponded to pyridine/picoline molecules. The loss of these donor molecules at such a high temperature indicated presence in the coordination sphere around the metal centre.

Molar conductance

The molar conductance value for the dioxomolybdenum (VI) complexes **(4.1)** to **(4.5)** lies in the range 1.8 – 5.0 $ohm^{-1}cm^2mol^{-1}$. Such a low value of molar

conductance for the above mentioned complexes indicates its non-electrolytic nature in DMSO **[19]**.

Magnetic moment

The room temperature magnetic susceptibility measurements of all the complexes were carried out in order to decide upon the magnetic behavior. All the dioxomolybdenum (VI) complexes mentioned in this chapter were found to be diamagnetic in nature which indicates that the molybdenum atom is present in +6 oxidation state with d^0 electronic configuration **[20]**.

Electronic spectra

The important electronic spectral bands for the homobimetallic molybdenum (VI) complexes along with molar extinction coefficients have been given in **Table 4.1**. The electronic spectra of the the complexes **(4.1)**, **(4.3)** and **(4.4)** have been shown in the **Figs. 4.4-4.6**.

The free ligand shows three bands at 293 nm, 303 nm and 340 nm. The band at 293 nm and 303 nm are assigned to intraligand $\pi \rightarrow \pi^*$ transition **[21-23]** while the band at 340 nm is assigned to $n \rightarrow \pi^*$ transition. The band at 340 nm is characteristic of salicyaldimine part **[24]** as has been reported in several monoacylhydrazones. The electronic spectra of the complexes were recorded in DMSO due to their poor solubility in common organic solvents. The electronic spectra of the complexes show three bands in the region 292 – 341 nm and an additional broad band in the region 417 – 432 nm. The bands in the region 292 – 341 nm are assigned to intraligand $\pi \rightarrow \pi^*$ and $n \rightarrow \pi^*$ and that in the region 417 – 432 nm is assigned to ligand-to-metal charge transfer (LMCT) transition due to its high molar extinction coefficients which lies in the range 1300-1710 $dm^3cm^{-1}mol^{-1}$. This ligand-to-metal charge transfer transition may have its origin from HOMO of phenolate oxygen atom to the LUMO of molybdenum **[25]**.

Proton nuclear magnetic resonance spectra

The ^{1}H NMR spectral data for the complexes **(4.1)** to **(4.5)** is presented in the **Table 4.2**. The spectra of the complexes **(4.1)**, **(4.2)** and **(4.3)** are shown in the **Figs. 4.7-4.9**. The two proton signals observed at δ12.64 ppm and δ11.00 ppm assigned to δ (-OH) and δ (>NH) protons, respectively, in free dihydrazone disappears in the dioxomolybdenum (VI) complexes **(4.1)** to **(4.5)**. The absence of signals around δ12.64 ppm and δ11.00 ppm due to -OH and >NH protons, respectively, in the metal complexes indicates the involvement of both the -OH and >NH groups of the dihydrazone in coordination to the molybdenum atom. The absence of signal due to -OH proton clearly suggests that the -OH group is involved in coordination with the molybdenum atom in the enol form through phenolate oxygen atoms via deprotonation. The absence of >NH proton signal in the ^{1}H NMR spectra of the complexes indicates destruction of >NH group and formation of NCO group via enolization which then coordinates to the molybdenum atom through oxygen atom. The signal due to azomethine proton is split into two doublets in the complexes **(4.1)** to **(4.5)** as compared to one singlet in the free dihydrazone. The doublets on an average show a downfield shift of about 0.11 ppm. The average downfield shift of the azomethine proton signals in the ^{1}H NMR spectra of the complexes indicates coordination of the azomethine nitrogens to the metal centre **[26]**. The appearance of two doublets due to azomethine protons in the dioxomolybdenum (VI) complexes **(4.1)** to **(4.5)** as compared to a singlet in free dihydrazone molecule suggests that the two hydrazone groups are oriented differently in the metal complexes. The difference between the two azomethine proton doublets is of the order of about 0.26 ppm which is quite reasonable for the existence of the dihydrazone in metal metal complexes in anti-cis configuration.

The multiplet appearing in the region δ7.81-6.90 ppm in all of the complexes is attributed to arise due to phenyl protons. Apart from the multiplets due to the phenyl protons, new signal appears at δ8.58, δ7.61 and δ7.35 in complex **(4.2)**. These signals are assigned to arise due to ortho, para and meta protons, respectively, of the

pyridyl ring **[27, 28]** of pyridine molecule. In complexes **(4.3)** and **(4.4)**, the ortho proton signal due to pyridyl ring **[27]** of 2-picoline and 3-picoline molecules appears at δ8.43 ppm and δ8.30 ppm respectively; whereas in complex **(4.5)**, the ortho proton signal due to pyridyl ring of 4-picoline molecule appears at δ8.41 ppm. The signal due to meta and para protons in complexes **(4.3)** to **(4.5)** is not clearly visible as it appears merged with the signals due to phenyl protons. The signal due to ortho protons of pyridyl ring of pyridine/picoline molecule is upfield shifted as compared to the ortho proton signal of free pyridine/picoline molecules, respectively **[29]**. The upfield shift of the ortho proton signal in complexes **(4.2)** to **(4.5)** indicates the possibility of coordination of pyridine and picoline molecules to the metal centre. As a result of coordination of the pyridyl nitrogen, the electron density on pyridyl nitrogen decreases which in turn decreases its electronegativity and consequently the electron density on various bonds of pyridyl ring i.e. C-N, C-C, C-H, drifts away from nitrogen atom. This increases the electron density on various carbon atoms and protons away from nitrogen atom. As a result, the electron density on various types of pyridyl protons is increased which results in the upfield shift of the signals due to these protons in the ^{1}H NMR spectra of the complexes **(4.2)** to **(4.5)**. In complexes **(4.3)** and **(4.4)**, a new signal appears at δ2.50 ppm and δ2.45 ppm, respectively, which are assigned to arise due to methyl protons of 2-picoline and 3-picoline molecules respectively. However, in complex **(4.5)**, the methyl proton signal due to 4-picoline molecule appears at δ2.30 ppm. Methyl proton signals are also upfield shifted in the complexes as compared to their position in the free picoline molecules, respectively. This is due to coordination of the pyridyl nitrogen atoms to the metal centre and hence further discussion on the matter is redundant.

Complexes **(4.1)** to **(4.5)** show a triplet in the region δ1.03-1.06 ppm, quartet in the region δ3.21-3.43 and another triplet in the region δ4.35-4.37 ppm. These signals are assigned to methyl protons, methylene protons and -OH protons of ethanol molecules **[30]** present in the lattice structure of the complexes.

Infrared spectra

Some of the structurally significant IR spectral data for the complexes have been set out in the **Table 4.3**. The IR spectra of the complexes **(4.1)**, **(4.2)** and **(4.3)** have been shown in the **Figs. 4.10-4.12**. The bands at 3278 and 3204 cm^{-1} assigned to stretching vibrations of phenolic -OH and secondary >NH group, respectively, in the ligand are absent in the metal complexes **(4.1)** to **(4.5)**. The absence of band around 3278 cm^{-1} in the complexes suggests the involvement of phenolic -OH group in coordination to the metal centre via deprotonation. Further the absence of band around 3204 cm^{-1} indicates the destruction of secondary >NH group upon coordination with the metal centre. The appearance of a new medium to strong intensity band in the region 3448 – 3436 cm^{-1} in the complexes have been attributed to arise due to the stretching vibration of the -OH group of ethanol molecules present in the complexes. In the complex **(4.1)**, the band is attributed to have contribution due to coordinated water molecules as well. The υ (>C=O) band which appears at 1667 cm^{-1} in the ligand is also absent in the complexes **(4.1)** to **(4.5)**. The disappearance of υ (>C=O) band in the complexes indicates that the ligand coordinates to the metal centre through >C=O group via enolization. Enolization of >C=O group is also supported by the absence of NH group in the metal complexes. The absence of band due to υ (>C=O), υ (>NH) and υ (-OH) indicates that both the hydrazone part of the ligand molecule are involved in bonding to the metal centre through >C=O group via enolization and phenolic -OH group via deprotonation.

A single strong band in the ligand appearing at 1534 cm^{-1} has been assigned to the stretching vibration of amide II + υ (C-O) group. This band is split into two strong intensity bands and appears around 1553 and 1535 cm^{-1}, respectively. One of the bands is shifted to higher frequency in all of the complexes and appears in the region around 1553 cm^{-1} whereas the other band appearing around 1535 cm^{-1} is almost unshifted in all of the complexes. The higher frequency shift of this band is related to bonding between phenolate oxygen atom and molybdenum atom whereas the unshifted band at 1535 cm^{-1} is assigned to stretching vibration of newly formed NCO

group produced as a result of enolization of the ligand upon complexation with the molybdenum atom. Enolization of the ligand is confirmed by the absence of bands due to stretching vibration of secondary >NH group and >C=O group in the infrared spectra of the complexes. The stretching vibration of >C=N- group appearing as a two strong intensity band at 1627 and 1603 cm^{-1} in the free dihydrazone on an average is shifted to lower frequency by 11-14 cm^{-1} and appears in the region 1604 – 1602 cm^{-1} in all of the dioxomolybdenum (VI) complexes. The shift of the band due to υ (>C=N-) to lower frequency indicates coordination of the azomethine nitrogen atom to the metal centre **[31]**. The band at 1262 cm^{-1} assigned to the stretching vibration of (C-O) group **[32]** in the ligand shows high frequency shift by 11 – 12 cm^{-1} in the complexes indicating the coordination of the (C-O) group to the metal centre via deprotonation of the phenolic -OH group. The region below 1200 cm^{-1} has been scrutinized for locating υ (N–N) vibration and various C–H vibrations. The weak band observed at 1035 cm^{-1} in the ligand can be assigned to υ (N–N) vibration. This band remains almost unshifted in position in the metal complexes indicating coordination of only one nitrogen atom of N-N group. Two strong bands appearing in the region 951 – 912 cm^{-1} in complexes **(4.1)** to **(4.5)** are assigned to the stretching vibration of the cis-MoO_2^{2+} group **[33]**. The band in the region 951 – 933 cm^{-1} is due to the symmetric stretching vibration of cis-MoO_2^{2+} group while the band in the region 916 – 902 cm^{-1} is due to the antisymmetric stretching vibration of the cis-MoO_2^{2+} group.

The uncoordinated pyridine bases absorb at around 604 cm^{-1}due to in-plane ring deformation mode **[34]**. In the complexes a new medium to weak band is observed in the region 600 – 620 cm^{-1}. This band is assigned to arise due to in-plane deformation mode of pyridine and substituted pyridine indicating their coordination to the metal centre. The molybdenum (VI) complexes **(4.2)** to **(4.5)** also show a weak intensity band in the region 1060-1003 cm^{-1}, which is assigned to ring stretching mode of pyridine, 2-picoline, 3-picoline and 4-picoline molecules **[35]**.

Conclusion

In this chapter five homobimetallic molybdenum (VI) complexes have been prepared and characterized on the basis of data obtained from physico-chemical and spectroscopic studies. The complexes were prepared by reacting $MoO_2(acac)_2$ with the ligand (H_4slox) in 3:1 molar ratio in ethanol. The ligand in the complexes was found to exist in enol form adopting anti-cis configuration. Whereas one metal atom occupies the N_2O_2 coordination chamber (two phenolate oxygen atoms and two azomethine nitrogen atoms). The other metal atom occupies either O_2O_2 coordination chamber (two oxygen atom from enolate carbonyl oxygen atoms and two from water molecules) or N_2O_2 coordination chamber (two oxygen atoms from enolate oxygen atoms and two nitrogen atoms from pyridyl nitrogen atoms). All the complexes are suggested to have anti-cis configuration with octahedral geometry around molybdenum centre. The tentative structure for the complexes is shown in the **Fig. 4.13**.

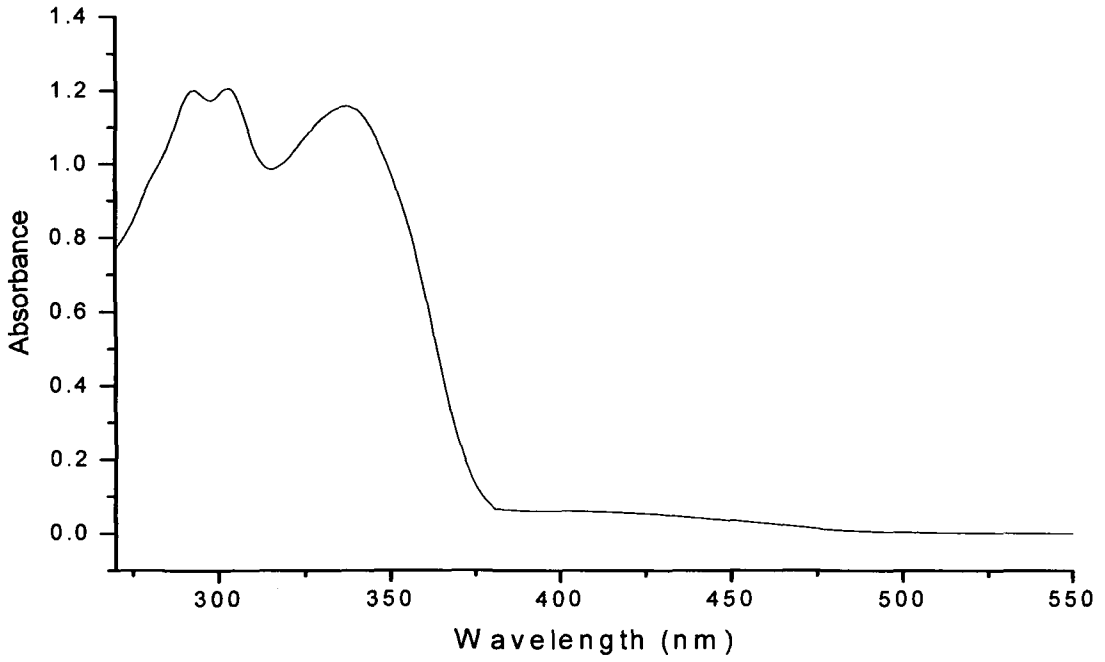

Fig. 4.4 Electronic spectrum of $[MoO_2)_2(slox)(H_2O)_2].C_2H_5OH$ **(4.1)**.

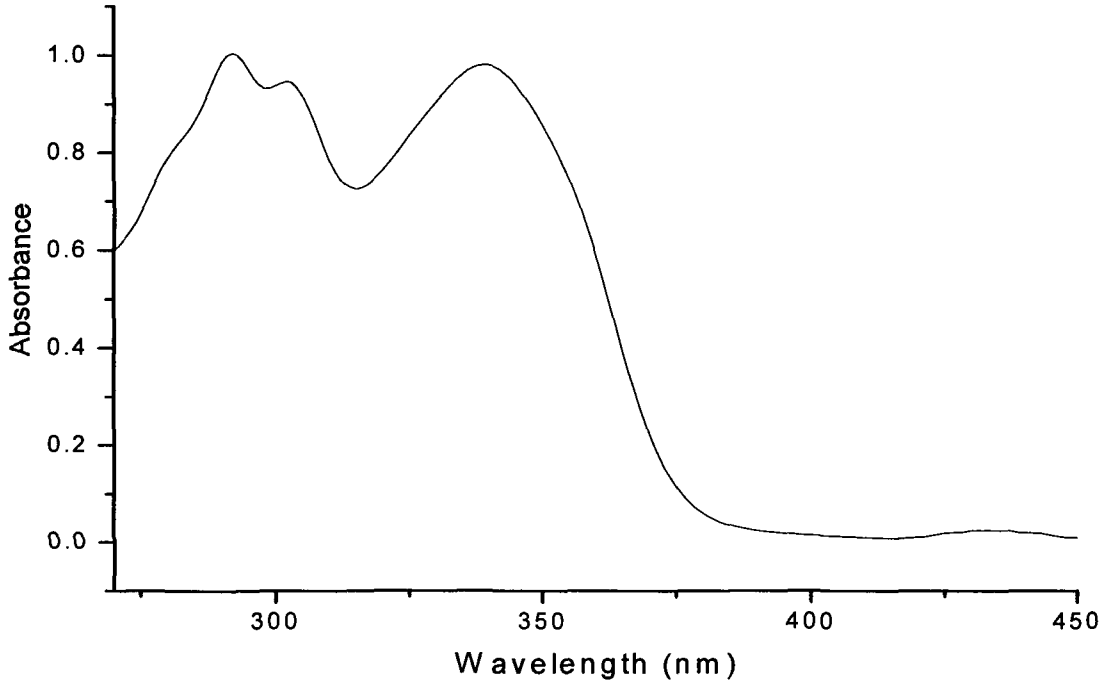

Fig. 4.5 Electronic spectrum of $[MoO_2)_2(slox)(2\text{-pic})_2].C_2H_5OH$ **(4.3)**.

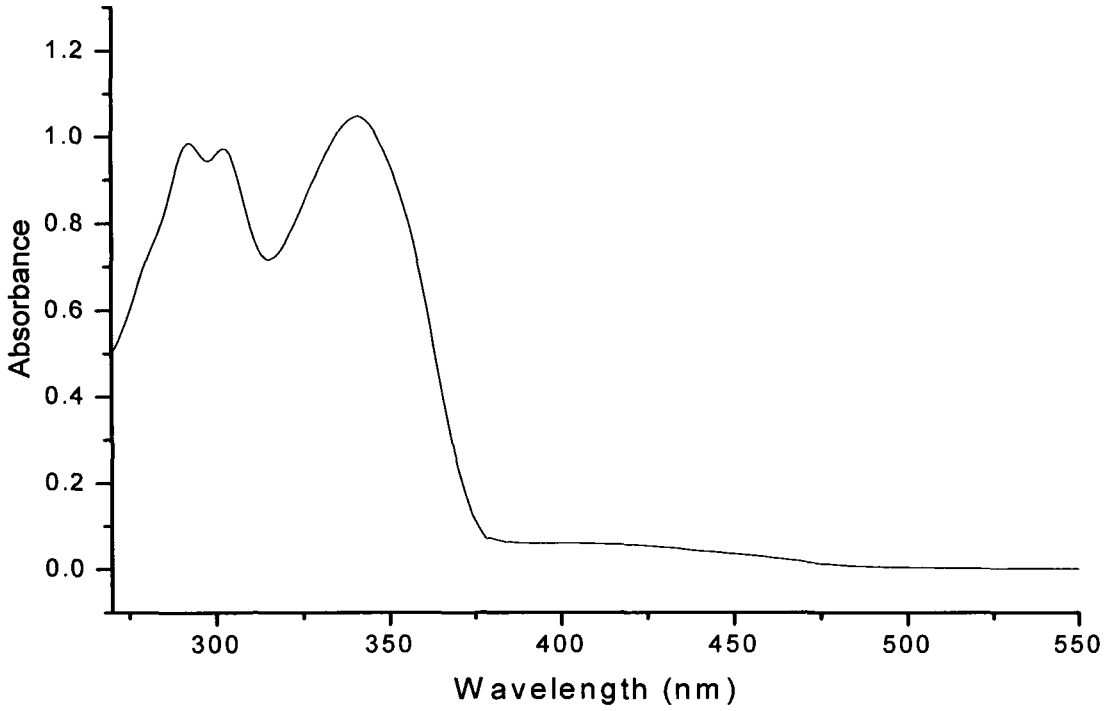

Fig. 4.6 Electronic spectrum of $[MoO_2)_2(slox)(3\text{-}pic)_2].C_2H_5OH$ **(4.4)**.

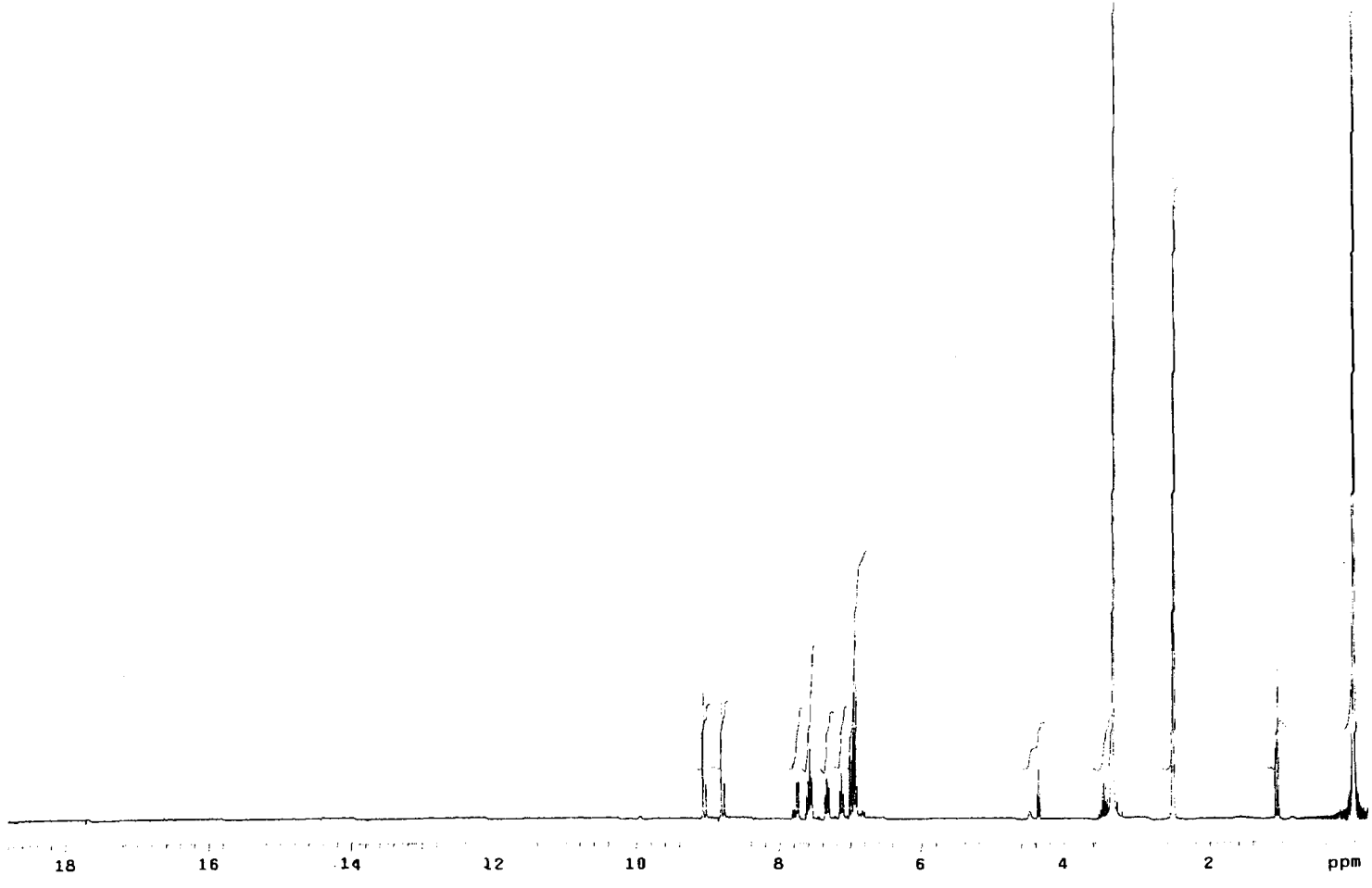

Fig. 4.7 ^{1}H NMR spectrum of $[MoO_2)_2(slox)(H_2O)_2].C_2H_5OH$ **(4.1)** in DMSO-d_6.

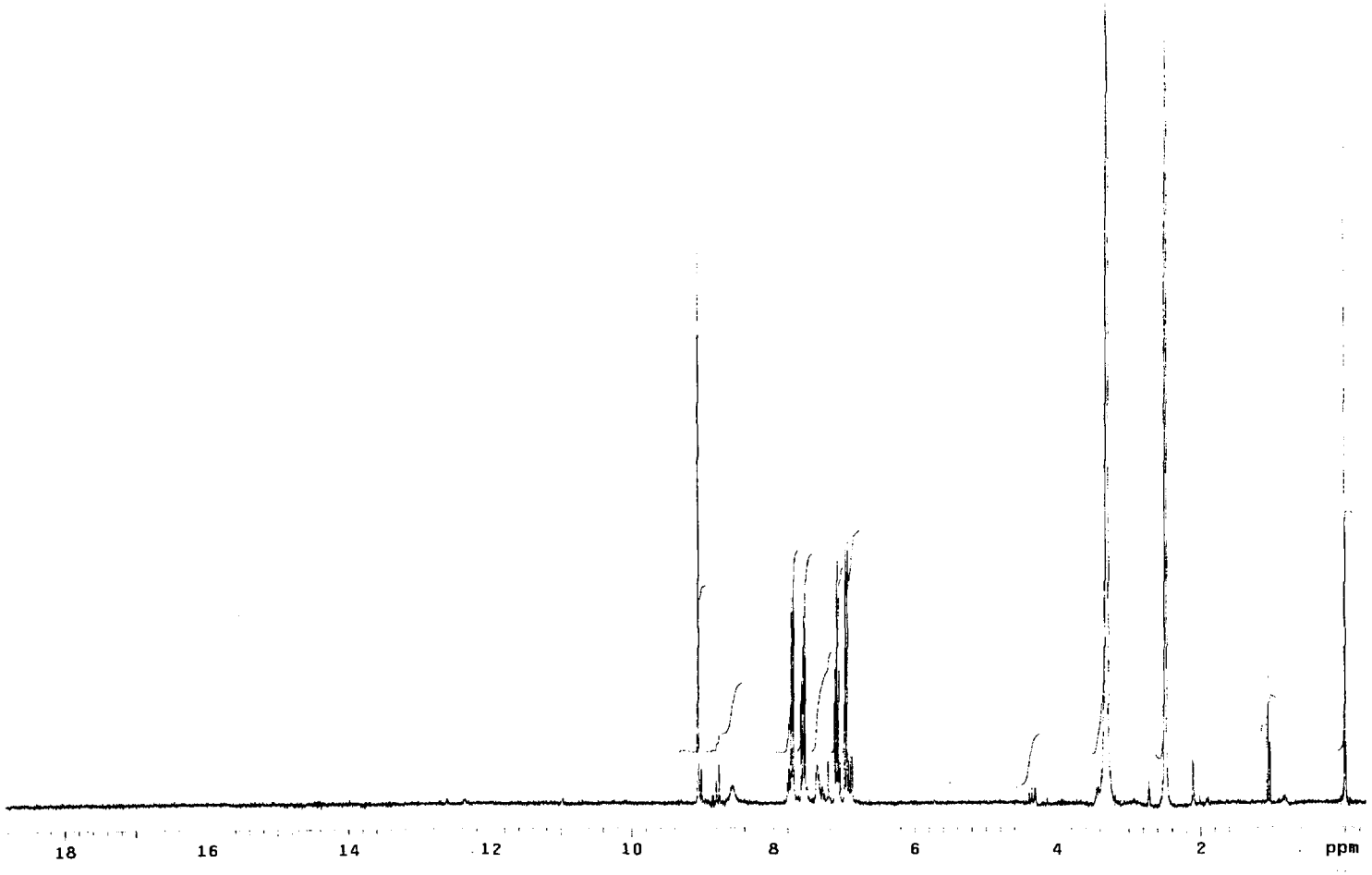

Fig. 4.8 ^{1}H NMR spectrum of $[MoO_2)_2(slox)(py)_2].C_2H_5OH$ **(4.2)** in DMSO-d_6.

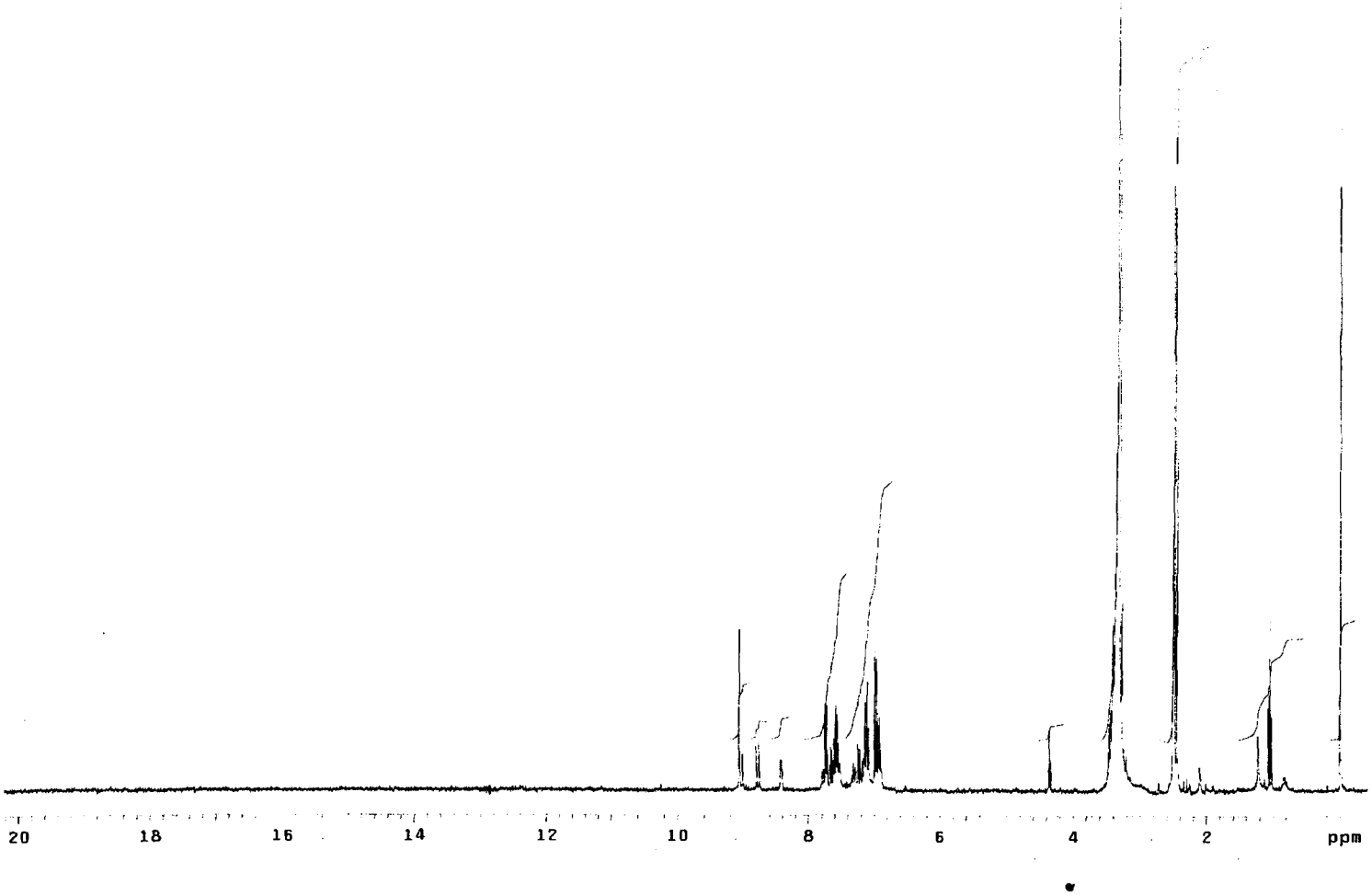

Fig. 4.9 ^{1}H NMR spectrum of $[MoO_2)_2(slox)(2\text{-pic})_2].C_2H_5OH$ **(4.3)** in DMSO-d_6.

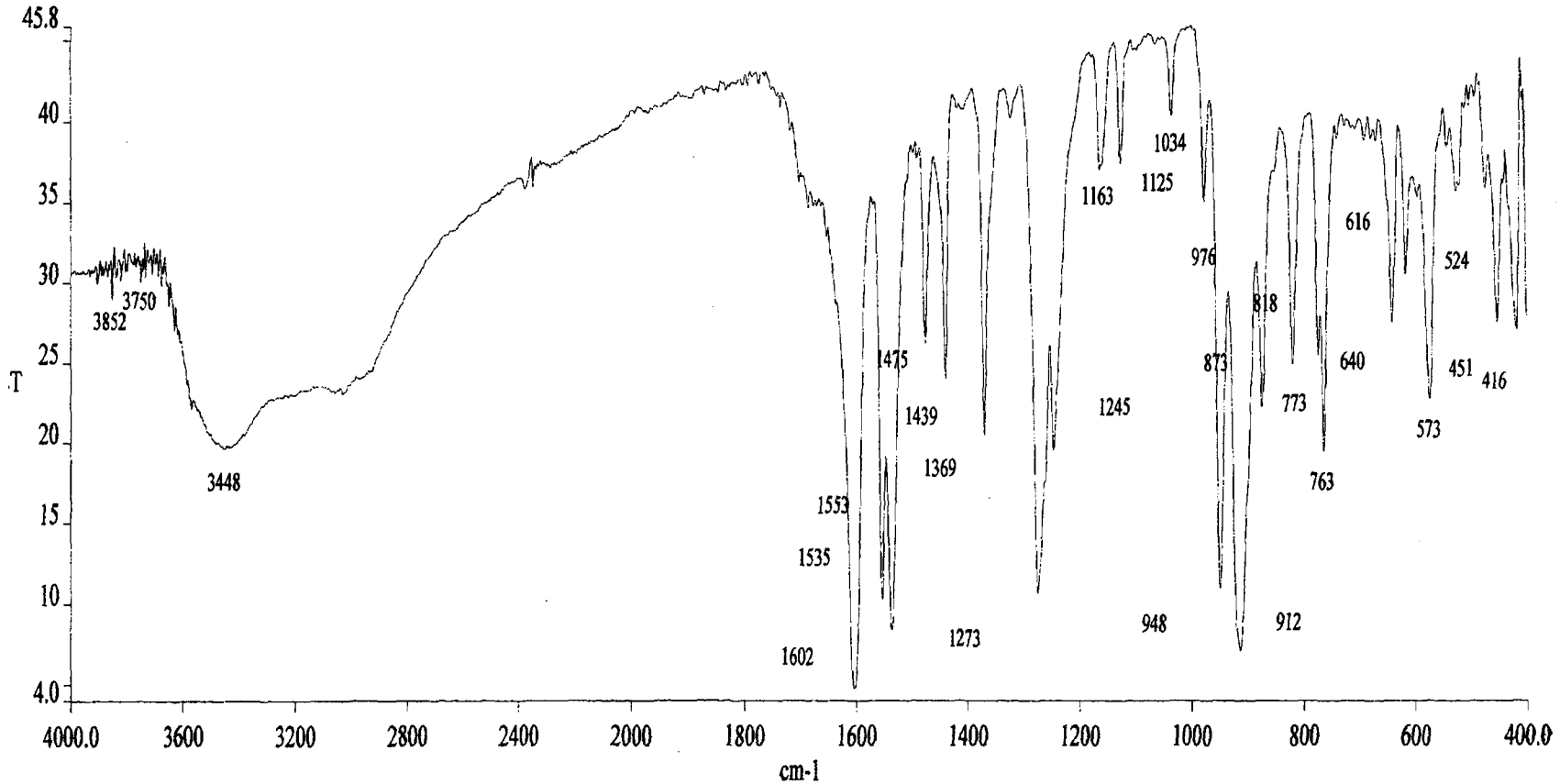

Fig. 4.10 Infrared spectrum of $[MoO_2)_2(slox)(H_2O)_2].C_2H_5OH$ **(4.1)** in KBr.

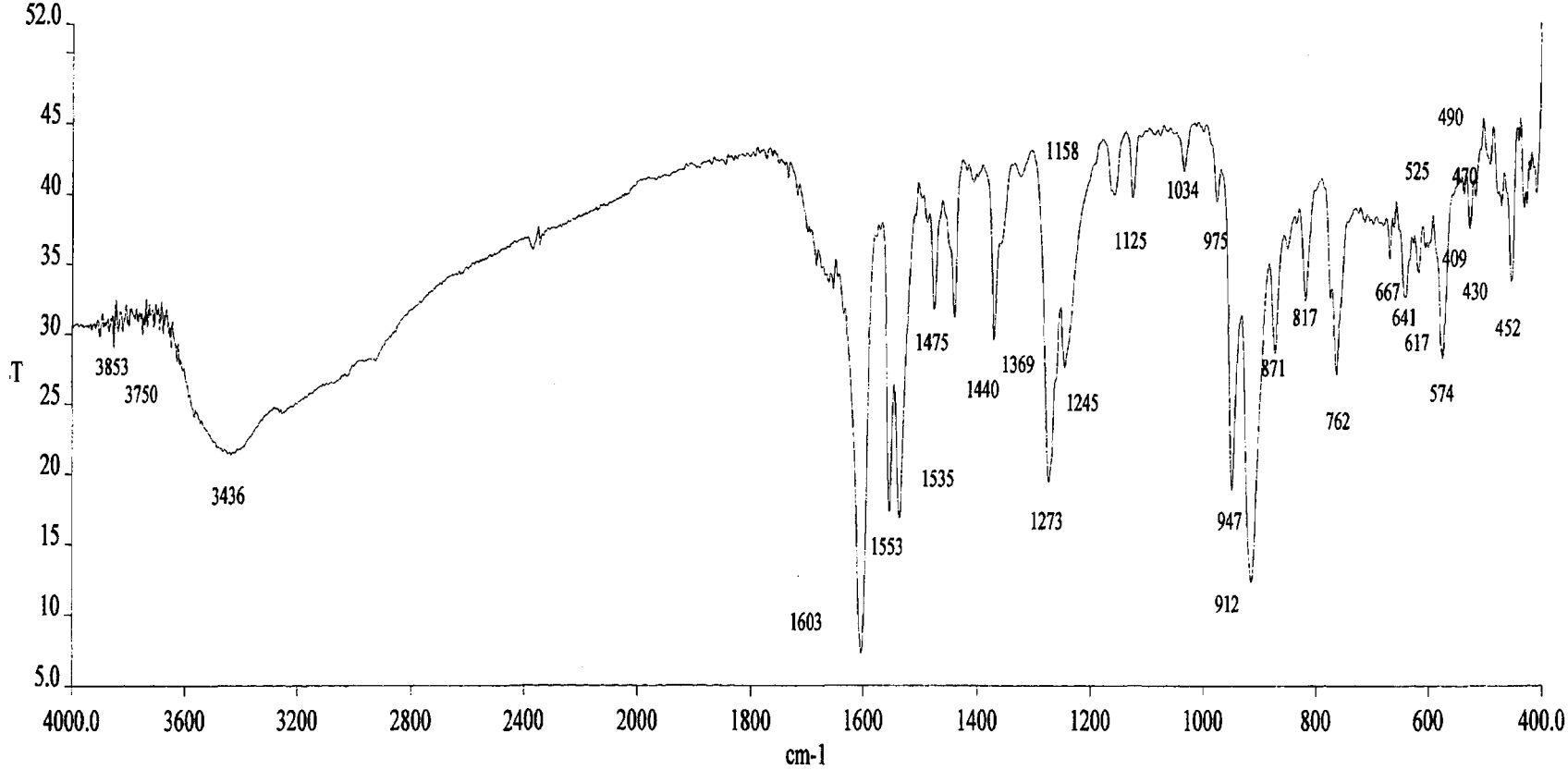

Fig. 4.11 Infrared spectrum of $[MoO_2)_2(slox)(py)_2].C_2H_5OH$ **(4.2)** in KBr.

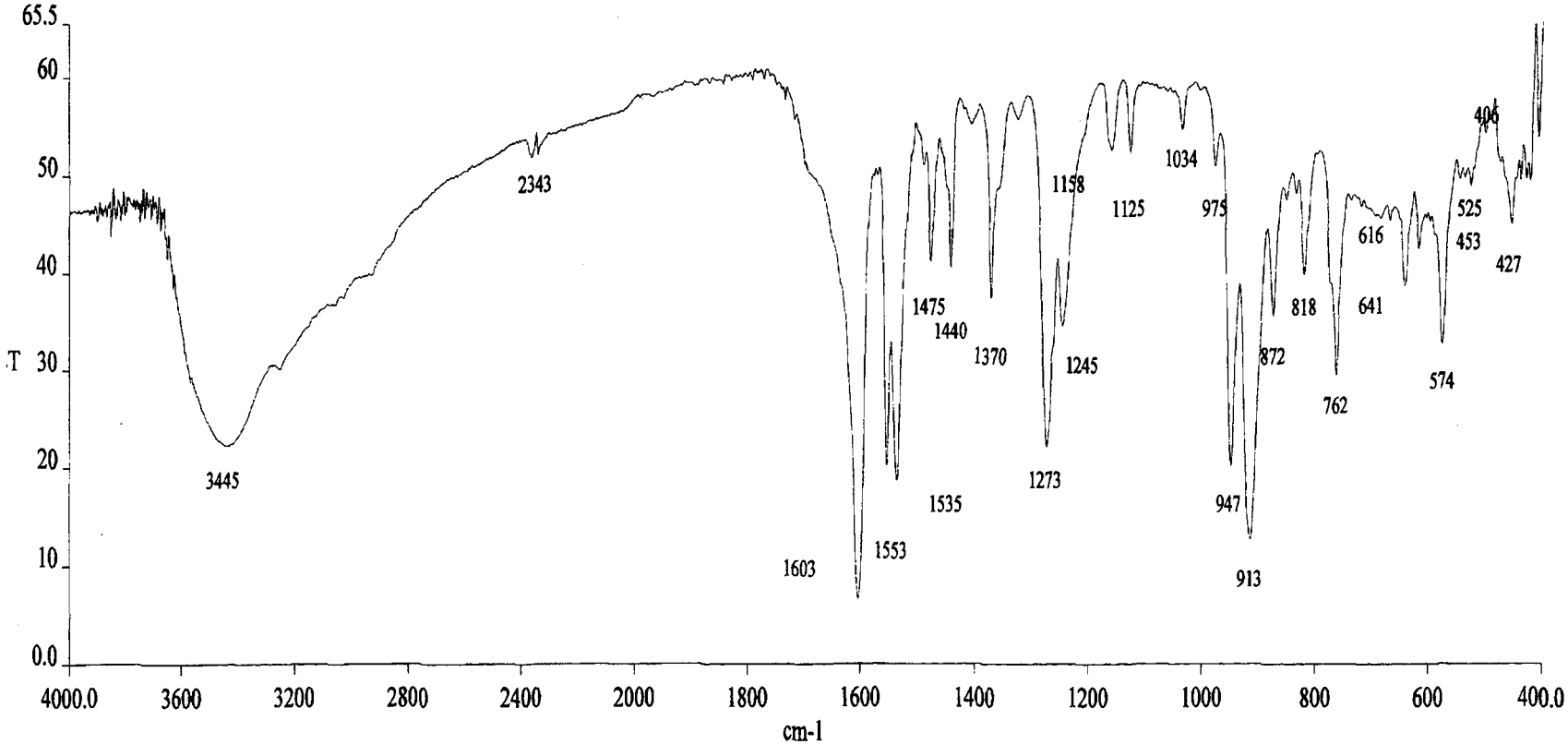

Fig. 4.12 Infrared spectrum of $[MoO_2)_2(slox)(2\text{-pic})_2].C_2H_5OH$ **(4.3)** in KBr.

Table 4.1: Analytical, colour, decomposition point, molar conductance and electronic spectral data for homobimetallic molybdenum (VI) complexes.

Sl No	Complex (Colour)	D.P (°C)	Elemental Analyses: Found (Calcd)%				Molar conductance Λ_M (ohm^{-1} cm^2mol^{-1})	Electronic spectral band λ_{max}(nm) (ε_{max})(dm^3 $mol^{-1}cm^{-1}$)
			M	C	H	N		
4.1	$[(MoO_2)_2(slox)(H_2O)_2].C_2H_5OH$ (Yellow)	>300	30.88 (30.56)	30.96 (30.69)	2.27 (2.25)	9.13 (8.92)	1.8	294(14950) 304(14988) 337(14462) 427(1310)
4.2	$[(MoO_2)_2(slox)(py)_2].C_2H_5OH$ (Yellow)	>300	26.01 (25.58)	41.98 (41.63)	2.70 (2.68)	10.98 (11.20)	3.2	292(13710) 302(13380) 338(13350) 424(1620)
4.3	$[(MoO_2)_2(slox)(2\text{-}pic)_2].C_2H_5OH$ (Yellow)	>300	25.02 (24.66)	43.75 (43.21)	3.33 (3.36)	11.21 (10.80)	2.4	292(14358) 303(13500) 340(14258) 432(1710)
4.4	$[(MoO_2)_2(slox)(3\text{-}pic)_2].C_2H_5OH$ (Yellow)	>300	24.92 (24.66)	43.57 (43.21)	3.34 (3.36)	11.01 (10.80)	3.8	293(15375) 303(15173) 341(16363) 424(1450)
4.5	$[(MoO_2)_2(slox)(4\text{-}pic)_2].C_2H_5OH$ (Yellow)	>300	25.12 (24.66)	43.66 (43.21)	3.39 (3.36)	10.51 (10.80)	5.0	293(15800) 303(15300) 341(15900) 417(1300)

Table 4.2: ^{1}H NMR spectral data for homobimetallic molybdenum (VI) complexes.

Sl No	Ligand/Complex	δ(OH)	δ(NH)	δ(CH=N)	δ(phenyl protons)	δ(pyridyl protons)		C_2H_5OH		
						o-proton	δ(CH_3)	δ(CH_3)	δ(CH_2)	δ(OH)
	H_4slox	12.64(s)	11.00(s)	8.81(s)	7.57 – 6.84(m)	--	--	--	--	--
4.1	$[(MoO_2)_2(H_2slox)(H_2O)_2].C_2H_2OH$	--	--	9.05(d, 13.8Hz) 8.79(d, 12.3Hz)	7.81 – 6.90(m)	--	--	1.06(t)	3.46(q)	4.35(t)
4.2	$[(MoO_2)_2(slox)(py)_2].C_2H_2OH$	--	--	9.05(d, 14.1Hz) 8.79(d, 12.9Hz)	7.81 – 6.90(m)	8.58 (8.61)[a]	--	1.06(t)	3.43(q)	4.36(t)
4.3	$[(MoO_2)_2(slox)(2\text{-}pic)_2].C_2H_2OH$	--	--	9.05(d, 13.5Hz) 8.79(d, 12.6Hz)	7.81 – 6.93(m)	8.43 (8.48)[a]	2.50 (2.55)[b]	1.06(t)	3.43(q)	4.37(t)
4.4	$[(MoO_2)_2(slox)(3\text{-}pic)_2].C_2H_2OH$	--	--	9.05(d, 15.3Hz) 8.78(d, 15.0Hz)	7.81 – 6.90(m)	8.30 (8.44 and 8.42)[a]	2.45 (2.32)[b]	1.04(t)	3.43(q)	4.36(t)
4.5	$[(MoO_2)_2(slox)(4\text{-}pic)_2].C_2H_2OH$	--	--	9.05(d, 14.4Hz) 8.79(d, 10.2Hz)	7.76 – 6.92(m)	8.41 (8.60)[a]	2.30 (2.32)[b]	1.25(t)	3.21(q)	4.35(t)

a, δ values for o-pyridyl proton of free pyridine and substituted pyridine.
b, δ values for methyl protons of free substituted pyridine molecule.

Table 4.3: Infrared spectral data for homobimetallic molybdenum (VI) complexes.

Sl. No.	Ligand/complex	ν(OH) + ν(NH)	ν(C=O)	ν(C=N)	AmideII + ν(C-O) (phenolic)	ν(NCO)	ν(C-O)	ν(N-N)	ν(MoO_2^{2+})	ν(M-O) (phenolic)	ν(M-O) (enolic)
	H_4 slox	3278(s) 3204(s) 3050(s)	1667(s)	1627(s) 1603(s)	1534(s)	--	1262(s)	1054(m) 1035(m)	--	--	--
4.1	$[(MoO_2)_2slox(H_2O)_2].C_2H_5OH$	3448(m)	--	1602(s)	1553(s)	1535(s)	1273(s)	1034(w)	948(s) 912(s)	573(m)	451(m)
4.2	$[(MoO_2)_2slox\ (py)_2].C_2H_5OH$	3436(m)	--	1603(s)	1553(s)	1535(s)	1273(s)	1034(w)	947(s) 912(s)	574(m)	452(m)
4.3	$[(MoO_2)_2slox(2\text{-}pic)_2].C_2H_5OH$	3445(s)	--	1603(s)	1553(s)	1535(s)	1273(s)	1034(w)	947(s) 913(s)	574(m)	453(w)
4.4	$[(MoO_2)_2slox(3\text{-}pic)_2].C_2H_5OH$	3436(s)	--	1603(s)	1553(s)	1537(s)	1274(s)	1034(w)	948(s) 912(s)	574(m)	451(w)
4.5	$[(MoO_2)_2slox(4\text{-}pic)_2].C_2H_5OH$	3437(m)	--	1604(s)	1553(s)	1535(s)	1273(s)	1034(w)	947(s) 913(s)	573(m)	452(w)

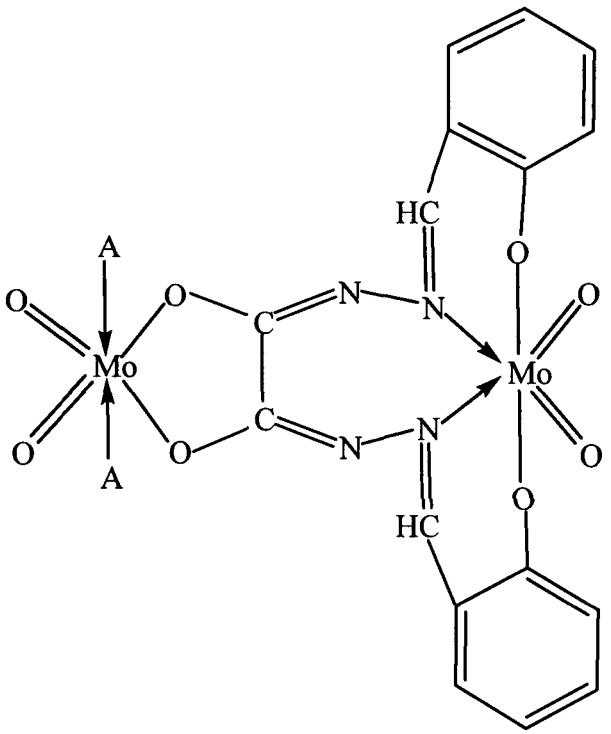

Fig. 4.13 Tentative structure of the complexes $[(MoO_2)_2(slox)(A)_2]$ {*where A = H_2O* **(4.1)**, *pyridine* **(4.2)**, *2-picoline* **(4.3)**, *3-picoline* **(4.4)**, *4-picoline* **(4.5)**}.

References

1. G. C. Tucci, J. P. Donahue and R. H. Holm, *Inorg. Chem.*, **37**, 1602 (1998).
2. H. M. Hoyt, F. E. Michael and R. G. Bergman, *J. Am. Chem. Soc.*, **26**, 1018 (2004).
3. C. J. Carrano, B. S. Chohan, B. S. Hammes, B. W. P. Kail, V. N. Namykin and P. Basu, *Inorg. Chem.*, **42**, 5999 (2003).
4. Z. G. Hubert-pfalzgraf, *New J. Chem.*, **11**, 663 (1987).
5. J. M. Mitchell and N. S. Linney, *J. Am. Chem. Soc.*, **123**, 862 (2001).
6. W. A. Nugent and J. M. Mayer, *Metal-ligand Multiple Bonds*; Wiley Interscience; New York (1988).
7. T. A. Albright, J. K. Burdett and M. H. Whaugbo, *Orbital Interactions in Chemistry*; Wiley: New York, p. 321 (1985).
8. R. R. Schrock, *In Handbook of Olefin Metathesis*; R. H. Grubbs, Ed., Wiley-VCH: Weinheim, Germany, p. 15 (2003).
9. B. E. Schultz, S. F. Gheller, M. C. Muellertics, M. J. Scott and R. H. Holm, *J. Am. Chem. Soc.*, **115**, 2714 (1993).
10. R. Hille, *Chem. Rev.*, **96**, 2757 (1996).
11. J. C. Boyington, V. N. Gladyshev, S. V. Khangnlov, T. C. Stadtman and P. D. Sun, *Science*, **275**, 1305 (1997).
12. K. H. Chang, C. C. Huanf, Y-H. Liu, Y-H. Hu, P-T. Chou and Y-C. Liu, *J. Chem. Soc. Dalton Trans.*, **31**, 173 (2004); D. A. Atwood and M. J. Harvey, *Chem. Rev.*, **101**, 37 (2001).
13. G. D. Fallon, B. M. Gatehouse, P. J. Maruni, K. S. Murray and B. O. Wesh, *J. Chem. Soc. Dalton Trans.*, 2733 (1984).
14. R. L. Dutta and Md. M. Hossain, *J. Scient. Ind. Res.*, **44**, 635 (1985).
15. G. Merf, Y. Lu, Y. He and Y. Guan, *Tetrahedron, Assym.*, **11**, 4255 (2000).
16. K. K. Narang and R. A. Lal, *Curr. Sci.*, **46**, 401 (1977).
17. R. A. Lal, A. N. Siva, S. Adhikari, M. K. Singh and U. S. Yadav, *Synth. React. Inorg. Met-Org. Chem.*, **26(2)**, 321-337 (1996); F. Feigel, V. Anger and R. E. Oesper, "*Spot Test in Organic Analysis*", 7th Ed., Elseiver

Publishing Company, Amsterdam, The Netherlands, p. 173, 384 (1966) (Indian Reprint, 2005).

18. R. A. Lal, J. Chakraborty, A. Kumar, S. Bhaumik, R. K. Nath and D. Ghosh, *Indian J. Chem.*, **43A**, 516 (2004); R. A. Lal, J. Chakraborty, S. Bhaumik and A. Kumar, *Indian J. Chem.*, **41A**, 1157 (2002).
19. W. J. Geary, *Coord. Chem. Rev.*, **7**, 81 (1971).
20. E. I. Stiefel, G. Wilkinson, (Ed.) "*Comprehensive Coordination Chemistry*"; R. D. Gillard and J. A. McCleverty (Eds.), Pergamon, Oxford, vol. **1**, p. 1375 (1987).
21. C. M. Metzler, A. Cahill, D. E. Metzler, *J. Am. Chem. Soc.*, **102**, 6075 (1980).
22. J. W. Lewis, C. Sandorfy, *Can. J. Chem.*, **60**, 1727 (1982).
23. D. Gegiou, E. Lambi, E. Hadjoudis, *J. Phys. Chem.*, **100**, 1762 (1996).
24. R. A. Lal, D. Basumatary, A. K. de and A. Kumar, *Trans. Met. Chem.*, **32**, 481 (2007).
25. D. G. McCollum, L. Hall, C. White, R. Ostrander, A. L. Rheingold, J. Whelam and B. Bosnich, *Inorg. Chem.*, **33**, 924 (1994).
26. R. A. Lal and A. Kumar, *Indian J. Chem.*, **37A**, 924 (1998).
27. L. M. Jackman and S. Sternhell, "*Applications of Nuclear Magnetic Resonance Spectroscopy in Organic Chemistry*", Chapter 3, Vol. **10**, 2nd Ed., Perganion Press, Amsterdam (1978).
28. J. C. N. Ma, E. W. Warnhoff, *Can. J. Chem.*, **43**, 143 (1961).
29. T. K. Wu, B. P. Daily, *J. Chem. Phys.* **41**, 1849 (1961).
30. Spectral Database for Organic Compounds, SDBS, National Institute of Advanced Industrial Science and Technology (AIST), Japan, www.aist.go.jp.
31. O. Pouralimardan, A. C. Chamayou, C. Janiak and H. H. Monfarad, *Inorg. Chim. Acta*, **360**, 1559 (2007); K. R. Barnard, M. Bruch, H. Susan, J. H. Enemark, R. W. Gable and A. G. Wedd, *Inorg. Chem.*, **36**, 637 (1997).
32. K. R. Barnard, M. Bruch, H. Susan, J. H. Enemark, R. W. Gable and A. G. Wedd, *Inorg. Chem.*, **36**, 637 (1997).
33. J. Topic and J. C. Bachert, *Inorg. Chem.*, **31**, 511 (1992).

34. K. Nakamoto, "*Infrared and Raman Spectra of Inorganic and Coordination Compounds*", 4th Ed., John Wiley and Sons, New York (1986).

35. R. A. Lal, M. L. Pal and S. Adhikari, *Synth. React. Met-Org. Chem.*, **26**, 997 (1996).

CHAPTER V

Synthesis and Characterization of Monometallic Copper (II) Complexes derived from Polyfunctional Disalicyaldehyde oxaloyldihydrazone

Introduction

In the previous chapters III and IV, we have described the monometallic and homobimetallic molybdenum molybdenum (VI) complexes derived from the Schiff base dihydrazone disalicylaldehyde oxaloyldihydrazone, respectively. Although, the dihydrazone is a potential hexadentate ligand, yet it showed only dibasic tridentate behavior in monometallic molybdenum (VI) complexes, bonding to the metal centre through phenolate oxygen atom, enolate oxygen atom and azomethine nitrogen atom through one half hydrazone part in enol form in staggered configuration while the other half hydrazone remained unbonded in keto form. On the other hand, in the homobimetallic complexes, the dihydrazone was found to bind the metal centres as a tetrabasic hexadentate ligand in enol form in anti-cis configuration through phenolate and enolate oxygen atoms and azomethine nitrogen atoms. Copper is the second metal selected in the present study for complexation purposes because of its biological and technological relation to molybdenum. At this stage, it appears pertinent to present the rationale for the selection of this particular metal i.e. its relationship to molybdenum prior to describing the synthesis and characterization of copper complexes.

Copper occurs in nature in combination with molybdenum in the unique heterobimetallic enzyme carbon monoxide dehydrogenase (CODH) **[1, 2]**. This enzyme catalyzes the oxidation of CO to CO_2, thereby providing carbon and energy to the organism and maintaining the sub-toxic levels of CO in troposphere **[1, 2]**. Further, molybdenum ions show antagonistic function with regard to copper in humans and animals **[3-8]**. Moreover, molybdenum and copper based heterometal systems are important in material sciences such as molecular scale memory devices

[9] or switches **[10]** or ferroelectrics **[11]**. A high-spin molecule $MoCu_6$ based on copper and octacyanomolybdate shows photoswitchable property **[12]**. Another Mo and Cu based compound $Cu_2[Mo(CN)_8].8H_2O$ shows property of ferroelectricity **[13]**. The coordination nanoparticles like $[Mo(CN)_8CuNi]$ act as photomagnetic particles **[14]** and have revealed the possibility of triggering supermagnetism **[15]** by ligand. It has been shown that the molybdenum-copper complexes or tungsten-copper complexes combining polyfunctional ligand constitute an interesting system of research due to their diverse structural chemistry **[16, 17]** and their relevance to biological systems and photonic materials **[18, 19]**.

Besides the above importance in combination with molybdenum in biological systems, material sciences and structural chemistry, copper plays significant roles either in combination with some other metals like zinc and iron or alone in the active sites of centres of several enzymes. Thus copper occurs in superoxide dismutase in combination with zinc where it catalyzes disproportionation of superoxide, produced in biological systems from action of enzymes on O_2 to O_2 and H_2O **[24]**. Copper also occurs in cytochrome oxidase in combination with iron **[25]** where it catalyzes oxidation of Fe^{2+} to Fe^{3+}. On the other hand, copper occurs alone in the active site centres of laccase, ceruloplasmin, ascorbate oxidase and particulate methane monooxygenase (pMMO) coupled sites where copper is often present in di-, or trinuclear assemblies. It has been proposed that the copper centres of pMMO are organized into a trinuclear catalytic or electron transfer cluster on the basis of magnetic susceptibility data. The electron paramagnetic resonance (EPR) spectra of fully oxidized enzymes obtained from three different pMMO-containing bacteria have also supported this formulation **[26-28]**. However, a mononuclear active centre as well has been supported by another interpretation of EPR spectra from similarly isolated pMMO samples **[29]**. Morover a crystallographic study of a membrane preparation of pMMO at 2.3 Å resolution has identified only one mononuclear and one distant, possibly dinuclear, metal site per enzyme unit **[30]**.

Copper is essential for the proper functioning of copper dependent enzymes, including cyctochrome C oxidase (energy production), superoxide dismutase (antioxidant protection), tyrosinase (pigmentation), dopamine hydroxylase (catecholamine production), lysyloxidase (collagen and elastin formation), clotting factor V (blood clotting) and ceruloplasmin (antioxidant protection), iron metabolism and copper transport **[31]**. Copper complexes have been explored for their anti-inflammatory activity. They have also shown potential to be used as a physiological approach to the treatment of numerous chronic diseases. This potential has been expanded to include, in addition to inflammatory diseases, gastrointestinal ulcers, cancers, carcinogenesis and diabetes. In these conditions, most of the research interest has centered on the finding that many copper complexes demonstrate superoxide dismutase (SOD) activity. Because of this, many of these compounds have been designated as SOD mimetics.

A survey of literature reveals that the majority of the complexes from dihydrazones have been prepared from reaction of metal salts with the preformed dihydrazone **[32]**. However, the report on the metal complexes of dihydrazones prepared by template methods is quite meager **[33-35]** yet the complexes prepared by template method are expected to have different bonding characteristics as well as properties as compared to those prepared from preformed dihydrazone.

In view of the above relation of copper with molybdenum, importance of the copper complexes and few isolated studies on metal complexes synthesized by template method and the fact that the chapters III and IV describes the monometallic and homobimetallic molybdenum (VI) complexes, the present chapter aims at synthesizing some copper complexes of the title ligand by template method and their characterization by various physic-chemical and spectroscopic techniques. Accordingly, the present chapter presents an account of synthesis and characterization of monometallic copper complexes of the title dihydrazone. The electron transfer reactions of the complexes have also been studied by cyclic voltammetry.

Experimental

Preparation of [Cu(H_2slox)] (5.1)

Oxaloyldihydrazine, ODH (0.60 g, 5.08 mmol) was dissolved in H_2O (20 mL). To this solution, $Cu(OAc)_2.2H_2O$ (1.00 g, 5.01 mmol) dissolved in methanol (60 mL) was added slowly and slowly accompanied by gentle stirring and the resulting solution was refluxed for 1/2h. This yielded a bluish green precipitate which was filtered in hot condition, washed several times with hot water, followed by three to four times with methanol (30 mL each time). The precipitate obtained was again suspended in methanol (60 mL) and the mixture was gently stirred for 30 minutes to make it homogeneous. This suspension was added to 1.6 mL of salicylaldehyde in methanol (30 mL) drop by drop over a period of 30 minutes accompanied by vigorous stirring. This precipitated a green coloured compound which was refluxed for 15 minutes, then filtered, washed three times with methanol (30 mL each time) followed by ether and finally dried over anhydrous $CaCl_2$. Yield 80 %.

Preparation of [Cu(H_2slox)(A)] *{where A = pyridine (py)* **(5.2)**, *2-picoline (2-pic)* **(5.3)**, *3-picoline(3-pic)* **(5.4)** *and 4-picoline (4-pic)* **(5.5)***}*

In order to prepare pyridine complex [Cu(H_2slox)(py)], [Cu(H_2slox)] (1.00 g, 2.47 mmol) was suspended in methanol (60 mL) and stirred for about 10 minutes to make it homogeneous. To this suspension 2.03 mL of pyridine was added slowly accompanied by vigorous stirring and the resulting mixture was refluxed for 1h, which precipitated a green coloured compound. The green coloured compound was filtered in hot condition, washed three to four times with 20 mL methanol followed by ether and dried over anhydrous $CaCl_2$. Yield 78 %.

The compounds [Cu(H_2slox)(2-pic)], [Cu(H_2slox)(3-pic)] and [Cu(H_2slox)(4-pic)] were also prepared by essentially the above procedure using 2.4 mL each of 2-picoline, 3-picoline and 4-picoline instead of pyridine. Yield 72 -79 %.

Results and discussion

The complexes described in this chapter together with colour, decomposition point, analytical, molar conductance, magnetic moment and electronic spectral data have been set out in **Table 5.1**. In order to synthesize the complexes, first oxaloyldihydrazine (ODH) in methanol was allowed to react with copper acetate in 1:1.1 molar ratios, under reflux for about 30 minutes. This led to precipitation of a bluish green coloured compound which was filtered in hot condition, washed several times with hot water, followed by three to four times with methanol. The precipitate so obtained was treated at room temperature with salicylaldehyde in 1:2.5 molar ratios in methanol by stirring for about 30 minutes to give a green coloured precipitate to which was then added pyridine and substituted pyridine molecules and then the resulting mixture was refluxes. On the basis of various elemental analyses, the complexes have been suggested to have the composition: $[Cu(H_2slox)]$ **(5.1)**, $[Cu(H_2slox)(A)]$ {*where A = pyridine (py)* **(5.2)**, *2-picoline (2-pic)* **(5.3)**, *3-picoline (3-pic)* **(5.4)** *and 4-picoline (4-pic)* **(5.5)**}.

These complexes are green coloured and air stable. They decompose above 300°C without melting. All the complexes are insoluble in common organic solvents such as methanol, ethanol chloroform, carbon tetrachloride, ether and benzene etc. They are soluble though not completely in highly coordinating solvents such as DMF and DMSO. A consistent effort to crystallize the complexes either from a saturated solution or by diffusion into saturated solutions in CH_3CN, DMSO and DMF in a closed system led to the precipitation of amorphous products. Such behaviour of the complexes with regard to their crystallization prevented their analysis by X-ray crystallography.

Thermal analyses

Decomposition studies **[36]** of the complexes were carried out in the temperature range 70 – 250° C and the vapours evolved were identified by passing through a

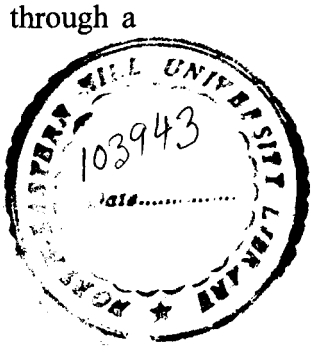

separate test tube containing anhydrous copper sulfate, a solution of sodium hydroxide and chloroform, a solution of iodine and sodium hydroxide and cyanogen bromide solution respectively. Complexes **(5.1)** to **(5.5)** do not show any weight loss either in the temperature range 100 – 120°C or in the temperature range 160 -180°C ruling out the possibility of water molecule in the lattice structure as well as in the first coordination sphere. The vapours evolved in the complex **(5.2)** in the temperature range 220 – 240°C turned $CHCl_3$ and NaOH solution red confirming that they originate from pyridine. On the other hand, vapours evolved in the complex **(5.4)** in this temperature range turned the colour of cyanogen bromide solution to green-violet on treatment with phloroglucinol solution suggesting the presence of 3-picoline molecule while the vapours evolved in the complex **(5.5)** turned the colour of cyanogen bromide solution to blue on treatment with phloroglucinol solution suggesting the presence of 4-picoline molecules in the complex. Complexes **(5.2)** to **(5.5)** show weight loss corresponding to one pyridine/picoline molecules respectively in this temperature range. The loss of weight at such a high temperature shows that these donor molecules are coordinated to the metal centre **[37]**.

Molar conductance

The complexes **(5.1)** to **(5.5)** have molar conductance values in the range of 1.2 – 1.8 $ohm^{-1}cm^2mol^{-1}$ in DMSO at 10^{-3} M dilution. These values are consistent with their non-electrolytic nature in this solvent **[38]**.

Magnetic moment

The magnetic moment values for the complexes isolated in the present study have been given in the **Table 5.1**.

At room temperature the present copper (II) complexes **(5.1)** to **(5.5)** have magnetic moment values in the range 1.71 – 1.79 BM. According to Figgis **[39]**, magnetic moment values less than 1.90 BM indicate square planar as well as octahedral

stereochemistry and magnetic moment value greater than 1.90 BM indicate tetrahedral stereochemistry. When magnetic moment value is close to spin only value of 1.73 BM then there is no appreciable spin-spin coupling between unpaired electrons belonging to different copper atoms. The magnetic moment values for all of the complexes lie close to spin only value of 1.73 BM indicating no appreciable spin-spin interaction between copper atoms. The magnetic moment value of the complexes suggests square planar geometry for the complexes.

Electronic spectra

The electronic spectral data of the complexes have been presented in **Table 5.1**. The electronic spectra of the complexes **(5.2)**, **(5.3)** and **(5.4)** have been shown in the **Figs. 5.1-5.3**. The electronic spectra of the complexes **(5.1)** to **(5.5)** show three bands in the region 290 – 340 nm region assigned to intraligand $\pi \rightarrow \pi^*$ and $n \rightarrow \pi^*$ transitions similar to that observed in the free dihydrazone ligand **[40-45]**. In addition to the ligand bands a new band appeas in the region 420 – 423 nm in all the complexes. This band has a high molar extinction coefficient in the range 1276 – 3718 $dm^3mol^{-1}cm^2$. In view of the high molar extinction coefficient of this band, it is assigned to arise due to the ligand-to-metal charge transfer transition, most probably, from phenolate oxygen atom to the copper centre **[46-49]**. This ligand-to-metal charge transfer band, which is strongly influenced by the chemical nature of the ligand within a given stereochemistry, is responsible for the appearance of the colour of the complexes.

All the complexes also show a single broad band in the 636 – 661 nm regions with a comparatively very low molar extinction coefficient in the range 59 – 90 $dm^3mol^{-1}cm^2$. Hence, this band is assigned to d-d transition **[50]**. In the octahedral **[51, 52]** and tetrahedral **[53]** complexes of copper (II), the band due to d-d transition occurs at ~800 nm and ~1200 nm, respectively. The 800 nm bands in octahedral complexes is considerably blue shifted due to Jahn-Teller distortion and in extreme cases, it falls in the range 600 – 700 nm reported for the square planar complexes **[54]**. Thus in all

of the copper (II) complexes a single broad band in the range 636 - 661 nm with a low molar extinction coefficient is assigned to have its origin from d-d transition. The essential feature of this band in the 630 – 660 nm regions suggests that it is the combination of three transitions ($^2B_{1g} \rightarrow {}^2A_{1g}$, $^2B_{1g} \rightarrow {}^2B_{2g}$ and $^2B_{1g} \rightarrow {}^2E_g$) Thus it may be concluded that all the copper (II) complexes have square-planar geometry **[50]**.

Electron paramagnetic resonance spectra

As we could not get well-shaped single crystals, the EPR spectra were recorded only for powder and solution samples for the Schiff base complexes at RT and LNT; the results are described in **Table 5.2**. The EPR spectra of the complexes **(5.1)**, **(5.3)** and **(5.4)** have been shown in **Figs. 5.4-5.6**. Hamiltonian parameters $g_{\|}$, $g_{\perp}$, $A_{\|}$ and $A_{\perp}$ were calculated and are included in **Table 5.3**. The $g_{\|}$ values for the copper (II) complexes **(5.1)** to **(5.5)** lie in the range 2.318 – 2.330 at RT and 2.314 – 2.339 at LNT, while the $g_{\perp}$ value lies in the range 2.111 – 2.119 at RT and 2.104 – 2.125 at LNT. The EPR spectra of the complexes at RT in DMSO solution are isotropic and show copper hyperfine splitting due to interaction of unpaired electron of copper (II) ion with the nuclear spin (I = 3/2) Although four hyperfine lines should be observed in the copper (II) complexes but, in practice, only three components are observable in the present case with average hyperfine coupling constant A_{av} = 107 – 112. The isotropic nature of the EPR spectra is due to the tumbling motion of the molecules in DMSO solution at room temperature. However, at LNT, since the molecules are sufficiently frozen, the complexes show anisotropic spectral features. The EPR spectra of all the complexes contain the characteristic copper hyperfine structures at LNT also in DMSO, in the $g_{\|}$ and $g_{\perp}$ regions due to the interaction of unpaired electron of Cu (II) ion with the nuclear spin (I=3/2). Only two copper hyperfine structures are observed in complexes at LNT. The location of the $g_{\perp}$ component prevents resolutions of all four $g_{\|}$ hyperfine lines. The superhyperfine structure in the $g_{\perp}$ region has been observed in the copper (II) complexes at LNT and is attributed to the interaction of the unpaired electron of copper (II) ion with the nuclear spin of the

N atom from the ligand molecule. The superhyperfine structures shows seven lines in the complex **(5.1)** with superhyperfine coupling constant $A_{|N}$ = 12G, corresponding to the coupling of electron spin with the nuclear spin of two nitrogen atom. This indicates coordination of two nitrogen atoms of the dihydrazone ligand. The appearance of seven lines in the EPR spectrum shows that the nitrogen atoms which are bonded to the metal centre are in different environment. This observation reveals that the two nitrogen atoms which coordinate to the metal centre originate from two different ligand molecules.

The shifting of g values from 2.0023 in a transition metal complex is due to mixing, via spin-orbit coupling of the metal orbitals involved in molecular orbitals containing the unpaired electron(s), with the empty or filled ligand orbitals. When the mixing is with the empty ligand orbitals, the result is negative g shift, whereas the mixing with the filled ligand orbitals leads to a positive g shift. The shift depends on the amount of the unpaired electron density at the donor sites of the ligands, i.e., on the degree of covalency of the complex. The in-plane σ covalency parameter, α^2_{Cu} was calculated for the copper (II) complexes **(5.1)** to **(5.5)** using the following equations **[55-57]** and the values obtained are listed in the table.

$$\alpha^2_{Cu} = - (A_{||}/0.036) + (g_{||} - 2.0023) + 3/7(g_{|} - 2.0023) + 0.04$$

The α^2_{Cu} value accounts for a fraction of the unpaired electron density on the copper (II) ion. The smaller the value of α^2_{Cu}, the more covalent is the bonding. For example α^2_{Cu} = 0.5 indicates complete covalent bonding, but α^2_{Cu} = 1.0 suggests complete ionic bonding. The α^2_{Cu} values for the copper (II) complexes **(5.1)** to **(5.5)** are in the range of 0.878 – 0.929 < 1 indicating that the copper (II) complexes have some covalent character.

The $A_{||}$ values for the copper (II) complexes **(5.1)** to **(5.5)** are in the range of 174 - 180 cm^{-1}. The ratio of $g_{||}/A_{||}$ is used to find the structure of the coordination complex. The ratio obtained for the copper (II) complexes **(5.1)** to **(5.5)** lies in the range 129.9

– 132.9 cm, which falls in the range 90 – 140 cm for square-planar copper (II) complexes **[57]**. All of the copper (II) complexes have $g_{||}>g_{|}>2.0023$ indicating that the unpaired electron lies in the $d_{x^2-y^2}$ orbital.

V. Suresh Babu et al **[58]** reported that $g_{||}$ is 2.4 for copper-oxygen bonds and 2.3 for copper-nitrogen bonds. The copper (II) complexes **(5.1)** to **(5.5)** have $g_{||}$ values between 2.3 – 2.4 and in agreement with the presence of mixed copper-oxygen and copper-nitrogen bonds.

The nature of the ligand forming the complex is evaluated from G values obtained by using the following equation;

$$G = (g_{||} - 2)/ (g_{|} - 2)$$

If $G < 4.0$, the ligand forming the complex is regarded as a strong field ligand. For the square planar complexes G is usually in the range **[57]** of 2.03-2.45. G value for the complexes **(5.1)** to **(5.5)** lies in the range 2.80-2.94 at RT and 2.74-3.09 at LNT which is in good agreement with the result reported for the square planar complexes of copper (II).

Infrared spectra

A comparative study of IR spectra of the complexes **(5.1)** to **(5.5)** with the preformed ligand shows that the ligand is present in keto-enol form in all of them except complex **(5.1)** where it is present in keto-form. The IR spectral data of the complexes have been illustrated in **Table 5.3**. The IR spectra of the complexes **(5.1)**, **(5.3)** and **(5.4)** have been shown in **Figs. 5.7-5.9**.

The free hydrazide shows strong bands at 3292, 1651 and 1588 cm^{-1}. The band at 3292 cm^{-1} is characteristic of ν (>NH) vibrations while the bands at 1651 and 1588 cm^{-1} are characteristic of stretching vibrations of >C=O group and bending

vibrations of $-NH_2$ groups. The essential features of these bands suggest that >C=O and $-NH_2$ groups of dihydrazide are involved in strong intramolecular H-bonding. The reaction of $Cu(OAc)_2.2H_2O$ with oxaloyldihydrazine in 1: 1 molar ratio followed by salicylaldehyde keeping Cu^{2+}: ODH: salicylaldehyde molar ratio at 1: 1: 2.5 yields a complex **(5.1)** which shows IR spectral features entirely different from that of ODH and similar to that of uncoordinated dihydrazone **[59, 60]**. The complex **(5.1)** shows a band at 3204 cm^{-1} which bears similarity with the preformed ligand band at the same position. This shows that secondary >NH groups are present in the complex. Further, the complex **(5.1)** shows another strong band at 1679 cm^{-1}. This band is essentially similar in features as compared to the ligand band at 1651 cm^{-1} in ODH and 1667 cm^{-1} in H_4slox. Hence this band is assigned to stretching vibration of >C=O group. The position of this band is higher as compared to the ν (>C=O) band in ODH and H_4slox. This rules out the possibility of coordination of >C=O group to the metal centre and suggest the absence of intramolecular hydrogen bonding involving >C=O group. In addition, the complex **(5.1)** shows a new band at 1613 cm^{-1} which is similar in nature to the band at 1627 and 1603 cm^{-1} in the free ligand and falls in the region in which >C=N- group in hydrazone metal complexes has been reported to absorb. Hence, this band is assigned to ν (>C=N-) **[61]**.

All these pieces of evidences suggest that $-NH_2$ group of dihydrazide and >C=O group of aldehyde condense with one another generating the dihydrazone in metal complex. A point of crucial importance in the IR spectrum of the complex **(5.1)** is that the ν (>C=O) band is decreased in intensity while ν (>C=N-) band has increased in intensity as compared to the corresponding band in the free dihydrazone. Another important feature of the IR spectrum of the complex **(5.1)** is that it shows a new band at 1527 cm^{-1} which masks the preformed ligand band at 1534 cm^{-1}. This band is assigned to stretching vibration of newly created NCO group produced as a result of enolization **[62]**. Such a feature associated with the IR spectrum of the complex **(5.1)** suggests that the half part of the dihydrazone produced has, most probably undergone enolization. The intensity of >C=N- is increased due to reinforcement of the band due to newly created NCO group giving rise to >C=N-N=C< group. The

strong band at 1276 cm^{-1} is assigned to ν (C-O) (phenolate) in the complex **(5.1)** as against the band at 1262 cm^{-1} in the free dihydrazone. This indicates bonding of phenolate oxygen atom to the metal centre **[63]**.

A weak band at 1035 cm^{-1} in the ligand has been assigned to υ (N–N) vibration. This band shifts to higher frequency in the complexes by 8-21 cm^{-1} indicating involvement of only one nitrogen atom of N–N group in coordination **[64]**. The υ (C–N) vibration at 1054 cm^{-1} in the ligand appearing as a weak band is also shifted to higher frequency in the complexes.

Clark et al **[65]** carried out extensive study of the M-N stretching mode of the various nitrogen donor ligands with metal halides and concluded that the υ (M-N) modes are strongly dependent on the grouping to which nitrogen atom is attached. Sacconi et al **[66]** suggested the M-N stretching mode in MCl_2-hydrazine complexes (where M = Mn^{II}, Fe^{II}, Co^{II}, Ni^{II}, Zn^{II} or Cd^{II}) in the range 440-325 cm^{-1}.

Percy et al **[67, 68]** al have studied the infrared spectra of 4-coordinate tetrahedral cobalt (II), zinc (II) and square planar nickel (II) and copper (II) chelates derived from salicylaldimines. Their assignment is based on ^{15}N-labelling of the copper (II) complexes of N-p-tolylsalicylaldimines. Two frequencies in the metal complexes in the low region are sensitive to isotopic substitution and have been assigned to υ (M-N). They propose two general υ (M-N) ranges as 560 – 490 cm^{-1} and 480 – 400 cm^{-1}. The electron withdrawing groups shift the υ (M-N) to higher cm^{-1}. However, the octahedral complexes show υ (M-N) at lower frequencies. The same authors predict υ (M-N) for the copper (II) and cobalt (II) complexes of N-salicylaldimine in the 520 -450 and 490 -390 cm^{-1} region respectively.

Nakamoto and coworkers **[69, 70]** have confirmed unequivocally, the metal-nitrogen stretching frequency by isotopic substitution method and proved the above sequence true for 8-hydroxyquinoline complexes. Lever et al **[71]** have studied the octahedral complexes by isotopic substitution method and suggested that the highest energy υ

(M-N) mode falls in the general sequence NO_3 > halogens > NCS as far as the dependence upon the counter ion is concerned. Thus the metal-nitrogen modes in the high spin octahedral cobalt (II), nickel (II) and copper (II) complexes are expected below 400 cm^{-1} and certainly not above 500 cm^{-1}. From the consideration of the molecular models Schiff bases complexes of hydrazine derivatives should lie at similar or perhaps, the lower energies than the corresponding modes in metal-hydrazine complexes because of the substitutions.

Martell et al **[72]** assigned a strong band in the 460 – 420 cm^{-1} region in divalent metal acetylacetonate complexes to metal-oxygen stretching vibrations. Nakamoto and Martell **[73]** carried out normal coordinate analysis on the copper (II) acetylacetonate complex and predicted thereotically a band at 455 cm^{-1} to Cu-O stretching frequency. Subsequently Nakamoto et al **[74]** studied the acetylacetonate complexes of various transition metals and calculated the metal-oxygen stretching frequency by use of perturbation method. They demonstrated the effect of changing the metal ion on the metal-oxygen stretching frequency. They compared the calculated values with the observed stretching frequency and found that a number of metal-acetylacetonates shows metal-oxygen stretching frequency in the range 470 – 420 cm^{-1}. The complex **(5.1)** shows new bands at 598(m) and 482(w) cm^{-1}. These bands are assigned to ν (M-O) (phenolate) and ν (M-O) (enolate) respectively.

The essential features of the IR spectra of the complexes **(5.2)** to **(5.5)** containing pyridine and substituted pyridines are essentially similar to that of the complex **(5.1)** attesting the signatures of coordinated dihydrazone in keto-enol form except the band due to coordinated pyridines. Hence, further discussion on this aspect is redundant.

The free pyridine bases absorb at around ~ 604 cm^{-1} due to in-plane ring deformation. In the complexes **(5.2)** to **(5.5)**, a new medium to weak band is observed in the region 605-640 cm^{-1}. This band is assigned to arise due to in-plane ring deformation mode of pyridine bases.

Cyclic voltammogram

The electrochemical properties of the complexes have been studied in DMSO due to their poor solubility in other organic solvents. The redox behaviors of copper (II) complexes have been examined using Pt electrode versus s.c.e at a scan rate 100 mVs^{-1}, with 0.1 M TBAP as a supporting electrolyte. The electrochemical data for the complexes along with that of free ligand is summarized in **Table 5.4**. The cyclic voltammograms of the dihydrazone and its copper (II) complexes **(5.1)**, **(5.3)** and **(5.4)** are shown in **Figs. 5.10-5.13**.

The ligand H_4slox is electroactive and shows reductive waves at +0.40, -0.31 and -0.93 V only. The potential of the Cu^{II}/Cu^{I}, Cu^{I}/Cu^{0} systems depend upon the stability of the complexes and are therefore influenced by the structure of the ligand and its electronic properties. Since in this study only one ligand is used only the structural aspects of the complex can affect the stability and thus the value of the redox potential. Complexes **(5.1)** and **(5.2)** show three reductive waves centered at -0.95, -1.45, -1.80 V and -0.82, -1.12, -1.78 V, respectively, during the cathodic potential scan. However, during the reverse anodic potential scan only two oxidative waves at -0.71, +0.95 V and -0.72, +0.75 V are observed. The reductive wave at -0.95 V and -0.82 V in the complexes are close to the reductive wave of the ligand at -0.93 V. Hence, these waves at -0.95 and -0.82 V in complexes **(5.1)** and **(5.2)** are attributed to be due to the electron transfer reactions centered on the ligand molecule. The other two waves are considered to arise due to the metal-centered electron transfer reactions. The reductive waves at -1.45 and -1.12 V and the oxidative waves at +0.95 and +0.75 V in the complexes **(5.1)** and **(5.2)**, respectively, are attributed to arise due to Cu^{II}/Cu^{I} redox couple while the reductive waves at -1.80 and -1.78 V and oxidative waves at -0.71 and -0.72 V are attributed to arise due to Cu^{I}/Cu^{0} redox couple. On the other hand complexes **(5.3)** and **(5.4)** show five reductive waves at +0.25, -0.80, -1.18, -1.51, -1.70 V and -0.12, -0.78, -1.28, -1.60, -1.71 V, respectively, during the cathodic potential scan while only two oxidative waves at -0.70, +0.65 and -0.69, +0.68 V in the anodic potential scan. The waves at +0.25 and

-0.80 V in the complex **(5.3)** and -0.12 and -0.78 V in the complex **(5.4)** are close to the reductive waves at +0.40 and -0.95 V in the free ligand. Hence, these reductive waves are attributed to arise due to electron transfer reactions centered on the ligand. The reductive waves at -1.51 and -1.60 V in the complexes **(5.3)** and **(5.4)**, respectively, do not have any corresponding oxidative waves in the anodic potential scan. It appears that these reductive waves arise due to formation of some unstable species which reverts back to its original state. Apart from these reductive waves the waves at -1.18 and -1.70 V in complex **(5.3)** and at -1.28 and -1.71 V in complex **(5.4)** arise due to electron transfer reactions centered on metal. These reductive waves are assigned to Cu^{II}/Cu^{I} and Cu^{I}/Cu^{0} redox couples, respectively. The corresponding oxidative waves appear at +0.65 and -0.70 V in complex **(5.3)** and at +0.68 and -0.69 V in complex **(5.4)** during the reverse anodic scan. The electrode reactions corresponding to the redox couples Cu^{II}/Cu^{I} and Cu^{I}/Cu^{0} are shown below:

$$[Cu^{II}(H_2slox)(A)] \underset{}{\overset{+e}{\rightleftharpoons}} [Cu^{I}(H_2slox)(A)]^{-1} \underset{}{\overset{+e}{\rightleftharpoons}} [Cu^{0}(H_2slox)(A)]^{-2}$$

Complex **(5.5)** shows only two reductive waves at -0.85 and -1.25 V during the cathodic scan. The waves at -1.21 V are attributed to arise due to electron transfer reactions centered on metal. The reductive wave at -0.85 V is close to the reductive wave centered on the ligand. Hence, this reductive wave at -0.85 V appears to have contribution due to the reductive wave at -0.93 V due to electron transfer reaction centered on ligand.

Conclusion

In this chapter it has been shown that the reaction of $Cu(OAc)_2.2H_2O$ with oxaloyldihydrazine in 1:1 molar ratio followed by salicylaldehyde in 1: 1: 2.5 molar ratio in methanol yields a copper (II) complex with the composition $[Cu(H_2slox)]$. On further reaction of this complex with excess of pyridine and substituted pyridines, the complexes having the composition $[Cu(H_2slox)(A)]$ (*where A = pyridine, 2-*

picoline, 3-picoline and 4-picoline) were obtained. The magnetic moment measurements suggested these complexes to be normal paramagnetic. All these complexes occupy the NNO coordination chamber with the fourth axial site occupied by either pyridine or substituted pyridine molecules except complex **(5.1)** in which the fourth coordination position around copper is occupied by azomethine nitrogen atom from second complex molecules. Electronic and EPR spectral data suggest that these complexes are square planar in nature. The complexes show Cu^{II}/Cu^{I} and Cu^{I}/Cu^{0} redox couples in their cyclic voltammogram. The tentative structures for these complexes are shown in **Figs. 5.14 and 5.15**.

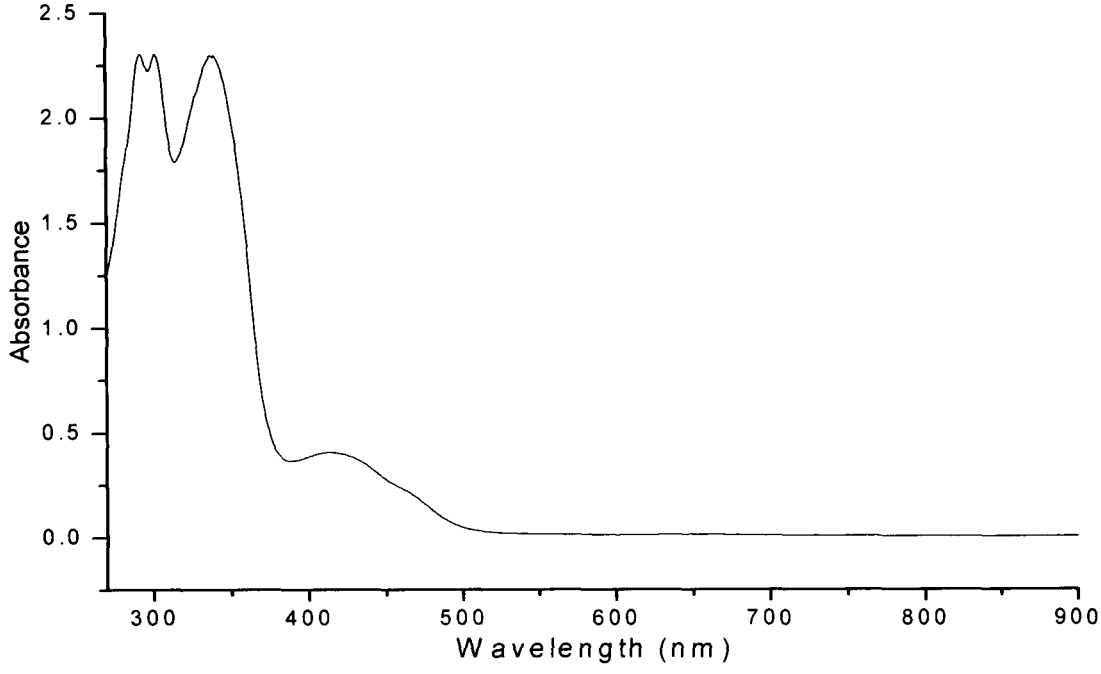

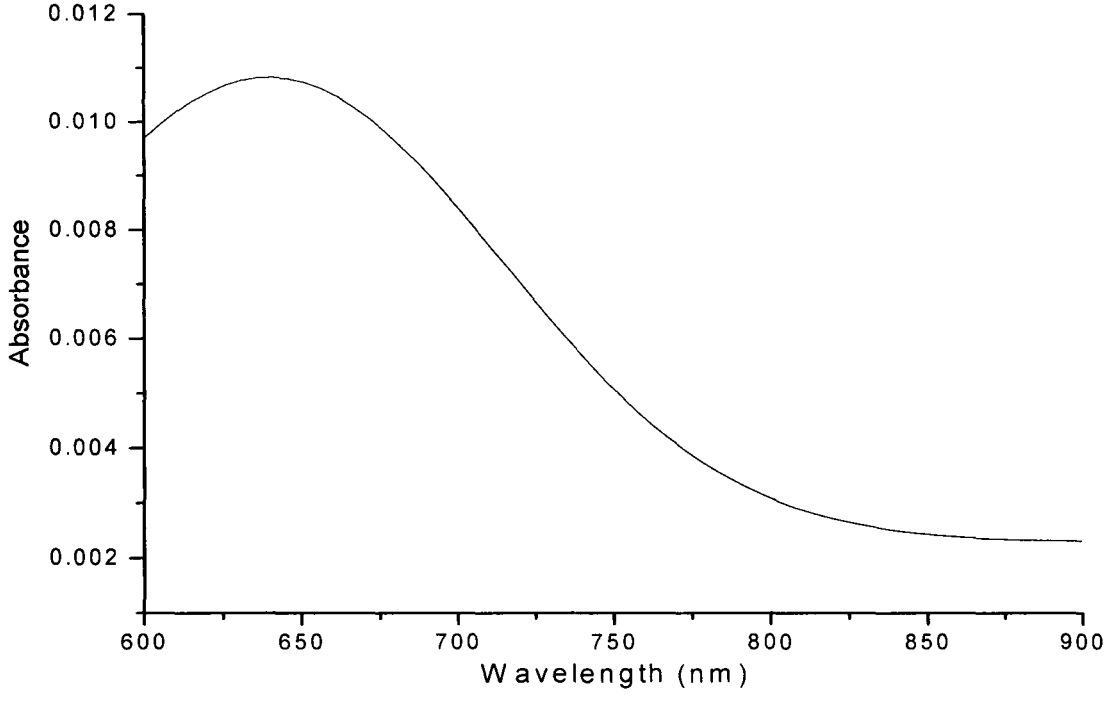

Fig. 5.1 Electronic spectrum of [Cu(H_2slox)(py)] **(5.2)**.

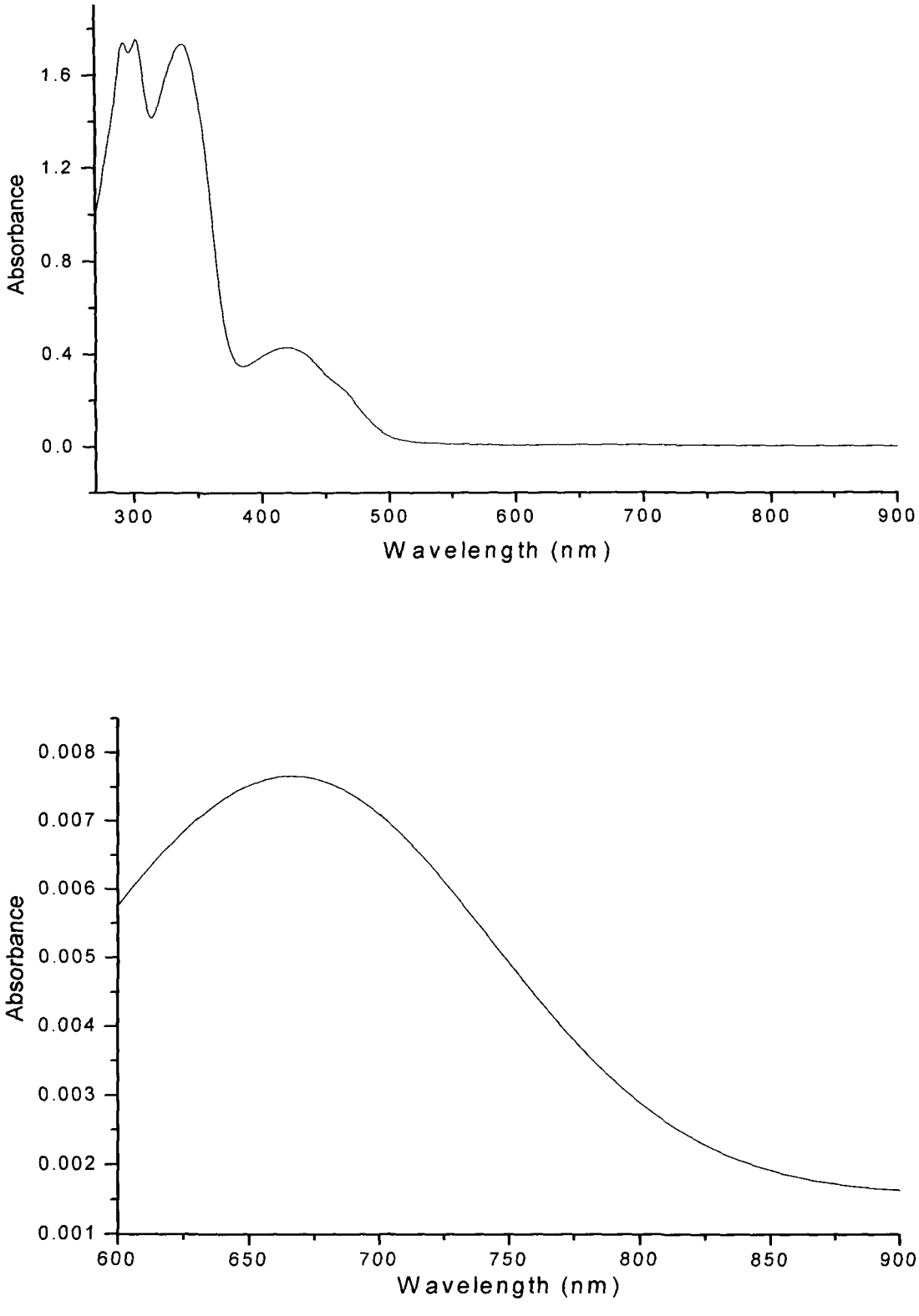

Fig. 5.2 Electronic spectrum of [Cu(H_2slox)(2-pic)] **(5.3)**.

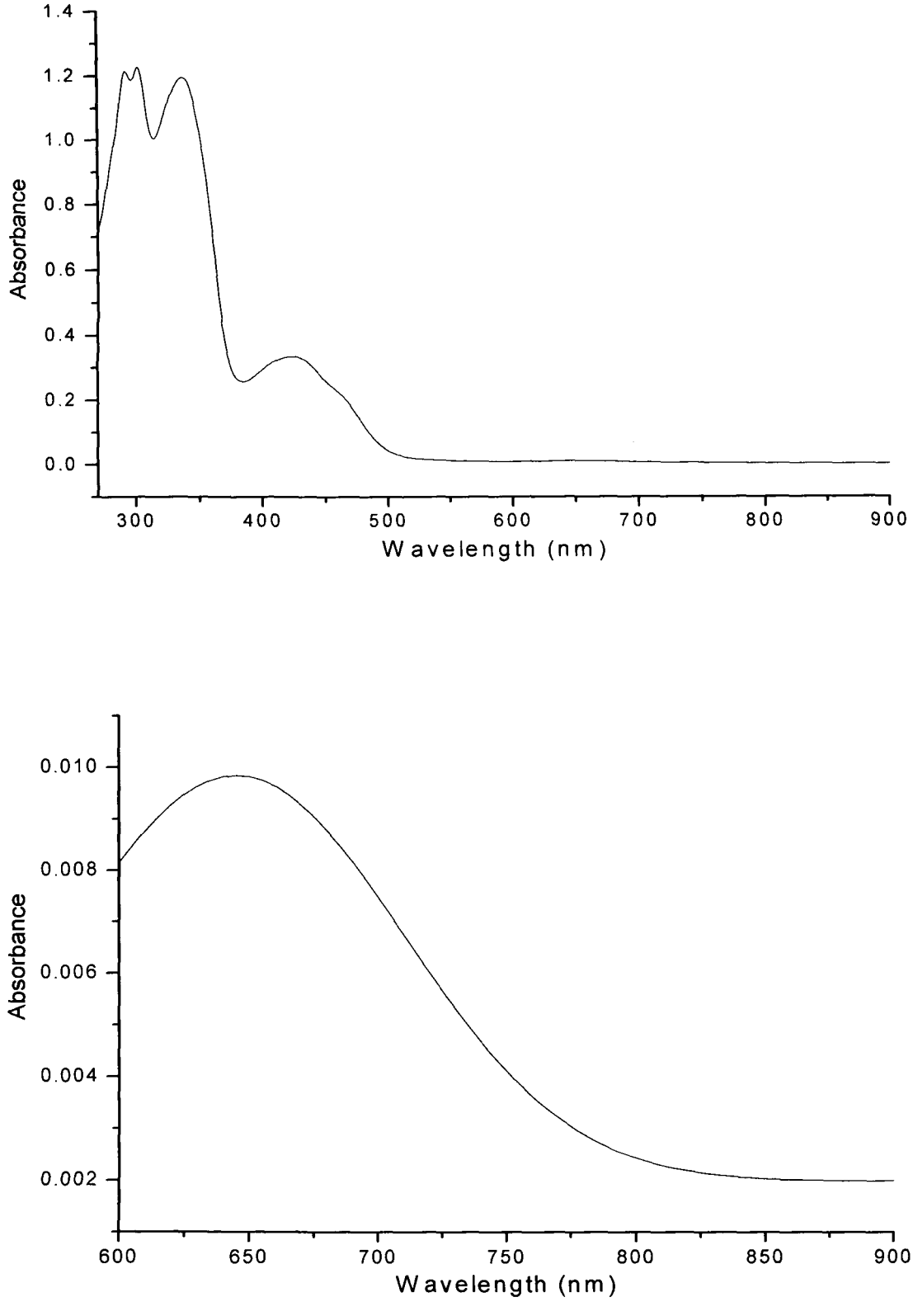

Fig. 5.3 Electronic spectrum of [Cu(H_2slox)(3-pic)] **(5.4)**.

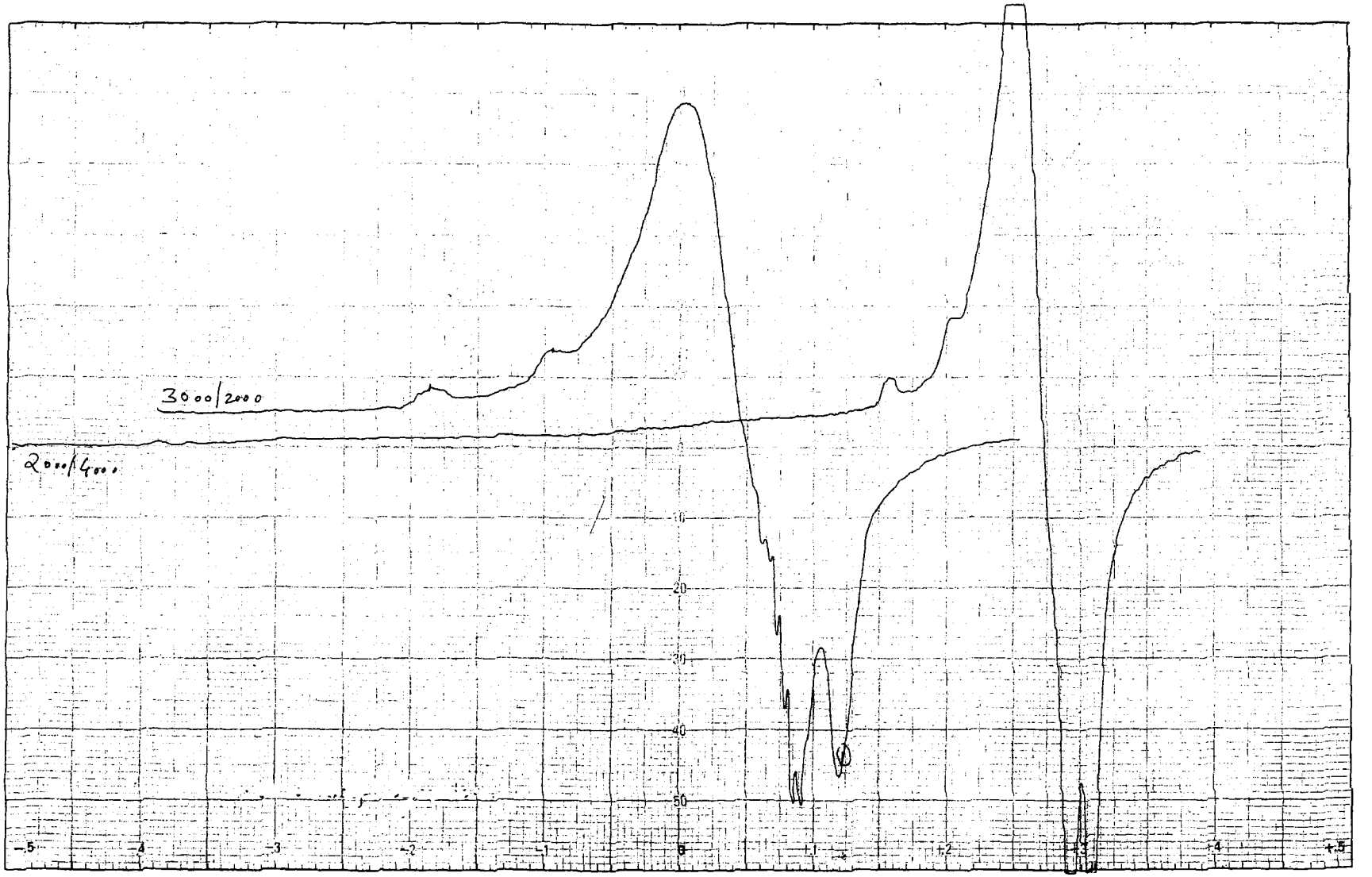

Fig. 5.4 (a) EPR spectrum of [Cu(H_2slox)] **(5.1)** in DMSO at Temperature: LNT; Frequency: 9.1 GHz; Scan Range: 2000 G; Field Set: 3000 G.

Fig. 5.4 (b) EPR spectrum of [Cu(H_2slox)] **(5.1)** in DMSO at Temperature: RT; Frequency: 9.1 GHz; Scan Range: 2000 G; Field Set: 3200 G.

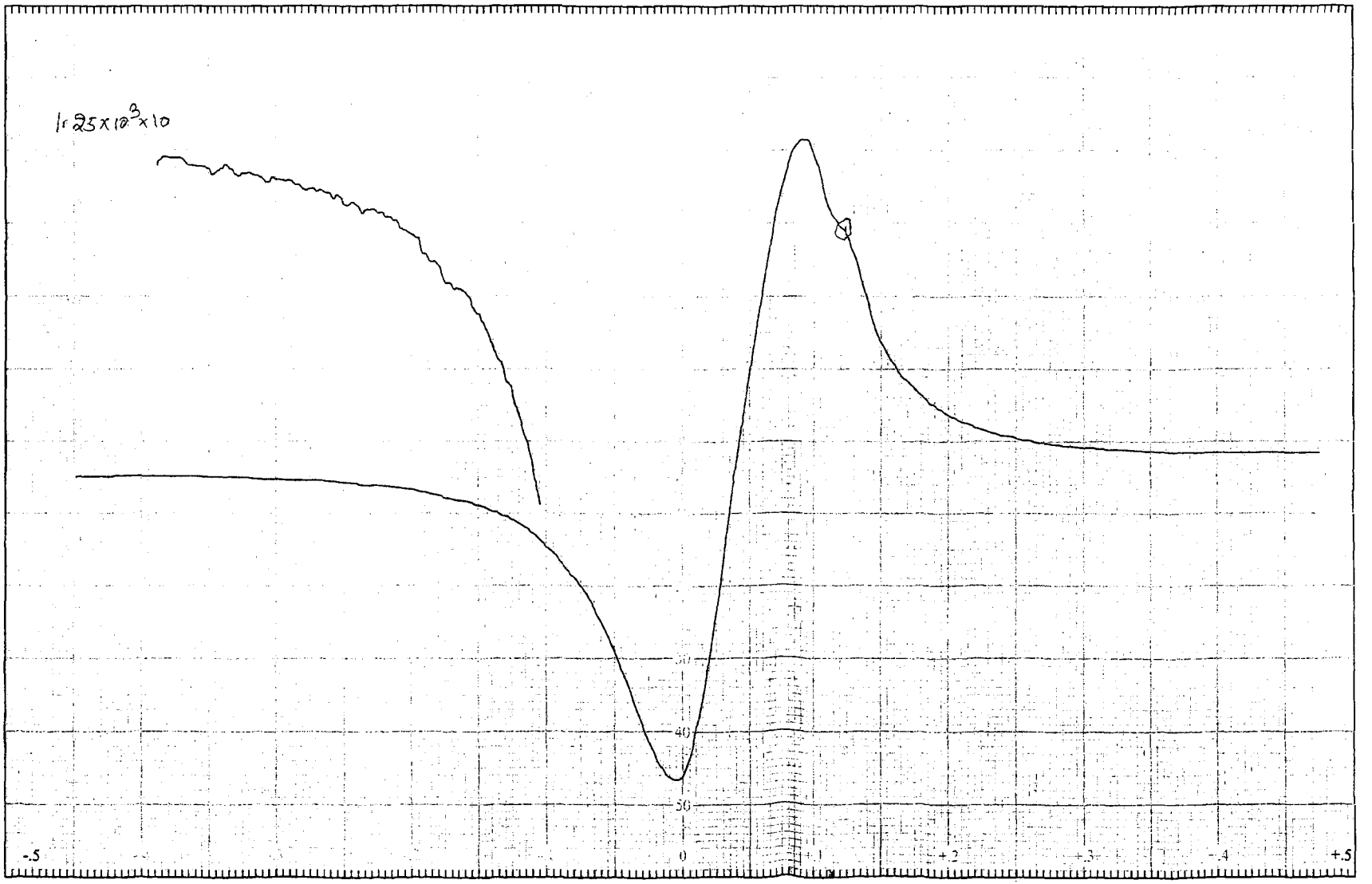

Fig. 5.5 (a) EPR spectrum of [Cu(H_2slox)(2-pic)] **(5.3)** in DMSO at Temperature: LNT; Frequency: 9.1 GHz; Scan Range: 2000 G; Field Set: 3000 G.

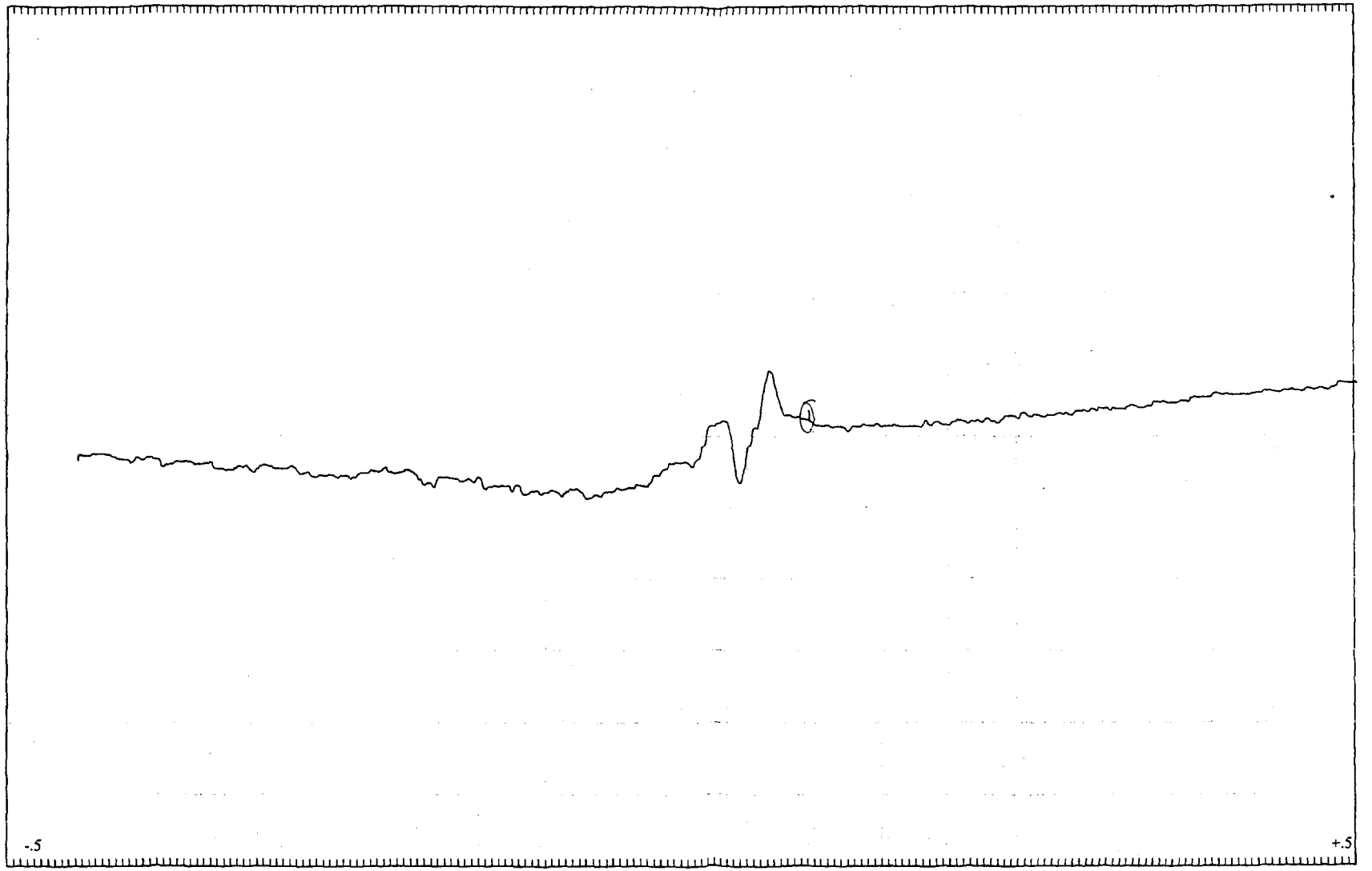

Fig. 5.5 (b) EPR spectrum of [Cu(H_2slox)(2-pic)] **(5.3)** in DMSO at Temperature: RT; Frequency: 9.1 GHz; Scan Range: 2000 G; Field Set: 3200 G.

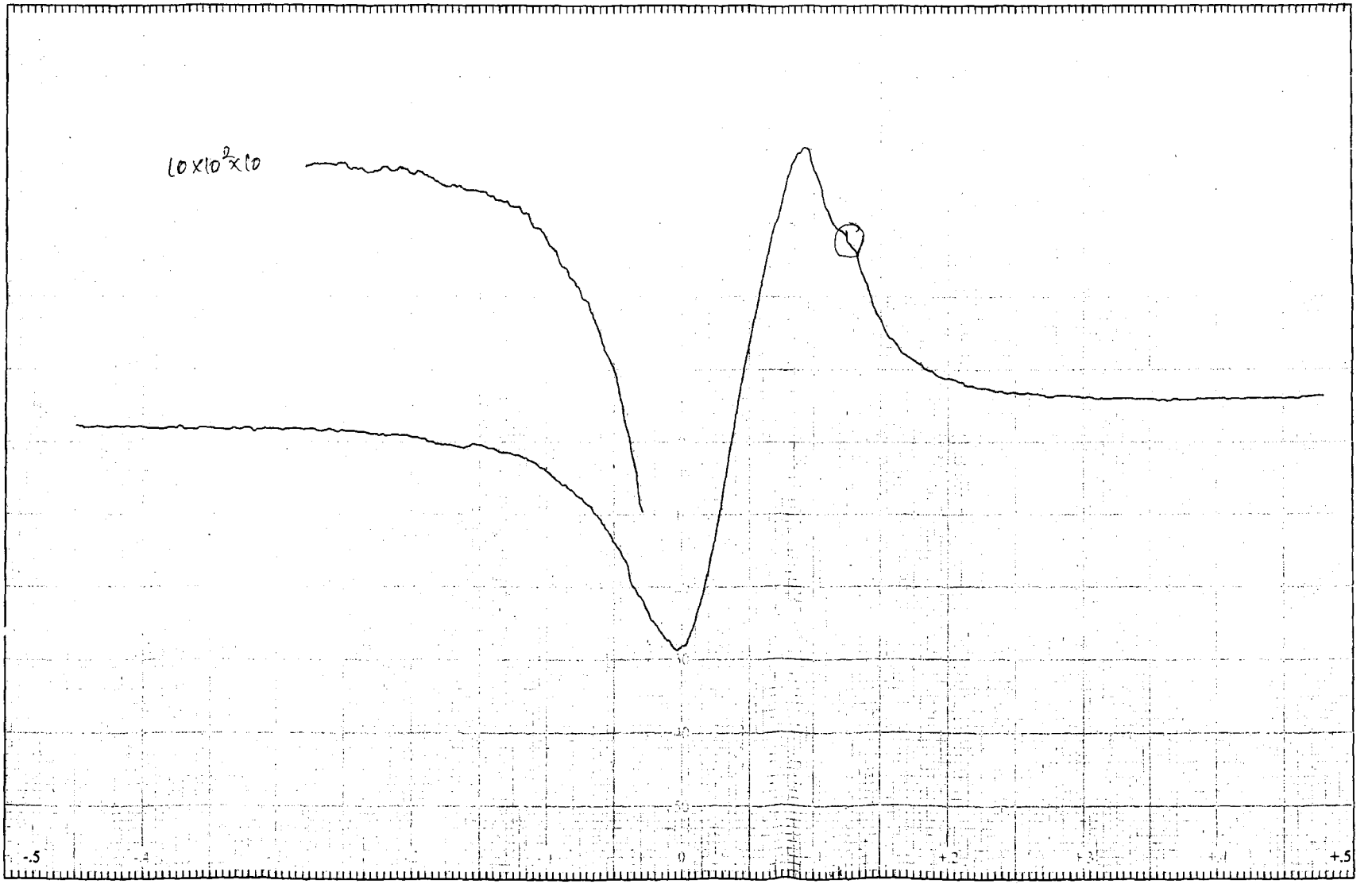

Fig. 5.6 (a) EPR spectrum of [Cu(H_2slox)(3-pic)] **(5.4)** in DMSO at Temperature: LNT; Frequency: 9.1 GHz; Scan Range: 2000 G; Field Set: 3000 G.

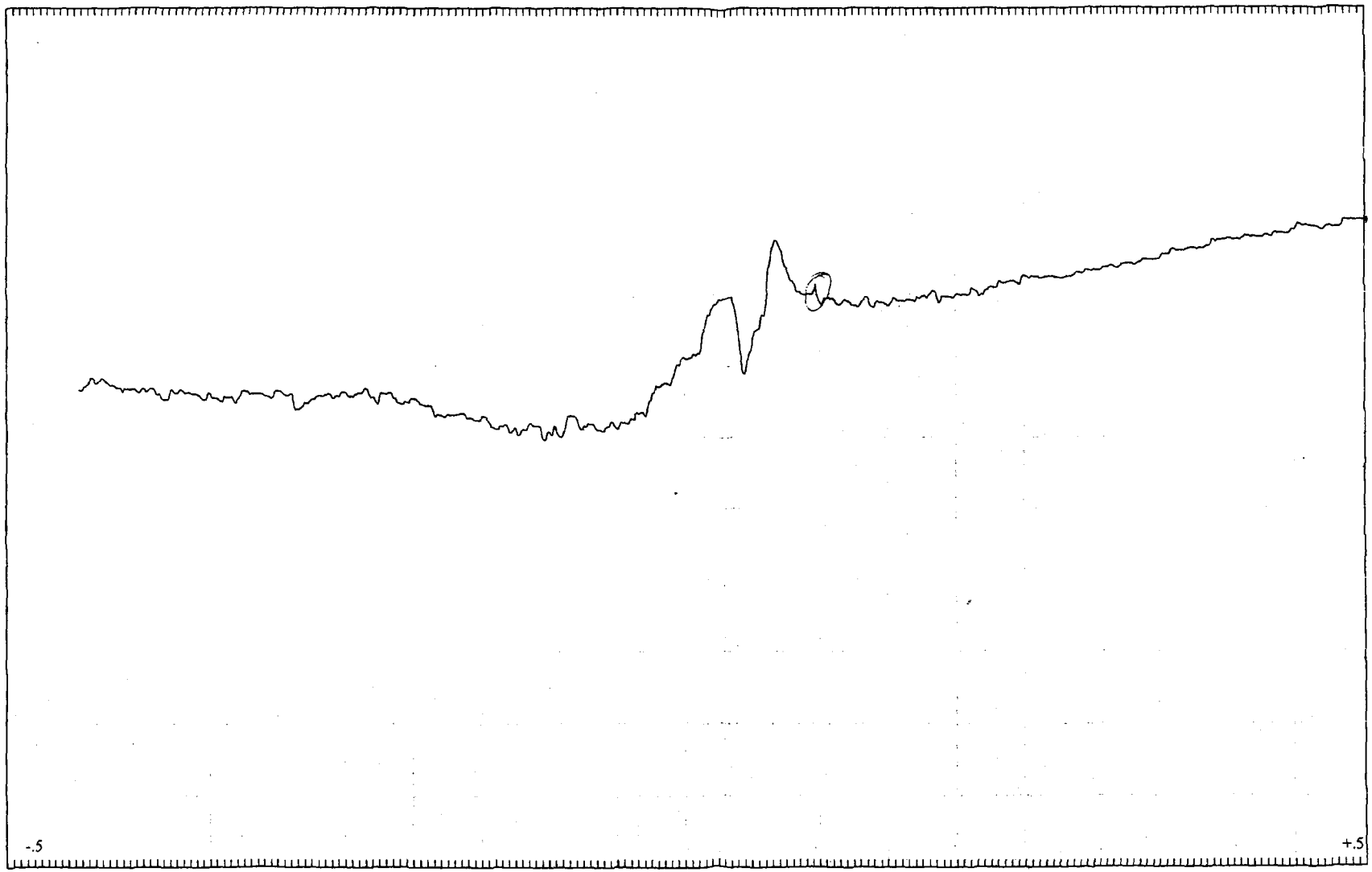

Fig. 5.6 (b) EPR spectrum of [Cu(H_2slox)(3-pic)] **(5.4)** in DMSO at Temperature: RT; Frequency: 9.1 GHz; Scan Range: 2000 G; Field Set: 3200 G.

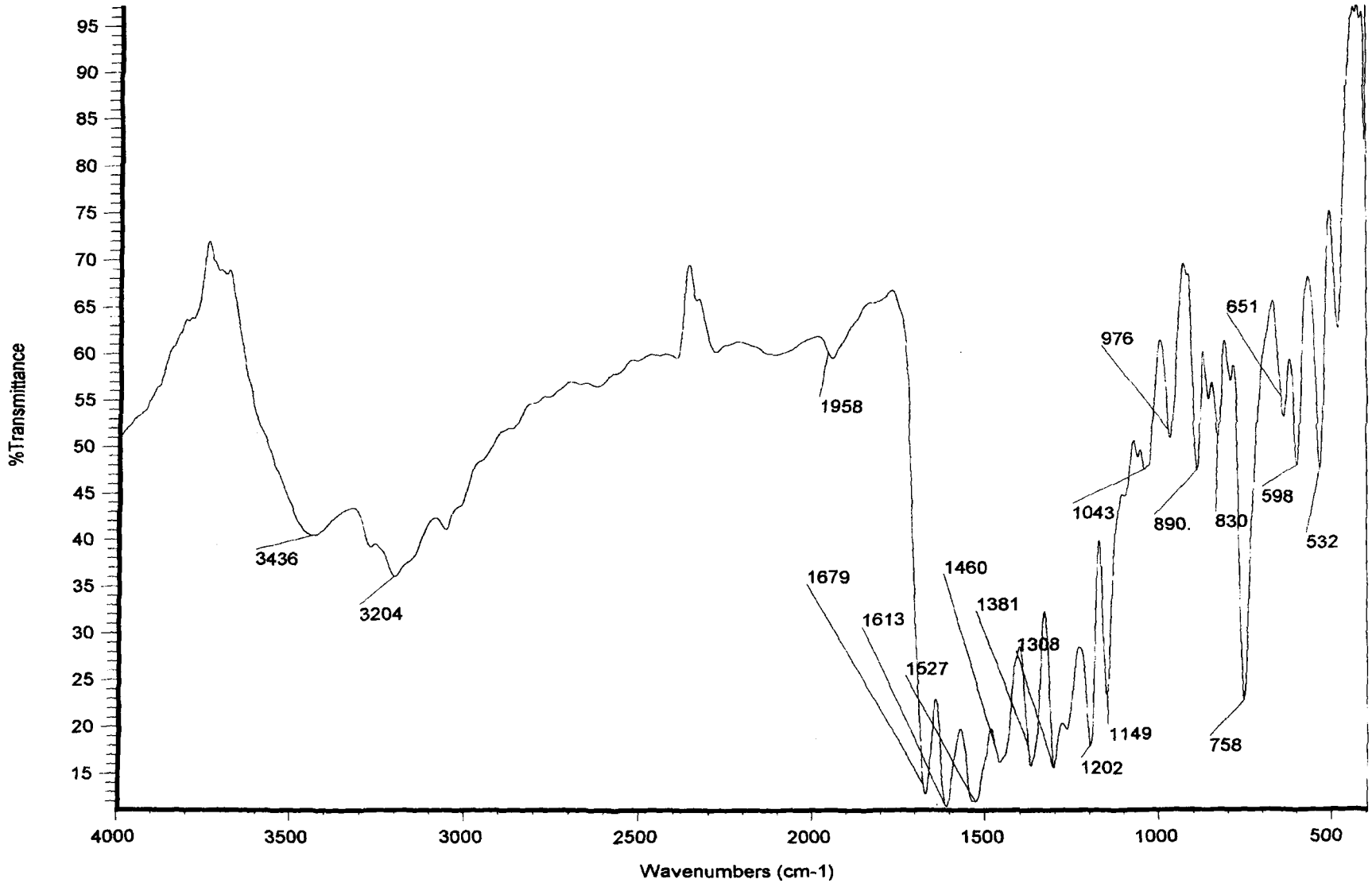

Fig. 5.7 Infrared spectrum of [Cu(H_2slox)] **(5.1)** in KBr.

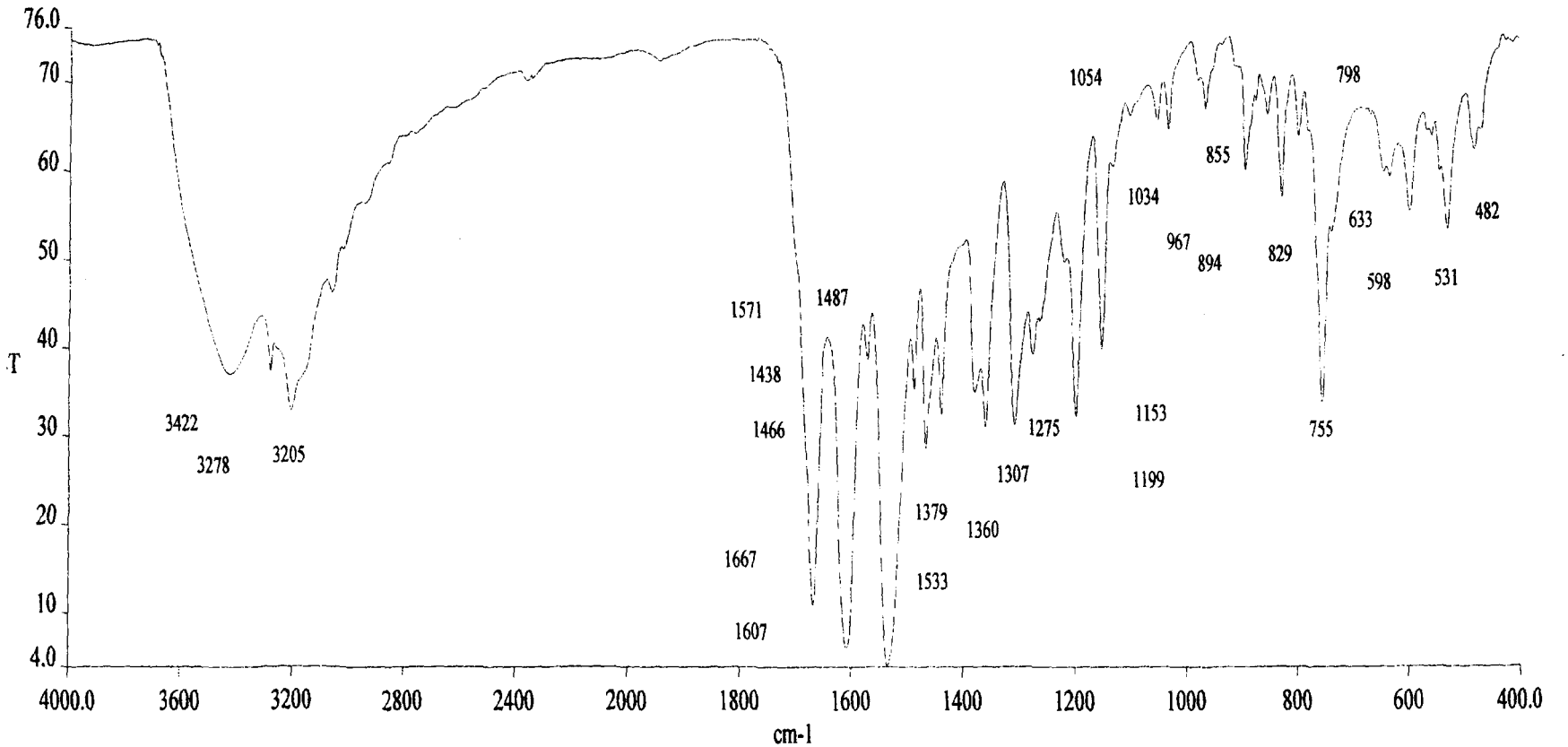

Fig. 5.8 Infrared spectrum of [Cu(H_2slox)(2-pic)] **(5.3)** in KBr.

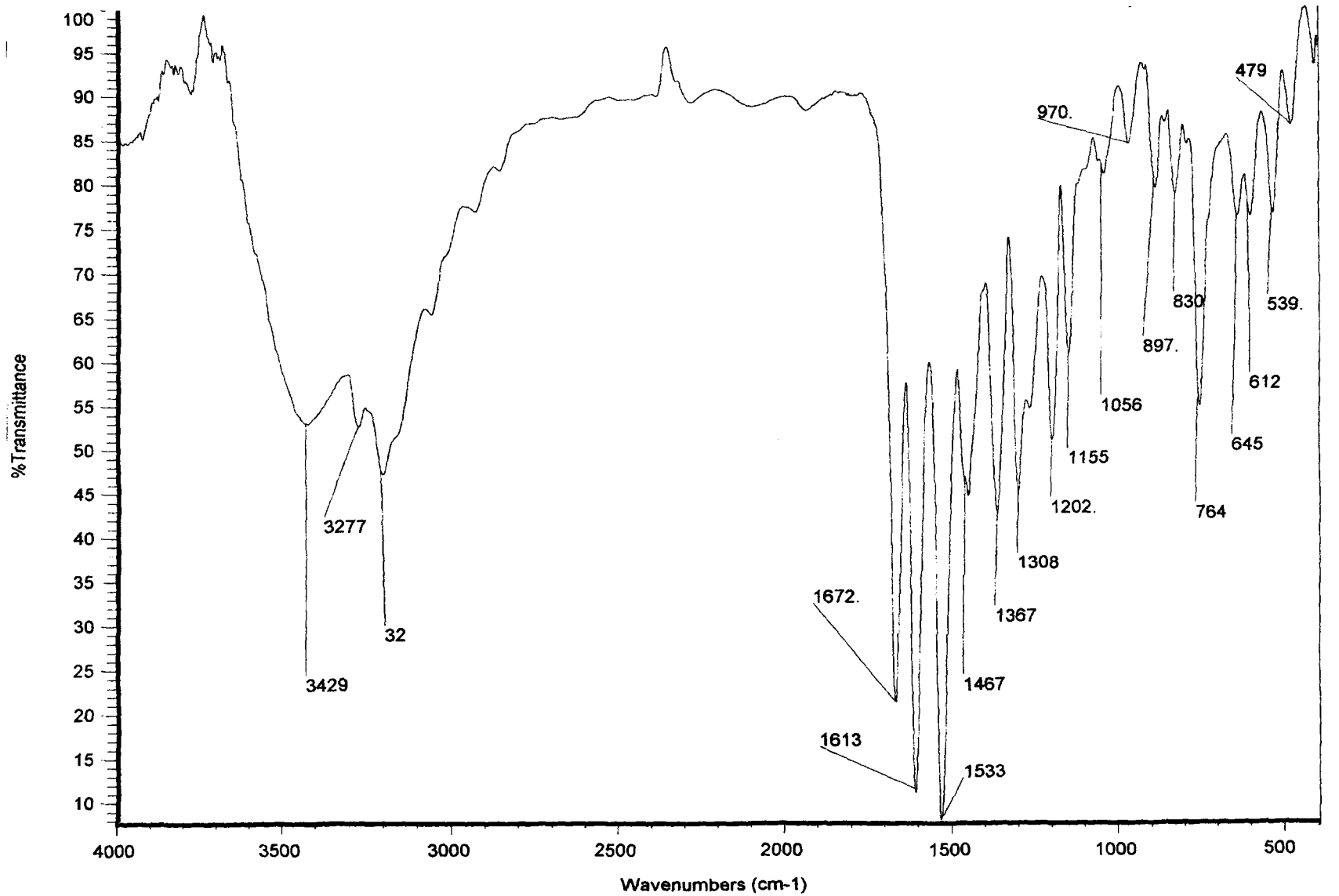

Fig. 5.9 Infrared spectrum of [Cu(H_2slox)(3-pic)] **(5.4)** in KBr.

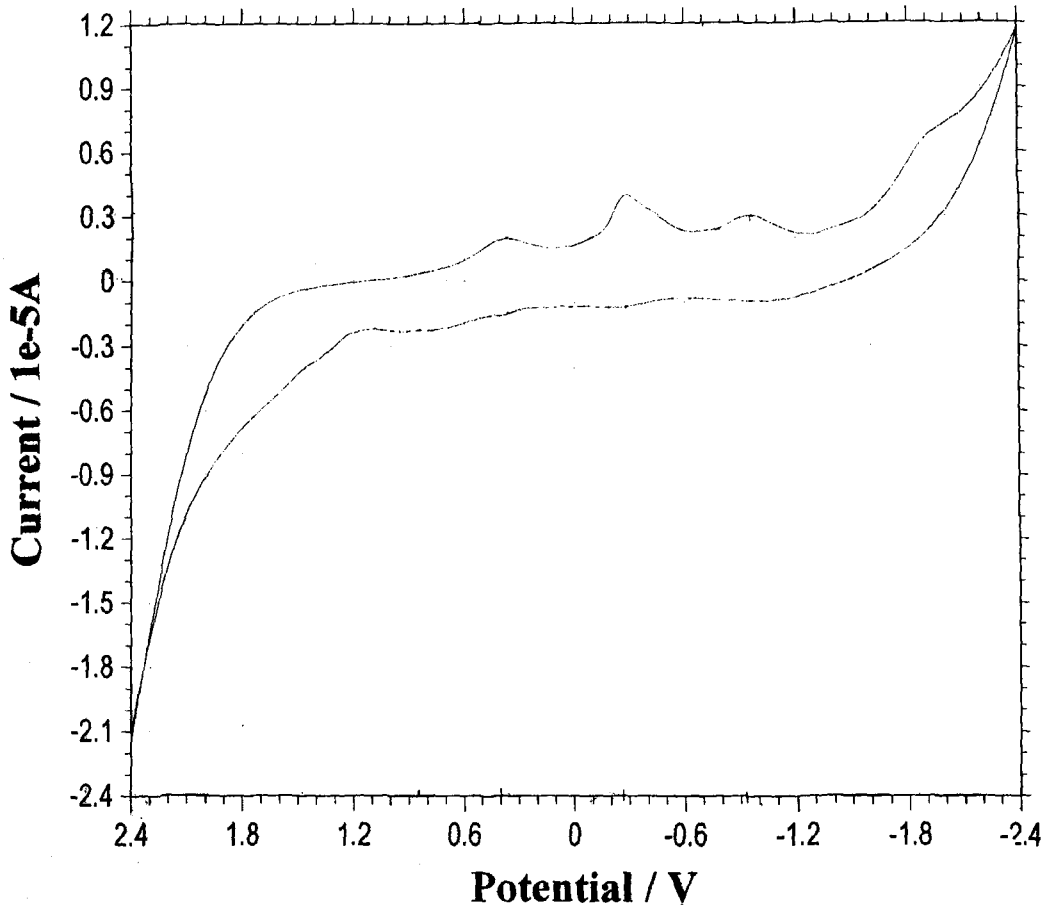

Fig. 5.10 Cyclic voltammogram of disalicylaldehyde oxaloyldihydrazone (H_4slox) at scan rate 100 mV/s.

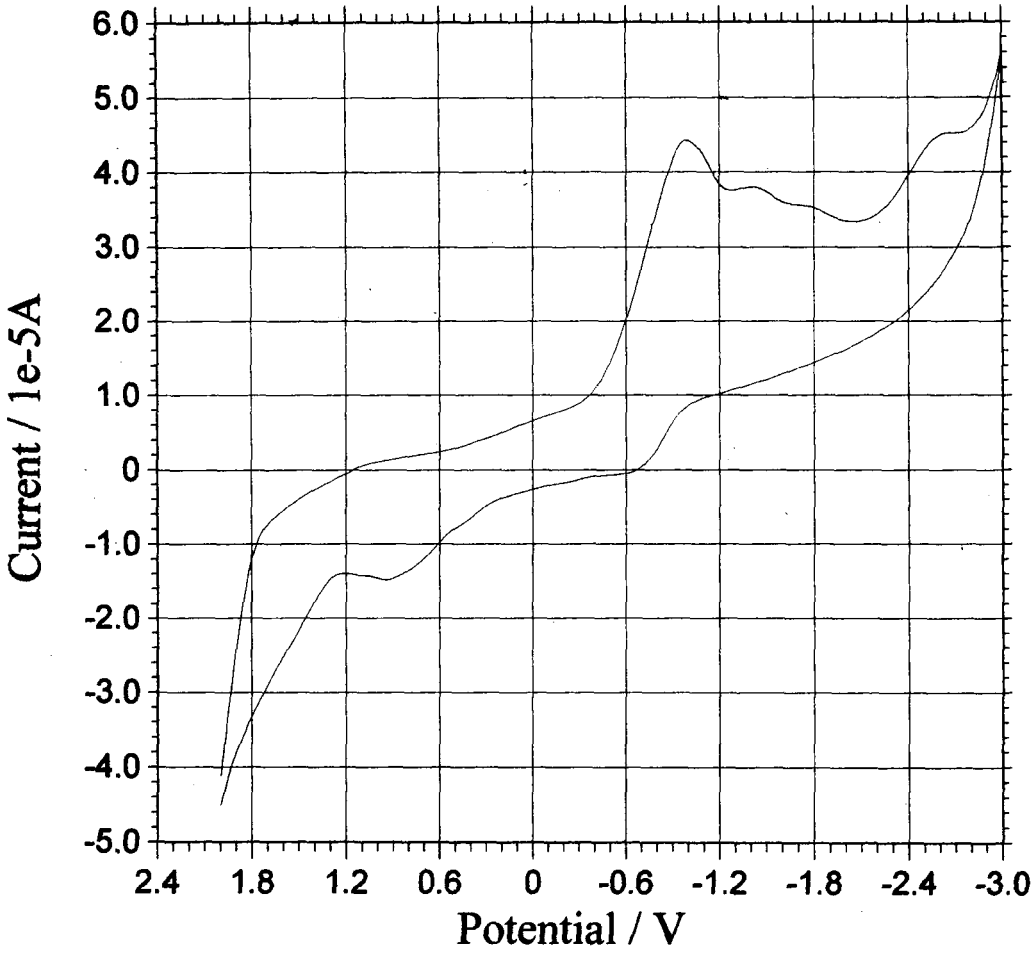

Fig. 5.11 Cyclic voltammogram of [Cu(H_2slox)] **(5.1)** at scan rate 100 mV/s.

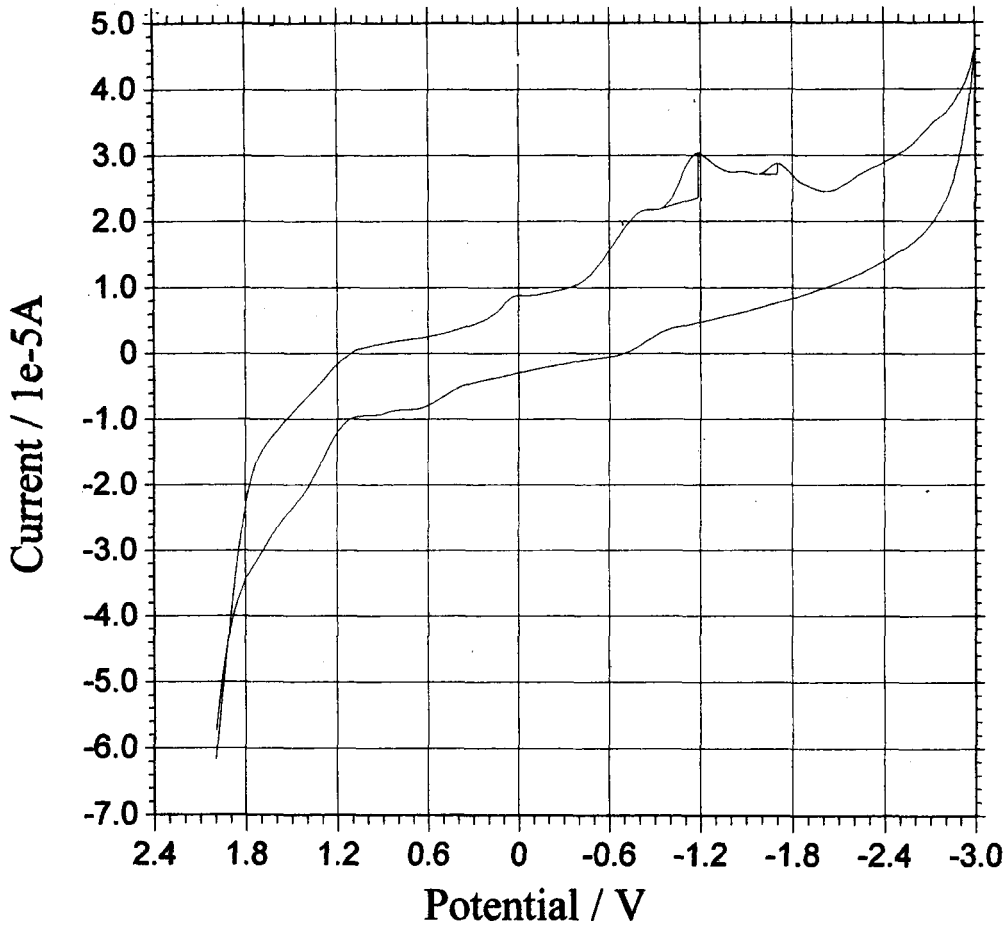

Fig. 5.12 Cyclic voltammogram of [Cu(H_2slox)(2-pic)] **(5.3)** at scan rate 100 mV/s.

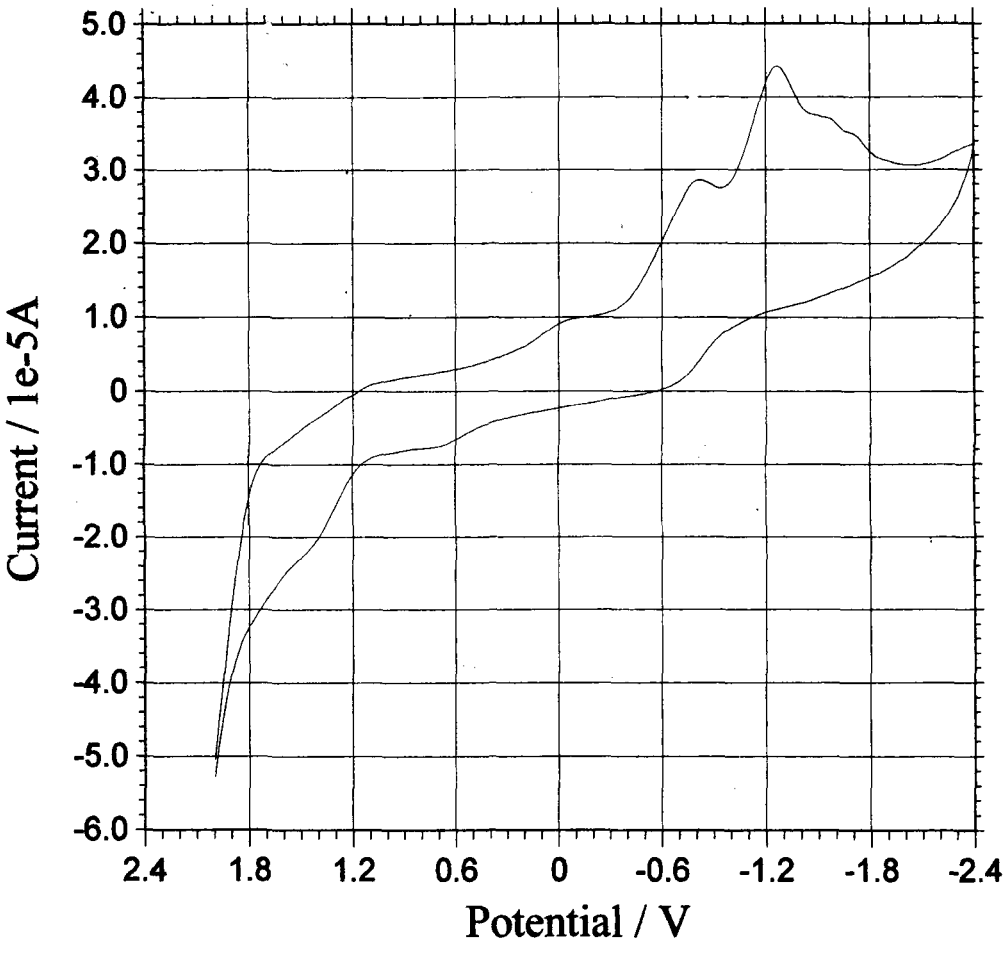

Fig. 5.13 Cyclic voltammogram of [Cu(H_2slox)(3-pic)] **(5.4)** at scan rate 100 mV/s.

Table 5.1: Complex, colour, decomposition point, analytical, molar conductance, magnetic moment and electronic spectral data for monometallic copper (II) complexes.

Sl. No.	Complex (colour)	D. P. (°C)	Elemental Analyses: Found (Calcd)%				Molar conductance Λ_M (ohm^{-1} cm^2mol^{-1})	Magnetic moment μ_{eff} (BM)	Electronic spectral band λ_{max}(nm) (ε_{max}) (dm^3 $mol^{-1}cm^{-1}$)
			M	C	H	N			
5.1	[Cu(H_2slox)] (Dark green)	>300	16.83 (16.40)	49.78 (49.59)	3.09 (3.12)	14.90 (14.46)	1.8	1.79	293(8554), 303(8518), 339(8743), 423(1276), 618(65)
5.2	[Cu(H_2slox)(py)] (Dark green)	>300	13.57 (13.62)	54.54 (54.05)	3.64 (3.67)	15.21 (15.01)	1.2	1.74	293(14381), 302(14394), 338(14350), 420(2505), 641(68)
5.3	[Cu(H_2slox)(2-pic)] (Dark green)	>300	13.70 (13.22)	55.10 (54.97)	3.96 (3.98)	14.86 (14.57)	1.5	1.71	292(13400), 303(13477), 336(13300), 420(3300), 661(59)
5.4	[Cu(H_2slox)(3-pic)] (Dark green)	>300	13.52 (13.22)	55.22 (54.97)	4.01 (3.98)	14.09 (14.57)	1.8	1.79	291(10050), 303(10192), 340(9892), 421(2777), 645(82)
5.5	[Cu(H_2slox)(4-pic)] (Dark green)	>300	12.81 (13.22)	54.67 (54.97)	4.03 (3.98)	14.62 (14.57)	1.4	1.75	294(15072), 304(15038), 339(14939), 423(3718), 636(90)

Table 5.2: EPR spectral data of monometallic copper (II) complexes at RT and LNT in DMSO solution.

Sl. No.	Complex	Temp	$g_{\|\|}$	$g_{\perp}$	g_{av}	$A_{\|\|} \times 10^{-4}$ (cm^{-1})	$A_{\perp} \times 10^{-4}$ (cm^{-1})	A_{av}	$g_{\|\|}/A_{\|\|}$	G	α^2
5.1	[Cu(H_2slox)]	RT	2.322	2.111	2.181	--	--	--	--	2.94	--
		LNT	2.339	2.125	2.196	180	70	107	129.9	2.74	0.929
5.2	[Cu(H_2slox)(py)]	RT	2.330	2.118	2.189	-	--	--	--	2.83	--
		LNT	2.326	2.107	2.180	175	--	--	132.9	3.09	0.895
5.3	[Cu(H_2slox)(2-pic)]	RT	2.318	2.114	2.182	--	--	--	--	2.83	--
		LNT	2.325	2.112	2.183	--	--	--		2.94	--
5.4	[Cu(H_2slox)(3-pic)]	RT	2.323	2.116	2.185	--	--	--	--	2.82	--
		LNT	2.314	2.104	2.174	174	75	108	132.9	3.06	0.878
5.5	[Cu(H_2slox)(4-pic)]	RT	2.329	2.119	2.189	--	--	--	--	2.80	--
		LNT	2.320	2.111	2.181	175	80	112	132.6	2.92	0.890

Table 5.3: Infrared spectral data for monometallic copper (II) complexes.

Sl. No.	Ligand/Complex	ν(OH) + ν(NH)	ν(C=O)	ν(C=N)	Amide II + ν(C-O) (phenolic)	ν(NCO)	ν(C-O)	ν(N-N)	ν(M-O) (phenolic)	ν(M-O) (enolic)
	H_2slox	3278(m) 3204(m)	1667(s)	1627(s) 1603(s)	1534(s)	--	1262(s)	1035(w)	--	--
5.1	[Cu(H_2slox)]	3436(m) 3278(m) 3204(m)	1679(s)	1613(s)	--	1527(s)	1276(s)	1043(w)	598(m)	482(w)
5.2	[Cu(H_2slox)(py)]	3423(m) 3277(m) 3211(m)	1672(s)	1613(s)	--	1533(s)[a]	1269(s)	1049(w)	605(m)	486(w)
5.3	[Cu(H_2slox)(2-pic)]	3422(m) 3278(m) 3205(m)	1667(s)	1607(s)	--	1533(s)[a]	1275(m)	1054(w)	598(m)	482(w)
5.4	[Cu(H_2slox)(3-pic)]	3249(m) 3277(m) 3200(m)	1672(s)	1613(s)	--	1533(s)[a]	1268(m)	1056(w)	612(m)	479(w)
5.5	[Cu(H_2slox)(4-pic)]	3423(m) 3264(m) 3204(m)	1679(s)	1613(s)	--	1533(s)[a]	1268(m)	1043(w)	605(m)	492(w)

a, ν(NCO) band merged with Amide II + ν(C-O) bands

Table 5.4: Electrochemical data for the monometallic copper (II) complexes.

Sl. No.	Ligand/Complex	E_{pc}	E_{pa}
	H_4slox	+0.40, -0.31, -0.93	--
5.1	[Cu(H_2slox)]	-0.95, -1.45, -1.80	-0.71, +0.95
5.2	[Cu(H_2slox)(py)]	-0.82, -1.12, -1.78	-0.72, +0.75,
5.3	[Cu(H_2slox)(2-pic)]	+0.25, -0.80, -1.18, -1.51, -1.70	-0.70, +0.65,
5.4	[Cu(H_2slox)(3-pic)]	-0.12, -0.78, -1.28, -1.60, -1.71	-0.69, +0.68
5.5	[Cu(H_2slox)(4-pic)]	-0.85, -1.25	--

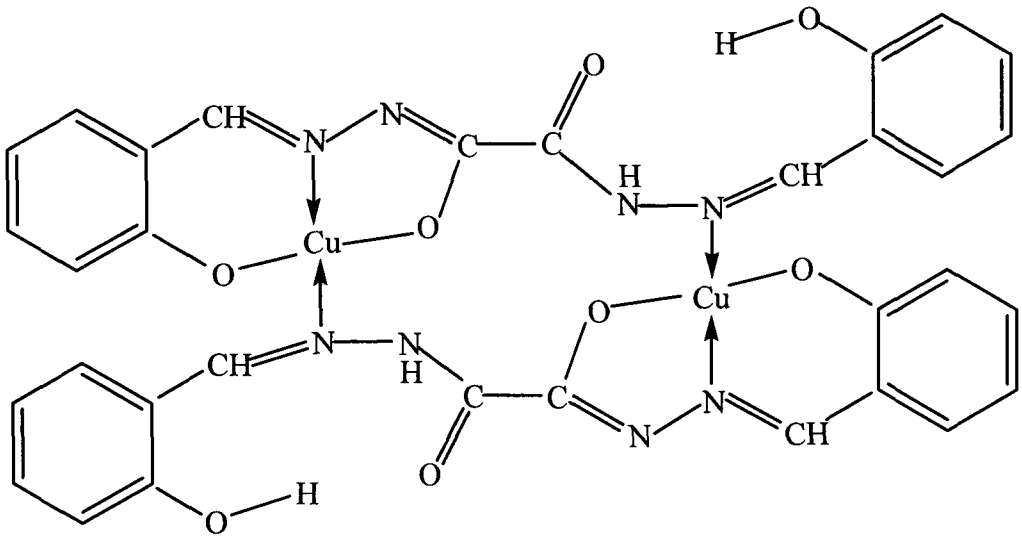

Fig. 5.14 Tentative structure of [Cu(H_2slox)] **(5.1)**.

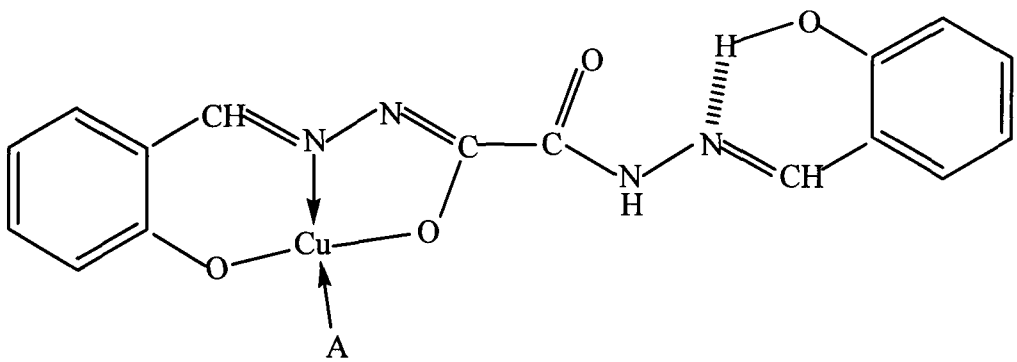

Fig. 5.15 Tentative structure of [Cu(H_2slox)(A)] {*where A = pyridine* **(5.2)**, *2-picoline* **(5.3)** ,*3-picoline* **(5.4)** *and 4-picoline* **(5.5)**}.

Refrences

1. H. Dobbek, L. Gremmer, O. Meyer and R. Huber, "*In Handbook of Metallo-proteins*"; A. Messerschmidt, R. Huber, K. Weighardt and T. Poulos, Eds., Wiley, Chiechester, U.K., **Vol. 2**, p. 1136-1147 (2001).
2. A. Siegel and H. Siegel, Eds., "*Metal Ions in Biological Systems*", Marcel Dekkar, New York, **Vol. 39** (2002).
3. C. Gourlay, D. J. Nielsen, J. M. White, Z. Knottenbelt, M. L. Kirk and C. G. Young, *J. Am. Chem. Soc.*, **128**, 2164 (2006).
4. A. N. Papadopoulos, A. G. Hatzidimitriou, A. Gourdon and D. P. Kessissglou, *Inorg. Chem.*, **33**, 2073 (1994).
5. F. de Silva and R. J. P. Williams, "*The Biological Chemistry of the Elements*", Clarendon Press; Oxford, England, p. 417, 540 (1991).
6. J. C. Bailer, H. J. Emeleus, R. Nyholeu, X. Trotman-Dickenson, "*In Comprenhensive Inorganic Chemistry*", G. Wilkinson, Eds., Perganion: Oxford, England, **Vol. 3**, Chapter 36 (1973).
7. C. F. Mills, *Philos. Trans. R. Soc. London, Ser.* B, **228**, 1 (1979).
8. C. F. Mills, *Chem. Ber.*, b, 512 (1979).
9. S. Sahe and J. F. Stoddart, *Chem. Soc. Rev.*, **36**, 77-92 (2007).
10. M. Irie, *Chem. Rev.*, **100**, 1683 (2000).
11. "*Ferroelectric Polymers: Chemistry, Physics and Applications*", H. S. Naleva, Eds., Marcel Dekker, Inc: New York (1995); C. M. E. Lines and A. M. Glass, "*Principles and Applications of Ferroelectrics and Related Materials*", the International Series of Monographs on Physics; Clarendon Press: Oxford, U.K. (1977).
12. J. M. Herrera, V. Marvand, M. Verdaguer, J. Manot, M. Kalisz and C. Mathomieve, *Angew. Chem. Int. Ed.*, **43**, 5468-5471 (2004).
13. K. Nakagawa, H. Tokoro and S. Ohkoshi, *Inorg. Chem.*, **47**, 10810 (2008).
14. D. Brinzei, L. Catala, C. Mathoniere, W. Wemsdorfer, A. Gloster, O. Stephan and T. Malla, *J. Am. Chem. Soc.*, **129**, 3778-3779 (2007).

15. J. Long, L. M. Chauoreau, C. Mathoniere and V. Marvand, *Inorg. Chem.*, **48**, 22 (2009).

16. M. A. Ansavi and J. A. Ibers, *Coord. Chem. Rev.*, **100**, 223-226 (1990); X. T. Wu, "*Inorganic Assembly Chemistry*", Science Press: Beijing, China, pp. 1-179 (2004).

17. C. Zhang, Y. L. Song and X. Wang, *Coord. Chem. Rev.*, **251**, 111-141 (2007); S. Shi, "*In Optoelectronic Properties of Inorganic Compounds*", D. M. Roundhill and J. P. Fackler, Eds., Plenum, New York, p. 55-105 (1998); B. J. Coc, "*In Comprehensive Coordination Chemistry II*", J. A. McCleverty and T. J. Meyer, Eds., Elsevier: Oxford, U.K., **Vol. 9**, p. 621-687 (2004).

18. R. H. Holm, *Adv. Inorg. Chem.*, **38**, 1-71 (1992); "*Molybdenum Enzymes Cofactors and Model Systems*", E. I. Stiefel, D. Coucouvarins and W. E. Newton, Eds., ACS Symposium Series 535, American Chemical Society: Washington D.C. (1993); "*Transition Metal Sulfur Chemistry, Biological and Industrial Significances*", E. I. Stiefel and K. Matsumoto, Eds., ACS Symposium Series 653, American Chemical Society: Washington D.C. (1996).

19. M. Takuma, Y. Ohki and K. Tatsumi, *Inorg. Chem.*, **44**, 6034 (2005); G. N. George, I. J. Pickering, H. H. Harris, J. Gailer, D. Klein, J. Lichtmannegger and K. H. Summer, *J. Am. Chem. Soc.*, **125**, 1704 (2003).

20. Y. Y. Niu, H. G. Zhang and X. L. Xui, *Coord. Chem. Rev.*, **248**, 169-183 (2004).

21. J. Y. Yang, J. H. Gu, Y. L. Song, G. Shi, Y. X. Wang, W. H. Zhang and J. P. Lang, *J. Physc. Chem.*, **111B**, 7987-7993 (2007); J. Wang, Z. R. Sun, L. Deng, Z. H. Wei, W. H. Zhang and J. P. Lang, *Inorg. Chem.*, **46**, 11381-11389 (2007).

22. W. H. Zhang, Y. L. Song, Z. G. Rev, H. X. Li, L. L. Li, Y. Zhang and J. P. Lang, *Inorg. Chem.*, **46**, 6647-6660 (2007).

23. J. P. Lang, X. F. Xu, Z. N. Chen and B. F. Abrahams, *J. Am. Chem. Soc.*, **125**, 12682-12683 (2003).

24. I. Fridovich, *J. Biol. Chem.*, **272**, 18515-18517 (1997).

25. S. Yoshikawa, "*Advances in Protein Chemistry*", **Vol. 60**, p. 341-342 (2002); J. Stenesh, "*Biochemistry*", p. 299 (1998).

26. G. Mezei, R. G. Raptis and J. Teser, *Inorg. Chem.*, **45**, 8841 (2008).

27. E. I. Solomon, U. M. Swedaram and T. E. Machonkin, *Chem. Rev.*, **96**, 2563 (1996).

28. H. H. T. Nguyen, S. J. Elliot, J. H. K. Yip and S. I. Chan, *J. Biol. Chem.*, **273**, 7957 (1998).

29. J. D. Sewran, D. Zolandz, M. E. Lindstrom and S. I. Chan, *J. Inorg. Biochem.*, **58**, 235 (1995); H. H. T. Bguyen, K. H. Nakagawa, B. Hedman, S. J. Elliot, M. E. Lindstrom, K. D. Hodgson and S. I. Chan, *J. Am. Chem. Soc.*, **118**, 12766 (1996).

30. S. S. Lewos, H. Yuan, M. L. P. Collins and W. E. Antholine, *Curr. Top. Biophys.*, **26**, 43 (2002); R. L. Liebermann and A. C. Rosenziolig, *Nature (London)*, **434**, 177 (2005).

31. N. W. Solomons, *J. Am. Coll. Nutr.* **4**, 83-105 (1985).

32. R. L. Dutta and Md. M. Hossain, *J. Scient. Ind. Res.*, **44**, 635 (1985).

33. R. A. Lal, S. Adhikari, A. Kumar, J. Chakraborty and S. Bhaumik, *Synth. React. Inorg. Met-Org. Chem.*, **32**, 81 (2002).

34. R. A. Lal, A. Kumar and J. Chakraborty, *Indian J. Chem.*, **40A**, 422 (2001).

35. R. A. Lal, L. M. Mukherjee, A. N. Siva, A. Pal, S. Adhikari, K. K. Narang and M. K. Singh, *Polyhedron*, **12**, 2351 (1993).

36. R. A. Lal, A. N. Siva, S. Adhikari, M. K. Singh and U. S. Yadav, *Synth. React. Inorg. Met-Org. Chem.*, **26 (2)**, 321 (1996); F. Feigel, V. Anger and R. E. Oesper, "*Spot Test in Organic Analysis*", 7th Ed., Elsevier Publishing Company, Amsterdam, Netherlands, p. 173, 384 (1996), (Indian Reprint, 2005).

37. M. Hussain, S. S. Bhattacharjee, K. B. Singh and R. A. Lal, *Polyhedron*, **10**, 779 (1991).

38. W. J. Geary, *Coord. Chem. Rev.*, **7**, 81 (1971).

39. B. N. Figgis, *Nature*, **182**, 1568 (1958).

40. M. D. Cohen and S. Flavian, *J. Chem. Soc.*, B **317**, 321, 329 and 334 (1967).

41. C. M. Metzler, A. Cahill and D. E. Metzler, *J. Am. Chem. Soc.*, **102**, 6075 (1980).

42. J. W. Lewis and C. Sandorfy, *Can. J. Chem.*, **60**, 1727 (1982).

43. D. Gegiou, E. Lambi and E. Hadjoudis, *J. Phys. Chem.*, **100**, 17762 (1996).

44. T. Kawasaki, T. Kamata, H. Ushjima, M. Kanakuba, S. Murata, F. Mizukami, Y. Fujii and Y. Usui, *J. Chem. Soc. Perkin Trans.*, **2**, 193 (1999).

45. T. N. Sorrell, *Tetrahedron*, 54 (1989).

46. T. N. Sorrell, D. L. Jameson and C. J. O'Conner, *Inorg. Chem.*, **33**, 456 (1994).

47. T. N. Sorrell, C. J. O'Conner, O. P. Anderson and J. H. Reibnenspies, *J. Am. Chem. Soc.*, **107**, 4199 (1985).

48. K. J. Oberhausen, J. F. Richardson, R. M. Bachanan, J. M. McCusker, D. N. Hendrickson and J. Mare Latour, *Inorg. Chem.*, **30**, 1357, (1991).

49. S. Teipel, K. Griesa, W. Haase and B. Kerbs, *Inorg. Chem.*, **33**, 456 (1994).

50. B. J. Hathaway, "*In Comprehensive Coordination Chemistry*", p. 594-774, Vol. **5**; G. W. Wilkinson, R. D. Gillard and J. A. McLeverty, Ed. Perganion Press, Oxford, New York (1987).

51. A. B. P. Lever, "*Inorganic Electronic Spectroscopy*", Elsevier (1968).

52. A. A. G. Tomlinson and B. J. Hathaway, *Coord. Chem. Rev.*, **5**, 142 (1970).

53. T. M. Dunn, "*The Visible and Ultraviolet Spectra of Complex Compounds*", in Modern Coordination Chemistry, Ed. J. Lewis and R. G. Wilkins.

54. L. Sacconi and M. Ciampolini, *J. Chem. Soc.*, A, 273 (1964).

55. D. Kivelson and R. Neiman, *J. Chem. Phys.*, **35**, 149 (1961).

56. S. Sujatha, T. M. Rajendiran, R. Kannappan, R. Venkatesan and P. Sambasiva Rao, *Proc. Indian Acad. Sci.*, **112 (6)**, 559 (2000).

57. A. Syamal. R. L. Dutta, "*Elements of Magneto Chemistry*", East West Press Pvt. Ltd., New Delhi (1993).

58. V. Suresh Babu, A. Ramesh, P. Raghuram and R. Raghava Naidu, *Polyhedron*, **16**, 607-612 (1997); S. Djebbar-Sid, O. Benalibaitich and J. P. Deloume, *Polyhedron*, **16**, 2175 (1997).

59. R. M. Silverstein and G. C. Bassler, "*Spectroscopic Identification of Organic Compounds*", Wiley, New York (1967).

60. C. N. R. Rao, "*Chemical Application of Infrared Spectroscopy*", Academic Press, New York (1963).

61. S. Naskar, D. Mishra, R. J. Butcher and S. K. Chattopadhyay, *Polyhedron*, **26**, 3703 (2007).

62. P. K. Radhakrishnan, P. Indrazenan and C. G. R. Nair, *Polyhedron*, **3**, 67 (1984); R. K. Aggarwal and J. Prakash, *Polyhedron*, **10**, 2567 (1991).

63. R. M. Issa, K. Y. El-Baradie and S. A. El-Koni, *J. Coord. Chem.*, **57**, 1611 (2004).

64. R. Gup and B. Kurkan, *Spectrochim. Acta A*, **62**, 1188 (2005).

65. R. J. H. Clark, *J. Chem. Soc.*, 1377 (1962); R. J. H. Clark and C. S. Williams, *Inorg. Chem.*, **4**, 350 (1965).

66. L. Sacconi, A. Sabatini and P. Gans, *Inorg. Chem.*, **3**, 1772 (1964).

67. G. C. Percy and D. A. Thornton, *J. Inorg. Nucl. Chem.*, **35**, 3357 (1972).

68. G. C. Percy and D. A. Thornton, *J. Inorg. Nucl. Chem.*, **34**, 3369 (1972).

69. N. Okhaku and K. Nakamoto, *Inorg. Chem.*, **10**, 798 (1971).

70. B. Hutchinson, J. Takemoto and K. Nakamoto, *J. Am. Chem. Soc.*, **92**, 3335 (1975).

71. A. B. P. Lever and E. Mantovani, *Can. J. Chem.*, **51**, 1567 (1973).

72. A. E. Martell, K. Nakamoto and P. J. McCarthy, *Nature*, **183**, 459 (1959).

73. K. Nakamoto and A. E. Martell, *J. Chem. Phys.*, **32**, 588 (1960).

74. K. Nakamoto, P. J. McCarthy, A. Duby and A. E. Martell, *J. Am. Chem. Soc.*, **83**, 1066, 1272 (1961).

CHAPTER VI

Synthesis and Characterization of Homotrimetallic Copper (II) Complexes derived from Polyfunctional Disalicyaldehyde oxaloyldihydrazone

Introduction

Chapter V describes the synthesis and characterization of monometallic copper complexes of H_4slox synthesized by template method. The title ligand being a polyfunctional ligand is capable of binding more than one metal atom if an excess of metal salt is used in the reaction. This is considered to be the most plausible possibility because copper occurs in the biological systems with few exceptions as binuclear or multinuclear systems. Hence, it was considered worthwhile to investigate the reactions of the polyfunctional dihydrazone ligand with the excess of metal salt and to explore the structures of the resulting complexes. In fact, in the present study, a monometallic complex described in the previous chapter has been used as a metal complex ligand and allowed to react with the excess of the metal salt and the products have been isolated and characterized. It appears appropriate at this stage, before we proceed for the synthesis of multimetallic copper (II) complexes to brief the importance of copper in multimetallic systems.

The importance of homobimetallic and polymetallic copper (II) complexes stems from the fact that copper is an essential bio-element responsible for numerous catalytic processes in living organism where it is often present in di- or trinuclear assemblies. The multinuclear arrays of copper centres at the active sites of copper oxidases and oxygen transport proteins are invariably present. Multinuclear copper oxidases are an important class of enzymes found in bacteria, fungi, plants and animals. Copper is present in enzymes in biological systems either alone or in combination with some other metal ions to discharge their biological functions. When copper is present alone in enzymes in biological systems, it occurs either as a

couple of ions or more than a couple of ions. Thus hemocyanin and tyrosinase contains binuclear copper sites while laccase, ascorbate oxidase, human ceruloplasmin, fungal laccase, FET 3 and phenoxazinase synthase etc. contain more than two copper atoms. Ceruloplasmin (Cp) is the only multicopper oxidase found in human [ferroxidase iron (II): dioxidoreductase EC] in which it is present in combination with iron. The physiological role of Cp is still somewhat in dispute, however, a consensus is emerging that it is a plasma ferroxidase **[1-4]**. All multicopper oxidases utilize at least four Cu ions to couple the four electron reduction of O_2 to H_2O with four sequential one-electron substrate oxidations. Multicopper oxidases contain four copper ions of the following types: atleast one blue copper or Type 1 site (T1) **[5]**, a normal or Type 2 site (T2) and a Type 3 copper pair (T3) involving strong antiferromagnetic coupling leading to the lack of EPR signal. The T2 and T3 site form a trinuclear cluster which is the site for dioxygen reduction. The function of the T1 site is to transfer electrons from substrate to the trinuclear cluster and this is the site for substrate oxidation. Substitution of the blue copper site by a redox innocent mercuric ion significantly impedes O_2 bond cleavage by the fully reduced trinuclear site. The absence of this fourth reducing equivalent stabilizes an intermediate in which dioxygen has been reduced by $2e^-$ to the peroxide level **[6]**. A $3e^-$ reduced O_2 species is apparently not thermodynamically preferred; as the peroxide is ligated directly to an easily oxidized Cu (I) species **[7]**. These data support the notion that dioxygen bond cleavage in the native trinuclear enzymes occur in two sequential $2e^-$ steps, with each of the four coppers providing 1 e^- **[8]**.

Ceruloplasmin is unique among the multicopper oxidases in that it contains additional copper sites beyond the four required for oxidase activity. Huber and Frieden were among the first to establish that human Cp contains six copper per molecule, with an additional labile copper-binding site that does not alter the oxidase activity **[9]**. Ortel et.al. **[10]** and later Messerschmidt and Huber **[11]** examined the sequence homology among the various multicopper oxidase and plastocyanin and noted that there are three putative T1 binding sites, one with a leucine in place of methionine. The crystal structure of Zeifseva etal confirms this basic stoichiometry

of six integral coppers (a trinuclear cluster and seventh labile copper) distributed between the two cation binding sites **[12]**.

Despite the extensive number of multicopper oxidases that have been structurally and spectroscopically characterized, several functionally relevant questions regarding the chemical nature of the trinuclear Cu cluster remains. One has to do with the nature of the water-derived ligand at the T2 site, its protonation state and its relation to the pH dependence of the enzyme reactivity. Moreover, the origin of the coordination unsaturation of the T2 and T3 sites is not fully understood (both have open positions directed inside the cluster) and some controversy exists regarding the nature and identity of the paramagnetic centre of the cluster **[13-16]**. The nature of the exogeneous ligand binding to the cluster has been studied in detail by spectroscopic methods in solution and it is clear that these ligands bridge the cluster **[6, 17, 18]**. However, the crystal structures of the azide and peroxide-bound forms show an uncoupling of T3 Cu (i.e. two Cu^{2+} centres at ~ 5Å with no bridge) **[5, 19, 20]**. Azide and peroxide bind to the cluster with low affinity while one of the unique features of the trinuclear cluster is its extremely high affinity for fluoride **[21-23]**. Finally, the crystal structures of the resting trinuclear cluster show open coordination positions at both the T2 and T3 centres indicating that a water or hydroxide ligand from the accessible solvent does not bind within the cluster even though the T2 Cu^{II} is three coordinate. Further, it has been shown that nitrous oxide reductase has a tetracopper active centre containing one capping sulfide and two terminal water (hydroxide ligand) **[24]**. Multicopper complexes are important for catalysis **[25]** as well as magnetic aspect **[26]**.

The polymetallic copper complexes have also become important because of their relevance in the development of novel functional materials showing molecular ferromagnetism **[27]** and specific catalytic properties **[28]**. Homotrimetallic copper (II) complexes also enjoy a clear fascination of the magnetochemists, as the complexes offer the opportunities to test magnetic exchange models on more complicated systems than the extensively studied binuclear **[29]** types. Many of these

complexes have $[Cu_3(\mu\text{-}X)(\mu\text{-}L)_3]$ ($X = O^{2-}$, OH^-, OCH_3^-, CO_3^{2-}, Cl^-, etc) triangular core **[30-35]** with L-bridges and they exhibit interesting magnetic properties. These studies offer opportunities to focus our attention on the properties of spin quartet ground states in ferrogmagnetic exchanged coupled systems or more complex behaviours due to spin-frustations.

In view of the above importance of the multicopper complexes, in biological systems, catalysis and magnetochemistry and polyfunctional nature of the dihydrazone ligand and the fact that the previous chapter has described monometallic copper (II) complexes synthesized by template method of the title ligand, it was of interest to synthesize multimetallic copper complexes and to characterize them by various physico-chemical and spectroscopic techniques. Several synthetic approaches have been proposed to design discrete polynuclear complexes. One of them consists of the introduction of bidentate or tridentate terminal ligands **[36]** and multi-atom bridging ligands **[37, 38]**. Another consists of the use of compartmental ligands, which are organic molecules able to hold together two or more metal ions **[39]**. Third approach uses metal complexes as ligands **[40]**.

A survey of literature shows that the homobimetallic copper complexs have been synthesized and characterized to a great extent. Further, although some work has been done on oligomeric copper (II) complexes with more than two copper ions **[41-51]**, yet the work on homotrimetallic copper (II) compounds containing linear arrangement of metal ions is quite scanty **[52, 53]**.

Majority of the copper complexes derived from dihydrazones are either monometallic or homobimetallic in nature but not even a single homotrimetallic complex has been synthesized and characterized **[54]**. In view of the above importance of the homotrimetallic copper complexes and absence of work on homotrimetallic copper complexes of dihydrazones, the present chapter aims at the synthesis and characterization of some homotrimetallic copper complexes of disalicylaldehyde oxaloyldihydrazone (H_4slox) using "complex as ligand" approach

[55]. The monometallic copper (II) complex [Cu(H_2slox)] **(5.1)** prepared in the previous chapter has been used as a precursor for the preparation of multimetallic copper complexes. Accordingly the complex [Cu(H_2slox)] was allowed to react with $CuCl_2.2H_2O$ in 1: 2.5 molar ratio in methanol under reflux. The isolated multimetallic copper (II) complexes were further reacted with pyridine and substituted pyridines and the structure of the isolated complexes were mainly discussed in the light of the elemental analyses, conductivity, magnetic moment, EPR, IR and electronic spectral data. The electron transfer reactions of the complexes have also been studied by cyclic voltammetry.

Experimental

Preparation of [Cu_3(slox)$Cl_2(H_2O)_2$] (6.1)

[Cu(H_2slox)] (1.00 g, 2.47 mmol) was suspended in methanol (30 mL) by stirring for about 10 minutes to make it homogenous. $CuCl_2.2H_2O$ (1.09 g, 6.39 mmol) was dissolved in methanol (30 mL) by stirring for 10 minutes accompanied by gentle heating. [Cu(H_2slox)] suspension was than added to $CuCl_2.2H_2O$ solution over a period of 30 minutes and the resulting mixture was refluxed for 1/2h. This gave a dark green coloured compound, which was filtered, washed with methanol followed by ether and dried over anhydrous $CaCl_2$.

Preparation of [Cu_3(slox)$Cl_2(A)_2$] {*where A = pyridine (py)* **(6.2)**, *2-picoline (2-pic)* **(6.3)**, *3-picoline (3-pic)* **(6.4)** *and 4-picoline (4-pic)* **(6.5)**}

In order to prepare [Cu_3(slox)$Cl_2(py)_2$], [Cu_3(slox)$Cl_2(H_2O)_2$] (0.50g, 0.81 mmol) was suspended in methanol (30 mL) and stirred for about 10 minutes to make it homogeneous. To this suspension 0.61 mL of pyridine was added slowly and the resulting mixture was refluxed for 1/2h. This gave a greenish coloured compound which was filtered, washed with methanol followed by ether and dried over anhydrous $CaCl_2$.

The compound $[Cu_3(slox)Cl_2(2\text{-}pic)_2]$, $[Cu_3(slox)Cl_2(3\text{-}pic)_2]$ and $[Cu_3(Slox)Cl_2(4\text{-}pic)_2]$ were also prepared by essentially the above procedure using 0.71 mL each of 2-picoline, 3-picoline and 4-picoline instead of pyridine.

Results and discussion

In this chapter we have prepared some homotrimetallic copper (II) complexes. The "complex as ligand" method was employed to synthesize the homotrimetallic complexes. The monometallic complex $[Cu(H_2slox)]$ prepared in the earlier chapter was used as the ligand. The monometallic complex was allowed to react with $CuCl_2.2H_2O$ in methanol which yielded homotrimetallic copper (II) complex. The homotrimetallic complex was than reacted with pyridine and substituted pyridine to check whether the pyridine/substituted pyridine molecule occupies the coordination sphere or not and to note the changes brought about. The complexes prepared in this chapter were found to have the compositions: $[Cu_3(slox)Cl_2(A)_2]$ {*where A = H_2O* **(6.1)**, *pyridine (py)* **(6.2)**, *2-picoline (2-pic)* **(6.3)**, *3-picoline (3-pic)* **(6.4)** *and 4-picoline (4-pic)* **(6.5)**}.

All these complexes are dark green in colour and decompose above 300°C. They are air stable and insoluble in common organic solvents. The solubility of these complexes in highly coordinating solvents such as DMSO and DMF is also poor. The compositions of the complexes were mainly determined from elemental analyses, and the stereochemistry of the complexes around Cu atom was determined from electronic and magnetic measurements.

Thermal analyses

Detail decomposition studies **[56]** of the copper (II) complexes **(6.1)** to **(6.5)** were carried out in the temperature range of 70 – 250°C, the vapours evolved were identified by passing through a separate test tube containing, anhydrous copper

sulphate, a solution of sodium hydroxide, a solution of iodine and sodium hydroxide and cyanogen bromide solution.

The vapours evolved by heating the complexes in the temperature range 70 -250°C were allowed to pass through a four separate test tube containing different solutions. No vapours evolved in the temperature range of 90-120°C which could turn the test tube containing anhydrous copper sulphate blue dismissing the possibility of presence of lattice water molecules **[57]** in these complexes. The vapours evolved at 160-180°C in the complex **(6.1)** turned the anhydrous copper sulphate blue indicating the presence of coordinated water molecule **[58]**. Complexes **(6.2)** to **(6.5)** did not show any weight loss around 180°C and did not give a positive test with anhydrous copper sulphate solution indicating the absence of water molecule inside the coordination sphere.

The vapours evolved in the complex **(6.2)** in the temperature range 220 – 240°C turned $CHCl_3$ and NaOH solution red confirming that they originate from pyridine. The vapours evolved in the complex **(6.4)** in this temperature range turn the colour of cyanogens bromide solution to green-violet on treatment with phloroglucinol solution suggesting the presence of 3-picoline molecule. Similarly the vapours evolved in the complexes **(6.5)** turn the colour of cyanogen bromide solution to blue on treatment with phloroglucinol solution. This suggests the presence of 4-picoline molecules in the complexes. Complexes **(6.2)** to **(6.5)** show weight loss corresponding to one pyridine/picoline molecule in the range 220-240°C, indicating their presence inside the coordination sphere of the complexes **[57]**.

Molar conductance

The molar conductance values for the copper (II) complexes **(6.1)** to **(6.5)** were carried out in DMSO due to poor solubility of the complexes in common organic solvents. The molar conductance values for the complexes are shown in **Table 6.1**. The molar conductance values obtained were found to lie in the range 1.3 – 2.0 ohm^{-}

$^{1}cm^{2}$ mol^{-1}. Such a low value of molar conductance indicates the non-electrolytic nature **[59]** of the complexes in DMSO. Due to poor ionic mobility of the complexes in solution the molar conductance value for the copper (II) complexes **(6.1)** to **(6.5)** fall far below that required for 1:1 electrolyte. The non-electrolytic nature of the complexes is also due to the large size of complexes apart from poor ionic mobility.

Magnetic moment

The room temperature magnetic susceptibility measurements were carried out for the complexes **(6.1)** to **(6.5)** and are illustrated in **Table 6.1**. The magnetic moment values for these complexes were found to be in the range 2.23 – 2.56 BM i.e., 0.74 – 0.85 BM per Cu atom. The observed magnetic moment values for these complexes are lower than the spin only value of 1.73 BM per Cu atom. This indicates that the copper (II) complexes undergo some kind of interaction leading to lower magnetic moment values. The lowering of magnetic moment values in these complexes may be due to direct metal-metal interaction via the overlap of suitable metal orbitals or due to super exchange arising from the transfer of paramagnetic spin density from one metal ion through the orbital overlap of the diamagnetic bridging atoms to an adjacent metal ion. Further decrease in magnetic moment may also occur due to super exchange via overlap of the metal d-orbital with the orbital of the bridging oxygen atom apart from the metal-metal interaction due to stacking of one molecule over the other.

Electronic absorption spectra

The electronic absorption spectra are often very helpful in the evaluation of results furnished by other methods of structural investigation. The electronic spectral measurements were used for assigning the stereochemistries of metal ions in the complexes based on the position and number of d-d transition peaks. The electronic spectral data for the complexes **(6.1)** to **(6.5)** are set out in **Table 6.1**. The electronic spectra of complexes **(6.1)**, **(6.2)** and **(6.3)** are shown in **Figs. 6.1-6.3**. A solution

electronic spectrum of the free ligand in DMSO shows three bands at 293 nm, 303 nm and 340 nm. The bands at 293 nm and 303 nm are assigned to intraligand $\pi \rightarrow \pi^*$ transition while the band at 340 nm is assigned to $n \rightarrow \pi^*$ transition **[60]**. The electronic spectra of the copper (II) complexes **(6.1)** to **(6.5)** also shows band in the 317 – 325 nm region due to different L – L* transitions of the coordinated ligand. A new band appears in the metal complexes in the region 429 – 435 nm having a high molar extinction coefficient in the range of 9000-10233 $dm^3\ mol^{-1}\ cm^{-1}$. This band has been assigned to ligand-to-metal charge transfer transition. This ligand-to-metal charge transfer band is responsible for the appearance of green colour of the copper (II) complexes. The spectra of copper (II) complexes mentioned in this chapter also display a relatively less intense broad band at 628 -660 nm that arises from the different d-d transitions of copper (II) **[61]**. The molar extinction coefficient for the d-d transition band (68-80 $dm^3mol^{-1}cm^{-1}$) is very low as compared to other bands present in the complexes. The position and intensity of the d-d absorption bands suggests a distorted square planar environment around the copper (II) with a $^2B_{1g}$ ground state **[61]**.

Electron paramagnetic resonance spectra

The EPR parameters for the complexes **(6.1)** to **(6.5)** are set out in **Table 6.2**. The EPR spectra of the complexes **(6.1)**, **(6.4)** and **(6.5)** are shown in **Figs. 6.4-6.6** as a representative example. The EPR spectra of the complexes **(6.1)** to **(6.5)** were recorded in DMSO both at RT and LNT. The analysis of magnetic moment data suggest that the three copper atoms interact with each other at room temperature. This is possible only if the dihydrazone coordinates to the metal centre in the syn-cis conformation. Consequently, the three copper ions are assumed to lie in in the same plane in the arrangement as shown in **Fig. 6.7** below.

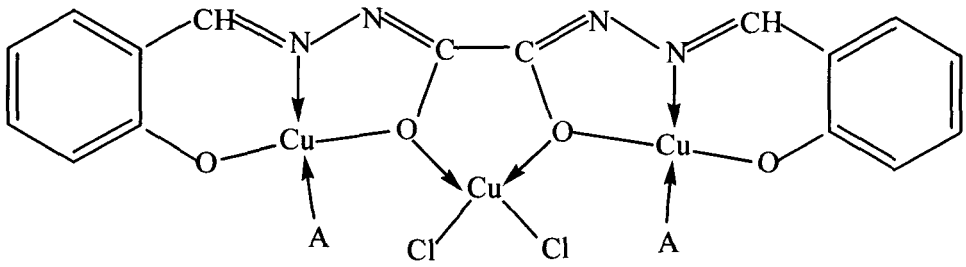

Fig. 6.7

The spin-hamiltonian appropriate to describe the exchange interaction in a linear symmetric fashion has the form **[62, 63]**

$$H = J\,(\overrightarrow{S1}.\overrightarrow{S2} + \overrightarrow{S2}.\overrightarrow{S3}) + J'\,\overrightarrow{S1}.\overrightarrow{S3}$$

where J describes the interaction between adjacent nuclei and J' describes the interaction between non-adjacent nuclei. The spin states can be labeled according to the eigen-values of the square of the total spin operator $S = S_1 + S_2 + S_3$. The resulting spin multiplets are two doublets and one quartet, $S = ½$ and $S = 3/2$, respectively. The two doublets can be identified by an intermediate coupling quantum number, S*, defined through the reaction $S^* = S_1 + S_3$. The energies of the three spin states are shown in **Fig. 6.8** which utilizes the contribution of the three individual species. As long as the homotrimetallic complex has two equivalent ions, as in the present case, the two spin doublets are not mixed and the g-values for the various multiplets can be easily expressed as a linear combination of the g-values of the individual ions, through an extension of methods reported for pairs of metal ions **[64, 65]**.

$1/2\ J - 1/4\ J'$ ——————————— (3/2, 1)

$-\ 3/4\ J'$ ——————————— (1/2, 0)

$-\ J + 1/4\ J'$ ——————————— (1/2, 1)

Fig. 6.8: Energies of the three spin states for linear symmetric three (S = 1/2) spin-coupled systems.

If the two equivalent Cu_1 and Cu_3 are coupled first, a singlet and a triplet are obtained and the g-values of the triplet can be easily calculated. If these states are coupled then with the doublet of Cu_2, then from the usual spin-projection techniques **[66]**, one derives the g-tensors for the ground and the excited states as shown in **Table 6.3**, in terms of the local g-tensors.

Table 6.3: g-Tensors of Homotrimetallic Complexes Containing Two Equivalent Metal Ions as a Function of the g-Tensors of the Individual Ions[a].

spin multiplet[b]	g-tensor	Spin-multiplet	g-tensor
|3/2>	1/3 g_1 + 1/3 g_2 + 1/3 g_3	|1/2, 0>	g_2
|1/2, 1>	2/3 g_1 – 1/3 g_2 + 2/3 g_3		

a The subscripts refer to the metal ions as indicated in Fig. 6.8

b The two spin doublets are labeled as |S, S*> . S* is defined as $S^* = S_1 + S_3$.

The coefficients 2/3 and -1/3 of the g-tensor in the ground state show that the local g_1 and g_3 of the terminal ions dominate the g-values of the homotrimetallic complex.

The magnetic exchange properties of the homotrimetallic copper (II) species resulting from the antiferromagnetic interactions, very often causes no EPR signals to be observed at RT (apparently because relaxation phenomenon hamper the observation) and only badly resolved spectra at low temperatures **[67-69]**. However, the spectra of the complexes in the present study are isotropic in DMSO solution at room temperature. The g-value falls in the region 2.188-2.241. This indicates interaction between adjacent metal centres in the structural unit of the complexes. It appears that the room temperature narrowing is of intramolecular nature, due to the thermal population of the two doublet and the quartet spin states. A confirmation of this interpretation comes from the fact that the EPR spectra at LNT, where only the

lowest doublet is populated, are exchange narrowed by intermolecular interactions and not broadened **[70]**. The hyperfine splitting could not be observed due to badly resolved spectra at room temperature.

On the other hand, the complexes show anisotropic spectra at LNT characteristic of the systems having axial symmetry. LNT EPR spectra are typical for S = ½ spin systems. The complexes show copper hyperfine splitting in $g_{\|}$ and $g_{\perp}$ regions. All of the hyperfine splitting constants fall in the region 120-150 G. The $g_{\|}$ values fall in the region 2.407-2.442 while the $g_{\perp}$ values fall in the range 2.176-2.208. Further, the $g_{\|}/A_{\|}$ values are also found to lie in agreement with the proposed distorted square planar geometry around copper atom. The $g_{\|}/A_{\|}$ values for the present complexes are found to lie in the range 162 – 200 cm, slightly higher than that required for a square planar geometry **[71]**. The G values for the complexes **(6.1)** to **(6.5)** are less than 4.0 indicating that the ligand forming the complex is a strong field ligand. For all the complexes at LNT, the G values were found to be less than 3.0. For square planar complexes G is usually in the range of 2.03 – 2.45 **[71]**. The G values in all the complexes were found to be in agreement with the above given range for square planar complexes. If we assume that the g-components of the individual sites do not differ too much, at least the numerical order of the components $g_{\|}$ and $g_{\perp}$, measured by EPR, is determined by the terminal copper ions. This allows us to draw some conclusions about the highest 3d-orbitals of the copper (II) ions in the trimer. The complexes show a ground state of total spin S= ½. The difference in the essential feature of EPR spectra at RT and LNT show that the ground state is energetically well separated from excited doublet and quartet states. The EPR spectra of monometallic copper (II) complexes exhibiting two types of g-values, $g_{\|} \neq g_{\perp}$, have been used to distinguish unambiguously between $(d_x^2\text{-}_y^2)$ and (d_z^2) ground states; the $d_x^2\text{-}_y^2$ orbital yields $g_{\|} > g_{\perp}$, while d_z^2 yields $g_{\perp} > g_{\|}$. The homotrimetallic copper (II) complexes **(6.1)** and **(6.3)** show four hyperfine split signals while the remaining complexes show three hyperfine split signals in the $g_{\|}$ region. The EPR spectra are also split in the $g_{\perp}$ region. The complex **(6.3)** shows two hyperfine split signals while the complexes **(6.4)** and **(6.5)** show three hyperfine split signals in the $g_{\perp}$ region with

the hyperfine splitting constant $A_{|}$ falling in the region 20-40 G, respectively. Such EPR spectra are typical of a d^9 complex possessing axial symmetry with the unpaired electron present in a $d_x^2-y^2$ orbital. The spectra of these complexes do not show any half field ($\Delta Ms = 2$) transition or fine structure and look like a spectrum associated with isolated S = ½ states.

Infrared spectra

The IR spectra of the complexes **(6.1)** - **(6.5)** shows similar features as that of the free ligand with some slight modification, which arises due to coordination of the ligand to the metal centre in enol form. The IR spectral data of the complexes are given in **Table 6.4**. The IR spectra of the complexes **(6.1)**, **(6.4)** and **(6.5)** are shown in **Figs. 6.9-6.11**.

The bands at 3270 cm^{-1} assigned to the stretching vibration of phenolic -OH group and the bands at 3204 cm^{-1} assigned to the stretching vibration of secondary >NH group in the free ligand is absent in the metal complexes. The absence of band around 3270 cm^{-1} in the complexes indicates that the phenolic -OH group is involved in coordination via de-protonation. Similarly the absence of υ (>NH) vibration in the IR spectra of the metal complexes indicates that the >NH group is destroyed upon complex formation. A strong band appearing in the region 3243-3433 cm^{-1} in the complexes **(6.1)** - **(6.5)** is due to the stretching vibration of υ (-OH) group of the water molecules. The presence of water molecule in the complexes **(6.1)** - **(6.5)** was confirmed by heating the complexes in the temperature range of 90 - 180°C and passing the evolved vapours through a trap containing anhydrous copper sulfate. Only complex **(6.1)** showed weight loss ~ 180°C. The weight loss at ~180°C corresponds to coordinated nature of water molecules. In rest of the complexes the band in the above region is probably due to the υ (-OH) vibration of water molecules absorbed by KBr during pellet preparation.

The υ (>C=O) (amide I) bands appearing at 1667 cm^{-1} in the ligand, disappears in all the complexes **(6.1)** - **(6.5)**. The disappearance of υ (>C=O) bands in the complexes indicates that the ligand coordinates to the metal centre through >C=O group via enolization. Enolization of >C=O group is also supported by the absence of >NH group in the metal complexes. The absence of bands due to υ (>C=O), υ (>NH) and υ (-OH) indicates that both the hydrazone part of the ligand molecule is involved in coordination to the metal centre through >C=O group via enolization and phenolic -OH group via de-protonation.

A single strong band appearing in the region 1533 cm^{-1} in all the complexes **(6.1)** - **(6.5)** is due to the presence of NCO group obtained as a result of enolization of the ligand. The amide II + υ (C-O) vibration appears merged with the vibration due to υ (NCO) group.

A very strong intensity band appearing at 1627 cm^{-1} and 1603 cm^{-1} in the dihydrazone are assigned to arise due to >C=N- group. The bands due to azomethine (>C=N-) group appears in the region 1613-1606 cm^{-1} in the complexes **(6.1)** - **(6.5)** which is shifted to lower frequency on an average by 7-12 cm^{-1}. The shift of the band due to azomethine group to lower frequency indicates the coordination of azomethine nitrogen atom to the metal centre. The spectral changes caused by the formation of the metal complexes are most apparent in the 1300-1100 cm^{-1} range. The υ (C–O) vibration in the ligand has been assigned at 1262 cm^{-1}. In the metal complexes these band show considerable higher shift and appear as a single strong intensity band in the region 1310-1301 cm^{-1} indicating involvement of C–O group in bonding to the metal complexes via oxygen atom.

The region below 1200 cm^{-1} has been scrutinized for locating υ (N–N) vibration and various C–H vibrations. The weak band observed at 1035 cm^{-1} in the ligand can be assigned to υ (N–N) vibration. This band either remains unshifted or shifts to higher frequency in the metal complexes.

The IR spectra of the copper (II) complexes **(6.1)** to **(6.5)** shows a new medium intensity bands in the region around 530-535 cm^{-1} and 480 – 485 cm^{-1}, which has been assigned to arise due to the υ (M–O) (phenolic) and υ (M–O) (enolic), **[72]** respectively. The existence of this band in the IR spectra of the copper (II) complex indicates that the ligand molecule is coordinated to the Cu atom through phenolic oxygen atom as well as through enolic oxygen atom.

The metal chlorine stretching frequency occurs in the region 400-200 cm^{-1} in monomeric octahedral complexes **[73]**. In polymeric complexes, the bridging υ (M–Cl) stretching frequency occurs as low as 184 and 174 cm^{-1} **[74]**. On the other hand, in the square planar complexes of second and third transition series, the terminal υ (M–Cl) stretching frequency appears in the region 330-370 cm^{-1} while the bridging υ (M–Cl) appear in the form of two bands in the region 290- 330 and 240-330 cm^{-1}, respectively **[75, 76]**. In the first transition series metal complexes, the bridging υ (M–Cl) frequencies appear in the regions 170-180 and 180-200 cm^{-1}, respectively. In the present complexes, the two new non-ligand bands appear ~ 180 and ~ 200 cm^{-1}, respectively **[77]**. These bands are assigned to arise due to bridging Cu-Cl stretching vibration. The occurrence of these two bands suggests that the chlorides are bridged between central Cu and terminal Cu atoms.

Cyclic voltammogram

The redox properties of the complexes have been investigated by cyclic voltammetry in DMSO and the electrochemical data for all the complexes alongwith those of the free ligand and precursor monometallic complexes are summarized in **Table 6.5**. The cyclic voltammogram of the complexes **(6.1)**, **(6.2)** and **(6.5)** are shown in **Figs. 6.12-6.14**. The ligand H_4*slox is electroactive and shows only reductive waves at* +0.40, -0.30 and -1.0V respectively. The precursor complex shows three reductive waves centered at -0.95, -1.45 and -1.80 V, respectively during the cathodic potential scan while only two oxidative waves at -0.71 and +0.95 V, respectively.

The complex **(6.1)** shows four successive reduction waves at E_{pc} = +0.40, -0.50, -0.80 and -1.10 V, respectively. However, in the reverse anodic scan only one oxidative wave appears at -0.40 V. This shows that the complex undergoes only one oxidation at potential of -0.40 V. Hence, it must undergo one corresponding reduction also. Accordingly the reductive wave at +0.40, -0.50 and -1.10 V are assigned to arise due to ligand centred electron transfer processes. The reductive wave at -0.80 V may be associated with oxidative wave at -0.40 V and may be attributed to arise due to metal centered electron transfer reaction. Accordingly, this redox couple is assigned to $Cu^{II}Cu^{II}$ Cu^{II}/ $Cu^{I}Cu^{II}Cu^{II}$ redox reaction.

On the other hand, when pyridine and substituted pyridines are coordinated to the metal centre, one additional redox couple arise which may be associated with metal centered redox reactions. Complex **(6.2)** shows four reductive waves at E_{pc} = +0.40, -0.40, -0.80 and -1.10 V, on cathodic potential scan while the anodic potential scan shows only two oxidative waves at -0.23 and -0.52 V, respectively. This waves at +0.40, -0.40 and -1.10 V are close to the waves at +0.40, -0.30 and -1.0 V in free ligand. Hence, these waves are assigned to arise due to ligand centered electron transfer reactions. The wave at -0.80 V is assigned to arise due to metal centered electron transfer reactions which may be associated with oxidative wave at -0.52 V. Further, the essential features of the reduction wave at -0.40 V also suggests that it appears to have contribution due to metal centered electron transfer reactions. Hence, the reductive wave at -0.40 V may also be associated with oxidative wave at -0.23 V. These redox couples are assigned to $Cu^{II}Cu^{II}$ Cu^{II}/ $Cu^{I}Cu^{II}Cu^{II}$ and $Cu^{I}Cu^{II}$ Cu^{II}/ $Cu^{I}Cu^{II}Cu^{I}$ redox reactions. The complex **(6.3)** also shows almost the same essential features in its cyclic voltammogram as the complex **(6.2)**. Hence, further discussion on this complex is redundant.

The complex **(6.4)** and **(6.5)** also show almost identical features yet different from those of the complexes **(6.1)** to **(6.3)**. Both the complexes show three reductive waves in the cathodic potential scan while two oxidative waves in the anodic potential scan. The oxidative waves may be assigned to arise due to electron

transfers centered on metal atom. It appears that the reductive waves due to metal centered electron transfer reactions are merged with the reductive waves due to ligand centered electron transfer reactions. Hence, these complexes are also believed to undergo similar type of electron transfer behavior as in the complexes **(6.2)** and **(6.3)**. The redox reactions may be represented as below:

$$Cu^{II}\,Cu^{II}\,Cu^{II} \underset{-e^-}{\overset{+e^-}{\rightleftharpoons}} Cu^{I}\,Cu^{II}\,Cu^{II} \underset{-e^-}{\overset{+e^-}{\rightleftharpoons}} Cu^{I}\,Cu^{II}\,Cu^{I}$$

It is imperative to mention that the complex **(6.1)** shows only one metal centered redox couple while the remaining complexes show two metal centered redox couples. The appearance of two metal centered redox couples in the complexes **(6.2)** to **(6.5)** is the consequence of coordination of pyridine and substituted pyridines to the metal centre. The peak separations between the redox couples are usually very large. This is attributed to originate from a slow heterogeneous electron exchange rather than an interfering homogeneous reaction **[78]**.

Conclusion

In this chapter five homotrimetallic complexes of copper have been isolated by the reaction of $[Cu(H_2slox)]$ with $CuCl_2.2H_2O$ in 1: 2.5 molar ratio in methanol as such or in the presence of excess of nitrogen donor bases such as pyridine and substituted pyridine molecules.. The complexes have been found to have magnetic moment much less than that required for three copper (II) atoms having one unpaired electron each. This value of magnetic moment indicates considerable amount of interaction between the copper (II) ions in the complexes. The electronic and EPR spectral evidences suggests the presence of three copper (II) ions per ligand molecule with a square planar geometry. The presence of three copper (II) ions per ligand molecule is also supported by the analytical and magnetic moment data. The IR spectra of the complexes **(6.1)** to **(6.5)** do not show any band due to ν (>C=O), ν (>NH) or ν (-OH) groups suggesting the presence of ligand molecule in enol form in these complexes. Based on the above discussion, the tentative structures of the complexes have been shown in the **Fig. 6.15**.

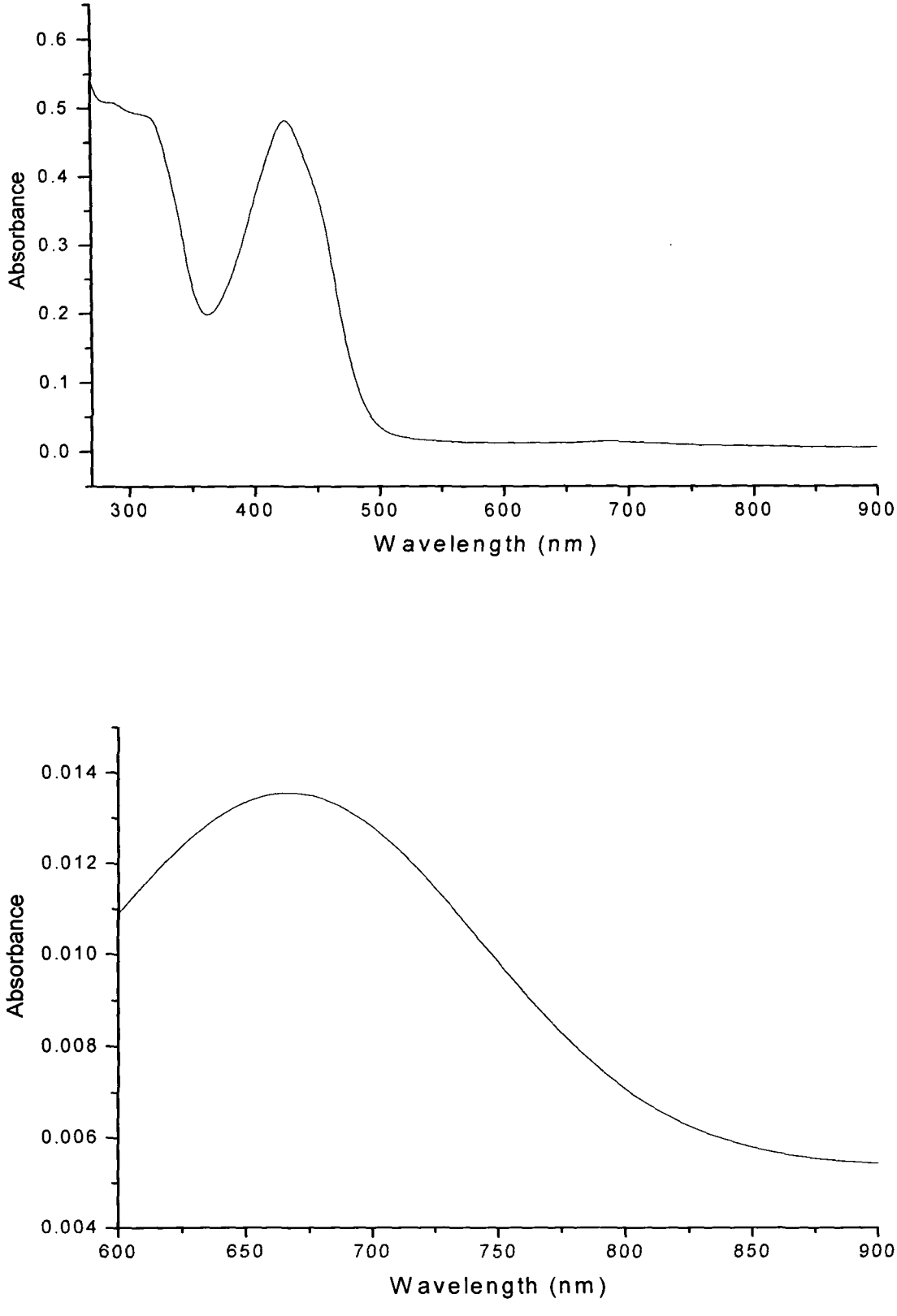

Fig. 6.1 Electronic spectrum of $[Cu_3(slox)Cl_2(H_2O)_2]$ **(6.1)**.

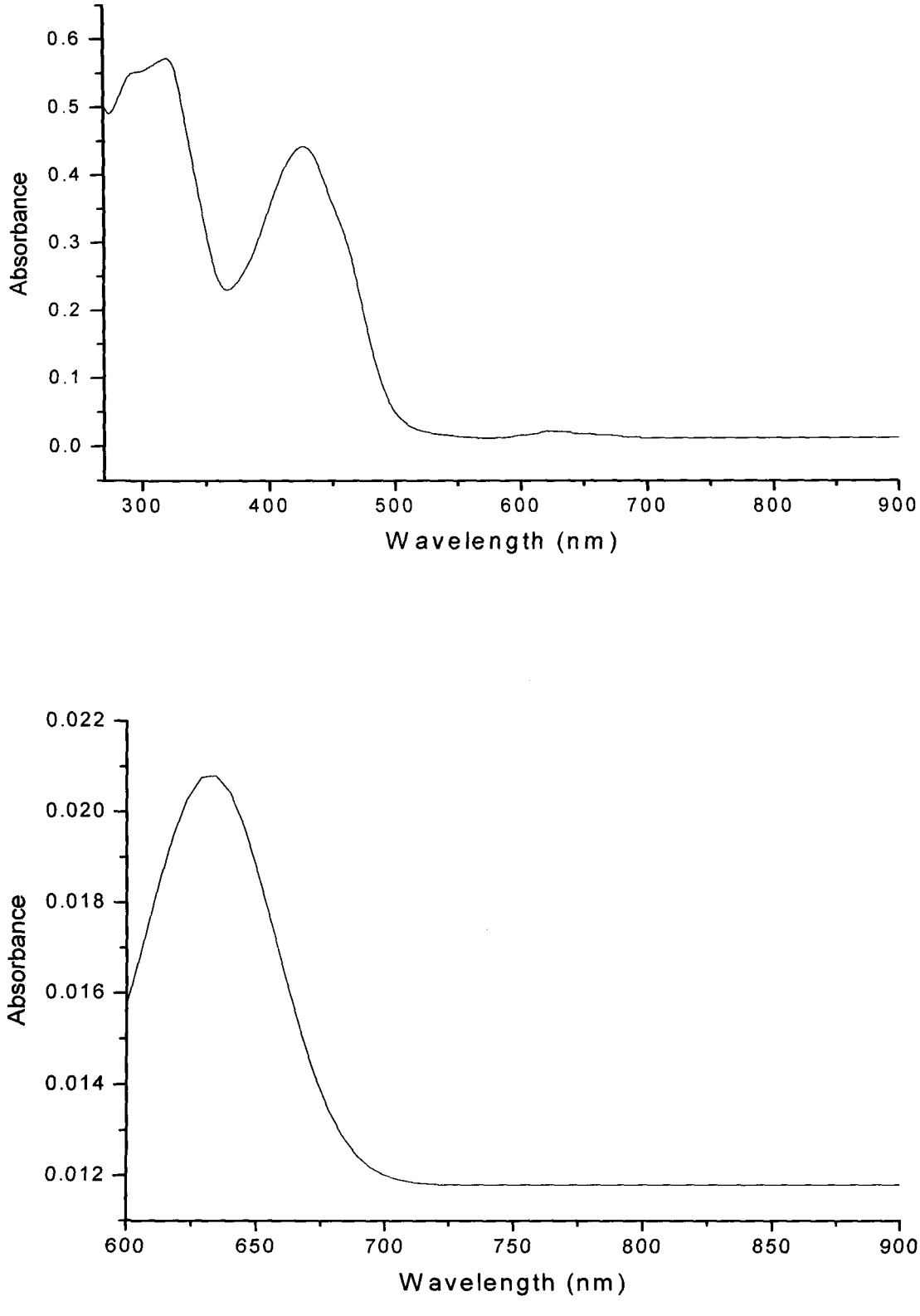

Fig. 6.2 Electronic spectrum of $[Cu_3(slox)Cl_2(py)_2]$ **(6.2)**.

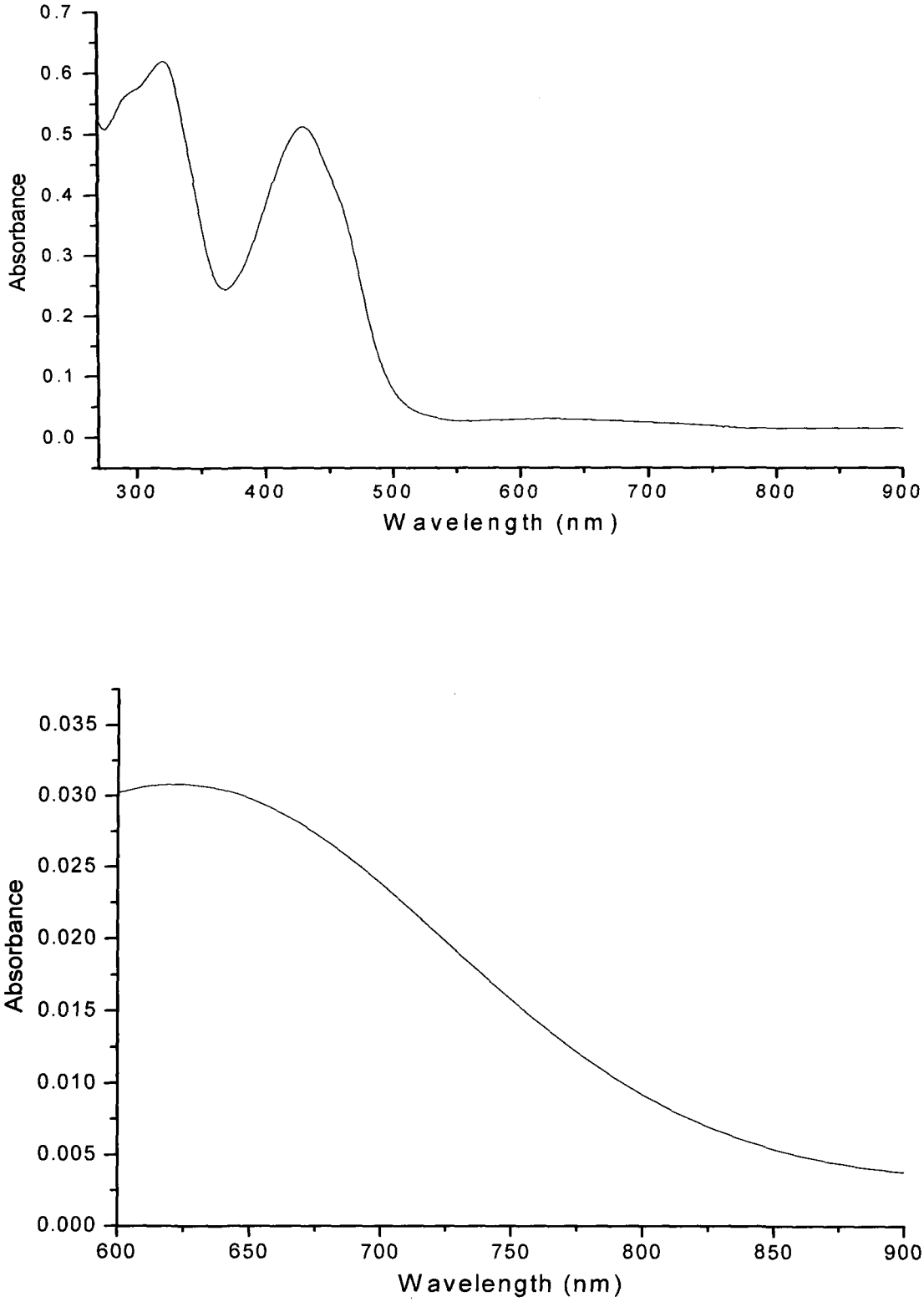

Fig. 6.3 Electronic spectrum of $[Cu_3(slox)Cl_2(2\text{-pic})_2]$ **(6.3)**.

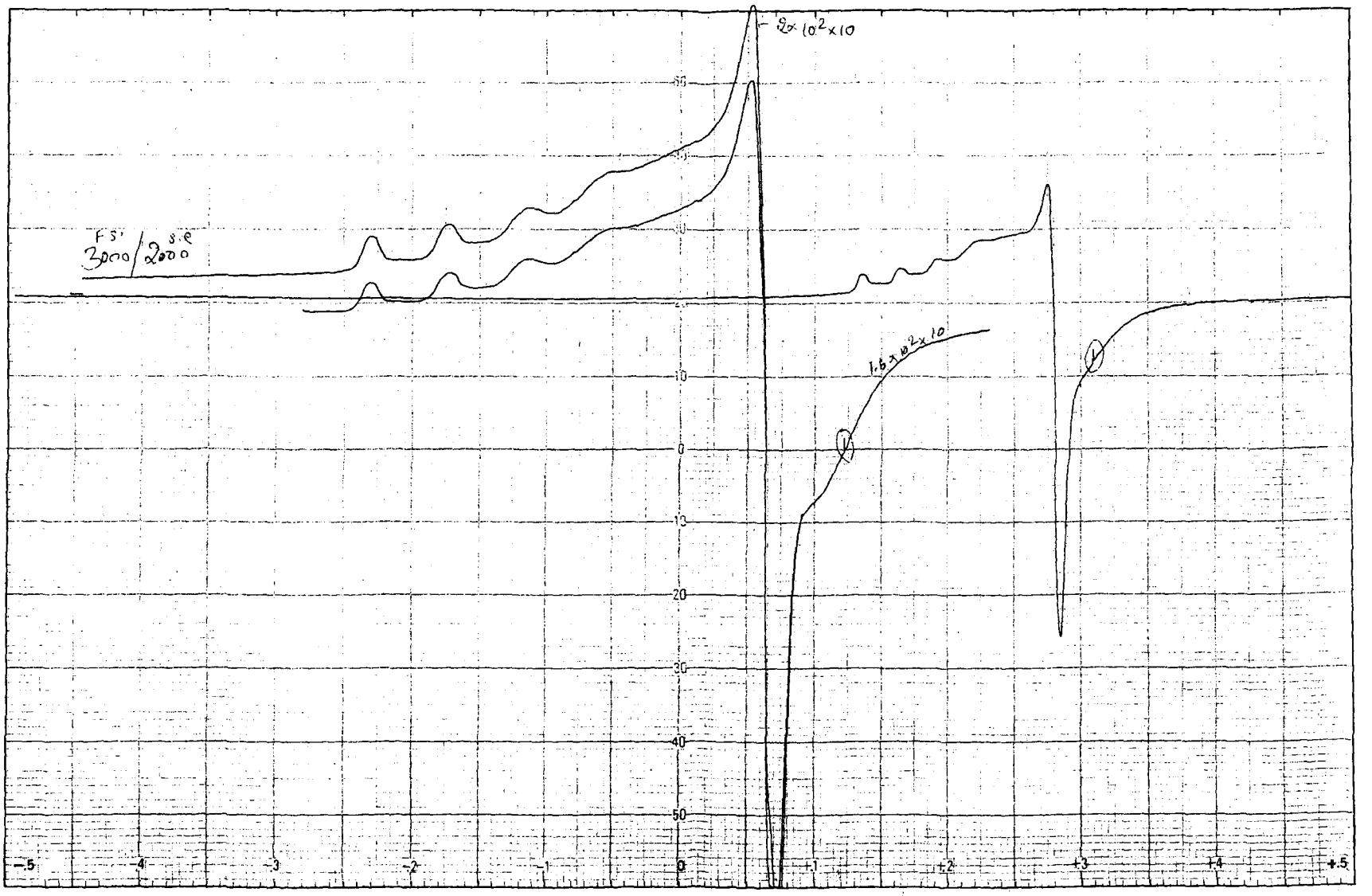

Fig. 6.4 (a) EPR spectrum of $[Cu_3(slox)Cl_2(H_2O)_2]$ **(6.1)** in DMSO at Temperature: LNT; Frequency: 9.1 GHz; Scan Range: 4000 G; Field Set: 2000 G.

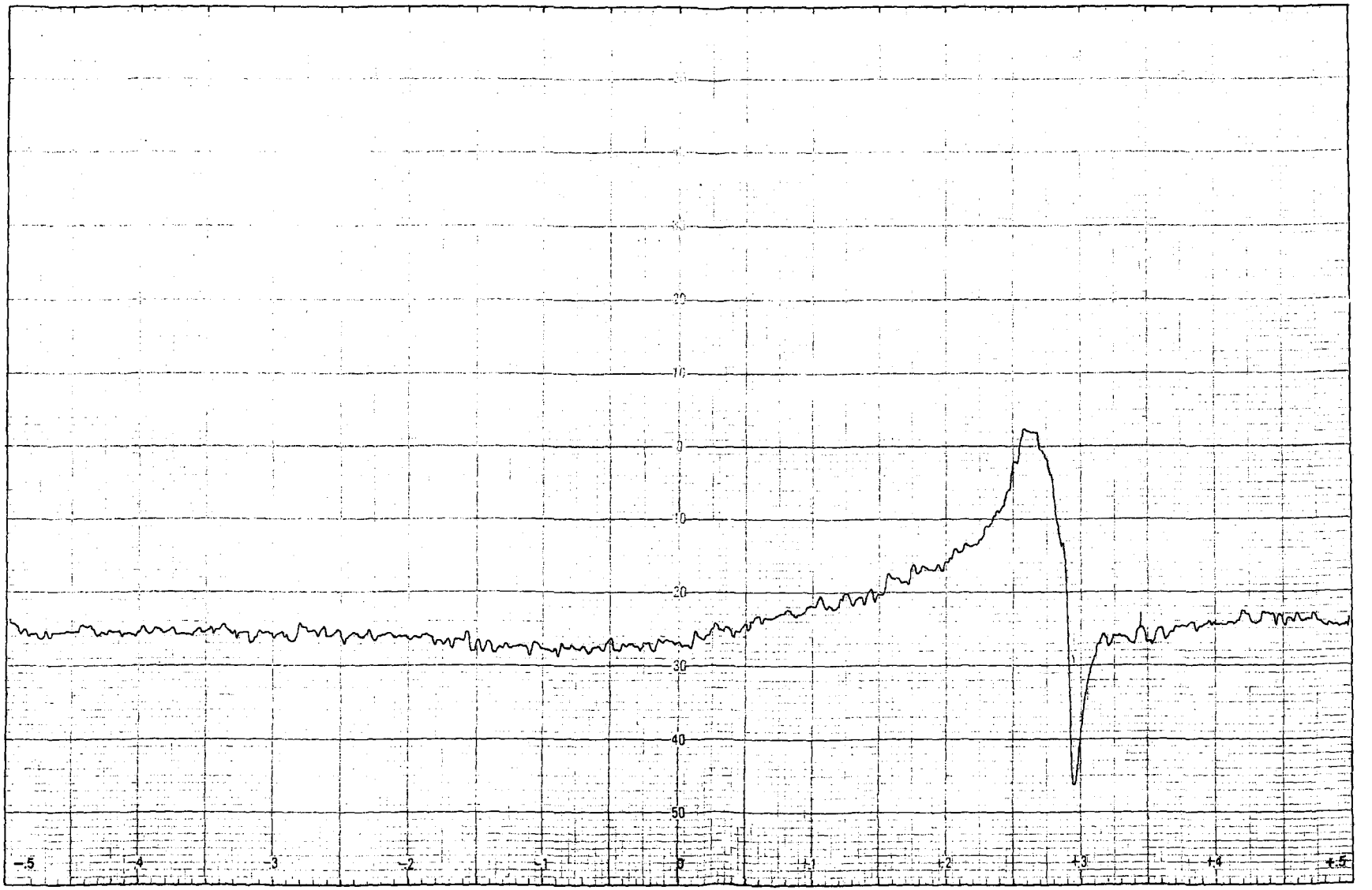

Fig. 6.4 (b) EPR spectrum of $[Cu_3(slox)Cl_2(H_2O)_2]$ **(6.1)** in DMSO at Temperature: RT; Frequency: 9.1 GHz; Scan Range: 4000 G; Field Set: 2000 G.

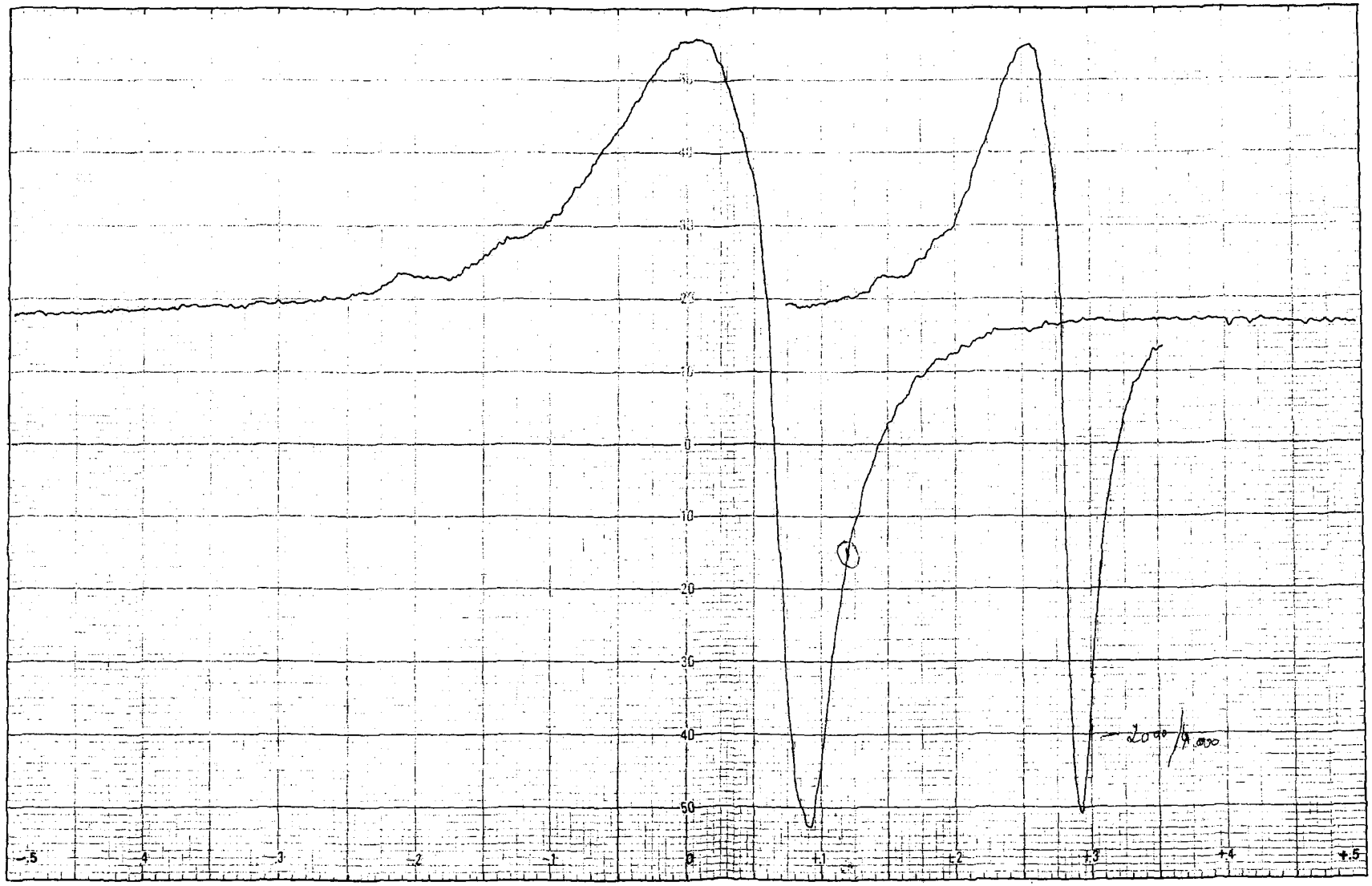

Fig. 6.5 (a) EPR spectrum of $[Cu_3(slox)Cl_2(3\text{-}pic)_2]$ **(6.4)** in DMSO at Temperature: LNT; Frequency: 9.1 GHz; Scan Range: 2000 G; Field Set: 3000 G.

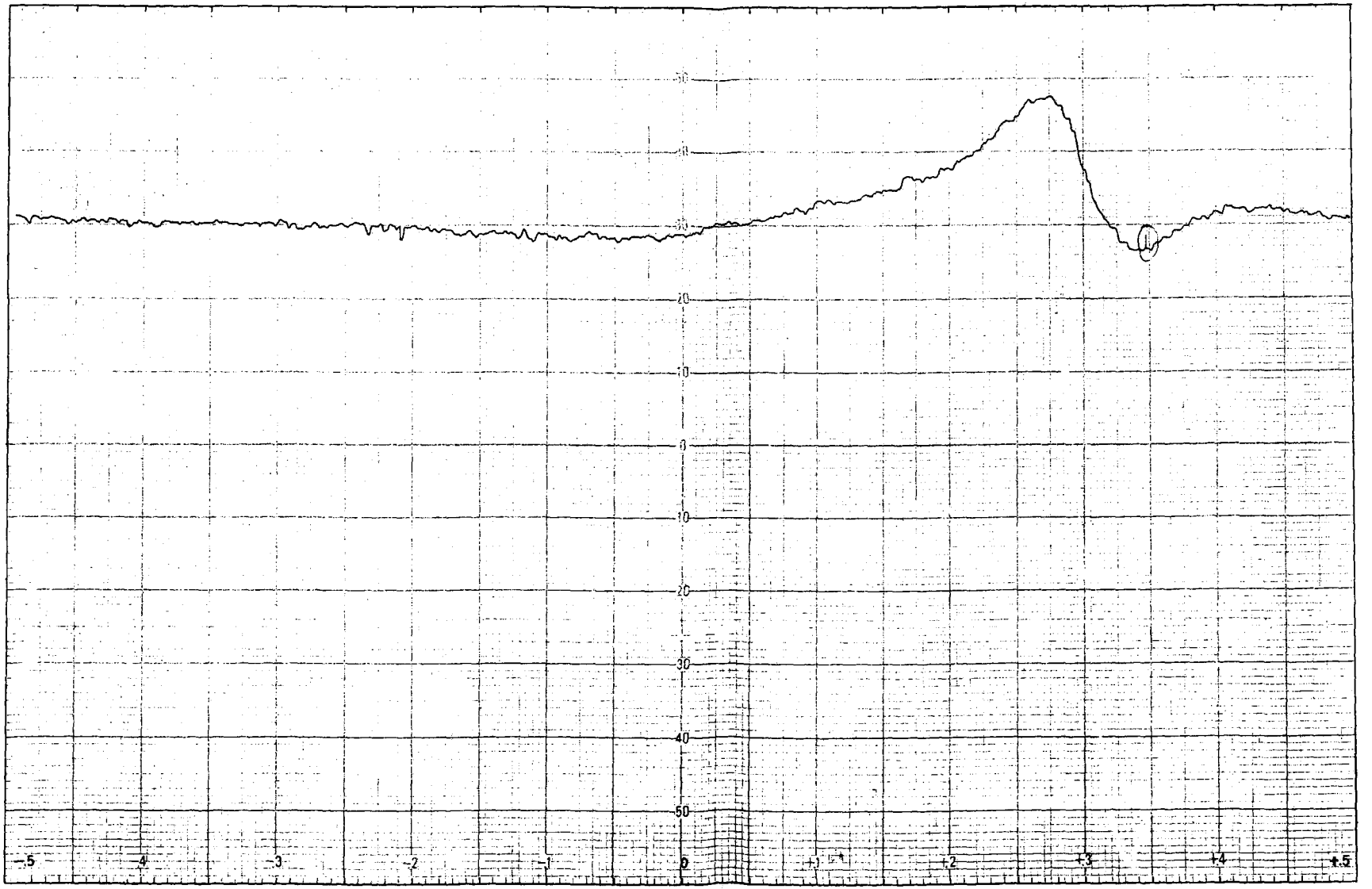

Fig. 6.5 (b) EPR spectrum of $[Cu_3(slox)Cl_2(3\text{-}pic)_2]$ **(6.4)** in DMSO at Temperature: RT; Frequency: 9.1 GHz; Scan Range: 4000 G; Field Set: 2000 G.

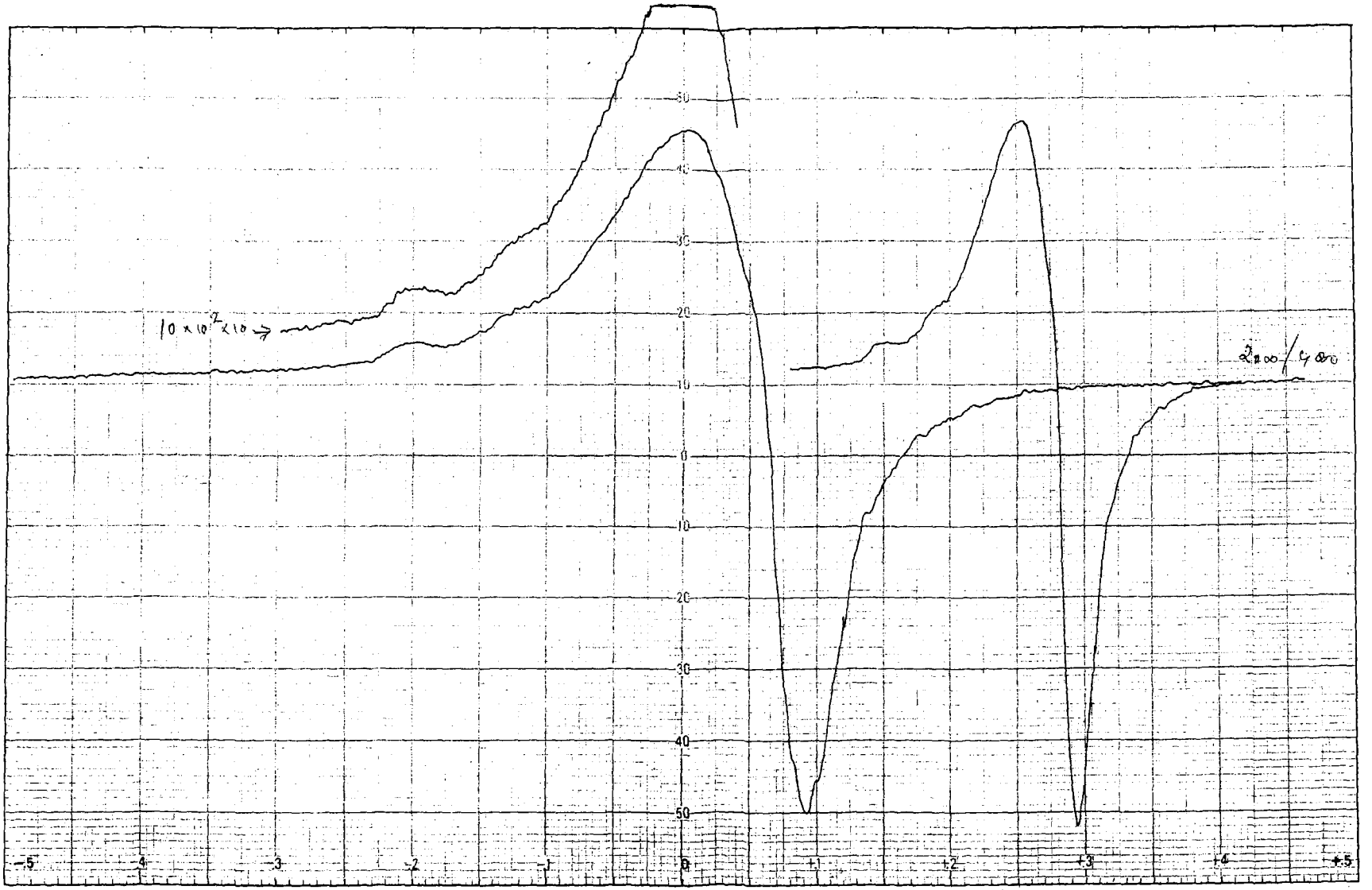

Fig. 6.6 (a) EPR spectrum of $[Cu_3(slox)Cl_2(4\text{-pic})_2]$ **(6.5)** in DMSO at Temperature: LNT; Frequency: 9.1 GHz; Scan Range: 2000 G; Field Set: 3000 G.

Fig. 6.6 (b) EPR spectrum of $[Cu_3(slox)Cl_2(4\text{-}pic)_2]$ **(6.5)** in DMSO at Temperature: RT; Frequency: 9.1 GHz; Scan Range: 4000 G; Field Set: 2000 G.

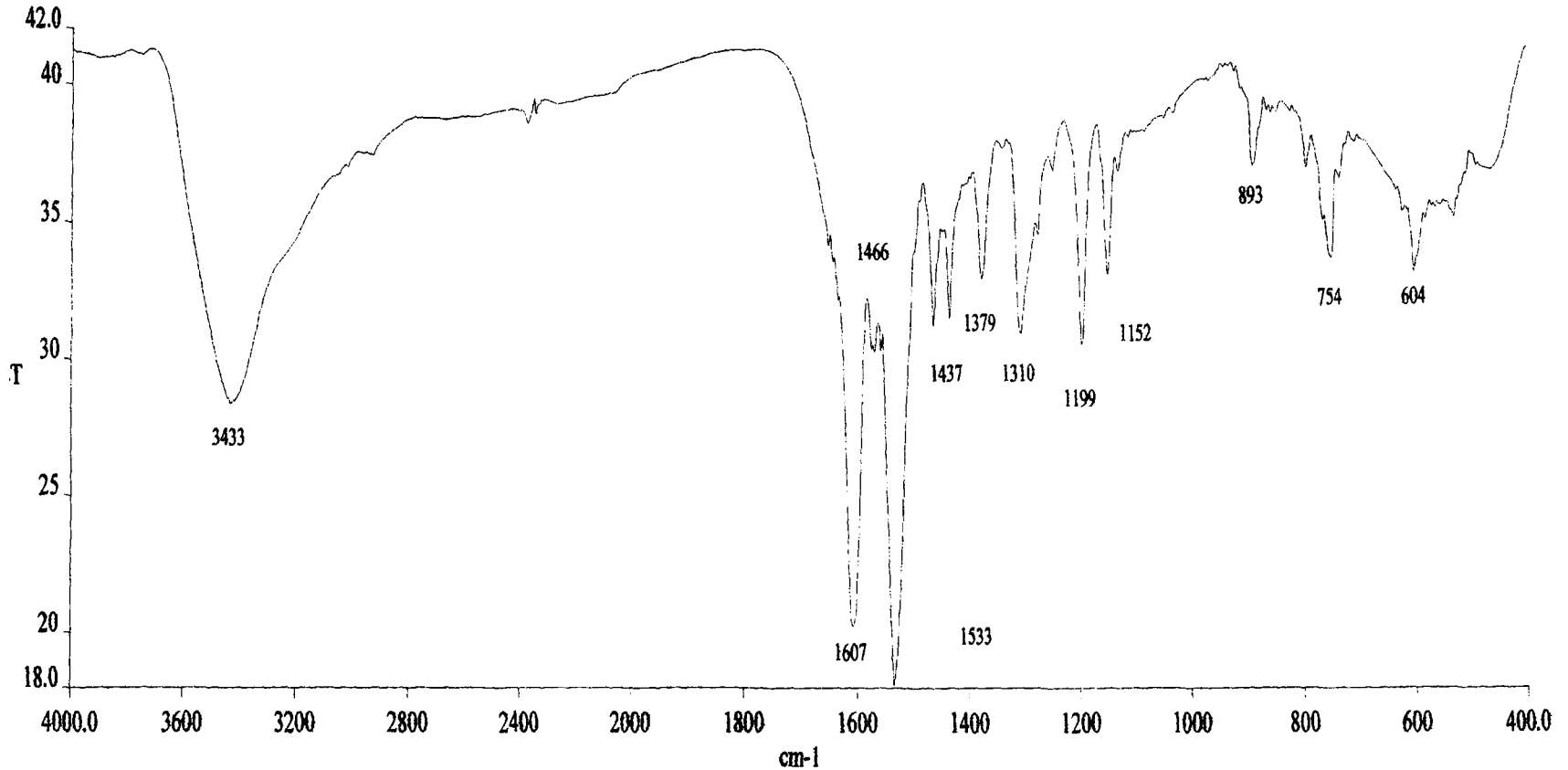

Fig. 6.9 (a) Infrared spectrum of $[Cu_3(slox)Cl_2(H_2O)_2]$ **(6.1)** in KBr.

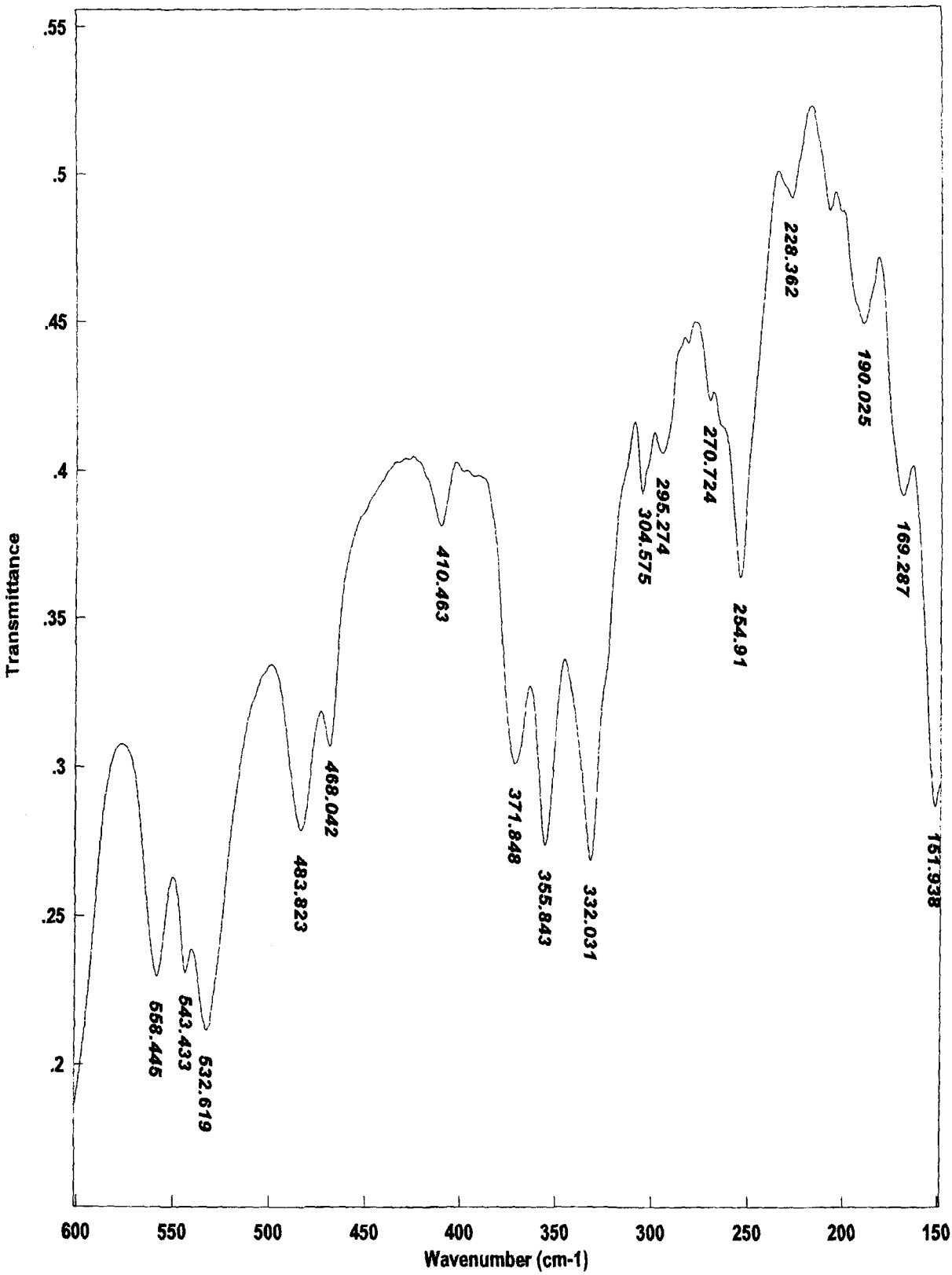

Fig. 6.9 (b) Infrared spectrum of $[Cu_3(slox)Cl_2(H_2O)_2]$ **(6.1)** in CsI.

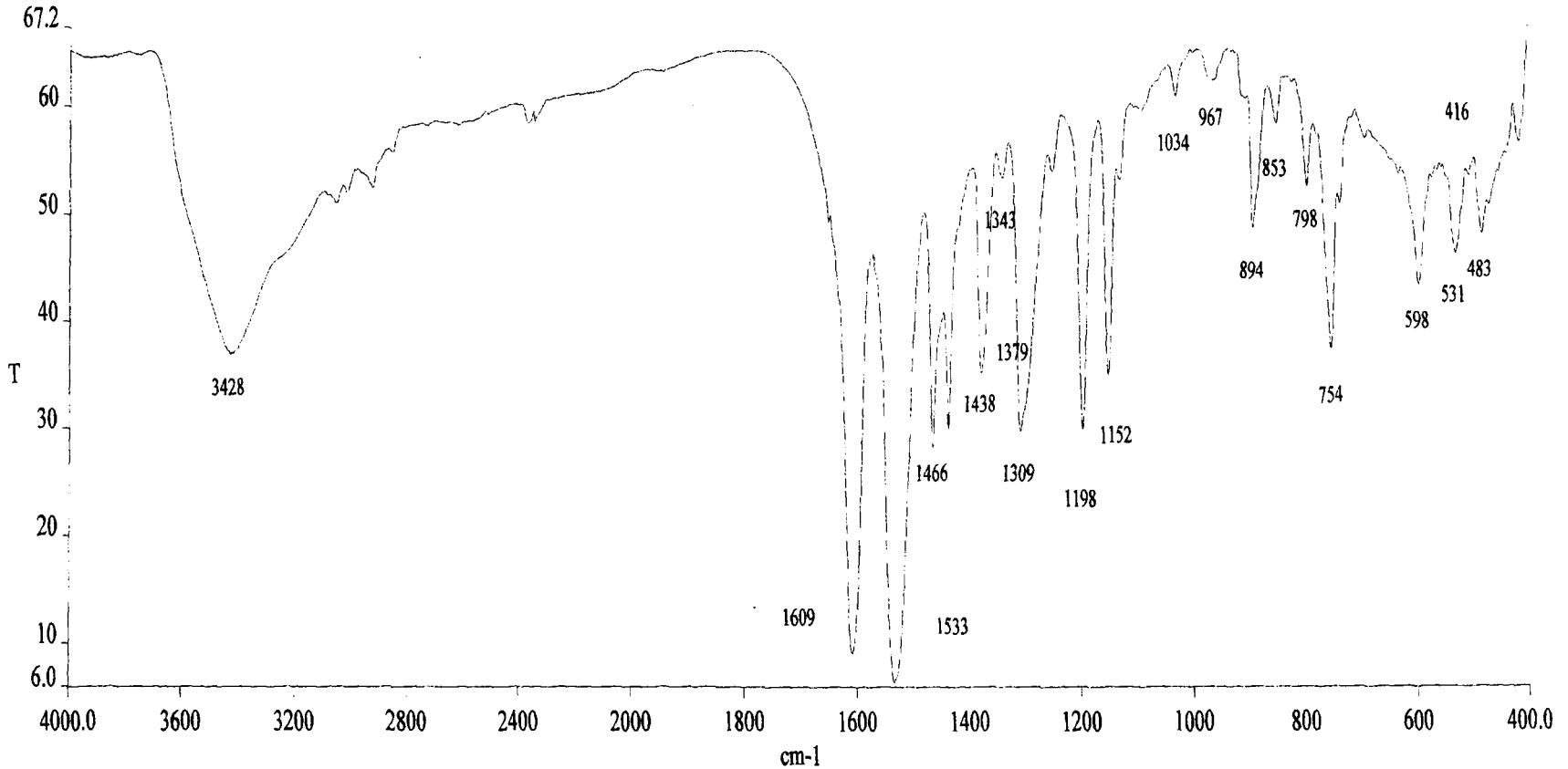

Fig. 6.10 (a) Infrared spectrum of $[Cu_3(slox)Cl_2(3\text{-}pic)_2]$ **(6.4)** in KBr.

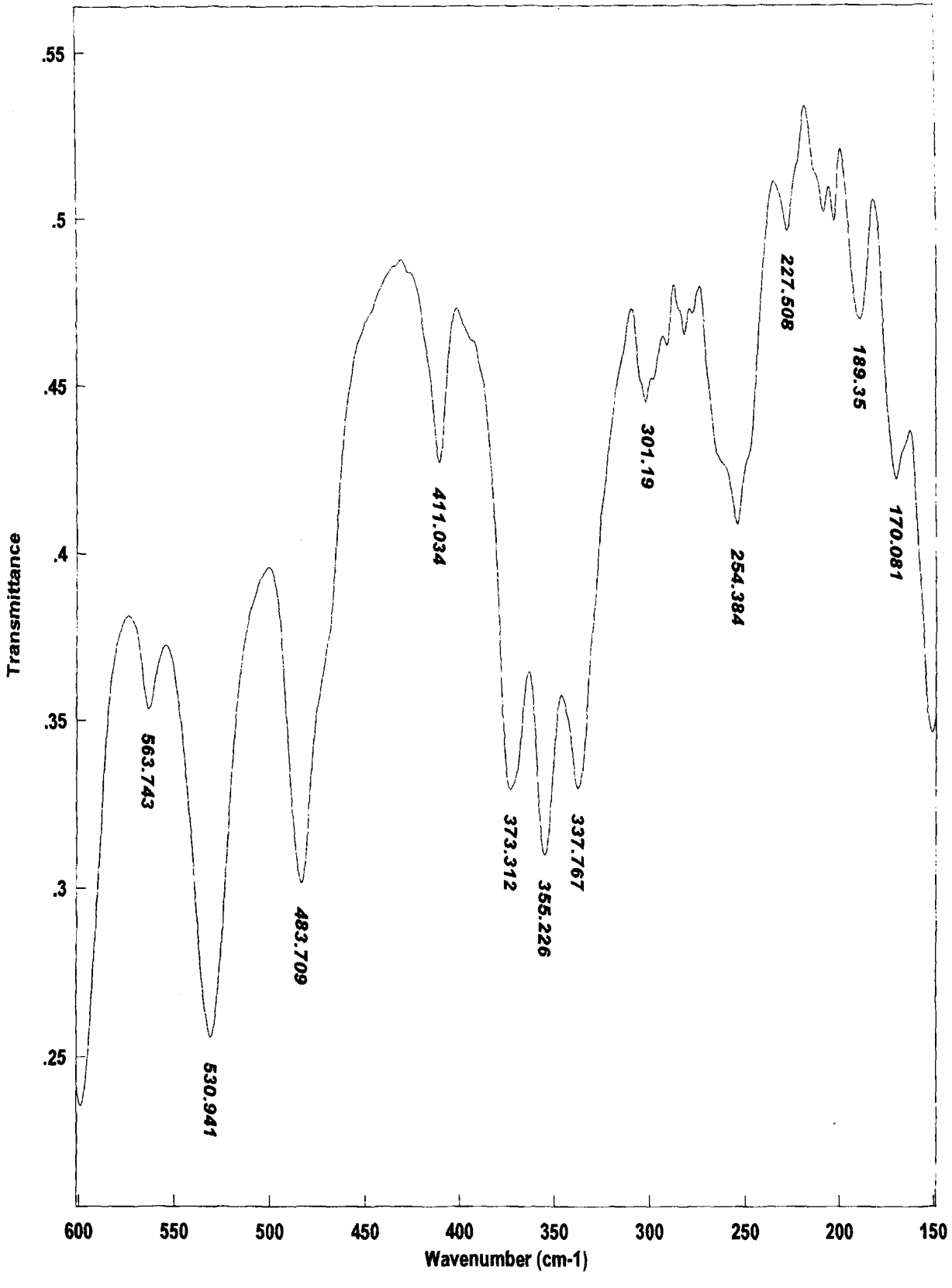

Fig. 6.10 (b) Infrared spectrum of $[Cu_3(slox)Cl_2(3\text{-}pic)_2]$ **(6.4)** in CsI.

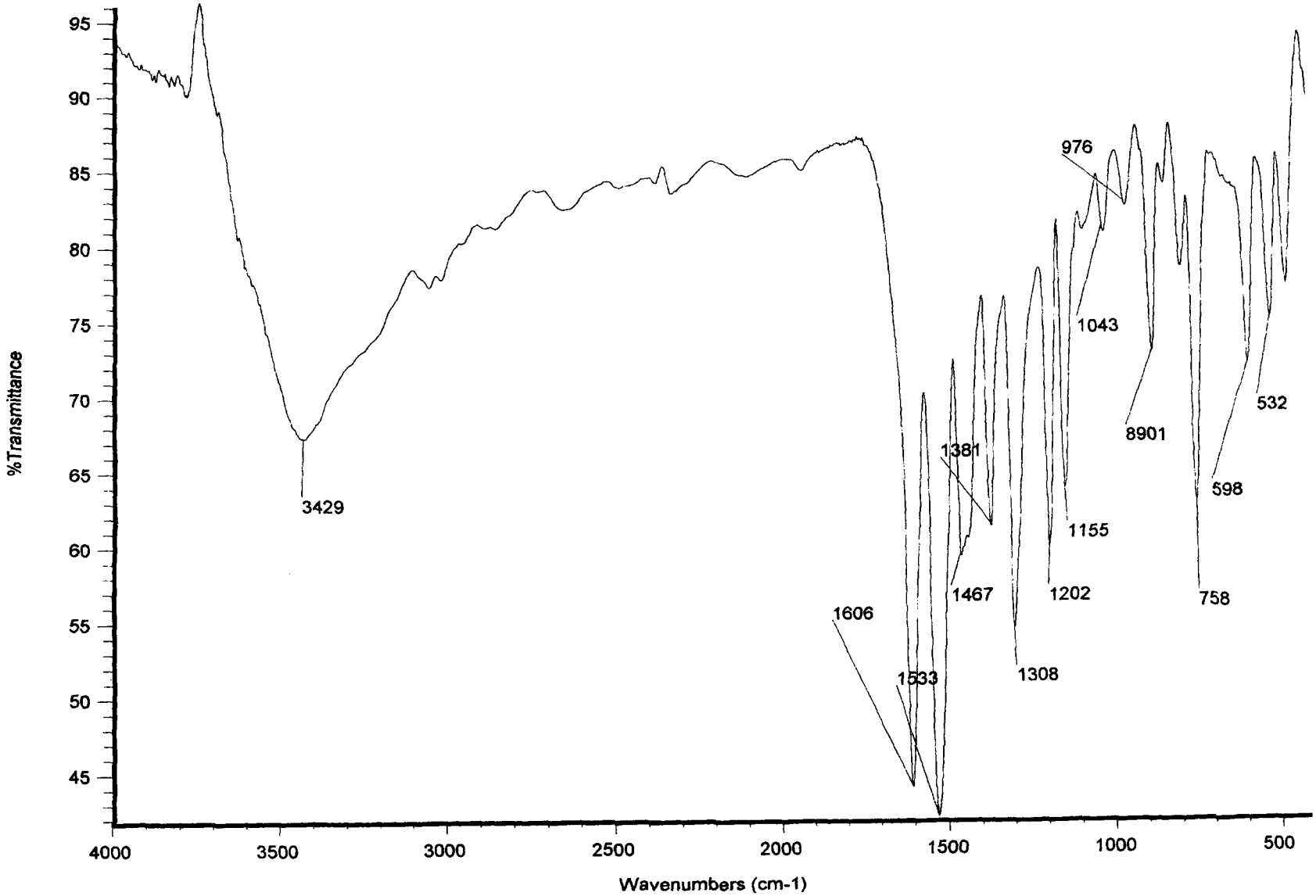

Fig. 6.11 (a) Infrared spectrum of $[Cu_3(slox)Cl_2(4\text{-pic})_2]$ **(6.5)** in KBr.

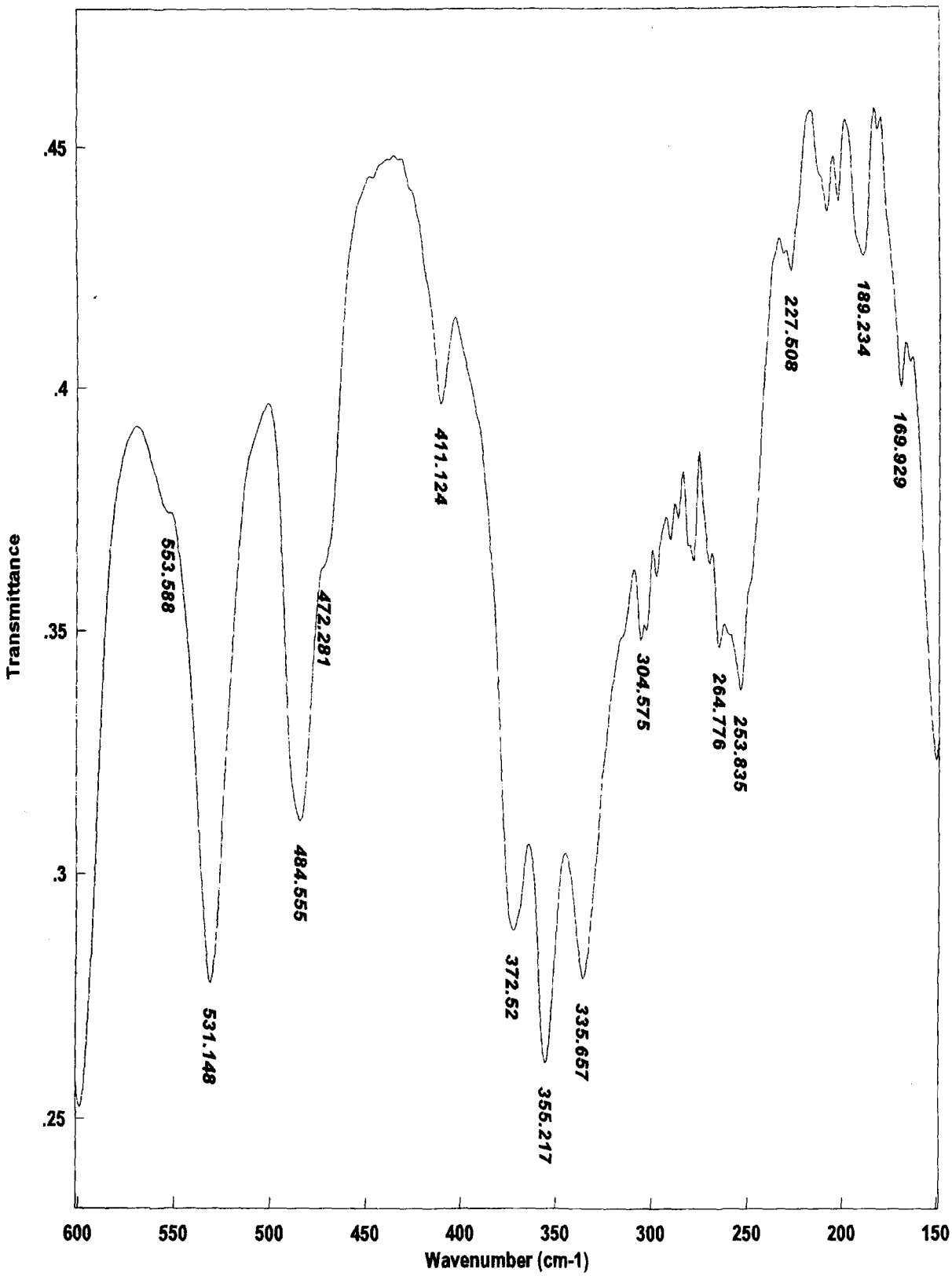

Fig. 6.11 (b) Infrared spectrum of $[Cu_3(slox)Cl_2(4\text{-}pic)_2]$ **(6.5)** in CsI.

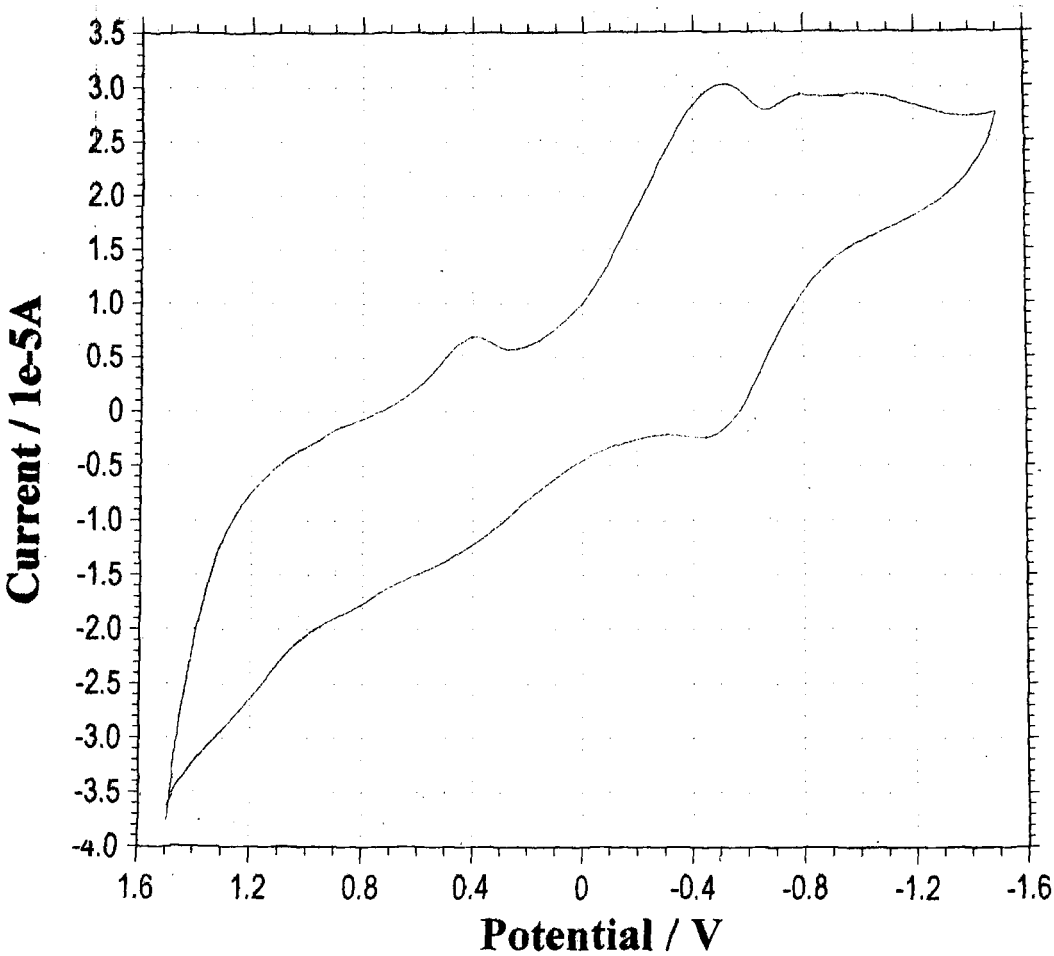

Fig. 6.12 Cyclic voltammogram of $[Cu_3(slox)Cl_2(H_2O)_2]$ **(6.1)** at scan rate 100 mV/s.

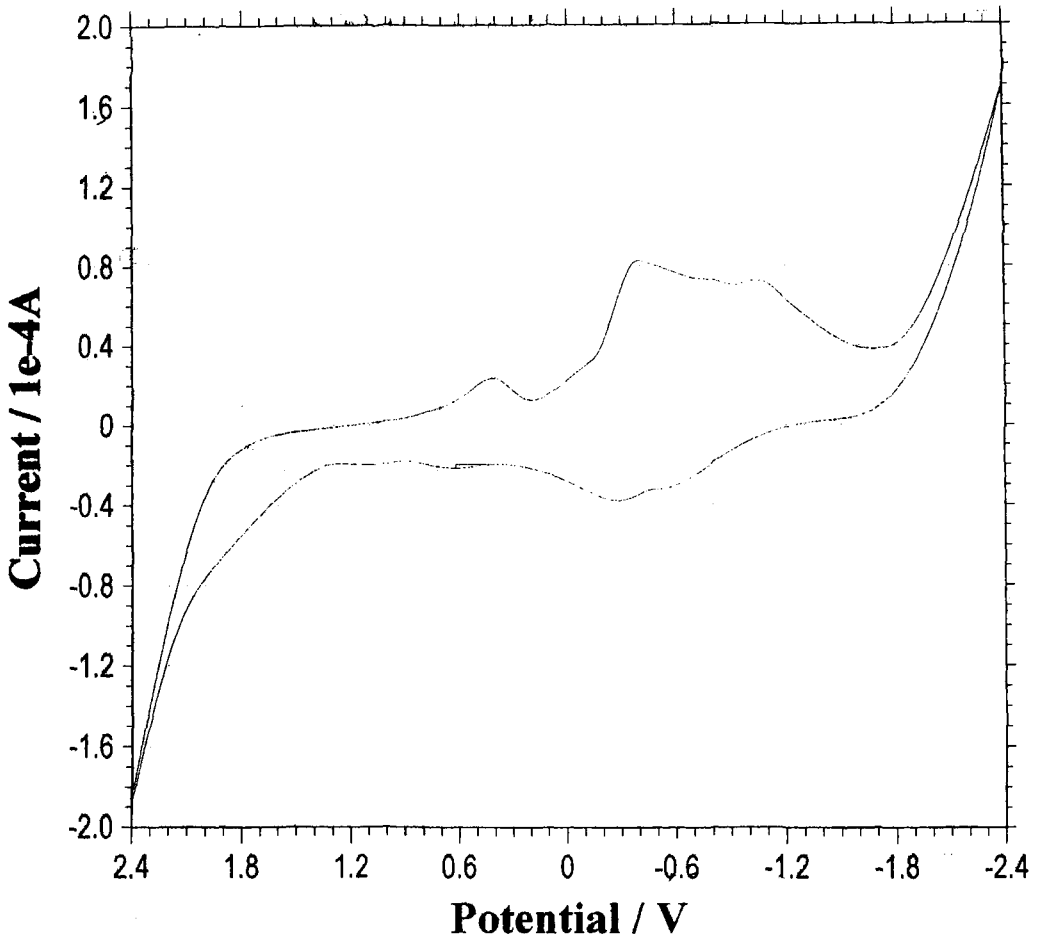

Fig. 6.13 Cyclic voltammogram of $[Cu_3(slox)Cl_2(py)_2]$ **(6.2)** at scan rate 100 mV/s.

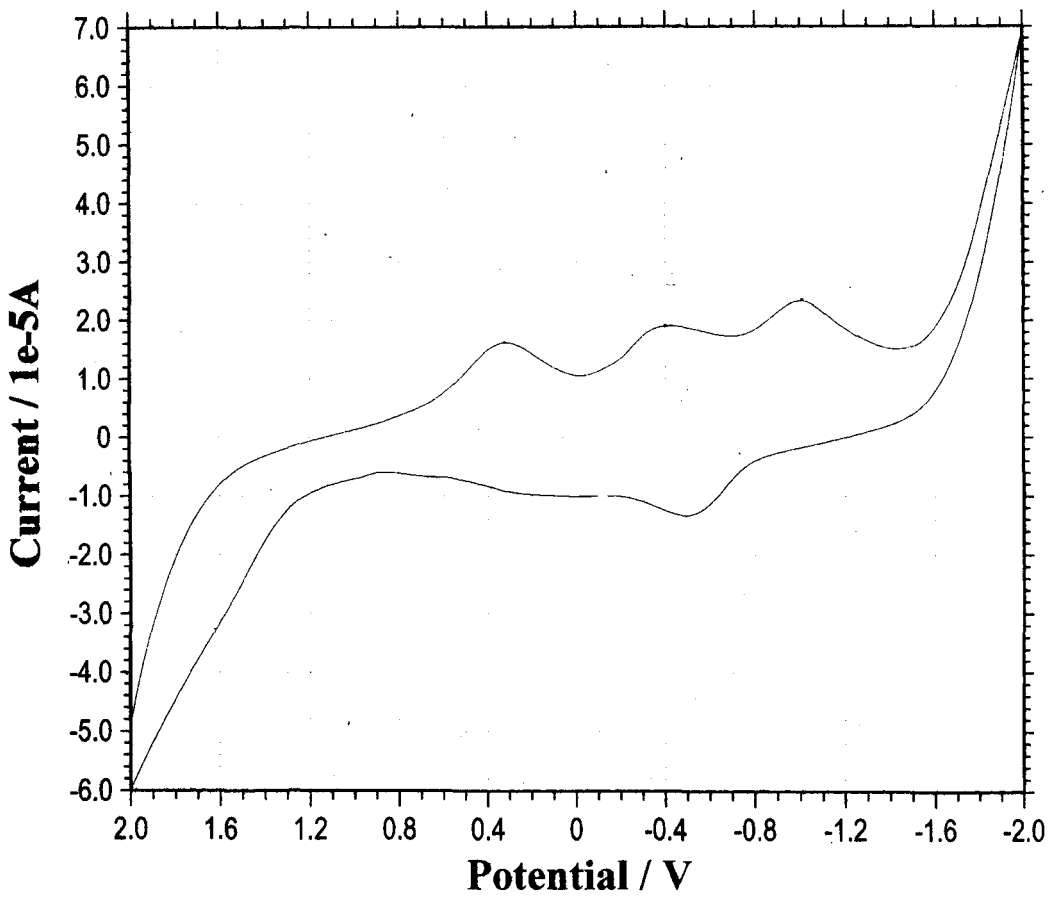

Fig. 6.14 Cyclic voltammogram of $[Cu_3(slox)Cl_2(4\text{-}pic)_2]$ **(6.5)** at scan rate 100 mV/s.

Table 6.1: Complex, colour, decomposition point, analytical, molar conductance, magnetic moment and electronic spectral data for homotrimetallic copper (II) complexes.

Sl. No.	Complex (Colour)	D. P. (°C)	Elemental Analyses: Found (Calcd)%					Molar conductance Λ_M (ohm^{-1} cm^2mol^{-1})	Magnetic moment μ_{eff} (BM)	Electronic spectral band λ_{max}(nm) (ε_{max}) ($dm^3mol^{-1}cm^{-1}$)
			M	C	H	N	Cl			
6.1	$[Cu_3(slox)Cl_2(H_2O)_2]$ (Dark green)	>300	30.94 (30.76)	31.44 (31.00)	2.25 (2.28)	8.77 (9.04)	11.56 (11.44)	2.00	2.23	322(10901) 435(9021) 660(72)
6.2	$[Cu_3(slox)Cl_2(py)_2]$ (Dark green)	>300	25.27 (25.69)	42.35 (42.09)	2.69 (2.72)	11.12 (11.33)	9.84 (9.56)	1.75	2.42	318(11024) 429(10233) 632(68)
6.3	$[Cu_3(slox)Cl_2(2\text{-}pic)_2]$ (Dark green)	>300	24.32 (24.76)	43.91 (43.67)	3.18 (3.14)	10.68 (10.91)	9.47 (9.21)	1.30	2.56	325(12134) 437(10010) 630(80)
6.4	$[Cu_3(slox)Cl_2(3\text{-}pic)_2]$ (Dark green)	>300	24.86 (24.76)	43.33 (43.67)	3.16 (3.14)	11.21 (10.91)	8.99 (9.21)	1.90	2.39	317(11222) 432(9878) 628(77)
6.5	$[Cu_3(slox)Cl_2(4\text{-}pic)_2]$ (Dark green)	>300	25.01 (24.76)	43.51 (43.67)	3.10 (3.14)	11.16 (10.91)	8.81 (9.21)	2.00	2.55	321(10679) 430(9000) 633(69)

Table 6.2: EPR spectral data for homotrimetallic copper (II) complexes at RT and LNT in DMSO solution.

Sl. No.	Complex	Temp	$g_{\|\|}$	$g_{\perp}$	g_{av}	$A_{\|\|} \times 10^{-4}$ (cm^{-1})	$A_{\perp} \times 10^{-4}$ (cm^{-1})	A_{av}	$g_{\|\|}/A_{\|\|}$	G	α^2
6.1	$[Cu_3(slox)Cl_2(H_2O)_2]$	RT	--	--	2.241	--	--	--	--	--	--
		LNT	2.407	2.176	2.253	120	--	--	200	2.31	0.852
6.2	$[Cu_3(slox)Cl_2(py)_2]$	RT	--	--	2.224	--	--	--	--	--	--
		LNT	2.442	2.204	2.283	125	--	--	195	2.17	0.913
6.3	$[Cu_3(slox)Cl_2(2\text{-}pic)_2]$	RT	--	--	2.202	--	--	--	--	--	--
		LNT	2.420	2.189	2.266	130	40	73.3	186	2.22	0.899
6.4	$[Cu_3(slox)Cl_2(3\text{-}pic)_2]$	RT	--	--	2.188	--	--	--	--	--	--
		LNT	2.428	2.197	2.274	150	15	60.0	162	2.17	0.966
6.5	$[Cu_3(slox)Cl_2(4\text{-}pic)_2]$	RT	--	--	2.219	--	--	--	--	--	--
		LNT	2.424	2.193	2.270	140	20	60.0	173	2.20	0.932

Table 6.4: Infrared spectral data for homotrimetallic copper (II) complexes.

Sl. No.	Ligand/Complex	ν(OH) + ν(NH)	ν(C=O)	ν(C=N)	Amide II + ν(C-O) (phenolic)	ν(NCO)	ν(C-O)	ν(N-N)	ν(M-O) (phenolic)	ν(M-O) (enolic)	ν(Cu-Cl) (bridging)
	H_2slox	3270(s) 3204(s)	1667(s)	1627(s) 1603(s)	1534(s)	--	1262(s)	1035(w)	--	--	--
6.1	$[Cu_3(slox)Cl_2(H_2O)_2]$	3433(s)	--	1607(s)	--	1533(s)	1310(s)	1033(w)	532(m)	483(m)	200(w) --
6.2	$[Cu_3(slox)Cl_2(py)_2]$	3423(s)	--	1613(s)	--	1533(s)	1308(s)	1035(w)	533(m)	484(m)	202(w) 195(w)
6.3	$[Cu_3(slox)Cl_2(2\text{-}pic)_2]$	3429(s)	--	1606(s)	--	1533(s)	1301(s)	1036(w)	531(m)	484(m)	200(w) 180(w)
6.4	$[Cu_3(slox)Cl_2(3\text{-}pic)_2]$	3428(s)	--	1609(s)	--	1533(s)	1309(s)	1034(w)	532(m)	484(m)	200(w) --
6.5	$[Cu_3(slox)Cl_2(4\text{-}pic)_2]$	3429(s)	--	1606(s)	--	1533(s)	1308(s)	1043(w)	531(m)	485(m)	200(w) 180(w)

Table 6.5: Electrochemical data for the homotrimetallic copper (II) complexes.

Sl. No.	Ligand/Complex	E_{pc}	E_{pa}
	H_4slox	+0.40, -0.31, -0.93	--
	[Cu(H_2slox)]	-0.95, -1.45, -1.80	-0.71, +0.95
6.1	[Cu_3(slox)Cl_2(H_2O)$_2$]	+0.40, -0.50, -0.80, -1.10	-0.40
6.2	[Cu_3(slox)Cl_2(py)$_2$]	+0.40, -0.40*, -0.80, -1.10	-0.52, -0.23
6.3	[Cu_3(slox)Cl_2(2-pic)$_2$]	+0.45, -0.25, -0.40*, -1.10*	-0.90, -0.30
6.4	[Cu_3(slox)Cl_2(3-pic)$_2$]	+0.57, -0.30*, -1.10*	+0.65, -0.40
6.5	[Cu_3(slox)Cl_2(4-pic)$_2$]	+0.48, -0.40*, -1.00*	-0.50, +0.30

*reductive waves due to metal centered electron transfer reactions and the ligand centered electron transfer reactions merged.

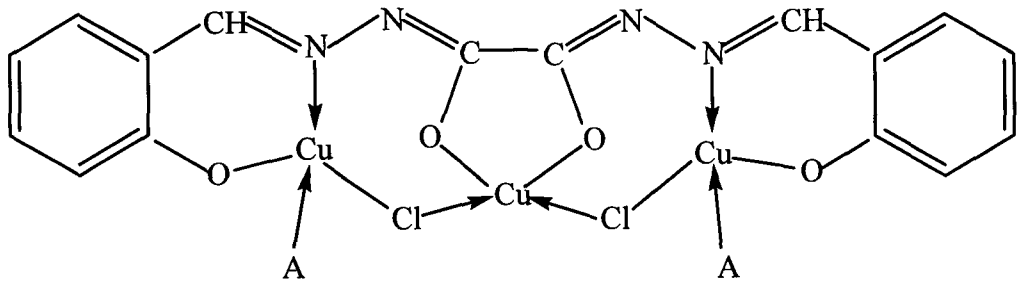

Fig. 6.15 Tentative structure of $[Cu_3(slox)Cl_2(A)_2]$ {*where A = H_2O* **(6.1)**, *pyridine* **(6.2)**, *2-picoline* **(6.3)**, *3-picoline* **(6.4)** *and 4-picoline* **(6.5)**}.

References

1. T. E. Machonkin, H. H. Zhang, B. Hedman, K. O. Hodgson and E. I. Solomon, *Biochemistry*, **37**, 9570 (1998).
2. G. K. Mukhopadhyay, Z. K. Attich and P. L. Fox, *Science*, **279**, 714 (1998).
3. H. A. Regan, S. Nacht, G. R. Lee, C. R. Bishop and G. E. Cartwright, *Am. J. Physiol*, **217**, 1320 (1969).
4. S. Osatav and D. A. Johnson, *J. Biol. Chem.*, **244**, 5757 (1969).
5. E. I. Solomon, U. M. Sundaram and T. E. Machonkin, *Chem. Rev.*, **96**, 2563 (1996).
6. D. J. Spira-Solomon, M. D. Allendorf and E. I. Solomon, *J. Am. Chem. Soc.*, **108**, 5318 (1990); P. F. Lindley, G. Cerd, I. Zaitseva, V. Zaitsev, B. Reinhammar, E. Selin-Lindgren and K. Yoshida, *J. Biol. Inorg. Chem.*, **2**, 454 (1977).
7. J. L. Cole, G. O. Tan, E. K. Yang, K. O. Hodgson and E. I. Solomon, *J. Am. Chem. Soc.*, **112**, 2243 (1990); W. Shin, U. M. Sundaram, J. L. Cole, H. H. Zhang, B. Hedman, K. O. Hodgson and E. I. Solomon, *J. Am. Chem. Soc.*, **118**, 3202 (1996).
8. A. Messerschmidt, R. Lederstein, R. Huber, M. Bolognesi, L. Augliano, R. Petruzzelli, A. Rossi and A. Finazzi-Agro, *J. Mol. Biol.*, **224**, 179 (1992); M. D. Allendorf, D. J. Spira and E. I. Solomon, *Proc. Natl. Acad. Sci., U.S.A.*, **82**, 3063 (1985).
9. C. T. Huber and E. Frieden, *J. Biol. Chem.*, **245**, 3973 (1970).
10. T. L. Ortel, N. Takoshi and F. W. Patnam, *Proc. Natl. Acad. Sci., U.S.A.*, **81**, 476 (1984).
11. A. Messerschmidt and R. Huber, *Eur. J. Biochem.*, **187**, 341 (1990).
12. I. Zaitseva, V. Zaitsev, G. Cerd, K. Mohkov, B. Bax, A. Ralph and P. Lindley, *J. Biol. Inorg. Chem.*, **1**, 15 (1996).
13. M. M. Morie-Bebel, D. R. McMillin and W. E. Antholine, *J. Biochemistry*, **235**, 415 (1986).

14. T. L. Fraterrigo, C. Miller, B. Reinhammar and D. R. McMillin, *J. Biol. Inorg. Chem.*, **4**, 183 (1999).

15. J. Li, D. R. McMillin and A. W. E. Antholine, *J. Am. Chem. Soc.*, **114**, 725 (1992).

16. R. P. Bonomo, B. M. G. Castronovo and A. M. Santoro, *J. Chem. Soc., Daltons Trans.*, **1**, 104 (2004).

17. J. L. Cole, P. A. Clark and E. I. Solomon, *J. Am. Chem. Soc.*, **112**, 9538 (1990).

18. U. M. Sundaram, H. H. Zhang, B. Hedman, K. O. Hodgson and E. I. Solomon, *J. Am. Chem. Soc.*, **119**, 12525 (1997).

19. A. Messerschimdt, H. Luecke and R. Huber, *J. Mol. Biol.*, **230**, 997 (1993).

20. V. N. Zaitsev, I. Zaitseva, M. Papiz and P. L. Lindley, *J. Biol. Inorg. Chem.*, **4**, 579 (1999).

21. R. Branden, B. G. Maliustrom and T. Vamgard, *Eur. J. Biochem.*, **36**, 195 (1973).

22. L. Bewntanar, J. Yoon, C. P. Aznar, A. E. Palmer, K. K. Andersson, R. D. Britt and E. I. Solomon, *J. Am. Chem. Soc.*, **127**, 13822 (2005).

23. A. Messerschmidt, "*In Bioinorganic Chemistry of Copper*", Eds., K. D. Karlin, Z. Tyeklar, Chapman and Hall, New York, 471 (1993).

24. M. L. Alvarez, J. Ai, W. Zumft, J. Sander Loher and D. M. Dooley, *J. Am. Chem. Soc.*, **123**, 576 (2001).

25. A. K. Sah, T. Tanese and M. Mikuriya, *Inorg. Chem.*, **45**, 2083 (2006); G. A. Ardizzoia, S. Cenini, G. LaMonica, N. Masciocchi and M. Moret, *Inorg. Chem.*, **33**, 1458 (1994).

26. P. A. Agaridis, P. Baran, R. Boca, F. Carvantes-lee, W. Haase, G. Mezei, R. G. Raptis and R. Warner, *Inorg. Chem.*, **41**, 2219 (2002); S. Mukhopadhyay, D. Mandal, P. B. Chatterjee, C. Desplanches, J. P. Sutter, R. J. Butcher and M. Chaudhury, *Inorg. Chem.*, **43**, 8501 (2004).

27. "*Magnetic Molecular Materials*", D. Gatteschi, O. Kahn, J. S. Miller and F. Palacio, Eds., NATO ASI Series 198, Kluwer Academic Publishers: Dordrecht, The Netherlands (1991).

28. G. A. Ardizzoia, S. Cenini, G. LaMonica, N. Masciocchi and M. Moret, *Inorg. Chem.*, **33**, 1458 (1994); G. A. Ardizzoia, M. A. Angoroui, G. LaMonica, F. Cariati, S. Cenini, M. Moret and N. Masciocchi, *Inorg. Chem.*, **30**, 4347 (1991).

29. "*Magneto-Structural Correlations in Exchange Coupled Systems*", R. D. Willet, D. Gatteschi and O. Kahn, Eds., NATO ASI Series, No. 140, Reidel: Dordrecht, The Netherlands, (1985); O. Kahn, "*Molecular Magnetism*", VCH Publishers, New York, (1993).

30. J. Sanmartin, M. R. Bermejo, A. M. Garcia-Deibe, O. Piro and E. E. Castellano, *Chem. Commun.*, 2145 (1999); J. Sanmartin, M. R. Bermejo, A. M. Garcia-Deibe, O. R. Nascimento, L. Lezama and T. Rojo, *J. Chem. Soc., Daltons Trans.*, 1030, (2002).

31. L. Castro, M. L. Calatayud, F. Lloret, J. Sletten and M. Julve, *J. Chem. Soc., Daltons Trans.*, 2397 (2002).

32. R. J. Butcher, C. J. O'Connor and E. Sinn, *Inorg. Chem.*, **20**, 537 (1981).

33. F. B. Hulsbergen, R. W. M. Ten Hoedt, J. Verschoor, J. Reedijk and A. L. J. Spek, *J. Chem. Soc., Daltons Trans.*, 539 (1983).

34. H. Lopez-Sandoval, R. Contreras, A. Escuer, R. Vicente, S. Bernes, H. Noth, G. J. Leigh and N. Barba-Behrens, *J. Chem. Soc., Daltons Trans.*, 2648 (2002).

35. H. D. Bian, W. Gu, J.-Y. Xu, F. Bian, S.-P. Yan, D.-Z. Liao, Z.-H. Jiang and P. Cheng, *Inorg. Chem.*, **42**, 4265 (2003).

36. R. Costa, A. Garcia, J. Ribas, T. Mallah, Y. Journaux, J. Sletten, X. Xolans and V. Rodriquez, *Inorg. Chem.*, **32**, 3733 (1993).

37. J. C. Liu, D. G. Fu, J. Z. Zhuang, C. Y. Duan and X. Z. You, *J. Chem. Soc., Daltons Trans.*, 2337 (1999).

38. E. Colacio, J. M. Donunquez-Vara, R. Kivekas, J. M. Moreno, A. Romerosa and J. Reuiz, *Inorg. Chim. Acta*, **212**, 115 (1993).

39. X. Chen, S. Zhan, C. Hu, B. Meng and Y. Liu, *J. Chem. Soc., Daltons Trans.*, 245 (1997); F. Tuna, l. Patron, Y. Journaux, M. Andrich, W. Plass and J. C. Trombe, *J. Chem. Soc., Daltons Trans.*, 539 (1999).

40. V. Y. Kukwhkiu and A. J. L. Pombeiro, *Coord. Chem. Rev.*, 181, 147 (1999).

41. L. Spiccia, B. Graham, M. T. W. Hearn, G. Lazarev, B. Moubaraki, K. S. Murray and E. R. T. Tiekink, *J. Chem. Soc., Daltons Trans.*, 4089 (1997).

42. P. Chaudhuri, M. Winter, B. P. C. Della Vedova, E. Bill, A. Trautwein, S. Gehring, P. Fleischhauer, B. Nuber and J. Weiss, *Inorg. Chem.*, **30**, 2148 (1991).

43. E. Colacio, J. M. Dominguez-Vera, A. Escuer, M. Klinga, R. Kivekas and A. Romerosa, *J. Chem. Soc., Daltons Trans.*, 343 (1995).

44. P. Fleischhauer, S. Gehring, C. Saal, W. Haase, Z. Tomkowicz, C. Zachini, D. Gatteschi, D. Dravidov and A. L. Bara, *J. Magn. Mater*, 159, 166 (1996); S. Gehring, P. Fleischhauer, H. Paulus and W. Haase, *Inorg. Chem.*, **32**, 54 (1993).

45. L. Zhao, L. K. Thompson, Z. Xu, D. O. Miller and D. R. Stirling, *J. Chem. Soc., Daltons Trans.*, 1706 (2001).

46. P. A. Angaridis, P. Baran, R. Boca, F. Cervantes-Lee, W. Hasse, G. Mezei, R. G. Raptis and R. Werner, *Inorg. Chem.*, **41**, 2219 (2002).

47. A. Escuer, R. Vicente, E. Penalba, X. Solans and M. Font-Bardia, *Inorg. Chem.*, **35**, 248 (1996).

48. X. Liu, M. P. Miranda, E. J. L. McInnes, C. A. Kilner and M. A. Halcrow, *J. Chem. Soc., Daltons Trans.*, 59 (2004).

49. K. Sakai, Y. Yamada, T. Tsubomura, M. Yabuki and M. Yamaguchi, *Inorg. Chem.*, 35, 542 (1996).

50. S. Ferrer, J. G. Haasnoot, J. Reedjik, E. Muller, M. B. Cingi, M. Lanfranchi, A. M. M. Lanfredi and J. Ribas, *Inorg. Chem.*, **39**, 1859 (2000).

51. S. Mukhopadhyay, D. Mandal, P. B. Chatterjee, C. Desplanches, J.-P. Sutter, R. J. Butcher and M. Chaudhury, *Inorg. Chem.*, **43**, 8501 (2004).

52. C. A. Koch, C. A. Reed, G. A. Brewer, N. P. Rath, W. R. Scheidt, G. Gupta and G. Lang, *J. Am. Chem. Soc.*, 111, 7645 (1989); E. Colacio, J. M. Donunguez-Vera, M. Ghazi, R. Kivekas, M. Klinga and J. M. Moreno, *Inorg. Chem.*, **37**, 3040 (1998).

53. E. Colacio, M. Ghazi, R. Kivekas, M. Klinga, F. Lloret and J. M. Moreno, *Inorg. Chem.*, **39**, 2770 (2000).

54. R. L. Dutta and Md. M. Hossain, *J. Scient. Ind. Res.*, **44**, 635 (1985).

55. V. Y. Kukushkin, D. Tudela, and A. J. L. Pombeiro, *Coord. Chem. Rev.*, 156, 333 (1996).

56. R. A. Lal, A. N. Siva, S. Adhikari, M. K. Singh and U. S. Yadav, *Synth. React. Inorg. Met-Org. Chem.*, **26(2)**, 321 (1996); F. Feigel, V. Anger and R. E. Oesper, "*Spot Test in Organic Analysis*", 7th Ed., Elsevier Publishing Company, Amsterdam, Netherlands, p. 173, 384 (1996), (Indian Reprint, 2005).

57. R. A. Lal, D. Basumatary, S. Adhikari and A. Kumar, *Spectrochim. Acta A*, **69**, 706 (2008).

58. R. A. Lal, J. Chakraborty, A. Kumar, S. Bhaumik, R. K. Nath and D. Ghosh, *Indian J. Chem.*, **43A**, 516 (2004); R. A. Lal, J. Chakraborty, S. Bhaumik and A. Kumar, *Indian J. Chem.*, **41A**, 1157 (2002).

59. W. J. Geary, *Coord. Chem. Rev.*, **7**, 81 (1971).

60. M. D. Cohen and S. Flavian, *J. Chem. Soc.*, B, 317, 321, 329 and 334 (1967); (b) D. Gegiou, E. Lambi and E. Hadjoudis, *J. Phys. Chem.*, **100**, 17762 (1996); (c) T. N. Sorrell, *Tetrahedron*, 54 (1989).

61. B. J. Hathaway, "*In Comprehensive Coordination Chemistry*", p. 594-774 Vol. 5; G. W. Wilkinson, R. D. Gillard and J. A. McLeverty, Ed. Perganion Press, Oxford, New York (1987).

62. L. Banci, A. Bencini and D. Gatteschi, *Inorg. Chem.*, **22**, 2681 (1983).

63. J. S. Griffith, *Struct. Bonding (Berlin)*, **10**, 87 (1972).

64. J. Scaringe, D. J. Hodgson and W. E. Hatfield, *Mol. Phys.*, **35**, 701 (1978).

65. D. Gatteschi, "*The Coordination Chemistry of Metallo-enzymes*", I. Bertini, R. S. Drago and C. Luchirat, Eds., D. Reidel Publishing Co., Dordrecht, p. 215 (1983).

66. P. Chaudhuri, M. Writer, B. P. C. Della Vedova, E. Bill, A. Transtwein, S. Gehring, P. Fleischhauer, B. Nuber and J. Weiss, *Inorg. Chem.*, **30**, 2148 (1991).

67. F. B. Hulsbergen, R. W. M. Ten Hoedt, J. Verschoor, J. Reedijik and A. L. J. Spek, *J. Chem. Soc., Dalton Trans.*, 539 (1983).

68. Y. Agnus, R. Louis, B. Metz, C. Boudon, J. P. Gisselbrecht and M. Gross, *Inorg. Chem.*, **30**, 3155 (1991).

69. W. Vreugdenhil, *Ph. D. Thesis*, Leiden University, Netherlands (1987).

70. L. Banci, A. Bencini and D. Gatteschi, *Inorg. Chem.*, **22**, 4018 (1983).

71. A. Syamal and R. L. Dutta, "*Elements of Magneto Chemistry*", East West Press Pvt. Ltd., New Delhi (1993).

72. M. Mashima, *Bull. Chem. Soc. Japan*, 35, 332, 338, 2020 (1962).

73. K. Nakamoto, "*Infrared and Raman Spectra of Inorganic and Coordination Compounds*", John Wiley and Sons, Inc., New York, pp 184 (1997).

74. D. A. Thornton, *Coord. Chem. Rev.*, **104**, 251 (1970).

75. D. M. Adams, M. Goldstein and E. F. Mooney, *Trans. Faraday Soc.*, **59**, 2228 (1963).

76. D. M. Adams and P. J. Chandler, *Chem. Comm.*, 69 (1966).

77. M. Goldstein and W. D. Unsworth, *Inorg. Chim. Acta*, **4**, 342 (1970).

78. T. K. Paine, T. Weybermiller, E. Bothe, K. Weighardt and P. Chaudhury, *J. Chem. Soc. Daltons Trans.*, 3136 (2003).

CHAPTER VII

Synthesis and Characterization of Monometallic and Homobimetallic Nickel (II) Complexes derived from Polyfunctional Disalicylaldehyde oxaloyldihydrazone

Introduction

Third and fourth chapter describe monometallic and homobimetallic molybdenum (VI) complexes while fifth and sixth chapter describe monometallic and homotrimetallic copper (II) complexes of disalicylaldehyde oxaloyldihydrazone. Nickel is the third metal selected in the present study because a nickel or cobalt promoted molybdenum catalyst is important in industrial catalysis; particularly in the hydrosulfurization process where organo sulfur compounds in petroleum feed stocks are heterogeneously desulfurized with dihydrogen **[1-3]**. Mixed metal molybdenum oxides are used as efficient and selective catalysts for potential oxidation of light alkanes in petrochemistry **[4]**. The coordination nanoparticles like $[Mo(CN)_8CuNi]$ acts as photomagnetic particles and have revealed the possibility of triggering supermagnetism by ligands. Besides these relationships of nickel with molybdenum, nickel alone plays a prominent role in several areas of material chemistry. Some typical interplay between nickel coordination chemistry and material science exists in the use of Ni-containing alkoxides for the synthesis of ceramic materials MOCUD and sol-gel processes, the preparation of nanoscopic dendrimers incorporating nickel, the construction of 3D hybrid inorganic-organic porous materials with Ni-coordination units and the fabrications of supported Ni catalysts and Ni nanostructures through nanotechnology. Paramagnetic high spin nickel (II) has been found particular attention in the field of molecular magnetism, culminating in the recent discovery of the first single molecule magnets based on nickel (II) centres **[5]**.

The role of nickel in biology has also been recognized since the discovery of urease as a nickel enzyme in 1975 by Werner. The list of nickel-dependent enzyme includes

urease, E. Coli glyoxalase I, [Ni-Fe]-hydrogenase, methyl-CoM reductase (MCR), CO dehydrogenase (CODH) and acetyl CoA synthase (ACS), all of which has been crystallographicaly characterized. In addition, a Ni-containing superoxide dismutase has been reported, and some enzymes such as peptide deformylase are active with Ni while not known to naturally occur as a Ni enzyme **[5]**.

A survey of literature reveals that few complexes of the nickel (II) ion with the dihydrazone derived from the condensation of salicylaldehyde and related o-hydroxy aromatic aldehydes and ketones with malonoyldihydrazine and other acyldihydrazines, aroyldihydrazines and pyridoyldihydrazines have been reported **[6-9]**, yet it has failed to locate any study on metal complexes of the dihydrazone ligand containing oxaloyl-fragments and bulky salicyloyl fragment in its molecular skeleton.

In view of such an importance of nickel alone and in combination with molybdenum and zinc in industrial processes and biological systems, and in view of the fact that the previous chapters describes molybdenum and copper complexes, it was thought of interest to study the nickel (II) complexes with the title ligand. The complexes were synthesized in methanol and characterized by elemental analyses, IR spectra, electronic spectral data and magnetic moment and are described in this chapter.

Experimental

Preparation of $[Ni(H_2slox)(H_2O)_2]$ (7.1)

H_4slox (1.00 g, 3.07 mmol) was suspended in methanol (60 mL) with constant stirring for a period of 15-20 minutes to make the homogeneous suspension. To this homogeneous suspension was added slowly a solution of $Ni(OAc)_2.4H_2O$ (0.84 g, 3.38 mmol) in methanol (30 mL) with constant stirring over a period of 30 minutes maintaining $Ni(OAc)_2.4H_2O$ and H_4slox molar ratio at 1:1.1. The resulting mixture was refluxed for about 1 1/2 h which precipitated a light yellowish green coloured

compound. This light yellowish green coloured compound was then suction filtered and purified by washing several times with 10 mL hot methanol each time followed by ether and finally dried over anhydrous $CaCl_2$. Yield: 86.5%.

Preparation of $[Ni_2(slox)(H_2O)_4]$ (7.2)

The preformed ligand, H_4slox (0.50 g, 1.53 mmol) was suspended in methanol (30 mL) with continous stirring under hot condition to make a homogeneous paste. This homogeneous suspension was added to a solution of $Ni(OAc)_2.4H_2O$ (1.14 g, 4.58 mmol) in methanol (40 mL) in hot condition over a period of 15-20 minutes accompanied with constant stirring and the mixture was subjected to reflux for about 3 h. This yielded a greenish yellow precipitate which was suction filtered under hot condition and purified by washing several times with 10 mL hot methanol each time followed by ether and finally dried over anhydrous $CaCl_2$. Yield: 82.3%.

Preparation of $[Ni_2(slox)(A)_4]$ {*where A = pyridine (py)* **(7.3)**, *2-picoline (2-pic)* **(7.4)**, *3-picoline (3-pic)* **(7.5)** *and 4-picoline (4-pic)* **(7.6)**}.

A homogeneous suspension of $[Ni_2(slox)(H_2O)_4]$ **(7.2)** (1.00 g, 1.96 mmol) in methanol (40 mL) was prepared with constant stirring for a period of 15-20 minutes. To a stirring suspension of $[Ni_2(slox)(H_2O)_4]$ in methanol was added 1.55 mL of pyridine drop by drop over a period of 30 minutes. The mixture was then put to reflux for about 1 h when a greenish yellow complex was precipitated. This was purified by filtering under suction in hot condition and washing several times with 10 mL hot methanol each time followed by ether and finally dried over anhydrous $CaCl_2$. Yield: 76.8%.

The complexes **$[Ni_2(slox)(A)_4]$** {*where A = 2-picoline (2-pic)* **(7.4)**, *3-picoline (3-pic)* **(7.5)** *and 4-picoline (4-pic)* **(7.6)**} were also prepared essentially by the above procedure by taking 1.82 mL of 2-picoline, 3-picoline and 4-picoline respectively instead of 1.55 mL of pyridine. Yield: 74.9-76.2%.

Preparation of $[Ni_2(slox)(phen)_3]$ (7.7) and $[Ni_2(slox)(bpy)_3]$ (7.8) {*where phen = 1,10-phenanthroline and bpy = 2,2'-bipyridine*}.

In order to isolate $[Ni_2(slox)(phen)_3]$ **(7.7)**, 1.00 g (1.96 mmol) of $[Ni_2(slox)(H_2O)_4]$ **(7.2)** was suspended in 50 mL methanol with constant stirring over a period of 15-20 minutes to make it homogeneous. To this suspension was added 1,10-phenanthroline (1.17 g, 5.90 mmol) solution slowly in methanol (40 mL) with constant stirring for a period of about 30 minutes. The mixture was then subjected to reflux for about 1 h, which precipitated a brown compound. This brown compound was suction filtered in hot condition and purified by washing several times with 10 mL hot methanol each time followed by ether and finally dried over anhydrous $CaCl_2$. Yield: 70.7%

The complex $[Ni_2(slox)(bpy)_3]$ **(7.8)** was prepared essentially by following the above mentioned procedure using 0.92 g (5.89 mmol) of 2,2'-bipyridine instead of 1.17 g (5.90 mmol) of 1,10-phenanthroline which yielded a brown coloured complex. Yield: 72.3%.

Result and discussion

The complexes described in this chapter together with their colour, decomposition point, analytical data, molar conductance, magnetic moment and electronic spectral data are set out in the **Table 7.1**. As only two method of preparation for the complexes have been used in the present chapter, only two types of complexes have been obtained. The composition of the complexes has been decided based on the data obtained from elemental analyses. The general compositions of the complexes are:

$[Ni(H_2slox)(H_2O)_2]$ **(7.1)**, $[Ni_2(slox)(A)_4]$ {*where A = H_2O* **(7.2)**, *pyridine (py)* **(7.3)**, *2-picoline (2-pic)* **(7.4)**, *3-picoline (3-pic)* **(7.5)** *and 4-picoline (4-pic)* **(7.6)**}, $[Ni_2(slox)(NN)_3]$ {*where NN = 1,10-phenanthroline (phen)* **(7.7)**, *and 2,2'-bipyridine (bpy)* **(7.8)**}.

These complexes are light greenish yellow, greenish yellow or brown in colour and have a very high decomposition point. All the complexes are insoluble in common organic solvents but soluble in highly coordinating solvents such as DMF and DMSO and are air stable.

Thermal analyses

The detailed decomposition studies **[10]** of all the complexes described in this chapter were carried out in the temperature range of 70-250°C. The vapours evolved on heating the complexes were allowed to pass through four separate test tubes containing anhydrous copper sulfate, chloroform solution containing a drop of 5M sodium hydroxide, solution of iodine and sodium hydroxide and cyanogen bromide solution respectively. No vapours were evolved in the temperature range 70-120°C which could turn anhydrous copper sulfate blue, dismissing the possibility of presence of water molecule in the lattice structure of the complexes. Further, the vapours evolved on heating the complexes **(7.1)** and **(7.2)** in the temperature range 160-180°C turned the test tube containing anhydrous copper sulfate blue confirming its origin from water molecules. The vapours evolved at such a high temperature suggest that the water molecules are coordinated to the metal centre. The loss of weight in the temperature range 160-180°C corresponded to two coordinated water molecule in complex **(7.1)** and four coordinated water molecule in complex **(7.2)**. The remaining complexes **(7.3)** to **(7.8)** did not show any weight loss in the above temperature range of 160-180°C suggesting the absence of coordinated water molecules. The complexes **(7.3)**, **(7.5)** and **(7.6)** showed further weight loss in the temperature range 220-240°C. The vapours evolved at this temperature range were passed through the above mentioned test tubes and it was found that in the complex **(7.3)** the colour of the test tube containing chloroform solution with a drop of 5M sodium hydroxide turned red. This confirmed the presence of pyridine molecule in the coordination sphere of the complex **(7.3)**. The vapours evolved in complexes **(7.5)** and **(7.6)** turned the colour of cyanogen bromide solution to green-violet and blue respectively on treatment with phloroglucinol solution suggesting the presence

of 3-picoline and 4-picoline molecules **[10, 11]**. The loss of weight at this temperature were found to be due to four pyridine molecule in complex **(7.3)** and four 3-picoline and 4-picoline molecules respectively in complexes **(7.5)** and **(7.6)**.

Molar conductance

The molar conductivity values for all the complexes in DMSO were in the range 2.5-3.9 $ohm^{-1}cm^2 mol^{-1}$ suggesting them to be non-electrolytes **[12]**.

Magnetic moment

The effective electronic configuration of nickel (II) is $3d^8$. Nickel exhibits a magnetic moment higher than that expected for two unpaired electrons in octahedral and tetrahedral environment whereas diamagnetism of the nickel (II) complexes leads to a square planar stereochemistry. The effective magnetic moment reported for high spin octahedral nickel (II) complexes is in the range 3.00 – 3.50 BM while for the tetrahedral complexes it ranges from 3.5 – 4.0 BM **[13]**. The reason for this deviation is attributed to arise from spin-orbit coupling which cause an orbital contribution in the quenched $^3A_{2g}$ ground state of nickel (II) ion in octahedral environment and not due to contribution from the orbital angular momentum of the electrons because the orbital angular momentum does not affect the $^3A_{2g}$ state. On the contrary, in case of tetrahedral nickel (II) complexes, the orbital angular momentum contributes strongly to the magnetic moment leading to magnetic moment value as high as 4.0 BM. The paramagnetism of the nickel (II) complexes **(7.1)** to **(7.8)** rules out the possibility of the square planar structure and the tetrahedral structure can be discarded on the basis of the magnitude of the magnetic moment. The nickel (II) complex **(7.1)** has magnetic moment value of 3.10 BM which falls in the range reported for high-spin octahedral nickel (II) complexes **[14]**.

In the complexes **(7.2)** to **(7.8)**, two nickel (II) ions are present for each ligand molecule. The magnetic moment values for the complexes **(7.2)** to **(7.6)** lie in the

range 2.94 – 3.10 BM i.e. 1.47-1.55 BM per nickel (II) ion. Such a low value of magnetic moment in these complexes certainly rules out low-spin square planar stereochemistry. But these values are considerably less than the values expected for two spin-free nickel (II) ions present in the same molecular unit. This indicates strong metal-metal interaction in the structural unit of the complexes. Anomalous magnetic moment values in the solid state have been explained on the basis of absorption spectra by proposing mixed octahedral and square planar stereochemistry due to molecular association **[15]**, but the electronic spectra of the complexes described in this chapter are consistent with the tetragonally distorted octahedral stereochemistry. Since, the hydrazine bridges do not cause any lowering of the magnetic moment **[16]**, therefore, it is reasonable to believe that the lowering of magnetic moment in these complexes **(7.2)** to **(7.6)** is due to the presence of oxo-bridged structure and as a result of this nickel (II) complexes attain a tetragonally distorted octahedral stereochemistry.

The complexes **(7.7)** and **(7.8)** have higher magnetic moment values of 4.95 and 4.80 BM, respectively. The magnetic moment value for these complexes is 2.48 and 2.40 BM per metal ion respectively. The μ_{eff} value per metal ion is again less than the value required for two unpaired electrons. This value suggests that some antiferromagnetic interaction is present between the two metal centres in the complexes. It is imperative to mention that the antiferromagnetic interaction in these complexes is less than those in the complexes **(7.2)** to **(7.6)** which may be attributed to coordination of 1,10-phenanthroline and bipyridine in these complexes which due to their bulky nature do not allow the two nickel (II) ions to come close to each other via oxo-bridging. These values further, suggests that spin exchange is not passed even through bridging ligand backbone.

Electronic spectra

The free ligand and its nickel (II) complexes **(7.1)** to **(7.8)** are insoluble in non-coordinating organic solvents, which prevented recording of electronic spectra of the

ligand and the nickel (II) complexes derived from the title ligand in these solvents. Hence, the electronic spectra were recorded in DMSO. The important electronic spectral bands for the title ligand and the nickel (II) complexes derived from it are presented in the **Table 7.1**, along with their molar extinction coefficient. The electronic spectra of the complexes **(7.1)** to **(7.4)** and **(7.7)** are shown in the **Figs. 7.1-7.5**.

The free ligand molecule exhibits three bands in the region 290 – 340 nm. The bands at 293 nm and 303 nm are assigned to intraligand $\pi \rightarrow \pi^*$ transition **[17-21]** while the band at 340 nm is assigned to $n \rightarrow \pi^*$ transition. The band at 340 nm is characteristic of salicylaldimine part as has been reported in several monoacylhydrazones **[22]**. The electronic spectra of the complexes **(7.1)** to **(7.8)** exhibit three bands in the region 295 – 432 nm. The bands in the region 295 – 333 nm are attributed to arise due to intraligand transition and are considerably red shifted in position in the nickel (II) complexes mentioned in this chapter. The red shift of the ligand band gives a good indication of chelation of dihydrazone ligand to the metal centre. A new band in the region 397 – 432 nm, with high molar extinction coefficient is assigned to have its origin in the ligand to metal charge transfer transition **[23-26]**. This ligand to metal charge transfer transition is strongly influenced by the chemical nature of the ligand within a given stereochemistry and is responsible for the appearance of coloured complexes.

Nickel complexes show three bands in the octahedral environment corresponding to the transitions $^3A_{2g} \rightarrow {}^3T_{2g}$ (F) (ν_1), $^3A_{2g} \rightarrow {}^3T_{1g}$ (F) (ν_2) and $^3A_{2g} \rightarrow {}^3T_{1g}$ (P) (ν_3) **[27]**. Since the transition $^3A_{2g} \rightarrow {}^3T_{1g}$ (P) (ν_3) generally occurs in the region 330 – 400 nm in which the bands due to organic fraction of the complexes arise as well. Therefore, this region is not useful from the point of view of drawing any conclusion about the stereochemistry **[28]**. However, the first two low energy bands observed in the 615 – 950 nm range in the complexes **(7.1)** to **(7.8)** are characteristic of nickel (II) in octahedral environment. The octahedral environment around nickel (II) in

these complexes is further supported by the value of $\nu_2/\ \nu_1$ ratio which lie in the region of 1.49 – 1.51 **[29]**.

A comparison of the absorption bands of the nickel (II) complexes **(7.1)** to **(7.8)** mentioned in the present study with the corresponding bands in the spectra of $[Ni(H_2O)_6]^{2+}$ at 1175, 740 **[30]** and $[Ni(NH_3)_6]^{2+}$ at 935, 570 **[30]** suggest that the first absorption band (ν_1) bears similarity with those of nitrogen donor ligands while the second band (ν_2) is intermediate between those observed for oxygen as well as nitrogen donor ligands.

The ligand field parameters **[31]** viz. Racah inter-electronic repulsion parameter (B), ligand field splitting energy (10Dq), covalency factor (β) and ligand field stabilization energy (LFSE) have been calculated for the nickel (II) complexes **(7.1)** to **(7.8)** and are illustrated in **table 7.2**. The Ligand field splitting energy (10Dq) and the Racah inter-electronic repulsion parameter (B) were calculated by the equation given by Lever **[13]**.

$^3A_{2g} \rightarrow {}^3T_{2g}\ (F)\ (\nu_1) = 10Dq$

$^3A_{2g} \rightarrow {}^3T_{1g}\ (F)\ (\nu_2) = 7.5B + 15Dq - \frac{1}{2}(225B^2 + 100Dq^2 - 180DqB)^{1/2}$

$^3A_{2g} \rightarrow {}^3T_{1g}\ (P)\ (\nu_3) = 7.5B + 15Dq + \frac{1}{2}(225B^2 + 100Dq^2 - 180DqB)^{1/2}$

The Racah inter-electronic repulsion parameter (B) was also calculated using the following equation **[32]** and the values obtained were found to be the same as calculated using the equation given by Lever.

$B_{complex} = (2\nu_1^2 + \nu_2^2 - 3\ \nu_1\nu_2)(15\nu_2 - 27\nu_1)$

The covalency factor (β) was obtained by the following equation

$\beta = B/B'$ (where B' is the free ion value = 1038 cm^{-1}) **[33]**

The ligand field stabilization energy (LFSE) expressed by the equation

LFSE = 10Dq, is also calculated and expressed in Kcal/mol in the table.

The percentage lowering of energy of 'P' state in the complexes as compared to its value in the free gaseous ion (β^o) is obtained by the equation:

$\beta^o = 100 - (\beta \times 100)$

The evaluation of B for the nickel (II) complexes **(7.1)** to **(7.8)** from the above equation lies in the range 564.75 – 619.61 cm^{-1}, which is very low as compared to the free ion value (1038 cm^{-1}). Such a low value of B indicates considerable covalent character in the nickel (II) complexes. The covalency factor β, for the complexes lie in the range 0.544 – 0.597, which is less than unity suggesting the presence of considerable amount of covalent character in the metal-ligand bonds. The percentage lowering of the energy of 'P' state in the complexes compared to its value in the free gaseous ion (β^o) is in the range 40.3 – 45.6% which shows a high degree of covalency.

The values of $\nu_2/\ \nu_1$ for tetragonal complexes are found significantly higher than the usual range for octahedral complexes and sometimes greater than the theoretical limit of 1.80 for octahedral symmetry. The interaction between $^3T_{1g}$ (P) and $^3T_{1g}$ (F) states **[34]** gradually lowers the ratio $\nu_2/\ \nu_1$ from the theoretical value of 1.80 to 1.50 – 1.70 and values of 1.60 – 1.70 are common for nickel (II) complexes of octahedral symmetry. In the present complexes the $\nu_2/\ \nu_1$ values lie in the range 1.49 – 1.51 which is slightly lower than the lower limit for usual octahedral complexes but are within the range reported for octahedral complexes **[35]**. These low value indicates a strong interaction between $^3T_{1g}$ (P) and $^3T_{1g}$ (F) states of the nickel (II) complexes. The ligand field stabilization energy for the nickel (II) complexes **(7.1)** to **(7.8)** in the present study lays in the range 36.2 – 37.0 kcal/mol.

Infrared spectra

A comparison of the IR spectra of the free dihydrazone (H_4slox) with those of the complexes suggests that it is present in keto form in complex **(7.1)** and enol form in the remaining complexes. The important IR spectral bands for the dihydrazone (H_4slox) and the nickel (II) complexes are shown in the **Table 7.3**. As a representative example the IR spectra of the complexes **(7.1)** to **(7.4)** and **(7.7)** are shown in **Figs. 7.6-7.10**.

The band at 3278 and 3204 cm^{-1} in the ligand arise due to the stretching vibration of phenolic -OH and secondary >NH group, respectively. The IR spectra of the complexes **(7.2)** to **(7.8)** do not show any band in this region which could be assigned to the stretching vibration of phenolic -OH or secondary >NH group. The absence of band due to phenolic -OH group in the IR spectra of the complexes indicates the involvement of -OH group in bonding to the metal centre via deprotonation while the absence of band due to stretching vibration of secondary >NH group indicates that the secondary >NH group is destroyed upon complexation with the metal atom, most probably, via enolization. The IR spectra of all the complexes contains a strong broad band in the region 3450-3300 cm^{-1} which is absent in the free dihydrazone ligand. The essential features of this band in all of the complexes suggest that it owes it origin either from the stretching vibration of water molecules present in the lattice structure as well as inside the coordination sphere or moisture absorbed during the preparation of KBr pellets. In order to decide upon whether the band in this region is due to moisture absorbed by KBr pellet or due to the presence of lattice or coordinated water molecules, thermal analyses were carried out. Thermal analyses showed the absence of lattice water molecules in all the complexes. Furthermore, only complexes **(7.1)** and **(7.2)** showed the presence of coordinated water molecules. Based on the thermal analyses experiment, the band in the region 3450-3300 cm^{-1} were assigned to arise due to the moisture absorbed by KBr pellets except complexes **(7.1)** and **(7.2)** where it has contribution from the stretching vibration of coordinated water molecules.

The ν (>C=O) (amide I) band appears at 1667 cm^{-1} in the present ligand as a very strong band. This band appears at 1668 cm^{-1} as a medium intensity band in the complex **(7.1)**. The intensity of this band is considerably reduced in the complex **(7.1)**. From these observation, it may be concluded that in this complex, one >C=O group is involved in coordination via enolization while the other >C=O group remains unbonded. Further, the amide I band at 1667 cm^{-1} in uncoordinated dihydrazone disappears in the remaining complexes **(7.2)** to **(7.8)**. This shows the distruction of amide structure of the ligand in the complexes and its involvement in coordination through carbonyl oxygen atoms via enolization.

The present ligand shows two very strong bands at 1627 and 1603 cm^{-1} due to stretching vibration of >C=N- group. This band appears in the form of a single strong band at 1608 cm^{-1} in the complex **(7.1)** while in the remaining complexes it appears as a couple of strong intensity band in the region 1626-1598 cm^{-1}. The average position of the ν(>C=N-) band shifts to lower frequency by 2-7 cm^{-1} in all of the complexes except complexes **(7.7)** and **(7.8)** where the shift to lower frequency is of about 17 and 11 cm^{-1}, respectively. The shift of ν (>C=N-) band to lower frequency indicates coordination of the dihydrazone through azomethine group to the metal centre **[36]**. It is imperative to mention that ν (>C=N-) band appears as a single band in the complex **(7.1)**, while it is split into two bands in the remaining complexes **(7.2)** to **(7.8)**. The appearance of ν (>C=N-) vibration as a single band in the complex **(7.1)** suggests that the dihydrazone coordinates to the metal centre in staggered configuration while the splitting of ν (>C=N-) vibration into two bands in the complexes **(7.2)** to **(7.8)** suggests that the dihydrazone is bonded to the metal centre in anti-cis configuration.

The free dihydrazone shows a strong band at 1534 cm^{-1}. This band is assigned to have a composite character due to mixed contribution of the amide II and ν (C-O) bands. This band shifts to higher frequency by 3 cm^{-1} in the complex **(7.1)** and appears at 1537 cm^{-1}. Such a small positive shift of this band indicates coordination

of phenolate atoms to the metal centre but at the same time dismissing the possibility of involvement of phenolate oxygen atom in bridge formation. However, a positive shift of about 17-24 cm^{-1} is observed for this band in the complexes **(7.2)** to **(7.6)**. A positive shift of more than 10 cm^{-1} is indicative of involvement of phenolate C-O group in bonding with metal ion accompanied by oxo-bridging **[37]**. The shift of ν (C-O) (phenolate) by about 17-24 cm^{-1} indicates that the phenolate oxygen atom is involved in bonding to the metal ion in the complexes **(7.2)** to **(7.6)**. A new strong intensity band appearing in the region 1503-1533 cm^{-1} in all of the complexes except complex **(7.1)** has been assigned to stretching vibration of the newly created NCO group **[36]**. The appearance of ν (NCO) group in the IR spectra confirms the presence of dihydrazone in enol form in the complexes **(7.2)** to **(7.8)**. It is imperative to mention that the intensity of the band at 1537 cm^{-1} is considerably increased in the complex **(7.1)**. It appears that this band has contribution both due to ν (C-O) (phenolate) and ν (NCO). This suggests involvement of phenolate C-O and enolate C-O groups in bonding via enolization of half part of the dihydrazone molecule.

In the dihydrazone a strong intensity band appears at 1262 cm^{-1} due to ν(C-O) (phenolic) vibration **[38]**. This band is shifted to higher frequency by 13-45 cm^{-1} in all of the complexes and appears in the region 1275-1307 cm^{-1} as a strong band and masks a medium intensity ligand band at 1306 cm^{-1}. Such a feature associated with ν(C-O) band indicates bonding through (C-O) oxygen atom of the dihydrazone to the nickel atom **[38]** via deprotonation of phenolic –OH group.

The region below 1200 cm^{-1} has been scrutinized and υ (N–N) vibration has been located. The weak band observed at 1035 cm^{-1} in the ligand is assigned to υ (N–N) vibration. This band shifts to higher frequency by 5-14 cm^{-1} in the metal complexes indicating involvement of only one nitrogen atom of N-N group in coordination **[39]**. The complexes **(7.2)** to **(7.6)** show a weak band in the region 810-820 cm^{-1}. This band is observed neither in the IR spectra of the uncoordinated ligand nor in those of the complexes **(7.1)**, **(7.7)** and **(7.8)**. Hence this band is assigned to stretching

vibration of tetraatomic species 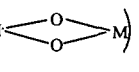 indicating presence of oxo-bridging in the complexes involving phenoxide oxygen atom **[40]**.

The new weak to medium intensity band appearing in the region 560-599 cm^{-1} and a weak intensity band in the region 434-476 cm^{-1} in the complexes **(7.1)** to **(7.8)** have been assigned to the stretching vibration of Ni-O (phenolic) and Ni-O (enolized carbonyl) bond indicating coordination of phenolate oxygen atom and enolized carbonyl oxygen atom to the metal centre, respectively. We were unable to assign Ni-N stretching vibration in the complexes because it falls in the region beyond the range of instrument employed for recording IR spectra.

The free pyridine bases absorb around 604 cm^{-1}due to in-plane ring deformation mode **[41]**. In the complexes a new weak band is observed in the region 600 – 620 cm^{-1}. This band is assigned to arise due to in-plane deformation mode of pyridine and substituted pyridine indicating their coordination to the metal centre. The nickel (II) complexes **(7.3)** to **(7.6)** also shows a weak intensity band in the region 1020-1010 cm^{-1}, which is assigned to ring stretching mode of pyridine, 2-picoline, 3-picoline and 4-picoline molecules **[42]** indicating their presence inside the coordination sphere of the complexes **[42]**. In the complex **(7.7)** strong intensity bands are observed at 726 cm^{-1} and 848 cm^{-1} which are assigned to the out of plane motion of the hydrogen atoms on the heterocyclic rings and the hydrogen atoms on the centre ring of 1,10-phenanthroline molecule, respectively **[43]**. In the Ni (II) bipyridyl complex only one band is observed at 736 cm^{-1} due to out-of-plane motion of the hydrogen atoms as expected for two identical groups of four hydrogen atoms each **[44]**. Apart from these bands complex **(7.7)** and complex **(7.8)** also show a medium broad band at 648 and 652 cm^{-1}which is assigned to arise due to in-plane ring deformation mode of 1,10-phenanthroline and 2,2'-bipyridine indicating their coordination to the metal centre.

Conclusion

In this chapter a monometallic and some homobimetallic complexes of nickel (II) have been prepared and characterized on the basis of data obtained from various physico-chemical and spectroscopic studies. The ligand coordinates to the metal centre in complex **(7.1)** as a dibasic tridentate ligand coordinating through one phenolate oxygen atom, one enolate oxygen atom and azomethine nitrogen atom. On the other hand, in the remaining complexes, the dihydrazone coordinates to the metal centre as a tetrabasic hexadentate ligand through both the phenolate oxygen atoms, both the enolate oxygen atoms and both the azomethine nitrogen atoms. In the complexes **(7.2)** to **(7.6)** the different metal atoms are bonded to one another through oxo-bridging involving phenoxide ions while no such oxo-bridging is present in the complexes **(7.7)** and **(7.8)**, most probably, due to coordination of bulky bipyridine and 1,10-phenanthroline. The dihydrazone coordinates to the metal centre in staggered configuration in complex **(7.1)** while in the anti-cis configuration in complexes **(7.2)** to **(7.8)**. Water, pyridine, substituted pyridine and bidentate donor molecules bpy and phen are coordinated to the metal centre. The complex **(7.1)** is normal paramagnetic corresponding to the presence of one nickel (II) ion while the complexes **(7.2)** to **(7.6)** possess anomalously low value of magnetic moment indicating metal-metal interaction in the structural unit via oxo-bridging. On the other hand, the complexes **(7.7)** and **(7.8)** possess magnetic moment values corresponding to two nickel (II) ion per ligand molecule with no metal-metal interaction. All of the complexes possess distorted octahedral stereochemistry around the metal centre. The tentative structures for the complexes are shown in **Figs. 7.11-7.13** respectively.

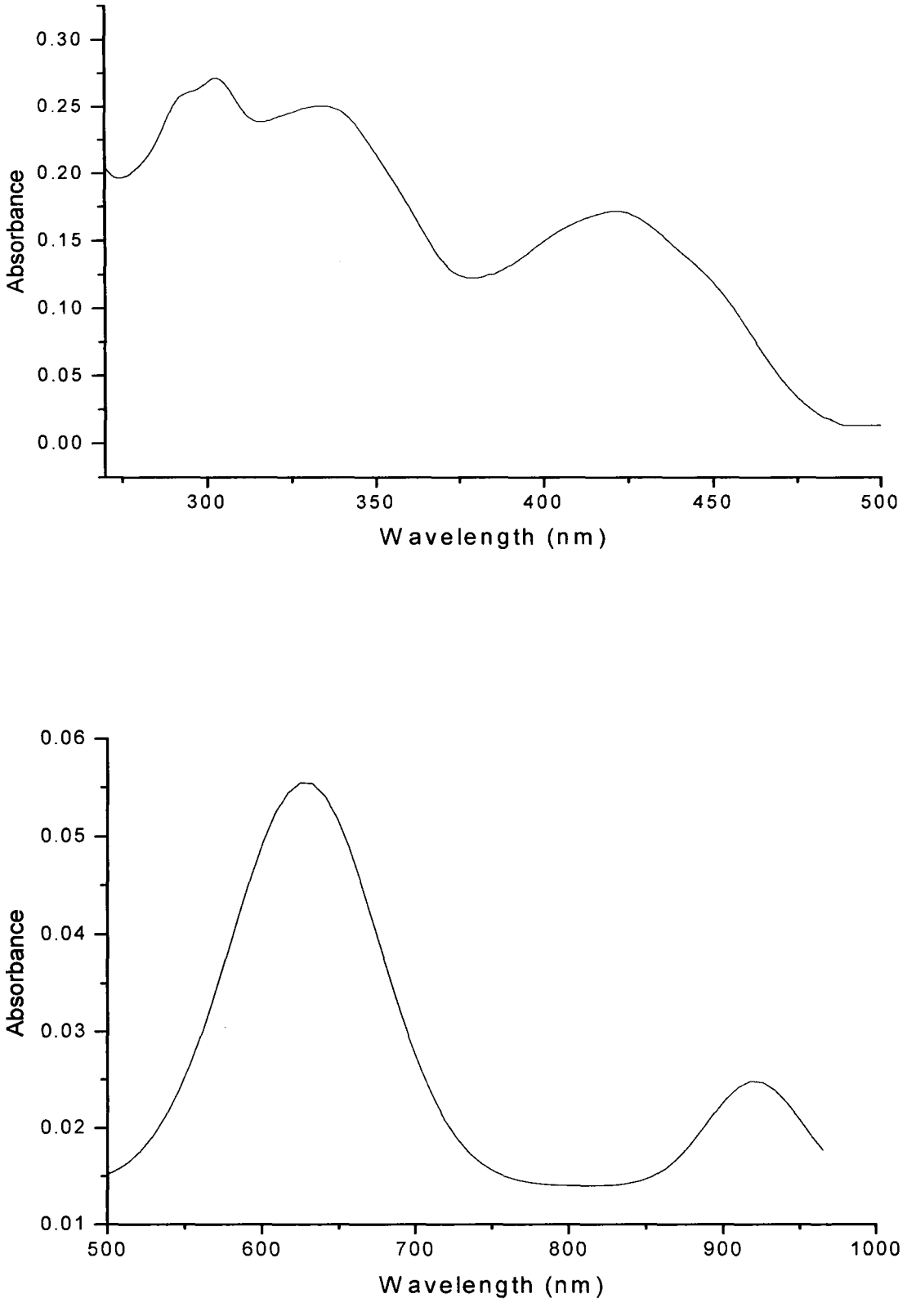

Fig. 7.1 Electronic spectrum of $[Ni(H_2slox)(H_2O)_3]$ **(7.1).**

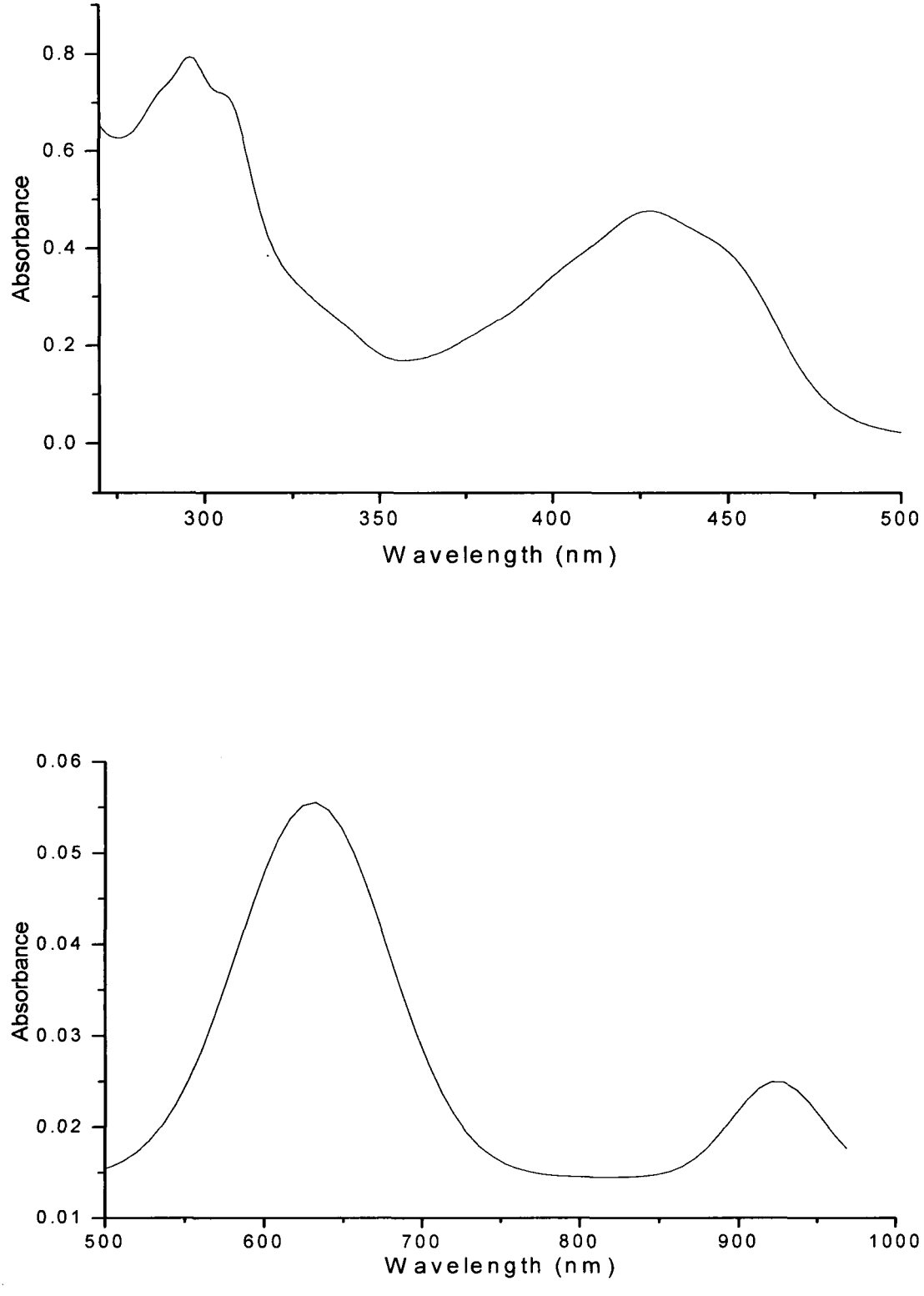

Fig. 7.2 Electronic spectrum of $[Ni_2(slox)(H_2O)_4]$ **(7.2)**.

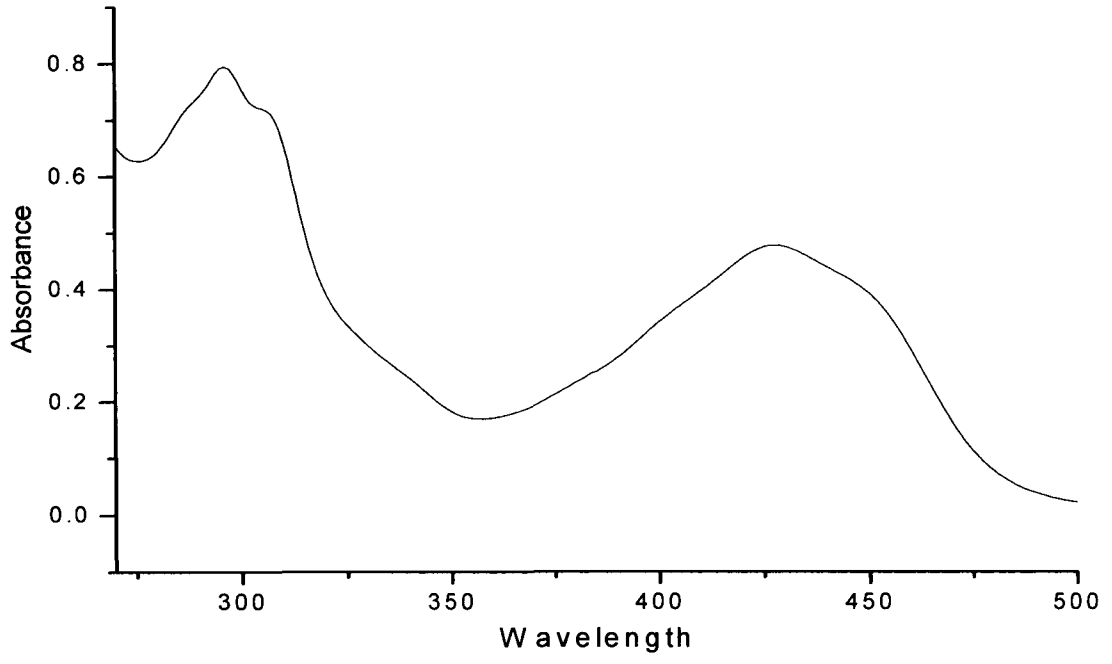

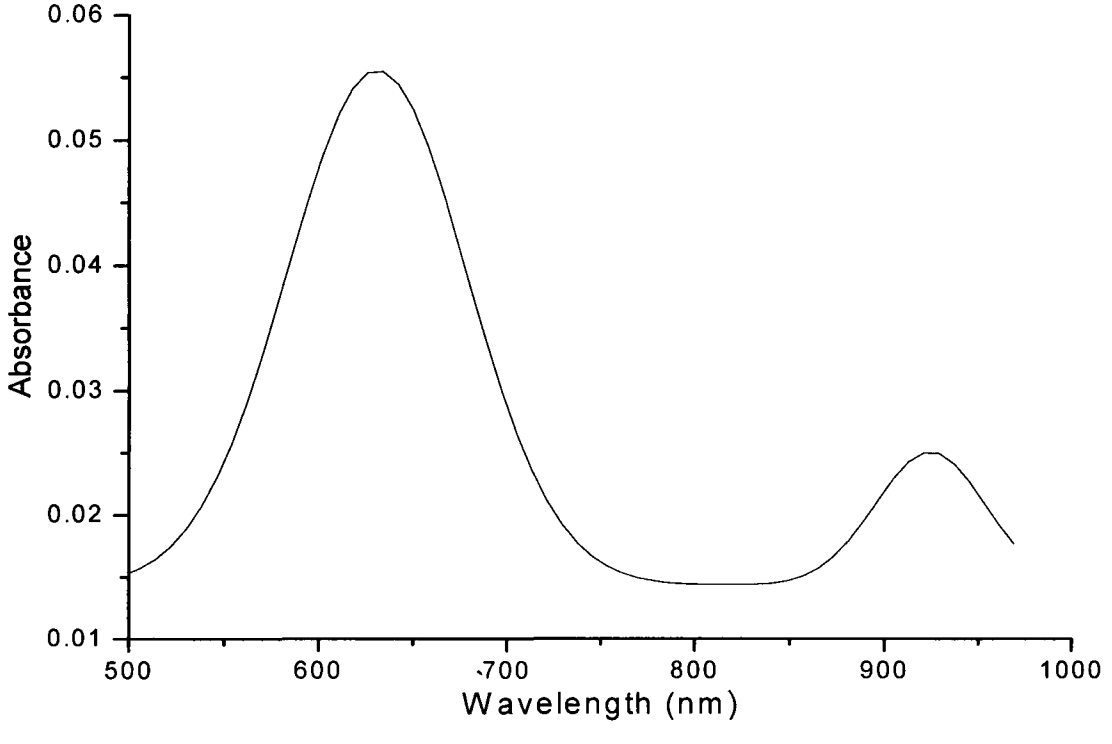

Fig. 7.3 Electronic spectrum of $[Ni_2(slox)(py)_4]$ **(7.3)**.

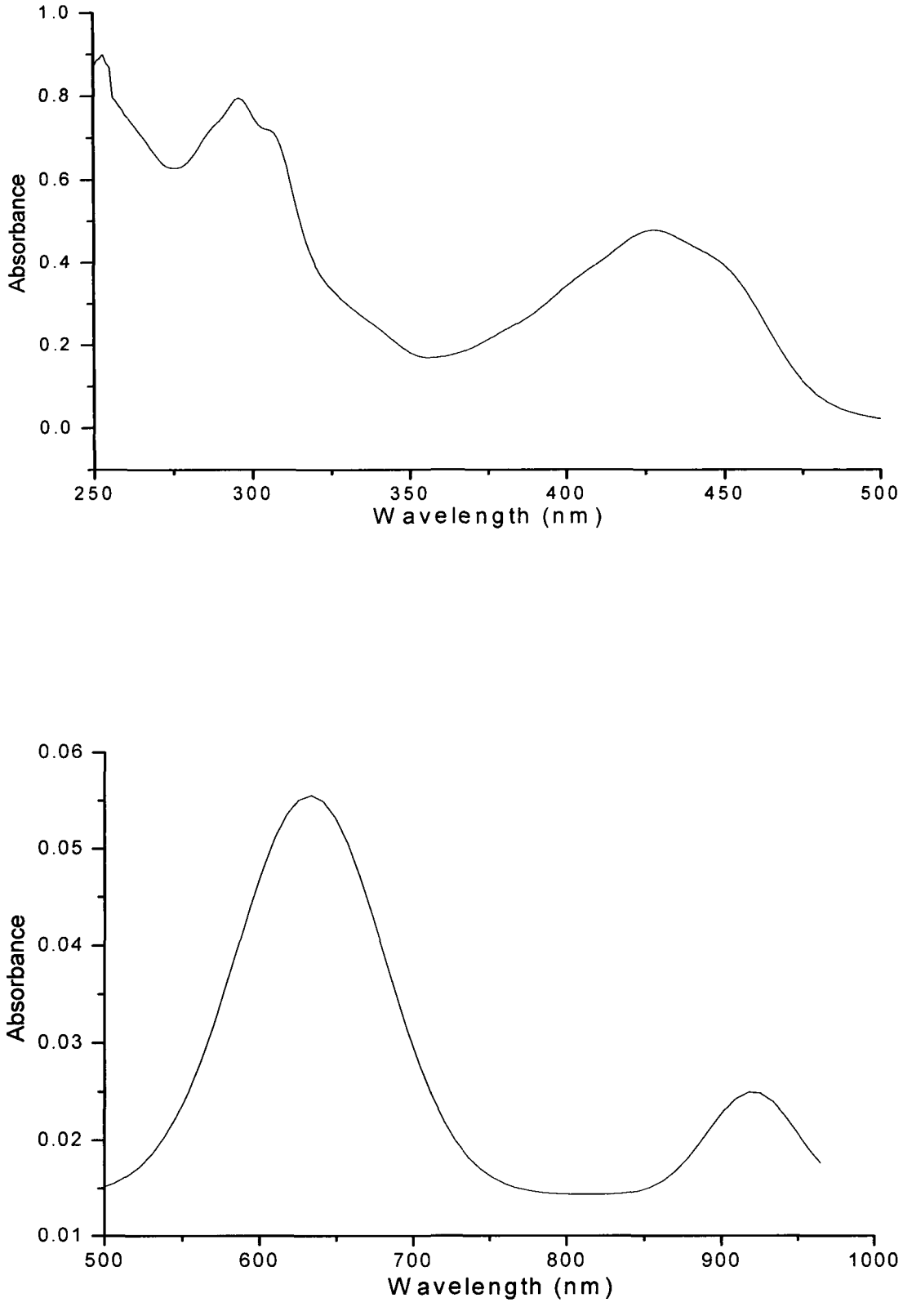

Fig. 7.4 Electronic spectrum of $[Ni_2(slox)(2\text{-}pic)_4]$ **(7.4)**.

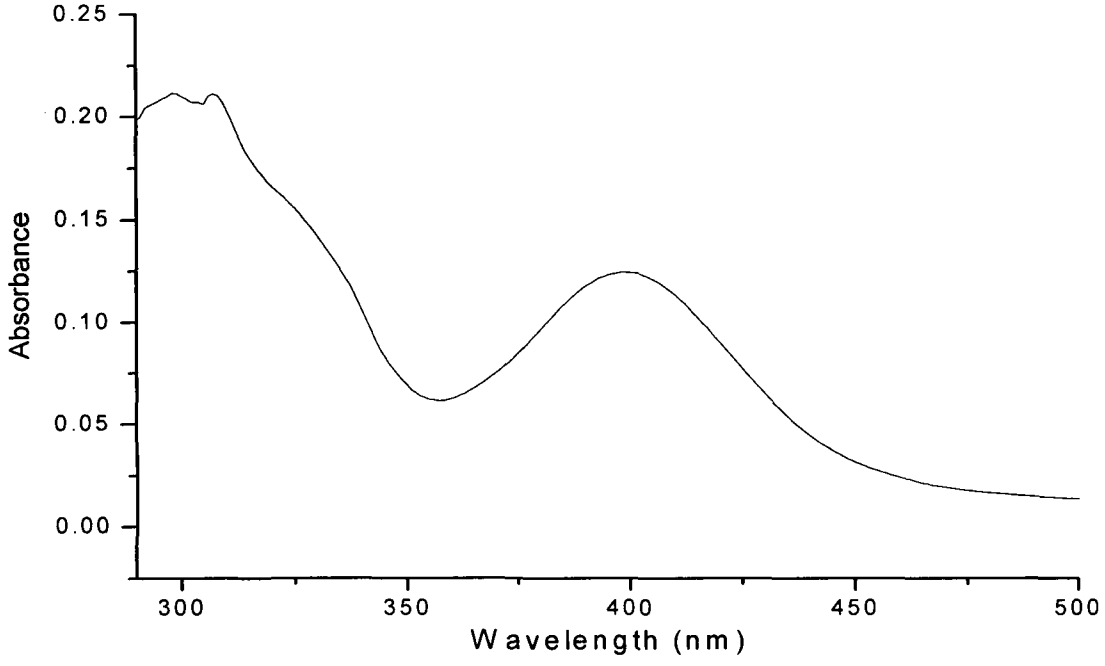

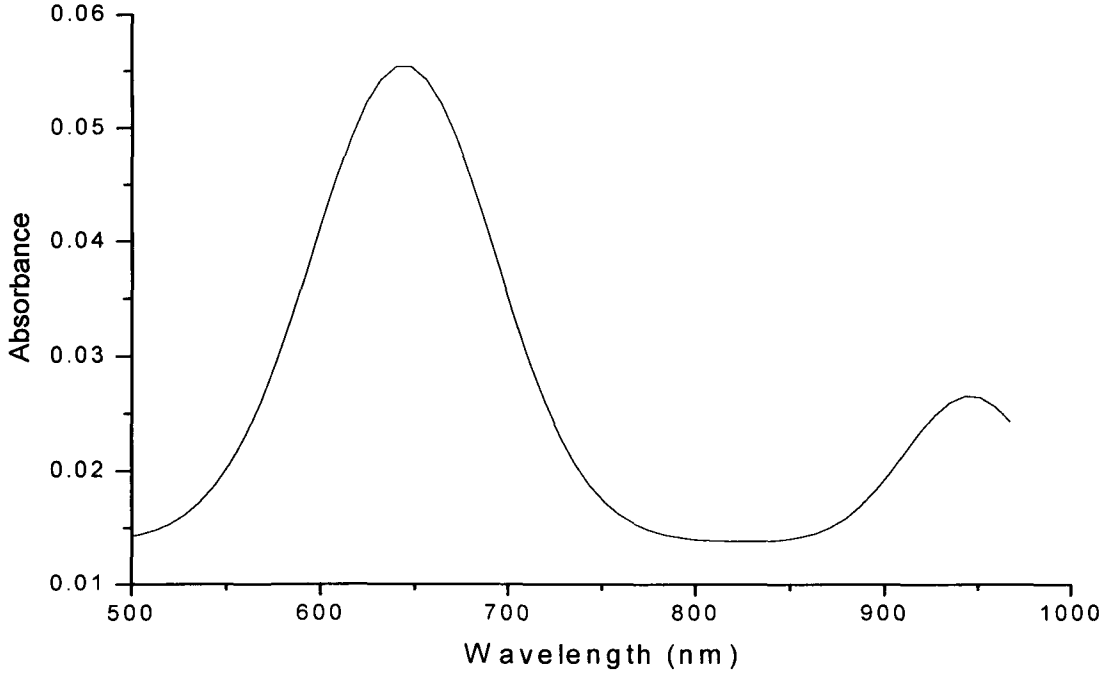

Fig. 7.5 Electronic spectrum of $[Ni_2(slox)(phen)_3]$ **(7.7)**.

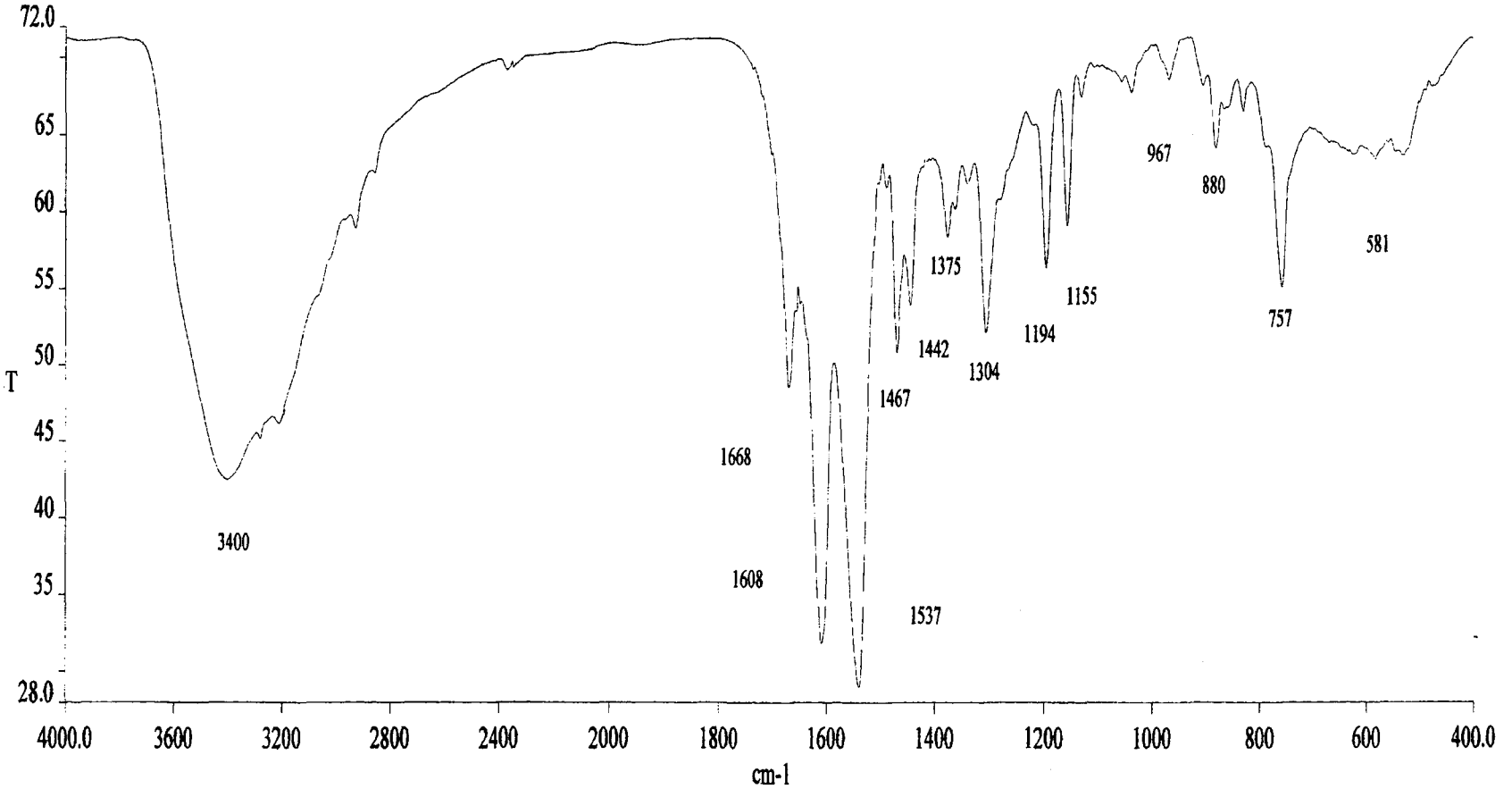

Fig. 7.6 Infrared spectrum of $[Ni(H_2slox)(H_2O)_3]$ **(7.1)** in KBr.

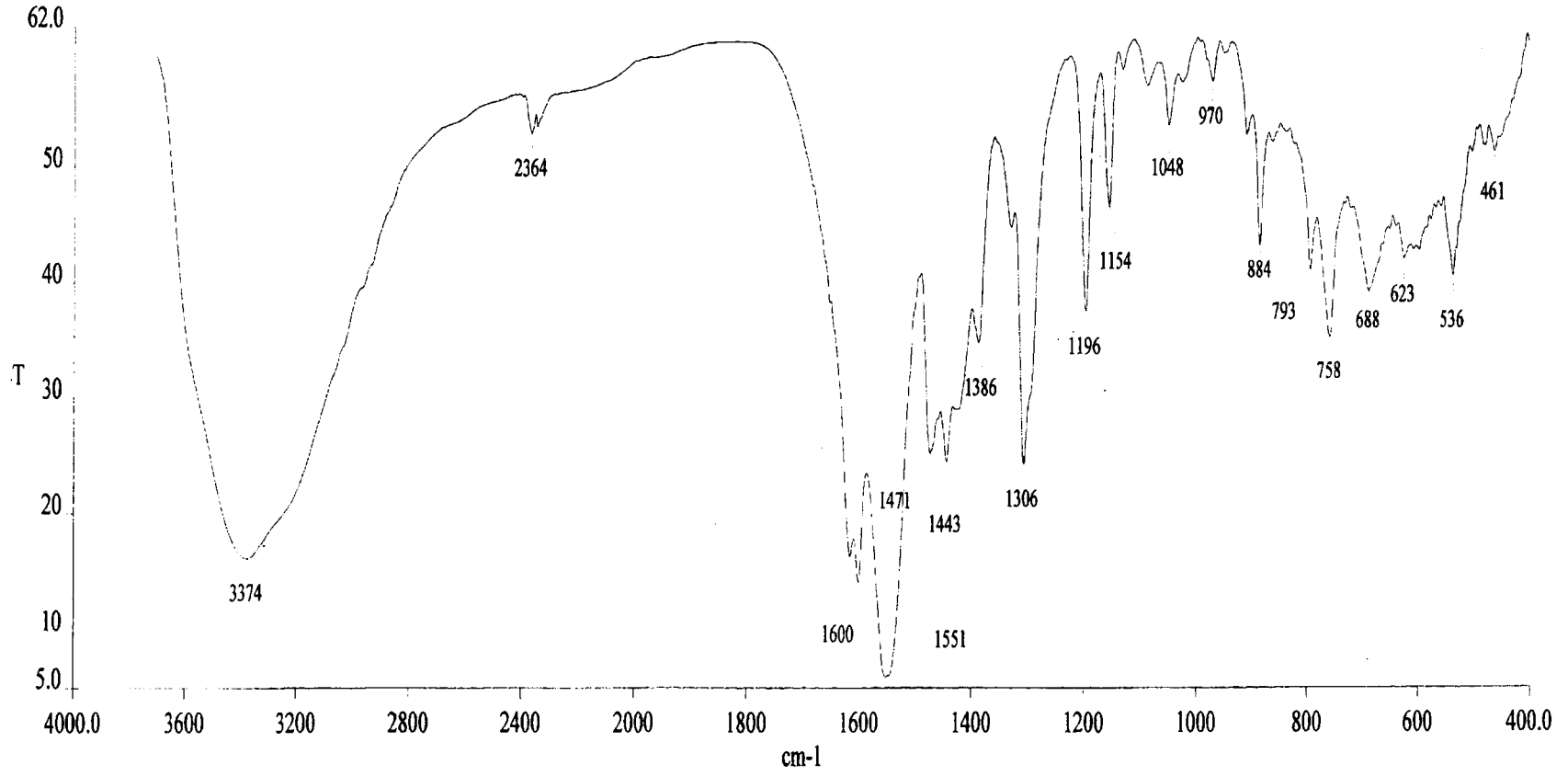

Fig. 7.7 Infrared spectrum of $[Ni_2(slox)(H_2O)_4]$ **(7.2)** in KBr.

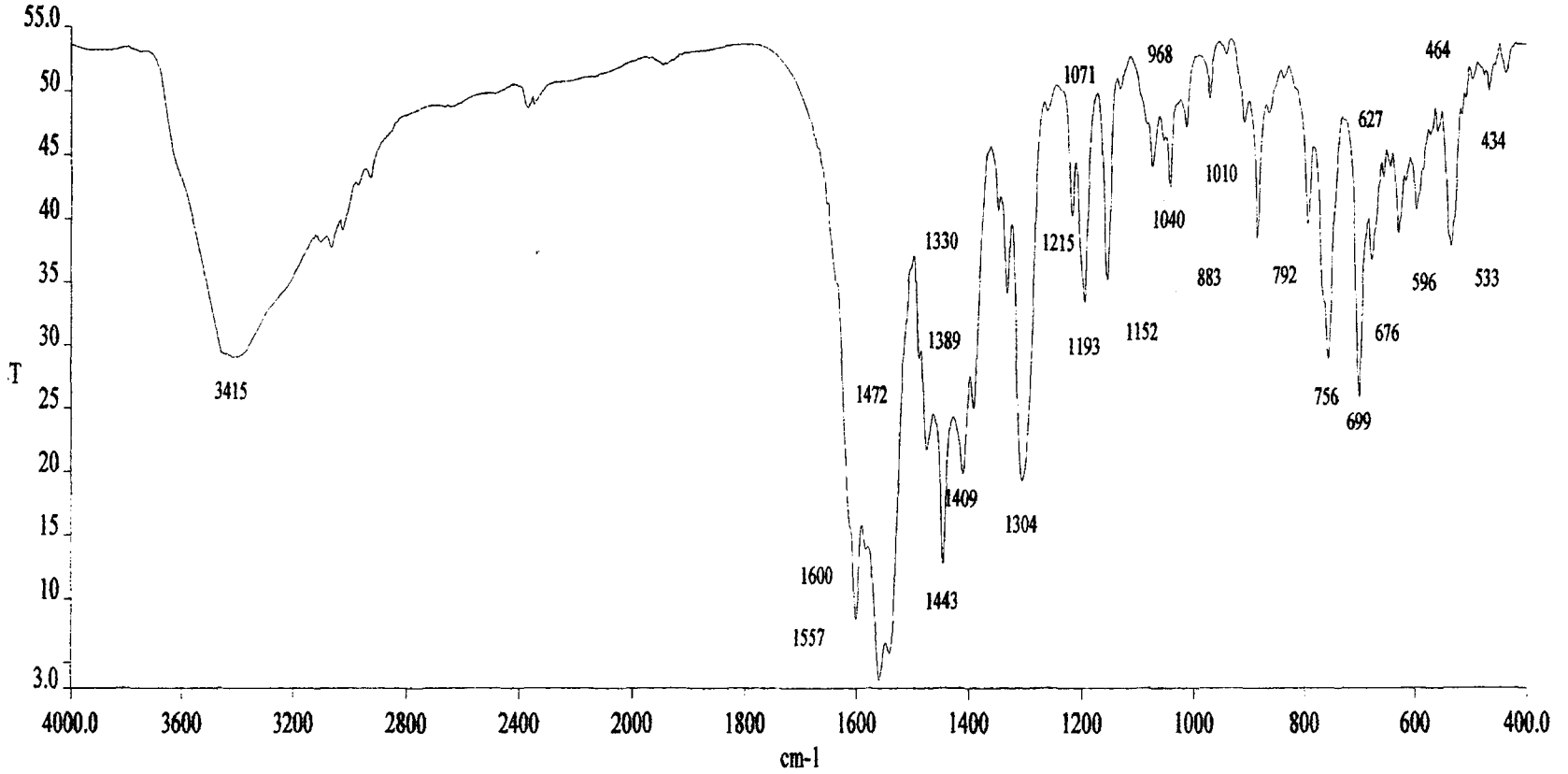

Fig. 7.8 Infrared spectrum of $[Ni_2(slox)(py)_4]$ **(7.3)** in KBr.

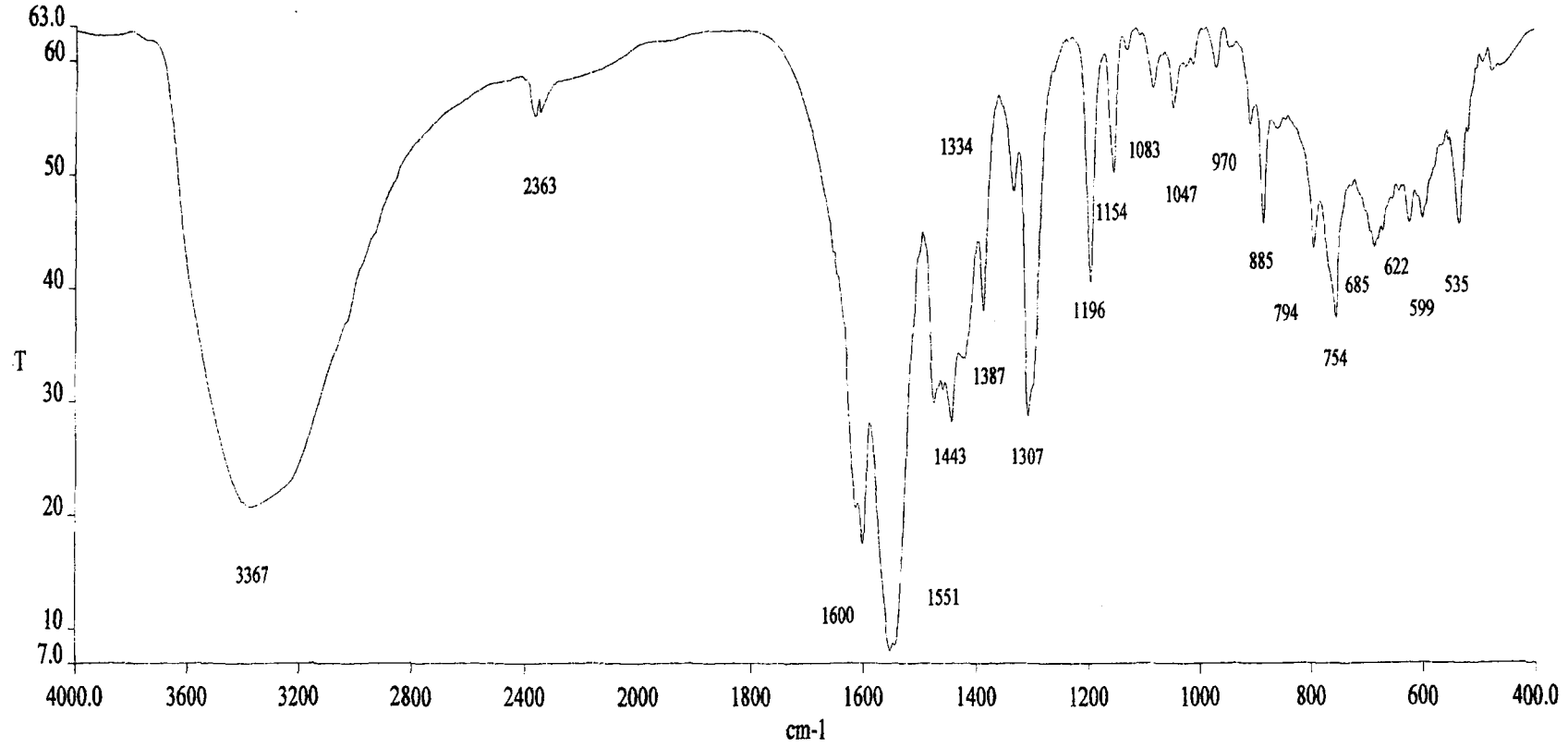

Fig. 7.9 Infrared spectrum of $[Ni_2(slox)(2\text{-pic})_4]$ **(7.4)** in KBr.

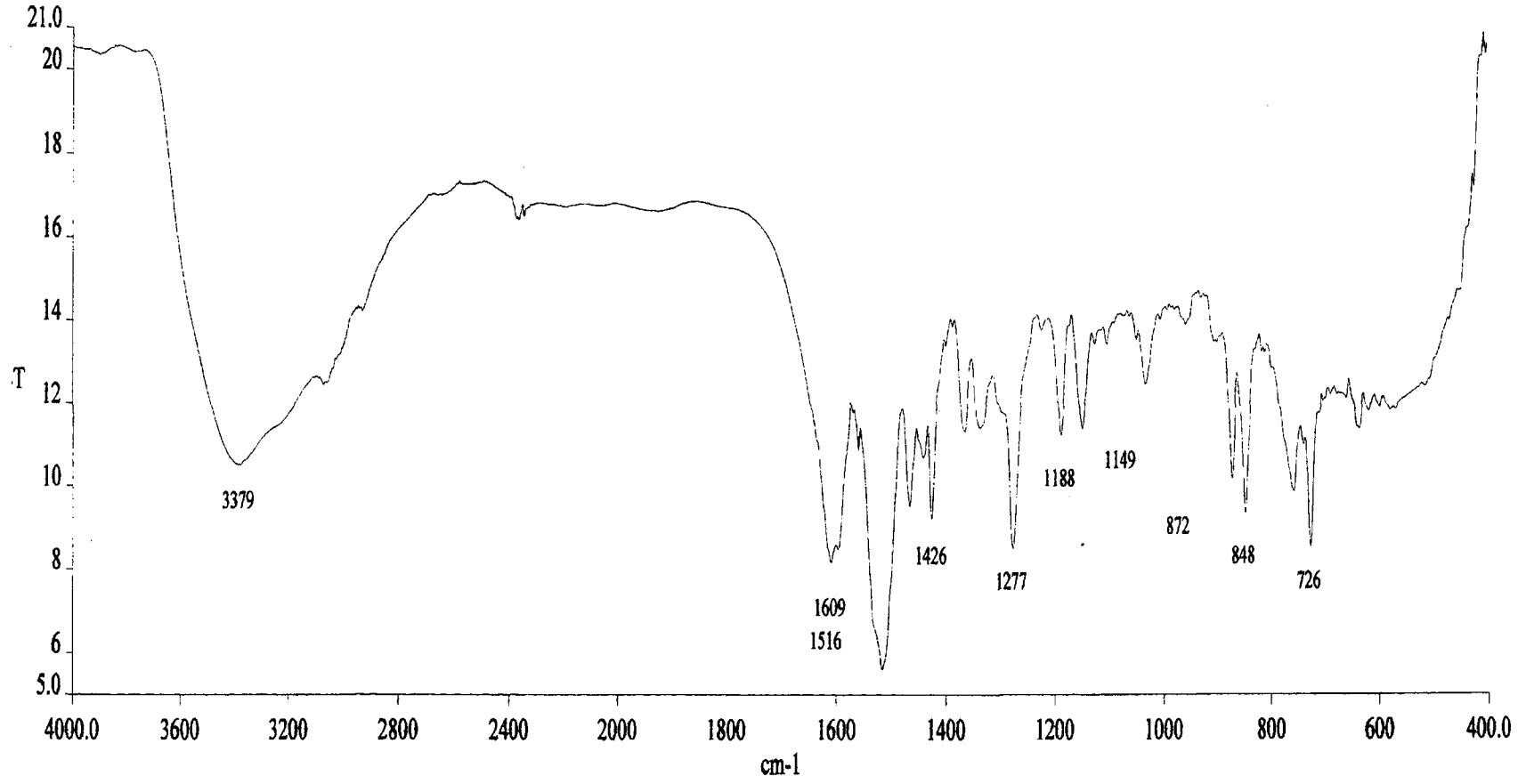

Fig. 7.10 Infrared spectrum of $[Ni_2(slox)(phen)_3]$ **(7.7)** in KBr.

Table 7.1: Complex, colour, decomposition point, analytical, molar conductance, magnetic moment and electronic spectral data for nickel (II) complexes.

Sl. No.	Complex (Colour)	D.P. (°C)	Elemental analyses: Found (Calcd)%				Molar conductance Λ_M (ohm^{-1} cm^2 mol^{-1})	Magnetic moment μ_{eff} (BM)	Electronic spectral band λ_{max}(nm) (ε_{max}) (dm^3 $mol^{-1}cm^{-1}$)
			M	C	H	N			
7.1	$[Ni(H_2slox)(H_2O)_3]$ (Light greenish yellow)	>300	13.76 (13.44)	44.25 (43.97)	4.10 (4.12)	13.11 (12.82)	2.5	3.10	303(9053) 333(8350) 420(5720) 619(95) 932 (55)
7.2	$[Ni_2(slox)(H_2O)_4]$ (Greenish yellow)	>300	22.62 (22.95)	38.00 (37.55)	3.17 (3.13)	11.15 (10.95)	3.1	2.94	297(9786) 306(8971) 432(5884) 615(69) 929(32)
7.3	$[Ni_2(slox)(py)_4]$ (Greenish yellow)	>300	15.93 (15.53)	57.41 (57.16)	3.68 (3.70)	14.66 (14.82)	2.9	2.96	295(9903) 307(8895) 431(5884) 617(69) 931(33)
7.4	$[Ni_2(slox)(2\text{-}pic)_4]$ (Greenish yellow)	>300	14.91 (14.46)	59.60 (59.12)	4.40 (4.43)	13.92 (13.79)	2.6	2.99	297(9899) 308(8746) 429(5959) 628(69) 946(31)
7.5	$[Ni_2(slox)(3\text{-}pic)_4]$ (Greenish yellow)	>300	14.82 (14.46)	58.82 (59.12)	4.47 (4.43)	14.05 (13.79)	3.0	2.98	296(9939) 307(8895) 426(5951) 633(67) 941(31)
7.6	$[Ni_2(slox)(4\text{-}pic)_4]$ (Greenish yellow)	>300	14.06 (14.46)	58.75 (59.12)	4.41 (4.43)	14.13 (13.79)	2.9	3.10	298(9898) 307(8890) 412(5947) 623(70) 940(32)
7.7	$[Ni_2(slox)(phen)_3]$ (brown)	>300	11.81 (11.35)	60.51 (60.35)	3.04 (3.09)	13.84 (13.54)	3.7	4.95	297(7000) 307(7043) 397(4137) 629(86) 950(52)
7.8	$[Ni_2(slox)(bpy)_3]$ (brown)	>300	13.26 (12.93)	60.32 (60.80)	3.55 (3.52)	15.17 (15.42)	3.9	4.80	297(9900) 308(8746) 426(5955) 622(69) 932(43)

Table 7.2: Ligand field parameters for the nickel (II) complexes.

Sl. No.	Complex	$^3A_{2g} \rightarrow {}^3T_{2g}$ (F)		$^3A_{2g} \rightarrow {}^3T_{1g}$ (F)		Dq	ν_2/ν_1	B	β	β^o	LFSE
7.1	$[Ni(H_2slox)(H_2O)_3]$	10730	932	16155	619	1073.0	1.506	607.36	0.585	41.5	36.9
7.2	$[Ni_2(slox)(H_2O)_4]$	10764	929	16260	615	1076.4	1.511	619.61	0.597	40.3	37.0
7.3	$[Ni_2(slox)(py)_4]$	10741	931	16207	617	1074.1	1.509	614.75	0.592	40.8	36.9
7.4	$[Ni_2(slox)(2\text{-}pic)_4]$	10571	946	15924	628	1057.1	1.506	599.95	0.578	42.2	36.3
7.5	$[Ni_2(slox)(3\text{-}pic)_4]$	10627	941	15798	633	1062.7	1.487	564.72	0.544	45.6	36.5
7.6	$[Ni_2(slox)(4\text{-}pic)_4]$	10638	940	16051	623	1063.8	1.509	608.75	0.586	41.4	36.5
7.7	$[Ni_2(slox)(phen)_3]$	10526	950	15898	629	1052.6	1.510	605.42	0.583	41.7	36.2
7.8	$[Ni_2(slox)(bpy)_3]$	10730	932	16077	622	1073.0	1.500	592.79	0.571	42.9	36.9

Table 7.3: Infrared spectral data for nickel (II) complexes.

Sl. No.	Ligand/complex	ν(OH) + ν(NH)	ν(C=O)	ν(C=N)	AmideII + ν(C-O) (phenolic)	ν(NCO)	ν(C-O)	ν(N-N)	ν(M-O) (phenolic)	ν(M-O) (enolic)	ν(M<O>M)
	H_4 slox	3278(s) 3204(s) 3050(s)	1667(s)	1627(s) 1603(s)	1534(s)	--	1262(s)	1035(m)	--	--	--
7.1	$[Ni(H_2slox)(H_2O)_3]$	3400(s) 3279(s) 3200(s)	1668(m)	1608(s)	1537(s)[a]	--	1304(s)*	1042(w)	581(w)	469(w)	--
7.2	$[Ni_2(slox)(H_2O)_4]$	3374(s)	--	1625(s) 1600(s)	1551(s)	1533(s)	1306(s)*	1048(w)	592(m)	461(w)	810(w)
7.3	$[Ni_2(slox)(py)_4]$	3415(s)	--	1600(s)	1557(s)	1530(s)	1304(s)*	1040(w)	596(m)	464(w)	812(w)
7.4	$[Ni_2(slox)(2\text{-}pic)_4]$	3367(s)	--	1626(s) 1600(s)	1551(s)	1533(s)	1307(s)*	1047(w)	599(m)	463(w)	818(w)
7.5	$[Ni_2(slox)(3\text{-}pic)_4]$	3392(s)	--	1622(s) 1600(s)	1553(s)	1532(s)	1307(s)*	1049(w)	598(m)	476(w)	816(w)
7.6	$[Ni_2(slox)(4\text{-}pic)_4]$	3410(s)	--	1618(s) 1599(s)	1551(s)	1503(s)	1299(s)	1040(w)	597(w)	493(m)	814(w)
7.7	$[Ni_2(slox)(phen)_3]$	3379(s)	--	1609(s) 1598(s)	1555(s)	1516(s)	1277(s)	1045(w)	565(w)	441(w)	--
7.8	$[Ni_2(slox)(bpy)_3]$	3375(s)	--	1610(s) 1598(s)	1558(s)	1513(s)	1275(s)	1024(m)	560(w)	434(w)	--

* merged with ligand

[a] ν (NCO) merged with Amide II + ν(C-O)

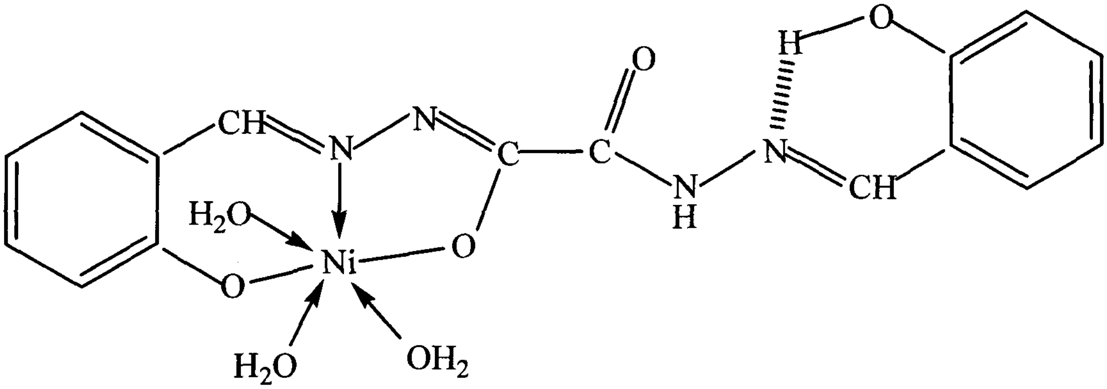

Fig. 7.11 Tentative structure for [Ni(H_2slox)(H_2O)$_3$] **(7.1)**.

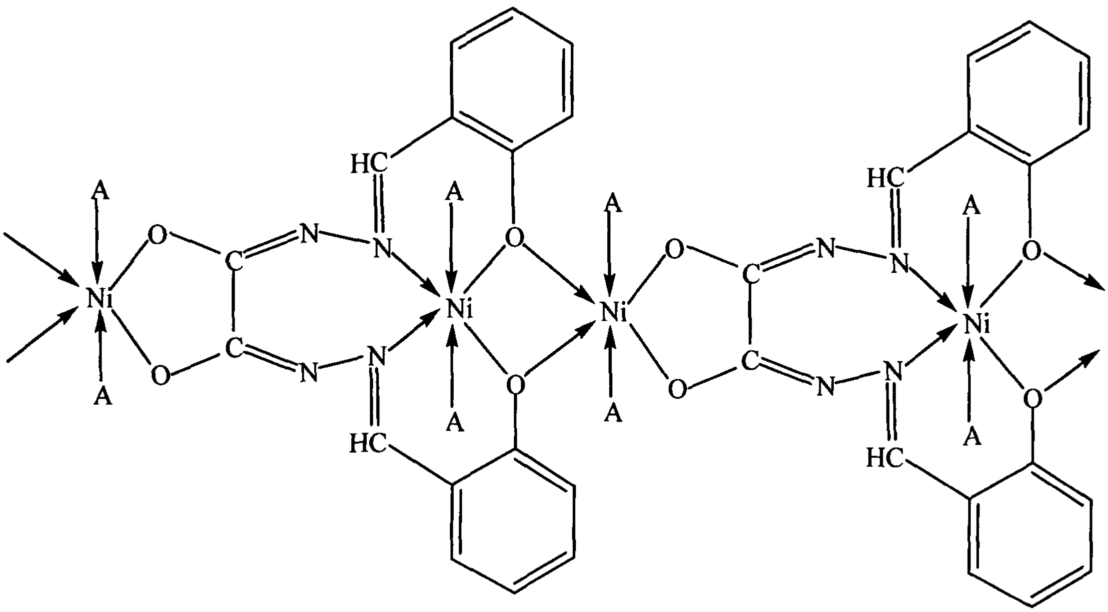

Fig. 7.12 Tentative structure for [Ni_2(slox)(A)$_4$] {*where A = H_2O* **(7.2)**, *pyridine* **(7.3)**, *2-picoline* **(7.4)**, *3-picoline* **(7.5)** *and 4-picoline* **(7.6)**}.

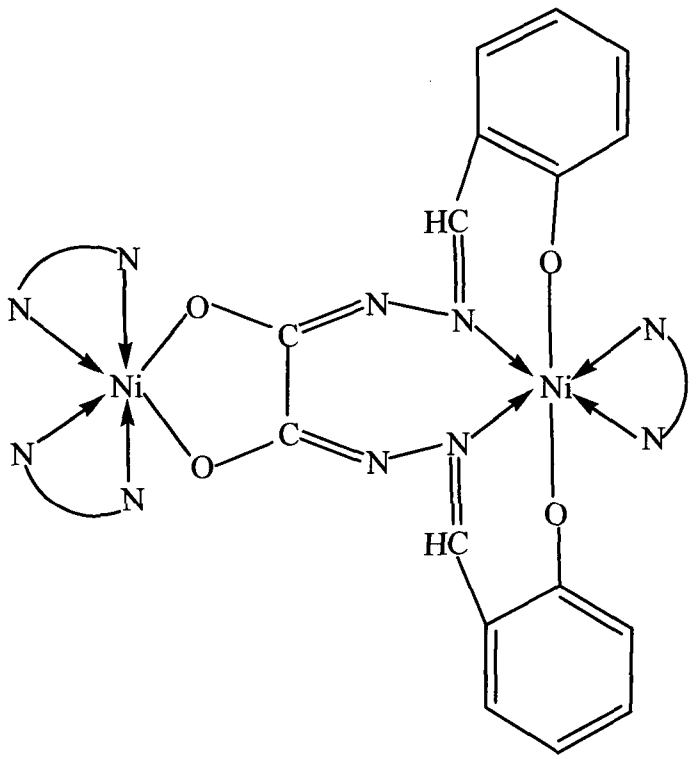

Fig. 7.13 Tentative structure for $[Ni_2(slox)(NN)_3]$ {*where NN = phenanthroline* **(7.7)** *and bipyridine* **(7.8)**}.

References

1. R. R. Chianeli, *Catal., Rev. Sci. Eng.*, **26**, 361 (1984).
2. R. J. Angelici, *Acc. Chem. Res.*, **21**, 387 (1988).
3. M. Lewandowski, A. Kolasa, P. Da Costa and C. Sayag, *Catal. Today*, **119**, 31 (2007).
4. P. Concepcion, P. Botella, J. M. Nieto, *Appl. Catal. A: Gen*, **278**, 45 (2004).
5. "*Comprehensive Coordination Chemistry II*", Elsevier (Pergamon), Vol. 6, p. 249-554 (2004).
6. K. K. Narang and M. K. singh, *Trans. Met. Chem.*, **12**, 385 (1987).
7. A. Bonardi, S. Ianelli, C. Pelizzi, G. Pelizzi and C. Solinar, *Inorg. Chim. Acta*, 232, 211 (1995).
8. D. P. Singh, M. N. Ansari and V. B. Rana, *J. Indian. Chem. Soc.*, **74**, 448 (1997).
9. G. Paolucci, S. Telluto, S. Sitran, D. Aju, F. Benetollo, A. Polo and G. Bombieri, *Inorg. Chim. Acta*, 193, 57 (1992).
10. R. A. Lal, A. N. Siva, S. Adhikari, M. K. Singh and U. S. Yadav, *Synth. React. Inorg. Met-Org. Chem.*, **26(2)**, 321-337 (1996); F. Feigel, V. Anger and R. E. Oesper, "*Spot Tests in Organic Analysis*", 7th Ed., Elseiver Publishing Company, Amsterdam, Netherland, p. 173, 384 (1996) (Indian reprint, 2005).
11. R. A. Lal, D. Basumatary, S. Adhikari and A. Kumar, *Spectrochim. Acta*, **69**, 706 (2008).
12. J. W. Geary, *Coord. Chem. Rev.*, **7**, 81 (1971).
13. A. B. P. Lever, "*Inorganic Electronic Spectroscopy*", Amsterdam: Elseiver (1984); V. P. Singh, P. Gupta and N. Lal, *Russ. J. Coord. Chem.*, **34**, 270-277 (2008).
14. S. M. E. Khalil, H. S. Seleem, B. A. El-Shetary and M. Shebl, *J. Coord. Chem.* **55**, 883 (2002).
15. S. C. Nyburg and J. C. Wood, *Inorg. Chem.*, **3**, 748 (1964); V. V. Sawant, J. Gopalkrishnan and C. C. Patel, *Inorg. Chem.*, **9**, 748 (1970); H. L. Nigam and

K. B. Pandeya, *Curr. Sci. (India)*, **41**, 449 (1972); W. Levason and C. A. McAuliffa, *Inorg. Chim. Acta*, 18, L5 (1975).

16. R. C. Aggarwal and K. K. Narang, *Inorg. Chim. Acta*, **7**, 651 (1973); *Indian J. Chem.*, **15A**, 64 (1967); **9**, 1413 (1971).
17. M. D. Cohen and S. Flavian, *J. Chem. Soc.*, B, 317, 321, 329 and 334 (1967).
18. C. M. Metzler, A. Cahill and D. E. Metzler, *J. Am. Chem. Soc.*, **102**, 6075 (1980).
19. J. W. Lewis and C. Sandorfy, *Can. J. Chem.*, **60**, 1727 (1982).
20. D. Gegiou, E. Lambi and E, Hadjoudis, *J. Phys. Chem.*, **100**, 17762 (1996).
21. T. Kawasaki, T. Kamata, H. Ushjima, M. Kanakuba, S. Murata, F. Mizukami, Y. Fujii and Y. Usui, *J. Chem. Soc. Perkin Trans.*, **2**, 193 (1999).
22. R. L. Dutta and M. M. Hussain, J. *Sci. Ind. Res.*, **44**, 635 (1985); M. Mohan, N. K. Gupta, M. Kumar, N. K. Jha and W. E. Antholine, *Inorg. Chim. Acta*, **197**, 39 (1992); S. C. Chan, L. L. Koh, P. H. Leung, J. D. Ranford and K. Y. Sim, *Inorg. Chim. Acta*, **236**, 101 (1995); T. N. Sorrell, *Tetrahedron*, 54 (1989).
23. T. N. Sorrell, D. L. Jameson and C. J. O'Conner, *Inorg. Chem.*, **33**, 456 (1994).
24. T. N. Sorrell, C. J. O'Conner, O. P. Anderson and J. H. Reibnenspies, *J. Am. Chem. Soc.*, **107**, 4199 (1985).
25. K. J. Oberhausen, J. F. Richardson, R. M. Bachanan, J. M. McCusker, D. N. Hendrickson and J. Mare Latour, *Inorg. Chem.*, **30**, 1357 (1991).
26. S. Teipel, K. Griesa, W. Haase and B. Kerbs, *Inorg. Chem.*, **33**, 456 (1994).
27. F. A. Cotton, G. Wilkinson, C. A. Murillo and M. Bochmann, "*Advanced Inorganic Chemistry*", New York: John Wiley and Sons Inc. (2003).
28. A. B. P. Lever, "*Inorganic Electronic Spectroscopy*", 2nd Ed., Vol. 33, Elsevier, Amsterdam (1984).
29. T. M. A. Ismail, *J. Coord. Chem.*, **58**, 141 (2005); N. Al-Awadi, N. M. Shuaib and A. El-Dissouky, *Spectrochim. Acta A*, **65**, 36 (2006).
30. O. Bostrop and C. K. Jorgensen, *Acta Chem. Scand.*, **11**, 1223 (1957).

31. R. S. Drago, "*Physical Methods in Inorganic Chemistry*", Reinhold Publishing Corporation, New York (1968).

32. B. Adhikari, S. Liu and C. R. Lucas, *Inorg. Chem.*, **32**, 5957 (1993).

33. V. V. Pavlishchuk, S. V. Kolotilov, A. W. Addison, E. Sinn and M. J. Prushan, *Russ. J. Inorg. Chem.*, **45**, 544 (2000).

34. A. B. P. Lever, *Coord. Chem. Rev.*, **3**, 119 (1968).

35. Z. H. Abd El-Wahab, *Spectrochim. Acta A*, **67**, 25 (2007).

36. P. K. Radhakrishnan, P. Indrasenan and C. G. R. Nair, *Polyhedron*, **3**, 67 (1984); R. K. Aggarwal and J. Prakash, *Polyhedron*, **10**, 2567 (1991).

37. U. Casellato, P. Guerriero, S. Tamburini, P. A. Vigato and S. Sitran, *J. Chem. Soc. Dalton Trans.*, 2145 (1991).

38. K. R. Barnard, M. Bruch, H. Susan, I. H. Enemark, R. W. Gable and A. G. Wedd, *Inorg. Chem.*, **36**, 637 (1997); G. G. Mohamed and C. M. sharaby, *Spectrochim. Acta A*, **66**, 949 (2007).

39. R. Gup and B. Kirkan, *Spectrochim. Acta A*, **62**, 1188 (2005).

40. V. L. Pecoraro, D. P. Kessissoglou and W. M. Butler, *Inorg. Chem.*, **26**, 495 (1987).

41. K. Nakamoto, "*Infrared and Raman Spectra of Inorganic and Coordination Compounds*", 4th Ed., John Wiley and Sons, New York (1986).

42. R. A. Lal, M. L. Pal and S. Adhikari, *Synth. React. Inorg. Met-Org. Chem.*, **26**, 997 (1996).

43. Mudasir, N. Yoshioka and H. Inoue, *Trans. Met. Chem.*, **24**, 210 (1999).

44. A. K. Boudalis, U. Nastopoulos, S. P. Perlepes, C. P. Raptopoulu and A. Terzis, *Trans. Met. Chem.*, **26**, 276 (2001).

CHAPTER VIII

Synthesis and Characterization of Heterobimetallic Copper, Molybdenum and Nickel Complexes derived from Polyfunctional Disalicylaldehyde oxaloyldihydrazone

Introduction

In the previous chapters, we described the monometallic molybdenum (VI), homobimetallic molybdenum (VI), monometallic copper (II), homotrimetallic copper (II) and nickel (II) complexes derived from the title dihydrazone ligand. We observed that the ligand exists either in keto-enol form or in enol form in these complexes. Because of the importance of heterobimetallic complexes in several areas of chemistry and meager amount of work done on it, it was thought of importance to synthesize and characterized some heterobimetallic complexes from the title ligand. It appears appropriate at this stage, before we proceed for the synthesis of heterobimetallic complexes to brief the importance of heterobimetallic systems.

Heterobimetallic chemistry is an area of active research due to the importance of heterobimetallic complexes in homogeneous catalysis **[1]**, heterogeneous catalysis **[2]**, and multimetallic enzymes **[3-5]**. The efficacy of heterobimetallic complexes in the asymmetric activation of carbon dioxide and related molecules has been demonstrated **[6]**. In homogeneous catalysis, a heterobimetallic complex containing an electron deficient metal atom and an electron rich metal atom presents the possibility of Lewis acid activation of a substrate molecule bound to the electron rich metal centre. The heterobimetallic complexes which have such types of properties are usually derived from widely divergent transition metals. Further, the heterobimetallic complexes have the potential to mediate certain chemical reactions of industrial relevance either more efficiently than or in a different manner to isolate metal centres **[7]**. Heterobimetallic complexes might prove helpful in investigating

the mutual influence of the two metal centres on the electronic, magnetic and redox properties of such systems **[8]**.

Heterobimetallic complexes are also important in the preparation of ceramic materials favouring an intimate mixing of the elements which can enable reactions at lower temperatures rather than for traditional route or the preparation of purer inaccessible solid state phases **[9]**. The high temperature superconductors may be prepared from soluble precursors owing to their low costs, the possibility to coat large unusually shaped objects and high homogeneity and purity **[10]**. Thus the heterobimetallic (heteropolymetallic) complexes may be reduced under ordinary conditions to yield alloys and other materials of industrial and technological importance.

In view of the above importance of the heterobimetallic (heteropolymetallic) complexes and quite meager work on heterobimetallic complexes of dihydrazones, the present chapter describes the synthesis of some heterobimetallic complexes of copper-molybdenum and nickel-molybdenum derived from the title dihydrazone. The complexes were mainly characterized on the basis of elemental analyses. The structure of the complexes has been discussed in the light of conductivity, IR spectra, magnetic moment, EPR and electronic spectral data.

Experimental

Preparation of $[Ni(slox)MoO_2(H_2O)_4]$ (8.1)

The complex $[Ni(H_2slox)(H_2O)_3]$ (1.00 g, 2.32 mmol) was suspended in methanol (60 mL) with constant stirring for about 30 minutes to make the suspension homogeneous. This suspension was then slowly added to a solution of $MoO_2(acac)_2$ (0.86 g, 2.64 mmol) in 30 mL methanol over a period of 30 minutes accompanied by constant stirring. The resulting mixture was put to reflux for about 5 h. This precipitated a dirty yellow colored complex which was suction filtered in hot

condition, washed three to four times with 20 mL hot methanol each time followed by ether and then finally dried over anhydrous $CaCl_2$.

Preparation of [Ni(slox)$MoO_2(A)_4$] {*where A = pyridine (py)* **(8.2)**, *2-picoline (2-pic)* **(8.3)**, *3-picoline (3-pic)* **(8.4)** *and 4-picoline (4-pic)* **(8.5)**}.

In order to prepare the complex [Ni(slox)$MoO_2(py)_4$] **(8.2)**, [Ni(slox)$MoO_2(H_2O)_4$] (1.00 g, 1.71 mmol) was suspended in methanol (50 mL) with constant stirring over a period of 10-15 minutes. The stirring was further continued for another 30 minutes to make the suspension homogeneous. To this homogeneous suspension was added 1.36 mL of pyridine drop by drop over a period of 30 minutes and the resulting mixture was refluxed for about 1 h. This precipitated a dirty yellow colored complex which was suction filtered in hot condition, washed three to four times with hot methanol followed by ether and finally dried over anhydrous $CaCl_2$.

The complexes [Ni(slox)$MoO_2(A)_4$] {*where A = 2-picoline (2-pic)* **(8.3)**, *3-picoline (3-pic)* **(8.4)** *and 4-picoline (4-pic)* **(8.5)**}, were also prepared essentially by following the above procedure using 1.60 mL of 2-picoline and 4-picoline molecules instead of 1.36 mL of pyridine.

Preparation of [Ni(slox)$MoO_2(NN)_2$] {*where NN = 2,2'-bipyridine (bpy)* **(8.6)** *and 1,10-phenanthroline (phen)* **(8.7)**}

The complex [Ni(slox)$MoO_2(H_2O)_4$] (1.00 g, 1.71 mmol) was suspended in methanol (60 mL) with constant stirring for about 30 minutes to make homogeneous suspension. To this homogeneous suspension was added a solution of bipyridine (0.82 g, 5.25 mmol) in 30 mL methanol drop by drop over a period of 30 minutes with constant stirring. The mixture was then subjected to reflux for a period of about 1 h when a yellow colored compound precipitated. The complex was isolated following the usual procedure.

The complex [Ni(slox)MoO_2(phen)$_2$] **(8.7)** was also isolated following the above procedure using 1.03 g (5.20 mmol) of phenanthroline instead of 0.82 g (5.25 mmol) of bipyridine.

Preparation of [Cu(slox)$MoO_2(H_2O)_2$] (8.8)

About 1.00 g (2.48 mmol) of the complex [Cu(H_2slox)] was suspended in methanol (60 mL) with constant stirring for about 15-20 minutes to make homogeneous suspension. To this homogeneous suspension was added a solution of $MoO_2(acac)_2$ (1.00 g, 3.07 mmol) in methanol (20 mL) drop by drop over a period of 30 minutes and the mixture thus obtained was refluxed for about 1 h. This yielded a greenish yellow colored compound which was isolated following the usual procedure.

Preparation of [Cu(slox)$MoO_2(A)_2$] {*where A = pyridine (py)* **(8.9)**, *2-picoline (2-pic)* **(8.10)**, *3-picoline (3-pic)* **(8.11)** *and 4-picoline (4-pic)* **(8.12)**}

In order to prepare the complex [Cu(slox)$MoO_2(py)_2$], about 1.00 g (1.82 mmol) of the complex [Cu(slox)$MoO_2(H_2O)_2$] was suspended is methanol (50 mL) with constant stirring to make homogeneous suspension. To this homogeneous suspension was then added 1.44 mL of pyridine drop by drop over a period of 30 minutes accompanied by constant stirring. The mixture was then subjected to reflux for about 1 h when a greenish yellow colored compound precipitated. This compound was suctioned filtered in hot condition and washed several times with minimum quantity of hot methanol followed by ether and finally dried over anhydrous $CaCl_2$.

The complex [Cu(slox)$MoO_2(A)_2$] {*where A = 2-picoline (2-pic)* **(8.10)**, *3-picoline (3-pic)* **(8.11)** *and 4-picoline (4-pic)* **(8.12)**}was also prepared by following essentially the above procedure using 1.70 mL of 2-picoline instead of 1.44 mL of pyridine.

Preparation of [Cu(slox)MoO_2(NN)] {*where NN = 2,2'-bipyridine (bpy)* **(8.13)** *and 1,10-phenanthroline (phen)* **(8.14)**}

The complex [Cu(slox)$MoO_2(H_2O)_2$] (1.00 g, 1.82 mmol) was suspended in methanol and stirred for about 10-15 minutes to make the suspension homogeneous. To this homogeneous suspension was added a solution of bipyridine (0.80 g, 5.12 mmol) in methanol (20 mL) drop by drop over a period of 30 minutes. The mixture was then reflux for about 1 h which precipitated the complex. The complex so precipitated was isolated by the usual procedure.

The complex [Cu(slox)MoO_2(phen)] **(8.14)** was also obtained by following the above procedure using 1.02 g (5.15 mmol) of phenanthroline instead of 0.80 g (5.12 mmol) of bipyridine.

Results and discussion

Synthesis of the pure samples of heterobimetallic complexes is a difficult task in the field of heterobimetallic chemistry. It is important to ensure that the metals are not scrambled giving rise to considerable quantities of other undesired bimetallic products. The synthesis of heterobimetallic products is accessible by the strategies developed by Lintvedt etal **[11]** via a monometallic complex intermediate by the use of polyfunctional ligands and Davies etal **[12]** via transmetallation beginning with a complex of discrete molecularity as target and another metal complex as transmetallator. Accordingly, reactions of preformed disalicylaldehyde oxaloyldihydrazone with $Cu(OAc)_2.H_2O$ and $Ni(OAc)_2.4H_2O$ in 1:1.1 molar ratio in methanol precipitated Cu(II) and Ni(II) complexes [$Cu(H_2slox)$] **(5.1)** and [$Ni(H_2slox)(H_2O)_3$] **(7.1)** respectively. Reactions of the Cu(II) complex **(5.1)** and Ni(II) complex **(7.1)** with $MoO_2(acac)_2$ in 1:1.1 molar ratio in methanol yielded Cu(II)-Mo(VI) and Ni(II)-Mo(VI) heterobimetallic complexes. These complexes were then treated with nitrogen donor bases such as pyridine, substituted pyridine, phenanthroline and bipyridine molecules which led to the substitution of water

molecule(s) by these nitrogen donor bases. The complexes isolated in the present chapter, together with their color, decomposition point, analytical data, magnetic moment, molar conductance and electronic spectral data are presented in **Table 8.1**. The analytical data of the complexes reveal that they have the compositions $[Ni(slox)MoO_2(A)_4]$ {*where A = H_2O* **(8.1)**, *pyridine (py)* **(8.2)**, *2-picoline (2-pic)* **(8.3)**, *3-picoline (3-pic)* **(8.4)** *and 4-picoline (4-pic)* **(8.5)**}, $[Ni(slox)MoO_2(NN)_2]$ {*where NN = 2,2'-bipyridine (bpy)* **(8.6)** *and 1,10-phenanthroline (phen)* **(8.7)**}, $[Cu(slox)MoO_2(A)_2]$ {*where A = H_2O* **(8.8)**, *pyridine (py)* **(8.9)**, *2-picoline (2-pic)* **(8.10)**, *3-picoline (3-pic)* **(8.11)** *and 4-picoline (4-pic)* **(8.12)**} and $[Cu(slox)MoO_2(NN)_2]$ {*where NN = 2,2-bipyridine (bpy)* **(8.13)** *and 1,10-phenanthroline (phen)* **(8.14)**}. The Ni(II)-Mo(VI) complexes are yellow while Cu(II)-Mo(VI) complexes are green or dark green in color. All the complexes are air stable, insoluble in water and common organic solvents such as EtOH, MeOH, CH_3COCH_3, CCl_4, $CHCl_3$, Et_2O, C_6H_6, CH_2Cl_2 and CH_3CN, but soluble in DMF and DMSO. The complexes decompose above 300°C.

Thermal analyses

Detailed decomposition studies **[13]** of the complexes were carried out in the temperature range of 70-250°C and the vapors evolved were identified by passing through a test tube containing anhydrous copper sulfate, a test tube containing chloroform solution with a drop of 5M sodium hydroxide, a test tube containing solution of iodine and sodium hydroxide and a test tube containing cyanogen bromide solution. None of the complexes showed loss of weight in the temperature range 100-120°C ruling out the possibility of presence of lattice water molecules but the complexes **(8.1)** and **(8.8)** showed loss of weight in the temperature range 160-180°C. The vapors evolved in this temperature range turned the test tube containing anhydrous copper sulfate blue confirming its origin from water molecules. The loss of weight at such a high temperature indicates the presence of water molecules inside the coordination sphere **[14]** of the complexes. The weight loss at this temperature corresponds to the presence of four water molecules in the complex **(8.1)** and two

water molecules in the complex **(8.8)** respectively. Complexes **(8.2)** to **(8.5)** and **(8.9)** to **(8.12)** showed weight loss at 220°C corresponding to pyridine, 2-picoline, 3-picoline and 4-picoline molecules. The vapours evolved at this temperature in the complex **(8.2)** and **(8.9)** turned a solution of $CHCl_3$ containing a drop of 5M NaOH solution red confirming that they originated from pyridine bases **[13]**. The vapours evolved in the complexes **(8.5)** and **(8.12)** at this temperature turned the color of cyanogen bromide solution to blue on treatment with phloroglucinol solution suggesting its origin from 4-picoline molecule **[13]**. The expulsion of these donor molecules at such a high temperature indicates that they are coordinated to the metal centre **[14]**.

Molar conductance

Molar conductance values for the complexes in DMSO at 10^{-3} M dilution are in the range 4.5-8.9 $ohm^{-1}cm^2mol^{-1}$. These values are consistent with non-electrolytic nature of the complexes in this solvent **[15]**.

Magnetic moment

The magnetic moment values for the complexes have been set out in **Table 8.1**. The room temperature magnetic moment for the heterobimetallic complexes **(8.1)** to **(8.7)** is in the range 2.87-3.10 BM while for the complexes **(8.8)** to **(8.14)** it is in the range 1.69-1.82 BM. This value of magnetic moment for the complexes **(8.1)** to **(8.7)** is close to the magnetic moment value required for two unpaired electrons in octahedral environment around nickel (II) centre **[16]**. This indicates that the nickel (II) ion is coordinated in octahedral fashion in the heterobimetallic complexes. In the complexes **(8.8)** to **(8.14)** the magnetic moment values is close to the spin-only value of 1.73 BM indicating that there is no appreciable spin-spin interaction between metal atoms. According to Figgis **[17]**, magnetic moment values less than 1.90 BM indicate square planar as well as octahedral stereochemistry and magnetic moment value greater than 1.90 BM indicate tetrahedral stereochemistry. On the basis of the

magnitude of magnetic moment the heterobimetallic complexes $[Ni(slox)MoO_2(A)_4]$ and $[Ni(slox)MoO_2(NN)_2]$ have been suggested to have octahedral geometry around nickel (II) centre while the heterobimetallic complexes $[Cu(slox)MoO_2(A)_2]$ and $[Cu(slox)MoO_2(NN)]$ have square planar geometry around copper (II) centre.

Electronic spectra

All the heterobimetallic complexes have been characterized by electronic spectroscopy and their electronic spectral data are listed in **Table 8.1**. The complexes are soluble in DMSO. Hence their electronic spectra were recorded in this medium in the range 200-1000 nm. The electronic spectra of the complexes **(8.1)** to **(8.3)**, **(8.7)**, **(8.8)**, **(8.9)** and **(8.13)** have been shown in **Figs. 8.1-8.7** as a representative example.

The electronic spectra of the complexes show three bands in the region 290-341 similar to those observed in the free dihydrazone ligand. These bands have been assigned to arise due to intraligand $\pi \rightarrow \pi^*$ and $n \rightarrow \pi^*$. Apart from these ligand bands three non ligand bands are observed in the nickel (II) heterobimetallic complexes **(8.1)** to **(8.7)** in the region 413-423, 618-626 and 931-952 nm respectively, whereas in the copper (II) heterobimetallic complexes **(8.8)** to **(8.14)** only two non-ligand bands are observed in the region 414-424 and 608-666 nm respectively. The bands in the region 415-425 nm have molar extinction coefficient values in the region 2330- 4460 $dm^3mol^{-1}cm^{-1}$. In view of very high molar extinction coefficient values for this band, it is assigned to have its origin due to ligand-to-metal charge transfer (LMCT) transition. The two low energy bands observed in the region 618-626 and 931-952 nm with molar extinction coefficients below 100 $dm^3 mol^{-1}cm^{-1}$ in the complexes **(8.1)** to **(8.7)** correspond to $^3A_{2g} \rightarrow {}^3T_{2g}$ (F) (ν_1) and $^3A_{2g} \rightarrow {}^3T_{1g}$ (F) (ν_2) transitions which are characteristics of nickel (II) in octahedral environment **[18]**. The complexes **(8.8)** to **(8.14)** show a single broad band in the 610 – 670 nm regions with a comparatively very low molar extinction coefficient in the range 60 – 100 $dm^3mol^{-1}cm^2$. Hence, this band is assigned to have its origin due to $^2E_g \rightarrow {}^2T_{2g}$ transition. In the octahedral and tetrahedral complexes of copper (II), the band due to

d-d transition occurs at ~800 nm and ~1200 nm, respectively. The 800 nm bands in octahedral complexes is considerably blue shifted due to Jahn-Teller distortion and in extreme cases, it falls in the range 600 – 700 nm reported for the square planar complexes **[19]**. The position of ligand field band in the complexes **(8.8)** to **(8.14)** in the region 610-670 nm suggests that they all have square planar stereochemistry around the copper (II) centre. The essential feature of this band in the 610 – 670 nm regions suggests that it is the combination of three transitions ($^2B_{1g} \rightarrow {}^2A_{1g}$, $^2B_{1g} \rightarrow {}^2B_{2g}$ and $^2B_{1g} \rightarrow {}^2E_g$) **[20]**.

The ligand field parameters **[21]** viz. Racah inter-electronic repulsion parameter (B), ligand field splitting energy (10Dq), covalency factor (β) and ligand field stabilization energy (LFSE) have been calculated for the complexes **(8.1)** to **(8.7)** and are listed in **Table 8.2**. The Ligand field splitting energy (10Dq) and the Racah inter-electronic repulsion parameter (B) were calculated by the equation given by Lever **[22]**.

$^3A_{2g} \rightarrow {}^3T_{2g}$ (F) (ν_1) = 10Dq

$^3A_{2g} \rightarrow {}^3T_{1g}$ (F) (ν_2) = 7.5B + 15Dq – ½($225B^2 + 100Dq^2 - 180DqB)^{1/2}$

$^3A_{2g} \rightarrow {}^3T_{1g}$ (P) (ν_3) = 7.5B + 15Dq + ½($225B^2 + 100Dq^2 - 180DqB)^{1/2}$

The Racah inter-electronic repulsion parameter (B) was also calculated using the following equation **[23]** and the values obtained were found to be the same as calculated using the equation given by Lever.

$B_{complex} = (2\nu_1^2 + \nu_2^2 - 3\,\nu_1\nu_2)\,(15\nu_2 - 27\nu_1)$

The covalency factor (β) was obtained by the following equation

β = B/B' (where B' is the free ion value = 1038 cm^{-1}) **[24]**

The ligand field stabilization energy (LFSE) expressed by the equation

LFSE = 10Dq, is also calculated and expressed in Kcal/mol in the table 8.2.

The percentage lowering of energy of 'P' state in the complexes as compared to its value in the free gaseous ion (β^o) is obtained by the equation:

$$\beta^o = 100 - (\beta \times 100)$$

The evaluation of B for the complexes **(8.1)** to **(8.7)** from the above equation lies in the range 593.56-625.85 cm^{-1}, which is very low as compared to the free ion value (1038 cm^{-1}). Such a low value of B indicates considerable covalent character in the complexes. The covalency factor β, for the complexes lie in the range 0.572-0.603, which is less than unity suggesting the presence of considerable amount of covalent character in the metal-ligand bonds. The percentage lowering of the energy of 'P' state in the complexes compared to its value in the free gaseous ion (β^o) is in the range 39.7-42.8 % which shows a high degree of covalency.

The values of $\nu_2/\ \nu_1$ for tetragonal complexes are found significantly higher than the usual range for octahedral complexes and sometimes greater than the theoretical limit of 1.80 for octahedral symmetry. The interaction between $^3T_{1g}$ (P) and $^3T_{1g}$ (F) states **[25]** gradually lowers the ratio $\nu_2/\ \nu_1$ from the theoretical value of 1.80 to 1.50 – 1.70 and values of 1.60 – 1.70 are common for nickel (II) complexes of octahedral symmetry. In the complexes **(8.1)** to **(8.7)** the $\nu_2/\ \nu_1$ values lie in the range 1.48 – 1.52 which is slightly lower than the lower limit for usual octahedral complexes but are within the range reported for octahedral complexes **[26]**. These low value indicates a strong interaction between $^3T_{1g}$ (P) and $^3T_{1g}$ (F) states of the complexes. The ligand field stabilization energy for the complexes **(8.1)** to **(8.7)** in the present study is in the range 36.09 – 36.90 kcal/mol.

Electron paramagnetic resonance spectra

The EPR spectrum of heterobimetallic copper (II)-molybdenum (VI) complex was

recorded in DMSO at RT and LNT. The EPR spectra of the complexes **(8.8)**, **(8.9)** and **(8.13)** are shown in **Figs. 8.8-8.10**. The frozen solution spectrum shows hyperfine lines both at RT and LNT and no features characteristics for a homobimetallic copper (II) complexes. This is also supported by the magnetic moment of the heterobimetallic copper (II)-molybdenum (VI) complexes (1.69-1.82 BM) which confirms the presence of only one copper atom per ligand molecule in the heterodinuclear complexes **(8.8)** to **(8.14)**. The spin Hamiltonian parameters, calculated for the copper (II)-molybdenum (VI) heterobimetallic complexes **(8.8)** to **(8.10)**, **(8.13)** and **(8.14)** from the spectra, are given in **Table 8.3**. The g tensor values of this copper (II)-molybdenum (VI) complexes can be used to derive the ground state. In square–planar complexes, the unpaired electron lies in the $d_{x^2-y^2}$ orbital giving $g_{\|} > g_{|} > 2.0023$ while the unpaired electron lies in the d_{z^2} orbital giving $g_{|} > g_{\|} > 2.0023$. From the observed values, it is clear that $g_{\|} > g_{|} > 2.0023$ suggesting that the complex is square–planar around copper centre. This is also supported by the fact that the unpaired electron lies predominantly in the $d_{x^2-y^2}$ orbital, as evident from the value of the exchange interaction term G, estimated from the expression:

$$G = (g_{\|} - 2)/(g_{|} - 2)$$

If G > 4·0, the local tetragonal axes are aligned parallel or only slightly misaligned. If G < 4·0, significant exchange coupling is present and the misalignment is appreciable. The observed value for the exchange interaction parameter for the complexes **(8.8)** to **(8.10)**, **(8.13)** and **(8.14)** (G = 2.15-3.04) suggests that the local tetragonal axes are misaligned, and the unpaired electron is present in the $d_{x^2-y^2}$ orbital.

The in-plane σ covalency parameter, α^2_{Cu} was calculated for the heterobimetallic copper (II)-molybdenum (VI) complexes **(8.8)** to **(8.10)**, **(8.13)** and **(8.14)** using the following equations and the values obtained are listed in the table 8.3.

$$\alpha^2_{Cu} = - (A_{\|}/0.036) + (g_{\|} - 2.0023) + 3/7(g_{|} - 2.0023) + 0.04$$

The α^2_{Cu} value accounts for a fraction of the unpaired electron density on the copper (II) ion. The smaller the value of α^2_{Cu}, the more covalent is the bonding. For example $\alpha^2_{Cu} = 0.5$ indicates complete covalent bonding, but $\alpha^2_{Cu} = 1.0$ suggests complete ionic bonding. The α^2_{Cu} values for the complexes **(8.8)**, **(8.9)** and **(8.14)** are in the range of $0.716 - 0.940 < 1$ indicating that these heterobimetallic complexes have some covalent character.

Infrared spectra

Some structurally significant IR bands for uncoordinated dihydrazone, precussor monometallic and heterobimetallic complexes have been set out in **Table 8.4**. The IR spectra of the heterobimetallic complexes **(8.1)** to **(8.3)**, **(8.7)**, **(8.8)** to **(8.10)** and **(8.13)** have been shown in **Figs. 8.11-8.18**. The strong bands at 3278 and 3204 cm^{-1} in the IR spectrum of free dihydrazone and at 3279 and 3200 cm^{-1} in the IR spectrum of the precussor monometallic $[Ni(slox)(H_2O)_3]$ complex and at 3278 and 3204 cm^{-1} in the IR spectrum of [Cu(slox)] complex assigned to the stretching vibration of -OH of salicylaldehyde part of the dihydrazone and >NH groups respectively, disappear in the IR spectra of the heterobimetallic complexes.which are assigned to stretching vibration of -OH of salicylaldehyde part of the dihydrazone and >NH group, respectively. This suggests the involvement of -OH group in bonding and collapse of amide structure of the ligand and its presence in enol form in these complexes. A strong broad band in the region 3386-3438 cm^{-1} might be due to ν (-OH) vibration of either lattice or coordinated water molecules or due to ν (-OH) of moisture absorbed by KBr during pellet preparation. In order to decide upon whether the bands in this region arise due to water molecules or due to moisture absorbed by KBr pellets, the compounds were subjected to thermal analysis. The thermo-analytical data suggest the presence of water molecules inside the coordination sphere of the complexes **(8.1)** and **(8.8)**. Hence, it can be said that the strong broad band in the region 3386-3438 cm^{-1} arise due to the presence of coordinated water molecules in the complexes **(8.1)** and **(8.8)** whereas in rest of the complexes the band in this region arise due to the moisture absorbed by KBr during pellet preparation.

The ν (>C=O) band at 1667 cm^{-1} in the free dihydrazone ligand and at 1668 and 1679 cm^{-1} in the precussor monometallic [Ni(slox)$(H_2O)_3$] and [Cu(slox)] complexes respectively are also absent in the IR spectra of the heterobimetallic complexes confirming the enol form of the dihydrazone in these complexes. The two very strong bands centred at 1627 and 1603 cm^{-1} due to the stretching vibration of azomethine (>C=N-) group shift to lower frequency by 6-13 cm^{-1} in all of the complexes. The shifts of the ν (>C=N-) band appearing in the region 1602-1609 cm^{-1} to lower frequency by 6-13 cm^{-1} indicates bonding between azomethine nitrogen atom and the metal centre **[27]**. The ν (>C=N-) band in the heterobimetallic Ni-Mo complexes **(8.2)**, **(8.3)**, **(8.5)** to **(8.7)** remains almost unshifted in position while shifts to lower frequency by 3 and 6 cm^{-1} in the complexes **(8.1)** and **(8.4)** as compared to their position in the precussor [Ni(slox)$(H_2O)_3$] complex. On the other hand, in the Cu-Mo heterobimetallic complexes, this band shifts to lower frequency by 5-10 cm^{-1} as compared to their position in the precussor [Cu(slox)] complex. Such a feature associated with the ν (>C=N-) band indicates that the strength of metal-ligand bond in the complexes **(8.2)**, **(8.3)**, **(8.5)** to **(8.7)** remains same as that in the monometallic complexes while a negative shift of about 3-10 cm^{-1} in the remaining complexes suggests that the metal-ligand bond is stronger in these complexes as compared to those in the precussor monometallic complexes.

The IR spectra of the ligand shows a strong band at 1534 cm^{-1} with composite character due to mixed contribution of the amide II and ν (C-O) (phenolic) bands. In all of the complexes a very strong band appears in the region 1512-1552 cm^{-1} except complex **(8.1)**, **(8.6)** and **(8.7)** which shows a couple of bands in this region. In the complexes **(8.1)** to **(8.7)** the amide II+ ν (C-O) (phenolic) bands shifts to higher frequency by 11-18 cm^{-1} and appears in the region 1545-1552 cm^{-1} whereas in rest of the complexes this band remains almost unshifted and appears in the region 1531-1534 cm^{-1}. The position of this band is consistent with the occurrence of bonding through phenolate oxygen atoms. However, the intensity of the band in this region is considerably increased as compared to that in the free ligand as well as in the precussor complexes suggests that this band has contribution from the band due to

stretching vibration of NCO group produced as a result of enolization of the ligand. In the complexes **(8.1)**, **(8.6)** and **(8.7)**, the band in the 1512-1530 and 1545-1552 cm^{-1} regions are assigned to the stretching vibration of ν (NCO) and amide II + ν (C-O) (phenolic), respectively, whereas in rest of the complexes these bands appears merged with one another.

The strong intensity band due to ν (C-O) (phenolic) at 1262 cm^{-1} in free dihydrazone splits into two component in the heterobimetallic complexes and appears in the region 1303-1310 cm^{-1} and 1270-1278 cm^{-1} respectively. Both these bands appear at higher position as compared to the band at 1262 cm^{-1}. This shows that the phenolate oxygen atom is bonded to the metal centre. The splitting of this band into two components is the effect of the formation of heterobimetallic complex. The ν (C-O) (phenolate) band appear as a single band ar 1304 and 1276 cm^{-1} in the monometallic precussor nickel (II) and copper (II) complexes respectively.

The complexes **(8.1)** to **(8.7)** show a couple bands in the region 881-924 cm^{-1} while the complexes **(8.8)** to **(8.14)** show a couple of bands in the region 884-948 cm^{-1}. The appearance of couple of bands in this region is characteristic of occurance of cis-MoO_2^{2+} group in the complexes. These bands are assigned to arise due to the symmetric and asymmetric stretching vibration of cis-MoO_2^{2+} group.

The complexes **(8.2)** to **(8.5)** and **(8.9)** to **(8.12)** show a very weak band in the region 1000-1070 cm^{-1} which is assigned to ring stretching mode of pyridine and substituted pyridine molecules **[28]**. Complexes **(8.7)** and **(8.14)** show two strong intensity bands at 725-727 and 841-849 cm^{-1} region which are assigned to the out-of-plane motion of the hydrogen atoms on the heterocyclic rings and the hydrogen atoms on the central ring, respectively. In the complexes **(8.6)** and **(8.13)** only one strong band is observed at 756 - 758 cm^{-1} due to out-of-plane motion of the hydrogen atoms as expected for two identical groups of four hydrogen atoms each. Apart from these bands, complexes **(8.6)**, **(8.7)**, **(8.13)** and **(8.14)** also show very strong bands at 632, 634, 631 and 632 cm^{-1} which are assigned to arise due to in-plane ring deformation

mode of phenanthroline and bipyridine molecules indicating their coordination to the metal centre **[29, 30]**.

The ν (M-O) (phenolic) may be expected at higher frequencies than ν (M-O) (enolized carbonyl) for difference in bond order. On examining the spectra of the ligand and precussor monometallic complexes and heterobimetallic complexes **(8.1)** to **(8.14)** below 600 cm^{-1}, the new band appearing in the 572-574 cm^{-1} region is tentatively assigned to ν (M-O) (phenolic). In the complexes **(8.13)** and **(8.14)** this band appears merged with the in-plane ring deformation mode of bipyridine and phenanthroline molecules respectively. The new band in the region 527-546 cm^{-1} is assigned to the ν (M-O) (enolized carbonyl).

Conclusion

In the present chapter some heterobimetallic Ni (II)-Mo (VI) and Cu (II)-Mo (VI) complexes have been synthesized using monometallic complexes $[Ni(H_2slox)(H_2O)_3]$ and $[Cu(H_2slox)]$ as the precussors. The complexes have been characterized on the basis of data obtained from various physico-chemical and spectroscopic studies. The absence of band due to ν (>C=O) group in the IR spectra of the complexes indicates enolization of the ligand as a consequence of the formation of heterobimetallic complexes. In all of the complexes, the dihydrazone coordinates to the metal centre as a tetrabasic hexadentate ligand. The electronic spectral data together with magnetic moment data indicate that the Ni (II) atom has an octahedral stereochemistry in the heterobimetallic complexes **(8.1)** to **(8.7)** similar to that in the precussor monometallic complex $[Ni(H_2slox)(H_2O)_3]$. Similarly copper (II) atom has a square planar stereochemistry in the heterobimetallic complexes **(8.8)** to **(8.14)** similar to that in the precussor monometallic complex $[Cu(H_2slox)]$. Out of the three metal ions MoO_2^{2+}, Cu (II) and Ni (II) ions, MoO_2^{2+} is a hard acid while Ni (II) and Cu (II) are relatively soft acids. Hence, given an opportunity to bind the donor atoms of the polyfunctional dihydrazone ligand, MoO_2^{2+} would prefer to bind hard carbonyl oxygen atom in enol form while Ni(II) and Cu(II) ions would prefer to

bind relatively soft phenolate oxygen atom and azomethine nitrogen atoms in the heterobimetallic complexes. Assuming that nickel (II) binds phenolate oxygen atoms and azomethine nitrogen atoms in the heterobimetallic complexes **(8.1)** to **(8.7)** occupying N_2O_2 coordination chamber, and the presence of two monodentate donor atoms around the metal centre in view of its octahedral stereochemistry, only two monodentate donor molecules are left for MoO_2^{2+} ion. Taking into consideration the bonding of two monodentate donor molecules, two enolate carbonyl oxygen atoms and two Mo=O oxygen atoms for Mo centre an octahedral stereochemistry is proposed for the molybdenum centre. On the basis of the similar reasoning, copper is assumed to occupy N_2O_2 coordination chamber giving rise to square planar stereochemistry. Taking into consideration that two monodentate donor molecules are bonded to the metal centre in heterobimetallic Cu (II)-Mo (VI) complexes, it is plausible to suggest that these two will be bonded to molybdenum centre. Considering the bonding of two monodentate donor molecules, two enolate carbonyl oxygen atoms and two Mo=O oxygen atoms, it is reasonable to suggest that the molybdenum centre again has an octahedral stereochemistry in the heterobimetallic complexes **(8.8)** to **(8.14)**. The tentative structures for the complexes have been shown in **Figs. 8.19-8.22**.

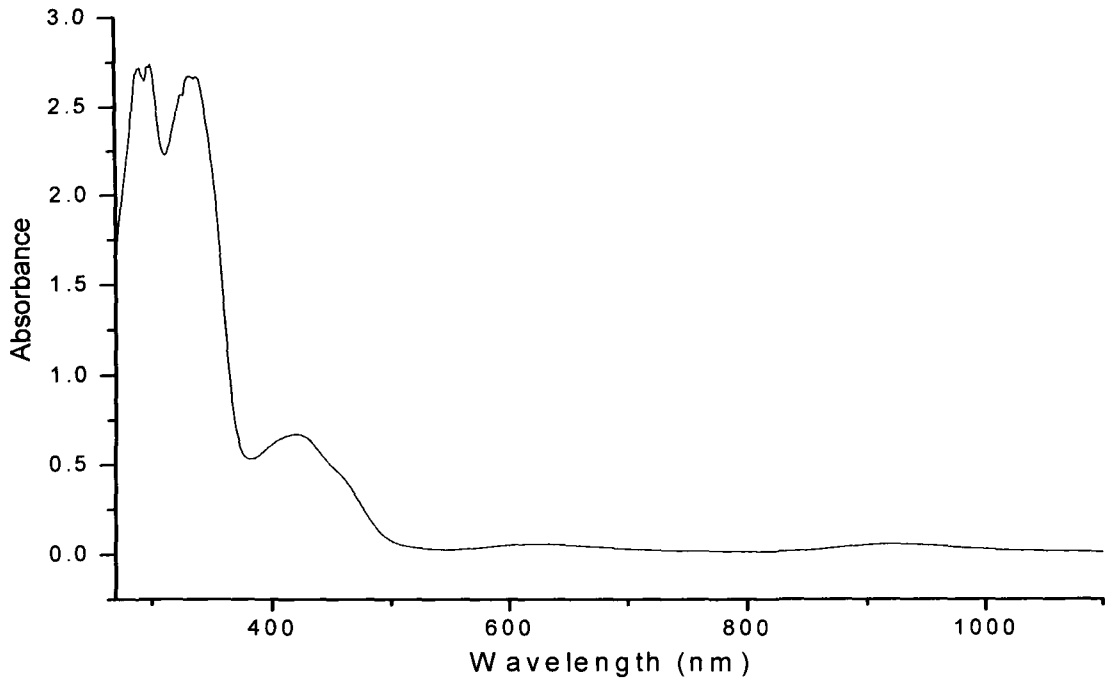

Fig. 8.1 Electronic spectrum of $[Ni(slox)MoO_2(H_2O)_4]$ **(8.1)**.

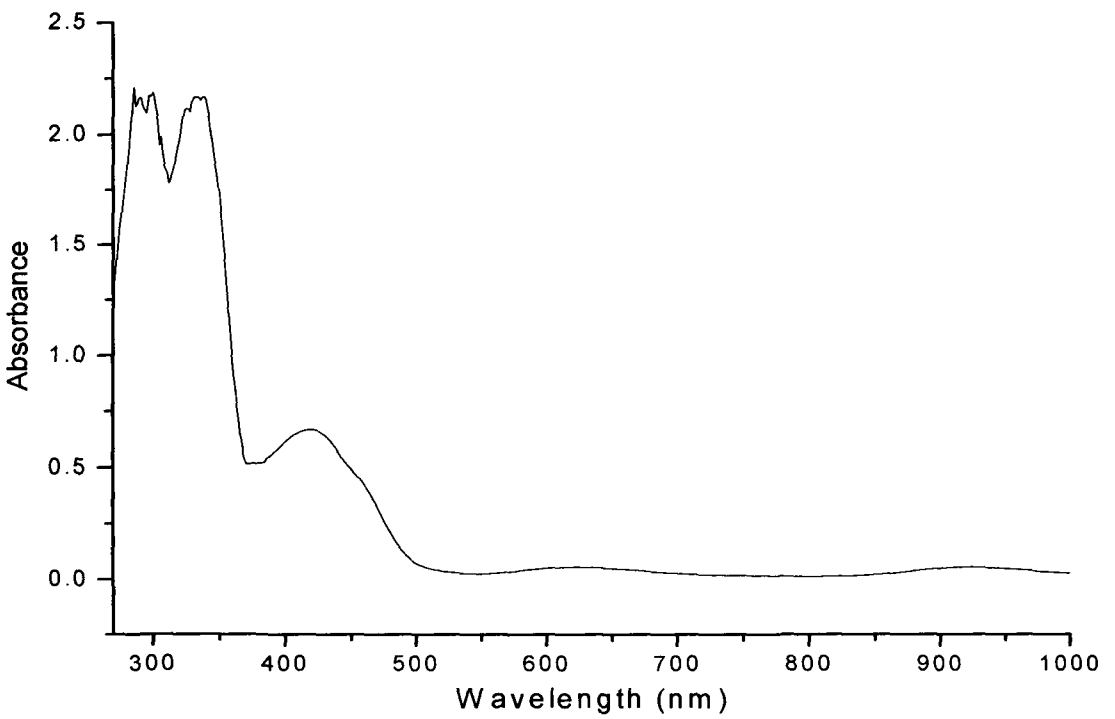

Fig. 8.2 Electronic spectrum of $[Ni(slox)MoO_2(py)_4]$ **(8.2)**.

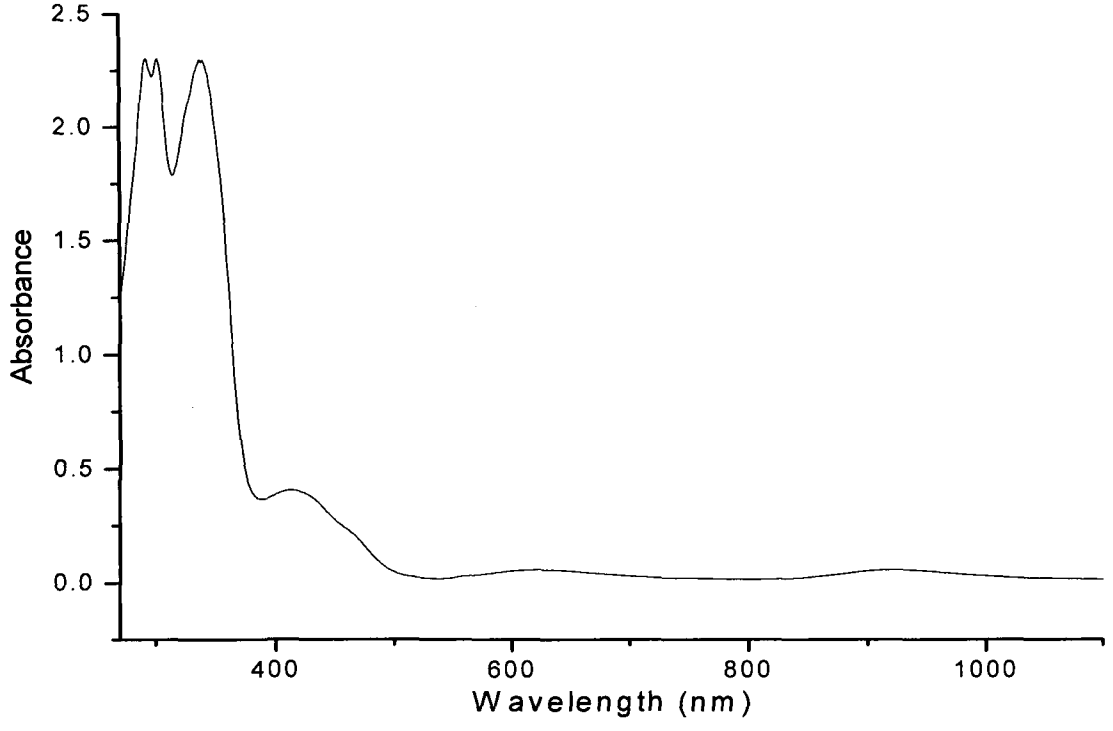

Fig. 8.3 Electronic spectrum of [Ni(slox)MoO_2(2-pic)$_4$] **(8.3)**.

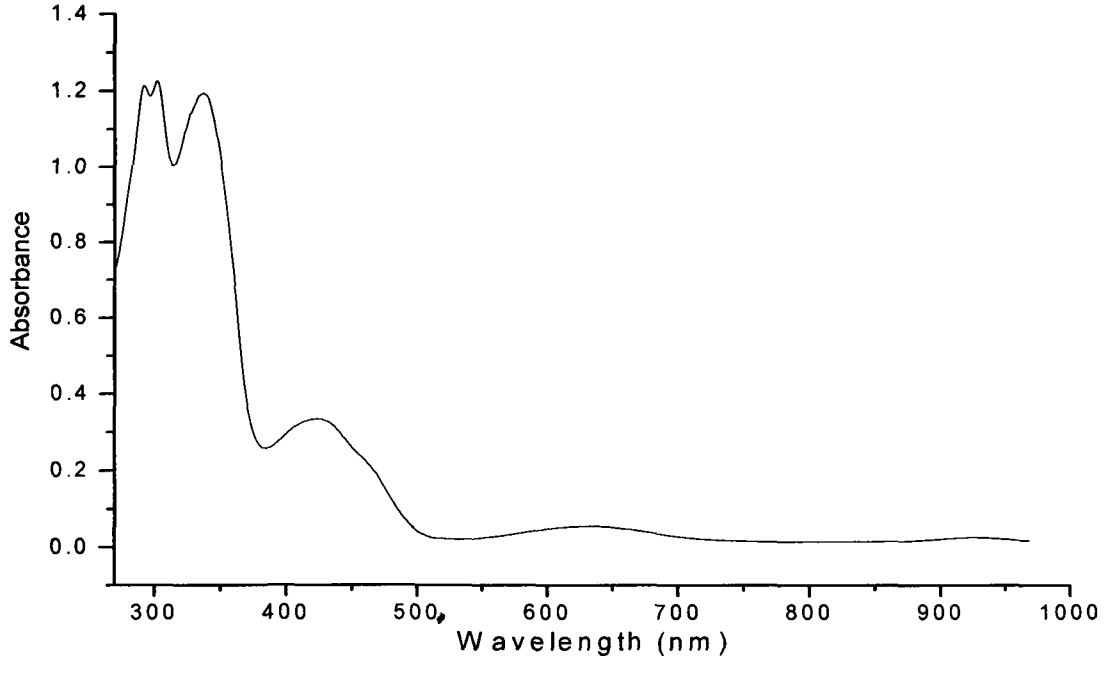

Fig. 8.4 Electronic spectrum of [Ni(slox)MoO_2(phen)$_2$] **(8.7)**.

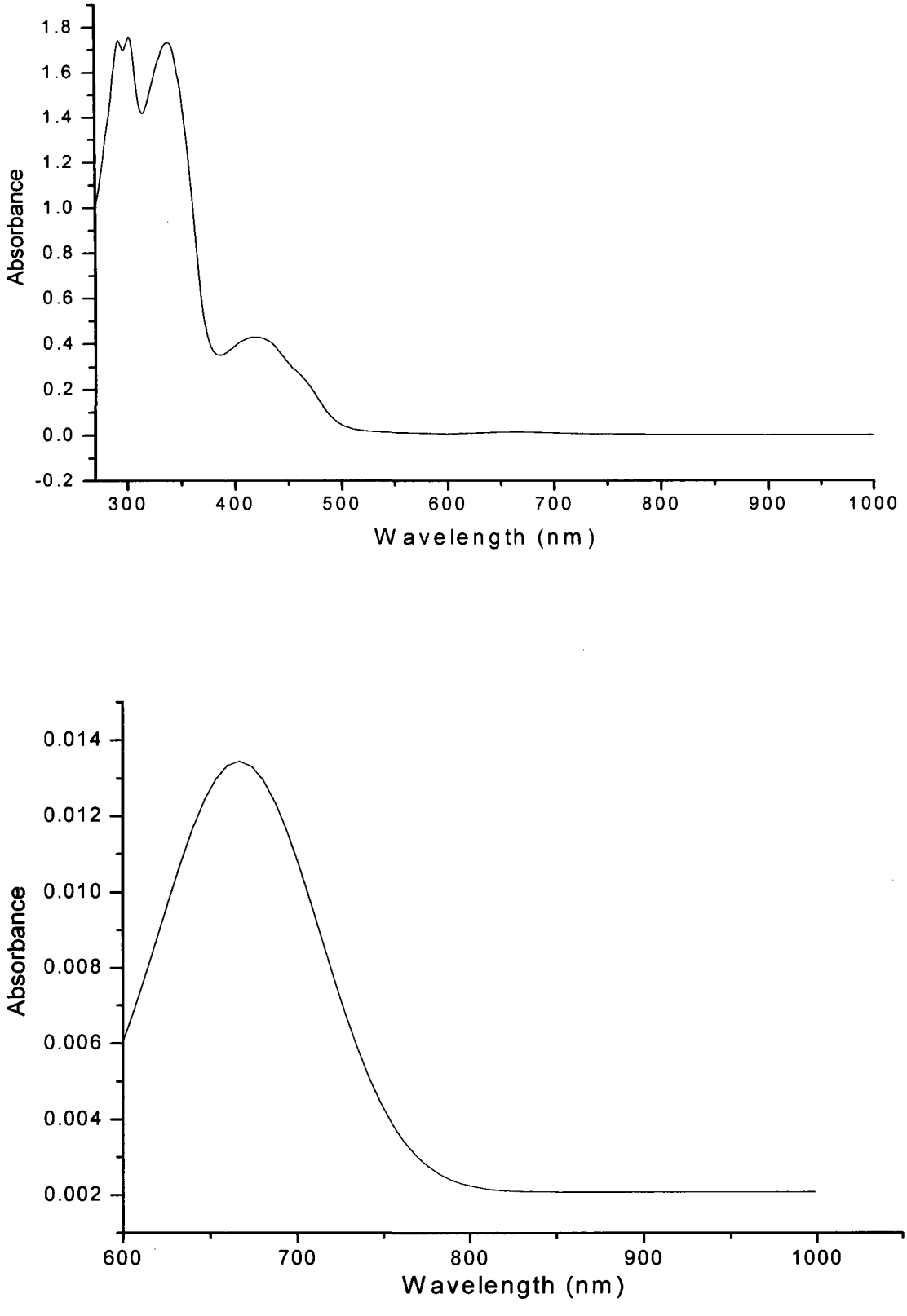

Fig. 8.5 Electronic spectrum of $[Cu(slox)MoO_2(H_2O)_2]$ **(8.8)**.

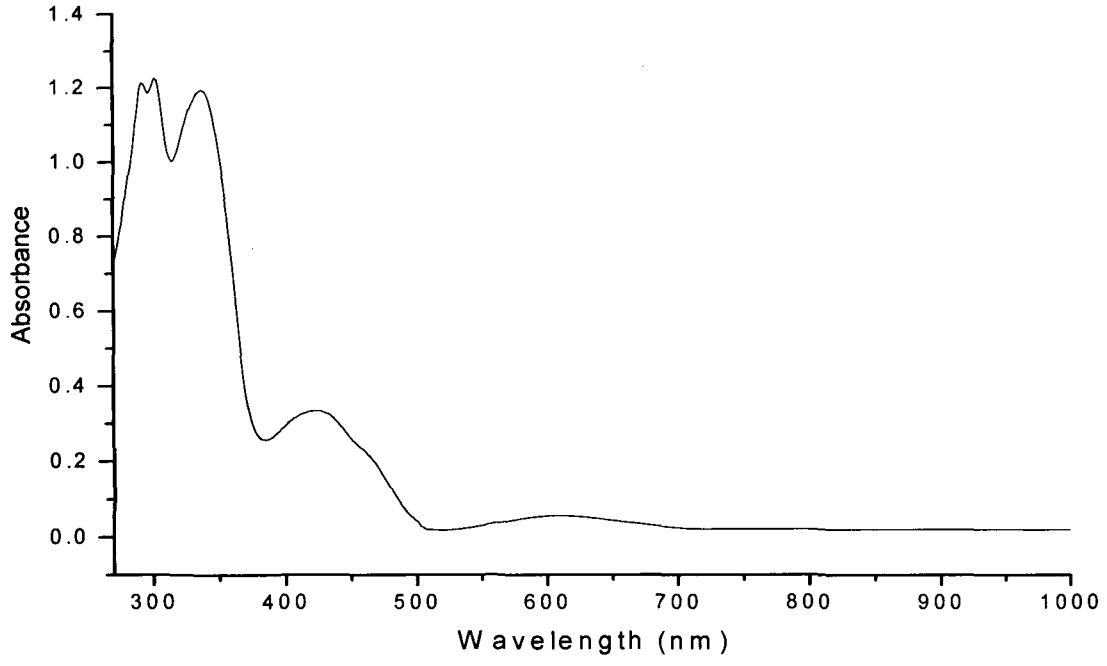

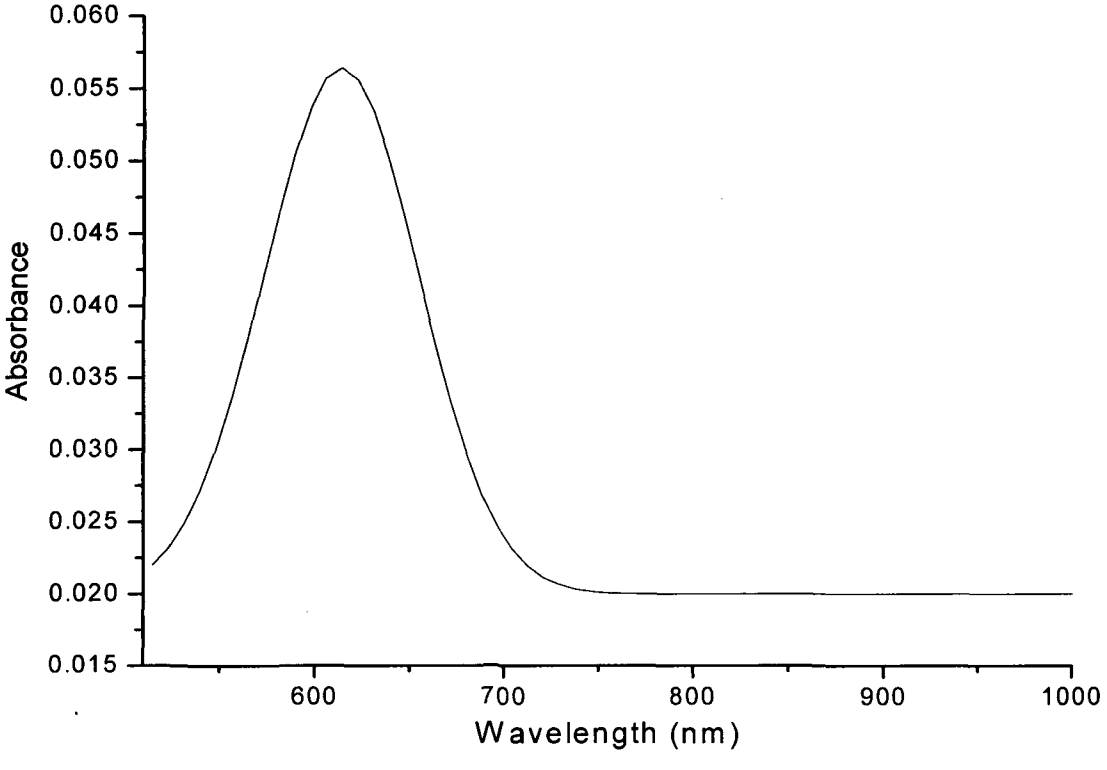

Fig. 8.6 Electronic spectrum of $[Cu(slox)MoO_2(py)_2]$ **(8.9)**.

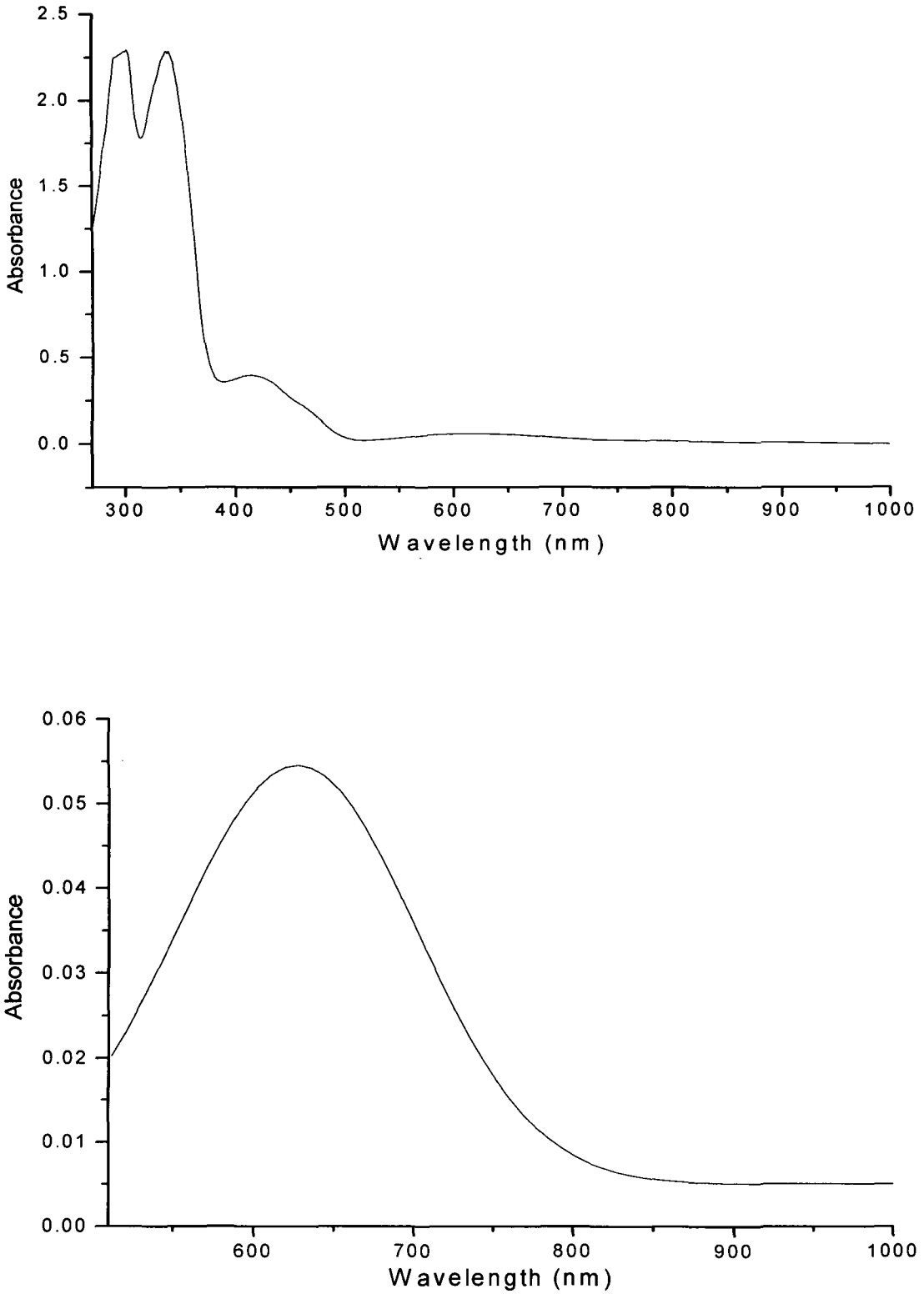

Fig. 8.7 Electronic spectrum of [Cu(slox)MoO_2(bpy)] **(8.13)**.

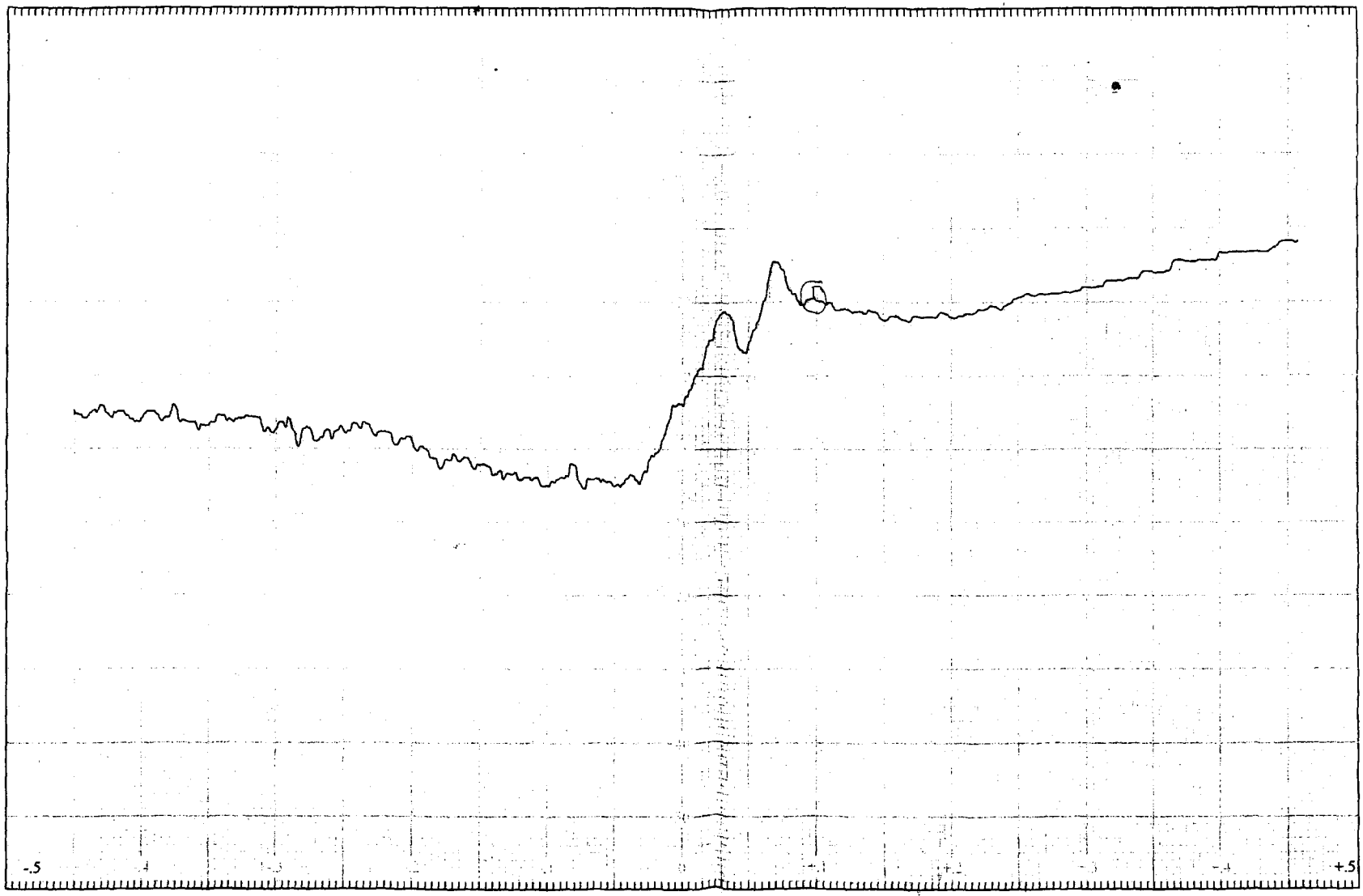

Fig. 8.8 (a) EPR spectrum of $[Cu(slox)MoO_2(H_2O)_2]$ **(8.8)** in DMSO at Temperature: RT; Frequency: 9.1 GHz; Scan Range: 2000 G; Field Set: 3200 G.

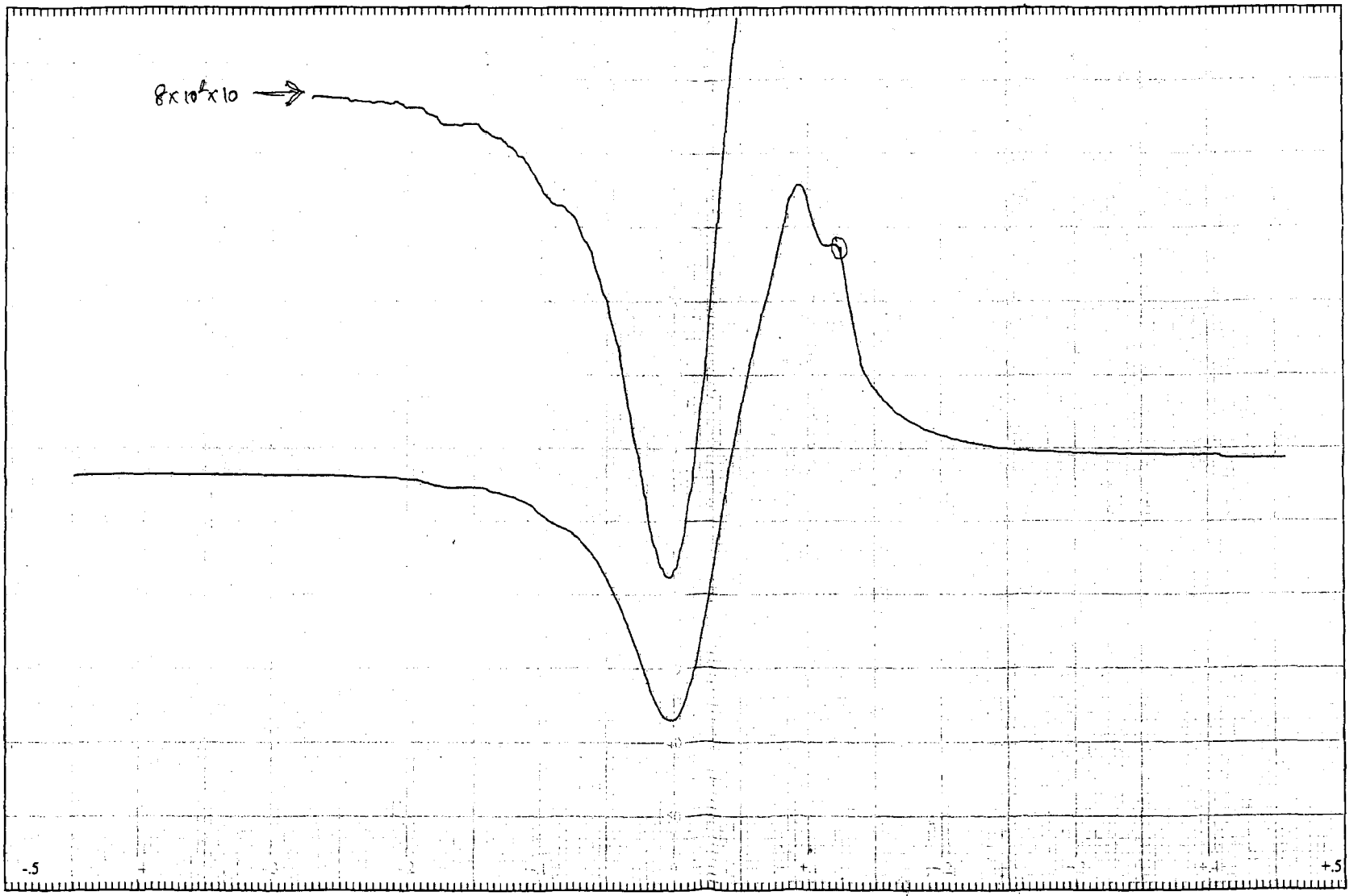

Fig. 8.8 (b) EPR spectrum of [Cu(slox)$MoO_2(H_2O)_2$] **(8.8)** in DMSO at Temperature: LNT; Frequency: 9.1 GHz; Scan Range: 2000 G; Field Set: 3000 G.

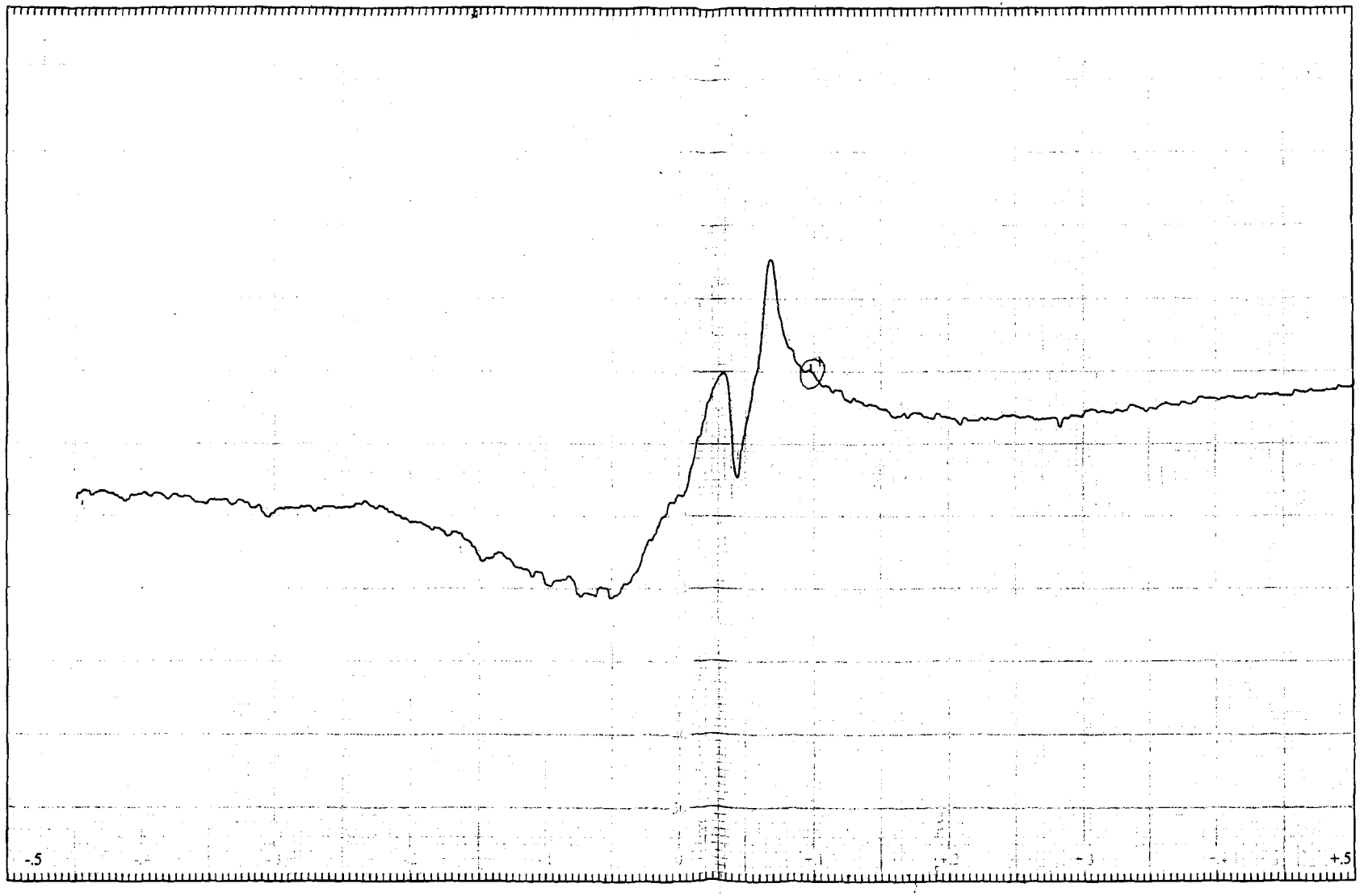

Fig. 8.9 (a) EPR spectrum of [Cu(slox)$MoO_2(py)_2$] **(8.9)** in DMSO at Temperature: RT; Frequency: 9.1 GHz; Scan Range: 2000 G; Field Set: 3200 G.

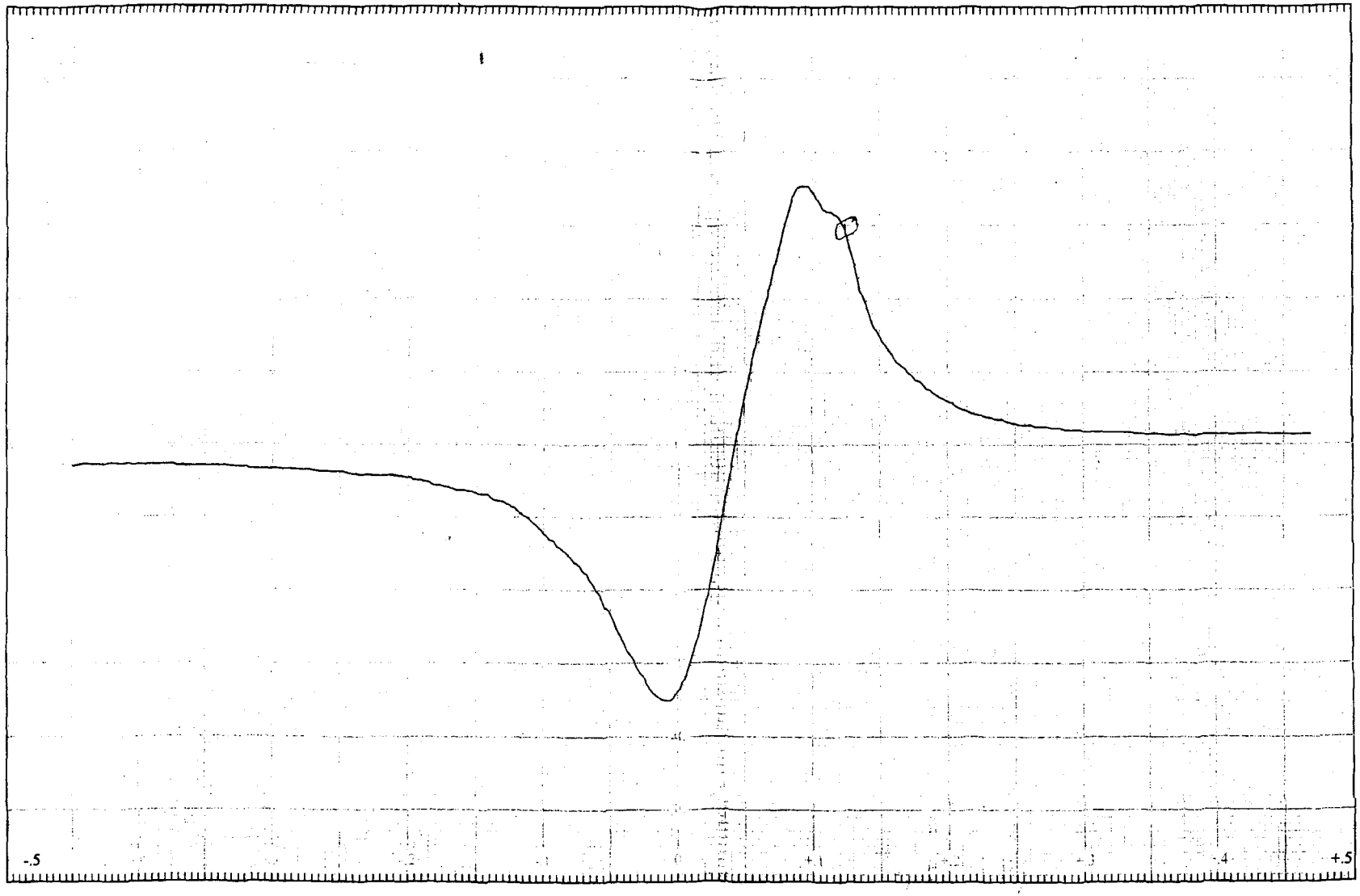

Fig. 8.9 (b) EPR spectrum of $[Cu(slox)MoO_2(H_2O)_2]$ **(8.9)** in DMSO at Temperature: LNT; Frequency: 9.1 GHz; Scan Range: 2000 G; Field Set: 3000 G.

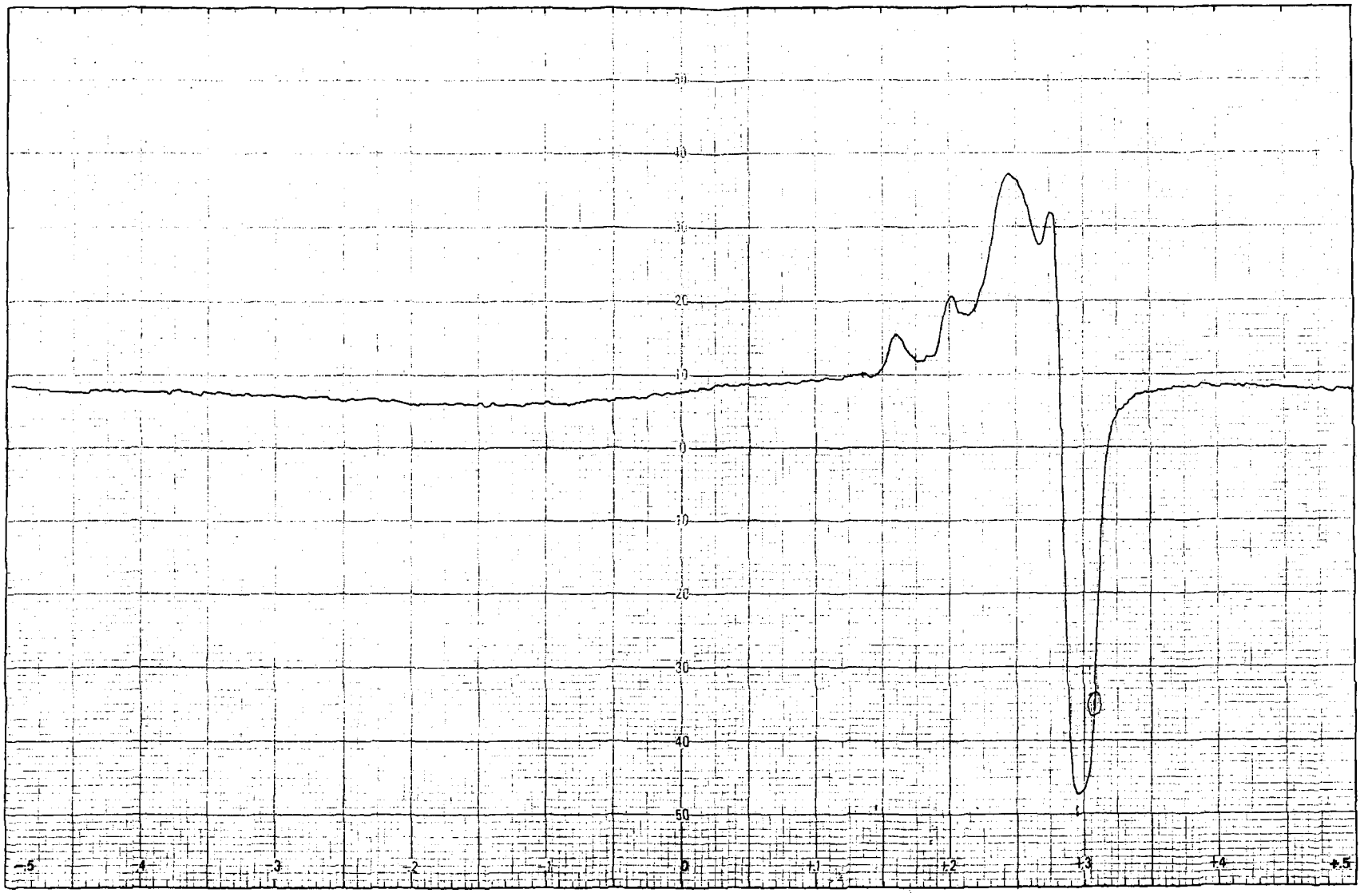

Fig. 8.10 EPR spectrum of [Cu(slox)MoO_2(bpy)] **(8.13)** in DMSO at Temperature: LNT; Frequency: 9.1 GHz; Scan Range: 4000 G; Field Set: 2000 G.

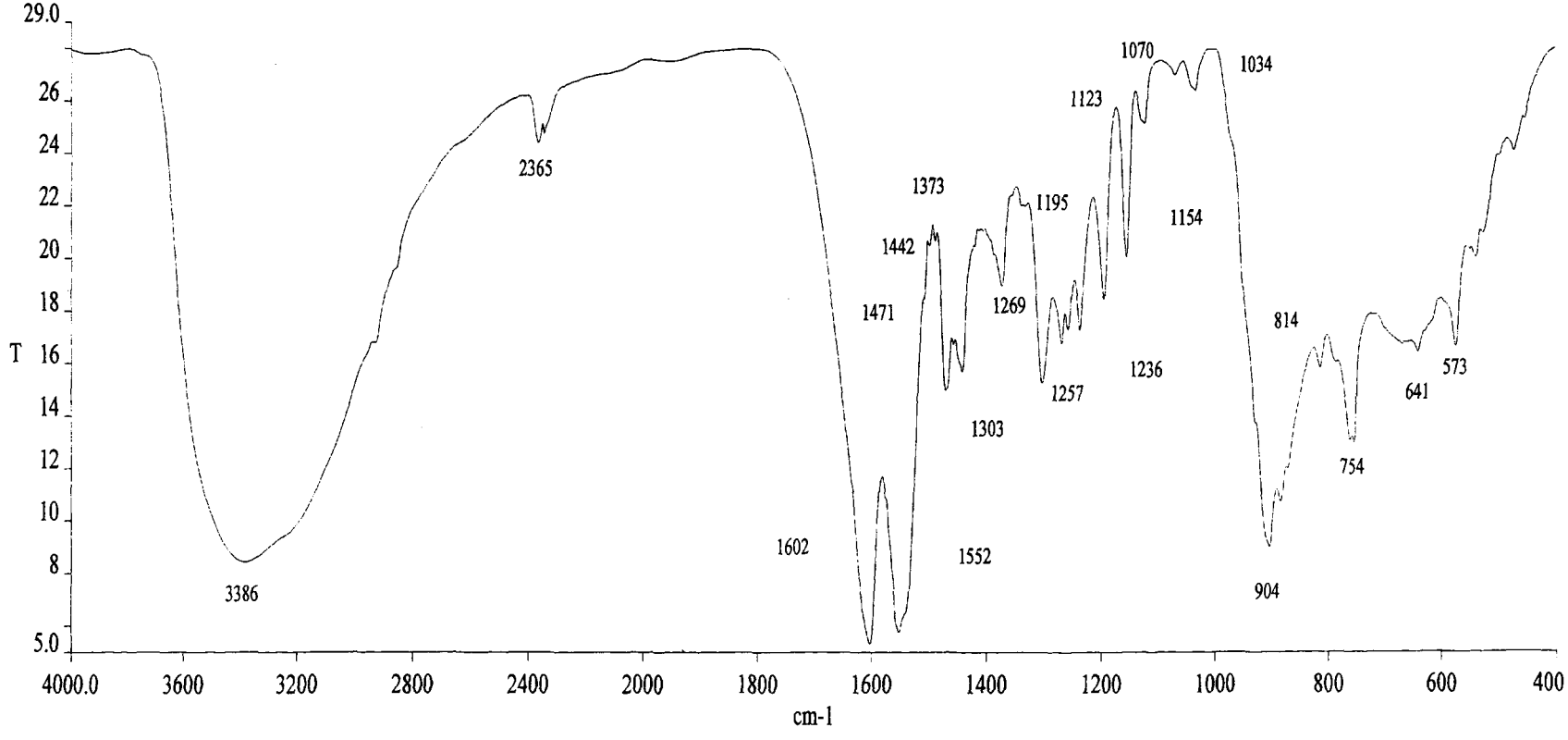

Fig. 8.11 Infrared spectrum of $[Ni(slox)MoO_2(H_2O)_4]$ **(8.1)** in KBr.

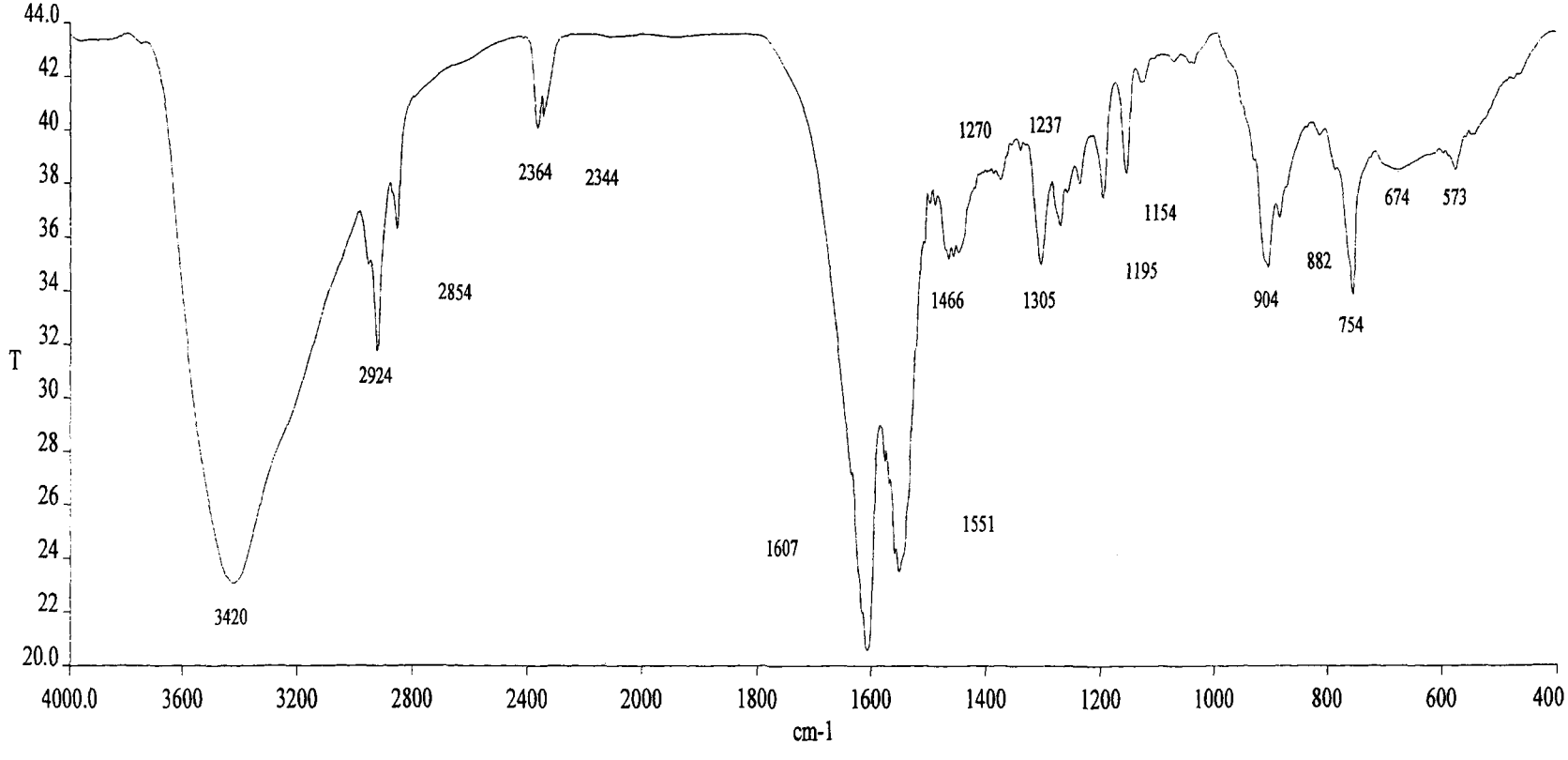

Fig. 8.12 Infrared spectrum of $[Ni(slox)MoO_2(py)_4]$ **(8.2)** in KBr.

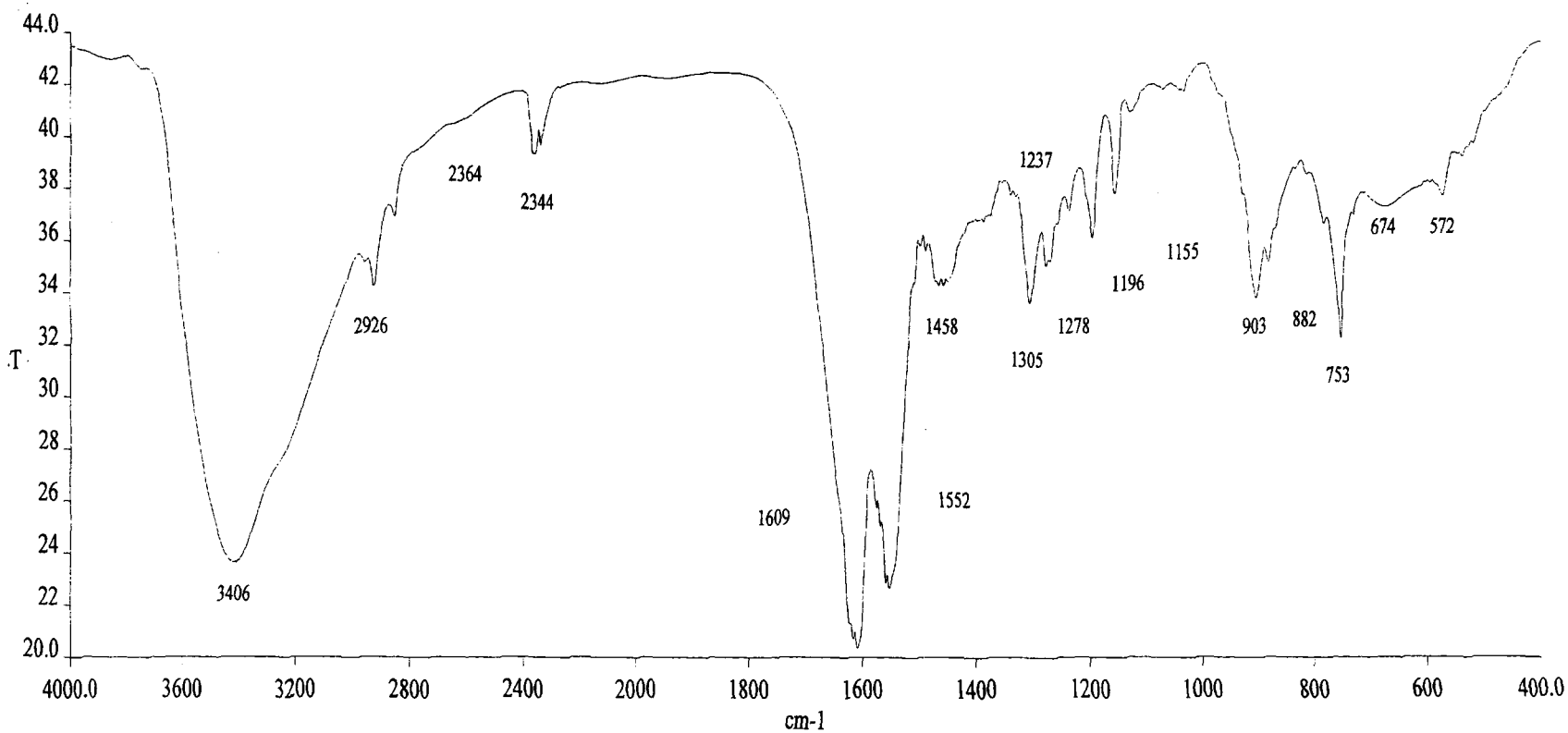

Fig. 8.13 Infrared spectrum of [Ni(slox)MoO_2(2-pic)$_4$] **(8.3)** in KBr.

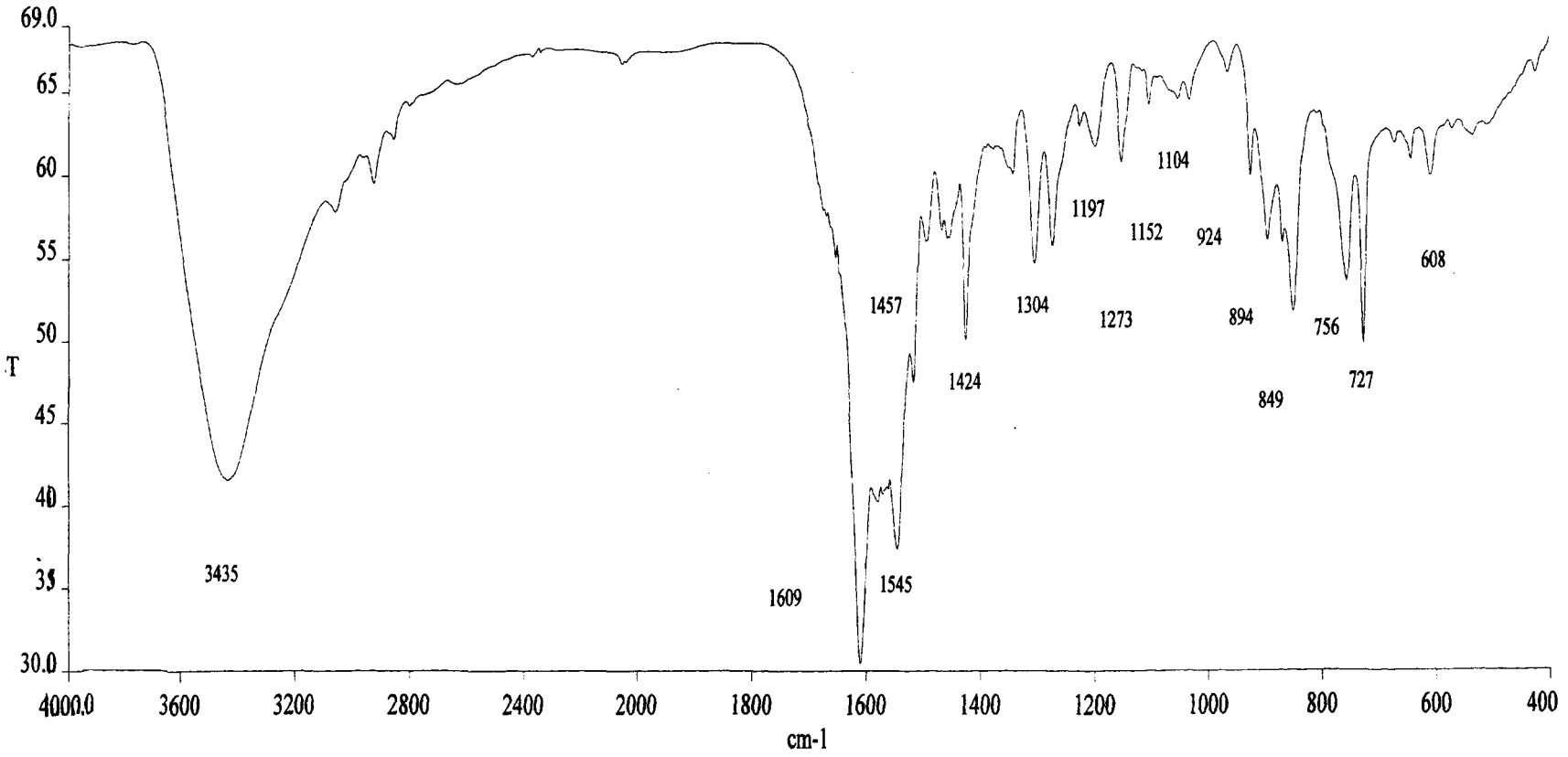

Fig. 8.14 Infrared spectrum of $[Ni(slox)MoO_2(phen)_2]$ **(8.7)** in KBr.

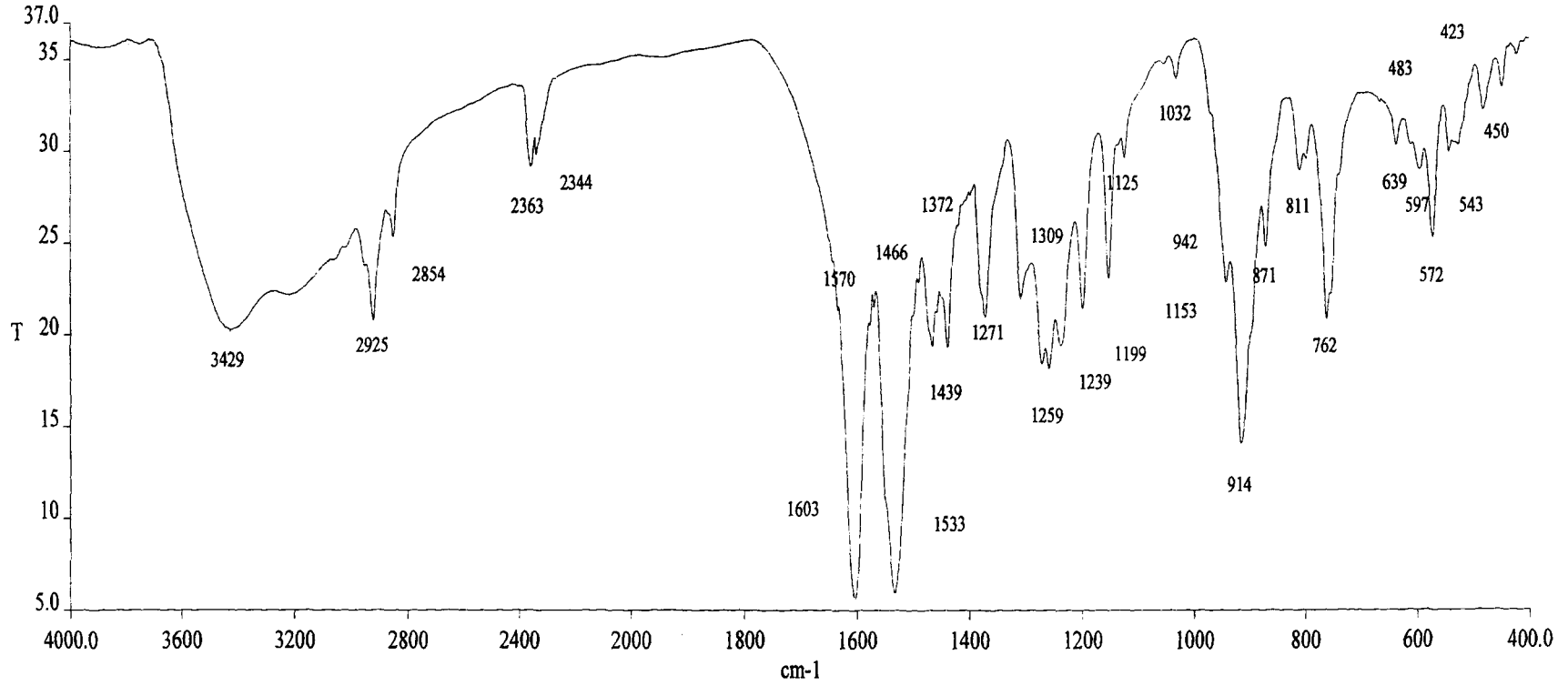

Fig. 8.15 Infrared spectrum of $[Cu(slox)MoO_2(H_2O)_2]$ **(8.8)** in KBr.

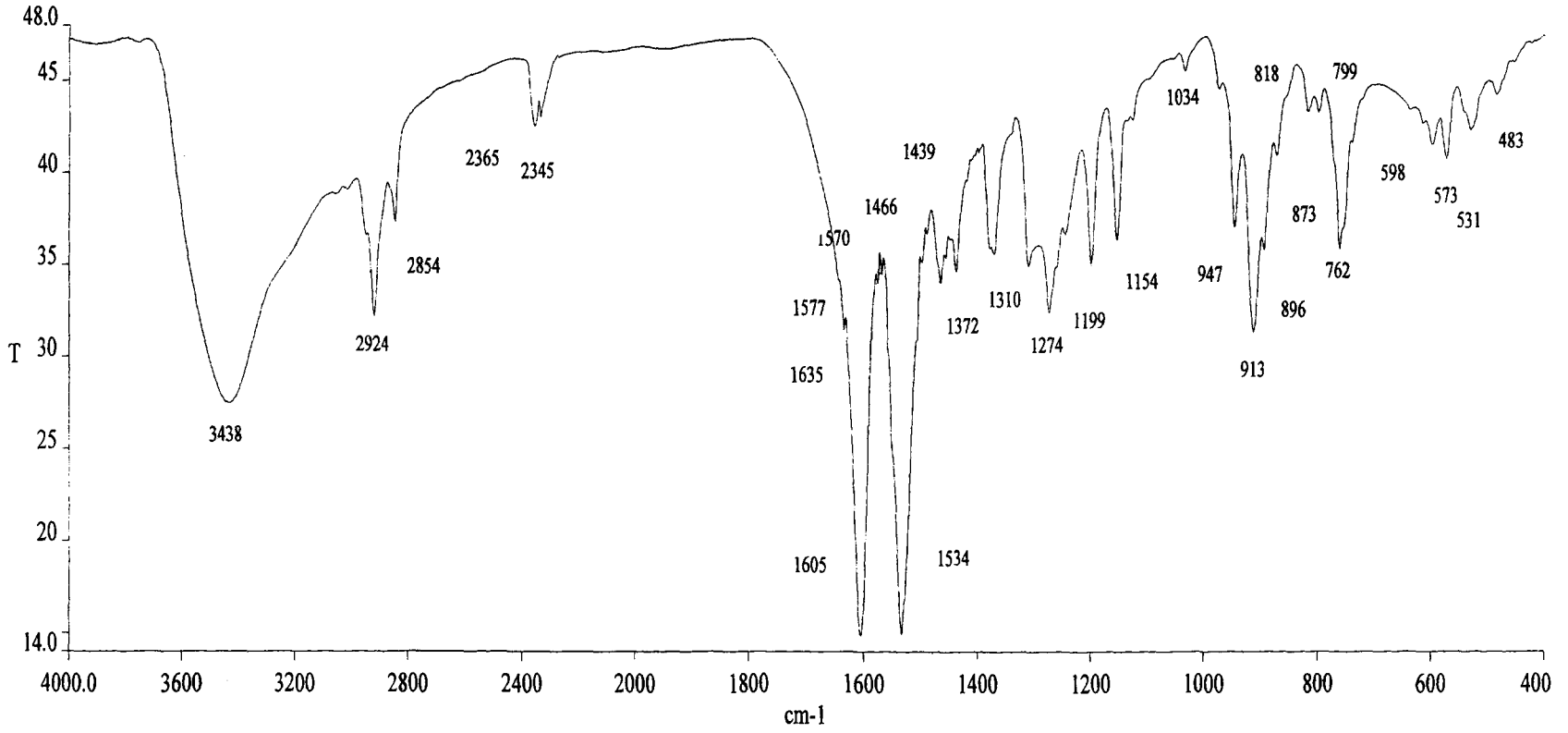

Fig. 8.16 Infrared spectrum of $[Cu(slox)MoO_2(py)_2]$ **(8.9)** in KBr.

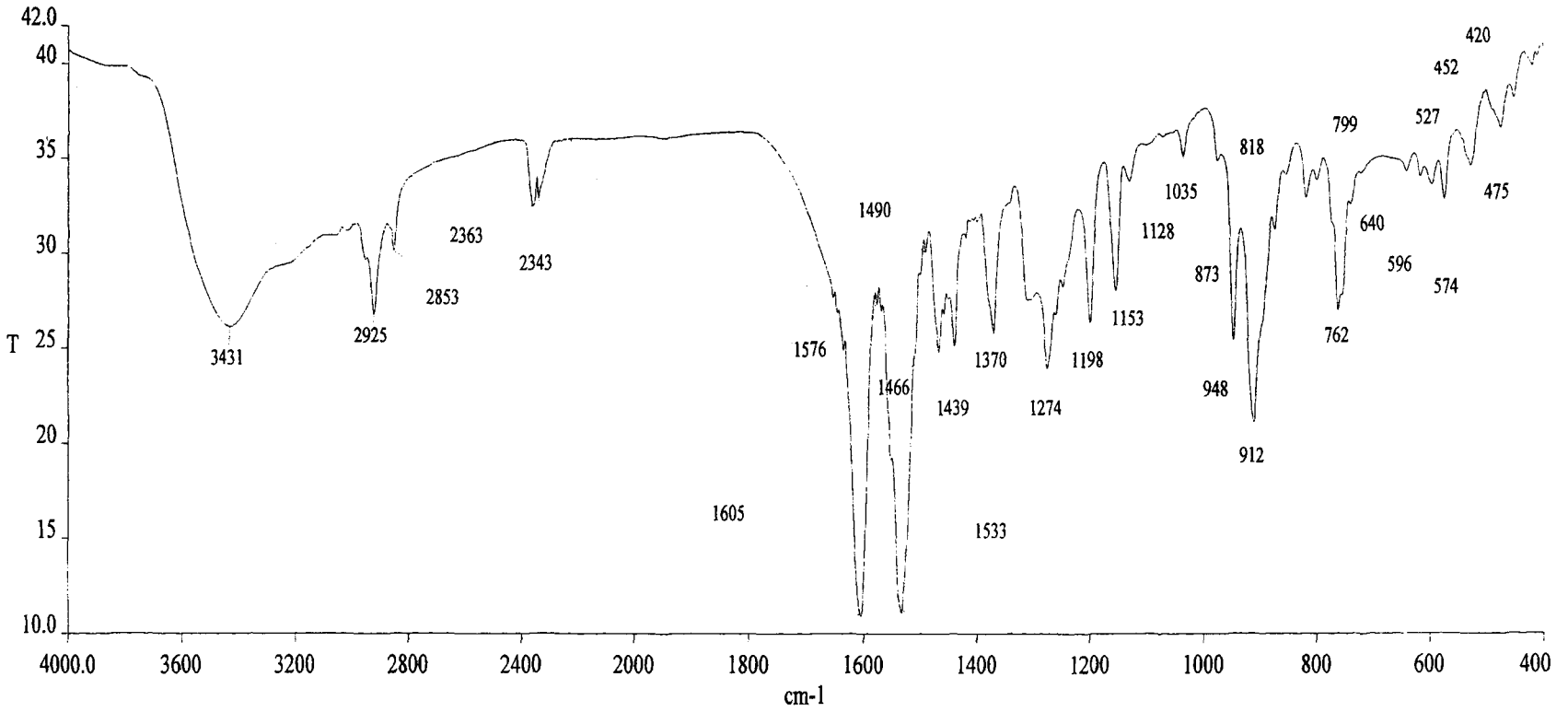

Fig. 8.17 Infrared spectrum of $[Cu(slox)MoO_2(2\text{-pic})_2]$ **(8.10)** in KBr.

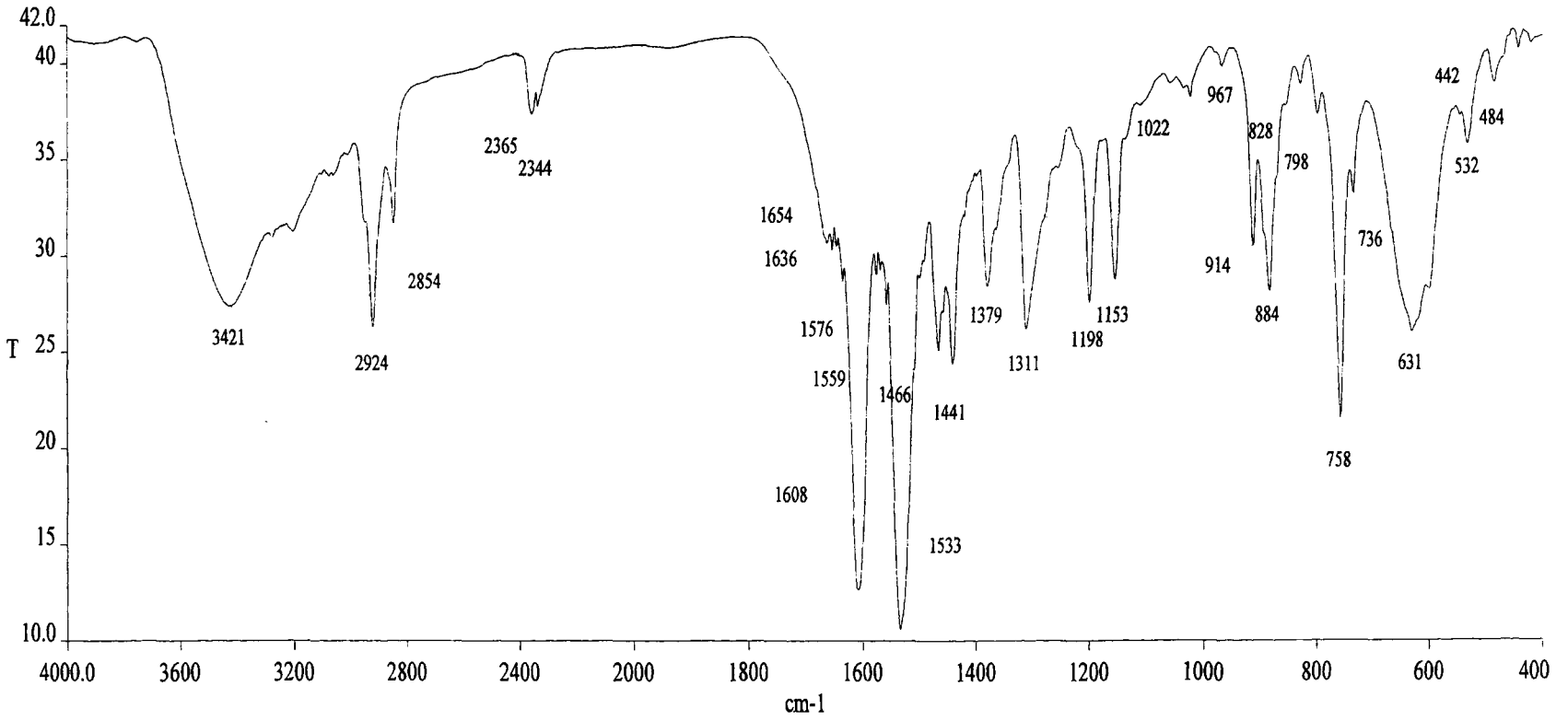

Fig. 8.18 Infrared spectrum of [Cu(slox)MoO_2(bpy)] **(8.13)** in KBr.

Table 8.1: Complex, colour, decomposition point, analytical, molar conductance, magnetic moment and electronic spectral data for heterobimetallic complexes.

Sl. No.	Complex (Color)	D.P (°C)	Elemental analyses: Found (Calcd)%					Molar cond Λ_M (ohm^{-1} cm^2mol^{-1})	Magnetic moment μ_{eff} (BM)	Electronic spectral band λ_{max}(nm) (ε_{max}) (dm^3 $mol^{-1}cm^{-1}$)
			Ni/Cu	Mo	C	H	N			
8.1	[Ni(slox)$MoO_2(H_2O)_4$] (dirty yellow)	>300	10.01 (10.11)	16.92 (16.52)	33.18 (33.09)	3.16 (3.12)	9.73 (9.65)	8.2	3.07	290(18052) 300(17988) 339(17445) 420(3769) 623(87) 937(92)
8.2	[Ni(slox)$MoO_2(py)_4$] (dirty yellow)	>300	6.92 (7.11)	11.78 (11.63)	52.45 (52.41)	3.62 (3.66)	13.80 (13.58)	4.5	2.96	293(16620) 304(16684) 335(16646) 421(3500) 618(93) 933(87)
8.3	[Ni(slox)MoO_2(2-pic)$_4$] (dirty yellow)	>300	6.43 (6.66)	11.11 (10.89)	54.62 (54.52)	4.31 (4.35)	12.69 (12.72)	5.2	2.87	292(16464) 302(16450) 338(16400) 413(2892) 622 (86) 931(81)
8.4	[Ni(slox)MoO_2(3-pic)$_4$] (dirty yellow)	>300	6.76 (6.66)	10.96 (10.89)	54.73 (54.52)	4.38 (4.35)	13.01 (12.72)	5.7	2.96	293(16500) 303(16521) 339(16550) 413(2901) 620(89) 942(87)
8.5	[Ni(slox)MoO_2(4-pic)$_4$] (dirty yellow)	>300	6.35 (6.66)	11.23 (10.89)	54.77 (54.52)	4.33 (4.35)	13.12 (12.72)	6.8	2.98	294(18086) 304(18046) 341(17933) 423(4460) 626(63) 952(45)
8.6	[Ni(slox)MoO_2(bpy)$_2$] (yellow)	>300	6.93 (7.15)	12.00 (11.69)	52.46 (52.67)	3.21 (3.19)	13.16 (13.65)	7.0	3.05	293(15954) 303(15902) 339(16670) 424(2801) 618(90) 934(65)
8.7	[Ni(slox)MoO_2(phen)$_2$] (yellow)	>300	6.88 (6.75)	11.51 (11.04)	55.39 (55.28)	3.06 (3.02)	12.78 (12.89)	7.3	3.10	292(16240) 302(16356) 337(16002) 423(2796) 624(93) 936(68)
8.8	[Cu(slox)$MoO_2(H_2O)_2$] (Greenish yellow)	>300	11.24 (11.56)	17.63 (17.46)	35.12 (34.97)	2.60 (2.57)	10.45 (10.20)	6.6	1.79	292(12442) 302(12550) 337(12371) 420(3064) 666(59)
8.9	[Cu(slox)$MoO_2(py)_2$] (Greenish yellow)	>300	9.75 (9.46)	14.01 (14.28)	46.61 (46.49)	3.03 (3.00)	12.67 (12.51)	4.9	1.69	292(12140) 302(12270) 337(11950) 423(3340) 608(97)
8.10	[Cu(slox)MoO_2(2-pic)$_2$] (Greenish yellow)	>300	8.83 (9.08)	13.99 (13.71)	48.32 (48.06)	3.49 (3.46)	12.29 (12.01)	7.1	1.75	291(12211) 303(12310) 338(12000) 424(3128) 612(82)
8.11	[Cu(slox)MoO_2(3-pic)$_2$] (Greenish yellow)	>300	8.96 (9.08)	13.46 (13.71)	48.17 (48.06)	3.42 (3.46)	11.88 (12.01)	5.4	1.76	292(12321) 303(12432) 338(11900) 423(3024) 614(88)
8.12	[Cu(slox)MoO_2(4-pic)$_2$] (Greenish yellow)	>300	9.49 (9.08)	13.63 (13.71)	48.40 (48.06)	3.44 (3.46)	12.34 (12.01)	6.5	1.78	292(12911) 304(12951) 340(12040) 416(2424) 625(76)
8.13	[Cu(slox)MoO_2(bpy)] (light green)	>300	9.72 (9.49)	14.02 (14.33)	46.35 (46.63)	2.74 (2.71)	12.76 (12.55)	8.0	1.82	302(12738) 338(12694) 414(2189) 619(87)
8.14	[Cu(slox)MoO_2(phen)] (light green)	>300	8.95 (9.16)	14.17 (13.83)	48.50 (48.48)	2.58 (2.62)	12.41 (12.11)	8.9	1.76	293(12560) 304(12442) 340(11600) 418(2331) 622(78)

Table 8.2: Ligand field parameters for the heterobimetallic nickel (II)-molybdenum (VI) complexes.

Sl. No.	Complex	$^3A_{2g} \rightarrow {}^3T_{2g}$ (F) (ν_1)		$^3A_{2g} \rightarrow {}^3T_{1g}$ (F) (ν_2)		Dq (cm^{-1})	ν_2/ν_1	B (cm^{-1})	β	β^o (%)	LFSE (Kcal/mol)
		cm^{-1}	nm	cm^{-1}	nm						
8.1	$[Ni(slox)MoO_2(H_2O)_4]$	10672	937	16051	623	1067.2	1.504	600.92	0.579	42.1	36.67
8.2	$[Ni(slox)MoO_2(py)_4]$	10718	933	16181	618	1071.8	1.509	615.12	0.593	40.7	36.82
8.3	$[Ni(slox)MoO_2(2\text{-}pic)_4]$	10741	931	16077	622	1074.1	1.497	603.16	0.581	41.9	36.90
8.4	$[Ni(slox)MoO_2(3\text{-}pic)_4]$	10615	942	16129	620	1061.5	1.519	629.66	0.607	39.3	36.47
8.5	$[Ni(slox)MoO_2(4\text{-}pic)_4]$	10504	952	15974	626	1050.4	1.521	625.85	0.603	39.7	36.09
8.6	$[Ni(slox)MoO_2(bpy)_2]$	10707	934	16181	618	1070.7	1.511	617.70	0.595	40.5	36.78
8.7	$[Ni(slox)MoO_2(phen)_2]$	10684	936	16026	624	1068.4	1.500	593.56	0.572	42.8	36.71

Table 8.3: EPR spectral data for heterobimetallic copper (II)-molybdenum (VI) complexes at RT and LNT in DMSO solution.

Sl. No.	Complex	Temp	$g_{\|}$	$g_{\perp}$	g_{av}	$A_{\|} \times 10^{-4}$ (cm^{-1})	G	α^2
8.8	$[Cu(slox)MoO_2(H_2O)_2]$	RT	2.197	1.958	2.038	180	--	0.716
		LNT	2.314	2.104	2.174	150	3.02	0.812
8.9	$[Cu(slox)MoO_2(py)_2]$	RT	2.242	1.961	2.055	190	--	0.789
		LNT	2.307	2.101	2.170	180	3.04	0.887
8.10	$[Cu(slox)MoO_2(2\text{-}pic)_2]$	LNT	2.442	2.190	2.274	160	2.33	1.005
8.13	$[Cu(slox)MoO_2(bpy)]$	LNT	2.424	2.162	2.249	170	2.62	1.002
8.14	$[Cu(slox)MoO_2(phen)]$	LNT	2.406	2.189	2.261	150	2.15	0.940

Table 8.4: Infrared spectral data for the heterobimetallic complexes.

Sl. No	Ligand/complex	ν(OH)+ ν(NH)	ν(C=O)	ν(C=N)	Amide II + ν(C-O) (phenolic)	ν(NCO)	ν(C-O)	ν(N-N)	$\nu(MoO_2^{2+})$	ν(M-O) (phenolic)	ν(M-O) (enolic)
	H_4 slox	3278(s) 3204(s)	1667(s)	1627(s) 1603(s)	1534(s)	--	1262(s)	1035(w) 1054(m)	--	--	--
	$[Ni(H_2slox)(H_2O)_3]$	3400(s) 3279(s) 3200(s)	1668(m)	1608(s)	1537(s)	--	1304(s)	1042(w)	--	581(w)	469(w)
	$[Cu(H_2slox)]$	3436(m) 3278(m) 3204(m)	1679(s)	1613(s)	1527(s)	--	1276(s)	1043(w)	--	598(m)	482(w)
8.1	$[Ni(slox)MoO_2(H_2O)_4]$	3386(s)	--	1602(s)	1552(s)	1530(s)	1303(s)	1034(w)	904(s) 881(s)	573(w)	540(w)
8.2	$[Ni(slox)MoO_2(py)_4]$	3420(s)	--	1607(s)	1551(s)	--	1305(s) 1270(m)	1037(w)	904(s) 882(s)	573(w)	544(w)
8.3	$[Ni(slox)MoO_2(2\text{-}pic)_4]$	3406(s)	--	1609(s)	1552(s)	--	1305(s) 1278(m)	1035(w)	903(s) 882(s)	572(w)	536(w)
8.4	$[Ni(slox)MoO_2(3\text{-}pic)_4]$	3419(s)	--	1605(s)	1550(s)	--	1303(s) 1271(m)	1036(w)	905(s) 886(s0	572(w)	542(w)
8.5	$[Ni(slox)MoO_2(4\text{-}pic)_4]$	3411(s)	--	1607(s)	1550(s)	--	1304(s) 1270(m)	1034(w)	904(s) 882(s)	573(w)	538(w)
8.6	$[Ni(slox)MoO_2(bpy)_2]$	3430(s)	--	1608(s)	1547(s)	1513(s)	1305(s) 1271(s)	1033(w)	921(s) 890(s)	574(w)	540(w)
8.7	$[Ni(slox)MoO_2(phen)_2]$	3435(s)	--	1609(s)	1545(s)	1512(s)	1304(s) 1273(s)	1031(w)	924(s) 894(s)	572(w)	546(w)

8.8	$[Cu(slox)MoO_2(H_2O)_2]$	3429(s)	-	1603(s)	-	1533(s)	1309(s) 1270(s)	1032(w)	942(s) 914(s)	572(w)	543(w)
8.9	$[Cu(slox)MoO_2(py)_2]$	3438(s)	-	1605(s)	-	1534(s)	1310(s) 1274(s)	1034(w)	947(s) 913(s)	573(w)	531(w)
8.10	$[Cu(slox)MoO_2(2\text{-}pic)_2]$	3431(s)	-	1605(s)	-	1533(s)	1309(s) 1274(s)	1035(w)	948(s) 912(s)	574(w)	527(w)
8.11	$[Cu(slox)MoO_2(3\text{-}pic)_2]$	3436(s)	-	1606(s)	-	1532(s)	1308(s) 1270(s)	1030(w)	946(s) 913(s)	574(w)	540(w)
8.12	$[Cu(slox)MoO_2(4\text{-}pic)_2]$	3439(s)	-	1604(s)	-	1531(s)	1310(s) 1272(s)	1035(w)	944(s) 912(s)	572(w)	529(w)
8.13	$[Cu(slox)MoO_2(bpy)]$	3421(s)	-	1608(s)	-	1533(s)	1311(s)	1022(w)	914(s) 884(s)	-	532(w)
8.14	$[Cu(slox)MoO_2(phen)]$	3410(s)	-	1608(s)	-	1531(s)	1306(s)	1035(w)	910(s) 891(s)	-	531(w)

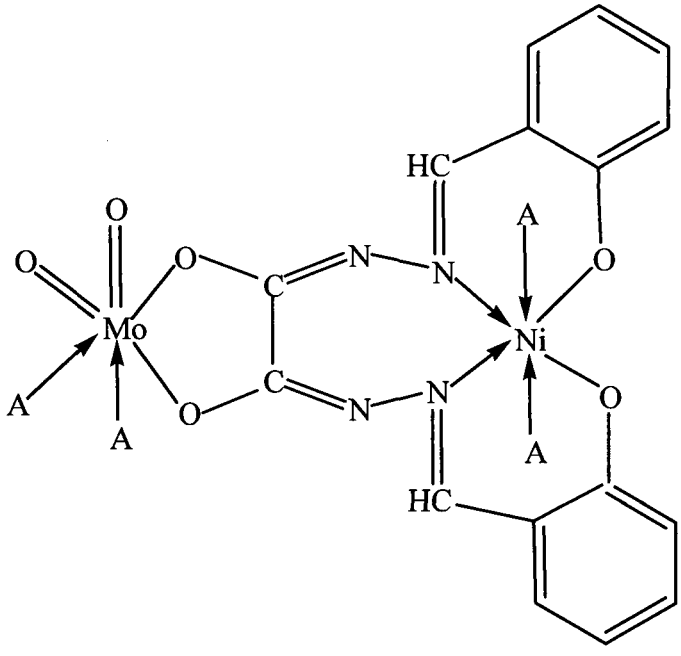

Fig. 8.19 Tentative structure of the complexes $[Ni(slox)MoO_2(A)_4]$ {where A = H_2O **(8.1)**, *pyridine* **(8.2)**, *2-picoline* **(8.3)**, *3-picoline* **(8.4)** *and 4-picoline* **(8.5)**}.

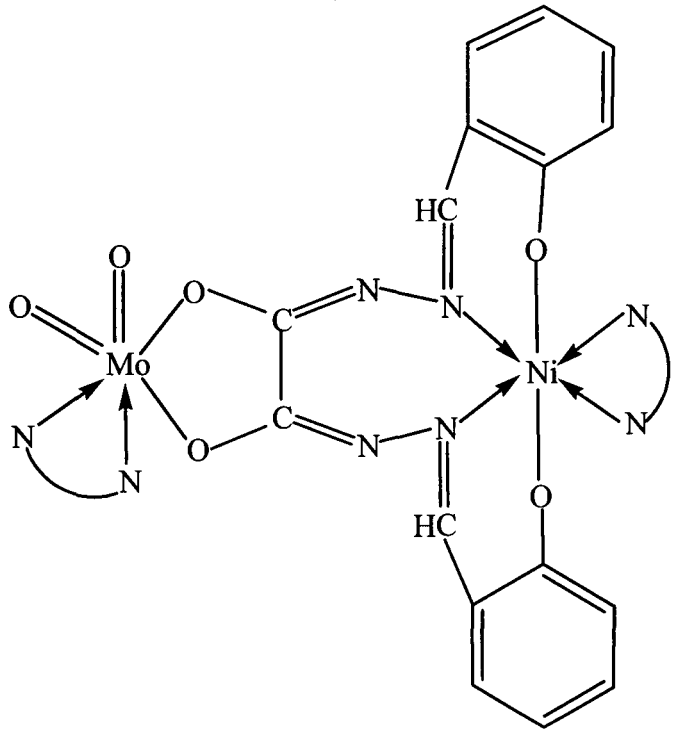

Fig. 8.20 Tentative structure of the complexes $[Ni(slox)MoO_2(NN)_2]$ {*where A = bipyridine* **(8.6)** *and phenanthroline* **(8.7)**}.

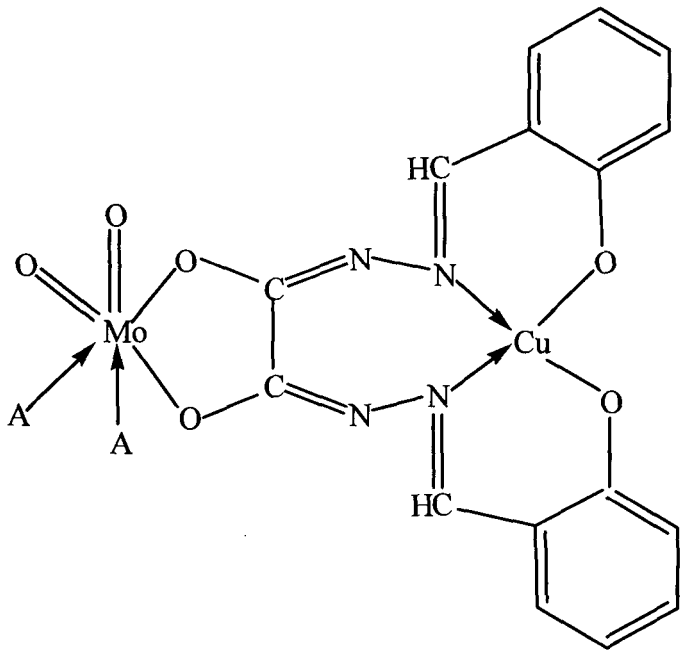

Fig. 8.21 Tentative structure of the complexes $[Cu(slox)MoO_2(A)_2]$ {*where A = H_2O* **(8.8)**, *pyridine* **(8.9)**, *2-picoline* **(8.10)**, *3-picoline* **(8.11)** *and 4-picoline* **(8.12)**}.

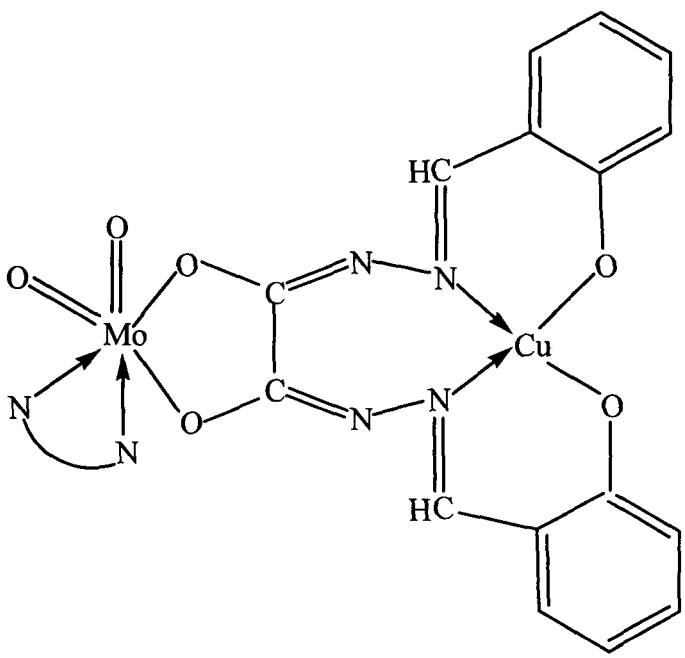

Fig. 8.22 Tentative structure of the complexes $[Cu(slox)MoO_2(NN)]$ {*where A = bipyridine* **(8.13)** *and phenanthroline* **(8.14)**}.

References

1. L. Sun, H. Berglund, R. Bavydov, T. Norrby, L. Hammarstorm, P. Korall, A. Borje, C. Philouze, K. Berg, A. Tray, M. Andersson, G. Stenhagen, J. Martensson, M. almgren, S. Styring and B. Akermark, *J. Am. Chem. Soc.*, **119**, 6996 (1997).
2. D. W. Stephen and T. A. Wark, *Inorg. Chem.*, **26**, 363 (1987).
3. J. Baker and B. Andersson, *Nature*, 370, 31 (1994).
4. Y. Lu, J. A. Roe, C. J. Bedder, J. Peisach, L. Banci, I. Bertini, E. B. Gralla and J. S. Valentine, *Inorg. Chem.*, **35**, 1692 (1996).
5. R. L Lintvedt, W. F. Lynch and J. K. Zehetmair, *Inorg. Chem.*, **29**, 3009 (1990).
6. S. R. Breeze and S. Wang, *Inorg. Chem.*, **3**, 5113 (1994); C. P. Love, C. L. Torardi and C. J. Page, *Inorg. Chem.*, **31**, 1784 (1992).
7. A. El-Toukhy, C. Z. Cai, G. Davies, T. R. Gilbert, K. D. Oman and M. Veidis, *J. Am. Chem. Soc.*, **106**, 4596 (1984); G. Davies, M. A. El-Sayed and El-Toukhy, *Comments Inorg. Chem.*, **8**, 203 (1989).
8. J. B. Carlson, G. Davies and P. Vorous, *Inorg. Chem.*, **33**, 2334 (1994).
9. G. Davies, M. A. El-Sayed and A. El-Toukhy, *Chem. Soc. Rev.*, **21**, 101 (1992); J. B. Carlson, G. Davies and P. Vorous, *Inorg. Chem.*, **33**, 2334 (1994).
10. U. Casellato, P. Guerriero, S. Tamburini, S. sitran and P. A. Vigato, *J. Chem. Soc. Dalton Trans.*, 2145 (1991); D. G. McCollum, C. Fraser, R. Ostrander, A. L. Reingold and B. Bosnich, *Inorg. Chem.*, **33**, 2383 (1994).
11. R. L. Lintvedt, W. E. Lynch and J. K. Zehetmair, *Inorg. Chem.* **29**, 3009 (1990).
12. G. Davies and A. G. Wedd, "*In Encyclopaedia of Inorganic Chemistry*", Ed. R. B. King; Wiley, New York, p. 2330 (1994).
13. R. A. Lal, A. N. Siva, S. Adhikari, M. K. Singh and U. S. Yadav, Synth. React. Inorg. *Met-Org. Chem.*, **26(2)**, 321-337 (1996); F. Feigl, V. Anger and

R. E. Oesper, "*Spot Tests in Organic Analysis*", 7th Ed., Elseiver Publishing Company, Amsterdam, Netherland, p. 173, 384 (1996) (Indian reprint, 2005).

14. M. K. Singh, N. K. Kar and R. A. Lal, *J. Coord. Chem.*, **61(19)**, 3158-3171 (2008).
15. W. J. Geary, *Coord. Chem. Rev.*, **7**, 81 (1971).
16. E. Vin˜uelas-Zahı´nos, M. A. Maldonado-Rogado, F. Luna-Giles and F. J. Barros-Garcı´a, *Polyhedron*, **27**, 879–886 (2008).
17. B. N. Figgis, *Nature*, **182**, 1568 (1958).
18. F. A. Cotton, G. Wilkinson, C. A. Murillo, and M. Bochmann, "*Advanced Inorganic Chemistry*", New York: John Wiley and Sons Inc. (2003).
19. L. Sacconi and M. Ciampolini, *J. Chem. Soc.*, A, 273 (1964).
20. B. J. Hathaway, "*In Comprehensive Coordination Chemistry*", p. 594-774, Vol. **5**; G. W. Wilkinson, R. D. Gillard, J. A. McLeverty, Ed. Perganion Press, Oxford, New York (1987).
21. R. S. Drago, "*Physical Methods in Inorganic Chemistry*", Reinhold Publishing Corporation, New York (1968).
22. A. B. P. Lever, "*Inorganic electronic spectroscopy*", Amsterdam: Elseiver (1984); V. P. Singh, P. Gupta and N. Lal, *Russ. J. Coord. Chem.*, **34**, 270-277 (2008).
23. B. Adhikari, S. Liu and C. R. Lucas, *Inorg. Chem.*, **32**, 5957 (1993).
24. V. V. Pavlishchuk, S.. V. Kolotilov, A. W. Addison, E. Sinn and M. J. Prushan, *Russ. J. Inorg. Chem.*, **45**, 544 (2000).
25. A. B. P. Lever, *Coord. Chem. Rev.*, **3**, 119 (1968).
26. Z. H. Abd El-Wahab, *Spectrochim. Acta A*, **67**, 25 (2007).
27. R. Gup and V. Kirman, *Spectrochim. Acta A*, **62**, 1188 (2005); K. R. Barnard, M. Bruch, H. Susan, J. H. Enemark, R. W. Gable and A. G. Wedd, *Inorg. Chem.*, **36**, 637 (1997).
28. R. A. Lal, M. L. Pal and S. Adhikari, *Synth. React. Met-Org. Chem.*, **26**, 997 (1996).
29. Mudasir, N. Yoshioka and H. Inoue, *Trans. Met. Chem.*, **24**, 210 (1999).

30. A. K. Boudalis, U. Nastopoulos, S. P. Perlepes, C. P. Raptopoulu and A. Terzis, *Trans. Met. Chem.*, **26**, 276 (2001).

ABSTRACT

CHAPTER I

Introduction and Literature Survey

This chapter gives a brief account of the importance of copper, molybdenum and nickel complexes. Pertinent literature on the transition and non-transition metal complexes of acyl, aroyl and pyridoyl dihydrazones derived from condensation of acyl-, aroyl-, and pyridoyl dihydrazines, respectively, with variety of aldehydes and ketones has also been presented in this chapter. An attempt has been made to survey literature on these ligands upto date.

CHAPTER II

Experimental

In this chapter the experimental details regarding the preparation of disalicylaldehyde oxaloyldihydrazone have been described. Procedure for elemental analyses, physico-chemical techniques and the instruments used are also presented.

CHAPTER III

Synthesis and Characterization of Monometallic Molybdenum (VI) Complexes derived from Polyfunctional Disalicylaldehyde oxaloyldihydrazone

This chapter deals with the synthesis and characterization monometallic molybdenum (VI) complexes derived from polyfunctional disalicylaldehyde oxaloyldihydrazone (H_4slox).

The monometallic complexes of the compositions: $[MoO_2(H_2slox)(A)]$ {where A = H_2O **(3.1)**, py **(3.2)**, 2-pic **(3.3)**, 3-pic **(3.4)** and 4-pic **(3.5)**} and

$[(MoO_2)_2(H_2slox)_2(NN)]$ {where NN = phen **(3.6)** and bpy **(3.7)**}, have been isolated and described.

All the complexes are either yellow or white in colour, air stable and decompose above 300°C. The complexes are non-electrolyte in DMSO. They are diamagnetic in nature consistent with d^0 electronic configuration of molybdenum.

The electronic spectrum of the free ligand shows bands in the region 290-342 nm assigned to $\pi \rightarrow \pi^*$ and $n \rightarrow \pi^*$ transitions. The complexes show an additional band in the region 413-431 nm assigned to ligand-to-metal charge transfer (LMCT) transition.

The free ligand shows two proton resonance at δ 12.64 (s), 11.00 (s), 8.81 (s) and eight proton resonance in the region 7.57-6.84 (m) ppm, respectively. The signals at δ 12.64, δ 11.00 and δ 8.81 ppm are assigned to arise due to -OH, >NH and -CH=N- protons, respectively, in the ligand. The multiplet in the region δ 7.57-6.84 ppm is assigned to arise due to protons of phenyl ring of the ligand molecule. The ^{1}H NMR spectra of the complexes show one proton resonances in the regions δ 12.64-12.67 and δ 10.98-11.31 ppm, respectively, due to -OH and >NH protons and two proton resonances in the region δ 8.63-9.06 due to -CH=N- protons. The complexes **(3.2)** to **(3.5)** also show an additional resonance in the region δ 8.35-8.54 ppm which have been assigned to arise due to the o-proton of pyridyl ring of the nitrogen donor bases. The ^{1}H NMR spectra of complexes **(3.6)** and **(3.7)** shows new signals at δ 7.89 and δ 8.80 due to phenanthroline and bipyridine protons. The resonance in the region 2.27-2.50 in the complexes **(3.3)** to **(3.5)** has been assigned to methyl protons of substituted pyridine molecules.

The IR spectrum of the ligand shows two bands at 3278 and 3204 cm^{-1}, respectively. The essential feature of this band suggests that they arise from phenolic -OH and >NH groups. A strong band at 1667 cm^{-1} is due to ν (>C=O) group while those at 1627 and 1603 cm^{-1} is due to ν (>C=N-) group. The IR spectra of the complexes also

show bands due to ν (-OH), ν (>NH), ν (>C=O) and ν (>C=N-) groups. Further, the complexes show new band in the region 1518-1533 cm^{-1}. This band is assigned to stretching vibration of NCO group produced as a result of enolization of the half part of the dihydrazone ligand upon coordination to the metal centre. The appearance of strong bands in the region 883-939 cm^{-1} in the IR spectra of the complexes is due to the presence of cis-MoO_2^{2+}. Complexes **(3.2)** to **(3.5)** show an additional new band in the region 1060-1003 cm^{-1} assigned to the ring stretching mode of pyridine and substituted pyridine molecules. Complex **(3.6)** shows two new strong bands at 725 and 840 cm^{-1} while complex **(3.7)** shows only one band at 758 cm^{-1}. These bands are due to the out-of-plane motion of the hydrogen atoms on the heterocyclic rings. The in-plane ring deformation mode of the phenanthroline and bipyridine occurs at 634 and 632 cm^{-1} in complexes **(3.6)** and **(3.7)** respectively.

On the basis of results obtained from various physico-chemical and spectral studies, the tentative structures for the complexes have been proposed at the end of the chapter.

CHAPTER IV

Synthesis and Characterization of Homobimetallic Molybdenum (VI) Complexes derived from Polyfunctional Disalicylaldehyde oxaloyldihydrazone

This chapter deals with the synthesis and characterization of homobimetallic molybdenum (VI) complexes derived from polyfunctional disalicylaldehyde oxaloyldihydrazone.

On the basis of various analytical and physico-chemical data, the complexes isolated in the present chapter are suggested to have the compositions: $[(MoO_2)_2(slox)(A)_2]$ {where A = H_2O **(4.1)**, py **(4.2)**, 2-pic **(4.3)**, 3-pic **(4.4)** and 4-pic **(4.5)**}.

All the complexes are yellow coloured and are air stable. They decompose above 300°C and have molar conductance value in the range 1.8-5.0 $ohm^{-1}cm^2mol^{-1}$ in

DMSO indicating that they are non-electrolyte in this solvent. All the complexes are diamagnetic in nature.

The electronic spectra of the complexes show three bands in the region 292 – 341 nm and an additional broad band in the region 417 – 432 nm. The bands in the region 292 – 341 nm are assigned to intraligand $\pi \rightarrow \pi^*$ and $n \rightarrow \pi^*$ and that in the region 417 – 432 nm is assigned to ligand-to-metal charge transfer (LMCT) transition.

The two proton -OH and >NH signals in the uncoordinated dihydrazone ligand at δ 12.64 and δ 11.00 ppm disappear in the complexes indicating the coordination of the ligand to the metal via deprotonation of phenolic -OH group and via enolized carbonyl group. The singlet at δ 8.81 ppm in the ligand undergoes splitting in the metal complexes. One signal is downfield shifted by about 0.24 ppm and the other signal remains at almost the same position as that in the free ligand. The splitting of >CH=N- signal into two in the ^{1}H NMR of the complexes is a good evidence of the existence of ligand molecule in anti-cis configuration. The complexes **(4.1)** to **(4.5)** show triplet in the region 1.04 -1.25 ppm, quartet in the region 3.21-3.46 ppm and another triplet in the region 4.35-4.37 ppm which are assigned to the $-CH_3$, $-CH_2$ and -OH protons of ethanol molecule. The o-proton signal of pyridyl ring of pyridine or substituted pyridine occurs in the region 8.30-8.58 ppm in the complexes **(4.2)** to **(4.5)**. These complexes except complex **(4.1)** and **(4.2)** also show a new signal in the region 2.30-2.50 ppm which are assigned to arise due to the protons of methyl group of substituted pyridine molecules.

The bands due to phenolic -OH and >NH groups are absent in the IR spectra of the complexes suggesting its involvement in coordination with the metal centre. A new broad band at 3448 cm^{-1} in the IR spectrum of the complex **(4.1)** is due to stretching vibration of -OH group of coordinated water molecules. The IR spectra of the complexes do not show bands due to stretching vibration of (>C=O) group suggesting its involvement in coordination with the metal centre via enolization. Enolization of the ligand is also evident from the appearance of new band due to ν

(NCO) group in the region 1535-1537 cm^{-1} in the complexes. The ν (>C=N-) band on an average shifts to lower frequency by 11-13 cm^{-1} in the metal complexes suggesting the coordination of azomethine nitrogen atom to the metal centre. The complexes **(4.2)** to **(4.5)** also show a weak intensity band in the region 1060-1003 cm^{-1}, which is assigned to ring stretching mode of pyridine, 2-picoline, 3-picoline and 4-picoline molecules. Two strong bands appearing in the region 951 – 912 cm^{-1} in complexes are assigned to the stretching vibration of the cis-MoO_2^{2+} group. The band in the region 951 – 933 cm^{-1} is due to the symmetric stretching vibration of cis-MoO_2^{2+} group while the band in the region 916 – 902 cm^{-1} is due to the asymmetric stretching vibration of the cis-MoO_2^{2+} group.

Based on physico-chemical data and spectral studies, the tentative structures of the complexes have also been suggested at the end of the chapter.

CHAPTER V

Synthesis and Characterization of Monometallic Copper (II) Complexes derived from Polyfunctional Disalicylaldehyde oxaloyldihydrazone

This chapter deals with the synthesis and characterization of monometallic copper (II) complexes derived from polyfunctional disalicylaldehyde oxaloyldihydrazone.

On the basis of various analytical and physico-chemical data, the complexes are suggested to have the compositions: [Cu(H_2slox)] **(5.1)**, [Cu(H_2slox)(A)] {where A = py **(5.2)**, 2-pic **(5.3)**, 3-pic **(5.4)** and 4-pic **(5.5)**}, respectively.

All the complexes are dark green in colour, air stable and decompose above 300°C. The complexes have molar conductance value in the range 1.2-1.8 $ohm^{-1}cm^2mol^{-1}$ in DMSO at 10^{-3} M dilution indicating their non-electrolytic nature. The room temperature magnetic moment values for the complexes are in the range 1.69-1.75 BM which is close to the spin only value of 1.73 BM indicating no appreciable spin-spin interaction between copper atoms.

Apart from the ligand bands, the complexes show a single broad band in the 636 – 661 nm regions with a comparatively very low molar extinction coefficient in the range 59 – 90 $dm^3mol^{-1}cm^2$. Hence, this band is assigned to d-d transition. The essential feature of this band in the 630 – 660 nm regions suggests that it is the combination of three transitions ($^2B_{1g} \rightarrow {}^2A_{1g}$, $^2B_{1g} \rightarrow {}^2B_{2g}$ and $^2B_{1g} \rightarrow {}^2E_g$) It is concluded that all the copper (II) complexes have square-planar geometry.

The $g_{\|}$ value for the copper (II) complexes **(5.1)** to **(5.5)** lies in the range 2.318 – 2.330 at RT and 2.314 – 2.339 at LNT, while the $g_{|}$ value lies in the range 2.111 – 2.119 at RT and 2.104 – 2.125 at LNT, respectively. The EPR spectra of the complexes at RT as well as at LNT in DMSO solution show copper hyperfine splitting due to interaction of unpaired electron of copper (II) ion with the nuclear spin (I = 3/2). The superhyperfine structure at high field has been observed in the copper (II) complex **(5.1)** at LNT and is attributed to the interaction of the unpaired electron of copper (II) ion with the nuclear spin of the N atom from the ligand molecule. The superhyperfine coupling constant $A_{|N}$ = 12G, corresponds to the coupling of electron spin with the nuclear spin of two nitrogen atoms.

The α^2_{Cu} values for the copper (II) complexes **(5.1)** to **(5.5)** are in the range of 0.878 – 0.929 < 1 indicating that the copper (II) complexes have some covalent character. The $A_{\|}$ values for the copper (II) complexes **(5.1)** to **(5.5)** are in the range of 174 - 180 cm^{-1}. The $g_{\|}/A_{\|}$ for the copper (II) complexes **(5.1)** to **(5.5)** lies in the range 129.9 – 132.9 cm, which falls in the range 90 – 140 cm for square-planar copper (II) complexes. All of the copper (II) complexes have $g_{\|}>g_{|}>2.0023$ indicating that the unpaired electron lies in the d_{x2-y2} orbital. G value for the complexes **(5.1)** to **(5.5)** lies in the range 2.80-2.94 at RT and 2.74-3.09 at LNT which is in good agreement with the result reported for the square planar complexes of copper (II).

The essential features of the IR spectra of the complexes **(5.1)** to **(5.5)** in the region 3000 – 3300 cm^{-1} is almost same as that of the ligand. The υ (>NH) band in the complexes remains almost unshifted in position ruling out the possibility of

coordination of ligand to the metal centre through secondary >NH nitrogen atom. The complexes show a very strong band in the region 1533-1527 cm^{-1} in the IR spectra. Although the IR spectrum of the ligand also shows a strong band at 1534 cm^{-1}, yet the intensity of the band in the region 1533-1527 cm^{-1} in the complexes is considerably enhanced as compared to that in the uncoordinated ligand. Hence this band appears to have contribution due to both υ (C-O) (phenolate) and υ (NCO) produced as a result of enolization. The presence of both υ (NCO) group and υ (>C=O) group in the complexes suggests that only one >C=O group undergoes enolization and the other >C=O group remains as such. The υ (>C=N-) band observed at 1627 and 1603 in the free dihydrazone shifts to lower frequency on an average by 2-8 cm^{-1} in the complexes indicating coordination through azomethine nitrogen atom to the metal centre.

The redox behaviors of copper (II) complexes **(5.1)** to **(5.5)** have been studied with the help of cyclic voltammetry.

Based on physico-chemical data and spectral studies, the tentative structures of the complexes have also been suggested at the end of the chapter.

CHAPTER VI

Synthesis and Characterization of Homotrimetallic Copper (II) Complexes derived from Polyfunctional Disalicylaldehyde oxaloyldihydrazone

This chapter deals with the synthesis and characterization of homotrimetallic copper (II) complexes derived from polyfunctional disalicylaldehyde oxaloyldihydrazone.

The complexes were isolated and characterized on the basis of various physico-chemical and spectral studies and were suggested to have the composition $[Cu_3(slox)Cl_2(A)_2]$ {where A = H_2O **(6.1)**, py **(6.2)**, 2-pic **(6.3)**, 3-pic **(6.4)** and 4-pic **(6.5)**}.

The complexes are either green or dark green in colour and decompose above 300°C without melting. The molar conductance values for the complexes in DMSO lies in the region 1.3 – 2.0 $ohm^{-1}cm^2mol^{-1}$ indicating their non-electrolytic nature in this solvent. The magnetic moment value of the complexes **(6.1)** to **(6.5)** lies in the region 2.23-2.56 BM i.e. 0.74 – 0.85 BM per copper atom indicating considerable amount of interaction between the copper atoms in these complexes.

The electronic spectra of the complexes show a new non-ligand band in the region 429 – 435 nm which have high molar extinction coefficient. This band has been assigned to arise due to ligand-metal charge transfer (LMCT) transition. The band in the region 628 – 660 nm is due to d-d transition which indicates square planar environment around copper (II) atom with $^2B_{1g}$ ground state.

The EPR spectra of the complexes in the present study are isotropic in DMSO solution at room temperature. The complexes show anisotropic spectra at LNT characteristic of the systems having axial symmetry. LNT EPR spectra are typical for S = ½ spin systems. The hyperfine splitting constants fall in the region 120-150 G. The $g_{\|}$ values fall in the region 2.407-2.442 while the $g_{|}$ values fall in the range 2.176-2.208. Further, the $g_{\|}/A_{\|}$ values are also found to lie in agreement with the proposed distorted square planar geometry around copper atom. The $g_{\|}/A_{\|}$ values for the present complexes are found to lie in the range 162 – 200 cm, slightly higher than that required for a square planar geometry. Such EPR spectra are typical of a d^9 complex possessing axial symmetry with the unpaired electron present in a $d_{x^2-y^2}$ orbital. The spectra of these complexes do not show any half field ($\Delta Ms = 2$) transition or fine structure and look like a spectrum associated with isolated S = ½ states.

The υ (-OH) and υ (>NH) vibrations disappear in the complexes indicating the coordination of -OH group via deprotonation and involvement of >NH group in coordination via enolization. The disappearance of band due to >C=O group and appearance of new band in the region around 1533 cm^{-1} due to newly created (NCO)

group further supports the enolization of the ligand molecule upon coordination with the metal centre. The bands due to azomethine (>C=N-) group appears in the region 1613-1606 cm^{-1} in the complexes **(6.1)** - **(6.5)** which is shifted to lower frequency on an average by 7-12 cm^{-1}. The shift of this band to lower frequency indicates the coordination of azomethine nitrogen atom to the metal centre. Complexes **(6.1)** to **(6.5)** show two new bands in the low frequency region ~ 180 and ~200 cm^{-1} assigned to arise due to stretching vibration of bridged Cu-Cl group.

The redox behaviors of copper (II) complexes **(6.1)** to **(6.5)** have been examined by cyclic voltammetry.

On the basis of various physico-chemical data and spectral studies, the tentative structures of the complexes have been suggested at the end of the chapter.

CHAPTER VII

Synthesis and Characterization of Nickel (II) Complexes derived from Polyfunctional Disalicylaldehyde oxaloyldihydrazone

This chapter describes the synthesis and characterization of monometallic and homobimetallic nickel (II) complexes derived from polyfunctional disalicylaldehyde oxaloyldihydrazone.

The complexes of the compositions $[Ni(H_2slox)(H_2O)_3]$ **(7.1)**, $[Ni_2(slox)(A)_4]$ {where A = H_2O **(7.2)**, py **(7.3)**, 2-pic **(7.4)**, 3-pic **(7.5)** and 4-pic **(7.6)**, $[Ni_2(slox)(NN)_2]$ {where NN = phen **(7.7)** and bpy **(7.8)**} have been described in this chapter.

The complexes are light greenish yellow, greenish yellow or brown in colour, air stable and have a very high decomposition point (>300°C). The complexes are non-electrolyte in DMSO. The magnetic moment values for the complexes at room temperature is found to lie in the range 2.94-3.10 BM i.e. 1.47-1.55 BM per nickel

(II) ion in complexes **(7.2)** to **(7.6)** while complex **(7.1)** has magnetic moment value of 3.10 BM which falls in the range reported for high-spin octahedral nickel (II) complexes. The magnetic moment values for complexes **(7.2)** to **(7.6)** are considerably less than the values expected for two spin-free nickel (II) ions present in the same molecular unit. This indicates strong metal-metal interaction in the structural unit of the complexes via oxo-bridging which causes substantial lowering of magnetic moment. Complexes **(7.7)** and **(7.8)** have magnetic moment value of 4.95 and 4.80 BM, respectively. The magnetic moment value for these complexes is very near to the theoretical value for four electron spin systems.

Apart from the ligand and charge transfer bands the nickel (II) complexes **(7.1)** to **(7.8)** show two bands in the 615-950 nm range corresponding to the transition $^3A_{2g} \rightarrow {}^3T_{2g}$ (F) (ν_1), and $^3A_{2g} \rightarrow {}^3T_{1g}$ (F) (ν_2), respectively. These two low energy bands observed in the complexes are characteristic of nickel (II) in octahedral environment. The octahedral environment around nickel (II) in these complexes is further supported by the value of $\nu_2/\ \nu_1$ ratio which lies in the region of 1.49-1.51.

The IR spectra of the complexes **(7.2)** to **(7.8)** do not show any band due to ν (-OH) and ν (>NH) groups suggesting the involvement of -OH group in coordination via deprotonation and destruction of amide structure via enolization. The ν (>C=O) band occurs at 1668 cm^{-1} in the complex **(7.1)** with reduced intensity whereas in the rest of the complexes this band is absent. The absence of band due to ν (>C=O) group indicates enolization of the ligand molecule and its coordination to the metal centre via enolized >C=O group in these complexes. The ν (>C=N-) band appears as a single strong band at 1608 cm^{-1} in the complex **(7.1)** while in the remaining complexes it appears as a couple of strong intensity band in the region 1626-1598 cm^{-1}. The appearance of ν (NCO) group in the IR spectra of all the complexes confirms the presence of dihydrazone in enol form. The presence of both ν (>C=O) and ν (NCO) bands in the IR spectrum of the complex **(7.1)** indicates that in this complex only one hydrazone part is enolized while the other hydrazone part remains uncoordinated in keto-form. The nickel (II) complexes **(7.3)** to **(7.6)** also show a

weak intensity band in the region 1020-1010 cm^{-1}, characteristic of ring stretching mode of pyridine, 2-picoline, 3-picoline and 4-picoline molecules.

Based on the various physico-chemical and spectral studies, the tentative structures of the complexes have been assigned at the end of the chapter.

CHAPTER VIII

Synthesis and Characterization of Heterobimetallic Copper, Molybdenum and Nickel Complexes derived from Polyfunctional Disalicylaldehyde oxaloyldihydrazone

This chapter describes the synthesis and characterization of heterobimetallic nickel (II)-molybdenum (VI) and copper (II)-molybdenum (VI) complexes derived from polyfunctional disalicylaldehyde oxaloyldihydrazone.

The complexes of the compositions $[Ni(slox)MoO_2(A)_4]$ {where A = H_2O **(8.1)**, py **(8.2)**, 2-pic **(8.3)**, 3-pic **(8.4)** and 4-pic **(8.5)**}, $[Ni(slox)MoO_2(NN)_2]$ {where NN = bpy **(8.6)** and phen **(8.7)**}, $[Cu(slox)MoO_2(A)_2]$ {where A = H_2O **(8.8)**, py **(8.9)**, 2-pic **(8.10)**, 3-pic **(8.11)** and 4-pic **(8.12)**} and $[Cu(slox)MoO_2(NN)_2]$ {where NN = bpy **(8.13)** and phen **(8.14)**} have been described in this chapter.

The Ni(II)-Mo(VI) complexes are yellow while Cu(II)-Mo(VI) complexes are green or dark green in color. All the complexes are air stable, decompose above 300°C and are non-electrolytic in nature in DMSO. The room temperature magnetic moment for the heterobimetallic complexes **(8.1)** to **(8.7)** is in the range 2.87-3.10 BM while for the complexes **(8.8)** to **(8.14)**, it is in the range 1.69-1.82 BM.

Three non-ligand bands are observed in the nickel (II)-molybdenum(VI) heterobimetallic complexes **(8.1)** to **(8.7)** in the region 413-423, 618-626 and 931-952 nm respectively, whereas in the copper (II)-molybdenum(VI) heterobimetallic complexes **(8.8)** to **(8.14)** only two non-ligand bands are observed in the region 414-

424 and 608-666 nm respectively. The two low energy bands observed in the region 618-626 and 931-952 nm in the complexes **(8.1)** to **(8.7)** correspond to $^3A_{2g} \rightarrow {}^3T_{2g}$ (F) (ν_1) and $^3A_{2g} \rightarrow {}^3T_{1g}$ (F) (ν_2) transitions, characteristic of nickel (II) in octahedral environment. The band in the 610 – 670 nm regions in the complexes (8.8) to (8.14) suggests that it is the combination of three transitions ($^2B_{1g} \rightarrow {}^2A_{1g}$, $^2B_{1g} \rightarrow {}^2B_{2g}$ and $^2B_{1g} \rightarrow {}^2E_g$).

The EPR spectra of the complexes **(8.8)** to **(8.14)** give g values in the order $g_{\|} > g_{|} >$ 2.0023 indicating square planar stereochemistry around copper centre with the unpaired electron lying predominantly in the $d_{x^2-y^2}$ orbital, as evident from the value of the exchange interaction term G.

The IR spectra of the complexes do not show any band due to ν (-OH), ν (>NH) and ν (>C=O) groups. The ν (>C=N-) band appears in the region 1602-1609 cm^{-1}. This band remains either unshifted or shifts to lower frequency in the complexes as compared to the precursor complexes. The band in the region 1512-1552 cm^{-1} is due to ν (NCO) obtained as a result of enolization of the ligand. The couple of new strong intensity bands appearing in the region 881-948 cm^{-1} are characteristic of occurrence of cis-MoO_2^{2+} group in the complexes. A weak intensity band in the region 1000-1070 cm^{-1} is assigned to ring stretching mode of pyridine and substituted pyridine molecules. Complexes **(8.7)** and **(8.14)** show two strong intensity bands at 725-727 and 841-849 cm^{-1} region which are assigned to the out-of-plane motion of the hydrogen atoms on the heterocyclic rings and the hydrogen atoms on the central ring, respectively. In the complexes **(8.6)** and **(8.13)** only one strong band is observed at 756 - 758 cm^{-1} due to out-of-plane motion of the hydrogen atoms as expected for two identical groups of four hydrogen atoms each.

Based on the various physico-chemical and spectral studies, the tentative structures of the complexes have been assigned at the end of the chapter.

LIST OF PUBLICATIONS

1. Synthesis, characterization and crystal structure of manganese (IV) complexes derived from salicylic acid, Ram A. Lal, Samhita Bhaumik, Aka Lemtur, Mahesh K. Singh, Debjani Basumatari, **Sanjesh Choudhury**, Arjun de and Arvind Kumar, *Inorg. Chim. Acta*, 359, 3105-3110 (2006).

2. Synthesis and crystal structure of $[Mn_2(H_2sal)_2(Hsal)_2(H_2O)_4]$. First example of reductive synthesis of binuclear manganese(I) salicylate complex, Ram A. Lal, Aka Lemtur, **Sanjesh Choudhury**, Mithun Chakrabarty, Debjani Basumatary, Mahesh K. Singh, Samhita Bhaumik, Arjun K. De and Arvind Kumar, *Trans. Met. Chem.*, 31, 423-428 (2006).

3. Synthesis and spectral studies of nickel (II) complexes derived from disalicylaldehyde oxaloyldihydrazone, R. A. Lal, **S. Choudhury**, A. Ahmed, M. Chakraborty, R. Borthakur and A. Kumar, *J. Coord. Chem.* (Under revision).

4. Synthesis and spectral characterization of homobimetallic molybdenum (VI) complexes derived from bis(2-hydroxy-1-naphthaldehyde)succinoyldihyarazone, Ram A. Lal, Mithun Chakrabarty, **Sanjesh Choudhury**, Roshmita Borthakur and Arvind Kumar, *J. Coord. Chem.* (Under Revision).

5. Synthesis and spectral studies of dioxomolybdenum (VI) complexes derived from disalicylaldehyde oxaloyldihydrazone, Ram A. Lal, **Sanjesh Choudhury**, Mithun Chakrabarty and Arvind Kumar (Communicated).

6. Synthesis and Characterization of Homobimetallic complex $[(MoO_2)_2(slox)(H_2O)].C_2H_5OH$ from Disalicylaldehyde oxaloyldihydrazone and its Reaction with Monodentate and Bidentate Electron Donor Bases, Ram. A. Lal, **Sanjesh Choudhury**, Mithun Chakrabarty and A. Kumar (Communicated).

ANNEXURE I

The complexes isolated in this paper were characterized mainly by IR, electronic, magnetic moment and conductivity measurements. The results have been considered for publication in the Journal of Coordination Chemistry, 2009.

Synthesis and spectral studies of nickel (II) complexes derived from disalicylaldehyde oxaloyldihydrazone

---

R. A. Lal, S. Choudhury, A. Ahmed, M. Chakraborty, R. Borthakur and A. Kumar.

Synthesis and spectral studies of nickel (II) complexes derived from disalicylaldehyde oxaloyldihydrazone

R. A. Lal[a]*, S. Choudhury[a], A. Ahmed[a], M. Chakraborty[a], R. Borthakur[a] and A. Kumar[b]

[a]Department of Chemistry, North-Eastern Hill University, Shillong 793022, Meghalaya, India.
[b]Institute of Chemistry, Academia Sinica, 128 Academia Road, Sec.2, Nankang, Taipei, 115 Taiwan, ROC.

Abstract

The mononuclear nickel (II) complex $[Ni(H_2slox)(H_2O)_3]$ (1) and polymeric dinuclear complexes $[Ni_2(slox)(A_4)]$ {A = H_2O (2), py (3), 2-pic (4), 3-pic (5) and 4-pic (6)} and the discrete binuclear complexes $[Ni_2(slox)(NN)_3]$ {NN = bpy (7) and phen (8)} have been synthesized from disalicylaldehyde oxaloyldihydrazone (H_4slox) in methanol medium. All of the complexes are non-electrolyte. The complexes (1), (7) and (8) are normal paramagnetic while the binuclear complexes (2) to (6) possess anomalously low μ_{eff} value indicating considerable metal-metal interaction in the structural unit. The discrete binuclear complexes (7) and (8) have no interaction between the two nickel (II) ions present in a single molecule. The anomalously low magnetic moment values in the complexes (2) to (6) is explained in terms of metal-metal interaction via phenoxide oxo-bridging. Such metal-metal interaction is less in the complexes (7) and (8) due to coordination of bulky bipyridine and phenanthroline molecules which do not allow the occurrence of phenoxide bridging. The dihydrazone is coordinated to the metal centre as a dibasic tridentate ligand in keto-enol form in staggered configuration in complex (1) while in the remaining complexes, the dihydrazone is coordinated as a tetrabasic hexadentate ligand in enol form in anti-cis configuration. The metal centre is suggested to have a tetragonally distorted octahedral stereochemistry in the complexes.

Keywords: Nickel complex; disalicylaldehyde oxaloyldihydrazone, molar conductance, magnetic moment, spectroscopic studies.

Introduction

In the last few years a renewed interest in metal based therapy has been raised: in fact, on coordination, bioactive ligands might improve their bioactivity profiles, while inactive ligands may acquire pharmacological properties **[1]**. In addition, metal coordination is one of the most efficient strategies in the design of repository, slow release or long acting drugs **[2]**. Furthermore, metal complexes have gained importance as enzyme inhibitors **[3]**. The synthesis, structural investigation and reaction of transition metal Schiff bases have received a special attention, because of their biological activities as antitumoral, antifungal and antiviral activities **[4]**. Schiff base hydrazones are interesting molecules from the point of view of pharmacology. Hydrazone derivatives are found to possess antimicrobial **[5]**, antitubercular **[6]**, anticonvulsant **[7]** and antiinfammatory **[8]** activities. In particular, the complexes of salicylaldehyde benzoylhydrazone were shown to be a potent inhibitor of DNA synthesis and cell growth **[9]**. This hydrazone also has mild bacteriostatic activity and a range of analogues has been investigated as potential oral ion chelating drugs for genetic

disorders such as thalasemia **[10]**. Further, the antibacterial and antifungal properties of 2, 6-diacetylpyridine bis(acylhydrazone) and their complexes with some first row transition metal ions was studied and reported by Carcelli et al. **[11]**. The iron complexes of the bis dihydrazones were found to be more active than the free ligands themselves.

Nickel is recognized as an important element in nature and so far six nickel-containing enzymes have been identified, which include CO-dehydrogenase, acetyl-CoA synthase, [Ni-Fe] hydrogenase, meyhyl –CoM reductase, urease and NiSOD**[12]**. Moreover, nickel plays a prominent role in several areas of material chemistry. Some typical interplay between nickel coordination chemistry and material science exists in the use of Ni-containing alkoxides for the synthesis of ceramic materials MOCUD and sol-gel processes, the preparation of nanoscopic dendrimers incorporating nickel, the construction of 3D hybrid inorganic-organic porous materials with Ni-coordination units and the fabrications of supported Ni catalysts and Ni nanostructures through nanotechnology. Paramagnetic high spin nickel (II) has found particular attention in the field of molecular magnetism, culminating in the recent discovery of the first single molecule magnets based on nickel (II) centres **[13]**.
Disalicylaldehyde oxaloyldihydrazone is a potential polyfunctional ligand containing amide, azomethine and phenol functions in duplicate. This is related to salicylaldehyde benzoylhydrazone in the sense the benzene ring of hydrazone part has been replaced by another acylhydrazone part. Thus in this dihydrazone, the two hydrazone parts are directly bonded to one another which gives it better multidentate character than salicylaldehyde benzoylhydrazone. Hence, depending upon the preferred stereochemical disposition of the metal valences and the nature of the bonds formed in the coordination process, it may offer several alternate modes of bonding and is capable of giving rise to mononuclear and polynuclear complexes involving ligand and phenolic oxygen bridging. Further, this dihydrazone is related to 2, 6-diacetylpyridine bis(acylhydrazones) in the sense that the oxaloyl-fragment of the ligand is capable of imposing planarity over the two hydrazone parts as the pyridyl ring exerts in 2, 6-diacetylpyridine bis(acylhydrazone).

A survey of literature reveals that although few complexes of the nickel (II) ion with the dihydrazone derived from the condensation of salicylaldehyde and related o-hydroxy aromatic aldehydes and ketones with malonoyldihydrazine and other acyldihydrazines, aroyldihydrazines and pyridoyldihydrazines have been reported **[14-17]**, yet it has failed to locate any study on metal complexes of the dislicylaldehyde dihydrazone containing oxaloyl-fragment.

In view of above medicinal importance of hydrazones and their metal complexes and importance of nickel in biological systems and material science and absence of work on metal complexes of disalicylaldeyde oxaloyldihydrazone (H_4slox, Fig. 1) and its relationship with salicylaldehyde benzoylhydrazone and 2, 6-diacetylpyridine bis(acylhydrazone), it was of interest to study the nickel (II) complexes with the title ligand. Accordingly, the present paper describes the synthesis, characterization and stereochemical investigation of metal complexes derived from reaction of nickel acetate with the title ligand under different experimental conditions.

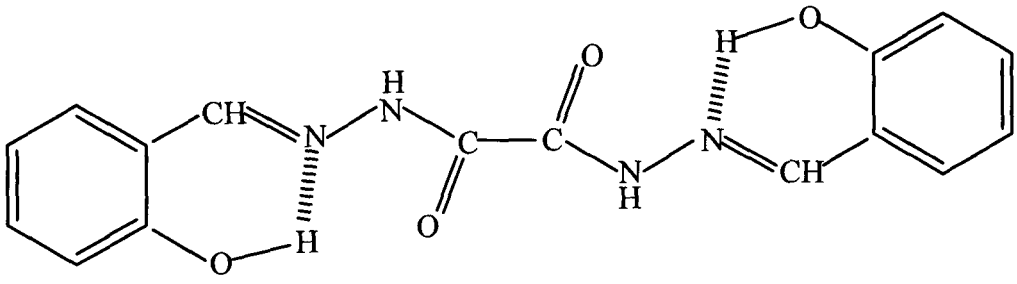

Fig.1. Disalicylaldehyde oxaloyldihydrazone (H_4slox)

Experimental

All the reagents were commercial grade materials and were used without further purification. The ligand disalicylaldehyde oxaloyldihydrazone (H_4L) was prepared in two steps. In the first step, oxaloyldihydrazine (ODH) was prepared by reacting diethyl oxalate (10.30 g, 7.33 mmol) in ethanol (30 mL) with hydrazine hydrate (7.70 g, 15.4 mmol). The product was recrystallized from hot water. In the second step, disalicylaldehyde oxaloyldihydrazone was prepared by reacting a warm dilute ethanol solution (100 mL) of oxaloyldihydrazine (2.00 g, 1.70 mmol) with salicylaldehyde (5.08 g, 4.24 mmol). The product was suction filtered, washed with ethanol and dried over anhydrous $CaCl_2$. [Yield: 82%] (m.p. 284°C). Anal. Calcd. for $C_{16}H_{14}N_4O_4$ (%): C, 58.90; H, 4.29; N, 17.18. Found: C, 58.42; H, 4.24, N, 17.17. λ_{max}(nm) (ε_{max}) (dm^3 $mol^{-1}cm^{-1}$): 293(10461), 303(10494), 340(11225).

Chemical analyses of carbon, hydrogen and nitrogen were performed by means of micro analytical methods using a Perkin-Elmer 240C microanalyser. The nickel content of the complexes was estimated gravimetrically as nickel dimethyl glyoximate **[18]**. IR spectra were recorded on either Perkin-Elmer model 983 spectrophotometer or Nicolet-Impact 410 FT-IR Spectrophotometer, from a KBr pellets in the 4000-400 cm^{-1} range. The UV-visible spectra for the complexes in the 200-1000 nm range were recorded on a Perkin-Elmer Lambda-25 spectrophotometer. Magnetic susceptibility measurements were performed using Sherwood Magnetic Susceptibility Balance. The molar conductance of the complexes at 10^{-4} M dilution in DMSO solution was measured on a Direct Reading Conductivity meter-304 with a dip type conductivity cell at room temperature.

Preparation of the complexes

Synthesis of [Ni(H_2slox)(H_2O)$_3$] (1)

H_4slox (1.00 g, 3.07 mmol) was suspended in methanol (60 mL) with constant stirring for a period of 15-20 minutes to make the homogeneous suspension. To this homogeneous suspension was added slowly a solution of $Ni(OAc)_2.4H_2O$ (0.77 g, 3.10 mmol) in methanol (30 mL) with constant stirring over a period of 30 minutes maintaining $Ni(OAc)_2.4H_2O$ and H_4slox molar ratio at 1.01:1. The resulting mixture was refluxed for about 1 1/2 h which precipitated a greenish yellow coloured compound which was then suction filtered and purified by washing several times with 10 mL hot methanol, each time, followed by ether and finally dried over anhydrous $CaCl_2$. Yield: 86.5%.

Synthesis of $[Ni_2(slox)(H_2O)_4]$ (2); $[Ni_2(slox)(A)_4]$ (where A = pyridine (py, 3), 2-picoline (2-pic, 4), 3-picoline (3-pic, 5), 4-picoline (4-pic, 6)); $[Ni_2(slox)(NN)_3]$ (where NN = 1,10-phenanthroline (phen, 7) and 2,2'-bipyridine (bpy, 8).

The preformed ligand, H_4slox (0.50 g, 1.53 mmol) was suspended in methanol (30 mL) with continous stirring under hot condition to make a homogeneous suspension. This homogeneous suspension was added to a solution of $Ni(OAc)_2.4H_2O$ (1.14 g, 4.58 mmol) in methanol (40 mL) in hot condition over a period of 15-20 minutes accompanied by constant stirring and the mixture was subjected to reflux for about 3 h. This yielded a greenish yellow precipitate which was suction filtered under hot condition and purified by washing several times with 10 mL hot methanol, each time, followed by ether and finally dried over anhydrous $CaCl_2$. Yield: 82.3%.

The complexes $[Ni_2(slox)(A)_4]$ (where A = pyridine (py, 3), 2-picoline (2-pic, 4), 3-picoline (3-pic, 5), 4-picoline (4-pic, 6)) were also prepared essentially by the above procedure by adding 1.82 mL of pyridine, 2-picoline, 3-picoline and 4-picoline respectively to the suspension of $[Ni_2(slox)(H_2O)_4]$ in methanol (30 mL) and refluxing the resulting solution for 1 h. Yield. 74-76%.
The complexes $[Ni_2(slox)(NN)_3]$ (where NN = 1,10-phenanthroline (phen, 7) and 2,2'-bipyridine (bpy, 8)) were prepared essentially by following the above mentioned procedure using 1.17 g (5.90 mmol) of 1,10-phenanthroline and 0.92 g (5.89 mmol) of 2,2'-bipyridine instead of pyridine maintaining molar ratio of $[Ni_2(slox)(H_2O)_4]$ and bidentate ligand at 1:3. Yield 70-72%.

Results and Discussion

The complexes together with their colour, decomposition point, analytical, molar conductance, magnetic moment and electronic spectral data are set out in the Table 1. The general compositions of the complexes are: $[Ni(H_2slox)(H_2O)_3]$ (1), $[Ni_2(slox)(A)_4]$ (where A = H_2O (2), pyridine (py, 3), 2-picoline (2-pic, 4), 3-picoline (3-pic, 5), 4-picoline (4-pic, 6)), $[Ni_2(slox)(NN)_3]$ (where = 1,10-phenanthroline (phen, 7), = 2,2'-bipyridine (bpy, 8)).

These complexes are greenish yellow, yellow or brown in colour and have a very high decomposition point. All the complexes are insoluble in common organic solvents but soluble in highly coordinating solvents such as DMF and DMSO and are air stable.

Thermal studies

Complexes (1) and (2) show loss of weight corresponding to three and four water molecules at 180°C indicating that they are coordinated to the nickel centre. On the other hand, complexes (3) to (8) show weight loss at 220°C corresponding to four pyridine/substituted pyridine molecules and three 1,10-phenanthroline/bipyridine molecules. The loss of these donor molecules at such a high temperature suggests that they are present in the first coordination sphere around the metal centre **[19]**.

Molar conductance

The molar conductivity values for all the complexes in DMSO were in the range 2.5-3.9 $ohm^{-1} cm^2 mol^{-1}$ suggesting them to be non-electrolytes **[20]**.

Magnetic moment

The nickel (II) complex (1) has magnetic moment value of 3.10 BM which falls in the range reported for high spin octahedral nickel (II) complexes **[21]**. The magnetic moment values for the complexes (2) to (6) lie in the range 2.94 – 3.10 BM i.e. 1.47-1.55 BM per nickel (II) ion. Such a low value of magnetic moment in these complexes rules out low-spin square planar stereochemistry. But these values are considerably less than the values expected for two spin-free nickel (II) ions present in the same molecular unit. This indicates strong metal-metal interaction in the structural unit of the complexes. Anomalous magnetic moment values in the solid state have been explained on the basis of absorption spectra by proposing mixed octahedral and square planar stereochemistry due to molecular association **[22]**, but the electronic spectra of the complexes are consistent with their tetragonally distorted octahedral stereochemistry. Hence, it is suggested that the lowering of magnetic moment in these complexes is due to the presence of oxo-bridged structure **[23]**.

The complexes (7) and (8) have higher magnetic moment values of 4.95 and 4.80 BM, respectively. The magnetic moment value for these complexes is 2.48 and 2.40 BM per metal ion respectively. The μ_{eff} value per metal ion is again less than the value required for two unpaired electrons. This value suggests that some antiferromagnetic interaction is present between the two metal centres in the complexes. It is imperative to mention that the antiferromagnetic interaction in these complexes is less than those in the complexes (2) to (6) which may be attributed to coordination of 1,10-phenanthroline and bipyridine in these complexes which due to their bulky nature do not allow the two nickel (II) ions to come close to each other via oxo-bridging.

Electronic Spectra

The important electronic spectral bands for the title ligand and the nickel (II) complexes derived from it are presented in the Table 1, along with their molar extinction coefficient.

All of the complexes show two weak bands in the regions 907-946 and 617-650 nm, respectively in addition to the ligand bands. These bands are described to $^3A_{2g} \rightarrow {}^3T_{2g}$ (F) and $^3A_{2g} \rightarrow {}^3T_{1g}$ (F), transitions, respectively. The positions of these bands suggest that these complexes have tetragonally distorted octahedral stereochemistry.

The ligand field parameters **[24]** viz. Racah inter-electronic repulsion parameter (B), ligand field splitting energy (10Dq), covalency factor (β) and ligand field stabilization energy (LFSE) have been calculated for the nickel (II) complexes **(1)** to **(8)** and the values have been presented in Table 2.

The values of v2/ v1 for tetragonal complexes are found significantly higher than the usual range for octahedral complexes and sometimes greater than the theoretical limit of 1.80 for octahedral symmetry. The interaction between $^3T_{1g}$ (P) and $^3T_{1g}$ (F) states **[25]** gradually

lowers the ratio ν_2/ν_1 from the theoretical value of 1.80 to 1.50 – 1.70 and values of 1.60 – 1.70 are common for nickel (II) complexes of octahedral symmetry. In the present complexes the ν_2/ν_1 values lie in the range 1.49 – 1.51 which is slightly lower than the lower limit for usual octahedral complexes but are within the range reported for octahedral complexes **[26]**. These low value indicates a strong interaction between $^3T_{1g}$ (P) and $^3T_{1g}$ (F) states of the nickel (II) complexes. The ligand field stabilization energy for the nickel (II) complexes (1) to (8) lies in the range 36.2 – 37.0 kcal/mol.

Infrared Spectra

A comparison of the IR spectra of the free dihydrazone (H_4slox) with those of the complexes suggests that it is present in keto-enol form in complex (1) and enol form in the remaining complexes (Table 3).

The bands at 3278, 3204 and 1667 cm^{-1} in the free ligand arise due to the stretching vibration of phenolic –OH, secondary –NH and >C=O groups, respectively, which are in accordance with the literature reports **[27-34]**. The IR spectrum of the complex (1) shows these bands are almost at the same position as in the uncoordinated dihydrazone but considerably reduced in intensity. This shows that the half portion of the ligand molecule remains unbonded in the complex. The reduction in intensity of these bands in the complex indicates that the other half portion of the dihydrazone is bonded to the metal ion, most probably, in the enolized form **[32]**. The IR spectra of the complexes (2) to (8) do not show any band in these regions. The absence of band due to phenolic –OH group in the IR spectra of the complexes indicates the involvement of –OH group in bonding to the metal centre via deprotonation while the absence of band due to stretching vibration of secondary –NH group and >C=O group indicates that the secondary –NH and carbonyl groups are destroyed upon complexation with the metal atom, most probably, via enolization **[27, 29, 34]**.

The present ligand shows two very strong bands at 1627 and 1603 cm^{-1} due to stretching vibration of >C=N group. This band appears in the form of a single strong band at 1608 cm^{-1} in the complex (1) while in the remaining complexes it appears as a couple of strong intensity band in the region 1626-1588 cm^{-1} **[34-36]**. The average position of the ν (C=N) band shifts to lower frequency by 2-7 cm^{-1} in all of the complexes except complexes (7) and (8) where the shift to lower frequency is of about 17 and 11 cm^{-1}, respectively. The shift of ν (C=N) band to lower frequency indicates coordination of the dihydrazone through azomethine group to the metal centre. It is imperative to mention that ν (C=N) band appears as a single band in the complex (1), while it is split into two bands in the remaining complexes (2) to (8). The appearance of ν (C=N) vibration as a single band in the complex (1) suggests that the dihydrazone coordinates to the metal centre in staggered configuration while the splitting of ν (C=N) vibration into two bands in the complexes (2) to (8) suggests that the dihydrazone is bonded to the metal centre in anti-cis configuration **[29, 37]**.

The free dihydrazone shows a strong band at 1534 cm^{-1}. This band is assigned to have a composite character due to mixed contribution of the amide II and ν (C-O) bands. This band shifts to higher frequency by 3 cm^{-1} in the complex (1) and appears at 1537 cm^{-1}. Such a small positive shift of this band indicates coordination of phenolate atoms to the metal

centre but at the same time dismissing the possibility of involvement of phenolate oxygen atom in bridge formation **[38]**. However, a positive shift of about 17-24 cm^{-1} is observed for this band in the complexes (2) to (6). A positive shift of more than 10 cm^{-1} is indicative of involvement of phenolate C-O group in bonding with metal ion accompanied by oxo-bridging **[39]**. The shift of ν (C-O) (phenolate) by about 17-24 cm^{-1} indicates that the phenolate oxygen atom is involved in bonding to the metal ion in the complexes (2) to (6) accompanied by oxo-bridging. A new strong intensity band appearing in the region 1503-1533 cm^{-1} in all of the complexes except complex (1) has been assigned to stretching vibration of the newly created NCO^- group **[40]**. The appearance of ν (NCO^-) group in the IR spectra confirms the presence of dihydrazone in enol form in the complexes (2) to (8). It is imperative to mention that the intensity of the band at 1537 cm^{-1} is considerably increased in the complex (1). It appears that this band has contribution both due to ν (C-O) (phenolate) and ν (NCO^-). This suggests involvement of phenolate C-O and enolate C-O groups in bonding via enolization of half part of the dihydrazone molecule.

The complexes (2) to (6) show a weak band in the region 810-820 cm^{-1}. This band is observed neither in the IR spectra of the uncoordinated ligand nor in those of the complexes (1), (7) and (8). Hence this band is assigned to stretching vibration of tetraatomic species 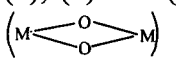 indicating presence of oxo-bridging in the complexes involving phenoxide oxygen atom **[41]**. The weak band observed at 1035 cm^{-1} in the ligand is assigned to υ (N–N) vibration. This band shifts to higher frequency by 5-14 cm^{-1} in the metal complexes indicating involvement of only one nitrogen atom of N-N group in coordination **[42]**. The new weak to medium intensity band appearing in the region 560-599 cm^{-1} and a weak intensity band in the region 434-476 cm^{-1} in the complexes (1) to (8) have been assigned to the stretching vibration of Ni-O (phenolic) and Ni-O (enolized carbonyl) bond indicating bonding of phenolate oxygen atom and enolized carbonyl oxygen atom to the metal centre, respectively **[43]**.

The free pyridine bases absorb around 604 cm^{-1}due to in-plane ring deformation mode **[43]**. In the complexes a new weak band is observed in the region 600 – 620 cm^{-1}. This band is assigned to arise due to in-plane deformation mode of pyridine and substituted pyridine indicating their coordination to the metal centre. In the complex (7) strong intensity bands are observed at 726 cm^{-1} and 848 cm^{-1} which are assigned to the out of plane motion of the hydrogen atoms on the heterocyclic rings and the hydrogen atoms on the centre ring of 1,10-phenanthroline molecule, respectively **[44]**. In the Ni (II) bipyridyl complex only one band is observed at 736 cm^{-1} due to out-of-plane motion of the hydrogen atoms as expected for two identical groups of four hydrogen atoms each **[45]**. Apart from these bands, complex (7) and complex (8) also show a medium broad band at 648 and 652 cm^{-1}which is assigned to arise due to in-plane ring deformation mode of 1,10-phenanthroline and 2,2'-bipyridine indicating their coordination to the metal centre.

Conclusion

In the present paper, we have described some mononuclear, binuclear and polynuclear complexes and characterized them on the basis of data obtained from physic-chemical and spectroscopic studies. The dihydrazone is bonded to metal centre in complex (1) as a dibasic

tridentate ligand through one phenolate oxygen atom, one enolate oxygen atom and one azomethine nitrogen atom, respectively. On the other hand, in the remaining complexes, the dihydrazone coordinates to the metal centre as a tetrabasic hexadentate ligand through both the phenolate oxygen atoms, both the enolate oxygen atoms and both the azomethine nitrogen atoms, respectively. In the complexes (2) to (8), one metal atom is bonded to two phenolate oxygen atoms and two azomethine nitrogen atoms occupying NNOO coordination chamber while the other metal atom is bonded to the two enolate oxygen atoms. In the complexe (2) to (6), the metal atom bonded to enolate oxygen atoms is tethered to another metal atom present in the NNOO coordination chamber from second complex molecule through phenoxide bridging leading to extended structure in two dimension giving rise to polynuclear character to the complexes. On the other hand, in the complexes (7) and (8), no such oxo-bridging is present, most probably, due to coordination of bulky bipyridine and phenanthroline molecules which give rise to discrete molecularity to these complexes. The dihydrazone coordinates to the metal centres in staggered configuration in complex (1) while in the anti-cis configuration in the remaining complexes (2) to (8). Water, pyridine, substituted pyridine and bidentate donor molecules bipyridine and phenanthroline are coordinated to the metal centre. The complex (1) is normal paramagnetic to the extent of two unpaired electrons corresponding to one high-spin nickel (II) ion while the complexes (7) and (8) possess magnetic moment values to the extent of four unpaired electrons corresponding to the presence of two nickel (II) ions per dihydrazone molecule with no metal-metal interaction. On the other hand, the complexes (2) to (6) possess anomalously low values of magnetic moment indicating metal-metal interaction in their structural unit via oxo-bridging. All of the complexes possess distorted octahedral stereochemistry around the metal centre. The tentative structures for the complexes are shown in Figs. 2, 3 and 4, respectively.

References

1. F. Lebon, M. Ledecq, Z. Benatallah, S. Sicsic, R. Lapouyade, O. Kahan, A. Garcon, M. Reboud-Ravaux, F. J. Durant, *J. Chem. Soc., Perkin Trans.*, **2**, 795 (1999).
2. N. Bharti, M. R. Maurya, F. Naqvi, A. Bhattacharya, S. Bhattacharya, A. Azam, *Eur. J. Med. Chem.*, **35**, 481 (2000).
3. A. Y. Louie, T. J. Meade, *Chem. Rev.*, **99**, 2711 (1999).
4. S. K. Sridhar, S. N. Pandeya, J. P. Stables, A. Ramesh, *Eur. J. Pharm. Sci.*, **16**, 129 (2002).
5. P. Vicini, F. Zani, P. Cozzini, I. Doytchinova, *Eur. J. Med. Chem.*, **37**, 553 (2002).
6. B. Kocyigit-Kaymakcioglu, S. Rollas, *Farmaco*, **57**, 595 (2002).
7. J. V. Ragavendran, D. Sriram, S. K. Patel, I. V. Reddy, N. Bharathwajan, J. Stables, P. Yogeeswari, *Eur. J. Med. Chem.*, **42**, 146 (2007).
8. S. Rollas, N. Gulerman, H. Erdeniz, *Farmaco*, **57**, 171 (2002).
9. D. K. Johnson, T. B. Murphy, N. J. Rose, W. H. Goodwin, L. Pickart, *Inorg. Chim. Acta*, **67**, 159 (1982).
10. J. L. Buss, B. T. Greene, J. Turner, F. M. Torti, S. V. Torti, *Curr. Top. Med. Chem.*, **4**, 1623 (2004).
11. M. Carcelli, P. Mazza, C. Pelizi, F. Zani, *J. Inorg. Biochem.*, **57**, 43 (1995).

12. A. Sigel, H. Sigel and R. K. O Siegel (Eds.), "*Nickel and Its Surprising Impact in Nature*", John Wiley and Sons, Ltd., Chichester, U. K., (2007); Metal Ions in Life Science, Vol. **2**.
13. C. G. Young in: J. A. McCleverty, T. J. Meyer, A. Wedd (Eds.), "*Comprehensive Coordination Chemistry II*", Vol. 6, Elsevier (Pergamon), p. 249-554 (2004).
14. R. A. Lal, D. Basumatary, S. Adhikari and A. Kumar, *Spectrochim. Acta*, **69A**, 706-714 (2008).
15. A. Bonardi, S. Ianelli, C. Pelizzi, G. Pelizzi and C. Solinar, *Inorg. Chim. Acta*, **232**, 211 (1995).
16. R. A. Lal and D. Basumatary, *Trans. Met. Chem.*, **32**, 481-493 (2007).
17. G. Paolucci, S. Telluto, S. Sitran, D. Aju, F. Benetollo, A. Polo and G. Bombieri, *Inorg. Chim. Acta.*, **193**, 57 (1992).
18. A. I. Vogel, "*Text book of Quantitative Inorganic Analysis*", (ELBS and Longman), 4th Ed., p. 379 (1978).
19. R. A. Lal, S. Adhikari, A. Kumar, J. Chakraborty and S. Bhaumik, *Synth. React. Inorg. Met-Org. Chem.*, **32(1)**, 81-96 (2002).
20. J. W. Geary, *Coord. Chem. Rev.*, **7**, 81 (1971).
21. S. M. E. Khalil, H. S. Seleem, B. A. El-Shetary, M. Shebl, *J. Coord. Chem.* **55**, 883 (2002).
22. V. V. Sawant, J. Gopalkrishnan and C. C. Patel, *Inorg. Chem.*, **9**, 748 (1970); W. Levason and C. A. McAuliff, *Inorg. Chim. Acta*, **18**, L5 (1975).
23. R. C. Aggarwal and K. K. Narang, *Inorg. Chim. Acta*, **7**, 651 (1973).
24. R. S. Drago, "*Physical Methods in Inorganic Chemistry*", Reinhold Publishing Corporation, New York (1968).
25. A. B. P. Lever, *Coord. Chem. Rev.*, **3**, 119 (1968).
26. Z. H. Abd El-Wahab, *Spectrochim. Acta*, **67A**, 25 (2007).
27. D. Y. Wu, G. Wu, W. Huang and C. Y. Duan, *Polyhedron*, **27**, 947 (2008).
28. A. Bolger, G. Ferguson, J. P. James, C. Long, P. McArdle and J. G. Vos, *J. Chem. Soc., Daltons Trans.*, 1577 (1993).
29. R. A. Lal, D. Basumatary, S. Adhikari and A. Kumar, *Spectrochim. Acta*, **69A**, 706 (2008).
30. L. Zhao, V. Niel, L. K. Thompson, Z. Xu, V. A. Milway, R. G. Harvey, D. O. Miller, G. D. Wilson, M. Leech, J. A. K. Howard and S. L. Heath, *J. Chem. Soc., Daltons Trans.*, 1446 (2004).
31. C. T. Yang, J. D. Ranford and J. J. Vittal, *Synth. React. Inorg. Met-Org. Nano-Met. Chem.*, **35**, 71 (2005).
32. V. P. Singh and P. Gupta, *J. Coord. Chem.*, **59**, 1483 (2006).
33. M. F. Iskander, A. F. M. Hefny, L. El-Sayed and S. E. Zayan, *J. Inorg. Nucl. Chem.*, **38**, 2209 (1976).
34. M. Carcelli, S. Ianelli, P. Pelagatte, G. Pelizzi, C. Solinas and M. Tegoni, *Inorg. Chim. Acta*, **358**, 903 (2005).
35. R. A. Lal, S. Adhikari, A. Pal, A. N. Siva and N. Kumar, *J. Chem. Res. (S)*, 122 (1997); *J. Chem. Res. (M)*, 749 (1997).
36. R. A. Lal, L. M. Mukherjee, A. N. Siva, A. Pal, S. Adhikari, K. K. Narang and M. K. Singh, *Spectrochim. Acta*, **50A**, 1005 (1994).

37. R. A. Lal, L. M. Mukherjee, A. N. Siva, A. Pal, S. Adhikari, K. K. Narang and M. K. Singh, *Polyhedron*, **12**, 2551 (1993).
38. S. Purohit, A. P. Koley, L. S. Prasad, P. T. Manoharan and S. Ghosh, *Inorg. Chem.*, **28**, 3935 (1989).
39. U. Casellato, P. Guerriero, S. Tamburini, P. A. Vigato and S. Sitran, *J. Chem. Soc. Dalton Trans.*, 2145 (1991).
40. K. R. Barnard, M. Bruch, H. Susan, I. H. Enemark, R. W. Gable and A. G. Wedd, *Inorg. Chem.*, **36**, 637 (1997).
41. V. L. Pecoraro, D. P. Kessissoglou and W. M. Butler, *Inorg. Chem.*, **26**, 495 (1987).
42. R. Gup and B. Kirkan, *Spectrochim. Acta*, **62A**, 1188 (2005).
43. K. Nakamoto, "*Infrared and Raman Spectra of Inorganic and Coordination Compounds*", 4th Ed., John Wiley and Sons, New York (1986).
44. Mudasir, N. Yoshioka and H. Inoue, *Trans. Met. Chem.*, **24**, 210 (1999).
45. A. K. Boudalis, U. Nastopoulos, S. P. Perlepes, C. P. Raptopoulu and A. Terzis, *Trans. Met. Chem.*, **26**, 276 (2001).

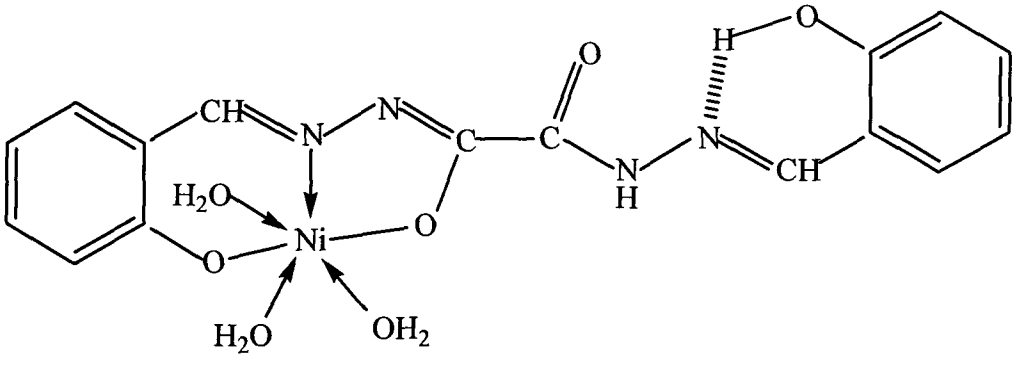

Fig. 2. Tentative structure for $[Ni(H_2slox)(H_2O)_3]$ (1)

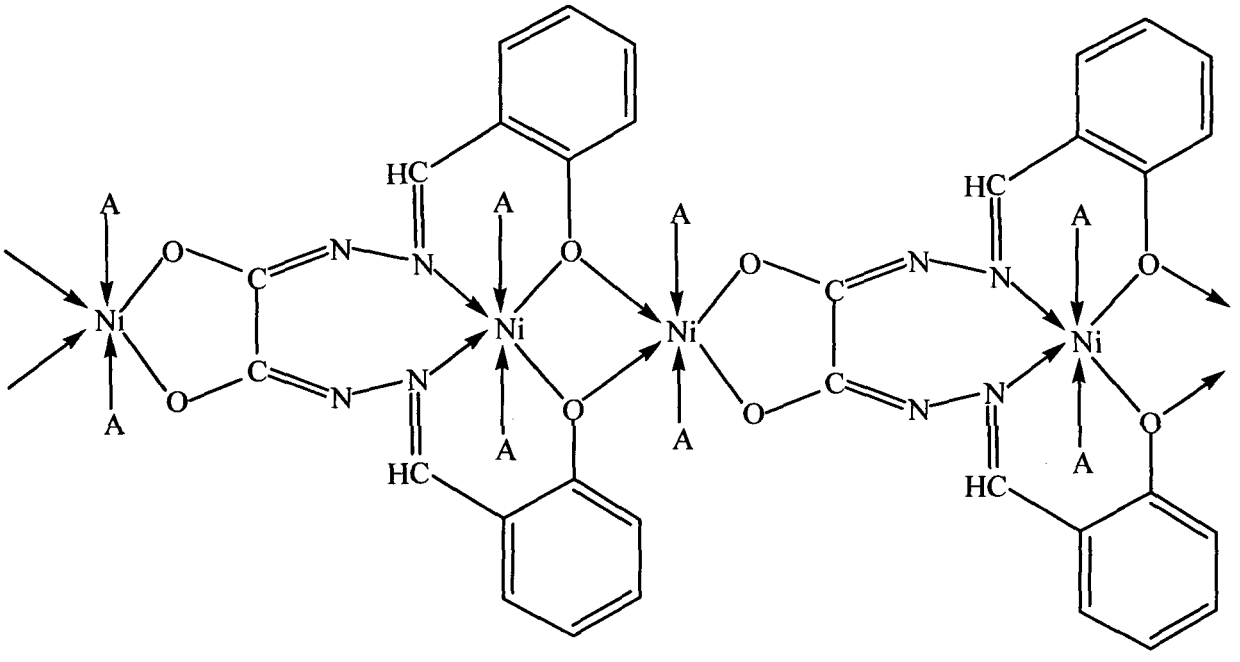

Fig. 3. Tentative structure for $[Ni_2(slox)(A)_4]$ (where A = H_2O (2), py (3), 2-pic (4), 3-pic (5), 4-pic (6)).

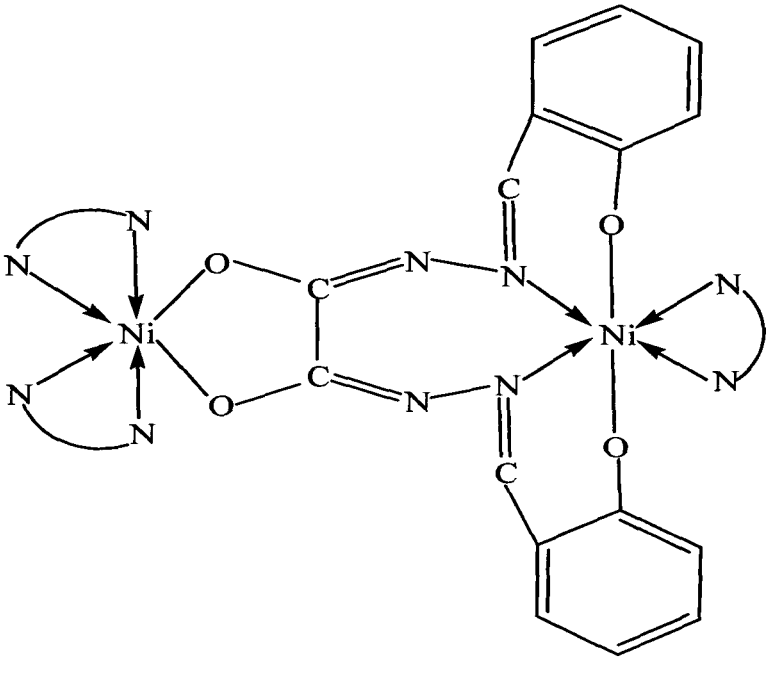

Fig. 4. Tentative structure for $[Ni_2(slox)(NN)_3]$ (where NN = phen (7) and bpy (8)).

Table 1. Complex, colour, decomposition point, analytical, molar conductance, magnetic moment and electronic spectral data for nickel (II) complexes.

Sl. No.	Complex/Colour	D.P. (°C)	Elemental Analysis: Found (Calcd)%				Molar conductance Λ_M (ohm^{-1} cm^2 mol^{-1})	Magnetic Moment μ_{eff} (BM)	Electronic spectral band λ_{max}(nm) (ε_{max}) (dm^3 $mol^{-1}cm^{-1}$)
			M	C	H	N			
1	$[Ni(H_2slox)(H_2O)_3]$	>300	13.76 (13.44)	44.25 (43.97)	4.10 (4.12)	13.11 (12.82)	2.5	3.10	303(9053) 333(8350) 420(5720) 619(95) 932 (55)
2	$[Ni_2(slox)(H_2O)_4]$	>300	22.62 (22.95)	38.00 (37.55)	3.17 (3.13)	11.15 (10.95)	3.1	2.94	297(9786) 306(8971) 432(5884) 615(69) 929(32)
3	$[Ni_2(slox)(py)_4]$	>300	15.93 (15.53)	57.41 (57.16)	3.68 (3.70)	14.66 (14.82)	2.9	2.96	295(9903) 307(8895) 431(5884) 617(69) 931(33)
4	$[Ni_2(slox)(2\text{-}pic)_4]$	>300	14.91 (14.46)	59.60 (59.12)	4.40 (4.43)	13.92 (13.79)	2.6	2.99	297(9899) 308(8746) 429(5959) 628(69) 946(31)
5	$[Ni_2(slox)(3\text{-}pic)_4]$	>300	14.82 (14.46)	58.82 (59.12)	4.47 (4.43)	14.05 (13.79)	3.0	2.98	296(9939) 307(8895) 426(5951) 633(67) 941(31)
6	$[Ni_2(slox)(4\text{-}pic)_4]$	>300	14.06 (14.46)	58.75 (59.12)	4.41 (4.43)	14.13 (13.79)	2.9	3.10	298(9898) 307(8890) 412(5947) 623(70) 940(32)
7	$[Ni_2(slox)(phen)_3]$	>300	11.81 (11.35)	60.51 (60.35)	3.04 (3.09)	13.84 (13.54)	3.7	4.95	297(7000) 307(7043) 397(4137) 629(86) 950(52)
8	$[Ni_2(slox)(bpy)_3]$	>300	13.26 (12.93)	60.32 (60.80)	3.55 (3.52)	15.17 (15.42)	3.9	4.80	297(9900) 308(8746) 426(5955) 622(69) 932(43)

Table 2. Electronic spectral bands and ligand field parameters for the nickel (II) complexes.

Sl. No.	Complex	$^3A_{2g} \rightarrow {}^3T_{2g}$ (F)		$^3A_{2g} \rightarrow {}^3T_{1g}$ (F)		Dq	ν_2/ν_1	B	β	β°	LFSE
1	$[Ni(H_2slox)(H_2O)_3]$	10730	932	16155	619	1073.0	1.506	607.36	0.585	41.5	36.9
2	$[Ni_2(slox)(H_2O)_4]$	10764	929	16260	615	1076.4	1.511	619.61	0.597	40.3	37.0
3	$[Ni_2(slox)(py)_4]$	10741	931	16207	617	1074.1	1.509	614.75	0.592	40.8	36.9
4	$[Ni_2(slox)(2\text{-}pic)_4]$	10571	946	15924	628	1057.1	1.506	599.95	0.578	42.2	36.3
5	$[Ni_2(slox)(3\text{-}pic)_4]$	10627	941	15798	633	1062.7	1.487	564.72	0.544	45.6	36.5
6	$[Ni_2(slox)(4\text{-}pic)_4]$	10638	940	16051	623	1063.8	1.509	608.75	0.586	41.4	36.5
7	$[Ni_2(slox)(phen)_3]$	10526	950	15898	629	1052.6	1.510	605.42	0.583	41.7	36.2
8	$[Ni_2(slox)(bpy)_3]$	10730	932	16077	622	1073.0	1.500	592.79	0.571	42.9	36.9

Table 3. Infrared spectral data for disalicylaldehyde oxaloyldihydrazone and its nickel (II) complexes.

Sl. No.	Ligand/complex	ν(OH) + ν(NH)	ν(C=O)	ν(C=N)	AmideII + ν(C-O)	ν(NCO^-)	ν(C-O)	ν(N-N)	ν(M-O) (phenolic)	ν(M-O) (carbonyl)	ν(M<O>M)
	H_4 slox	3278(s) 3204(s) 3050(s)	1667(s)	1627(s) 1603(s)	1534(s)	-	1262(s)	1035(m)	-	-	-
1	$[Ni(H_2slox)(H_2O)_3]$	3400(s) 3279(s) 3200(s)	1668(m)	1608(s)	1537(s)	-	1304(s)*	1042(w)	581(w)	469(w)	-
2	$[Ni_2(slox)(H_2O)_4]$	3374(s)	-	1625(s) 1600(s)	1551(s)	1533(s)	1306(s)*	1048(w)	592(m)	461(w)	810(w)
3	$[Ni_2(slox)(py)_4]$	3415(s)	-	1600(s)	1557(s)	1530(s)	1304(s)*	1040(w)	596(m)	464(w)	812(w)
4	$[Ni_2(slox)(2\text{-}pic)_4]$	3367(s)	-	1626(s) 1600(s)	1551(s)	1533(s)	1307(s)*	1047(w)	599(m)	463(w)	818(w)
5	$[Ni_2(slox)(3\text{-}pic)_4]$	3392(s)	-	1622(s) 1600(s)	1553(s)	1532(s)	1307(s)*	1049(w)	598(m)	476(w)	816(w)
6	$[Ni_2(slox)(4\text{-}pic)_4]$	3410(s)	-	1618(s) 1599(s)	1551(s)	1503(s)	1299(s)	1040(w)	597(w)	493(m)	814(w)
7	$[Ni_2(slox)(phen)_3]$	3379(s)	-	1609(s) 1588(s)	1555(s)	1516(s)	1277(s)	1045(w)	565(w)	441(w)	-
8	$[Ni_2(slox)(bpy)_3]$	3375(s)	-	1610(s) 1598(s)	1558(s)	1513(s)	1275(s)	1024(m)	560(w)	434(w)	-

* merged with ligand band